



***In Vitro* Cell Models of Vascular Calcification:
Integrative Roles for RANKL and TRAIL**

A dissertation submitted for the degree of Ph.D. by

Emma Harper, BSc.

Under the Supervision of Dr. Philip M. Cummins

September 2018

School of Biotechnology

Faculty of Science and Health

Dublin City University

DECLARATION

I hereby certify that this material, which I now submit for assessment on the programme of study leading to the award of Doctor of Philosophy, is entirely my own work, that I have exercised reasonable care to ensure that the work is original, and does not to the best of my knowledge breach any law of copyright, and has not been taken from the work of others save and to the extent that such work has been cited and acknowledged within the text of my work.

Signed: *Emma Harper* (Candidate)

Date: 15th May 2018

ID Number: 10313969

ACKNOWLEDGEMENTS

As the final touches are added to this thesis, there are a long list of thanks that I need to extend to the individuals who supported me over the course of this PhD project:

First and foremost, Phil – I can't thank you enough for your supervision and guidance from the first day I arrived in your office to discuss a PhD to finally writing this thesis. I imagine the scramble for last-minute funding back in 2014 added a few unnecessary grey hairs! At that stage I didn't realise what a positive and motivating experience it would be to spend four years in your lab (which I now consider a second home). It was both challenging and enjoyable and the best decision I could have made.

To the dynamic duo – Keith and Rob – my friends for life. Thank you both so much for the constant advice, laughs and distractions that have helped me through the past few years (with some serious science thrown in as well!). Because of your escapades I have endless (well-documented) happy memories to look back on, and I hope to receive regular red bucket updates and official invites to Scone Thursday.

I also want to sincerely thank the previous members of the trusty XB11/XB20 consortium: Hannah and Laura, who were always on hand for advice and encouragement, and Alisha, who provided a huge amount of guidance in the early stages of my PhD. I also have to extend this thanks to the School of Biotechnology as a whole, my support network of the past 8 years; what a talented School to be a part of and I have no doubt it can only get better!

Thank you to Dr. Diarmuid Smith of Beaumont Hospital, for driving this work from a clinical perspective; to Dr. Colin Davenport, whose solid research built the foundations for making this project a success. Special thanks also to the School of Health and Human Performance, in particular to Dr. Ronan Murphy, for the continuous collaborative support provided over the course of this project.

Thank you to the Irish Research Council and the DCU Daniel O'Hare Scholarship Scheme for having faith in and funding this research. Thanks also to the Irish Endocrine Society for providing a positive and encouraging platform to present my research on a regular basis. Thanks to the School of Biotechnology Orla Benson Memorial Scholarship Scheme for enabling me to travel to improve my research skills at the University of York, and to Arizona State University for facilitating my research visit to the BioDesign Institute. These experiences have shaped me as a researcher and I am extremely grateful for these opportunities.

Last but not least – thank you to my family. Mam, you have been such a strong support and inspiration to me long before this PhD, and I imagine listening to me talk about science for four years has not been easy! I appreciate everything you have done for me and having you and Nanny Harper with me has made this journey a lot easier. Sean, you have had to listen to my every worry since day one and you have experienced every bit as much of this adventure as I have. Thank you for being so positive and reassuring even when you had your own thesis to write! Finally, thank you to my extended family, friends and felines, for being so understanding and encouraging throughout this journey – it has helped more than you know!

PUBLICATIONS

Harper E, Rochfort KD, Forde H, Davenport C, Smith D, Cummins PM. Activation of the non-canonical NF- κ B/p52 pathway in vascular endothelial cells by RANKL elicits pro-calcific signalling in co-cultured smooth muscle cells. *Cell Signal* 2018;**47**:142-150.

Forde H, Davenport C, **Harper E**, Cummins PM, Smith D. The role of OPG/RANKL in the pathogenesis of diabetic cardiovascular disease. *Cardiovasc Endocrinol and Metab* 2018;**7**:28-33 [Review].

Davenport C, **Harper E**, Rochfort KD, Forde H, Smith D, Cummins PM. RANKL inhibits the production of OPG from smooth muscle cells under basal conditions and following exposure to cyclic strain. *J Vasc Res* 2018;**55**:111-123 [Joint First Author].

Harper E, Rochfort KD, Forde H, Davenport C, Smith D, Cummins PM. TRAIL attenuates RANKL-mediated osteoblastic signalling in vascular cell mono-culture and co-culture models. *PLoS One* 2017;**12**:e0188192.

Davenport C, **Harper E**, Forde H, Rochfort KD, Murphy RP, Smith D, Cummins PM. RANKL promotes osteoblastic activity in vascular smooth muscle cells by upregulating endothelial BMP-2 release. *Int J Biochem Cell Biol* 2016;**77(Pt A)**:171-180.

Harper E, Forde H, Davenport C, Rochfort KD, Smith D, Cummins PM. Vascular calcification in type-2 diabetes and cardiovascular disease: Integrative roles for OPG, RANKL and TRAIL. *Vascul Pharmacol* 2016;**82**:30-40 [Review].

Forde H, **Harper E**, Davenport C, Rochfort KD, Wallace R, Murphy RP, Smith D, Cummins PM. The beneficial pleiotropic effects of tumour necrosis factor-related apoptosis-inducing ligand (TRAIL) within the vasculature: A review of the evidence. *Atherosclerosis* 2016;**247**:87-96 [Review].

PRESENTATIONS

Harper E, Rochfort KD, Davenport C, Forde H, Smith D, Cummins PM. RANKL induces pro-calcific paracrine signalling via the non-canonical NF- κ B pathway in endothelial cells, promoting smooth muscle cell calcification. School of Biotechnology Research Day, DCU; January 26th 2018 [Poster Presentation].

Harper E, Forde H, Davenport C, Rochfort KD, Smith D, Cummins PM. TRAIL protects against RANKL-induced calcification in an *in vitro* vascular co-culture model, in part via attenuation of NF- κ B pro-calcific signalling. Irish Endocrine Society Annual Meeting, Malahide, Dublin; October 14th 2017 [Oral Presentation].

Harper E, Forde H, Davenport C, Rochfort KD, Smith D, Cummins PM. The protective effect of TRAIL on RANKL-induced vascular calcification in an *in vitro* co-culture model. School of Biotechnology Research Day, DCU; January 27th 2017 [Poster Presentation].

Harper E, Forde H, Davenport C, Rochfort KD, Smith D, Cummins PM. Investigating the protective effect of TRAIL on RANKL-induced calcification using a vascular cell co-culture model. Irish Endocrine Society Annual Meeting, Belfast, UK, October 13-14th 2016 [Poster Presentation]. *Winner of the Montgomery Medal for best poster.*

Harper E, Forde H, Davenport C, Smith D, Cummins PM. Type-2 diabetes: a “hard” act to beat. Tell It Straight Competition Final, St. Patrick’s College; April 28th 2016 [Oral Presentation].

Harper E, Forde H, Davenport C, Smith D, Cummins PM. Mechanisms of vascular calcification in type-2 diabetes and cardiovascular disease. School of Biotechnology Research Day, DCU; January 29th 2016 [Oral Presentation].

TABLE OF CONTENTS

Abbreviations	I
Units	VI
List of Figures	VII
List of Tables	X
Abstract	XI
1.0 Introduction	1
<i>1.1 Background</i>	2
1.1.1 Type-2 Diabetes Mellitus (T2DM) and Cardiovascular Disease (CVD)	2
1.1.1.1 The Progression of T2DM/CVD	3
1.1.1.2 Current T2DM/CVD Management	4
<i>1.2 Vascular Calcification (VC)</i>	5
1.2.1 VC – A Brief History	5
1.2.2 Forms of VC and their Location in the Vasculature	6
1.2.2.1 Intimal Calcification	6
1.2.2.2 Medial Calcification	7
1.2.3 Bone Morphogenesis	9
1.2.3.1 Bone Morphogenesis – A Balance of Osteoblasts and Osteoclasts	9
1.2.3.2 Molecular Players in Bone Morphogenesis – RANKL and OPG	11
1.2.3.3 Bone Morphogenesis – Key Mechanisms	12
1.2.4 VC Pathogenesis	13
1.2.4.1 VC Pathogenesis at the Cellular Level	13
1.2.4.2 VC Pathogenesis at the Molecular Level	14
1.2.4.2.1 Pro-calcific Transcription Factors	15
1.2.4.2.2 Downstream Protein Mediators	15
1.2.4.2.3 BMPs	16
1.2.4.2.4 Pro-inflammatory and Pro-oxidant Mediators	17
1.2.4.3 VC Pathogenesis – a Role for RANKL and OPG	18
1.2.4.4 VC Pathogenesis – a Role for TRAIL	20
1.2.4.4.1 TRAIL – Location, Function and Regulation	20
1.2.4.4.2 TRAIL in the Vasculature	22

1.2.4.5 VC Pathogenesis – Mechanistic Considerations for RANKL and TRAIL	24
1.2.4.5.1 NF- κ B Signalling	24
1.2.4.5.2 Oxidative Stress	28
1.3 VC Models	30
1.3.1 <i>In vitro</i> Studies	30
1.3.2 <i>In vivo</i> Studies	32
1.3.3 Clinical Research	33
1.3.3.1 OPG	34
1.3.3.2 RANKL	35
1.3.3.3 TRAIL	36
1.4 Therapeutic Considerations	37
1.4.1 Recombinant OPG Therapy	37
1.4.2 Anti-RANKL Therapy	38
1.4.3 TRAIL Administration	38
1.4.4 Additional Therapeutic Possibilities	39
1.5 Study Hypotheses and Objectives	40
1.5.1 Study 1: Profiling the Effects of RANKL +/- TRAIL in the Vasculature	40
1.5.2 Study 2: Profiling the Effects of RANKL/TRAIL under Pathological Conditions	40
1.5.3 Study 3: Investigating the Mechanisms of RANKL/TRAIL Function during VC	41
2.0 Materials and Methods	43
2.1 Materials	44
2.1.1 Consumables and Plasticware	44
2.1.2 Reagents and Chemicals	45
2.1.3 Apparatus and Equipment	50
2.1.4 Buffer Preparation	51
2.2 Methods	54
2.2.1 Cell Culture Methods	54
2.2.1.1 Sterile Conditions	54
2.2.1.2 Growth and Maintenance of Cells	54
2.2.1.3 Trypsinisation	55

2.2.1.4 Cryopreservation and Cryorecovery	55
2.2.1.5 Cell Counting	55
2.2.2 Cell Models and Treatments	56
2.2.2.1 Monoculture Models	56
2.2.2.2 Co-Culture Models	57
2.2.2.3 Calcification Models	58
2.2.2.4 siRNA Gene Knockdown Models	59
2.2.2.4.1 siRNA Transfection Optimisation	60
2.2.2.4.2 Co-culture Experiments: NFκB2 Knockdown	60
2.2.3 Gene Expression Analysis	60
2.2.3.1 RNA Isolation	60
2.2.3.2 DNase Treatment and cDNA Synthesis	62
2.2.3.3 RNA and DNA Quantification	62
2.2.3.4 Primer Design and Optimisation	63
2.2.3.5 Standard PCR	64
2.2.3.6 Agarose Gel Electrophoresis	67
2.2.3.7 Quantitative Real-Time PCR	67
2.2.3.8 Primer Efficiencies	69
2.2.4. Protein Analysis	70
2.2.4.1 Protein Extraction	70
2.2.4.2 BCA Assay	70
2.2.4.3 SDS-PAGE	71
2.2.4.4 Electrophoretic Transfer and Western Immunoblotting	72
2.2.4.5 Enzyme-linked Immunosorbent Assay (ELISA)	74
2.2.4.5.1 Standard ELISA protocol	75
2.2.5 Functional and Physiological Analysis	76
2.2.5.1 ALP Enzyme Activity Assay	76
2.2.5.2 Permeability Assay	76
2.2.6 Cell Staining	77
2.2.6.1 Alizarin Red S: Calcium Staining	77
2.2.6.1.1 Alizarin Red Staining for Microscopy	77
2.2.6.1.2 Alizarin Red Staining for Quantification by Absorbance	78
2.2.6.2 Immunofluorescence Microscopy: Oxidative Stress	78
2.2.7 Flow Cytometry	79

2.2.7.1 Apoptosis Assay	80
2.2.7.2 Oxidative Stress	82
2.2.8 Bioinformatics Search	82
2.2.9 Data Normalisation	83
2.2.10 Statistical Analysis	83
3.0 Profiling the Pro-calcific Effects of RANKL +/- TRAIL in Vascular Cell Mono- and Co-culture Models	85
<i>3.1 Introduction</i>	86
3.1.1 Background and Hypothesis Development	86
3.1.2 Study Aims	87
3.1.3 Experimental Design	87
<i>3.2 Preliminary Investigations</i>	89
3.2.1 Establishing Treatment Conditions	89
3.2.2 Expression of RANKL and TRAIL	91
3.2.2.1 HAECs	91
3.2.2.2 HASMCs	92
3.2.3 Expression of RANKL and TRAIL Receptors	92
3.2.4 Effects of RANKL and TRAIL on Cellular Integrity	92
3.2.4.1 Cell Morphology	93
3.2.4.2 Viability and Apoptosis	93
3.2.4.3 Endothelial Barrier Function	95
3.2.4.4 Phenotypic Analysis of Smooth Muscle Cells	95
3.2.5 Methodological Validation	95
3.2.5.1 qPCR	96
3.2.5.2 ELISA	96
3.2.5.3 Co-culture	96
3.2.6 Discussion: Preliminary Investigations	97
3.2.6.1 Selection of Optimal Treatment Conditions in HAECs	97
3.2.6.2 Expression of RANKL and TRAIL in HAECs and HASMCs	98
3.2.6.3 The Effects of RANKL and TRAIL on Cellular Integrity	99
3.2.6.4 Methodological Validation	101

3.3 HAEC Monoculture	102
3.3.1 The Effects of RANKL +/- TRAIL on the Expression of HAEC Gene Targets	102
3.3.2 The Effects of RANKL +/- TRAIL on the Expression of HAEC Protein Targets	102
3.3.3 The Effects of RANKL +/- TRAIL on HAEC NF- κ B Activation	104
3.3.4 HAEC Monoculture: Summary of Results	104
3.3.5 Discussion: HAEC Monoculture	105
3.3.5.1 The Effects of RANKL +/- TRAIL on BMP-2 Regulation	105
3.3.5.2 The Effects of RANKL +/- TRAIL on Pro-Calcific Markers	106
3.3.5.3 The Effects of RANKL +/- TRAIL on OPG Regulation	107
3.3.5.4 The Effects of RANKL +/- TRAIL on NF- κ B Activation	108
3.3.5.5 Summary: HAEC Monoculture	109
3.4 HASMC Monoculture	110
3.4.1 The Effects of RANKL +/- TRAIL on the Expression of HASMC Gene Targets	110
3.4.2 The Effects of RANKL +/- TRAIL on the Expression of HASMC Protein Targets	112
3.4.3 The Effects of RANKL +/- TRAIL on NF- κ B Activation	112
3.4.4 The Effects of β -glycerophosphate on the Expression of Gene/Protein Targets	112
3.4.5 The Effects of BMP-2 +/- Noggin on HASMC Gene/Protein Targets	113
3.4.6 HASMC Monoculture: Summary of Results	114
3.4.7 Discussion: HASMC Monoculture	115
3.4.7.1 The Effects of RANKL +/- TRAIL on Pro-Calcific Targets	115
3.4.7.2 The Effects of RANKL +/- TRAIL on OPG Regulation	117
3.4.7.3 The Effects of RANKL +/- TRAIL on NF- κ B Activation	119
3.4.7.4 Summary: HASMC Monoculture	119
3.5 HAEC:HASMC Co-culture	120
3.5.1 The Effects of RANKL +/- TRAIL on the Expression of HASMC Gene Targets	120
3.5.2 The Effects of RANKL +/- TRAIL on the Expression of HASMC Protein Targets	120
3.5.3 The Effects of RANKL +/- TRAIL on HASMC NF- κ B Activation	123
3.5.4 The Effects of RANKL +/- Noggin on the Expression of HASMC Targets	123
3.5.5 HAEC:HASMC Co-culture: Summary of Results	124
3.5.6 Discussion: Co-culture	125
3.5.6.1 The Effects of RANKL +/- TRAIL on Endothelial Paracrine Signalling	125
3.5.6.2 The Effects of EC Paracrine Signalling on HASMC Pro-Calcific Indices	126
3.5.6.3 The Effects of Paracrine Signalling on HASMC OPG Regulation	128

3.5.6.4 The Effects of Paracrine Signalling on HASMC NF- κ B Activation	129
3.5.6.5 Summary: Co-culture	130
3.6 Alizarin Red S Staining for End-point Calcification	131
3.6.1 Alizarin Red S Staining: MC3T3-E1 Pre-osteoblasts	131
3.6.2 Alizarin Red S Staining: HASMCs	131
3.6.3 Discussion: End-point Calcification	133
3.7 Summary and Conclusions	135
4.0 Profiling the Effects of RANKL and TRAIL in Vascular Cell Models under Inflammatory and Hyperglycemic Conditions	137
4.1 Introduction	138
4.1.1 Background and Hypothesis Development	138
4.1.2 Study Aims	139
4.1.3 Experimental Design	139
4.2 Preliminary Investigations	141
4.2.1 Expression of RANKL and TRAIL	141
4.2.1.1 HAECs	141
4.2.1.2 HASMCs	141
4.2.2 Effects of RANKL and TRAIL on Cellular Integrity	142
4.2.2.1 Cell Morphology	142
4.2.2.2 Viability and Apoptosis	144
4.2.2.3 Endothelial Barrier Function	144
4.2.2.4 Phenotypic Analysis of Smooth Muscle Cells	144
4.2.3 Methodological Validation	144
4.2.5 Discussion: Preliminary Investigations	145
4.2.5.1 Expression of RANKL/TRAIL under Pathological Conditions	145
4.2.5.2 The Effects of TNF α and Glucose on Cellular Integrity	146
4.3 HAEC Monoculture	148
4.3.1 The Effects of TNF α and Glucose on Pro-Calcific Targets in HAECs	148
4.3.2 The Effects of RANKL and TRAIL under Inflammatory Conditions in HAECs	148
4.3.3 The Effects of RANKL and TRAIL under Hyperglycemic Conditions in HAECs	152

4.3.4 HAEC Monoculture: Summary of Results	153
4.3.5 Discussion: HAEC Monoculture	154
4.3.5.1 The Effects of TNF α on VC Indices	154
4.3.5.2 The Effects of RANKL on VC Indices under Inflammatory Conditions	155
4.3.5.3 The Effects of TRAIL on VC Indices under Inflammatory Conditions	156
4.3.5.4 The Effects of Hyperglycemia on VC Indices	157
4.3.5.5 The Effects of RANKL on VC Indices under Hyperglycemic Conditions	158
4.3.5.6 The Effects of TRAIL on VC Indices under Hyperglycemic Conditions	158
4.3.5.7 HAEC Monoculture: Summary	159
4.4 HASMC Monoculture	160
4.4.1 The Effects of TNF α and Glucose on Pro-Calcific Targets in HASMCs	160
4.4.2 The Effects of RANKL and TRAIL under Inflammatory Conditions in HASMCs	160
4.4.3 The Effects of RANKL and TRAIL under Hyperglycemic Conditions in HASMCs	163
4.4.4 HASMC Monoculture: Summary of Results	165
4.4.5 HASMC Monoculture: Discussion	166
4.4.5.1 The Effects of TNF α on VC Indices	166
4.4.5.2 The Effects of RANKL on VC Indices under Inflammatory Conditions	167
4.4.5.3 The Effects of TRAIL on VC Indices under Inflammatory Conditions	168
4.4.5.4 The Effects of Hyperglycemia on VC Indices	169
4.4.5.5 The Effects of RANKL on VC Indices under Hyperglycemic Conditions	170
4.4.5.6 The Effects of TRAIL on VC Indices under Hyperglycemic Conditions	171
4.4.5.7 HASMC Monoculture: Summary	172
4.5 HAEC:HASMC Co-culture	173
4.5.1 The Effects of TNF α and Glucose on Pro-Calcific Targets in Co-culture	173
4.5.2 The Effects of RANKL and TRAIL under Inflammatory Conditions in Co-culture	173
4.5.3 The Effects of RANKL and TRAIL under Hyperglycemic Conditions in Co-culture	176
4.5.4 HAEC:HASMC Co-culture: Summary of Results	178
4.5.5 Co-culture: Discussion	179
4.5.5.1 The Effects of TNF α on VC Indices	179
4.5.5.2 The Effects of RANKL on VC Indices under Inflammatory Conditions	181
4.5.5.3 The Effects of TRAIL on VC Indices under Inflammatory Conditions	181
4.5.5.4 The Effects of Hyperglycemia on VC Indices	182

4.5.5.5 The Effects of RANKL on VC Indices under Hyperglycemic Conditions	183
4.5.5.6 The Effects of TRAIL on VC Indices under Hyperglycemic Conditions	184
4.5.5.7 Co-culture: Summary	185
4.6 Summary and Conclusions	186
5.0 Mechanisms of RANKL-induced Pro-calcific Signalling and TRAIL-mediated Protection in the Vasculature	187
5.1 Introduction	188
5.1.1 Background and Hypothesis Development	188
5.1.2 Study Aims	189
5.1.3 Study Overview	189
5.1.3.1 Identification of Novel VC Targets	189
5.1.3.2 Investigating the Role of Oxidative Stress in VC Regulation	191
5.1.3.3 Clarifying the Role of Non-canonical NF- κ B Signalling during VC	192
5.1.4 Experimental Design	192
5.2 Identification and Analysis of a Novel VC Target	194
5.2.1 Target Identification	194
5.2.2 The Effects of RANKL +/- TRAIL on TRACP5 Expression	196
5.2.3 The Effects of RANKL/TRAIL on TRACP5 Expression during Inflammation	198
5.2.4 The Effects of RANKL/TRAIL on TRACP5 Expression during Hyperglycemia	198
5.2.5 Discussion: TRACP5 Analysis	201
5.2.5.1 Identification of a Novel VC Target: TRACP5	201
5.2.5.2 The Function of TRACP5 in Bone and Vasculature	202
5.2.5.3 The Effects of RANKL +/- TRAIL on TRACP5 Expression	204
5.2.5.4 The Effects of RANKL/TRAIL on TRACP5 during Inflammation	205
5.2.5.5 The Effects of RANKL/TRAIL on TRACP5 during Hyperglycemia	206
5.2.5.6 TRACP5: Summary of Results	207
5.3 Identifying the Role of RANKL/TRAIL in Endothelial Oxidative Stress	208
5.3.1 The Expression of SOD1/SOD2 in HAECs	208
5.3.1.1 The Effects of RANKL +/- TRAIL on SOD1/SOD2 Expression	208
5.3.1.2 The Effects of RANKL/TRAIL on SOD1/SOD2 during Inflammation	209

5.3.1.3 The Effects of RANKL/TRAIL on SOD1/SOD2 during Hyperglycemia	210
5.3.2 The Effects of RANKL +/- TRAIL on Pro-/Anti-oxidant Gene Expression	210
5.3.3 The Effects of the Anti-Oxidant NAC on Pro-calcific Signalling in HAECs	211
5.3.3.1 The Effects of NAC on the Pro-calcific/Pro-oxidant Actions of RANKL	212
5.3.3.2 The Effects of NAC on the Pro-oxidant/Pro-calcific Actions of TNF α	212
5.3.4 The Effects of TRAIL on RANKL-induced ROS Generation in HAECs	212
5.3.5 Discussion: Oxidative Stress	215
5.3.5.1 The Effects of RANKL +/- TRAIL on SOD1/SOD2 Expression	215
5.3.5.2 The Effects of RANKL/TRAIL on SOD1/SOD2 during Inflammation	217
5.3.5.3 The Effects of RANKL/TRAIL on SOD1/SOD2 during Hyperglycemia	217
5.3.5.4 The Effects of RANKL +/- TRAIL on Redox Gene Expression	219
5.3.5.5 The Effects of NAC on the Pro-calcific/Pro-oxidant Actions of RANKL	222
5.3.5.6 The Effects of NAC on the Pro-calcific/Pro-oxidant Actions of TNF α	223
5.3.5.7 The Effects of TRAIL on RANKL-induced ROS Generation	223
5.3.5.8 Summary: Oxidative Stress	226
5.4 Investigating the Role of Non-canonical NF-κB Activation in HAECs	227
5.4.1 Optimisation of siRNA Knockdown	227
5.4.2 The Effects of NF- κ B/p52 Knockdown on Pro-Calcific Indices in HAECs	229
5.4.3 The Effects of NF- κ B/p52 Knockdown on Pro-Calcific Indices in Co-culture	230
5.4.4 The Effects of NF- κ B/p52 Knockdown on Pro/Anti-Oxidant Indices in HAECs	230
5.4.5 Discussion: Non-canonical NF- κ B Activation	232
5.4.5.1 The Effects of NF- κ B/p52 Knockdown on Pro-Calcific Indices	233
5.4.5.2 The Effects of NF- κ B/p52 Knockdown on Anti-oxidant Expression	235
5.5 Summary and Conclusions	237
6.0 Final Summary	239
6.1 Final Summary	240
6.1.1 Study 1: Key Findings	241
6.1.2 Study 2: Key Findings	242
6.1.3 Study 3: Key Findings	244
6.2 Future Directions	246

<i>6.3 Concluding Remarks</i>	248
Bibliography	249
Appendices	291

ABBREVIATIONS

ADAM™	Advanced Detection and Accurate Measurement
ALP	Alkaline Phosphatase
ANOVA	Analysis of Variance
ApoE	Apolipoprotein E
AR	Alizarin Red
BB	Binding Buffer
BCA	Bicinchoninic Acid
BioGRID	Biological General Repository for Interaction Databases
BMP	Bone Morphogenetic Protein
BSA	Bovine Serum Albumin
BSP	Bone Sialoprotein
cDNA	Complimentary Deoxyribonucleic Acid
CAC	Coronary Artery Calcium
CAD	Coronary Artery Disease
CKD	Chronic Kidney Disease
CO ₂	Carbon Dioxide
C _q	Quantification Cycle
C _t	Cycle Threshold
CVD	Cardiovascular Disease
DAPI	4',6-Diamidino-2-Phenylindole Dihydrochloride
DcR	Decoy Receptor
dH ₂ O	Distilled Water
DHE	Dihydroethidium
DMSO	Dimethyl Sulfoxide
DNA	Deoxyribonucleic Acid
dNTP	Deoxynucleotide Triphosphate
DR	Death Receptor
EC	Endothelial Cell

EDTA	Ethylenediaminetetraacetic Acid
ELISA	Enzyme Linked Immunosorbent Assay
eNOS	Endothelial Nitric Oxide Synthase
ERK	Extracellular Signal-Related Kinase
FACS	Fluorescence Automated Cell Sorting
FBS	Fetal Bovine Serum
FITC	Fluorescein Isothiocyanate
FSC	Forward Scatter
GAPDH	Glyceraldehyde 3-Phosphate Dehydrogenase
GLP-1RA	Glucagon-Like Peptide-1 Receptor Agonist
GLUT	Glucose Transporter
HAEC	Human Aortic Endothelial Cell
HASMC	Human Aortic Smooth Muscle Cell
HCl	Hydrochloric Acid
HEPES	4-(2-Hydroxyethyl)-1-Piperazineethanesulfonic Acid
HMOX	Heme Oxygenase
HRP	Horseradish Peroxidase
HUVEC	Human Umbilical Vein Endothelial Cell
IF	Immunofluorescence
Ig	Immunoglobulin
I κ B	Inhibitor of κ B enhancer
IKK	I κ B Kinase
IL	Interleukin
IMS	Industrial Methylated Spirits
IP	Immunoprecipitation
IPA	Isopropanol
LDL	Low Density Lipoprotein
MAPK	Mitogen-activated Protein Kinase
MGP	Matrix gla Protein

MI	Myocardial Infarction
MIQE	Minimum Information for Publication of Quantitative Real-Time PCR Experiments
mRNA	Messenger RNA
MSC	Mesenchymal Stem Cell
Msx2	Msh Homeobox 2
MWCO	Molecular Weight Cut Off
NAC	N-Acetyl- <i>L</i> -Cysteine
NADPH	Nicotinamide Adenine Dinucleotide Phosphate
NCBI	National Centre for Biotechnology Information
NF- κ B	Nuclear Factor of Activated B-cells
NFATc1	Nuclear Factor of Activated T-cells, Cytoplasmic 1
NGS	Normal Goat Serum
NIK	NF- κ B-Inducing Kinase
NO	Nitric Oxide
NOX	NADPH Oxidase
Nt-siRNA	Non-targetting siRNA
OCN	Osteocalcin
OD	Optical Density
OPG	Osteoprotegerin
OPN	Osteopontin
p-p65	Phosphorylated p65 Subunit
PAD	Peripheral Artery Disease
PBS	Phosphate Buffered Saline
Phox	Phagocytic Oxidase
(q) PCR	(Real Time) Polymerase Chain Reaction
PE	Phycoerythrin
PES	Polyethersulfone
pH	Power of Hydrogen

PI	Propidium Iodide
(P) P_i	Inorganic (Pyro)phosphate
pNPP	p-Nitrophenyl Phosphate
PS	Phosphatidylserine
PTH	Parathyroid Hormone
PVDF	Polyvinylidene Fluoride
RANK (L)	Receptor Activator of NF- κ B (Ligand)
RIPA	Radio Immunoprecipitation Assay
RISC	RNA-induced Silencing Complex
RNA	Ribonucleic Acid
ROS	Reactive Oxygen Species
rRNA	Ribosomal RNA
RT	Reverse Transcriptase
Runx2	Runt-Related Transcription Factor 2
SDS	Sodium Dodecyl Sulfate
SDS-PAGE	SDS-Polyacrylamide Gel Electrophoresis
SEM	Standard Error of the Mean
siRNA	Small Interfering RNA
SM	Smooth Muscle
SOD	Superoxide Dismutase
Sox9	Sex-Determining Region Y-Box 9
SSB	Sample Solubilisation Buffer
SSC	Side Scatter
STRING	Search Tool for the Retrieval of Interacting Genes and Proteins
t-p65	Total p65 Subunit
T2DM	Type-2 Diabetes Mellitus
TAD	Transcription Activation Domain
TAE	Tris Acetic Acid EDTA

TBS (-T)	Tris Buffered Saline (-Tween® 20)
TEE	Trans-Endothelial Exchange
TEMED	Tetramethylethylenediamine
TGF	Transforming Growth Factor
TMB	Tetramethylbenzidine
TNF	Tumour Necrosis Factor
TRACP5	Tartrate Resistant Acid Phosphatase 5
TRAF	TNF Receptor Associated Factor
TRAIL	TNF-related Apoptosis Inducing Ligand
αMEM	Modified Eagle Medium, alpha Modification
VC	Vascular Calcification
VEGF	Vascular Endothelial Growth Factor
VSMC	Vascular Smooth Muscle Cell
vWF	Von Willebrand Factor

UNITS

%	Percent
μg	Microgram
μL	Microlitre
μM	Micromolar
bp	Base Pair
g	Gram
IU	International Enzyme Unit
Kb	Kilobase
kDa	Kilodalton
L	Litre
M	Molar
M	Metre
mL	Millilitre
mM	Millimolar
mm	Millimetre
ng	Nanogram
nM	Nanomolar
nm	Nanometre
°C	Degrees Celcius
pg	Picogram
V	Volts
v/v	Volume per Volume
w/v	Weight per Volume
<i>xg</i>	Times Force of Gravity

LIST OF FIGURES

- Figure 1.1** Basic representation of the three distinct layers of the vascular wall.
- Figure 1.2** Intimal and medial calcification.
- Figure 1.3** Progression of bone morphogenesis.
- Figure 1.4** The regulation of pro-calcific genes and proteins in calcifying vascular cells.
- Figure 1.5** Interactions between OPG and RANKL in healthy and vessel.
- Figure 1.6** Interactions between OPG, RANKL and TRAIL in the vasculature.
- Figure 1.7** The canonical and non-canonical NF- κ B pathways activated by RANKL.
- Figure 1.8** Representation of the in vitro co-culture model.
-
- Figure 2.1** The ADAMTM Counter with an Accuchip resting in the loading bay.
- Figure 2.2** Schematic representation of the HAEC:HASMC co-culture model.
- Figure 2.3** The process of siRNA gene silencing.
- Figure 2.4** The three distinct phases of TrizolTM extractions.
- Figure 2.5** Example of a NanodropTM reading for cDNA quantification.
- Figure 2.6** Examples of amplification curves on LightCycler@96 software demonstrating the principle of qPCR.
- Figure 2.7** Representative melting curve.
- Figure 2.8** Layout of the fully assembled transfer cassette.
- Figure 2.9** The final steps of the ELISA protocol following TMB addition.
- Figure 2.10** Principle of the trans-endothelial permeability assay.
- Figure 2.11** The flow cell of a flow cytometer.
- Figure 2.12** Example output of the apoptosis assay.
-
- Figure 3.1** Typical morphology of HAECs and HASMCs in culture.
- Figure 3.2** Representation of the transwell co-culture model.
- Figure 3.3** Optimisation of RANKL and TRAIL exposure concentrations in HAEC monoculture.
- Figure 3.4** The effect of RANKL and TRAIL exposure on HAEC and HASMC apoptosis.
- Figure 3.5** Protein analyses in HAEC monoculture.
- Figure 3.6** mRNA and protein analyses in HASMC monoculture.
- Figure 3.7** NF- κ B activation in HASMC monoculture following RANKL +/- TRAIL treatment.

- Figure 3.8** The co-culture model.
- Figure 3.9** mRNA analyses of HASMCs in co-culture.
- Figure 3.10** Analysis of protein targets in co-cultured HASMCs.
- Figure 3.11** Summary of the key responses following endothelial exposure to RANKL +/- TRAIL in co-culture.
- Figure 3.12** Alizarin red staining of differentiated MC3T3-E1 and HASMC cells.
-
- Figure 4.1** Representation of the transwell co-culture model under inflammatory and hyperglycemic conditions.
- Figure 4.2** HAECs under control conditions and following exposure to TNF α .
- Figure 4.3** The effect of TNF α and glucose exposure on HAEC and HASMC apoptosis.
- Figure 4.4** The effects of TNF α on pro-calcific indices in HAEC monoculture.
- Figure 4.5** The effects of glucose on pro-calcific indices in HAEC monoculture.
- Figure 4.6** The effects of TNF α +/- RANKL/TRAIL on pro-calcific indices in HAECs.
- Figure 4.7** The effects of glucose +/- RANKL/TRAIL on pro-calcific indices in HAECs.
- Figure 4.8** Summary of the key findings following endothelial exposure to RANKL/TRAIL +/- TNF α /glucose.
- Figure 4.9** The effects of TNF α on pro-calcific indices in HASMC monoculture.
- Figure 4.10** The effects of glucose on pro-calcific indices in HASMC monoculture.
- Figure 4.11** The effects of TNF α +/- RANKL/TRAIL on pro-calcific indices in HASMCs.
- Figure 4.12** The effects of glucose +/- RANKL/TRAIL on pro-calcific indices in HASMCs.
- Figure 4.13** Summary of the key findings following smooth muscle exposure to RANKL/TRAIL +/- TNF α /glucose.
- Figure 4.14** The co-culture model.
- Figure 4.15** The effects of TNF α on pro-calcific indices in co-cultured HASMCs.
- Figure 4.16** The effects of glucose on pro-calcific indices in co-cultured HASMCs.
- Figure 4.17** The effects of TNF α +/- RANKL/TRAIL on pro-calcific indices in co-culture.
- Figure 4.18** The effects of glucose +/- RANKL/TRAIL on pro-calcific indices in co-culture.
- Figure 4.19** Summary of the key HASMC responses following endothelial exposure to RANKL/TRAIL +/- TNF α /glucose in co-culture.
-
- Figure 5.1** Schematic representation of the experiments and techniques employed in Chapter 5.

- Figure 5.2** Representation of the transwell co-culture model employed for TRACP5 analysis.
- Figure 5.3** The effects of RANKL +/- TRAIL on TRACP5 expression.
- Figure 5.4** The effects of RANKL/TRAIL on TRACP5 mRNA expression under inflammatory and hyperglycemic conditions.
- Figure 5.5** The effects of RANKL/TRAIL on TRACP5 protein expression under inflammatory and hyperglycemic conditions.
- Figure 5.6** Representation of the key findings of TRACP5 investigations.
- Figure 5.7** The effects of RANKL +/- TRAIL on SOD1 expression in HAECs.
- Figure 5.8** The effects of RANKL +/- TRAIL on pro/anti-oxidant mRNA expression in HAECs.
- Figure 5.9** The effects of RANKL +/- NAC on gene/protein expression in HAECs.
- Figure 5.10** The effects of RANKL +/- TRAIL on ROS generation in HAECs.
- Figure 5.11** Representation of the key findings of redox investigations.
- Figure 5.12** Representation of the transwell co-culture model employed following endothelial NF- κ B p52/p100 knockdown.
- Figure 5.13** Optimisation of NF- κ B2 siRNA knockdown.
- Figure 5.14** The effects of RANKL following endothelial siRNA knockdown in co-cultured HASMCs.
- Figure 6.1** Visual interpretation of the key findings from Studies 1-3.

LIST OF TABLES

Table 1.1	Non-exhaustive list of modifiable and non-modifiable risk factors common to type-2 diabetes and cardiovascular disease.
Table 1.2	Summary of the most relevant in vitro studies regarding the effects of RANKL, TRAIL and OPG in the vasculature.
Table 1.3	Summary of the most relevant in vivo studies regarding the effects of RANKL, TRAIL and OPG in the vasculature.
Table 2.1	Soluble factors, their source and concentration as employed for cell exposures.
Table 2.2	Reaction mixture for cDNA synthesis.
Table 2.3	Standard PCR reaction components.
Table 2.4	Standard PCR reaction parameters.
Table 2.5	Forward/reverse primer sequences employed in standard PCR and qPCR.
Table 2.6	Employed volumes of qPCR reaction components.
Table 2.7	qPCR reaction parameters.
Table 2.8	Components of resolving and stacking gels for SDS-PAGE.
Table 2.9	Details of antibodies employed in western immunoblotting.
Table 2.10	Detection limits for DuoSet® ELISA kits.
Table 3.1	Average percentages of viable, non-viable, and apoptotic HAECs and HASMCs post-treatment.
Table 3.2	The effects of RANKL +/- TRAIL in HAEC monoculture.
Table 3.3	The effects of RANKL +/- TRAIL in HASMC monoculture.
Table 3.4	The effects of RANKL +/- TRAIL in HAEC:HASMC co-culture.
Table 4.1	Average percentages of viable, non-viable, and apoptotic HAECs and HASMCs post-treatment.
Table 4.2	The effects of TNF α and glucose +/- RANKL or TRAIL in HAECs.
Table 4.3	The effects of TNF α or glucose +/- RANKL or TRAIL in HASMCs.
Table 4.4	The effects of TNF α or glucose +/- RANKL or TRAIL in co-cultured HASMCs.
Table 5.1	Key protein interactions and potential interactions with RANKL, OPG and TRAIL identified using the STRING bioinformatics database.

ABSTRACT

***In Vitro* Cell Models of Vascular Calcification: Integrative Roles for RANKL and TRAIL**

Emma Harper

Cardiovascular death remains the leading cause of mortality in type-2 diabetes mellitus, in which a high prevalence of vascular calcification (VC) is a significant risk factor. VC contributes to cardiovascular burden, with many diabetic sufferers succumbing to cardiac disease and stroke. Research indicates that key proteins observed in circulation, namely receptor-activator of NF- κ B ligand (RANKL) and tumour necrosis factor-related apoptosis-inducing ligand (TRAIL), interact with each other to regulate the calcification process. Whilst it is clear that RANKL promotes VC, in part via endothelial paracrine signalling, the precise role of TRAIL in this context remains undefined. Nonetheless, recent studies suggest a protective role for TRAIL in a vascular setting. Thus, we hypothesised that TRAIL inhibits VC via attenuation of RANKL-induced pro-calcific signalling. We also considered the individual effects of RANKL and TRAIL in the presence of relevant pathological stimuli (inflammation, hyperglycemia), and investigated how TRAIL may interfere with key pro-calcific pathways in the vasculature from a mechanistic perspective.

Human aortic endothelial cells (HAECs) and smooth muscle cells (HASMCs) were cultured in mono- and co-culture formats, the latter approximating the paracrine signalling axis of the vasculature. Both cell types were routinely exposed to RANKL +/- TRAIL. Following analysis of a wide range of VC-related indices, it was found that TRAIL co-incubation robustly attenuated RANKL-induced endothelial paracrine signalling, thereby preventing calcification in the underlying smooth muscle. Under inflammatory and hyperglycemic conditions, RANKL contributed to the promotion of pro-calcific signalling, whilst TRAIL exhibited a protective influence on vascular cells. Furthermore, it was found that RANKL induced non-canonical NF- κ B signalling and oxidative stress in the promotion of VC, whilst TRAIL exerted its protective influence via anti-oxidant effects and attenuation of the non-canonical NF- κ B pathway. This data therefore yields valuable mechanistic information on VC pathogenesis, and on the potential therapeutic value of TRAIL in this context.

Chapter 1

Introduction

1.1 Background

Cardiovascular disease (CVD) remains a leading cause of mortality among patients with type-2 diabetes mellitus (T2DM), in which a high prevalence of vascular calcification (VC) is a significant contributing risk factor (Rubin and Silverberg, 2004). The VC process, analogous to that of bone morphogenesis, can generally be described as a form of progressive arterial hardening that results in reduced vessel elasticity (Demer, 1991), ultimately increasing the risk of future cardiovascular events. There are two major forms of calcification; intimal calcification, which involves lipid and cholesterol accumulation under the damaged endothelial monolayer, and medial calcification, also known as Mönckeberg's sclerosis, which involves mineral deposition within the vessel smooth muscle layer (Proudfoot and Shanahan, 2001). The term "VC" conventionally refers to calcification within the medial arterial layer, the prime focus of this thesis, whilst intimal calcification has long been associated with atherosclerotic disease (Lehto *et al.*, 1996). It should be noted that, although T2DM-related calcification has been well-documented at the clinical level, the molecular mechanisms underlying the manifestation and progression of VC are still the subject of much debate. In this respect, this literature review will examine the VC phenomenon from three distinct perspectives: (i) to provide a concise overview of the pathogenesis of VC and the relevance of osteogenic pathways; (ii) to critically assess our understanding of the molecular players and mechanisms underpinning VC; and (iii) to consider calcification from a clinical perspective, highlighting potential novel therapeutic approaches to VC pathology. Finally, the primary objectives of this thesis will be outlined.

1.1.1 Type-2 Diabetes Mellitus (T2DM) and Cardiovascular Disease (CVD)

Type-2 diabetes mellitus (T2DM) accounts for 90-95% of all diabetes cases worldwide (Harris, 1998). According to Diabetes Ireland there are over 200,000 people living with T2DM in this country alone, a figure which is expected to rise to 278,850 by the year 2030 affecting 7.5% of our total population. In addition, according to the Healthy Ireland survey, there are approximately 1 million people over the age of 30 that are currently at risk of developing this disease if significant lifestyle changes are not made (Diabetes Ireland, 2018). These figures make T2DM the fastest growing health pandemic in Ireland, and the situation in this country reflects the global picture; T2DM therefore constitutes a major health challenge at both a national and international level. Furthermore, type-2 diabetics are much more likely to suffer

from conditions of the cardiovascular system, having detrimental consequences on T2DM mortality rates. The World Health Organization estimates that T2DM, with these associated cardiovascular complications, will be the 7th leading cause of death globally by the year 2030 (Morrish *et al.*, 2001). Many diabetic patients go on to suffer lethal cardiovascular events, including myocardial infarction (MI) or stroke, as underlying cardiovascular conditions often go unnoticed for long periods of time. The reasons for the high prevalence of cardiovascular issues in T2DM have not yet been fully delineated, and as such, a better understanding of disease pathophysiology combined with improvements in disease monitoring and treatment are therefore clearly warranted.

1.1.1.1 The Progression of T2DM/CVD

T2DM, at a most basic level, is a metabolic disorder primarily characterised by elevated blood glucose (hyperglycemia) and insulin resistance. In this respect, the hormone insulin controls blood sugar levels, enabling cellular glucose uptake from the circulation. During T2DM, this insulin may not work efficiently, or the pancreas may secrete insufficient amounts of insulin to adequately manage blood sugar levels, thereby resulting in hyperglycemia. While the precise explanation for the high prevalence of CVD among type-2 diabetic patients remain unclear, it may be attributed in part to the fact that several “modifiable” (i.e. controllable) and “non-modifiable” (i.e. uncontrollable) risk factors for CVD overlap with those for T2DM (Smulders *et al.*, 2008; World Heart Federation, 2017) (Table 1.1).

Table 1.1. Non-exhaustive list of modifiable and non-modifiable risk factors common to type-2 diabetes and cardiovascular disease.

Modifiable Risk Factors	Non-Modifiable Risk Factors
Obesity	Family History
Sedentary Lifestyle	Ethnicity
Smoking	Age
Dyslipidemia eg. High Cholesterol	Gender
Hypertension	History of Gestational Diabetes*
Dietary Factors eg. Alcohol Consumption	
Glucose Intolerance*	
Lack of Sleep*	

*Risk factor for type-2 diabetes only.

In addition to these common risk factors (Table 1.1), the presence of hyperglycemia among type-2 diabetic patients may also promote the development and progression of coinciding vascular complications. In this regard, hyperglycemia has been found to promote endothelial injury, rendering the innermost vascular layer dysfunctional; in this respect, endothelial dysfunction is a well-established precursor to a number of adverse clinical outcomes, as it promotes a pro-inflammatory, pro-atherogenic and pro-oxidant pathological vascular environment (Popov, 2010; Shi and Vanhoutte, 2017). Endothelial dysfunction is indeed considered a precursor to a number of macrovascular diseases common during T2DM, including angina, hypertension, coronary artery disease (CAD), carotid artery disease, peripheral artery disease (PAD) and ultimately (potentially fatal) acute MI or stroke (Ganz and Hsue, 2013; Versari *et al.*, 2009; Widmer and Lerman, 2013). Similarly, hyperglycemia and T2DM are associated with a number of microvascular diseases that can have detrimental effects on quality of life (Shi and Vanhoutte, 2017). It is extremely difficult for clinicians in practise to treat these conditions, however, given that the precise molecular processes underpinning the link between T2DM and CVD remain undefined.

1.1.1.2 Current T2DM/CVD Management

Currently, there are a number of relatively inefficient disease management options for diabetics suffering from CVD, focusing primarily on the concept of “modifiable” and “non-modifiable” risk factors as listed in Table 1.1. Non-modifiable risk factors are those that cannot be altered, such as a patient’s age, gender, and family history of T2DM/CVD (independently increasing diabetes risk by 2-6 fold) (Harrison *et al.*, 2003). Treatment is therefore centred around those modifiable factors that can be controlled, including obesity, hypertension, smoking, lack of exercise, dyslipidemia and alcohol consumption, with interventions generally consisting of both lifestyle changes and pharmaceuticals (eg. statins to control blood cholesterol levels) (Eldor and Raz, 2009). However, even with these interventions in place, risk factors are difficult to maintain under control, making this an ineffective treatment method for T2DM/CVD (Banegas *et al.*, 2011). As an additional point of relevance, there is no definitive widespread method of diagnosing cardiovascular complications in T2DM (or the extent of CVD) unless a patient suffers a cardiovascular event, in which case it is often too late for successful intervention. Therefore, a range of cardiovascular diseases of varying severity remain untreated during T2DM, ultimately contributing to the startling morbidity and mortality rates associated with this disease.

1.2 Vascular Calcification (VC)

Vascular calcification (VC), or “hardening of the arteries”, is one of the most prevalent cardiovascular complications among type-2 diabetics, and yet, this disorder remains unchallenged by current T2DM/CVD disease management. In recent years, it has been discovered that VC is not only an adverse side-effect of T2DM, but also participates in and accelerates the occurrence of acute cardiovascular complications (Demer and Tintut, 2008), making it and its mechanism of action a prime target for intervention. Recently, the potential of VC as both a biomarker of CVD risk and as a target for the inhibition and reversal of CVD has begun to emerge in the literature (Kapustin and Shanahan, 2009; Rennenberg *et al.*, 2009), but while considerable information has been gathered thus far on VC mechanisms, there is still much that is not understood (Muthu, 2013). If the precise mechanism(s) of action can be specified, it will bring us closer to the development and implementation of therapies that can either prevent or regress VC in diabetics, and ultimately improve the cardiovascular health and reduce the morbidity and mortality associated with T2DM worldwide.

1.2.1 VC – A Brief History

Calcification is a phenomenon primarily associated with bone formation. It is approximately 500 years since the first comparison was made between ossification and blood vessel hardening (Acierno, 1994), with the first elements of bone confirmed in the vasculature in 1906 (Bunting, 1906), however it is only in the past number of decades that the factuality of VC has started to emerge. Although it has long been appropriately associated with age, CVD and metabolic disorders such as diabetes, VC was until recently believed to be a passive degenerative disorder, with elevated calcium and phosphate levels resulting in mineral deposition as a form of arterial protection (Hayden *et al.*, 2005; Mizobuchi *et al.*, 2009; Valdivielso, 2011). Contrary to this belief, it is now known to be an active process involving the differentiation of vascular cells into osteoblast-like cells capable of mineralisation (Mizobuchi *et al.*, 2009). A number of mineralisation proteins have been identified in vascular cells, alongside mounting evidence that vascular smooth muscle cells (VSMCs) have the ability to simultaneously exhibit both physiological smooth muscle and pathophysiological osteogenic properties (Shanahan *et al.*, 2000). The growing evidence supporting this trans-differentiation of VSMCs has resulted in widespread recognition that VC is an actively regulated dynamic process sharing many similarities with that of bone morphogenesis.

1.2.2 Forms of VC and their Location in the Vasculature

VC can be broadly classified into two distinct forms depending upon its location within the vascular wall: intimal VC, affecting the tunica intima, and medial VC, affecting the tunica media; the latter form will be the prime focus of this thesis (Figure 1.1). A third form of VC, valvular calcification, can also affect aortic valves (Mohler *et al.*, 2001), but given the very specific nature of this complication, will not be included in the current literature review.

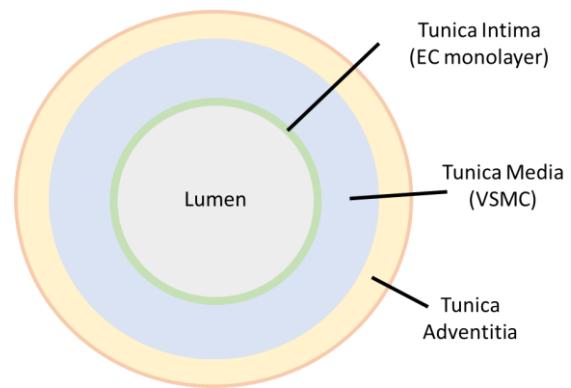


Figure 1.1. Basic representation of the three distinct layers of the vascular wall. EC, endothelial cell; VSMC, vascular smooth muscle cell.

1.2.2.1 Intimal Calcification

Intimal VC is more commonly referred to as atherosclerotic calcification, given that it co-locates with atherosclerotic plaque *in vivo* (Figure 1.2A). Atherosclerosis is a progressive inflammatory syndrome characterised by the formation of atheromata, or plaques, within the vascular intima. This plaque formation involves the gradual deposition and accumulation of oxidised low-density lipoprotein (LDL) and macrophages, in conjunction with VSMC migration and foam cell formation, to form a potentially rupture-prone plaque within the arterial lumen (Ross, 1999). Atherosclerosis (and thus intimal calcification) is generally limited to larger arterial vessels (e.g. aortic arch, thoracic aorta, coronary artery), often leading to diseases such as angina, CAD, carotid artery disease and PAD (Albrecht, 2013; Ford *et al.*, 2017; Thapar *et al.*, 2013). Moreover, atherosclerosis is strongly affected by arterial haemodynamic forces, and is more likely to develop at sites of disturbed shear stress such as that experienced at major arterial curvatures and bifurcations (Cunningham and Gotlieb, 2005). Indeed, the aorta is the most common vascular bed for intimal VC (Allison *et al.*, 2004; Doherty *et al.*, 2003).

It is thought that the presence of intimal VC, manifesting as small nodules of calcified material within atherosclerotic tissue, renders these plaques more prone to rupture and thus significantly increase the risk of a cardiovascular event (e.g. acute MI, stroke) (Abedin *et al.*, 2004; Budoff *et al.*, 2003; Johnson *et al.*, 2006; Virmani *et al.*, 1998). At a molecular level, intimal calcification is strongly dependent on pro-inflammatory cytokines present within atheromata

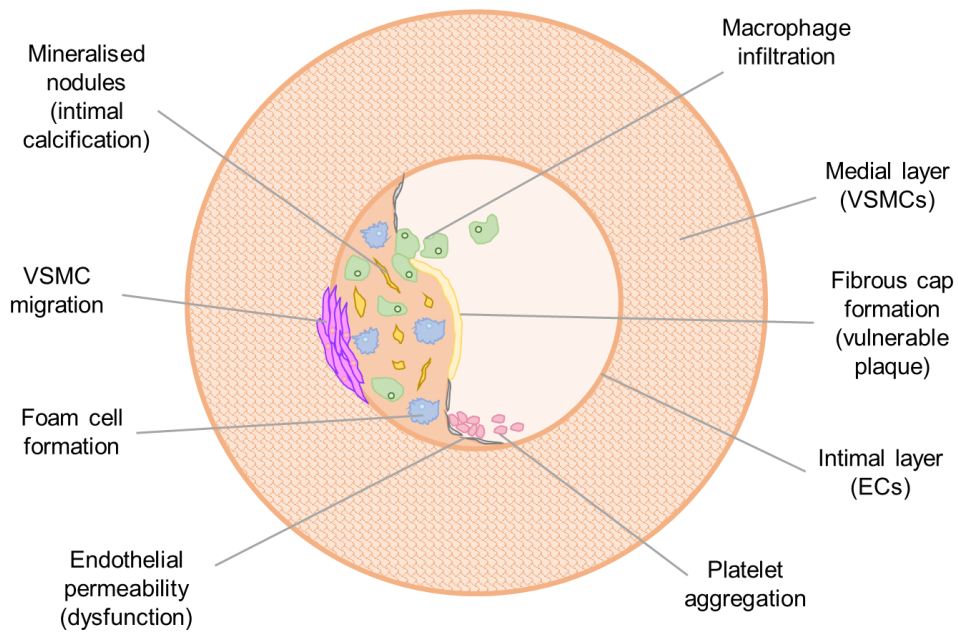
(Doherty *et al.*, 2003; Tintut *et al.*, 2000), which originate primarily from macrophages and foam cells prevalent in vulnerable plaques (Finn *et al.*, 2010). These infiltrating macrophages (and cytokines) can drive other pro-calcific and pro-oxidant signals, as can vascular cells themselves (Johnson *et al.*, 2006; Mody *et al.*, 2001), further promoting the progression of intimal VC. Whilst atherosclerotic calcification is highly prevalent in the general population (Allison *et al.*, 2004), diabetics with poorly-controlled blood glucose levels are at an even higher risk of developing intimal VC (Aronson and Rayfield, 2002).

1.2.2.2 Medial Calcification

Medial calcification, on the other hand, is a hydroxyapatite mineralisation process (Orimo, 2010) within the VSMC medial layer analogous to the process of endochondral ossification. Medial arterial calcification is the most common form of VC in T2DM, wherein arteries lose their elasticity due to the *circumferential mineral deposition within the smooth muscle cell layer* (Lehto *et al.*, 1996) (Figure 1.2B). Medial calcification can occur at any point within the arterial tree, including smaller vessels unlikely to be affected by atherosclerosis (Trouvin and Goëb, 2010). Thus far, medial VC has been implicated in multiple cardiovascular pathologies including hypertension, coronary insufficiency, left ventricular hypertrophy and an increased risk of atherosclerotic plaque rupture (Panizo *et al.*, 2009; Rubin and Silverberg, 2004; Singh *et al.*, 2012). Medial VC can also be driven by many of the same pro-calcific, pro-inflammatory and pro-oxidant signals as intimal VC, and also appears to be promoted by hyperglycemic conditions, given the higher prevalence of VC observed in diabetic patients (Stabley and Towler, 2017). Interestingly, although both intimal and medial VC can occur as independent entities, they share many risk factors and mechanistic similarities and often exist alongside one another in the same individual (McCullough *et al.*, 2008).

What makes medial VC a distinctly different process to intimal VC, however, is not only its location in the vasculature; the process of medial calcification is particularly similar to the process of bone formation, with smooth muscle cells taking on a distinctly “osteoblastic” phenotype (Kaden *et al.*, 2004; Ndip *et al.*, 2011; Panizo *et al.*, 2009) capable of inducing mineralisation. As such, the process of bone morphogenesis will first be summarised, before discussing in-depth the molecular signalling pathways and mechanisms underpinning medial VC (simply referred to as VC from this point forward).

A: Intimal VC



B: Medial VC

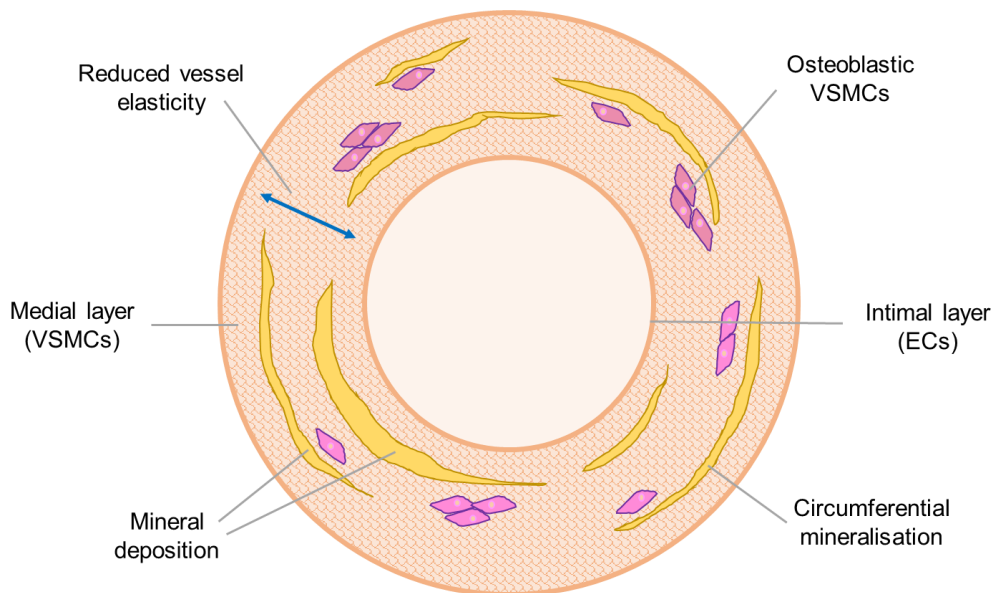


Figure 1.2. Intimal and medial calcification. (A) Intimal calcification occurs alongside atherosclerosis *in vivo*, manifesting as small nodules of calcified material rendering plaque vulnerable to rupture. Intimal VC coincides with several of the hallmarks of atherosclerotic disease; EC dysfunction and permeability, VSMC migration, foam cell formation, macrophage infiltration and platelet aggregation (Ross, 1999). (B) Medial VC exists as circumferential mineral deposits within the smooth muscle layer, a process promoted by “osteoblastic” VSMCs. This mineral deposition ultimately reducing vessel elasticity and promotes a number of vascular pathologies (Lehto *et al.*, 1996). Intimal and medial VC often coincide in the same vessel (McCullough *et al.*, 2008). EC, endothelial cell; VSMC, vascular smooth muscle cell.

1.2.3 Bone Morphogenesis

As noted, VC is now known to be a highly dynamic process involving the action of various hormones and cytokines upon multiple vascular cell types (Demer, 2001). Many of these proteins and their respective functions are traditionally associated with bone morphogenesis, and therefore before considering the pathogenesis of VC, it is critical to first understand the calcification process within this traditional physiological setting.

1.2.3.1 Bone Morphogenesis – A Balance of Osteoblasts and Osteoclasts

By way of overview, bone remodelling involves a complex equilibrium between anabolic bone formation (osteogenesis, ossification) and catabolic bone resorption, a key dynamic balance for healthy bone metabolism. This balance initially enables early bone development and thereafter maintains mineral homeostasis of calcium and phosphorus (Trouvin and Goëb, 2010), allowing continuous removal of old or damaged bone tissue alongside simultaneous growth of new bone. There are two cell types at the forefront of bone morphogenesis, namely bone-forming osteoblasts and bone-resorbing osteoclasts, which jointly regulate the remodelling process in conjunction with various hormones and cytokines. Osteoblasts are derivatives of bone marrow stem cells, whilst osteoclasts arise from the cytoplasmic fusion of immune precursors of monocyte/macrophage lineage to generate a multi-nucleated pre-osteoclast that forms a mature osteoclast upon activation (Ducy *et al.*, 2000; Teitelbaum, 2000) (Figure 1.3). Over-activation of bone-resorbing osteoclasts can lead to multiple pathological conditions including osteoporosis and rheumatoid arthritis (Kearns *et al.*, 2008), whilst diminished osteoclast function may result in osteopetrosis (excessive bone formation). These respective disease processes highlight the critical importance of maintaining a healthy balance between bone formation and resorption.

Central to this osteogenic balance are the serum glycoproteins, osteoprotegerin (OPG) and receptor activator of nuclear factor kappa-B ligand (RANKL), which function as part of a signalling triad with the RANK receptor to modulate cell function, differentiation and survival during bone morphogenesis (Boyce and Xing, 2007). Osteocytes, mature osteoblasts trapped within the bone matrix, are the predominant source of RANKL for the activation of osteoclast precursors, whilst osteoblasts are a significant source of OPG (Figure 1.3). RANKL has long been implicated in the promotion of osteoclastogenesis and bone resorption (Wada *et al.*, 2006); this function entails binding of RANKL to its cell surface RANK receptor, which is

widely expressed in both precursor and mature osteoclasts (Atkins *et al.*, 2006; Myers *et al.*, 1999). Within this context, OPG acts as a soluble decoy receptor for RANKL (Luan *et al.*, 2012), preventing RANK:RANKL interactions and blocking the resulting downstream osteoclastogenic cascade. Generally, when RANKL expression is induced, OPG levels are downregulated such that the RANKL:OPG ratio promotes osteoclastogenesis (Kearns *et al.*, 2008). Unsurprisingly, the RANKL:OPG ratio appears to be differentially regulated in pathological conditions compared to healthy physiological states (Liu *et al.*, 2010), highlighting a role for these proteins in the maintenance of bone homeostasis.

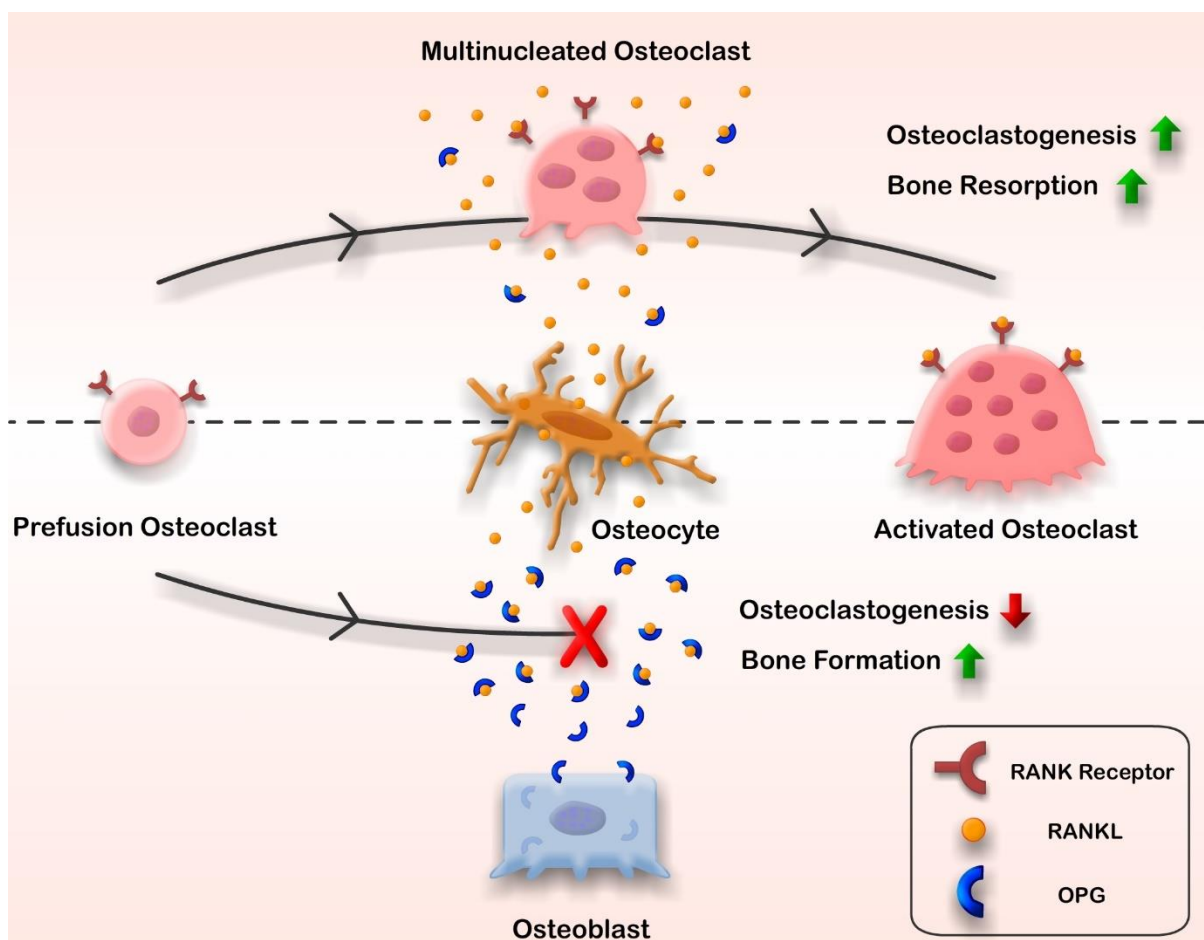


Figure 1.3. Progression of bone morphogenesis. Osteocytes are the primary source of RANKL in bone, a ligand with osteoclastic properties when bound to the RANK cell surface receptor (middle). Osteoclasts arise from the cytoplasmic fusion of immune precursors of monocyte/macrophage lineage (prefusion osteoclasts) to generate a multi-nucleated osteoclast; RANKL:RANK binding can then occur on the surface of this multi-nucleated osteoclast, to form a mature, activated osteoclast capable of bone resorption (top). Osteoblasts are the primary source of OPG in bone, a soluble decoy receptor for RANKL serving to prevent bone resorption. High levels of OPG prevent RANKL:RANK binding and prevent bone resorption (thereby promoting bone formation) (bottom). RANK, receptor activator of nuclear factor kappa-B; RANKL, receptor activator of nuclear factor kappa-B ligand; OPG, osteoprotegerin. Harper *et al.*, 2016.

1.2.3.2 Molecular Players in Bone Morphogenesis – RANKL and OPG

At a molecular level, RANKL is a type-II homotrimeric transmembrane protein (Boyce and Xing, 2007) and a member of the tumour necrosis factor (TNF) superfamily. RANKL typically remains membrane bound, but also exhibits at least two known active soluble forms that may arise either through proteolytic cleavage from the cell membrane or alternate mRNA splicing (Ikeda *et al.*, 2001). Both membrane-associated and secreted forms of RANKL are capable of promoting osteoclast formation (Lacey *et al.*, 2012). Structurally, RANKL has a small intracellular N-terminal domain, a transmembrane anchor, a connecting stalk and an extracellular receptor-binding domain, the latter of which typically arranges into a homotrimer in both membrane-bound and soluble form (Luan *et al.*, 2012). Whilst many cell types express RANKL, osteocytes appear to be the prominent source for *in vivo* activation of osteoclast precursors (Nakashima *et al.*, 2011). Additional sources of RANKL include vascular cells, stromal cells, T-cells and immune osteoclast precursors (monocytes, macrophages and dendritic cells) (Hofbauer and Schoppet, 2004; Kong *et al.*, 1999; Lacey *et al.*, 1998).

OPG, the decoy receptor for RANKL, is a soluble TNF receptor family member often referred to as an “osteoclastogenesis inhibitory factor” (Yasuda *et al.*, 1998). OPG is synthesized and secreted *in vivo* by most cell types including vascular cells (particularly smooth muscle cells), but osteoblasts and stromal cells exhibit the most prominent expression (Hofbauer and Schoppet, 2004). Structurally, OPG is a glycosylated cytokine with seven domains; four cysteine-rich domains (1-4) at the N-terminus are responsible for attenuating RANKL-induced osteoclast activation and activity (Luan *et al.*, 2012), while domains 5 and 6 are apoptosis-mediating regions. Domain 7 is responsible for cysteine-mediated dimerization, and can also bind the anticoagulant heparin (Yamaguchi *et al.*, 1998). OPG can also bind to and neutralise TNF-related apoptosis-inducing ligand (TRAIL), a pleiotropic molecule with a dominant role in the mediation of apoptosis. OPG is also considered an unusual member of the TNF receptor superfamily, as it lacks a transmembrane region and is exclusively secreted as a soluble protein (Luan *et al.*, 2012). OPG exists in serum as either a 60 kDa monomer or a 120 kDa disulphide-linked homodimer, with the latter more biologically active; it can also be detected in complex with any one of its ligands (Venuraju *et al.*, 2010).

1.2.3.3 Bone Morphogenesis – Key Mechanisms

At a mechanistic level, the key pathways involved in bone morphogenesis are complex, but several of the pathways that mediate ossification are particularly relevant to VC. As a brief overview, RANKL in its osteoclastic role in bone, is known to exert its function via NF- κ B (nuclear factor of activated B-cells) signalling. NF- κ B is a rapidly inducible transcription factor that exerts diverse functions in almost all animal cell types (Zhang *et al.*, 2017), and can be activated via two distinct pathways, canonical and non-canonical, that will be described in more detail in Section 1.2.4.5.1. In bone, NF- κ B plays a crucial role in osteoclastogenesis when activated by RANKL; at a basic level, RANKL binds to its cell surface receptor (RANK) to activate both canonical and non-canonical NF- κ B pathways, and the respective downstream components translocate to the nucleus to mediate osteoclastic gene expression (Boyce *et al.*, 2010). The role for OPG in bone formation involves the prevention of RANKL:RANK binding, therefore attenuating NF- κ B activation and the resulting osteoclastic gene upregulation.

In addition to NF- κ B, bone morphogenetic proteins (BMPs) are potent regulators of osteogenic differentiation; these osteo-inductive members of the transforming growth factor (TGF)- β superfamily function through binding to a heterodimeric transmembrane BMP receptor (I and II) complex; when a specific BMP binds to its specific type II receptor, the type I receptor becomes activated. Phosphorylation and nuclear translocation of Smad transcription factors ensue, resulting in gene transcription alterations (Hruska *et al.*, 2005) that regulate bone formation, maintenance and repair (Sykaras and Opperman, 2003). BMP-2, for example, functions through increasing the expression of the transcription factors runt-related transcription factor-2 (Runx2) (Sage *et al.*, 2010) and osterix (Lee *et al.*, 2003), which follows on to induce alkaline phosphatase (ALP), an enzyme involved in the mineralisation of bone.

Thirdly, oxidative stress plays an important role in bone remodelling, as redox signalling and reactive oxygen species (ROS) can regulate the natural balance between osteoblasts and osteoclasts (and therefore bone formation and resorption) (Domazetovic *et al.*, 2017). ROS are highly reactive chemical species that promote a pathological “pro-oxidant” environment, thereby promoting bone resorption (Huh *et al.*, 2006). Anti-oxidant signalling, leading to a reduction in ROS levels, therefore prevent bone resorption and allow bone formation to ensue (Jun *et al.*, 2008). Indeed, redox signalling in bone is closely associated with RANKL signalling and NF- κ B activation, as redox status has been found to directly regulate RANKL-induced osteoclastogenesis (Huh *et al.*, 2006).

1.2.4 VC Pathogenesis

While RANKL and OPG play pertinent roles in the regulation of bone turnover, they are also central to the development and progression of VC, as are a number of key mechanisms involved in bone morphogenesis. Thus, the role of these ligands and signalling pathways will now be discussed in detail from a vascular perspective, again maintaining focus on the VSMC layer (the established location of medial VC *in vivo*).

1.2.4.1 VC Pathogenesis at the Cellular Level

As a simplistic overview, VC is a gradual mineralisation process that occurs in arterial tissue, beginning with vascular wall damage and ultimately progressing to the deposition of hydroxyapatite within the medial arterial layer (Orimo, 2010). Many aspects of the metabolic syndrome associated with T2DM can promote this process, including oxidative stress, endothelial dysfunction, dyslipidemia, irregularities in mineral metabolism, and the heightened generation of pro-inflammatory cytokines (Singh *et al.*, 2009; Singh *et al.*, 2010; Singh *et al.*, 2012). At the cellular level, studies have indicated that VC primarily involves the phenotypic trans-differentiation of VSMCs into osteoblastic (bone-forming) or chondrocytic (cartilage-forming) cells, capable of expressing and releasing osteoblastic proteins that regulate the calcification process (Luo *et al.*, 1997; Speer *et al.*, 2009). Proteins in circulation also contribute to VSMC calcification, most likely through a combination of direct contact with VSMCs (as they diffuse through a dysfunctional endothelial monolayer), and through exhibiting their effects directly on healthy (non-dysfunctional) endothelial cells which signal in a paracrine manner to underlying VSMCs (Davenport *et al.*, 2016; Panizo *et al.*, 2009).

In culture, VSMCs are induced to calcify when exposed to elevated levels of calcium and phosphate, encouraging the osteochondrogenic phenotype and a loss of natural VSMC markers (Steitz *et al.*, 2001). Interestingly, VSMC differentiation is generally referred to as *osteoblastic*, however many recent studies now indicate that VC may more closely resemble a *chondrocytic* process (Speer *et al.*, 2009). Indeed, both osteoblastic and chondrocytic processes involve the upregulation of many of the same genes and proteins (Speer *et al.*, 2009; Tyson *et al.*, 2003), and as such, chondrocyte-like cells may be considered to have an osteoblastic phenotype when assessed in culture. In support of VSMC chondrocytic differentiation, Speer and colleagues (2009) used a fate-mapping approach in a murine model of VC to provide evidence that VSMCs are the main origin of chondrocytic cells seen in calcified vessels. Medial cells from

calcified vessels of 4-week old matrix gla protein (MGP)-deficient mice were shown to lack expression of VSMC lineage proteins (smooth muscle myosin heavy chain, smooth muscle α -actin (SM α -actin), smooth muscle-22 α (SM22 α)) however they did express osteochondrogenic proteins osteopontin (OPN) and type II collagen. These chondrocyte-like cells were involved in large calcific medial regions, and had previously expressed these smooth muscle markers, providing strong evidence that they had differentiated from VSMCs (Speer *et al.*, 2009). Given the similarity in phenotype between osteoblastic and chondrocytic cells, however, both terms will be considered to describe a “pro-calcific” VSMC phenotype throughout this thesis.

While VSMCs may be the main source of “calcifying” cell in the vasculature, a number of additional cell types also contribute to the establishment and progression of VC. As noted, the intimal endothelial monolayer is now considered to play a major role in the regulation of VC, known to communicate with the underlying HASMCs via paracrine signalling (Davenport *et al.*, 2016; Osako *et al.*, 2010). Thus, when the endothelium is exposed to pro-calcific proteins in circulation, or exposed to a pro-inflammatory, pro-oxidant environment such as that present during endothelial dysfunction (Higashi *et al.*, 2009; Zhang, 2008), the secretory profile of these cells can be altered to promote calcification within the medial arterial layer (Yao *et al.*, 2013). Furthermore, as mentioned, intimal VC and atherosclerotic plaque often co-locate with medial VC *in vivo* (McCullough *et al.*, 2008), and macrophages and foam cells within the atheroma can secrete pro-inflammatory cytokines that further promote the VC process (Barath *et al.*, 1990; McLaren *et al.*, 2011; Moore *et al.*, 2013).

1.2.4.2 VC Pathogenesis at the Molecular Level

There are numerous molecular components involved in the pathogenesis of calcification, described in detail by Sage and colleagues (2010), and a number of proteins relating to osteogenesis/chondrogenesis have been identified in arterial vascular cells (Papadopouli *et al.*, 2008). VC mechanisms are mediated by transcription factors that also control osteogenesis/chondrogenesis, such as Runx2, sex-determining region Y box-9 (Sox9) and osterix, and their downstream matrix components ALP, bone sialoprotein (BSP) and osteocalcin (OCN) (Tintut and Demer, 2006). Furthermore, BMPs, central regulators of osteogenic differentiation, are also known to have potent pro-calcific effects in the vasculature, as are a number of pro-inflammatory cytokines (e.g. TNF α , interleukin (IL)-6) (Al-Aly, 2008; Davenport *et al.*, 2016; Hénaut and Massy, 2018). The most relevant of these factors to the current research are described in more detail overleaf.

1.2.4.2.1 Pro-calcific Transcription Factors

There are several pro-calcific transcription factors involved in the regulation of bone morphogenesis that are also known to regulate VC. Runx2, for example, a “master regulator” of osteoblast differentiation and bone development, has been implicated as one of the central osteoblastic transcription factors involved in VC pathogenesis (Lin *et al.*, 2015). Runx2 is responsible for inducing the expression of a wide range of osteoblastic genes (Byon *et al.*, 2011; Pratap *et al.*, 2003; Weng and Su, 2013), and also trans-activates another osteoblastic transcription factor, osterix (Nishio *et al.*, 2006). Indeed, Runx2 has been shown to be elevated in calcified arteries (Moe *et al.*, 2003), and Runx2 deletion has been shown to attenuate osteochondrogenic differentiation and subsequent calcification in VSMCs (Lin *et al.*, 2015). Another transcription factor, msh homeobox 2 (Msx2) also plays a crucial role in osteoblastic differentiation of VSMCs, but is not believed to be necessary for subsequent calcification (Andrade *et al.*, 2017).

Sox9, a chondrocytic transcription factor with a primary role in chondrocyte differentiation, is also responsible for driving a number of pro-calcific genes (Akiyama *et al.*, 2002). Unlike Runx2, however, Sox9 has only recently been implicated in the VC process (Kauffenstein *et al.*, 2014) and is of particular interest given that the calcification process is now thought to closely resemble chondrocytic rather than osteoblastic differentiation (Speer *et al.*, 2009). Sox9 has also been detected in calcified vessels (Kauffenstein *et al.*, 2014) and is known to be expressed in cultured VSMCs (Tyson *et al.*, 2003). In a vascular context, the particular stimuli that induce Sox9 expression are relatively unclear, but it has been shown to potentiate BMP-2-induced cartilage formation (Liao *et al.*, 2014). Interestingly, Sox9 prevents Runx2-mediated osteoblastic gene expression in bone (Cheng and Genever, 2010), however, the expression of osteoblastic targets have been identified alongside Sox9 expression in calcified vascular cells (Tyson *et al.*, 2003). Thus, the role of this transcription factor in a vascular setting may vary considerably from their traditional roles in osteo/chondrogenesis and remain to be delineated.

1.2.4.2.2 Downstream Protein Mediators

There are a number of proteins downstream of these transcription factors that regulate the VC process. ALP, for example, is a metalloenzyme regulated by Runx2 that is actively involved in the mineralisation process, and is known to be highly expressed in calcified vascular tissue (Sheen *et al.*, 2015). ALP is localised to the extracellular side of the plasma membrane, but can

also be identified intracellularly (attached to matrix vesicles) and in secretory form (Davenport *et al.*, 2016; Golub and Boesze-Battaglia, 2007). Extracellular ALP is the most relevant to VC, given that it promotes mineralisation by reducing inorganic pyrophosphate (PP_i) levels (an inhibitor of mineralisation) and increasing inorganic phosphate (P_i) levels (a promoter of mineralisation) in the extracellular space (Schoppet and Shanahan, 2008). Budding matrix vesicles containing hydroxyapatite crystals (a calcium- and phosphate-containing mineral), which are then deposited into the extracellular matrix if the PP_i/P_i balance is correct (Orimo, 2010) (Figure 1.4). In addition to ALP, BSP and OCN, early and late markers of VC, respectively (Huang *et al.*, 2007), also promote the mineralisation process in VSMCs by promoting nucleation and binding of hydroxyapatite crystals (Hunter and Goldberg, 1994). As these osteoblastic markers are upregulated, natural VSMC markers (e.g., SM α -actin, SM22 α) are downregulated, resulting in a “calcifying” VSMC phenotype. A range of proteins are also involved in the negative regulation of VC; for example, MGP inhibits VC in its role as a BMP inhibitor (Boström *et al.*, 2001), while OPN binds strongly to calcium atoms to prevent mineralisation (Sodek *et al.*, 2000). However, upregulation of the aforementioned pro-calcific transcription factors have also been associated with a decrease in the expression of these proteins (Schinke *et al.*, 2000; Zhang *et al.*, 2012).

1.2.4.2.3 BMPs

BMPs are known to play a central role in the regulation of VC, and vascular cells have been shown to express BMP receptors (Kim *et al.*, 2013; Yu *et al.*, 2007). There are multiple BMPs involved in the regulation of osteoblastogenesis, some of which are particularly relevant in a vascular setting. BMP-2, for example, is known to induce the calcification process, and exerts its osteoblastic function by increasing the expression of the transcription factors Runx2 (Sage *et al.*, 2010) and osterix (Lee *et al.*, 2003), which follow on to induce ALP activity. BMPs exert their function via Smad phosphorylation and translocation, promoting osteoblastic gene expression (Hruska *et al.*, 2005). Of significant interest is the role for BMP-2 identified in endothelial:smooth muscle cell communication; in this respect, endothelial cells directly exposed to pro-calcific stimuli in circulation secrete BMP-2 as a pro-calcific paracrine signal to the underlying VSMCs (the location of medial VC *in vivo*) (Davenport *et al.*, 2016; Osako *et al.*, 2010). BMP-4 has also been implicated in the promotion of VC in smooth muscle (Panizo *et al.*, 2009), whilst BMP-7 has been shown to inhibit calcification (Mathew *et al.*, 2006).

1.2.4.2.4 Pro-inflammatory and Pro-oxidant Mediators

Inflammation is closely related to calcification, as immune/vascular cells at the site of atherosclerotic plaque release inflammatory cytokines that contribute to VC regulation (Johnson *et al.*, 2006; Mody *et al.*, 2001). In this respect, TNF α and IL-6 have both been shown to induce VC (Al-Aly, 2008; Hénaut and Massy, 2018) and can activate many of the aforementioned pro-calcific mediators in vascular cells (e.g. Runx2, ALP, BMP-2) (Illiandri *et al.*, 2016; Kurozumi *et al.*, 2016). Of further note, oxidative stress (induced by ROS) is a well-known inducer of pro-calcific and pro-inflammatory proteins in the vasculature (Al-Aly *et al.*, 2007; Byon *et al.*, 2008), and ROS are also known to be secreted by vascular cells under pro-calcific conditions (Clempus and Griendling, 2006; Farrar *et al.*, 2015). Of particular relevance to T2DM, hyperglycemia (a pro-oxidant, pro-inflammatory stimulus) has also been shown to stimulate chondrocytic trans-differentiation of human VSMCs, alongside increased levels of Runx2 and Sox9 expression, increased ALP activity and mineralisation (Bessueille *et al.*, 2015).

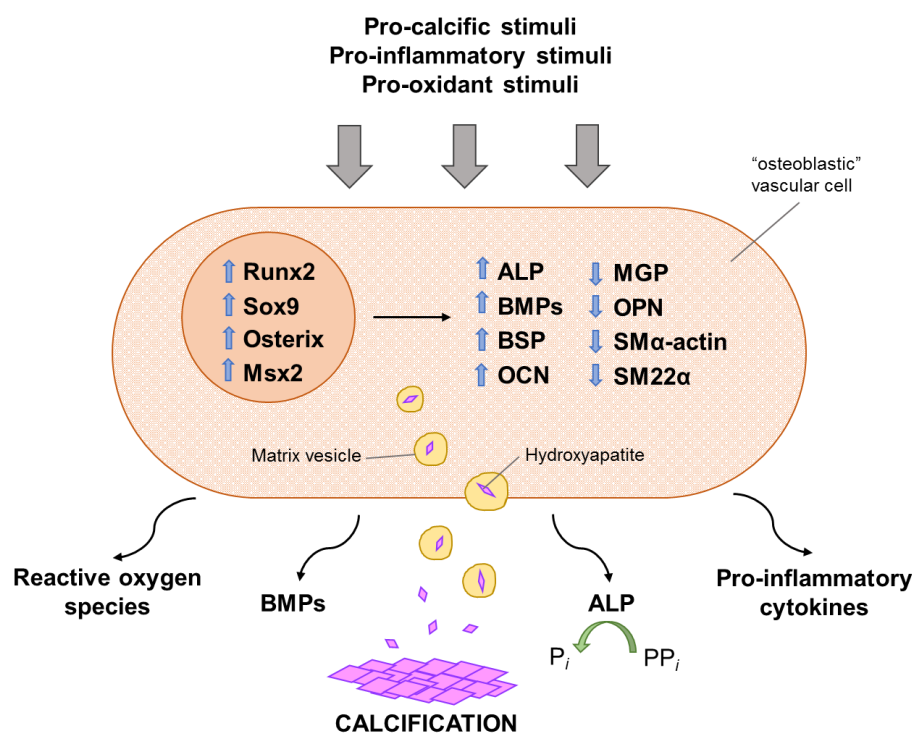


Figure 1.4. The regulation of pro-calcific genes and proteins in calcifying vascular cells. Pro-calcific stimuli, pro-inflammatory stimuli and pro-oxidant stimuli can induce a number of osteoblastic/chondrocytic transcription factors in vascular cells (Runx2, Sox9, osterix, Msx2). These transcription factors drive the expression of pro-calcific proteins (ALP, BMPs, BSP, OCN) and downregulate anti-calcific proteins (MGP, OPN) and smooth muscle markers (SM α -actin, SM22 α). ALP is secreted alongside hydroxyapatite (in matrix vesicles), and converts PP_i to P_i to promote mineral deposition. These osteoblastic vascular cells also secrete BMPs, pro-inflammatory cytokines and reactive oxygen species to further promote the calcification process. ALP, alkaline phosphatase; BMP, bone morphogenetic protein; BSP, bone sialoprotein; MGP, matrix gla protein; Msx2, msh homeobox 2; OPN, osteopontin; (P)P_i, inorganic (pyro)phosphate; Runx2, runt-related transcription factor-2; SM, smooth muscle; Sox9, sex determining region Y box-9.

1.2.4.3 VC Pathogenesis – a Role for RANKL and OPG

There is gathering evidence that the OPG/RANKL/RANK signalling axis is central to the manifestation and progression of VC (Papadopouli *et al.*, 2008). RANKL in circulation primarily originates from bone, but additional sources of vascular RANKL are thought to include circulating T-cells and vascular cells themselves (although this expression is believed to be relatively low) (Osako *et al.*, 2010; Collin-Osdoby *et al.*, 2001; Hofbauer and Schoppet, 2004; Ndip *et al.*, 2014). OPG, on the other hand, is expressed to a significant extent by smooth muscle cells (Corallini *et al.*, 2009), and to a lesser extent by endothelial cells (Davenport *et al.*, 2018), but circulating OPG originating from bone can also contribute to VC regulation within the vasculature. Furthermore, the RANK cell surface receptor is known to be expressed in vascular cells (Kavurma *et al.*, 2008), and thus RANKL can influence the vasculature by inducing endothelial paracrine signals (Davenport *et al.*, 2016), and also by direct contact with underlying VSMCs in areas of damage or dysfunctional endothelium.

As described, the role for RANKL in bone morphogenesis involves the induction of bone resorption, while OPG promotes bone formation by preventing RANKL:RANK binding (thereby preventing osteoclastic activity). In the vasculature, however, RANKL promotes *osteoblastic* rather than osteoclastic activity, acting as a key driver of VC, while OPG, in its *vasoprotective* role as a RANKL decoy receptor, prevents RANKL-induced pro-calcific signalling (Papadopouli *et al.*, 2008). Thus, ***both RANKL and OPG appear to exhibit contradictory effects during vascular calcification to those typically manifested by either of these ligands during bone remodelling, an apparent pathophysiological paradox that has yet to be fully understood.***

From a mechanistic perspective, RANKL can actively promote the calcification process in the vasculature by binding to the RANK receptor, inducing pathological differentiation of healthy VSMCs into calcified VSMCs with an osteoblastic phenotype (Kaden *et al.*, 2004; Ndip *et al.*, 2011; Panizo *et al.*, 2009). RANKL binds to its receptor in homotrimeric form, triggering the activation of both canonical and non-canonical NF- κ B pathways (Khavandgar *et al.*, 2014), although it has been suggested that RANKL exerts its pro-calcification actions primarily via non-canonical activation (Panizo *et al.*, 2009). NF- κ B then translocates to the nucleus (Ndip *et al.*, 2011) where it activates osteogenic gene expression and downregulates smooth muscle markers (e.g. smooth muscle α -actin) (Ndip *et al.*, 2014). The VSMC then becomes a calcifying cell with an osteochondrogenic phenotype, producing and secreting pro-calcific proteins that

drive the formation of a mineralised matrix (Ndip *et al.*, 2014) (Figure 1.5). RANKL has also been shown to be upregulated in calcified VSMCs (Kaden *et al.*, 2004) and atherosclerotic tissue (Higgins *et al.*, 2015); these findings indicate that, when serum RANKL levels are high, an acceleration of this differentiation process occurs, resulting in an increased mineral deposition within the medial arterial wall (Figure 1.5, right).

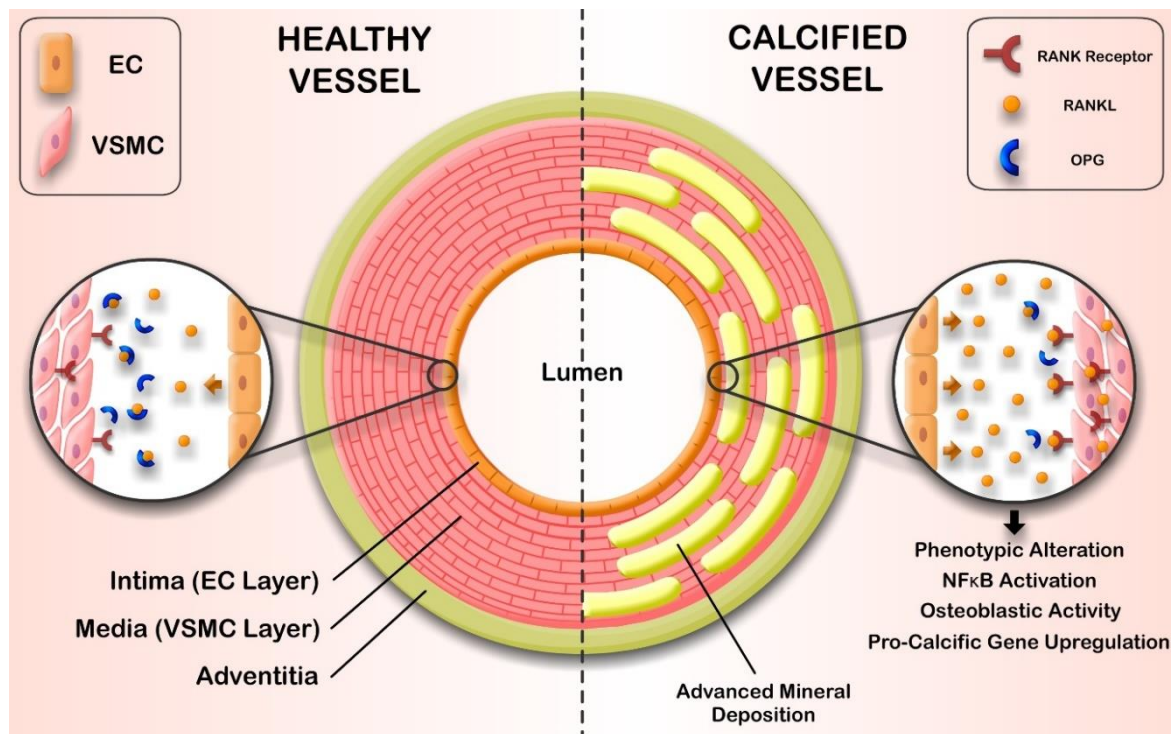


Figure 1.5. Interactions between OPG and RANKL in healthy (left) and calcified (right) vessel. In healthy vasculature, VSMCs secrete enough OPG to neutralise excess RANKL, originating from circulation and surrounding vascular cells. OPG prevents RANKL binding to the RANK receptor on the VSMC surface, thereby preventing RANKL-induced calcification (left). When RANKL levels are high, however, VSMCs cannot secrete enough OPG to neutralise RANKL, enabling RANKL:RANK binding and osteoblastic activation to ensue. This activation ultimately results in the formation of calcified mineral deposits within the medial arterial layer (right). EC, endothelial cell; VSMC, vascular smooth muscle cell; RANK, receptor activator of nuclear factor kappa-B; RANKL, receptor activator of nuclear factor kappa-B ligand; OPG, osteoprotegerin; NF- κ B, nuclear factor kappa-B. Harper *et al.*, 2016.

OPG, on the other hand, binds and neutralises RANKL (Collin-Osdoby, 2004), and this neutralization ameliorates the VC process and exerts an anti-calcific effect within the vasculature. In this respect, OPG prevents RANKL:RANK interaction and NF- κ B activation/translocation, resulting in a healthy non-calcified vessel (Figure 1.5, left). When RANKL levels are high, however, VSMCs cannot secrete enough OPG to neutralise the excess, thereby rendering the vessel prone to RANKL-induced calcification.

1.2.4.4 VC Pathogenesis – a Role for TRAIL

In recent years, a novel role has emerged for an additional ligand in the vasculature: namely, TRAIL. This ligand has been shown to interact with OPG and RANKL in the modulation of the calcification process (Schoppet *et al.*, 2004), and although its precise functions in this context are poorly defined, mounting evidence now points to a *vasoprotective role for TRAIL in the prevention of VC*. Prior to discussing the effects of TRAIL in a vascular context, some background will first be provided on the function and regulation of this complex ligand *in vivo*.

1.2.4.4.1 TRAIL – Location, Function and Regulation

As its name suggests, the primary function for TRAIL is as an inducer of apoptosis, and although originally believed to exert this function on malignant or transformed hematopoietic cells, it is now known to have diverse pleiotropic roles in multiple cell types (Forde *et al.*, 2016; Wiley *et al.*, 1995). TRAIL has been identified in multiple tissue locations including spleen, prostate and lung (Wiley *et al.*, 1995), but its mRNA and protein expression has thus far only been demonstrated in immune, vascular, hepatocytic and myocytic cells (Falschlehner *et al.*, 2009; Forde *et al.*, unpublished observations; Gochuico *et al.*, 2000; Sato *et al.*, 2006; Spierings *et al.*, 2004). TRAIL is also present in the circulation (albeit in the picomolar range), and interestingly, serum TRAIL has been shown to be inversely correlated with a number of pathologies including CVD (Volpato *et al.*, 2011).

At a molecular level, TRAIL, a member of the TNF ligand superfamily, is a type-II transmembrane protein with the ability to bind five different receptors found on numerous cell types, as well as a C-terminal domain that can also be cleaved from the cell surface (or secreted in vesicles) to release a soluble form (Ehrlich *et al.*, 2003). Both membrane-bound and soluble TRAIL can induce apoptosis, although soluble TRAIL is thought to exert a more potent apoptotic effect (Kim *et al.*, 2004). Two TRAIL receptors (DR4 and DR5) have a cytoplasmic death domain, whilst two decoy receptors (DcR1 and DcR2) lack a functional death domain; thus TRAIL-induced apoptosis via DR4 and DR5 is antagonised by the competitive inhibitory effect of DcR1 and DcR2 (Ravi *et al.*, 2001). OPG acts as an additional soluble decoy receptor for TRAIL (and vice-versa); therefore, OPG has a second protective function in addition to its ability to block RANKL-induced calcification, by virtue of its ability to block TRAIL-dependent apoptotic signalling (Emery *et al.*, 1998).

The regulation of TRAIL *in vivo* is mediated by a number of factors including the NF- κ B family of transcription factors (Wurzer *et al.*, 2004) and interferons (Kayagaki *et al.*, 1999; Miura *et al.*, 2006), described in detail by Forde *et al.* (2016). TRAIL receptor regulation, although not yet fully defined, appears to be mediated by many of the same pathways that regulate TRAIL (Kamohara *et al.*, 2004; Ravi *et al.*, 2001). TRAIL receptors are expressed at varying levels in a wide range of cells and tissues *in vivo* (hepatocytes, neurons, cardiac myocytes, colon, kidney, lung, vasculature, and pancreas among others) (Daniels *et al.*, 2005; Pan *et al.*, 1998; Zauli *et al.*, 2006), and as such, it is no surprise that TRAIL exerts complex pleiotropic functions dependent on the location-specific expression of death and decoy receptors (and the pathways activated by TRAIL:TRAIL receptor binding).

The mechanisms associated with TRAIL signalling are complex, but, as noted, TRAIL's primary function as an apoptosis-inducing ligand is best defined. Indeed, TRAIL's apoptotic function is initiated by DR4 and DR5 binding, resulting in the formation of the death-inducing signalling complex (Almasan *et al.*, 2003) and downstream caspase activation (Suliman *et al.*, 2001). There are also a number of signalling pathways activated by TRAIL, however, that result in anti-apoptotic functions, but these pathways are less understood. As a brief summary, TRAIL has the ability to induce NF- κ B activation, which can function to either promote cell survival or apoptosis depending on the cellular context (Degli-Esposti, 1999; Ravi *et al.*, 2001). In this respect, high concentrations of TRAIL (1 μ g/mL) cause the NF- κ B-dependent upregulation of anti-apoptotic proteins which may reduce cellular sensitivity to TRAIL-induced apoptosis (Almasan *et al.*, 2003). Secondly, TRAIL can initiate the mitogen activated protein kinase (MAPK)/extracellular signal-related kinase (ERK) signalling cascade (Falschlehner *et al.*, 2007), which results in an anti-apoptotic effect in vascular cells (Secchiero *et al.*, 2003). A third non-apoptotic signalling cascade activated by TRAIL is the protein kinase B/Akt pathway (Secchiero *et al.*, 2003); Akt activation also indirectly protects from apoptosis through P53 degradation and NF- κ B activation (Hausenloy *et al.*, 2004). While these pathways can be activated by DR4 and DR5 under the correct conditions, the decoy receptor DcR2 (while incapable of inducing apoptosis) is capable of activating other signalling pathways (e.g. NF- κ B) which may accentuate the anti-apoptotic role of TRAIL (Delgi-Esposti *et al.*, 1997).

For a comprehensive review on the pleiotropic roles of TRAIL *in vivo*, and an in-depth summary of the pathways that activate, and are activated by TRAIL, see Forde *et al.* (2016). For the purpose of the current review, however, a focus on the specific role for TRAIL in the vasculature will be maintained.

1.2.4.4.2 TRAIL in the Vasculature

The pro-survival role of TRAIL has led to the hypothesis that this ligand may exert pleiotropic roles in many cell types, including the circulatory system (Forde *et al.*, 2016). Although there is still much debate over whether or not TRAIL is expressed in the vascular endothelium (Secchiero and Zauli, 2008), TRAIL receptors are expressed by endothelial cells (Zauli *et al.*, 2006), and VSMCs express both TRAIL and TRAIL receptors (Cheng *et al.*, 2014; Harith *et al.*, 2016; Li *et al.*, 2016). Additionally, immune cells present at sites of atherosclerotic plaque and intimal calcification are sources of surface and soluble TRAIL (Ehrlich *et al.*, 2003; Kamohara *et al.*, 2004) while the TRAIL receptors on these cells are widely expressed (Guicciardi and Gores, 2009). As noted, TRAIL is also present in circulation (Volpato *et al.*, 2011), further supporting a physiological role for TRAIL in the vasculature.

An emerging hypothesis within the field of vascular research has proposed a *vasoprotective* role for TRAIL, possibly via the mediation of anti-atherogenic, anti-inflammatory and anti-oxidant effects. In this respect, TRAIL delivery has been shown to promote anti-atherosclerotic activity in diabetic mice, while TRAIL-deficient mice also developed accelerated medial VC (di Bartolo *et al.*, 2013). Furthermore, TRAIL deficiency has also been associated with increased atherosclerotic plaque size in Apolipoprotein E(ApoE)^{-/-} mice (Watt *et al.*, 2011), and Secchiero *et al.* (2006) also found that TRAIL reduced plaque mass and increased macrophage apoptosis within atherosclerotic lesions. Furthermore, TRAIL has been shown to exert anti-oxidant and anti-inflammatory effects on the endothelium via the modulation of endothelial nitric oxide synthase (eNOS) (Zauli *et al.*, 2003), and endothelial survival and proliferation has also been observed in response to TRAIL treatment (Pritzker *et al.*, 2004; Secchiero *et al.*, 2003). From a clinical perspective, decreased serum TRAIL levels correlate with acute cardiovascular events (including myocardial infarction, heart failure) and resulting mortality (Niessner *et al.*, 2009; Secchiero *et al.*, 2009; Volpato *et al.*, 2011), potentially implicating lower circulating TRAIL with poorer prognoses.

Contrastingly, however, some competing theories point to a potential role for TRAIL as an inducer of calcification. In this respect, elevated levels of TRAIL have been identified in vulnerable atherosclerotic plaque (Michowitz *et al.*, 2005; Schoppet *et al.*, 2004) and both TRAIL and its decoy receptor OPG have been identified at elevated levels alongside medial VC (Schoppet *et al.*, 2004). There is also evidence that TRAIL induces apoptosis in endothelial cells (Li *et al.*, 2003) and VSMCs (Sato *et al.*, 2006) *in vitro*, yet TRAIL has also been shown

to exhibit anti-apoptotic activity in these cells under certain conditions (Kavurma *et al.*, 2008; Secchiero *et al.*, 2003; Secchiero *et al.*, 2004). As such, the precise role(s) for TRAIL within the vasculature are as of yet unclear, and remain the focus of a complex debate within the field of vascular research.

As mentioned, OPG can also serve as a decoy receptor for TRAIL. Importantly, both TRAIL and RANKL compete for OPG with similar binding affinities, with OPG favouring the protein of greatest concentration, resulting in a competitive effect between the two ligands (Vitovski *et al.*, 2007). With excessive TRAIL levels, OPG:RANKL binding is reduced, allowing unopposed RANKL activity to ensue (and vice versa) (Figure 1.6). Therefore, the concentration of all three ligands are relevant to the ultimate biological effects within the vascular system, a fact which may be relevant in explaining the apparent contradictions in TRAIL function. Overall, there is evidence to suggest that TRAIL has substantive yet diverse functional roles within the vasculature (which may be dependent on or independent of OPG/RANKL), but further research is necessary to confirm if these effects are beneficial in the context of VC.

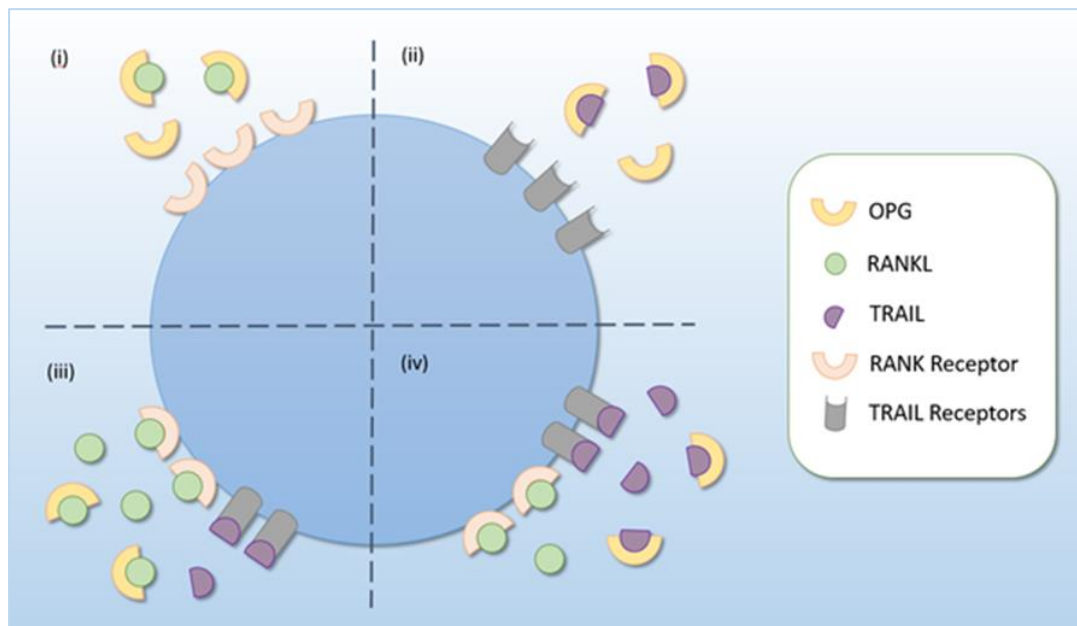


Figure 1.6. Interactions between OPG, RANKL and TRAIL in the vasculature. (i) OPG is in excess of RANKL, preventing RANKL:RANK binding. (ii) OPG is in excess of TRAIL, preventing TRAIL binding to its receptors. (iii) RANKL is in excess of OPG, thus excess RANKL can bind to RANK receptors. There is no OPG available to prevent TRAIL binding to its receptors. (iv) TRAIL is in excess of OPG, thus excess TRAIL can bind to receptors. There is no OPG available to prevent RANKL binding to its receptors. OPG, osteoprotegerin, RANK, receptor activator of nuclear factor kappa-B; RANKL, receptor activator of nuclear factor kappa-B ligand; TRAIL, tumour necrosis factor-related apoptosis-inducing ligand.

1.2.4.5 VC Pathogenesis – Mechanistic Considerations for RANKL and TRAIL

Whilst the mechanisms for both RANKL and TRAIL are well-established in the context of osteogenesis and apoptosis, respectively, the precise signalling pathways activated by these ligands in a vascular context remain relatively undefined. Indeed, both RANKL and TRAIL are known to activate NF- κ B, and there is evidence that they also do so in the vasculature (Kavurma *et al.*, 2008; Panizo *et al.*, 2009), but it is somewhat unclear *which* NF- κ B pathway (i.e. canonical or non-canonical) mediates their respective pro-calcific and (hypothesised) protective effects in vascular cells. Furthermore, evidence also exists pertaining to a role for redox signalling in the mediation of RANKL/TRAIL vascular function (Thummuri *et al.*, 2017; Zauli *et al.*, 2003), and indeed, VC is known to exist alongside a pro-oxidant environment (Byon *et al.*, 2008). These pathways (described in more detail below) have not yet been extensively studied in the context of RANKL/TRAIL function in a vascular setting, but further clarification of the mechanistic targets of these ligands may aid in the development of successful therapeutics to prevent or revert VC.

1.2.4.5.1 NF- κ B Signalling

By way of overview, the NF- κ B family of inducible transcription factors are known to mediate a number of physiological and pathological cellular processes, particularly with respect to inflammation, immunity, cell differentiation and survival (Oeckinghaus and Ghosh, 2009; Wong and Tergaonkar, 2009). This family consists of five members, similar in structure, that function together in a signalling cascade: p50, p52, p65 (RelA), RelB and c-Rel (Liu *et al.*, 2017; Moynagh 2005; Hoffmann *et al.*, 2006). These members have a homologous N-terminal Rel homology domain that allows for dimerisation and DNA binding, allowing varying combinations of hetero- and homodimers to modulate gene transcription via binding to a specific DNA element, κ B enhancer (Huxford *et al.*, 1999; Liu *et al.*, 2017). The subunits p50 and p52 are derived from larger precursors p100 and p105, respectively. RelB, c-Rel and p65 contain transcription activation domains (TADs), allowing them to activate gene expression, while p50 and p52 do not have this function; thus, p50 and p52 function to suppress gene transcription unless dimerised to a transcription factor containing a TAD (Oeckinghaus and Ghosh, 2009). There are also a number of I κ B (inhibitor of κ B enhancer) proteins in the cytoplasm that prevent NF- κ B activity, which also include precursor proteins p100 and p105; for example, in unstimulated cells, p100 binds to RelB to prevent nuclear translocation

(Oeckinghaus and Ghosh, 2009). Thus, NF- κ B regulation involves a complex balance of both positive and negative feedback mechanisms to achieve the appropriate response.

The NF- κ B family of transcription factors facilitate the activation of two signalling pathways, the *canonical* (classical) pathway, and the *non-canonical* (alternative) pathway. Both pathways involve the formation of an I κ B kinase (IKK) complex, which causes phosphorylation-induced degradation of I κ Bs, allowing NF- κ B subunits to translocate to the nucleus (Israël, 2010). The canonical pathway involves the phosphorylation and nuclear translocation of the p50/p65 heterodimer, while the non-canonical pathway involves the phosphorylation and cleavage of the p100 precursor and subsequent translocation of p52/RelB. In both cases, NF- κ B activation leads to the expression of I κ B α , which functions in a negative feedback manner to terminate NF- κ B signalling unless a permanent activation signal is present (Ruland, 2011) (Figure 1.7). In general, canonical NF- κ B mediates diverse cellular functions and can be rapidly activated in response to its stimuli; non-canonical activation, on the other hand, is slow and persistent, and exerts limited functions mediated by specific ligands (including RANK) (Sun, 2011).

As noted, RANKL is known to exert its osteoclastic functions in bone via NF- κ B signalling (Beristain *et al.*, 2012; Boyce *et al.*, 2015), and is also known to activate both NF- κ B pathways within a vascular setting (Khavandgar *et al.*, 2014; Panizo *et al.*, 2009). At a molecular level, RANKL binding to the RANK receptor results in the association of TNF receptor associated factors (TRAFs) with the cytoplasmic domain of RANK (Wong *et al.*, 1998). TRAFs are a family of adaptor proteins that interact with the intracellular domain of cell surface receptors to mediate downstream pathways (Arch *et al.*, 1998), and TRAFs 2, 5 and 6 can activate NF- κ B (Song *et al.*, 1997). TRAF6 appears to be most pertinent with regard to RANKL:RANK binding, which can then go on to activate both canonical and non-canonical NF- κ B pathways (Boyce *et al.*, 2015).

To activate the canonical pathway, recruited TRAF6 induces the formation of a complex of IKKs (specifically, IKK α , IKK β and IKK γ) that induce the phosphorylation and degradation of inhibitory I κ B α ; thus, the p65/p50 heterodimer is free to translocate to the nucleus. In osteoclastogenesis, the p65/p50 heterodimer then induces the expression of c-Fos and nuclear factor of activated T-cells cytoplasmic 1 (NFATc1), transcription factors necessary for osteoclast differentiation (Boyce *et al.*, 2015) (Figure 1.7, left). In the vasculature, however, the specific effects of p65/p50 translocation remain unclear, but NFATc1 has also been implicated in the development of oxidised LDL-induced VC (Goettsch *et al.*, 2011). To activate

the non-canonical pathway, TRAF6 directly activates the NF- κ B-inducing kinase (NIK), the first protein of the non-canonical signalling cascade (Darnay *et al.*, 1999). NIK forms a complex and activates IKK α , also promoting the binding of IKK α to its substrate, p100 (Xiao *et al.*, 2004). Once bound, p100 is cleaved to form p52, which then forms a heterodimer with RelB prior to nuclear translocation (Sun, 2011) (Figure 1.7, right). As with canonical activation, in osteogenesis, p52/RelB also drive the same osteoclastic genes as p50/p65 (i.e., c-Fos, NFATc1), but it is as of yet unclear what genes are regulated by RANKL-mediated p52/RelB in the vasculature.

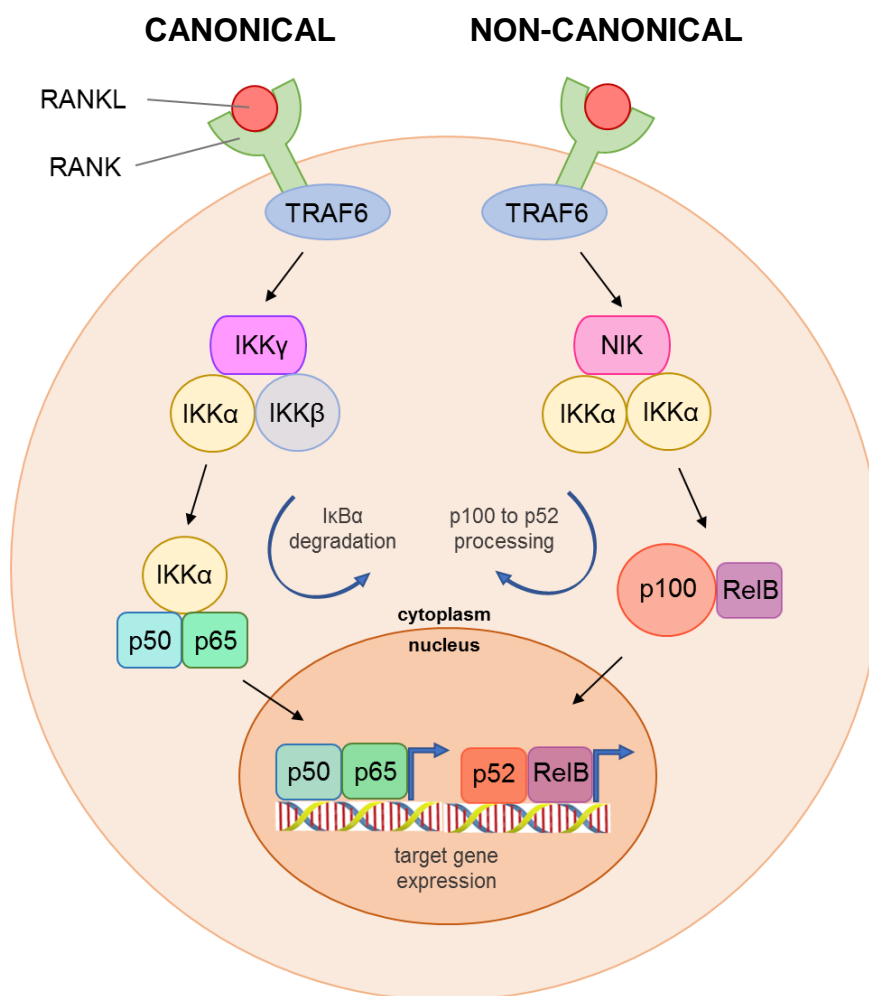


Figure 1.7. The canonical (left) and non-canonical (right) NF- κ B pathways activated by RANKL. (A) The canonical NF- κ B pathway involves TRAF6 association with the intracellular domain of RANK. This association recruits three members of the IKK family to induce the degradation of I κ B α , allowing p50/p65 translocation to the nucleus. **(B)** The non-canonical pathway also involves TRAF6 association with RANK, inducing NIK; NIK complexes with IKK α , promoting p100 binding and processing to p52. The p52/RelB heterodimer can then translocate to the nucleus. Once translocated, both p50/p65 and p52/RelB heterodimers can regulate gene expression. IKK, I κ B kinase; NIK, NF- κ B-inducing kinase; RANK(L), receptor activator of NF- κ B (ligand); TRAF, tumour necrosis factor receptor associated factor.

As noted, TRAIL can activate NF- κ B via DcR2, DR4 or DR5 binding (Delgi-Esposti *et al.*, 1997). TRAIL-mediated binding to its death receptors is mostly associated with caspase-mediated apoptosis (Wang and El-Deiry, 2003), but activation of NF- κ B has also been associated with both pro-apoptotic and pro-survival functions (Delgi-Esposti, 1999; Ravi *et al.*, 2001) and the induction of pro-inflammatory cytokines (Tang *et al.*, 2008). Unlike RANKL, however, no studies to date have yet associated non-canonical NF- κ B activation with TRAIL function; furthermore, there is limited data available regarding the downstream targets of TRAIL-induced NF- κ B outside the context of apoptosis/survival (summarised in detail by Forde *et al.*, 2016). TRAIL is known to have diverse pleiotropic functions in many cells and tissues, but as mentioned, its precise role(s) in the vasculature (and particularly those mediated by NF- κ B) remain to be delineated.

Of particular relevance, NF- κ B signalling has been associated with a number of pathological conditions relevant to VC. In this respect, NF- κ B has been implicated in a number of metabolic and vascular diseases due to its close association with the inflammatory response, including T2DM and atherosclerosis (Baker *et al.*, 2011; Baumgartl *et al.*, 2006; Rocha and Libby, 2009). Indeed, pro-inflammatory cytokines are widely accepted inducers and products of NF- κ B signalling, and are themselves known to promote VC (Al-Aly, 2008; Hénaut and Massy, 2018). Furthermore, these cytokines have been found to be present at high levels in atherosclerotic plaque (Barath *et al.*, 1990), the location of intimal VC *in vivo*, often coinciding with medial calcification (McCullough *et al.*, 2008). Interestingly, the NF- κ B pathway has previously been suggested as a potential therapeutic target for inflammatory vascular diseases (Pamukcu *et al.*, 2011), and with relevance to RANKL, NF- κ B blockade has been shown to prevent osteoclastogenesis *in vivo* (Jimi *et al.*, 2004). Additionally, the glucagon-like peptide-1 receptor agonist (GLP-1RA) exenatide has been found to protect from VC via attenuation of RANKL/NF- κ B activation (Zhan *et al.*, 2014), whilst induced activation of NF- κ B has been shown to accelerate VC (Zhang *et al.*, 2017; Zhao *et al.*, 2012). Unfortunately, however, these studies focus on canonical NF- κ B activation (or do not specify which pathway); thus, much remains to be delineated regarding the precise role for both canonical and non-canonical NF- κ B during VC pathogenesis. As both RANKL and TRAIL activate NF- κ B to modulate osteoclastogenesis and apoptosis/survival, respectively, it is highly likely that the aforementioned effects of these ligands in the vasculature may be mediated in some way by NF- κ B; more information on NF- κ B signalling may therefore aid in delineating VC mechanisms and ultimately developing a successful treatment.

1.2.4.5.2 Oxidative Stress

Oxidative stress has also been implicated in the pathogenesis of vascular diseases, and is known to be involved in RANKL/TRAIL signalling. Oxidative stress is exerted *in vivo* by ROS, metabolic by-products resulting from the reduction of oxygen. ROS is a cumulative term used to describe a number of chemically reactive oxygen-containing species that are naturally produced in the mitochondria during aerobic metabolism, including both free radicals (e.g. superoxide, hydroxyl, peroxy) and non-radicals (e.g. hydrogen peroxide) (Bayir, 2005). Under healthy conditions, these species mediate a number of physiological processes (Vara and Pula, 2014). Under certain pathological conditions, however, ROS may be overproduced (in both mitochondria and cytosol) to levels above those required to mediate physiological processes (Schieber and Chandel, 2014); elevated ROS then leads to irreversible damage to intracellular components (e.g. nucleic acids, proteins) resulting in cell dysfunction or cell death (Pitocco *et al.*, 2013). ROS levels are mediated by a number of pro-oxidant and anti-oxidant enzymes (Rahal *et al.*, 2014), and some of these enzymes are of particular relevance to the vasculature.

In vascular cells, ROS are primarily produced by membrane-associated nicotinamide adenine dinucleotide phosphate (NADPH) oxidases, often referred to as NOX enzymes (Pitocco *et al.*, 2013). There are multiple NOX isoforms, many of which are expressed by vascular cells (Meyer and Schmitt, 2000), and these isoforms are determined based on the specific arrangement of their phagocytic oxidase (phox) subunits (gp91, p22, p40, p47, p67) (Brandes and Kreuzer, 2005). Following assembly at the plasma membrane, NOX enzymes catalyse ROS generation by transferring electrons from NADPH to molecular oxygen, and can release ROS both intra- and extracellularly (Lassègue *et al.*, 2010; Raaz *et al.*, 2014). Xanthine oxidase, another enzyme involved in ROS generation in endothelial cells, produced ROS when converting (hypo)xanthine to uric acid (Madamanchi *et al.*, 2005). The third main source of ROS in the vasculature involves the uncoupling of endothelial nitric oxide synthase (eNOS)-mediated nitric oxide (NO) production from oxygen reduction; eNOS can then produce ROS in the form of superoxide and hydrogen peroxide (Yang *et al.*, 2009).

Interestingly, eNOS, under normal conditions, produces NO, a free radical responsible for the regulation of vascular homeostasis, VSMC proliferation and vasodilation (Sena *et al.*, 2013). As such, eNOS generally confers a protective influence on the vasculature (Albrecht *et al.*, 2003), highlighting a dual role for this enzyme in the regulation of ROS. Superoxide dismutase (SOD) enzymes also exert an anti-oxidant effect on the vasculature by converting superoxide

anions into less harmful compounds (Ighodaro and Akinloye, 2017; Zhang *et al.*, 2003). There are three isoforms of SOD; SOD1, responsible for scavenging cytosolic ROS, SOD2, responsible for scavenging mitochondrial ROS, and SOD3, responsible for scavenging extracellular ROS (Faraci and Didion, 2004; Fukai *et al.*, 2002; Zelko *et al.*, 2002). Finally, heme oxygenase-1 (HMOX1) exerts an anti-oxidant effect on the vasculature via the degradation of heme, a potent pro-oxidant (Jeney *et al.*, 2002) in response to oxidative stress and inflammation (True *et al.*, 2007). Thus, the regulation of ROS in the vasculature involves a complex balance of both pro- and anti-oxidant enzymes.

From a pathological perspective, many of these enzymes have been associated with vascular pathologies. In this respect, NADPH oxidases have been associated with the progression of endothelial dysfunction and CVD/T2DM (Higashi *et al.*, 2009; Kayama *et al.*, 2015; Pitocco *et al.*, 2013). More specifically, the expression of both gp91 and p47 phox subunits have been positively correlated with atherosclerosis and intimal calcification (Barry-Lane *et al.*, 2001; Meyer and Schmitt, 2000; Sorescu *et al.*, 2002), and p47 has been shown to be induced in endothelial cells under pro-inflammatory conditions common during VC (Li *et al.*, 2002). Furthermore, eNOS uncoupling has been shown to be prevalent in CVD/T2DM, contributing to vascular ROS (Guzik *et al.*, 2002; Yang *et al.*, 2009). Indeed, elevated ROS has been associated with the pathology of endothelial dysfunction and VC (Byon *et al.*, 2008; Faraci and Didion, 2004; Li and Shah, 2004; Madamanchi *et al.*, 2007; Towler, 2008), and with particular respect to T2DM, is known to be induced by hyperglycemia (Callaghan *et al.*, 2005).

Of relevance, RANKL has been shown to induce ROS formation in osteoclastogenesis (Thummuri *et al.*, 2017), and TRAIL is thought to exert its apoptotic function via the induction of oxidative stress in malignant cells (Lee *et al.*, 2002). Interestingly, an anti-oxidant role for TRAIL has also been considered in the vasculature (Zauli *et al.*, 2003), indicating that TRAIL may exert varying roles in normal versus tumour cells. No literature to date has yet investigated the effects of these ligands on oxidative stress in vascular cells, however, or assessed what the implications of this might be for VC. Of further note, redox signalling and NF- κ B have been shown to reciprocally interact (Morgan and Liu, 2011), and Zhao and colleagues (2011) have presented pertinent evidence describing the dual activation of both ROS and NF- κ B during VC. Pro-inflammatory cytokines, known activators of NF- κ B, are also well established pro-oxidant stimuli, and given that both RANKL and TRAIL can also activate NF- κ B, may highlight a role for RANKL/TRAIL-mediated oxidative stress during VC pathogenesis.

1.3 VC Models

There have been numerous vascular cell culture and animal models employed to date to highlight the critical importance of RANKL, TRAIL and their common decoy receptor OPG in the VC process, contributing to the overall mechanistic understanding of calcification. Although some data is conflicting, most studies endorse the pro-calcific effects of RANKL and the protective effects of both TRAIL and OPG within the vasculature. A summary of *in vitro* and *in vivo* models and their corresponding findings are discussed in the following sections 1.3.1 and 1.3.2, respectively.

1.3.1 *In vitro* Studies

There is a considerable body of *in vitro* evidence to support the proposed pro-calcific actions of RANKL and anti-calcification actions of OPG/TRAIL in vascular cells, as summarised in Table 1.2 overleaf. Firstly, Panizo and co-workers have provided clear evidence in cell culture models that RANKL directly increases VSMC calcification in a dose-dependent manner, a process that can be counteracted through co-incubation with OPG (Ndip *et al.*, 2011; Panizo *et al.*, 2009). Additionally, di Bartolo and colleagues have demonstrated OPG's ability to prevent calcium-induced calcification in cultured VSMCs (di Bartolo *et al.*, 2011). Anti-calcific effects are also a feature of TRAIL-mediated protection. As noted in Section 1.2.4.4, a considerable body of evidence points to an ant-atherogenic role for TRAIL. Specifically with respect to VC, studies employing VSMCs isolated from both wild-type and TRAIL-deficient mice revealed accelerated calcification in the latter, pointing to a putative role for TRAIL in preventing calcium-induced calcification of VSMCs. Moreover, this effect was shown to be calcium dose-dependent. After 24 hours of calcium exposure, wild-type VSMCs significantly increased RANKL mRNA with simultaneous inhibition of both OPG and TRAIL, demonstrating the differential regulation of RANKL, OPG and TRAIL in the modulation of VC *in vitro* (di Bartolo *et al.*, 2013). Furthermore, although not directly relevant in a vascular setting, Zauli and colleagues have pertinently illustrated that TRAIL can prevent bone resorptive activity induced by RANKL plus macrophage colony stimulating factor *in vitro* (Zauli *et al.*, 2004), potentially indicating a role for TRAIL in the mediation of RANKL function.

In contrast to these observations, it has also been claimed that neither OPG, RANKL nor TRAIL have any effect on VSMC calcification *in vitro* (Olesen *et al.*, 2012). In addition, it has

been noted that RANKL has no direct effect on VSMCs (Byon *et al.*, 2011), while Chasseraud and colleagues have demonstrated that TRAIL can actually enhance VSMC mineralisation in the presence of phosphate (Chasseraud *et al.*, 2011). The methodological approach of the investigator may therefore be pertinent to explaining these discrepancies. Many previous studies have employed phosphate-containing “calcifying” growth media to enhance calcification. However, phosphate itself induces osteoblastic activity, possibly confounding the observed cellular effects of OPG, RANKL and/or TRAIL. Additionally, calcium deposition is often relied upon as a calcification end-point assay, despite wide variability and lack of reproducibility across VSMC populations (Olesen *et al.*, 2012). Furthermore, endogenous OPG secretion (primarily by VSMCs (Corallini *et al.*, 2009)) leading to RANKL and TRAIL neutralization is often overlooked, whilst commonly-used static VSMC monocultures lack endothelial paracrine signalling inputs and shear-mediated conditioning effects that are undoubtedly present in the corresponding *in vivo* environment (Chiu *et al.*, 2009; Eddahibi *et al.*, 2006). Some or all of these confounders are features in many of the studies within the literature, and are potential sources of data misinterpretation.

Table 1.2. Summary of the most relevant *in vitro* studies regarding the effects of RANKL, TRAIL and OPG in the vasculature.

Study	Protein	Outcome
Panizo <i>et al.</i>, 2009	OPG	Anti-calcification
	RANKL	Pro-calcification
Di Bartolo <i>et al.</i>, 2011	OPG	Anti-calcification
Zauli <i>et al.</i>, 2004	RANKL	Pro-calcification
	TRAIL	Anti-calcification
Di Bartolo <i>et al.</i>, 2013	OPG	Anti-calcification
	RANKL	Pro-calcification
	TRAIL	Anti-calcification
Olesen <i>et al.</i>, 2012	OPG	No effect
	RANKL	No effect
	TRAIL	No effect
Byon <i>et al.</i>, 2011	RANKL	No effect
Chasseraud <i>et al.</i>, 2011	TRAIL	Pro-calcification
Davenport <i>et al.</i> 2016	RANKL	Pro-calcification*
Osako <i>et al.</i>, 2010	RANKL	Pro-calcification*

*Exerts this effect through endothelial cell paracrine signalling.

Using an advanced perfused capillary co-culture model approach that specifically addresses some of these confounders, our research group have recently determined that RANKL does not appear to directly affect osteogenic activity and/or calcification in VSMCs, rather it appears to stimulate ECs to release paracrine factors capable of inducing VSMC osteochondrogenic transformation (Davenport *et al.*, 2016). This is somewhat consistent with Osako and colleagues, who have provided evidence that RANKL may act indirectly on VSMCs through stimulating endothelial release of osteogenic paracrine signals including BMP-2 (Osako *et al.*, 2010). Thus, whilst the majority of *in vitro* research completed to date supports the respective pro-calcific and anti-calcific effects of RANKL and OPG/TRAIL (Table 1.2), the precise mechanisms through which this occurs are likely more complex than previously believed.

1.3.2 *In vivo* Studies

Numerous murine models have also been employed to illustrate the effects of OPG, RANKL and TRAIL in the VC process. In an early study by Bucay and colleagues, it was noted that OPG-deficient mice developed accelerated medial VC in large arteries (aortic and renal), where endogenous OPG production is typically prevalent, indicating a protective role for OPG in these locations (Bucay *et al.*, 1998). More recently, Callegari and colleagues have demonstrated that recombinant OPG delivery to OPG-deficient ApoE^{-/-} mice can reduce calcification in addition to reducing atherosclerotic lesion size (Callegari *et al.*, 2013), and further demonstrated that OPG inactivation increases calcification and lesion size in the same murine model (Callegari *et al.*, 2014). Interestingly, inactivation of RANKL signalling in OPG-deficient ApoE^{-/-} VSMCs counteracted this effect (Callegari *et al.*, 2014), whilst murine serum OPG has also been shown to be inversely correlated with free/unbound levels of RANKL (Secchiero *et al.*, 2006). To further support the proposed OPG/RANKL relationship, isolated murine OPG^{-/-}ApoE^{-/-} VSMCs developed increased calcification and exerted an upregulation of osteochondrogenic genes following RANKL treatment, while OPG^{+/+}ApoE^{-/-} VSMCs exhibited no such response (Callegari *et al.*, 2014). This basic model highlights the protective effect of OPG on VC through the modulation of RANKL's pro-calcific effects.

Although OPG can also act as a soluble decoy receptor for TRAIL, many *in vivo* studies have also highlighted the protective effects of TRAIL on the vasculature. For example, it has previously been shown that systemic delivery (both single/repeated injection) of recombinant TRAIL to ApoE^{-/-} diabetic mice demonstrated anti-atherosclerotic activity (Secchiero *et al.*,

2006). Elevated diabetic risk has also been linked to TRAIL deficiency, as high fat diet (HFD)-fed TRAIL^{-/-}ApoE^{-/-} and TRAIL^{-/-}ApoE^{+/+} mice showed multiple indicators of diabetes development after 12 weeks when compared to TRAIL^{+/+}ApoE^{-/-} mice (including increased weight, hyperglycemia and reduced plasma insulin) (di Bartolo *et al.*, 2011). In the aforementioned study by di Bartolo *et al.* (Section 1.3.1), advanced atherosclerotic lesions in HFD-fed TRAIL^{-/-}ApoE^{-/-} and ApoE^{-/-} mice were also monitored, revealing an increase in calcification and cartilaginous metaplasia at 20 weeks and an upregulation of pro-calcification proteins (including RANKL and BMP-2) at 12 weeks in TRAIL^{-/-}ApoE^{-/-} when compared to ApoE^{-/-} mice (di Bartolo *et al.*, 2013). On a final note, the previously reported ability of TRAIL to counteract RANKL's osteoclastic signals *in vitro* (Zauli *et al.*, 2004) was verified in a murine model (Zauli *et al.*, 2008), pointing to a vasoprotective role for TRAIL in the modulation of RANKL function. These studies are summarised below in Table 1.3.

Table 1.3. Summary of the most relevant *in vivo* studies regarding the effects of RANKL, TRAIL and OPG in the vasculature.

Study	Protein	Outcome
Bucay <i>et al.</i> , 1998	OPG	Anti-calcification
Callegari <i>et al.</i> , 2013	OPG	Anti-calcification
Callegari <i>et al.</i> , 2014	OPG	Anti-calcification
	RANKL	Pro-calcification
Secchiero <i>et al.</i> , 2006	TRAIL	Anti-calcification
Di Bartolo <i>et al.</i> , 2011	TRAIL	Anti-calcification
Di Bartolo <i>et al.</i> , 2013	RANKL	Pro-calcification
	TRAIL	Anti-calcification
Zauli <i>et al.</i> , 2008	RANKL	Pro-calcification
	TRAIL	Anti-calcification

1.3.3 Clinical Research

It is now widely accepted that VC constitutes a major risk factor in CVD-associated morbidity and mortality. In this respect, previous studies have specifically linked VC to cardiac death, as coronary artery calcification (CAC) in CAD has been shown to be significantly associated with mortality (Budoff *et al.*, 2010). Moreover, atherosclerotic calcification has been claimed to be an independent risk factor for cardiovascular death (Detrano *et al.*, 2008), often occurring

alongside medial VC (McCullough *et al.*, 2008). As CVD is the major cause of mortality among diabetes subjects (Morrish *et al.*, 2001), it is unsurprising that VC is a pathological condition frequently accelerated in this patient population (Sage *et al.*, 2010; Shao *et al.*, 2010). Additionally, clinical evidence is continuously emerging regarding the involvement of RANKL, TRAIL and their decoy receptor OPG in VC and associated cardiovascular events. Importantly, all three glycoproteins have been identified within vascular tissues, circulating blood, and calcified atherosclerotic lesions (Higgins *et al.*, 2015; Schoppet *et al.*, 2004; Van Campenhout and Golledge, 2009), with clinical observations supporting a likely role for these regulatory proteins in the VC process in patients with T2DM/CVD. Careful analysis of these protein targets within a clinical setting (addressed below) may unlock their potential value to CVD and T2DM with respect to risk assessment and disease management (di Bartolo and Kavurma, 2014; Sage *et al.*, 2010). A joint focus will be maintained on both T2DM and atherosclerosis in this approach, linked co-morbidities manifesting medial and intimal calcification, respectively.

1.3.3.1 OPG

Circulating OPG has thus far been positively correlated with a number of T2DM/CVD pathologies. High levels of plasma OPG have been shown to positively predict CVD morbidity and mortality (Reinhard *et al.*, 2010; Vik *et al.*, 2011), while circulating OPG is increased in patient groups with high levels of arterial calcification (O'Sullivan *et al.*, 2010). As part of the Dallas Heart Study, it was observed that CAC and aortic plaque volume could be independently (positively) associated with circulating OPG in an unselected population, thereby indicating its possible use as a biomarker for atherosclerosis (Abedin *et al.*, 2007). Moreover, high levels of OPG have been positively correlated with CAD (Schoppet *et al.*, 2003) and peripheral vascular disease (Zielger *et al.*, 2005), whilst Omland and co-workers have highlighted its potential use as a predictor of heart failure in patients who suffer from acute coronary syndromes (Omland *et al.*, 2008). Most recently, Higgins and colleagues have demonstrated that both tissue and serum OPG are strongly and inversely associated with calcification in human carotid atherosclerosis (Higgins *et al.*, 2015). Since OPG is a proposed inhibitor of RANKL-induced VSMC osteogenic differentiation (Morony *et al.*, 2008), increased circulating OPG levels may represent a protective phenomenon to tackle pro-inflammatory and pro-calcific events (Singh *et al.*, 2012); the role of this ligand as a decoy receptor for TRAIL, in this respect, is less clear.

Elevated serum OPG has also been linked to T2DM. In murine models for example, it has been shown that OPG levels increase shortly after induction of diabetes (Secchiero *et al.*, 2006), with a similar trend noted in clinical studies. Many studies have significantly correlated serum OPG elevation with worsening cardiovascular burden in T2DM, including CAC (Jung *et al.*, 2010), carotid intimal-medial thickness (Gaudio *et al.*, 2014), hypertension (Rozas Moreno *et al.*, 2013), CAD/PAD (Poulsen *et al.*, 2011), metabolic syndrome and microvascular complications (Tavintharan *et al.*, 2014). Elevated OPG has also been shown to invariably predict coronary artery VC progression in diabetics, and furthermore can be used to predict future cardiovascular events (Anand *et al.*, 2006; Anand *et al.*, 2007). Finally, a 2012 study into advanced carotid atherosclerosis illustrated that a history of diabetes and CAD (among other diseases) could independently predict circulatory plasma OPG levels (Giaginis *et al.*, 2012). Therefore, it is highly likely that serum OPG concentration may constitute an important and specific CVD biomarker in T2DM, but it is unclear what the potential therapeutic value of this protein may be given that OPG levels are already elevated in T2DM/CVD patients.

1.3.3.2 RANKL

Despite strong evidence supporting a role for OPG as a T2DM/CVD biomarker, clinical investigations focusing on RANKL have proven much more divisive, with varying clinical observations across the T2DM/CVD spectrum. It has been claimed for example that circulating RANKL levels exhibit no correlation with either advanced carotid atherosclerosis (Giaginis *et al.*, 2012) or carotid intimal-medial thickness (Gaudio *et al.*, 2014). More recently however, both serum and tissue RANKL have been positively correlated with carotid calcification in atherosclerotic lesions (Higgins *et al.*, 2015). With respect to T2DM, Gaudio and co-workers have reported that circulating RANKL levels were lower in diabetics than in control subjects (Gaudio *et al.*, 2014), whilst O'Sullivan and co-workers reported no change in plasma RANKL levels in T2DM (O'Sullivan *et al.*, 2010). In another recent study, the authors identified an inverse association between higher levels of total RANKL and CAC/triglycerides in post-menopausal women (Poornima *et al.*, 2014). It has also been reported that RANKL expression is upregulated and localized to areas displaying medial arterial calcification in patients with charcot neuroarthropathy (Ndip *et al.*, 2011), whilst soluble RANKL (sRANKL) has also been positively co-associated with well-known biomarkers of heart failure (Loncar *et al.*, 2010). Overall, however, based on these recent clinical findings, a definitive role for RANKL as a serum biomarker for T2DM/CVD remains inconclusive, and the primary clinical relevance for

this ligand may lie in the prevention of RANKL-mediated pro-calcific events during VC (well-defined both *in vitro* and *in vivo*).

1.3.3.3 TRAIL

There has been considerable clinical focus on circulating TRAIL levels in CVD. Secchiero and co-workers have found that levels of circulating TRAIL are decreased after acute MI and that lower TRAIL levels are independently associated with increased levels of cardiac death in the year following patient discharge (Secchiero *et al.*, 2009) - observations consistent with the vasoprotective anti-calcific role for TRAIL previously postulated from *in vitro* and animal studies. Furthermore, due to elevated OPG and decreased TRAIL in acute MI patients, these researchers proposed that the ratio between OPG/TRAIL may have potential use as a biomarker, as this balance was significantly associated with CAD. In support of its efficacy as a biomarker, follow-up patients who developed heart failure had a significantly elevated OPG/TRAIL ratio than those who did not, indicating that this ratio may be used to predict heart failure in acute MI patients (Secchiero *et al.*, 2009). TRAIL levels have also inversely predicted all-cause mortality in patients with advanced heart failure (Niessner *et al.*, 2009).

In other research, Mori and co-workers reported that serum TRAIL levels were significantly lower in CAD patients, and were inversely associated with CAD severity independently of other coronary risk factors (Mori *et al.*, 2010), while Volpato and colleagues found a significant inverse relationship between baseline serum TRAIL levels and all-cause CVD mortality (Volpato *et al.*, 2011). Kawano and co-workers have also previously reported that serum TRAIL levels were significantly and inversely correlated with carotid intimal-medial thickness in a subset of T2DM patients with macrovascular diseases (Kawano *et al.*, 2011). Notwithstanding these observations, inconsistencies between study findings are also evident from the literature. In this regard, O'Sullivan *et al.* found no change in TRAIL levels in T2DM subjects (2010), whilst Galeone *et al.* (2013) detected high levels of TRAIL in calcified aortic valves, as well as elevated levels of circulating TRAIL in these CVD patients compared to control subjects. The balance of clinical evidence, however, suggests that serum TRAIL levels may constitute an important predictor of CV burden in patients with T2DM and CVD. Thus, given the previously reported potential therapeutic value for TRAIL identified *in vivo*, it appears that this ligand's translational potential may be multi-faceted.

1.4 Therapeutic Considerations

The dynamic nature of VC offers significant potential for clinical intervention in patients with T2DM manifesting cardiovascular complications. Thus far, however, there are no treatment options available for VC across the T2DM/CVD patient spectrum, most likely due to an insufficient understanding of the precise molecular and cellular mechanisms involved, in conjunction with a lack of clinical studies. It is clear that the dynamic pathways involving RANKL, TRAIL and their decoy receptor OPG represent potential therapeutic targets for interference of the calcification process. To date, however, progress in exploring these therapeutic options (which could play a key role in the development of an effective treatment for VC) has been limited. Nonetheless, the anti-calcific effects of OPG/TRAIL, as well as the pro-calcific effects of RANKL, have been considered by some authors in the context of generating targets for VC intervention.

1.4.1 Recombinant OPG Therapy

Unsurprisingly, in view of its mechanism of action, OPG administration has been suggested as one potential treatment option for VC (Wu *et al.*, 2013). OPG functions to prevent osteoclastogenesis and resorption in bone, whilst also having a paradoxical function in preventing osteochondroblastic calcification within the vasculature, thus resulting in a context-specific dual protective function. In support of this, numerous murine studies have illustrated that OPG deficiency tends to increase the extent of VC and cardiovascular complications, and promisingly, a recombinant OPG fusion protein (Fc-OPG) has been shown to inhibit VC in an animal study (Morony *et al.*, 2008). In this latter study, *ldlr*^{-/-} mice were fed an atherogenic diet alongside Fc-OPG administration; calcification (as measured by the Von Kossa silver stain for calcium deposition) was specifically inhibited with no effect on atherosclerotic lesion number or size. It can be noted that Fc-OPG has also been safely employed in rat models to treat arthritis (Bolon *et al.*, 2002) and orthodontic issues (Fernández-González *et al.*, 2015), and administered to dogs (alongside BMP-2) to increase bone formation and healing (Yao *et al.*, 2011), although its specific pleiotropic effects on VC were not considered during these particular investigations. As noted, however, circulating OPG is significantly elevated during T2DM/CVD, and as such, the precise benefit of recombinant OPG treatment in human clinical studies remains to be determined.

1.4.2 Anti-RANKL Therapy

Due to the cross-over in molecular mechanisms between bone morphogenesis and VC, it is possible that a second prospective treatment for VC could be adapted from currently existing osteoporosis therapy (Wu *et al.*, 2013). Osteoporosis is a systemic skeletal disease in which the level of bone resorption is greater than that of bone formation, leading to continuous bone degradation and ultimately resulting in low bone mass and fragility (Miyazaki *et al.*, 2014). Denosumab, a human monoclonal antibody for RANKL, is one of the latest approved treatment options for osteoporosis (Suresh *et al.*, 2015; Wu *et al.*, 2013), although its effects on VC have not yet been fully assessed. Mimicking the natural actions of OPG, Denosumab binds and neutralizes RANKL (but not TRAIL), attenuating its osteoclastic effects and allowing osteoblastic build-up of bone to ensue (Kostenuik *et al.*, 2009). As RANKL promotes osteochondroblastic activity in VSMCs, anti-RANKL therapy could theoretically function to reduce the extent of calcification in the vasculature.

In support of this theory, it has been demonstrated that Denosumab reduced aortic calcium levels by half in a murine model of osteoporosis (Helas *et al.*, 2009), but contrastingly, the only corresponding human study completed to date has noted no influence of this therapy on aortic calcification progression over a three-year period (Samelson *et al.*, 2014). It is possible that this disparity is due to inconsistencies in calcification measurement, as Samelson and colleagues utilized a semi-quantitative method (lateral spine X-rays) as opposed to the quantitative measurement of aortic calcium deposition employed by Helas and co-workers (2009). However, as noted, the natural increase in circulating OPG during T2DM likely exerts the same influence as Denosumab *in vivo*, and (given that VC progresses alongside this elevated OPG) may not be sufficient to attenuate RANKL-mediated pro-calcific effects (indeed, it must be remembered that in both bone and vasculature, RANKL exerts its function despite the presence of endogenous OPG production). The potential of anti-RANKL therapy in VC treatment therefore awaits further clinical investigation, but it is likely that successful intervention for VC may lie outside of the RANKL:OPG axis.

1.4.3 TRAIL Administration

Although its potential therapeutic use in cardiovascular protection has been suggested (Volpato *et al.*, 2011), there have been no human clinical investigations conducted to date that address the potential of TRAIL for the treatment of VC. As noted however, recombinant TRAIL

administration to ApoE^{-/-} diabetic mice has been shown to significantly reduce atherosclerosis progression (Secchiero *et al.*, 2006), whilst TRAIL delivery protects against diabetic vascular injury in rats (Liu *et al.*, 2014). Also of relevance, TRAIL deficiency appears to promote VC and diabetes *in vivo* (di Bartolo *et al.*, 2011; di Bartolo *et al.*, 2013), and most relevantly, has been shown to attenuate RANKL-mediated function both *in vitro* and *in vivo* (Zauli *et al.*, 2004; Zauli *et al.*, 2008). Thus, the potential therapeutic value of TRAIL in the treatment of VC cannot be ignored, but further basic research is necessary to determine the precise mechanism(s) of TRAIL-mediated protection before clinical trials can be conducted.

1.4.4 Additional Therapeutic Possibilities

A range of potential therapeutic possibilities for VC unrelated to the OPG/RANKL/TRAIL axis have emerged in the literature, some of which are related to current treatments for osteoporosis, CVD, and chronic kidney disease (CKD) (Wu *et al.*, 2013). Firstly, like Denosumab, bisphosphonates (pyrophosphate analogs) are a successful osteoporosis treatment that have been considered as a potential VC therapy option due to their inhibitory effect on hydroxyapatite crystal formation (Boskey *et al.*, 2003). Additionally, teriparatide, a shortened recombinant human parathyroid hormone also employed for osteoporosis treatment, has been shown to reduce VC in *ldlr*^{-/-} mice (Shao *et al.*, 2003). Secondly, statins, which have been routinely employed to lower blood cholesterol and prevent vascular complications during CVD/T2DM, have also been considered as a potential treatment option for VC, in view of their inherent pleiotropic properties (Wu *et al.*, 2013). Indeed, statins have been shown to reduce levels of pro-calcific serum RANKL (Lenglet *et al.*, 2014) and to increase anti-calcific serum OPG (Mori *et al.*, 2010). Thirdly, GLP-1RAs, a new class of injectable glucose-lowering drugs, are currently employed in T2DM treatment (Mafong *et al.*, 2008), and thus far, the potential for GLP-1RAs in VC prevention have been promising (Zhan *et al.*, 2014). Furthermore, endothelin receptor agonists used to treat hypertension have also been shown to be effective against VC *in vitro* (Wu *et al.*, 2003) and *in vivo* (Essalihi *et al.*, 2004), while a monoclonal antibody to IL-1 β (01BSUR, Novartis) has been noted to reduce aortic calcification in *ldlr*^{-/-} mice (Awan *et al.*, 2016). Finally, owing to the similarity in calcification-driven pathogenesis, the range of existing therapies for CKD may also hold promise in the development of a successful VC treatment (Wu *et al.*, 2013). An extensive list of treatment options for VC are summarised in Appendix 1.1 for perusal (Harper *et al.*, 2016).

1.5 Study Hypotheses and Objectives

Accelerated VC observed during T2DM is a leading cause of morbidity and mortality, however, the key molecular events and signalling pathways underpinning this process remain to be fully defined. Evidence now points to a role for the signalling triad RANKL, TRAIL and their common decoy receptor OPG in the regulation of VC; in this respect, the pro-calcific and protective effects of RANKL and OPG, respectively, are well documented, but the role for TRAIL in a vascular setting remains under debate. Despite this, compelling evidence now points to a *vasoprotective* role for TRAIL, but further research is required to confirm its potential therapeutic relevance to VC. Furthermore, whilst the precise mechanisms underlying the physiological roles for RANKL and TRAIL are well defined, the interrelated mechanisms by which these ligands exert their function in the vasculature remain to be explored.

1.5.1 Study 1: Profiling the Effects of RANKL +/- TRAIL in the Vasculature

The pro-calcific effects of RANKL in the vasculature have been well described, exerting both direct effects on vascular cells (Panizo *et al.*, 2009) and indirect effects on VSMCs via endothelial paracrine signalling (Davenport *et al.*, 2016; Osako *et al.*, 2010). Furthermore, we note an interesting piece of evidence presented by Zauli and colleagues (2004; 2008) that TRAIL can attenuate RANKL-induced osteoclastogenesis, suggesting that TRAIL has the ability to regulate RANKL signalling. Thus, given the proposed vasoprotective properties of TRAIL, *we hypothesise that TRAIL may exert an anti-calcific influence on the vasculature via attenuation of RANKL-induced pro-calcific signalling.* As RANKL is known to promote VC both directly and via paracrine communication, the effects of RANKL +/- TRAIL on vascular cells in monoculture (endothelial/smooth muscle cells separately) and in co-culture (endothelial/smooth muscle cells in indirect contact) will be assessed (Figure 1.8A). A range of VC-related indices will be analysed following RANKL +/- TRAIL treatment at an mRNA and/or protein level by RT-qPCR, ELISA and Western blotting where appropriate.

1.5.2 Study 2: Profiling the Effects of RANKL and TRAIL under Pathological Conditions

We notice that the vast majority of studies to date assess the effects of RANKL and TRAIL under “healthy” conditions *in vitro*. In reality, however, RANKL and TRAIL during CVD/T2DM exert their function in the presence of pathological stimuli, primarily

hyperglycemia and inflammation. Thus, *we hypothesise that the influence of RANKL and TRAIL may vary considerably under pathological compared to healthy conditions.* In this respect, the effects of RANKL/TRAIL on the vasculature under pathological conditions will be analysed, which may aid in delineating the roles of RANKL and TRAIL during VC. Again, both monoculture and co-culture models will be included in order to recapitulate the paracrine signalling element of physiological vasculature (Figure 1.8B), and a range of VC-related indices analysed by RT-qPCR, ELISA and Western blotting within each model.

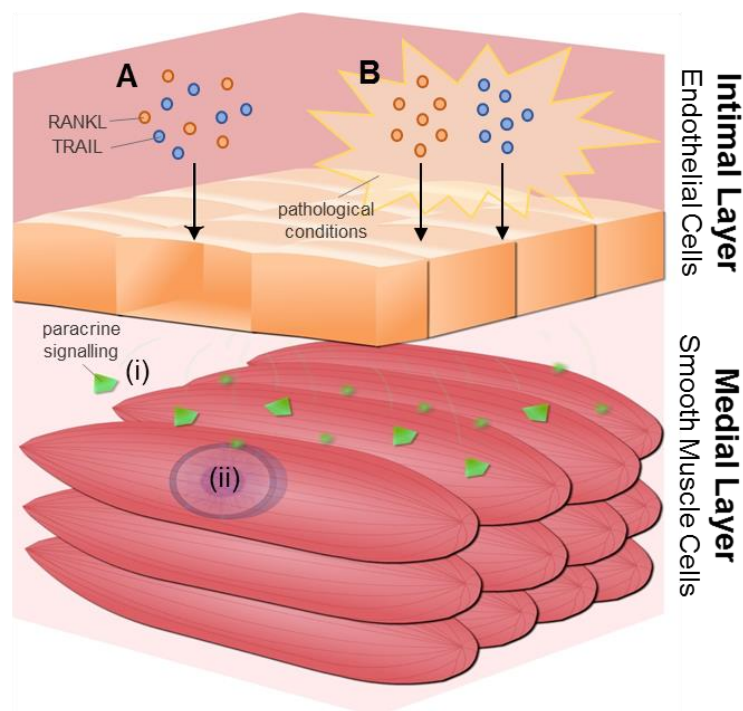


Figure 1.8. Representation of the *in vitro* co-culture model to be employed for studies 1 and 2. (A) Endothelial cells will be treated with RANKL +/- TRAIL, and (B) endothelial cells will be treated with RANKL or TRAIL under pathological conditions. (i) Endothelial:smooth muscle paracrine signalling and (ii) smooth muscle cell responses will be assessed in each case. RANKL, receptor activator of NF- κ B ligand; TRAIL, tumour necrosis factor-related apoptosis-inducing ligand. Image adapted from Harper *et al.*, 2018.

1.5.3 Study 3: Investigating the Mechanisms of RANKL and TRAIL Function during VC

From a mechanistic perspective, both RANKL and TRAIL function are known to involve NF- κ B signalling and oxidative stress, both of which have been implicated in vascular pathologies (Byon *et al.*, 2008; Folli *et al.*, 2011; Patel and Santani, 2009). However, the signalling pathways activated by these ligands during VC remain to be clarified. *We therefore hypothesise that both NF- κ B activation and redox signalling may regulate RANKL/TRAIL function during*

VC. Thus, we chose to investigate these pathways in the aforementioned *in vitro* models via analysis of a range of both VC-related and redox indices via RT-qPCR, ELISA and Western blotting where appropriate. Oxidative stress will also be assessed via analysis of reactive oxygen species by flow cytometry and fluorescence microscopy. Furthermore, the potential for the involvement of additional protein mediators not yet implicated in the VC process will be assessed via bioinformatics analyses (Section 2.2.8). Identifying the precise molecular mechanisms underpinning VC may ultimately lead to therapeutic development that will reduce T2DM/CVD-related mortality worldwide.

Chapter 2

Materials and Methods

2.1 Materials

2.1.1 Consumables and Plasticware

Becton Dickinson (New Jersey, USA)

Falcon® round-bottomed test tubes for flow cytometry 352054

Digital Bio Technology (Seoul, South Korea)

Accuchip 4x Kit AD4K-200

Merck Millipore (Massachusetts, USA)

Immobilon®-PSQ polyvinylidene fluoride 0.2 µm membrane ISEQ00010

Millicell® hanging cell culture transwell insert 0.4 µm MCHT06H48

Roche Diagnostics (Basel, Switzerland)

LightCycler® 480 plates 96-well 04729692001

Sarstedt AG & Co. (Nümbrecht, Germany)

10 µL pipette tips 70.1130

200 µL pipette tips 70.760.002

1000 µL pipette tips 70.762

0.2 mL PCR tubes 72.737.002

0.5 mL PCR tubes 72.735.002

1.5 mL microtubes 72.706.200

2 mL microtubes 72.695.500

15 mL centrifuge tubes 62.554.502

50 mL centrifuge tubes 62.559.001

10 mL serological pipettes 86.1254.001

100 x 20 mm tissue culture dishes 83.3902

6-well tissue culture plates 83.3920

12-well tissue culture plates 83.3921

24-well tissue culture plates 83.3922

96-well tissue culture plates 83.3924

Cell scrapers 83.1830

CryoPure tubes 72.380.992

Filtopur 0.2 µm syringe filters 83.1826.001

Thermo Fisher Scientific (Massachusetts, USA)

MicroAmp™ Optical adhesive film 4311971

Nunc® Immuno MaxiSorp™ 96-well plates 439454

White Microtiter™ plates 611F96WT

Terumo Medical (New Jersey, USA)

Terumo® 10 mL syringe without needle SS-10ES

2.1.2 Reagents and Chemicals

Becton Dickinson (New Jersey, USA)

FACS rinse solution 340346

FACSFlow™ sheath fluid 342003

BioAssay Systems (California, USA)

QuantiChrom™ alkaline phosphatase assay kit DALP-250

Bio-Rad (California, USA)

Coomassie Brilliant Blue R-250 161-0400

Cell Signalling Technologies (Massachusetts, USA)

Anti-human NF-κB p65 (D14E12) XP® rabbit monoclonal antibody 8242S

Anti-human phospho-NF-κB p65 (Ser536) rabbit monoclonal antibody 3031S

Anti-mouse HRP-linked antibody 7076S

Anti-rabbit HRP-linked antibody 7074S

Dharmacon Inc. (Colorado, USA)

DharmaFECT™ 1 transfection reagent 11571731

ON-TARGETplus™ GAPDH control siRNA D-001830-01-05

siGENOME™ non-targetting siRNA pool D-001206-13-05

SMARTpool™ ON-TARGETplus™ NF-κB2 siRNA L-003918-00-0005

Sterile RNase-free water B-003000-WB-100

Eurofins Genomics GmbH (Ebersberg, Germany)

Custom DNA primer oligonucleotides

Fisher Scientific (New Hampshire, USA)

Acetic acid glacial A35-500

Buffer solution pH 4 (phthalate) J/2825/15

Buffer solution pH 7 (phosphate) J/2855/15

Buffer solution pH 10 (borate) J/2885/15

Propan-2-ol/Isopropanol P/7490/15

InvivoGen (California, USA)

Primocin™ antimicrobial agent for primary cells ANT-PM-1

Lennox Laboratories Supplies (Dublin, Ireland)

Industrial methylated spirits CRTSI0330716

Merck Millipore (Massachusetts, USA)

Alizarin Red staining solution TMS-008-C

Anti-human NF-κB p52 rabbit monoclonal antibody 06-413

Anti-human SOD2 rabbit polyclonal antibody AB10346

Luminata™ Forte Western HRP substrate WBLUF0100

Recombinant human OPG GF120

PromoCell GmbH (Heidelberg, Germany)

Endothelial cell growth medium MV C-22020
Smooth muscle cell growth medium 2 C-22062
CryoSFM freezing medium C-29910

Research and Diagnostic (R&D) Systems Inc. (Minnesota, USA)

Human BMP-2 DuoSet® ELISA DY355
Human IL-6 DuoSet® ELISA DY206
Human OPG DuoSet® ELISA DY805
Human RANKL DuoSet® ELISA DY626
Human TNF α DuoSet® ELISA DY210
Human TRAIL DuoSet® ELISA DY375
Normal goat serum DY005
Recombinant human noggin protein 6057-NG
Recombinant human RANKL protein 390-TN
Recombinant human TRAIL protein 375-TL
Anti-human TRACP5 sheep polyclonal antibody AF3948
Anti-human GAPDH mouse monoclonal antibody MAB5718
Anti-human SOD1 mouse monoclonal antibody MAB3418

Roche Diagnostics (Basel, Switzerland)

Complete EDTA-free protease inhibitor cocktail tablets 04693132001
Fast Start essential DNA green master 06924204001

Santa Cruz Biotechnology (Texas, USA)

Anti-human RANKL mouse monoclonal antibody sc-377079
Anti-human TRAIL mouse monoclonal antibody sc-8440

Sigma-Aldrich (Dorset, UK)

Acrylamide/bis-acrylamide solution A3574

Agarose A5093

Albumin from bovine serum A2153

Ammonium bicarbonate A6141

Ammonium hydroxide 338818

Ammonium persulfate A9164

Ascorbic acid 2-phosphate 49752

Bovine serum albumin (for ELISA) A7638

Brilliant blue R B0149

Chloroform C2432

Custom DNA primer oligonucleotides

Deoxynucleotide set DNTP100

Dexamethasone D4902

D-glucose G8644

Dihydroethidium 37291

Dimethyl sulfoxide D8418

D-mannitol M4125

DNase 1 kit AMPD1

Dulbecco's phosphate-buffered saline D8537

Ethanol E7023

Ethylenediaminetetraacetic acid disodium salt dihydrate (EDTA) E5134

Fluorescein Isothiocyanate-Dextran 40kDa (FITC-Dextran) FD40S

Glycerol G6279

Glycine G8898

HEPES H4034

Human recombinant TNF α H8916

Hydrochloric acid H1758

L-glutamine G6392

Methanol 34860

Minimum Essential Medium Eagle, alpha modification (α MEM) M8042

N,N,N',N'-tetramethylethylenediamine (TEMED) T9281

N-acetyl-L-cysteine A9165

Paraformaldehyde P6148

Penicillin-streptomycin P0781

Phosphate-buffered saline tablets P4417

Ponceau S solution P7170

Potassium chloride P9541

Potassium phosphate monobasic P5655

Sodium azide 13412

Sodium chloride S3014

Sodium deoxycholate D6750

Sodium dodecyl sulphate L3771

Sodium fluoride S7920

Sodium hydroxide 72068

Sodium orthovanadate S6508

Sodium phosphate dibasic S3264

Tris acetate-EDTA buffer, 50X T9650

Tris base T1503

TritonTMX-100 X100

Trizma[®] base T6066

Trypsin-EDTA solution T4174

Tween[®]20 P1379

β -glycerophosphate G9422

2-mercaptoethanol M6250

4',6-diamidino-2-phenylindole dihydrochloride (DAPI) 32670

Thermo Fisher Scientific (Massachusetts, USA)

Dead Cell Apoptosis Kit with Annexin V Alexa Fluor® 488 & Propidium Iodide V13241

DreamTaq DNA polymerase kit EP0702

Fetal bovine serum 10106169

GeneRuler 100 bp plus DNA ladder SM0321

High capacity cDNA reverse transcription kit 4368814

MultiScribe™ reverse transcriptase 4311235

PageRuler™ Plus prestained protein ladder 26619

Pierce™ BCA protein assay kit 23225

Recombinant human BMP-2 PHC7145

RNaseZap™ RNase decontamination solution AM9780

SYBR Safe® DNA gel stain S33102

Trizol™ reagent 15596018

Western blot stripping reagent 10057103

2.1.3 Apparatus and Equipment

ADAM™ cell counter (Digital Bio, Seoul, South Korea)

Agarose gel rig (Apollo Scientific, Stockport, UK)

Benchtop pH meter SevenCompact™ (Mettler Toledo, Ohio, USA)

Block heater SBH130D (Stuart Scientific, Staffordshire, UK)

Clifton™ water bath (Nickel-Electro Ltd., Weston-super-Mare, UK)

ELx800 microplate reader (Biotek, Vermont, USA)

FACSAria™ flow cytometer (Becton Dickinson, New Jersey, USA)

G-Box chemi-luminescence analysis system (Syngene, Cambridge, UK)

HeraCell™ 150 incubator (Thermo Fisher Scientific, Massachusetts, USA)

HERASafe™ laminar flow cabinet class II (Thermo Fisher Scientific, Massachusetts, USA)

Large volume centrifuge 5804R (Eppendorf, Cambridge, UK)

LightCycler®96 real-time PCR system (Roche Diagnostics, Basel, Switzerland)

Liquid nitrogen storage container (Taylor-Wharton Cryogenics, Borehamwood, UK)

Mini orbital shaker SSM1 (Stuart Scientific, Staffordshire, UK)
Mini-PROTEAN® Tetra-cell gel casting module (Bio-Rad, California, USA)
Mini-PROTEAN® Tetra-Cell SDS-PAGE and transfer module (Bio-Rad, California, USA)
MJ Mini thermal cycler (Bio-Rad, California, USA)
Multiskan™ EX microplate reader (Thermo Fisher Scientific, Massachusetts, USA)
Nalgene® Mr. Frosty cryo-freezing container (Thermo Fisher Scientific, Massachusetts, USA)
Nanodrop™ 1000 spectrophotometer (Thermo Fisher Scientific, Massachusetts, USA)
Nikon Eclipse Ti fluorescent microscope (Nikon, Tokyo, Japan)
Nikon Eclipse TS100 phase-contrast microscope (Nikon, Tokyo, Japan)
PowerPac™ basic electrophoresis power supply (Bio-Rad, California, USA)
See-saw rocker SSL4 (Stuart Scientific, Staffordshire, UK)
Small volume centrifuge 5430R (Eppendorf, Cambridge, UK)
Synergy™ HT Fluorescent microplate reader (Bio-Tek, Vermont, USA)

2.1.4 Buffer Preparation

Radio Immunoprecipitation Assay (RIPA) stock (1.28X)

HEPES, pH7.5, 64 mM

Sodium chloride, 192 mM

Triton X-100, 1.28% (v/v)

Sodium deoxycholate, 0.64% (v/v)

SDS, 0.128% (w/v)

RIPA cell lysis buffer

1.28X RIPA stock, 1X

Sodium fluoride, 10 mM

EDTA, pH 8.0, 5 mM

Sodium phosphate, 10 mM

Sodium orthovanadate, 1 mM

Protease inhibitor cocktail, 1X

Running buffer for SDS-PAGE

Trizma® base, 25 mM

Glycine, 192 mM

SDS, 0.1% (w/v)

Transfer buffer

Tris-HCl, pH6.8, 25 mM

Glycine, 192 mM

Methanol, 20% (v/v)

Sample solubilisation buffer (SSB)

Tris-HCl, pH6.8, 250 mM

SDS, 8% (w/v)

Glycerol, 40% (v/v)

2-mercaptoethanol, 4% (v/v)

Bromophenol blue, 0.008% (w/v)

0.2 µm filter

Phosphate buffered saline (PBS) stock, 10X concentrate

Sodium chloride, 1.37 M

Potassium chloride, 27 mM

Sodium phosphate dibasic, 81 mM

Potassium phosphate monobasic, 15 mM

Adjust to pH 7.4

Tris buffered saline (TBS) stock, 10X concentrate

Tris base, 0.5 M

Sodium chloride, 1.5 M

Adjust to pH 7.6

Tris-HCl

Tris base, 1.5 M

Adjust to pH 6.8/pH 8.8 with HCl

Coomassie R-250 staining solution

Coomassie brilliant blue R250, 1% (w/v)

Glacial acetic acid, 10% (v/v)

Methanol, 40% (v/v)

Distilled water, 50% (v/v)

0.2 µm filter

Coomassie R-250 de-staining solution

Methanol, 20% (v/v)

Glacial acetic acid, 10% (v/v)

Distilled water, 70% (v/v)

FACS buffer

Fetal bovine serum, 2% (v/v)

Sodium azide, 0.1% (w/v)

PBS, 98% (v/v)

0.2 µm filter

2.2 Methods

2.2.1 Cell Culture Methods

2.2.1.1 Sterile Conditions

All cell culture work was carried out in a validated HERASafe™ laminar flow Class II biological safety cabinet. Equipment was routinely sanitised with 70% industrial methylated spirits (IMS) before use. All materials used in cell culture work, including pipette tips, microtubes and phosphate-buffered saline (PBS) were autoclaved as required, and reconstitution buffers for recombinant proteins subject to 0.2 µm filtration. Tissue culture plates, pipettes and centrifuge tubes were pre-sterilised. Standard aseptic technique was routinely employed.

2.2.1.2 Growth and Maintenance of Cells

Human aortic endothelial cells (HAECs) and human aortic smooth muscle cells (HASMCs) were obtained from PromoCell GmbH (Heidelberg, Germany). HAECs were donated by a 23 year-old Caucasian male and were cultured in endothelial cell growth medium MV (Promocell), with final concentrations of 0.05 mL/mL fetal bovine serum (FBS), 0.004 mL/mL endothelial cell growth supplement, 10 ng/mL recombinant human epidermal growth factor, 90 µg/mL heparin and 1 µg/mL hydrocortisone. HASMCs were donated by a 19 year-old Caucasian male and were cultured in smooth muscle cell medium 2 (Promocell) with final concentrations of 0.05 mL/mL FBS, 0.5 ng/mL recombinant human epidermal growth factor, 2 ng/mL recombinant human basic fibroblast growth factor and 5 µg/mL recombinant human insulin. Penicillin (100 U/mL) and streptomycin (100 µg/mL) were added to both growth media. Primocin™ antimicrobial agent, at a final concentration of 100 µg/mL, was included in place of these antibiotics for long-term incubation periods (providing protection from bacteria, mycoplasma and fungi). Primocin™ is validated for primary cell culture, and no differences were noted in cell morphology or viability when compared to antibiotic treatment.

HAECs/HASMCs of passage 5 to 12 were used for experimental procedures. Cells were maintained at 37°C and 5% CO₂. Fresh media was added to cells in culture every 2-3 days, and passaged at 80-90% confluency unless otherwise described. HAECs and HASMCs were visually analysed daily to monitor confluency and morphological changes using a Nikon Eclipse TS100 microscope at 10X and 40X magnification.

2.2.1.3 Trypsinisation

Trypsinisation is required to passage both HAEC and HASMC adherent cells. Spent media was removed from the cell culture dish and cells were washed twice with sterile Dulbecco's PBS to remove trypsin inhibitors. A small volume of pre-warmed 10% (v/v) trypsin-EDTA was added to cover the cell monolayer and incubated at 37°C for 2-3 minutes until the cells had visibly detached from the surface. An equal volume of culture media was then added to deactivate the trypsin enzyme. The cell suspension was transferred to a 15 mL centrifuge tube and subject to centrifugation at 50 *xg* for 5 minutes, supernatant media removed, and the resulting cell pellet re-suspended in fresh growth media. For both HAECs and HASMCs, the ratio of passage was 1:3.

2.2.1.4 Cryopreservation and Cryorecovery

To cryopreserve cell stocks, approximately 1×10^6 cells were trypsinised and subject to centrifugation at 100 *xg*. The resulting cell pellet was then re-suspended in 1 mL CryoSFM cryopreservation medium (Promocell), which contains a number of cryoprotectants including methylcellulose and dimethyl sulfoxide (DMSO). Re-suspended cells were transferred to a sterile CryoPure cryovial and placed in a Mr. Frosty™ isopropanol chamber at -80°C to ensure a cooling rate of -1°C per minute. The following day, cryovials were transferred to liquid nitrogen storage. When required, cells were recovered by rapid thawing of the vial in a 37°C water bath and immediate transfer to pre-warmed media, which was replaced with fresh media after 24 hours.

2.2.1.5 Cell Counting

Cells were routinely counted during trypsinisation to ensure appropriate seeding densities, or at the point of harvesting for viability measurement and data normalisation after experimental procedures. All cell counts were carried out using an Advanced Detection and Accurate Measurement (ADAM™) counter (Digital Bio), as pictured in Figure 2.1. The ADAM™ counter method applies fluorescent propidium iodide (PI) staining to cell suspensions in order to calculate: (i) total cell number (T), (ii) non-viable cell number (N), (iii) viable cell number (T-N), and (iv) percentage viability. PI intercalates with available DNA, but cannot penetrate

undamaged cell membranes. A small volume (15 μ L) of cell suspension was mixed with an equal volume of both solution N, containing PI only, and solution T, which contains both PI and lysis buffer to ensure disruption of intact membranes. A 15 μ L aliquot of each mixture was added to the appropriate channel in a microfluidic Accuchip, and the Accuchip loaded into the ADAM™ counter. Multiple images of the channels are taken, and the ADAM™ image analysis software determines average values for total and viable cell counts which are then displayed digitally.



Figure 2.1. The ADAM™ Counter with an Accuchip resting in the loading bay. Image courtesy of www.digital-bio.com.

2.2.2 Cell Models and Treatments

2.2.2.1 Monoculture Models

To identify direct effects of soluble factors on HAECs and HASMCs, standard monoculture experiments were employed. Cells were seeded into 6-well, 12-well or 24-well culture dishes at the required seeding density. At confluency, cells were washed with sterile PBS and fresh pre-warmed media added containing soluble factors at experimental concentrations. The following recombinant proteins were employed for cell exposures (Table 2.1):

Table 2.1. Soluble factors, their source and concentrations employed for cell exposures.

Soluble factor	Source	Concentration
TNFα	Sigma-Aldrich	100 ng/mL
RANKL	R&D Systems	5-50 ng/mL
TRAIL	R&D Systems	5-50 ng/mL
BMP-2	Thermo Fisher Scientific	5 ng/mL
Noggin	R&D Systems	100 ng/mL
Glucose	Sigma-Aldrich	15-30 mM
Mannitol	Sigma-Aldrich	30 mM
NAC	Sigma-Aldrich	5 mM

TNF, tumour necrosis factor; RANKL, receptor activator of NF- κ B ligand; TRAIL; TNF-related apoptosis inducing ligand; BMP, bone morphogenetic protein; NAC, N-acetyl-L-cysteine.

2.2.2.2 Co-Culture Models

In vivo, both HAECs and HASMCs thrive in close proximity to each other; thus, a co-culture model was employed to better recapitulate the paracrine signalling properties of the vessel wall. Representing the intimal layer of the vasculature, HAECs were directly treated with soluble factors and the resulting paracrine influences on underlying co-cultured HASMCs were monitored. ECs and VSMCs have been successfully employed in similar non-contact co-culture studies (Liu *et al.*, 2007; Nam *et al.*, 2011; Wang *et al.*, 2011).

For the majority of HAEC:HASMC co-culture experiments, HASMCs were first grown in standard 6-well culture dishes as described above. At confluency, transwell culture inserts (Merck Millipore) were placed in HASMC wells, and HAECs seeded into the wells at a density of 2×10^5 cells/insert to ensure tight monolayer formation. Transwell inserts support the endothelial monolayer above a 0.4 μm porous membrane, allowing HAEC:HASMC communication while maintaining separate luminal and subluminal compartments. A combination of HAEC and HASMC media was used for co-culture experiments (1:1 ratio) to ensure healthy maintenance of both cells, and a total of 6 mL media was required per well (2 mL apical/luminal, 4 mL basolateral/subluminal). After seeding, the co-culture was incubated for 24 hours pre-treatment to ensure endothelial monolayer formation and media volume equilibration. This method was altered for gene knockdown experiments (Section 2.2.2.4).

To initiate experimental conditions, relevant concentrations of soluble factors were added to the apical compartment. HAECs are in direct contact with these factors, as endothelial cells are exposed to circulating soluble factors in the vasculature, while HASMCs rely on the paracrine signalling of HAECs (through the subluminal compartment *in vitro* or through the intercellular space *in vivo*) to induce a response. After incubation, spent media from both luminal and subluminal compartments, along with protein/RNA from the HASMC culture, were harvested for analysis. A schematic diagram of the non-contact co-culture model is illustrated overleaf in Figure 2.2.

During co-culture development, a simple conditioned media transfer model was utilised (previously employed by Davenport *et al.*, 2016) to confirm consistency with previously published results. In this case, HAECs in standard 6-well culture dishes were exposed to soluble factors for 72 hours, and 50% endothelial conditioned media (+ 50% fresh HASMC media) was transferred to confluent reporter HASMCs for a further 72 hours. HASMCs were subsequently harvested for protein/mRNA analyses.

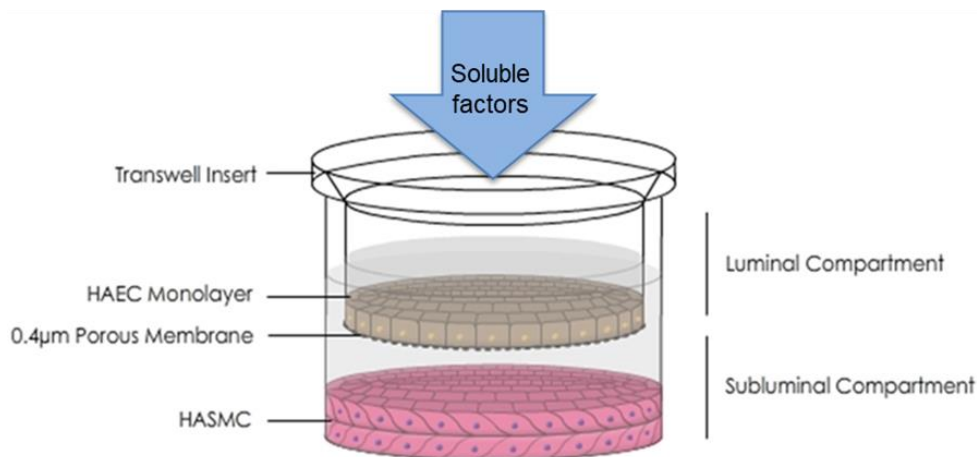


Figure 2.2. Schematic representation of the HAEC:HASMC co-culture model. Image adapted from Harper *et al.*, 2017. HAEC, human aortic endothelial cell; HASMC, human aortic smooth muscle cell.

2.2.2.3 Calcification Models

In order to investigate end-point calcification, HASMCs were subject to high phosphate-induced osteoblastic differentiation. Pro-osteogenic differentiation medium was employed, consisting of minimum essential medium eagle alpha modification (α MEM) supplemented with 0.292 g/L L-glutamine, 10% FBS and 1% penicillin/streptomycin, and the pro-osteogenic factors dexamethasone (100 nM), ascorbic acid 2-phosphate (50 μ M), and β -glycerophosphate (10 mM) (Langenbach and Handschel, 2013; Shioi *et al.*, 1995). This medium has previously been successfully employed for osteoblastic differentiation (Ghali *et al.*, 2015; Westhrin *et al.*, 2015). HASMCs were exposed to differentiation medium at approximately 60% confluency, and remained in culture for 21 days prior to treatment with soluble factors.

A murine osteoblastic precursor cell line (MC3T3-E1) was also employed as a positive control for osteogenic differentiation/mineral deposition. MC3T3-E1 cells, kindly donated for use by Dr. Steve Kerrigan (Cardiovascular Infection Research Group, RCSI), were cultured in standard α MEM supplemented with L-glutamine, FBS and antibiotics prior to differentiation. Cells were trypsinised and cryopreserved according to sections 2.2.1.3 and 2.2.1.4 respectively, and passages 24-28 were used for experimental purposes. MC3T3-E1 cells were exposed to differentiation medium for 21 days prior to analysis.

Control medium, consisting of α MEM supplemented with L-glutamine, FBS and antibiotics in the absence of pro-osteogenic factors, was routinely employed as a negative control for both HASMCs and MC3T3-E1 cells.

2.2.2.4 siRNA Gene Knockdown Models

HAECs were subject to small interfering (si) RNA knockdown of the NFκB2 gene, coding for the p100 subunit of the non-canonical NF-κB pathway (and thus the p52 cleaved product). siRNA knockdown, or gene ‘silencing’, involves the exogenous introduction of synthesised short double-stranded RNA sequences (~20-24 bp) into the cell cytoplasm. This siRNA, complementary to the target gene mRNA sequence, is processed by the RNA-induced silencing complex (RISC), and ultimately used to locate and bind the mRNA of interest. The target mRNA is then cleaved by argonaute 2 endonuclease (Chendrimada *et al.*, 2005), reducing mRNA copy number and thus transcription and translation of the target protein (Figure 2.3).

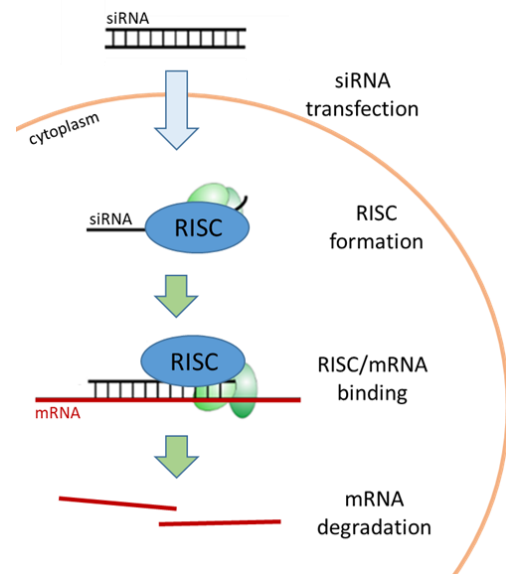


Figure 2.3. The process of siRNA gene silencing. RISC, RNA-induced silencing complex. Image adapted from www.biorresource.com.

DharmaFECT™ transfection reagents (Dharmacon), with self-reported minimal reagent toxicity, were chosen for transient lipid-based transfection. An intact endothelial monolayer is required for co-culture, and alternative physical techniques (eg. electroporation) can induce leakage of intracellular components and high percentage of cell death (Tsong *et al.*, 1991).

HAECs were trypsinised and seeded into 6-well dishes (optimisation) or transwell inserts (co-culture) for siRNA knockdown. In all cases, cells were re-suspended and plated in antibiotic-free medium, and left to adhere overnight. For the siRNA transfection procedure, 5 μM siRNA solution was prepared in sterile molecular grade water. DharmaFECT™ 1 transfection reagent and siRNA (Dharmacon) were individually diluted in antibiotic- and serum-free medium and incubated for 5 minutes at room temperature. Diluted DharmaFECT™ 1 and siRNA were mixed and incubated for a further 20 minutes at room temperature. The resulting mix was diluted with antibiotic-free complete medium, achieving a final concentration of 50 nM siRNA and a final volume of 10 μL DharmaFECT™ 1 per well. Spent media was removed from cultured HAECs, transfection medium added and cells were incubated for 48 hours (mRNA analysis) or 72 hours (protein analysis) unless otherwise described. DharmaFECT™ 1 has previously been used for the transfection of human primary cells (Chiang *et al.*, 2016; Dharmacon, 2015), while both GAPDH and NFκB2 siRNA sequences have been successfully employed for gene silencing (Bryant *et al.*, 2012; Nguyen *et al.*, 2015).

2.2.2.4.1 siRNA Transfection Optimisation

HAECs were seeded at a density of 2.5×10^6 cells per well for optimisation purposes. Initially, cells were assessed for gene knockdown receptivity using positive control siRNA for endogenous GAPDH. HAECs were exposed to the recommended 25 nM GAPDH siRNA across a range of 2.5-10 μL /well DharmaFECT™ 1 reagent volumes in order to assess reagent toxicity and suitability. For NF κ B2 gene knockdown optimisation, HAECs were exposed to 25 nM and 50 nM pooled NF κ B2 siRNA across a DharmaFECT™ 1 volume range of 2.5-10 μL /well to determine optimal transfection conditions. A non-targetting scrambled siRNA control pool was also included to expose non-specific effects. Cell viability, NF κ B2 mRNA expression and NF- κ B p100/p52 protein expression were measured post-knockdown to assess reagent toxicity and transfection/knockdown efficiency. Untransfected cells and non-targetting siRNA controls were included under all experimental conditions for comparison purposes.

2.2.2.4.2 Co-culture Experiments: NF κ B2 Knockdown

HASMCs were grown to confluency in standard 6-well culture dishes. HAECs were seeded into semi-permeable transwell inserts at a lower density of 1.5×10^6 cells per insert, and allowed to incubate for 24 hours before commencing siRNA knockdown in optimal transfection media. After 48 hours in culture, transwell inserts were removed from the transfection media and transferred to the dish of confluent HASMCs. Cells were allowed to recover for 6 hours in fresh media prior to treatment with recombinant RANKL. HAECs and HASMCs were co-cultured for a further 72 hours, prior to harvesting for analysis. Additionally, HAECs were assessed for responses post-exposure to both NF κ B2 siRNA and non-targetting siRNA, alongside HASMC responses to endothelial non-targetting siRNA treatment.

2.2.3 Gene Expression Analysis

2.2.3.1 RNA Isolation

To prevent RNA degradation by natural RNases, all surfaces, equipment and gloves were sprayed with RNaseZap™ and all pipette tips, centrifuge tubes and PBS were autoclaved for use in RNA work. If cell counting was not required, cells were washed three times with sterile PBS and Trizol™ reagent then added directly to the cell culture dish to a total of 1 mL per condition. If cell counting was required, cells were trypsinised and counted via ADAM™

counter before the addition of Trizol™ to the cell pellet after centrifugation. Trizol™ reagent degrades cellular components (including cell membranes), whilst maintaining RNA integrity, allowing the separation of high quality total RNA from DNA and protein. Trizol™ monophasic solution contains a mixture of phenol and guanidine isothiocyanate (among other proprietary components), and improves on the RNA isolation method originally developed by Chomczynski & Sacchi (1987).

After incubation, cells were scraped using a sterile cell scraper to ensure all cells were lysed and detached from the plate surface, and the total volume of Trizol™ was transferred to a centrifuge tube. If trypsinised, it was ensured that the resulting cell pellet was fully re-suspended in Trizol™ solution. In both cases, a 5-minute incubation at room temperature was included at this stage to ensure maximum RNA separation from protein complexes. Subsequently, 0.2 mL chloroform was added per 1 mL Trizol™ solution, samples were shaken vigorously for 15 seconds and incubated at room temperature for 15 minutes. Samples were then subject to centrifugation at 15,000 xg for 15 minutes at 4°C, resulting in sample separation

into three phases (Figure 2.4): (i) a lower organic phenol-chloroform phase containing DNA and protein, (ii) a thick white interphase, and (iii) an upper aqueous phase containing RNA. The aqueous phase was then carefully transferred into a fresh centrifuge tube and an equal volume of isopropanol (IPA) added to precipitate out the total RNA. Samples were then gently inverted 5-10 times to ensure equal mixing and stored overnight at -20°C.

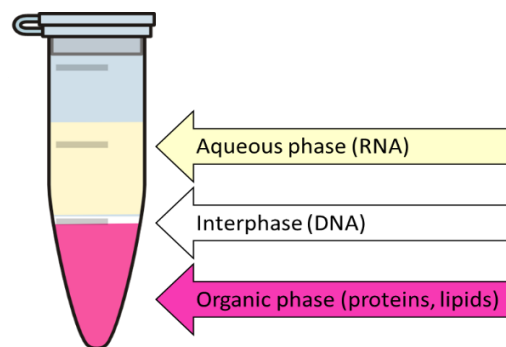


Figure 2.4. The three distinct phases of Trizol™ extractions. DNA, deoxyribonucleic acid; RNA, ribonucleic acid.

After re-equilibrating to room temperature, samples were centrifuged at 15,000 xg for 10 minutes at 4°C and the supernatant removed leaving a small precipitated RNA pellet. The pellet was detached from the wall of the centrifuge tube, washed with 100% ethanol to remove impurities, and then re-centrifuged (5 minutes, 15,000 xg , 4°C) to enable removal of the ethanol supernatant. After allowing the RNA pellet to air-dry, it was re-suspended in a small volume of RNase-free water and incubated at 60°C for 10 minutes to ensure sample homogenisation, then placed on ice prior to quantification/quality assessment with Nanodrop™ (Section 2.2.3.3). RNA samples were stored long-term at -80°C and were sporadically subject to RNA integrity checks via agarose gel electrophoresis (Section 2.2.3.6).

2.2.3.2 DNase Treatment and cDNA Synthesis

Prior to cDNA synthesis, RNA samples were subject to treatment with deoxyribonuclease 1 (DNase 1) enzyme to ensure degradation of any contaminating genomic double- or single-stranded DNA. First, 8 μL of 100 $\text{ng}/\mu\text{L}$ RNA was treated with 1 μL DNase 1 enzyme (10X) and 1 μL DNase buffer (10X), and incubated at room temperature for 15 minutes. Next, 1 μL of DNase stop solution was then added followed by a 10-minute incubation at 60°C to denature the DNase enzyme. Treated RNA samples were stored on ice for cDNA processing (final volume 11 μL). A High-capacity cDNA Reverse Transcription Kit (Applied Biosystems) was used to convert these RNA samples into cDNA using reverse transcriptase (RT) enzyme. For a final reaction volume of 20 μL , 9 μL of reaction mixture was added to each RNA sample containing the following:

Table 2.2. Reaction mixture for cDNA synthesis.

Reagent	Volume (20 μL)
10X RT buffer	2 μL
10X random primers	2 μL
Multiscribe™ RT (50 U/ μL)	1 μL
25X dNTP mix (100 mM)	0.8 μL
RNase-free water	3.2 μL

RT, reverse transcriptase. dNTP, deoxynucleotide triphosphate.

Samples were well mixed before placing on a thermal cycler and run on the specified RT programme of 25°C for 10 minutes, 37°C for 120 minutes and 85°C for 5 minutes. Samples were held at 4°C before Nanodrop™ quantification and final storage at -20°C.

2.2.3.3 RNA and DNA Quantification

The Nanodrop™ ND-1000 spectrophotometer (Thermo Fischer Scientific) was employed for nucleic acid analysis of both quantity and purity. RNA/cDNA (1 μL sample) is placed in between two fibre optic cables, and the light passed through is subject to spectrophotometric analysis at a range of wavelengths. The Nanodrop™ provides a concentration reading in $\text{ng}/\mu\text{L}$ and the ratio of absorbance at 260/280 and 260/230 nm is used to assess sample purity. Inaccurate ratios suggest the presence of impurities such as proteins or solvents used during RNA extraction. An example of the Nanodrop™ output for cDNA is illustrated in Figure 2.5.

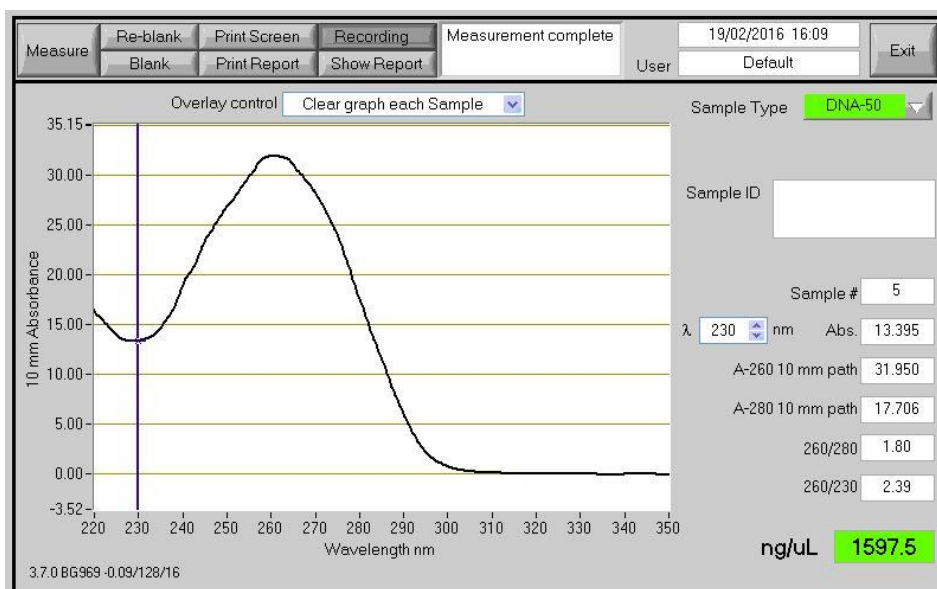


Figure 2.5. Example of a Nanodrop™ spectrophotometric reading for cDNA quantification. The final cDNA concentration is presented as ng/μL, while the purity is determined by 260/280 and 260/230 nm ratio.

2.2.3.4 Primer Design and Optimisation

For polymerase chain reaction (PCR), primer sequences were designed for BMP-2. The online Primer3 tool (<http://primer3.ut.ee/>) was used to identify potential primer sets for the coding region of human BMP-2, specifying optimal primer parameters for product size, primer size, melting temperature and GC content. The Northwestern BioTools OligoCalc website (<http://www.basic.northwestern.edu/biotools/OligoCalc.html>) was then used to confirm primer characteristics, ensure specificity for BMP-2 using BLAST, and check their structural integrity. Primer sets for GAPDH, 18S, IL-6, ALP, Runx2, OPG, RANKL and TRAIL were pre-published by our research group while Sox9 primers were designed and published by Alesutan *et al.* (2015). Primer sets for TRAIL receptors, SOD1, SOD2, HMOX1, gp91 and p47 were sourced from a colleague, Dr. Hannah Forde. All other primers utilised were sourced from the PrimerBank website and confirmed against the human mRNA sequence (<https://pga.mgh.harvard.edu/primerbank/>).

Standard PCR was employed for primer optimisation and to test primer specificity (i.e., to confirm no non-specific secondary product amplification or extensive primer-dimer formation). Annealing temperature and primer concentration were optimised for BMP-2 and re-confirmed for previously optimised primer sets. All primer product sizes were confirmed by agarose gel electrophoresis (Section 2.2.3.6) and assessed for efficiency via real-time PCR (Section 2.2.3.7). Primer sequences, their respective product sizes and optimal annealing temperatures are detailed overleaf in Table 2.5; primer efficiencies are listed in Appendix 2.1.

2.2.3.5 Standard PCR

Using the Nanodrop™ reading, cDNA samples were diluted to a final concentration of 500 ng/μL and the 25 μL PCR reaction mix was made up as follows (Table 2.3):

Table 2.3. Standard PCR reaction components.

Reagent	Volume (25 μL)
10X reaction buffer	2.5 μL
10 mM dNTPs	2 μL
DreamTaq DNA polymerase (5 U/μL)	0.2 μL
25 mM magnesium chloride	1.5 μL
cDNA (500 ng/μL)	2 μL
Forward/reverse primer (10 mM)	2 x 1μL
RNase-free water	14.8 μL

dNTP, deoxynucleotide triphosphate.

For each PCR reaction, two controls were included; a negative control containing water in place of cDNA, and a non-RT control (in which RT enzyme was omitted from cDNA synthesis reaction mix). PCR product in the non-RT control indicates the presence of contaminating genomic DNA in the sample preparation. Each reaction mix was then placed in a thermal cycler and subject to the following standard PCR temperature cycle (Table 2.4) before a cooling hold at 4°C. The annealing temperature was dependent on the primer set used, as detailed in Table 2.5 overleaf.

Table 2.4. Standard PCR reaction parameters.

Denature		95°C	5 minutes	
Cycling	Denature	95°C	15 seconds	Repeat x40-45
	Annealing	See Table 2.5	30 seconds	
	Extension	72°C	15 seconds	
Extension		72°C	5 minutes	

Table 2.5. Forward/reverse (F/R) primer sequences employed in standard PCR and qPCR.

Target Gene	Sequence (5'- 3')	Product Size (bp)	Annealing Temp. (°C)
GAPDH F	GAGTCAACGGATTTGGTCGT		
GAPDH R	TTGATTTTGGAGGGATCTCG	238	60
18S F	CAGCCACCCGAGATTGAGCA		
18S R	TAGTAGCGACGGGCGGTGTG	250	60
OPG F	GGCAACACAGCTCACAAGAA		
OPG R	CTGGGTTTGCATGCCTTTAT	241	58
RANKL F	AGAGCGCAGATGGATCCTAA		
RANKL R	TTCCTTTTGCACAGCTCCTT	180	58
TRAIL F	TTCACAGTGCTCCTGCAGTC		
TRAIL R	ACGGAGTTGCCACTTGACTT	170	60
ALP F	GCCTGGCTACAAGGTGGTG		
ALP R	GGCCAGAGCGAGCAGC	293	58
BMP-2 F	CAAGCCAAACACAAACAGCG		
BMP-2 R	CCAACGTCTGAACAATGGCA	199	57
Runx2 F	GGTACCAGATGGGACTGTGG		
Runx2 R	GAGGCCGGTCAGAGAACAAAC	315	59
Sox9 F	AGCGAACGCACATCAAGAC		
Sox9 R	CTGTAGGCGATCTGTTGGGG	85	60
IL-6 F	AAAGAGGCACTGGCAGAAAA		
IL-6 R	AGCTCTGGCTTGTTCCCTCAC	183	60
p52/p100 F	AGAGGCTTCCGATTTTCGATATGG		
p52/p100 R	GGATAGGTCTTTTCGGCCCTTC	89	60
TRACP5 F	GATCCCACAGACCAATGTGTC		
TRACP5 R	CCAGCACGTAGTCCTCCCT	179	60
SOD1 F	GTGGGGAAGCATTAAAGGACTGAC		
SOD1 R	CAATTACAGCACAAGCCAAACGAC	355	60
SOD2 F	GGGAGATGTTACAGCCCAGA		
SOD2 R	AGTCACGTTTGATGGCTTCC	149	60
eNOS F	TGATGGCGAAGCGAGTGAAG		
eNOS R	ACTCATCCATACACAGGACCC	129	60

SM α -actin F	CTATGAGGGCTATGCCTTGCC		
SM α -actin R	GCTCAGCAGTAGTAACGAAGGA	122	61
SM22 α F	CCGTGGAGATCCCAACTGG		
SM22 α R	CCATCTGAAGGCCAATGACAT	104	61
RANK F	CACCAAATGAACCCCATGTTTAC		
RANK R	GGACTCCTTATCTCCACTTAGGC	182	60
DcR1 F	TCCCCAAGACCCTAAAGTTCG		
DcR1 R	CAGTGGTGGCAGAGTAAGC	75	60
DcR2 F	GTTGGCTTTTCATGTCGGAAGA		
DcR2 R	CCCAGGAACTCGTGAAGGAC	129	60
DR4 F	ACCTTCAAGTTTGTCGTCGTC		
DR4 R	CCAAAGGGCTATGTTCCCATT	115	60
DR5 F	GCCCCACAACAAAAGAGGTC		
DR5 R	AGGTCATTCCAGTGAGTGCTA	128	61
gp91 F	GCTGTTCAATGCTTGTGGCT		
gp91 R	TCTCCTCATCATGGTGCACA	403	62
p47 F	AAGTGGTTTGACGGGCAG		
p47 R	TGGACGGAAAGTAGCCTG	597	62
HMOX 1 F	ATTGCCAGTGCCACCAAGTTCAAG		
HMOX 1 R	ACGCAGTCTTGGCCTCTTCTATCA	103	61
BSP F	GAACCTCGTGGGGACAATTAC		
BSP R	CATCATAGCCATCGTAGCCTTG	79	61
OCN F	GGCGCTACCTGTATCAATGG		
OCN R	GTGGTCAGCCAACTCGTCA	110	60
BSP (murine) F	ATGGAGACGGCGATAGTTCC		
BSP (murine) R	CTAGCTGTTACACCCGAGAGT	148	60
OCN (murine) F	CTGACCTCACAGATCCCAAGC		
OCN (murine) R	TGGTCTGATAGCTCGTCACAAG	187	61

GAPDH, glyceraldehyde 3-phosphate dehydrogenase; OPG, osteoprotegerin; RANK(L), receptor activator of NF- κ B (ligand); TRAIL, tumour necrosis factor-related apoptosis-inducing ligand; ALP, alkaline phosphatase; BMP, bone morphogenetic protein; Runx2, runt-related transcription factor-2; Sox9, sex determining region Y box-9; IL, interleukin; TRACP5, tartrate resistant acid phosphatase 5; SOD, superoxide dismutase; eNOS, endothelial nitric oxide synthase; SM, smooth muscle; DcR, decoy receptor; DR, death receptor; HMOX1, heme oxygenase 1; BSP, bone sialoprotein; OCN, osteocalcin. Respective primer efficiencies are presented in Appendix 2.1.

2.2.3.6 Agarose Gel Electrophoresis

Agarose gel electrophoresis was used to assess PCR products from standard PCR reactions. A 1% agarose gel was made by adding 1 g agarose to 100 mL TAE buffer (40 mM Tris-Acetate pH 8.2, 1 mM EDTA) and heating to dissolve. After cooling, 10 μ L SYBR Safe® gel stain was added to the liquid agarose, mixed well and transferred into a casting gel rig with the appropriate well comb. The gel was left to polymerise at room temperature in the dark (as SYBR Safe® is light sensitive) for approximately 30 minutes. The rig was then filled with TAE buffer and the comb removed to allow sample loading.

For PCR product visualisation, 10 μ L of PCR product was loaded into each well; wells containing 5 μ L GeneRuler™ 100 bp DNA Ladder was included for PCR product size determination. The gel was electrophoresed at 100 V, and when the PCR products had been sufficiently resolved, the bands were visualised using the Syngene G-Box imaging system.

For RNA integrity checks, 1 μ g RNA (diluted in 8 μ L RNase-free water) was loaded into each well for electrophoresis. Intact RNA can be visualised as two distinct bands: the 18S ribosomal RNA (rRNA) at 1.9 kb and the 28S rRNA at 4.5 kb (1:2 ratio). Degraded RNA will appear as a smear at the bottom of the gel.

2.2.3.7 Quantitative Reverse Transcription PCR (RT-qPCR)

After optimisation, the primer sets were employed in quantitative real-time PCR (qPCR) to assess reverse transcribed mRNA levels using the LightCycler®96 System (Roche Diagnostics). In qPCR, the level of gene amplification is tracked in real-time via the binding of SYBR Green 1 nucleic acid stain to double-stranded DNA. SYBR Green dye emits a green fluorescent signal when bound to DNA, and thus as PCR cycles progress and the product is amplified, this fluorescence accumulates. This signal is then graphed as a means of quantifying the level of gene amplification. To conduct relative gene quantification between samples, LightCycler® systems employ the second derivative maximum method, in which the quantification cycle (C_q) number acts as a measure of gene copy abundance. The C_q is defined as the point at which the curvature of the amplification plot is maximal. In this case, in contrast to the threshold cycle (C_t) method, no arbitrary threshold value needs to be assigned. The methodological principle is the same, as illustrated overleaf in Figure 2.6: the higher the expression of a gene in a sample, the faster the amplification of that gene will reach the C_q . The principles of the comparative C_t method ($\Delta\Delta C_t$) as described by Livak and Schmittgen (2001),

are first used to calculate the sample- and gene-specific ratio against the reference gene, and secondly to calculate the normalised ratio (or fold change) compared to the control sample. The same negative controls as used in standard PCR were also included in each qPCR run. Amplification curves with $C_q > 40$ were considered too low to accurately determine expression levels.

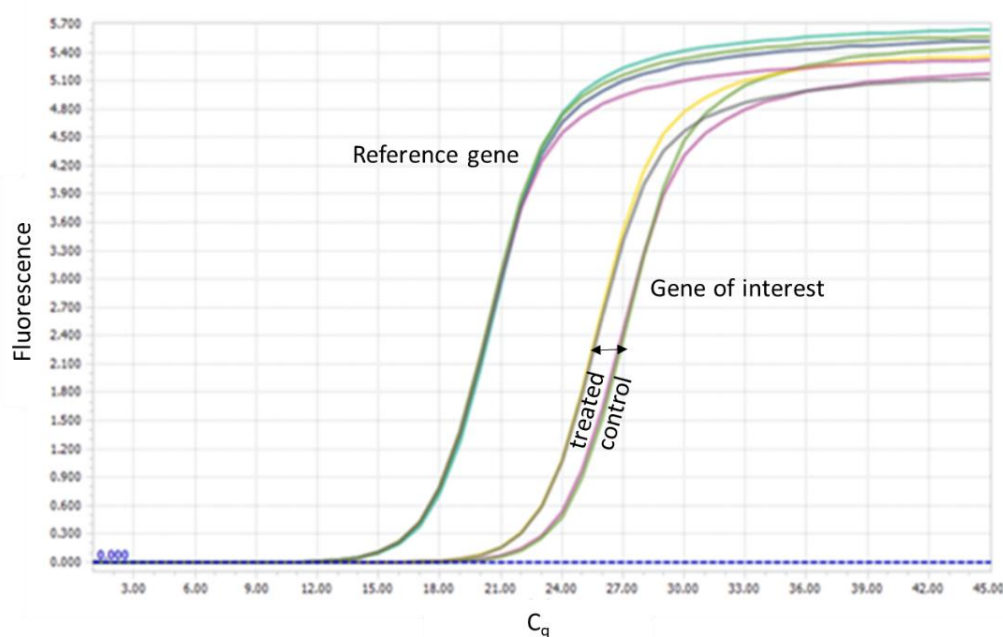


Figure 2.6. Examples of amplification curves on the LightCycler®96 software demonstrating the principle of qPCR. The gene of interest has a lower quantification cycle (C_q), and therefore higher expression levels, in the treated sample.

For each qPCR reaction, samples were assayed in duplicate or triplicate for both the gene of interest and the endogenous reference gene (GAPDH or 18S). Reaction constituents were as follows, according to the manufacturer’s specifications (Table 2.6). This mix was then subject to thermocycling under the conditions listed in Table 2.7.

Table 2.6. Employed volumes of qPCR reaction components.

Reagent	Volume (10 μ L)
Fast Start Essential DNA Green Master	5 μ L
cDNA (500 ng/ μ L)	2.5 μ L
F/R primer (10 μ M)	2 x 1 μ L
RNase-free water	1.5 μ L

Volumes listed are for one well of a 96-well PCR reaction plate.

Table 2.7. qPCR reaction parameters.

Pre-incubation		95°C	10 minutes	
Amplification	Denature	95°C	10 seconds	Repeat x45-55
	Annealing	See Table 2.5	10 seconds	
	Extension	72°C	10 seconds	

To ensure primer specificity, PCR amplicons were routinely checked via agarose gel electrophoresis to ensure correct product formation. In addition, melt curve analysis was carried out for every qPCR run. A single melting curve peak indicates single and specific product formation with no non-specific PCR products or primer-dimers present (Figure 2.7). Once product specificity was confirmed, results were analysed in accordance with The Minimum Information for publication of Quantitative real-time PCR Experiments (MIQE) guidelines.

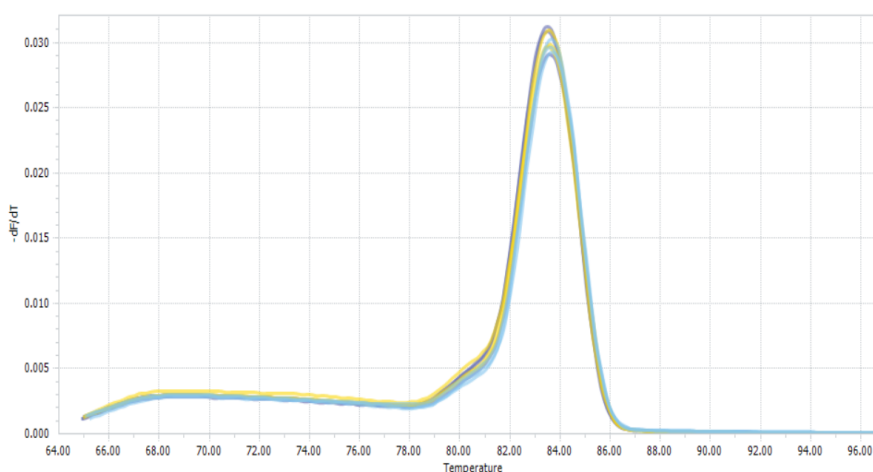


Figure 2.7. Representative melting curve (OPG primers).

2.2.3.8 Primer Efficiencies

Standard curve analysis was employed using the LightCycler® system to calculate primer efficiencies. After PCR amplification, the PCR product was subject to 1/1000-fold dilution in RNase-free water. A further 7-point 1/10 serial dilution followed. Each dilution was subject to qPCR according to the reaction mix and parameters detailed in Tables 2.6 and 2.7 respectively, in addition to a negative control (RNase-free water in place of cDNA). The resulting values

were used to plot a standard curve of C_q versus the relative number of gene copies. The primer efficiency, in percentage, was then calculated from the following formula:

$$\text{Primer efficiency} = 10^{\frac{1}{\text{slope}} - 1}$$

As specified in the MIQE guidelines, all primer sets were confirmed to have an acceptable efficiency of between 90% and 105% and were deemed suitable for gene expression analysis. The percentage efficiency of all primer sets are presented in Appendix 2.1.

2.2.4. Protein Analysis

2.2.4.1 Protein Extraction

Following exposure to soluble factors, cells were harvested for total intracellular protein. For routine analyses, if counting was not required, cells were washed 3 times with PBS and a small volume of 1X radioimmunoprecipitation assay (RIPA) buffer was added on ice. A cell scraper was used to aid in cellular lysis and to detach cells from the surface of the dish. The full volume was transferred to a centrifuge tube and the samples subject to rotation at 4°C for 1 hour. Samples were then centrifuged for 20 minutes at 10,000 xg at 4°C to remove any insoluble cellular debris. The protein supernatant was then removed to a fresh tube and stored at -80°C. If cell counting was required, cells were first trypsinised for the purpose of ADAM™ counter analysis, and then centrifuged to gather the cell pellet. RIPA buffer was added directly to the cell pellet, and re-suspended before rotation, centrifugation and storage.

For the purpose of ALP enzyme activity assay analysis, cells were harvested in the same manner but with 0.2% Triton X-100 in place of RIPA lysis buffer. The components of RIPA (chelating/denaturing agents, detergents) will inhibit enzyme activity and therefore should be avoided in sample preparation.

2.2.4.2 BCA Assay

The bicinchoninic acid (BCA) biochemical assay originally employed by Smith *et al.* (1985) is required prior to protein analysis for the purpose of data normalisation. This assay determines total protein concentration in whole cell lysates. For analysis, lysate samples are diluted 1:5 in RIPA lysis buffer to ensure they fall within the 0-2 mg/mL bovine serum albumin (BSA) standard curve. The samples and standards are then added in triplicate to a 96-well plate, and

200 μL BCA working reagent (1:50 dilution of reagent B (copper sulphate solution) in reagent A (alkaline bicarbonate solution), as part of a commercially available kit (ThermoScientific)) is added to each well. The plate is then incubated for 30 minutes in the dark at 37°C to allow two reactions to occur: the reaction of Cu^{2+} with protein in an alkaline environment to form Cu^+ , and a second reaction between Cu^+ and bicinchoninic acid. The latter results in a colour change from green to purple, the extent of which is dependent on the amount of copper ions (and therefore protein) present. The plate is then read at 570 nm, the wavelength at which this purple complex absorbs light, on a colorimetric plate reader and the unknown protein concentrations determined via standard curve.

2.2.4.3 SDS-PAGE

SDS-polyacrylamide gel electrophoresis (SDS-PAGE) was carried out using a 12% (v/v) resolving gel and a 5% (v/v) stacking gel, made up of the components listed in Table 2.8 below:

Table 2.8. Components of resolving and stacking gels for SDS-PAGE.

Component	12% Resolving Gel	5% Stacking Gel
Distilled water	3345 μL	5990 μL
1.5 M Tris-HCl, pH 8.8	2500 μL	-
1.5 M Tris-HCl, pH 6.8	-	2500 μL
30% Acrylamide/bis-acrylamide	4000 μL	1300 μL
10% SDS	100 μL	100 μL
10% Ammonium persulfate	50 μL	100 μL
TEMED	5 μL	10 μL
Total Volume	10 mL	10 mL

SDS, sodium dodecyl sulfate; TEMED, tetramethylethylenediamine.

Immediately after mixing, 5-6 ml of the resolving gel mixture was added between two 10x100 mm glass plates with a 1 mm spacer held in a Mini-PROTEAN® gel casting module (Bio-Rad). Once the gel was set, after approximately 45 minutes, the dH_2O was removed, the stacking gel was mixed and 1-2 mL poured on top of the resolving gel. The comb was immediately inserted, providing the sample wells, and the stacking gel allowed to polymerise for 15-30 minutes. SDS-PAGE was carried out using the Mini-PROTEAN® Tetra-Cell system (Bio-Rad) using the method of Laemmli (1970), all components of which were assembled as

described by the manufacturer. Once polymerised, the gels were placed in running buffer in a 1 L electrophoresis tank. Samples were diluted with distilled water as determined by the BCA assay and made up to a final volume of 25 μL , containing 25% (6.25 μL) sample solubilisation buffer (SSB). Samples were then boiled for 5 minutes at 95°C on a block heater and stored on ice until ready to load.

Before loading, the comb was gently removed to allow running buffer to fill the wells. The full sample volume was loaded into each well, ruled on either side by 2 μL PageRuler™ protein ladder (10-250 kDa). Samples were subject to electrophoretic separation for approximately 2 hours at 80 V.

2.2.4.4 Electrophoretic Transfer and Western Immunoblotting

A Mini-PROTEAN® Trans Blot module (Bio-Rad) was used for protein transfer to an Immobilon®-PSQ polyvinylidene fluoride (PVDF) 0.2 μm membrane (Millipore) according to the wet transfer method of Towbin *et al.* (1979). After separation, the resolving gel was removed from the glass plates, separated from the stacking gel, and placed in an assembled wet transfer cassette soaked in transfer buffer. The PVDF membrane, previously soaked in methanol and cut to the correct size, was placed on top, ensuring no air bubbles were present to affect successful protein transfer. The cassette, as illustrated in Figure 2.8, was then placed in the module in transfer buffer and the protein was transferred at 50 V overnight at 4°C.

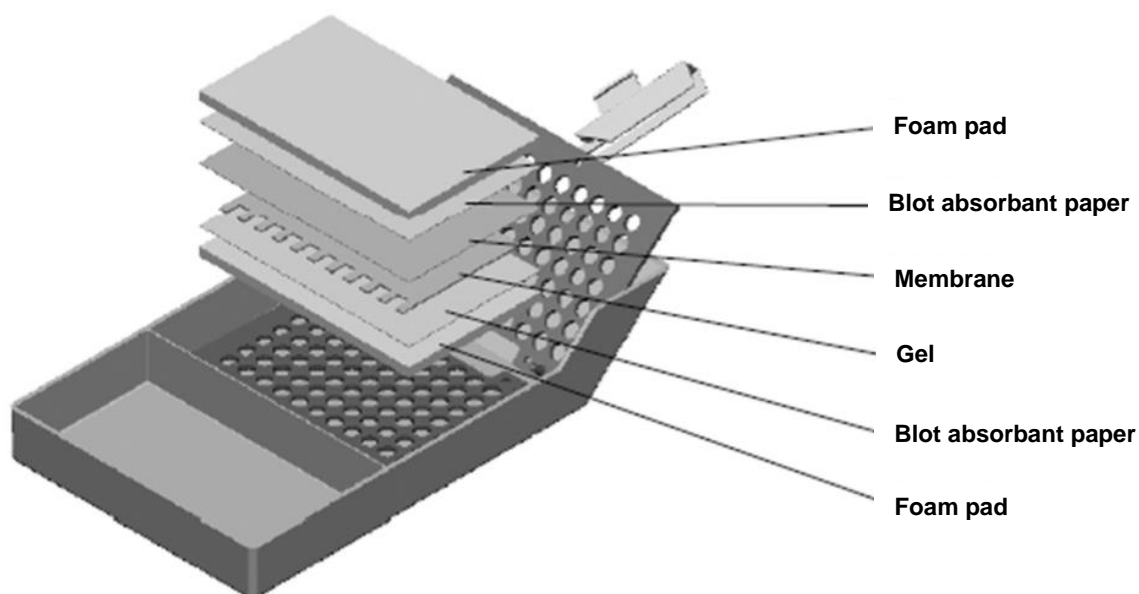


Figure 2.8. Layout of the fully assembled transfer cassette. Image courtesy of www.bio-rad.com.

On completion of wet transfer, the PVDF membrane was stained with Ponceau S solution (Sigma-Aldrich) to ensure successful and even transfer of the protein bands. Ponceau S negative stain interacts with the positively charged amino groups of proteins, staining them red, and can be unstained with repeated distilled water rinses for further analysis after visualisation of the protein bands. The resolving gel was also removed from the transfer cassette at this point and stained with Coomassie R-250 staining solution for 1 hour on a see-saw rocker, and a further 1 hour in Coomassie de-staining solution to confirm successful protein transfer.

After staining, the membrane was blocked for 1 hour in a 5% BSA tris-buffered saline solution plus 0.1% Tween®-20 detergent (TBS-T) with gentle rocking. The membrane was then cut into separate sections depending on the size of the protein of interest, and incubated overnight at 4°C on a see-saw rocker in the relevant primary antibody (diluted in 1% BSA in TBS-T) (Table 2.9).

Table 2.9. Details of the antibodies employed in Western immunoblotting.

Antibody Target	Protein Size	1° Species	1° Dilution	2° Dilution
GAPDH	37 kDa	Mouse	1:10,000	1:5000
Phospho-NF-κB p65	65 kDa	Rabbit	1:1000	1:1000
NF-κB p65	65 kDa	Rabbit	1:1000	1:1000
NF-κB p52/p100	52/100 kDa	Rabbit	1:1000	1:1000
SOD1	16 kDa	Mouse	1:1000	1:1000
SOD2	28 kDa	Rabbit	1:1000	1:1000
TRACP5	35-42 kDa	Sheep	1:2000	1:1000
RANKL	43-55 kDa	Mouse	1:1000	1:1000
TRAIL	32 kDa	Mouse	1:1000	1:1000

Prior to probing, primary and secondary antibody concentrations were optimised for use across a number of parameters: dilution factor, secondary antibody incubation time, and chemiluminescent exposure duration. GAPDH, glyceraldehyde 3-phosphate dehydrogenase; NF-κB, nuclear factor-κB; SOD, superoxide dismutase; TRACP5, tartrate-resistant acid phosphatase-5; RANKL, receptor-activator of NF-κB ligand; TRAIL, tumour necrosis factor-related apoptosis-inducing ligand.

Once the primary antibody was removed, the membrane was washed three times with TBS-T for 5 minutes each, and the relevant secondary antibodies (Cell Signalling) added and incubated on a see-saw rocker at room temperature for 2-3 hours. After this incubation, the wash steps were repeated. Antibodies were stored at -20°C and re-used up to 5 times. Luminata™ Forte Western Horseradish Peroxidase (HRP) chemiluminescent substrate (Millipore) was used for visualisation of the bound HRP-conjugated secondary antibodies. A minimal amount of this substrate was added to the membrane and imaged using GeneSnap software on a Syngene G-Box. Images were saved for densitometric analysis using freely available Image J software.

For proteins with a molecular weight in the range of 30-45 kDa, Western blot stripping reagent (Thermo Fisher) was employed to enable a second analysis for visualisation of overlapping GAPDH endogenous control bands. The stripping process was optimised to ensure complete removal of both primary and secondary antibodies. After imaging, membranes were incubated for 15 minutes in stripping buffer to remove bound antibodies, washed three times with TBS-T, and then re-blocked for 1 hour with 5% BSA in TBS-T. Primary and secondary antibodies for GAPDH were employed as normal and the blot subject to a second chemiluminescent analysis.

2.2.4.5 Enzyme-linked Immunosorbent Assay (ELISA)

An enzyme-linked immunosorbent assay (ELISA) was used for the quantification of OPG, BMP-2, RANKL and TRAIL in media and lysate samples, and IL-6 in media samples, using DuoSet® ELISA kits (R&D Systems). These kits are designed for the development of sandwich ELISAs to measure antigens from cell culture preparations, and their specificity and calibration confirmed by the manufacturer. Materials provided in the DuoSet® ELISA kit include capture antibody, detection antibody, recombinant human standard and Streptavidin-HRP (streptavidin conjugated to horseradish peroxidase). Additional solutions required included PBS, wash buffer (0.05% Tween®-20 in PBS, pH 7.2-7.4), normal goat serum (NGS), reagent diluent (1% BSA in PBS), tetramethylbenzidine (TMB) substrate solution, and stop solution (1 M sulfuric acid). Nunc® Microtitre 96-well plates were used for each assay.

All DuoSet® ELISA kits measure total levels of the protein target, including both free and bound forms. As OPG can act as a decoy receptor for RANKL and TRAIL, additional experiments were performed to confirm that endogenous OPG production or recombinant RANKL/TRAIL treatment did not interfere with ELISA measurements.

2.2.4.5.1 Standard ELISA protocol

For ELISA preparation, microtitre plates were first coated with capture antibody, sealed and incubated overnight at room temperature. The plate was then washed three times with wash buffer and blocked with reagent diluent for 1 hour to prevent non-specific binding. The plate was subject to a second wash step before the addition of samples and standards in duplicate or triplicate, and incubated overnight at 4°C. Samples were diluted in reagent diluent where appropriate to ensure readings fell within the range of the standard curve (Table 2.10).

Table 2.10. Detection limits for DuoSet® ELISA kits.

Protein Target	Detection Range
OPG	62.5 - 2000 pg/mL
RANKL	78.1 - 5000 pg/mL
TRAIL	23.4 - 1500 pg/mL
BMP-2	46.9 - 3000 pg/mL
IL-6	9.38 - 600 pg/mL
TNF α	15.6 - 1000 pg/mL

After this incubation, the plate was re-washed and loaded with the appropriate dilution of detection antibody for a 2-hour incubation at room temperature. Both OPG and TRAIL ELISA kits require an additional 2% NGS to aid stability of the detection antibody. After a subsequent wash, streptavidin-HRP was added to each well and incubated for 20 minutes, followed by the final wash step and TMB addition. The plate was incubated for approximately 20 minutes in the dark (TMB is light sensitive) before the addition of stop solution. These steps and the associated colour changes are illustrated in Figure 2.9. The plate was read immediately at dual wavelengths 450 nm and 570 nm; this wavelength correction allows for optical interference of the Nunc® plate. Concentrations were subsequently determined using standard curve analysis; a typical standard curve for each ELISA DuoSet® kit employed is presented in Appendix 2.2A.

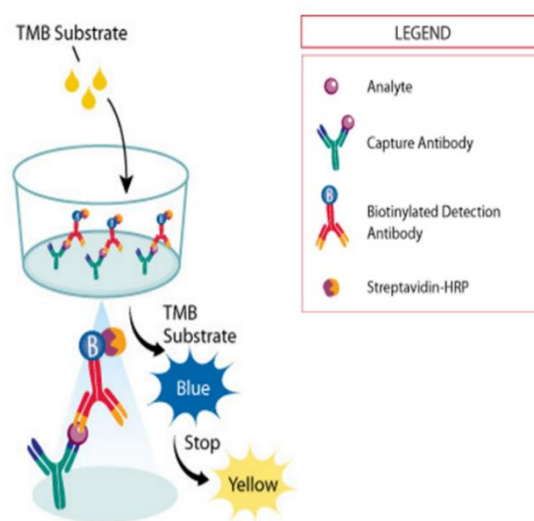


Figure 2.9. The final steps of the ELISA protocol. TMB, tetramethylbenzidine. Image courtesy of www.rndsystems.com.

2.2.5 Functional and Physiological Analysis

2.2.5.1 ALP Enzyme Activity Assay

A colorimetric Quantichrom™ ALP activity kit (Bioassay Systems) was employed to directly quantify ALP activity in media supernatant and lysate samples, as in previous publications (Davenport *et al.*, 2015, 2016). This assay is based on the following kinetic reaction: ALP hydrolyses *p*-Nitrophenyl phosphate (pNPP) into *p*-nitrophenol and phosphate, forming a yellow product with a maximum absorbance at 405 nm. The working solution for the assay consists of assay buffer pH 10.5, 0.2 M magnesium acetate and 1 M pNPP, which when added to the sample is subject to a 4-minute incubation at 37°C. The plate is read at 0 and 4 minutes, with distilled H₂O (negative control) and tartrazine (yellow liquid with a fixed absorbance) loaded for run calibration. All samples were assayed in duplicate. ALP activity (IU/L) is calculated from the colour change over the fixed time period using the following equation:

$$\text{ALP Activity} = \frac{(\text{OD}_{\text{SAMPLE } t} - \text{OD}_{\text{SAMPLE } 0}) \cdot \text{Reaction Vol}}{(\text{OD}_{\text{CALIBRATOR}} - \text{OD}_{\text{H}_2\text{O}}) \cdot \text{Sample Vol} \cdot t}$$

x 35.3 (media supernatant)
x 353 (lysate)

OD_{SAMPLE 0} and OD_{SAMPLE t} are average absorbance values at 0 minutes and 4 minutes respectively; OD_{H₂O} and OD_{CALIBRATOR} are the average absorbance values of dH₂O and tartrazine; reaction volume is 200 μL; sample volume is 50 μL volume for media supernatants and 5 μL volume for lysates; *t* is the incubation time (4 minutes). The multiplication factor is determined by a number of factors including light path length, incubation time, molar absorbance and sample volume, and is calculated by the kit manufacturer. Results are expressed as fold change to experimental control to account for microplate reader variations.

2.2.5.2 Permeability Assay

The trans-endothelial permeability/barrier assay was employed for physiological analysis of HAEC monolayers in transwell inserts, i.e., to assess the effect of soluble factors on endothelial monolayer integrity in co-culture. This method has been successfully implemented in previous publications (Rochfort *et al.*, 2014; Walsh *et al.*, 2011). HAECs were seeded into transwell inserts in usual co-culture format, and allowed to incubate for 24 hours to ensure tight monolayer formation. Following a 72-hour incubation period with the relevant soluble factors, spent media was removed and 4 mL fresh media added to the basolateral compartment.

Fluorophore media, containing 250 $\mu\text{g/mL}$ FITC-labelled Dextran (40 kDa), was prepared and 2 mL added to the apical compartment. Immediately, a small sample volume was collected from the basolateral compartment and diluted as necessary in fresh media. Samples were taken from the basal compartment every 30 minutes for 3 hours, diluted and loaded in triplicate on a white 96-well microplate (Figure 2.10). A positive control (diluted fluorophore media) and negative control (fresh media) were included on each plate. Samples were read on a fluorospectrophotometer (Bio-Tek), with an excitation wavelength of 490 nm and an emission of 520 nm. Results are expressed as percentage trans-endothelial exchange (TEE) of FITC-dextran, with the positive and negative controls representing 100% and 0% TEE respectively.

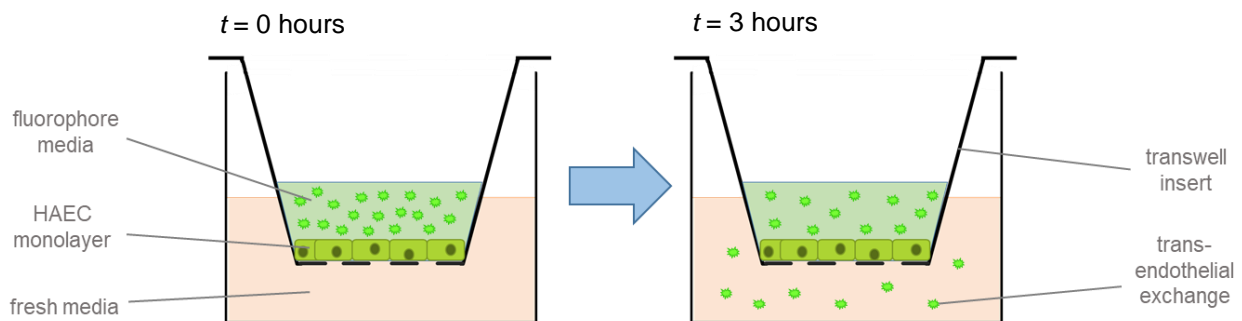


Figure 2.10. Principle of the trans-endothelial permeability assay. HAEC, human aortic endothelial cell; t , time.

2.2.6 Cell Staining

2.2.6.1 Alizarin Red S: Calcium Staining

Alizarin Red (AR) S, an anthraquinone derivative, is routinely employed as a marker of matrix mineralisation *in vitro*, as it is a potent stain for calcific deposits (and other minerals) in bone and other tissues (Puchtler *et al.*, 1969). Calcium forms an AR S-calcium complex through chelation, resulting in a bright red stain. AR staining was employed to identify and quantify crystalline and non-crystalline calcific deposits in differentiated HASMC and MC3T3-E1 cells.

2.2.6.1.1 Alizarin Red Staining for Microscopy

Post-treatment, spent media was removed and cells were washed three times with calcium- and magnesium-free PBS. Cells were then fixed with 3.7% paraformaldehyde for 15 minutes at room temperature, before being washed a further three times with distilled water. AR staining

solution (40 mM), at the optimal pH of 4.1 - 4.3, was added to the cells and incubated for 30 minutes in the dark with gentle agitation. After removal of the staining solution, cells were washed three times with distilled water and imaged at 0X, 4X, 10X and 40X magnification on a Nikon Eclipse phase-contrast microscope.

2.2.6.1.2 Alizarin Red Staining for Quantification by Absorbance

Following microscopic imaging, AR stain was quantified by absorbance. Acetic acid (10% (v/v)) was added to each well and incubated for 30 minutes in the dark with gentle agitation (stain extraction). Cells were scraped, transferred to microtubes, and vortexed for 30 seconds, before heating at 85°C for 10 minutes on a block heater. AR stain extractions were then cooled on ice, subject to centrifugation at 20,000 xg for 15 minutes, and the supernatant transferred to a fresh tube. Ammonium hydroxide solution (25% (v/v)) was then added to the sample for neutralisation, and 150 μ L sample added in triplicate to an opaque wall plate for analysis. An AR standard curve (0 - 4 mM) was included alongside the samples in triplicate for quantification (Appendix 2.2B), and the plate read at 405 nm.

2.2.6.2 Immunofluorescence Microscopy: Oxidative Stress

In order to measure active reactive oxygen species (ROS) levels, HAECs were stained with dihydroethidium (DHE) and analysed via immunofluorescent microscopy. DHE, a superoxide indicator, can enter the cytoplasm of living cells where it stains blue until it is oxidised by ROS. When oxidised, this reaction yields ethidium, which can intercalate with available DNA. In order to assess ROS levels via immunofluorescence (IF), HAECs were exposed to experimental treatments as required, and DHE added at 3 μ M concentration 30 minutes prior to the end of the incubation period. Media was then removed, cells washed three times with PBS and fixed for 15 minutes with 3.7% paraformaldehyde. Cells were washed a further three times and 4',6-diamidino-2-phenylindole dihydrochloride (DAPI) nuclear counterstain added for 3 minutes at 1/3000 dilution. The cells were re-washed before being coated in a thin layer of distilled water. Stained HAECs were imaged on a Nikon Eclipse Ti fluorescent microscope at 4X, 10X and 40X magnification, with exposure time kept constant for each condition. An unstained control was included for all microscopy work.

2.2.7 Flow Cytometry

Flow cytometry, a laser-based technology enabling single-cell analysis, was employed to investigate apoptosis and oxidative stress in response to soluble factors *in vitro*. In flow cytometry, the characteristics of each cell in suspension are investigated as they flow through a hydrodynamically-focused stream of liquid (sheath fluid); each particle or cell (“event”) is interrogated by a single-wavelength light beam. Detectors surrounding the laser beam measure a number of characteristics of each event at the point where the liquid stream and light beam meet. Forward light scatter (FSC), a measure of light refraction directly proportional to cell size, is measured by a detector in line with the light beam. Side light scatter (SSC), a measure of cell granularity, is measured by a number of detectors perpendicular to the light beam (as intracellular components can disperse light in all directions). Thus, FSC and SSC measurements help to identify cell populations based on size and internal complexity.

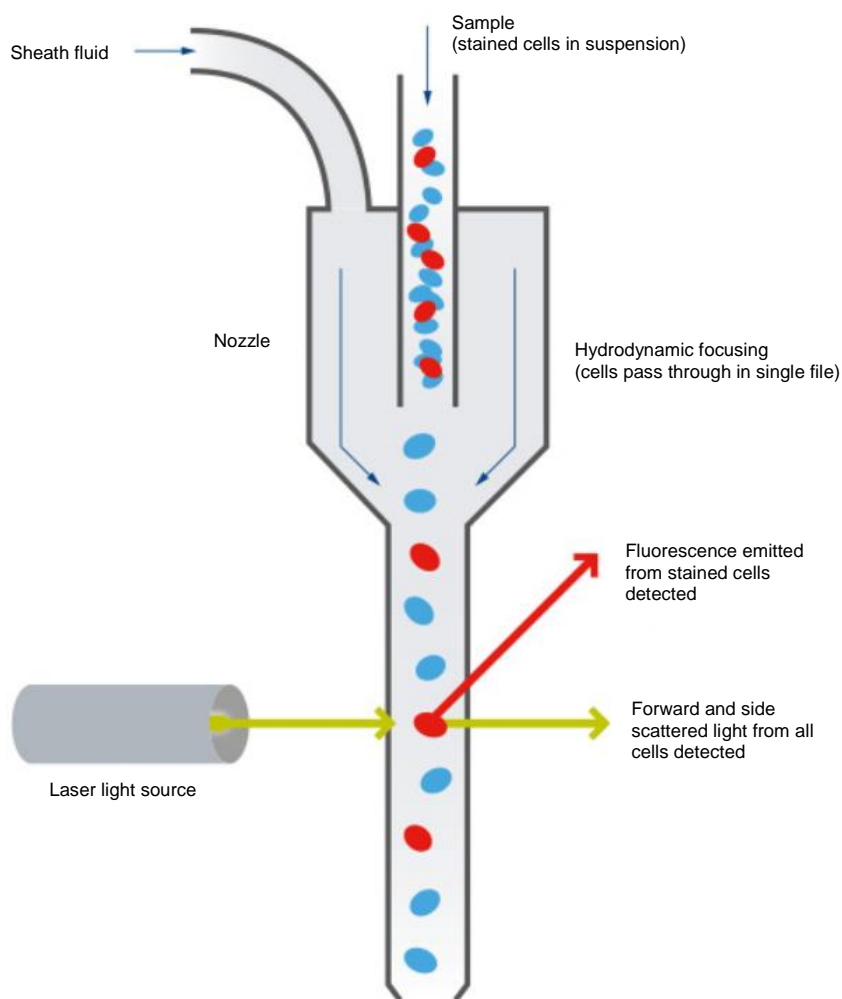


Figure 2.11. The flow cell of a flow cytometer. The cell suspension, which may be fluorescently labelled, enters the flow cell and is hydrodynamically focused in a stream of sheath fluid. Cells pass the laser light source where they are interrogated for fluorescence and light scattering, and the light and fluorescence emission collected by a number of detectors. Image courtesy of www.abcam.com.

In addition, cells can be specifically interrogated for the presence of fluorophores when fluorescent dyes (e.g. intercalating dyes for nucleic acids, fluorescence-linked antibodies) are employed in sample preparation. These fluorophores can be excited by the laser as the event passes through the beam, and fluorescent detectors measure scattered emissions at a longer wavelength. Optimised laser parameters (e.g. voltage and gain), specific FSC/SSC settings, and a strategic gating technique help to develop a biochemical profile of the cell suspension, as the signals are amplified and visualised digitally on the FACS Aria™ flow cytometer. The flow cell of a flow cytometer is depicted in Figure 2.11.

2.2.7.1 Apoptosis Assay

The Dead Cell Apoptosis Kit with Annexin V and PI (Thermo Fisher) was employed as in previous publications (Rochfort *et al.*, 2014) for apoptosis and viability measurements in HAECs and HASMCs following exposure to soluble factors. This kit not only distinguishes between live and dead cells, but measures the degree of apoptosis at the point of interrogation. This kit employs two fluorescent labels; first, PI, a red fluorescent dye that intercalates with available nucleic acid is used to distinguish between live and dead cells. Using the same logic as for cell counting (Section 2.2.1.5), PI cannot penetrate undamaged cell membranes and therefore is a suitable measure of the non-viable cell population. The second fluorescent dye, green Alexa Fluor®-488, is conjugated to recombinant Annexin V anticoagulant. In healthy live cells, a protein called phosphatidylserine (PS) is expressed on the inner surface cell membrane, while in apoptotic cells, PS is translocated to the extracellular surface. Annexin V phospholipid-binding protein has a high affinity for PS, and thus fluorescence-conjugated Annexin V acts as a suitable identifier of apoptotic cells. Using this dye combination in flow cytometry, viable non-apoptotic cells can be identified as having negligible fluorescence, viable apoptotic cells will have green fluorescence, and non-viable post-apoptotic cells have both red and green fluorescence (Figure 2.12). These distinct cell populations can be visualised using the 488 nm laser on the FACS Aria™, exciting both PI and Alexa Fluor®-488 dyes which have differing emission spectra.

For the apoptosis assay, cells were first exposed to experimental treatments as required; two untreated negative controls (stained, unstained) and one apoptotic positive control (20% DMSO, 30 minutes) were also included. Cells were trypsinised and washed in PBS while the Annexin V binding buffer (BB) (1/5 dilution of stock in dH₂O) and 100 µg/mL PI (1/20 dilution of PI stock in BB) were prepared. The cell suspension was re-centrifuged and re-suspended in

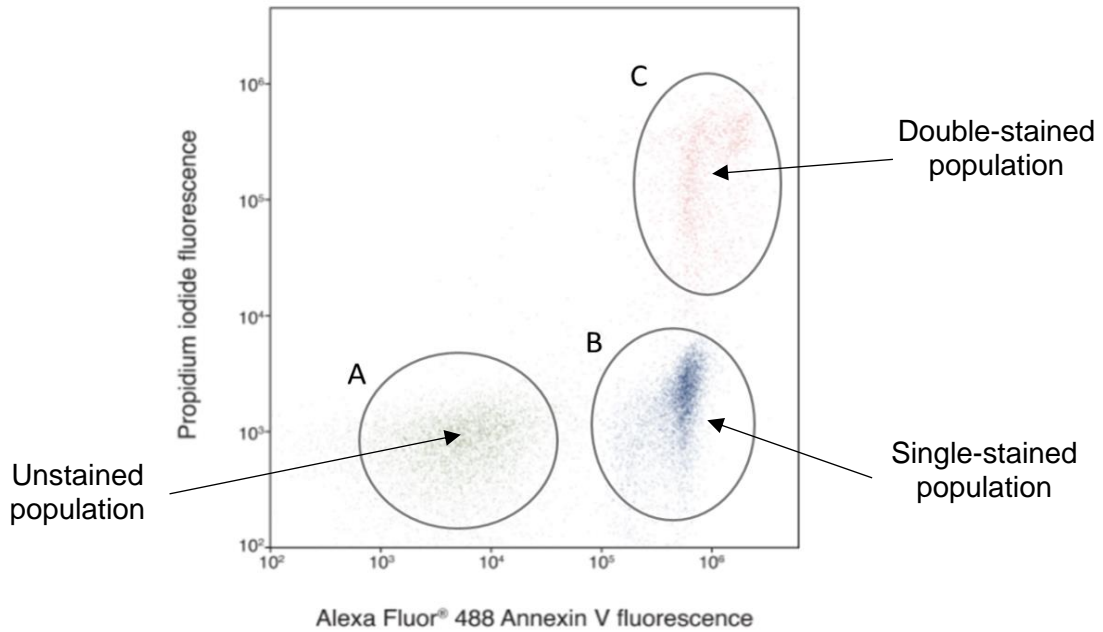


Figure 2.12. Example output of the apoptosis assay. (A) unstained live cells. (B) Alexa Fluor®-488 stained apoptotic cells. (C) Alexa Fluor®-488 and PI stained post-apoptotic non-viable cells. Image adapted from www.thermofisher.com.

100 μ L BB. Alexa Fluor®-488 Annexin V (5 μ L) and PI (1 μ L) were added to the suspension and incubated for 15 minutes at room temperature in the dark, with the exception of one untreated control. BB (400 μ L) was then added and the suspension transferred to sterile Falcon® tubes. Tubes were kept on ice in the dark until ready to read.

The negative unstained control was first processed to determine the optimal FSC/SSC settings for each cell type. The positive control was run to ensure all three cell populations (healthy, apoptotic and non-viable) were clearly within range. All samples were read on the FITC (~530 nm) and PE-Texas Red (~610 nm) detection channels to 10,000 events. As PI and Alexa Fluor®-488 have relatively close emission maxima, a compensation protocol was employed to remove bleed-through fluorescence between channels. To do this, single-stained cell suspensions for both PI and Alexa Fluor®-488 were analysed alongside a double-stained sample. The auto-compensation settings on the Becton-Dickinson FACSDIVA™ software automatically calculates and eliminates the percentage of overlapping fluorescence, improving result specificity. Quadrant and gating strategies (e.g. doublet discrimination) were employed as required for data analysis via FACSDIVA™ and freely available Cyflogic software.

2.2.7.2 Oxidative Stress

As for IF microscopy (Section 2.2.6.2), ROS levels were investigated using DHE staining by flow cytometry. Unlike qualitative microscopic analyses, ROS levels can be quantified using this technique by measuring the relative intensity of ethidium fluorescence, after DHE is oxidised, in control versus treated samples. In this case, HAECs were again exposed to 3 μ M DHE prior to the completion of the incubation period (an unstained control was also included). HAECs were then trypsinised and centrifuged to gather the cell pellet, washed in FACS buffer, re-centrifuged and re-suspended in 500 μ L FACS buffer. After transferring to Falcon® tubes, samples were excited using the 488 nm laser and emission spectra read on the PE-Texas Red channel for 10,000 events. No compensation settings were required for DHE single stain analysis. Gating strategies were employed as required and data analysed via FACSDIVA™ and Cyflogic.

2.2.8 Bioinformatics Search

In order to identify novel targets that may be involved in RANKL/TRAIL-mediated VC signalling, the Search Tool for the Retrieval of Interacting Genes/Proteins (STRING) database (version 10.0; accessed November 2016; <https://string-db.org/>) was primarily employed. The STRING database, developed by a consortium of academic institutions including the Swiss institute of Bioinformatics, the Novo Nordisk Foundation Centre for Protein Research, and the European Molecular Biology Laboratory, obtains protein association knowledge principally from experimental literature curation. Computational predictions of protein-protein interactions are also included in the STRING database, obtained via text mining methods and orthology. STRING provides a colour-coded network of known and predicted interactions for any given protein; the data is weighted and integrated and a confidence score calculated for each interaction based on available evidence. This confidence score represents how likely an interaction is to be true, with values ranging from 0 to 1 (with 1 being the highest possible confidence). Proteins interacting with RANKL, TRAIL and their soluble decoy receptor OPG were first investigated using the STRING database, while further analyses were conducted for additional pro-calcific proteins of interest. Searches were conducted within both *homo sapiens* and *mus musculus* species databases, and the 20 highest scored interactions for each database reviewed. The minimum required interaction score for each search was 0.900 (high confidence), with results identified experimentally or via text mining.

Secondly, the Biological General Repository for Interaction Datasets (BioGRID) database (version 3.4.142; accessed November 2016; <https://thebiogrid.org/>) was employed as a secondary search tool to confirm and expand on the protein-protein interactions identified via the STRING database. BioGRID is a public database of protein, chemical and genetic interactions curated from over 1.5 million entries within the biomedical literature. Searches conducted within BioGRID were filtered for physical rather than genetic interactions, and for interactions identified via high-throughput methods, a high confidence score (>0.900) was required.

Following protein identification, the Universal Protein Resource Knowledgebase (UniProtKB), a consortium consisting of the European Bioinformatics Institute, the Swiss Institute of Bioinformatics and the Protein Information Resource, was employed to compare the functions of proteins identified as potential interactants with RANKL and TRAIL. UniProtKB (accessed November 2016; <https://www.uniprot.org/>) contains functional protein information derived from the literature and genome sequencing projects, and biological functions identified via this database were used to direct further literature investigations.

2.2.9 Data Normalisation

For conditioned media analyses, absolute values for ELISA and enzyme activity assay were normalised to 10^5 cells, as measured by ADAM™ cell counter. For lysate analyses by ELISA and enzyme activity assay, absolute values were normalised to pg total cell lysate, as measured by BCA assay. For lysate analyses by Western blotting, samples were diluted to equal concentrations of total cell protein prior to SDS-PAGE, and further normalised post-analysis to endogenous control (GAPDH). For NF- κ B analyses, phosphorylated-p65 was also normalised to total p65, and the p52 cleaved subunit normalised to p100, to accurately determine pathway activation for canonical and non-canonical NF- κ B, respectively.

2.2.10 Statistical Analysis

All data was analysed and graphed using Microsoft Excel, expressed as the mean \pm standard error of the mean (SEM). Independent experiments were conducted to a minimum of $n = 3$. Control versus treated groups were analysed by analysis of variance (ANOVA) in conjunction

with a Dunnett's *post-hoc* test for multiple comparisons, and a Student's *t*-test was utilised for pairwise comparisons. A value of $p \leq 0.05$ was considered statistically significant.

Chapter 3

Profiling the effects of RANKL +/- TRAIL in vascular cell mono- and co- culture models

3.1 Introduction

3.1.1 Background and Hypothesis Development

Accelerated VC observed in systemic diseases (eg. T2DM) is widely associated with cardiovascular morbidity/mortality; however, the key pathological events driving this process have yet to be fully delineated. Accordingly, improved knowledge of the molecular and mechanistic pathways underpinning VC are essential if successful therapeutic interventions are to be developed.

A number of studies to date have considered the functions of RANKL and TRAIL in the vasculature, several of which form the basis of this chapter. As detailed in Chapter 1, RANKL has long been implicated as a promoter of medial VC, as it exhibits pro-calcific/osteoblastic actions in vascular smooth muscle (Kaden *et al.*, 2004; Ndip *et al.*, 2011; Panizo *et al.*, 2009). Furthermore, RANKL has been noted to exert pro-calcific effects on endothelial cells, inducing the release of osteoblastic paracrine signals such as BMP-2/4 to underlying VSMCs (Davenport *et al.*, 2016; Osako *et al.*, 2010). Correspondingly, RANKL expression has been observed in vascular cells and in circulation (Cheng *et al.*, 2015; Osako *et al.*, 2010), with elevated levels detected in calcified/atherosclerotic tissue (Higgins *et al.*, 2015). From a mechanistic perspective, RANKL function is known to involve NF- κ B signalling, and the non-canonical NF- κ B pathway has been implicated in pro-calcific events (Panizo *et al.*, 2009). Although the functions of RANKL in VC are well established, the precise role(s) of TRAIL in this process, and its mechanism of action, remain undefined.

Like RANKL, TRAIL has also been identified in serum and in vascular cells (Cheng *et al.*, 2014; Volpato *et al.*, 2011; Zauli *et al.*, 2006), and a growing body of evidence now points to a protective role for TRAIL in VC. From a clinical perspective, decreased serum TRAIL levels correlate with acute cardiovascular events (including myocardial infarction, heart failure) and resulting mortality (Niessner *et al.*, 2009; Secchiero *et al.*, 2009; Volpato *et al.*, 2011). *In vivo*, TRAIL administration has demonstrated anti-atherosclerotic activity in diabetic mice, with TRAIL deficiency promoting VC in TRAIL-null mice (di Bartolo *et al.*, 2013). Moreover, Zauli and colleagues have found that TRAIL has the ability to interfere with RANKL function, attenuating its role in bone resorption (Zauli *et al.*, 2004; Zauli *et al.*, 2008). Despite this, however, no such concept has been investigated in the vasculature to date. ***We therefore hypothesise that TRAIL exerts protective anti-calcific effects on the vasculature, in part via attenuation of RANKL-induced pro-calcific signalling.***

3.1.2 Study Aims

As noted, the function of TRAIL in the vasculature remains the subject of much debate. Former VC investigations in the literature rely heavily on cell models of minimal relevance *in vivo* (for example, vascular beds that are not susceptible to calcification), and limit their studies to a narrow range of pro-calcific markers (Corallini *et al.*, 2011; Osako *et al.*, 2010; Secchiero *et al.*, 2003). As the aorta is a long-established location for VC *in vivo* (Mackey *et al.*, 2007; Wexler *et al.*, 1996), primary human arterial endothelial/smooth muscle cells will be employed in this study, within which a wide range of recognised pro-calcific indices will be monitored in physiologically relevant *in vitro* models. Within these models, the hypothesised protective role of TRAIL on RANKL-induced pro-calcific signalling will be thoroughly evaluated.

To better understand the signalling processes surrounding VC, a number of specific study aims were defined:

1. To delineate the direct effects of RANKL and TRAIL on the intimal vascular endothelium, the primary target for circulatory protein interaction, and to investigate the potential for TRAIL protection in the intimal layer.
2. To define the direct effects of RANKL and TRAIL on medial vascular smooth muscle cells, the primary location of mineral deposition *in vivo*, and to investigate the potential for TRAIL protection in the medial layer.
3. To implement a physiologically relevant co-culture model in which to investigate the effects of RANKL and TRAIL on endothelial:smooth muscle paracrine signalling, and to monitor the potential for TRAIL protection within this model.

3.1.3 Experimental Design

To address study aims 1 and 2, primary human aortic endothelial cells (HAECs) and human aortic smooth muscle cells (HASMCs) respectively were cultured in standard 6-well dishes (Figure 3.1) and exposed to RANKL (5-25 ng/mL), TRAIL (5 ng/mL), or both for 72 hours. To address study aim 3, a non-contact

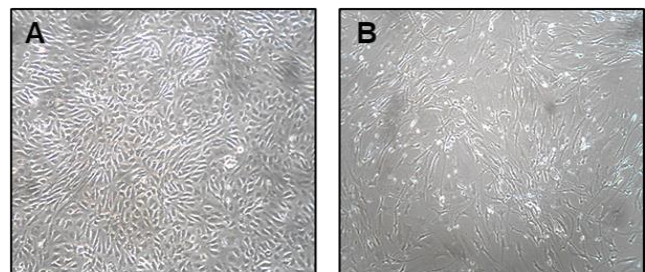


Figure 3.1. Typical morphology of HAECs and HASMCs in culture. (A) Cultured HAECs under control conditions displaying typical cobblestone morphology. (B) Cultured HASMCs under control conditions displaying their characteristic spindle shape. Images were taken using a Nikon Eclipse TS100 phase-contrast light microscope.

co-culture model was developed in which HASMCs were grown to confluency in standard 6-well culture dishes (subluminal compartment), while HAECs were seeded in semi-permeable transwell inserts (luminal compartment). Transwell inserts were suspended above confluent smooth muscle cells and exposed to RANKL (5-25 ng/mL), TRAIL (5 ng/mL) or co-incubated with both for 72 hours (Figure 3.2). In each case, mRNA, protein lysate and conditioned media were harvested as required for analyses by RT-qPCR, ELISA, enzyme activity assay and Western blotting where appropriate ($n = 3$). The following gene/protein targets previously implicated in the VC process were monitored in both mono- and co-culture:

- (i) BMP-2, an endothelial paracrine signalling molecule induced by RANKL (Davenport *et al.*, 2016);
- (ii) ALP, an enzyme involved in matrix mineralisation in the VC process (Hui and Tenenbaum, 1998);
- (iii) OPG, a soluble decoy receptor for both RANKL and TRAIL, shown to have cardioprotective properties (Van Campenhout and Golledge, 2009);
- (iv) IL-6, a pro-inflammatory cytokine, evidenced as a key driver of pro-calcific genes (Kurozumi *et al.*, 2016);
- (v) Runx2, an osteoblastic transcription factor responsible for driving pro-calcific genes (Pratap *et al.*, 2003);
- (vi) Sox9, a chondrocytic transcription factor responsible for driving pro-calcific/chondroblastic genes (Akiyama *et al.*, 2002);
- (vii) Canonical and non-canonical NF- κ B activation, central pathways involved in RANKL function (Panizo *et al.*, 2009; Yu *et al.*, 2011).

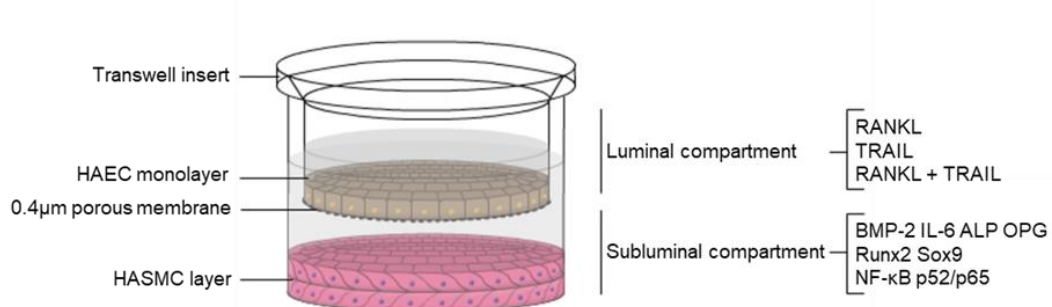


Figure 3.2. Representation of the transwell co-culture model. HASMCs were grown to confluency in standard 6-well culture dishes. HAECs were cultured in semi-permeable transwell inserts and suspended above the confluent smooth muscle layer when confluent. HAECs were exposed to RANKL (5-25 ng/mL), TRAIL (5 ng/mL) or both in the luminal compartment for 72 hours. Conditioned media in the subluminal compartment was assessed for BMP-2, IL-6, ALP and OPG release; HASMC protein lysates were harvested and analysed for BMP-2, ALP, OPG and NF- κ B p52/p65; the HASMC transcriptome was harvested and assessed for BMP-2, IL-6, ALP, OPG, Runx2 and Sox9 mRNA expression. Image adapted from Harper *et al.*, 2017.

3.2 Preliminary Investigations

This chapter will focus primarily on the effects of recombinant RANKL and TRAIL exposure on HAECs and HASMCs. A number of preliminary investigations were conducted to ensure suitable experimental design and correct interpretation of analyses: establishing optimal treatment conditions, determining basal expression levels of RANKL, TRAIL and their receptors, highlighting potential adverse cellular effects of recombinant protein exposure, and ensuring a valid methodological approach.

3.2.1 Establishing Treatment Conditions

Prior to implementing experimental conditions, raw HAEC and HASMC unconditioned media was subject to ELISA analysis to ensure negligible RANKL/TRAIL levels prior to recombinant protein addition. Both proteins proved undetectable in endothelial and smooth muscle media, with measurements below the lower limit of detection (data not shown).

In consideration of the experimental aims and the HAEC:HASMC co-culture investigations conducted by Davenport *et al.* (2016), optimal exposure conditions were primarily determined based on *maximal RANKL-induced endothelial BMP-2 secretion*. In this respect, Davenport *et al.* (2016) identified a role for BMP-2, but not BMP-4, in EC paracrine signalling in response to RANKL. Additional paracrine factors (extracellular ALP activity, OPG and IL-6 release) were also considered. Minimal direct effects of TRAIL on these paracrine factors was preferential so as not to disguise the pro-calcific effects of RANKL. As VC is a chronic process, an exposure duration of 72 hours was implemented to reflect *in vivo* pathological conditions while maintaining cell culture integrity. This duration has been successfully employed in previous VC signalling studies (Davenport *et al.*, 2016; Freise *et al.*, 2016).

By way of optimisation, RANKL concentrations that elicited measurable changes in VC parameters were required, to provide a model in which to investigate TRAIL-mediated protection. In this respect, physiological RANKL circulating levels of approximately 50 pg/mL as reported by Bilgir *et al.* (2018) were first investigated for suitability *in vitro*. HAECs and HASMCs were subject to treatment with 50 pg/mL of RANKL for 72 hours, however, no effects were noted in the release profiles of any of the paracrine signalling molecules measured (data not shown). Therefore, the higher dose range of 5-50 ng/mL previously utilised by Davenport *et al.* (2016) was employed for subsequent optimisation studies (Figure 3.3).

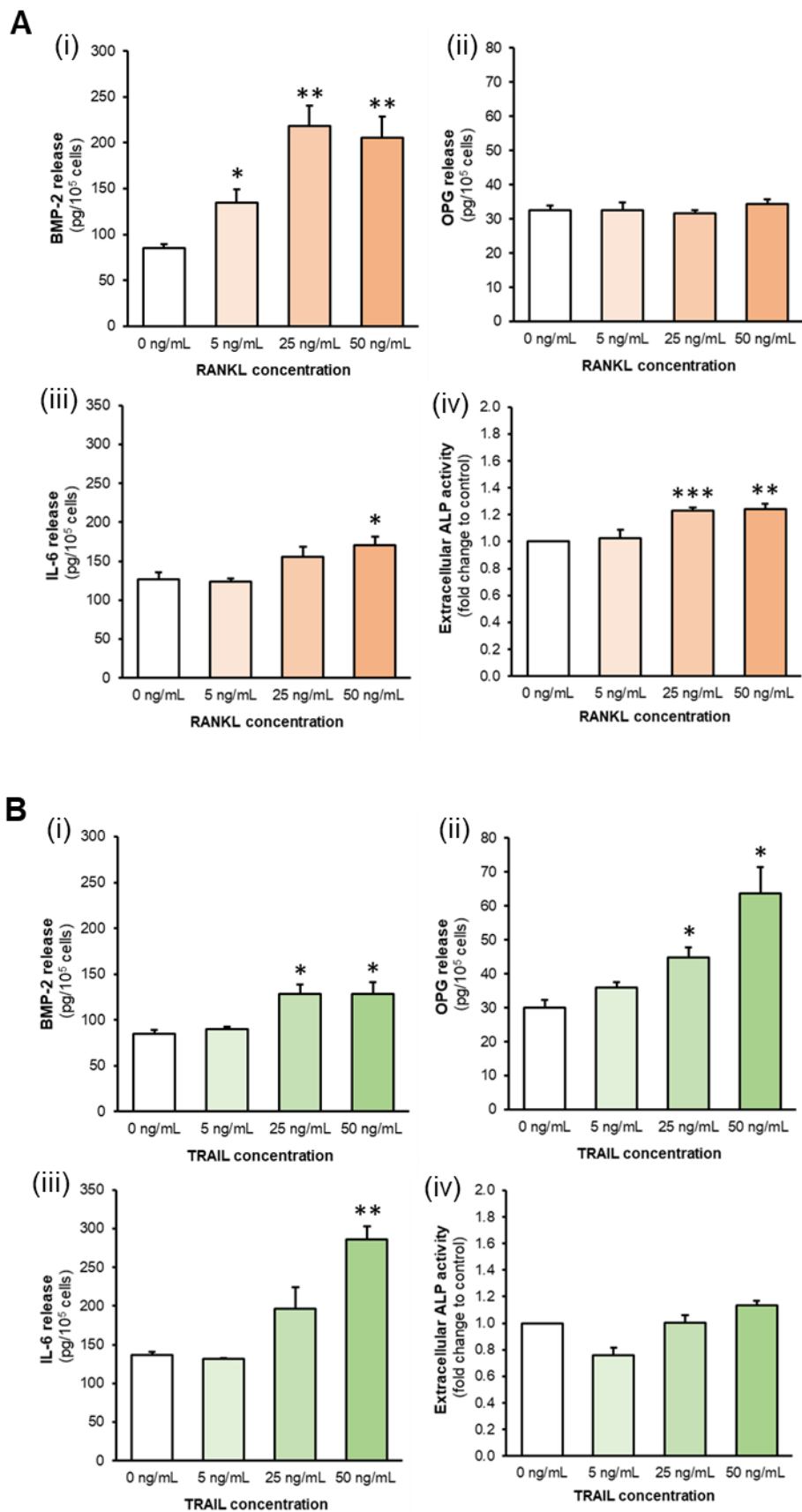


Figure 3.3. Optimisation of RANKL and TRAIL exposure concentrations in HAEC monoculture. HAECs were exposed to 5-50 ng/mL (A) RANKL or (B) TRAIL for 72 hours. (i) BMP-2, (ii) OPG and (iii) IL-6 release were monitored by ELISA; (iv) extracellular ALP activity was determined by activity assay. Absolute values normalised to 10⁵ cells. * $p < 0.05$; ** $p < 0.01$; *** $p < 0.001$ compared to 0 ng/mL control.

Following endothelial exposure to 5, 25 and 50 ng/mL RANKL, it was determined that 25 ng/mL RANKL elicited maximal BMP-2 release while also significantly increasing pro-calcific ALP activity in the conditioned media (Figure 3.3A). As such, this concentration was deemed optimal for *in vitro* studies. With respect to TRAIL, however, concentrations that elicited *minimal* effects on the measured indices were optimal, to ensure that RANKL-induced pro-calcific effects could be clearly monitored. In this regard, it was noted that TRAIL significantly increased BMP-2 and OPG secretion from HAECs at 25 ng/mL and above (Figure 3.3B). As such, a concentration of 5 ng/mL TRAIL was deemed optimal for *in vitro* studies. Given that the optimal RANKL concentration (25 ng/mL) was in excess of the optimal TRAIL concentration (5 ng/mL), a lower RANKL concentration of 5 ng/mL was also included; this ensured that the pro-calcific effects of RANKL would not overwhelm the potential protective influence of TRAIL. Neither RANKL nor TRAIL induced significant inflammatory IL-6 release under any of the optimal conditions chosen.

3.2.2 Expression of RANKL and TRAIL

In order to ensure accuracy of treatment concentrations, basal mRNA and protein expression of RANKL and TRAIL in HAECs and HASMCs was examined, alongside any potential differential effects when exposed to recombinant RANKL (25 ng/mL) or TRAIL (5 ng/mL) for 72 hours.

3.2.2.1 HAECs

With regard to mRNA expression, RANKL and TRAIL levels were undetectable both at basal levels and following RANKL/TRAIL exposure (data not shown). In endothelial conditioned media, soluble RANKL was detected by ELISA at an average concentration of 61.9 pg/mL per 10^5 cells, with TRAIL release approximately ten times less; neither RANKL (25 ng/mL) nor TRAIL (5 ng/mL) treatment exerted any observable effects on RANKL/TRAIL release into the conditioned media. Secreted RANKL and TRAIL levels were therefore deemed too low to affect treatment conditions in the 5-25 ng/mL range. Intracellular RANKL and TRAIL averaged 584.6 and 157.3 pg/mg lysate, respectively, and again no significant variations were noted in intracellular RANKL/TRAIL following exposure to these ligands. Furthermore, Western blotting analysis identified low-level expression of RANKL and undetectable levels of TRAIL in endothelial lysates (Appendix 3.1).

3.2.2.2 HASMCs

In HASMCs, RANKL and TRAIL mRNA were expressed at transcriptionally relevant levels compared to endogenous control, with no significant deviations in expression following exposure to RANKL/TRAIL (data not shown). In HASMC-conditioned media, secreted RANKL and TRAIL levels averaged 96.2 pg/mL and 212.5 pg/mL per 10^5 cells, respectively; RANKL treatment elevated TRAIL release by 23% and TRAIL induced a 31% increase in RANKL secretion. While these levels were deemed relatively insignificant compared to the excess ng/mL experimental concentrations, endogenous RANKL and TRAIL production was noted for subsequent HASMC analyses. Intracellular levels of RANKL (1329.5 pg/mL) and TRAIL (6188.4 pg/mL), were not altered by recombinant ligand exposure. Again, Western blotting confirmed the presence of both RANKL and TRAIL protein in HASMC lysate, at significantly higher levels than that of HAECs (Appendix 3.1).

3.2.3 Expression of RANKL and TRAIL Receptors

The mRNA expression of RANKL and TRAIL surface receptors were also confirmed in HAECs and HASMCs to ensure these recombinant ligands could exert direct physiological effects in culture. TRAIL receptors (decoy receptors DcR1 and DcR2, death receptors DR4 and DR5) were expressed at similar levels in both cell types compared to endogenous controls, while RANK receptor mRNA was approximately 10^4 fold more abundant in HASMCs than HAECs (data not shown). Indeed, all four cell surface receptors for TRAIL, along with the RANK receptor, are known to be expressed in both HAECs and HASMCs (Kavurma *et al.*, 2008; Secchiero *et al.*, 2003).

3.2.4 Effects of RANKL and TRAIL on Cellular Integrity

The potential adverse effects of recombinant RANKL and TRAIL on cellular integrity were also assessed prior to experimental treatment. To this end, cell morphology, viability and apoptosis, endothelial barrier function and the expression of phenotypic markers in smooth muscle cells were assessed.

3.2.4.1 Cell Morphology

HAECs and HASMCs were assessed via light microscopy pre- and post- exposure to RANKL and TRAIL for 72 hours. No changes in HAECs were noted with recombinant protein treatment or co-treatment, exhibiting a typical “cobblestone” morphology (Figure 3.1A). Similarly, no physical variations were noted in treated or co-cultured HASMCs which retained their characteristic spindle shape (Figure 3.1B). Morphological assessment was routinely employed throughout experimental procedures.

3.2.4.2 Viability and Apoptosis

Routine viability measurements were conducted via ADAM™ counter as required. Cell viability for both HAECs and HASMCs were maintained above 90% for all recombinant ligand treatments and co-treatments in mono- and co-culture (data not shown). Apoptosis was also monitored via flow cytometry as described in Section 2.2.7.1 to ensure that neither RANKL nor TRAIL at the employed concentrations were potent apoptotic inducers in HAECs or HASMCs. In HAECs, TRAIL treatment resulted in a very small but statistically significant 1.2% increase in apoptosis, while in HASMCs, RANKL exposure decreased apoptotic cells by 6.4% compared to control (Figure 3.4). Average values for viability and apoptotic measurements are summarised overleaf in Table 3.1.

3.2.4.3 Endothelial Barrier Function

As endothelial cells will ultimately be employed in co-culture, HAEC barrier function was assessed to ensure that RANKL nor TRAIL did not alter monolayer integrity or permeability over the 72-hour exposure time. HAECs were exposed to RANKL and/or TRAIL in transwell inserts for 72 hours. FITC-dextran was then added to the apical compartment as described in Section 2.2.5.2, and the percentage trans-endothelial exchange (TEE) monitored over a three-hour period. Untreated control cells permitted an average TEE of 3.0% FITC-dextran, and neither RANKL nor TRAIL treatment exhibited any significant difference on endothelial permeability, averaging 3.7% and 4.0% TEE, respectively (Appendix 3.2A).

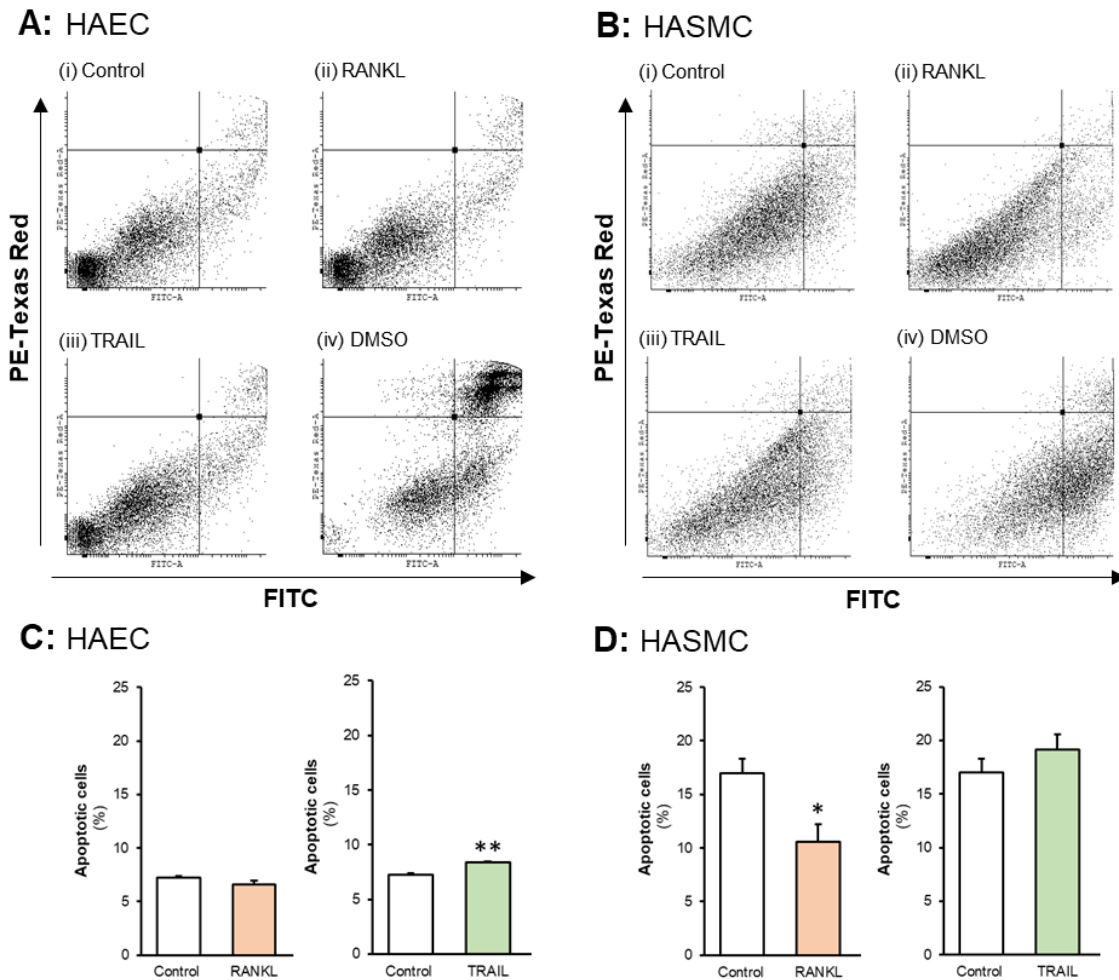


Figure 3.4. The effect of RANKL and TRAIL exposure on HAEC and HASMC apoptosis. (A) HAECs and (B) HASMCs were exposed to experimental concentrations of RANKL (25 ng/mL) and TRAIL (5 ng/mL) for 72 hours, or 20% DMSO for 30 minutes, prior to analysis by flow cytometry. Dot plots are presented for apoptosis measurements of (i) control, (ii) RANKL, (iii) TRAIL and (iv) DMSO. Quadrants determined by unstained control. Bar charts represent percentage apoptosis when (C) HAECs and (D) HASMCs were exposed to (i) RANKL and (ii) TRAIL for 72 hours. * $p < 0.05$; ** $p < 0.01$ compared to untreated control.

Table 3.1. Average percentages of viable, non-viable, and apoptotic HAECs and HASMCs post-treatment.

		Viable (%)	Non-viable (%)	Apoptotic (%)
HAECs	<i>Untreated</i>	96.58	3.41	7.23
	<i>25 ng/mL RANKL</i>	96.63	3.34	6.59
	<i>5 ng/mL TRAIL</i>	96.36	3.62	8.42**
	<i>DMSO</i>	48.42	49.15	17.8
HASMCs	<i>Untreated</i>	95.60	3.32	17.01
	<i>25 ng/mL RANKL</i>	98.36***	1.52***	10.60*
	<i>5 ng/mL TRAIL</i>	96.29	3.00	19.11
	<i>DMSO</i>	88.20	11.43	44.63

* $p < 0.05$; ** $p < 0.01$; *** $p < 0.001$ compared to untreated control.

3.2.4.4 Phenotypic Analysis of Smooth Muscle Cells

As noted, trans-differentiation of HASMCs away from smooth muscle and towards a pro-osteoblastic phenotype can occur under the correct conditions, particularly in the presence of pro-calcific factors such as RANKL. Thus, HASMCs were characterised for specific phenotypic markers under both control conditions and following exposure to recombinant ligands. In this respect, HASMCs were analysed for mRNA expression levels of two core smooth muscle markers: SM α -actin and SM22 α , and two markers of osteoblastic differentiation: BSP and OCN. No changes were noted in the expression levels of either smooth muscle or osteoblastic markers after 72 hours' treatment with RANKL or TRAIL (Appendix 3.2B), confirming that HASMCs maintain a characteristic smooth muscle phenotype for the experimental duration. Furthermore, no changes in the above phenotypic markers were noted in HASMCs in co-culture, despite the potential presence of pro-calcific endothelial paracrine signalling (data not shown).

3.2.5 Methodological Validation

Prior to experimentation, confirmatory experiments were carried out to ensure a valid methodological approach for RT-qPCR, ELISA and co-culture cell models. Validations were carried out at the optimal determined experimental concentrations for RANKL and TRAIL recombinant ligands.

3.2.5.1 qPCR

Prior to conducting gene expression analysis on experimental samples, it was confirmed that both GAPDH and 18S were appropriate endogenous controls for the treatment conditions employed. To this end, both reference genes were assessed for changes in expression levels in response to RANKL or TRAIL exposure for 72 hours. Both ligands were noted to have no effect on either GAPDH or S18 gene expression in HAECs or HASMCs (Appendix 3.3A), confirming their suitability in experimental qPCR analyses.

3.2.5.2 ELISA

As OPG can function as a soluble decoy receptor for both RANKL and TRAIL, it was considered that recombinant protein addition may interfere with extracellular OPG ELISA

readings. Reciprocally, endogenous OPG production may alter the analysis of RANKL and/or TRAIL release. In this regard, experimental concentrations of both RANKL and TRAIL were “spiked” into untreated HASMC conditioned media after 72 hours and subject to OPG ELISA analysis. Meanwhile, conditioned HASMC media was also spiked with recombinant human OPG at 20 ng/mL (doubling secreted OPG concentration), and RANKL/TRAIL release monitored by ELISA. No neutralisation effects were noted in RANKL, TRAIL, or OPG levels between control and spiked conditioned media (Appendix 3.3B, C), highlighting that neither recombinant protein addition nor endogenous OPG production interfere with ELISA analyses.

3.2.5.3 Co-culture

In addition to the endothelial permeability assay (Section 3.2.4.3), further validation was conducted prior to co-culture; namely, calculating recombinant protein leakage into the basal HASMC compartment. HAECs were exposed to recombinant ligands at experimental concentrations, and basal concentrations of RANKL and TRAIL determined by ELISA analysis at 24 and 72 hours. RANKL- and TRAIL-treated endothelial cells permitted an approximate 1.8% and 5.4% transfer, respectively, of total ligand from the luminal to the subluminal compartment after 72 hours in culture (Appendix 3.3D). In consideration of the larger media volume present in the subluminal compartment, these percentage values equate to absolute concentrations of 224.9 pg/mL RANKL and 135.7 pg/mL TRAIL at the termination of co-culture treatment.

3.2.6 Discussion: Preliminary Investigations

Extensive efforts were made to ensure robust and relevant *in vitro* models were employed alongside a sound methodological approach. In this respect, preliminary investigations primarily involved the optimisation of exposure conditions, identification of potential adverse effects, and the validation of experimental controls.

3.2.6.1 Selection of Optimal Treatment Conditions in HAECs

As noted, exposure conditions were primarily chosen based on optimal RANKL-induced BMP-2 release from HAECs, as previously characterised by Davenport *et al.* (2016), representing endothelial paracrine signalling to HASMCs in the vascular wall. Endothelial release of active ALP, a critical marker of osteoblastic activity, were also assessed; ALP promotes matrix mineralisation via PP_i clearance/increasing P_i levels in the extracellular space (Schoppet and Shanahan, 2008), and thus may contribute to RANKL-induced pro-calcific events in underlying HASMCs in co-culture. As HAECs have been previously noted to release low but detectable quantities of OPG decoy receptor under basal conditions (Davenport *et al.*, 2016), minimal extracellular OPG levels were preferential to facilitate uninterrupted RANKL/TRAIL function. Furthermore, negligible endothelial IL-6 release was required for multiple reasons: firstly, IL-6 has been shown to increase vascular permeability through VEGF production (Hashizume *et al.*, 2009; Tanaka *et al.*, 2014), an undesirable outcome in co-culture where a tight endothelial barrier is desired. Secondly, research indicates that IL-6 can directly induce ALP and Runx2 expression in VSMCs (Kurozumi *et al.*, 2016), an effect which may hinder the identification of RANKL-induced pro-calcific signalling. Thirdly, IL-6 has been shown to suppress RANK signalling during osteoclastic differentiation (Yoshitake *et al.*, 2008); although not directly relevant in a vascular setting, the overlapping functions of RANKL in bone and in the VC process (and thus the potential for interference in the employed cell models) must be considered. An exposure concentration of 25 ng/mL RANKL satisfied the above requirements, achieving substantial BMP-2/ALP secretion alongside negligible OPG/IL-6.

TRAIL's optimal exposure concentration was also determined by BMP-2/IL-6, as elevated release of both soluble markers was noted at 25 ng/mL and above. Thus, 5 ng/mL TRAIL was required so as not to interfere with RANKL-specific pro-calcific effects. This concentration-dependent BMP-2/IL-6 induction further supports the complex pleiotropic role of TRAIL in the vasculature (Forde *et al.*, 2016), and may go towards explaining some of the contrasting

effects noted with TRAIL exposure in the literature (Chasseraud *et al.*, 2011; Olesen *et al.*, 2012). Crucially, no significant effects on OPG/ALP secretion were detected at the optimal TRAIL dose. A significant and novel finding of this preliminary investigation is the dose-dependent release of cardioprotective OPG in response to TRAIL treatment, possibly the result of self-regulation in response to abundant extracellular TRAIL, but also a potential contributor to the growing theory of TRAIL-mediated vasoprotection. Interestingly, OPG (co-localised with von-Willebrand Factor) is subject to rapid release from Weibel-Palade bodies in response to endothelial inflammation (Zannettino *et al.*, 2005), potentially revealing an additional role for TRAIL at higher concentrations. This finding may also be of relevance in explaining TRAIL-induced BMP-2/IL-6 release, however this conjecture requires further research and is beyond the scope of the current study.

On an additional note, it is no surprise that reported circulating levels of RANKL (~50 pg/mL) did not induce endothelial pro-calcific paracrine responses in culture. Recorded concentrations of basal RANKL production in HAECs were of a similar magnitude, and low-level endogenous OPG production may contribute to RANKL neutralisation. Subsequently, the higher dose range of 5-50 ng/mL was considered suitable as it has previously been employed to investigate the effects of RANKL in HAECs, particularly regarding BMP-2 secretion (Davenport *et al.* 2016, Osako *et al.*, 2010). Moreover, higher levels of RANKL than that measured in circulation have been detected in atherosclerotic and calcified lesions (Dhore *et al.*, 2001; Morony *et al.*, 2008; Schoppet *et al.*, 2004) enhancing the physiological relevance of the employed RANKL concentration in the current study.

3.2.6.2 Expression of RANKL and TRAIL in HAECs and HASMCs

There are varying reports in the literature regarding the expression of RANKL and TRAIL in vascular cells. While both proteins have been identified in calcified arteries *in vivo*, whether this originates from circulating immune cells (Falschlehner *et al.*, 2009; Hofbauer and Schoppet, 2004) or from the vasculature itself is long under debate. Regarding the endothelium, RANKL mRNA/protein has been detected in HAECs (Osako *et al.*, 2010) and microvascular ECs (Collin-Osdoby *et al.*, 2001), while TRAIL mRNA/protein has been detected in microvascular ECs (Pritzker *et al.*, 2004) and pulmonary arteries (Spierings *et al.*, 2004). Contrastingly, the absence of RANKL (Zannettino *et al.*, 2005) and TRAIL (Secchiero *et al.*, 2006) in HUVECs has been reported at both transcriptional and translational level. To account for these divergences, Zannettino and colleagues (2005) highlight the potential differences in

microvascular EC and HUVEC responses, while Spierings *et al.* (2004) suggest that the expression of TRAIL is both tissue and cell-specific. Interestingly, previous studies in our own lab indicate that neither protein is expressed at detectable quantities in HAECs, despite the presence of mRNA transcripts (Davenport *et al.*, unpublished observations). While these cells were cultured under similar conditions, these studies by Davenport *et al.* employed primary HAECs from a different donor to those employed in the current investigation. Together with the findings from the present study in which low-level RANKL/TRAIL protein (but not transcript expression) was detected, we further support the proposition by Spierings *et al.* (2004) that while ECs in general can produce RANKL and TRAIL, their expression may be cell-specific and should be evaluated for each endothelial population.

There are more consistent reports in the literature regarding VSMC expression of RANKL and TRAIL. Concurring with our study, both RANKL mRNA and protein expression have been detected in murine aortic VSMCs (Chang *et al.*, 2015; Tseng *et al.*, 2010), while TRAIL transcripts/protein have been quantified in VSMCs (Harith *et al.*, 2016; Li *et al.*, 2016). In supernatant media, low concentrations of RANKL and TRAIL bound to OPG in human VSMC supernatant media have also been discovered (Nguyen *et al.*, 2007). Contrastingly, however, previous studies by Davenport *et al.* (2016) within our own research group have revealed a lack of RANKL/TRAIL production by HASMCs; this discrepancy may also be explained by the proposition of a VSMC population-specific production profile, as different HASMC donors were employed in each case. Moreover, primary HASMCs are notoriously heterogeneous in culture, with phenotypic characteristics dependent on the specific differentiation state of the explanted populations (Speer *et al.*, 2009). As with HAECs, RANKL and TRAIL produced by VSMCs may therefore contribute to that detected in calcified lesions *in vivo* (Dhore *et al.*, 2001; Morony *et al.*, 2008; Schoppet *et al.*, 2004), however, given the relatively overwhelming concentrations of OPG produced by HASMCs (Davenport *et al.*, 2016), their biologically significant effects at these levels are likely negated in culture. Nonetheless, the induction of RANKL/TRAIL secretion observed with TRAIL and RANKL exposure, respectively, is considered a significant finding of this study, providing, to our knowledge, the first evidence of inter-regulation between the two ligands in the vasculature.

3.2.6.3 The Effects of RANKL and TRAIL on Cellular Integrity

Despite the notorious roles of RANKL and TRAIL as potent inducers of calcification and apoptosis, respectively, both proteins exerted minimal effects on HAEC/HASMC viability and

integrity. No detrimental effects of recombinant ligand exposure on endothelial barrier function were noted, despite the claim that RANKL induces vascular permeability (Min *et al.* 2007). In HAECs exposed to TRAIL, a slight but significant increase in apoptosis was noted after 72 hours, an effect considered inconsequential for current cell models. Despite TRAIL's historical function as an "apoptosis-inducing ligand", the literature reveals conflicting results. While Cheng *et al.* (2014) have previously generalised that excessive TRAIL stimulates EC apoptosis, concurrent with studies by Li *et al.* (2013) and Sato *et al.* (2006), TRAIL has in some cases been shown to promote endothelial survival (Secchiero *et al.*, 2003). Unpublished studies in our lab have however revealed that higher concentrations of TRAIL (100 ng/mL) over a shorter exposure period (24 hours) induce an approximate 5% increase in apoptosis, potentially revealing concentration- and time-dependency in TRAIL's apoptotic function (Forde *et al.*, unpublished observations). While responses to TRAIL are likely to be somewhat concentration-dependent, varying responses to TRAIL treatment have been considered (Spencer *et al.*, 2009), further supporting a complex pleiotropic role for this protein *in vivo*. Therefore, the effects of TRAIL on endothelial integrity likely vary widely and involve a complex balance of both pro- and anti-apoptotic signalling pathways, a subject for further investigation outside the scope of this thesis (for review, see Forde *et al.*, 2016).

As an additional novel finding, RANKL exposure significantly decreased smooth muscle apoptosis and cell death. Although Bharti *et al.* (2003) present opposing evidence of RANKL-induced apoptosis, their study employed a murine monocytic cell line, and no comprehensive investigations have since clarified the role of RANKL in VSMC apoptosis. While not covered in the current study, further research is necessary to delineate the pro-survival properties of RANKL in smooth muscle.

As expected, neither RANKL nor TRAIL were noted to affect the expression of smooth muscle markers SM α -actin and SM22 α or the early (BSP) and late (OCN) markers of osteogenic differentiation in HASMCs after 72 hours' exposure. Despite RANKL's well-defined roles in pro-calcific signalling, differentiation processes generally require 14-21 days' differentiation in complex pro-osteogenic media to induce phenotypic changes in VSMCs (Patel *et al.*, 2016, Yang *et al.*, 2005). Therefore, transcriptional and translational variations pre-and post-exposure can be directly attributed to RANKL/TRAIL exposure and not to a weakened VSMC phenotype.

3.2.6.4 Methodological Validation

Regarding the choice of endogenous control, GAPDH and 18S were confirmed to be suitable for mRNA analysis post-exposure to RANKL/TRAIL, as no changes in these genes were noted in HAECs/HASMCs. These reference genes have also been previously employed following RANKL/TRAIL exposure in vascular cells (Davenport *et al.*, 2016; Panizo *et al.*, 2009; Patel *et al.*, 2013). On a separate note, no neutralisation effects were noted in RANKL, TRAIL, or OPG levels between control and spiked conditioned media following ELISA analyses. In agreement with the manufacturer's specifications, this suggests that these DuoSet™ ELISA systems measure both free and bound protein, a finding previously confirmed for the RANKL DuoSet™ kit by Davenport *et al.* (unpublished observations).

In relation to co-culture models, transwell inserts have been successfully employed in VC studies to demonstrate the paracrine interaction between VSMCs and various cell types (Hénaut *et al.*, 2016; Zhang *et al.*, 2014). However, additional efforts were made in this case to confirm a tight endothelial monolayer in co-culture, to ensure that recombinant RANKL/TRAIL could not leak through into the subluminal compartment in significant quantities to cause direct effects on underlying HASMCs. In consideration of the endothelial barrier function *in vitro*, endothelial protein uptake and degradation by natural proteases, minimal recombinant RANKL/TRAIL was expected to cross the HAEC monolayer. Indeed, after 72 hours, less than 2% and 6% total RANKL and TRAIL respectively were detected in the subluminal compartment; in combination with neutralising OPG secretion, these low pg/mL concentrations are unlikely to exert direct physiological effects on HASMCs in co-culture. The aforementioned permeability assay, viability and apoptosis measurements, and morphological assessments also support a robust physiologically relevant co-culture model in which to assess the effects of RANKL/TRAIL on the vasculature.

3.3 HAEC Monoculture

As noted, HAECs were first employed in monoculture to investigate the effects of RANKL +/- TRAIL, in order to profile the pro-calcific effects of RANKL and the potential protective effects of TRAIL on the vascular intima. A number of gene and protein targets were analysed as part of this study, listed in Section 3.1.3.

3.3.1 The Effects of RANKL +/- TRAIL on the Expression of HAEC Gene Targets

Following analyses by RT-qPCR, neither RANKL nor TRAIL altered the mRNA expression levels of BMP-2, ALP, Runx2 or IL-6 gene targets in endothelial monoculture after 72 hours (Appendix 3.4A). Both OPG and Sox9 mRNA were deemed undetectable in the HAEC transcriptome, with levels below that required for accurate detection. However, as elevated levels of BMP-2 and ALP protein were detected in the endothelial secretome in response to 25 ng/mL RANKL (Figure 3.3), the mRNA levels of these genes following 24 hours' incubation with RANKL were also investigated (in the event that mRNA changes had normalised after 72 hours). Again, no notable differences were detected in BMP-2 mRNA levels, but both ALP and Runx2 transcripts were significantly more abundant at the earlier time-point before returning to baseline levels at 72 hours (Appendix 3.5B).

3.3.2 The Effects of RANKL +/- TRAIL on the Expression of HAEC Protein Targets

With regard to protein release, RANKL was again confirmed to dose-dependently increase paracrine BMP-2 secretion and extracellular ALP activity. TRAIL had no effect on secretory BMP-2 levels, but reduced active ALP release by approximately 20%. Co-incubation with both RANKL and TRAIL resulted in complete attenuation of RANKL-induced BMP-2 release at both concentrations, while TRAIL significantly reduced ALP activity when compared to RANKL treatment alone (Figure 3.5A (i), (iii)). Regarding intracellular protein, again dose-dependent increases of BMP-2 and active ALP were noted in response to RANKL. In the case of BMP-2, while TRAIL treatment alone had no effect, co-incubation with both recombinant proteins significantly increased BMP-2 production when compared to RANKL exposure (Figure 3.5A (ii)). In the case of ALP, however, TRAIL co-incubation fully attenuated RANKL-induced activity at both concentrations (Figure 3.5A (iv)). No changes were noted at a translational level for OPG (Appendix 3.4B) or secretory IL-6 (data not shown).

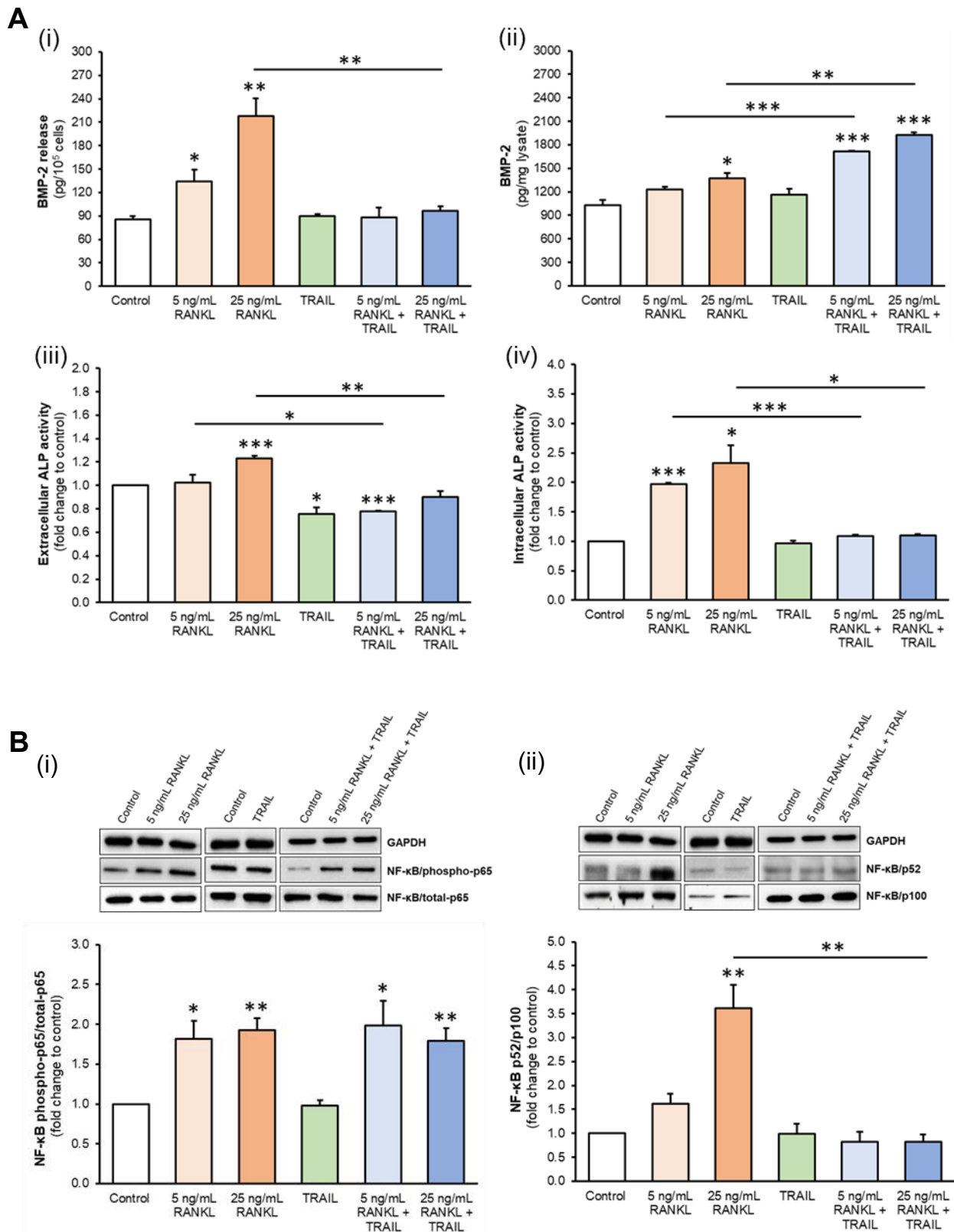


Figure 3.5. Protein analyses in HAEC monoculture. HAECs were exposed to RANKL (5-25 ng/mL) +/- TRAIL (5 ng/mL) for 72 hours. **(A)** (i) BMP-2 release and (ii) intracellular BMP-2 levels were analysed by ELISA. (iii) extracellular and (iv) intracellular ALP activity were determined by activity assay. **(B)** (i) Canonical and (ii) non-canonical NF-κB activation were determined by Western blotting, analysed by scanning densitometry and normalised to GAPDH. Blots are representative. Absolute values for media and lysate analysis are and normalised to 10⁵ cells and total protein respectively. * $p < 0.05$; ** $p < 0.01$; *** $p < 0.001$ compared to untreated control unless otherwise stated; bars indicate statistical significance between treatment groups.

3.3.3 The Effects of RANKL +/- TRAIL on HAEC NF- κ B Activation

Both canonical and non-canonical NF- κ B pathways were activated in response to RANKL. Phosphorylated p65 levels were similarly elevated in response to both 5 and 25 ng/mL RANKL, while cleaved p52 levels increased in a dose-dependent manner (Figure 3.5B). TRAIL itself had no effect on either NF- κ B pathway at the employed concentration in endothelial cells, and did not interfere with RANKL-induced canonical activation. However, TRAIL completely attenuated non-canonical signalling induced by RANKL exposure, at both 5 and 25 ng/mL concentrations. As an additional investigation, non-canonical activation was monitored over the earlier time course of 0-24 hours, to better profile pro-calcific NF- κ B signalling responses to RANKL. It was found that cleaved p52 levels are elevated as early as 15 minutes' post-exposure, peaking at approximately 6 hours, and this pathway remains active after 24 hours of treatment (Appendix 3.5A). Furthermore, β -glycerophosphate, a well-established inducer of calcification, was noted to significantly induce non-canonical NF- κ B activation while exerting minimal effect on canonical signalling after 72 hours' exposure. Elevated BMP-2 release and extracellular ALP activity were noted alongside this activation (Appendix 3.6).

3.3.4 HAEC Monoculture: Summary of Results

Differentially expressed indices in response to RANKL +/- TRAIL treatment in HAEC monoculture are summarised in Table 3.2 below.

Table 3.2. The effects of RANKL +/- TRAIL in HAEC monoculture.

		RANKL (25 ng/mL)	TRAIL (5 ng/mL)	RANKL + TRAIL
BMP-2	<i>Extracellular Protein</i>	↑	–	–
	<i>Intracellular Protein</i>	↑	–	↑↑
ALP	<i>Extracellular Activity</i>	↑	↓	–
	<i>Intracellular Activity</i>	↑	–	–
NF-κB (p52/p100)	<i>Activation</i>	↑	–	–
NF-κB (p-p65/t-p65)	<i>Activation</i>	↑	↑	↑

↑, upregulation; ↑↑, further upregulation relative to corresponding treatment conditions; ↓, downregulation; –, no change. p-p65, phospho-p65; t-p65, total p65.

3.3.5 Discussion: HAEC Monoculture

Firstly, the pro-calcific effects of RANKL and the proposed protective effects of TRAIL were explored in endothelial monolayer. Thus far, limited data exists regarding the process of VC in large artery ECs, as the majority of calcification studies to date employing RANKL and TRAIL have been completed in VSMC models. As such, there is minimal research data available to which our findings can be compared, and we present a number of novel findings regarding pro-calcific indices never before explored in human endothelial cell models. These studies are vital in addressing the current hypothesis as they aid in defining the endothelial contribution to vascular paracrine signalling, enhancing our ultimate understanding of more complex co-culture models. Given the comprehensive nature of this investigation, only the key findings of the presented HAEC monoculture studies (summarised in Table 3.2) will be discussed.

3.3.5.1 The Effects of RANKL +/- TRAIL on BMP-2 Regulation

BMP-2 has been defined as a pro-osteogenic protein known to act in a paracrine manner on underlying VSMCs in the vasculature. In this respect, and in agreement with the literature, RANKL was noted to dose-dependently induce BMP-2 release in HAEC monoculture (Davenport *et al.*, 2016; Osako *et al.*, 2010). At a translational level, this trend was maintained, however no concurrent transcriptional changes were observed. Given the induction of BMP-2 protein, BMP-2 mRNA levels were also investigated following 24 hours' RANKL treatment, and again no changes were detected in BMP-2 transcript expression at this earlier time point. Osako and colleagues, to our knowledge the only other research group to assess the effects of RANKL on BMP-2 expression in HAECs, noted an upregulation of BMP-2 mRNA expression at 6 hours, however they fail to report on gene expression levels at 24 hours and beyond. Additionally, while not directly relevant to our VC model, early-stage (6 hours) BMP-2 mRNA expression has also been induced by RANKL exposure in osteosarcoma cells (Wittrant *et al.*, 2006). It is therefore possible that BMP-2 mRNA transcription may be subject to early upregulation before returning to baseline levels, but this hypothesis requires further confirmation. This inconsistency between mRNA and protein levels also suggests that RANKL modulates long-term BMP-2 production at a translational rather than a transcriptional level, with BMP-2 mRNA levels likely irrelevant to chronic conditions such as VC.

With regard to TRAIL, no effects were observed in BMP-2 mRNA/protein following 72 hours' exposure, in agreement with our hypothesis. Indeed, despite the known pro-calcific effects of

RANKL and the ability of TRAIL to counteract RANKL function in osteoclastogenesis (Zauli *et al.*, 2004; Zauli *et al.*, 2008), no studies to date have investigated the combined effects of these ligands on BMP-2 release. We therefore present, for the first time, the ability of TRAIL to *completely attenuate RANKL-induced BMP-2 paracrine signalling in HAECs, even when RANKL is greatly in excess*. This novel finding provides the first evidence of TRAIL-mediated protection within the context of VC. Furthermore, with co-exposure to TRAIL, we report that TRAIL enhanced RANKL-induced intracellular BMP-2 levels (while blocking its release). Thus, TRAIL may exert an inhibitory effect on chronic RANKL-induced BMP-2 *secretion*, rather than production, having no effect on total protein turnover.

3.3.5.2 The Effects of RANKL +/- TRAIL on Pro-Calcific Markers

Interestingly, alongside BMP-2, RANKL is known to exert its pro-calcific function in the vasculature via upregulation of osteogenic transcription factors (eg. Runx2), subsequently increasing ALP expression/activity (Sage *et al.*, 2010). ALP is also independently recognised as an extracellular inducer of calcification, and is often used to assess mineralisation in vascular settings (Lieberman *et al.*, 2013). However, what the majority of the literature fails to address is the effect of RANKL on these pro-calcific indices in ECs, focusing instead on VSMC models. While VSMCs are indeed the primary location for mineralisation *in vivo*, the endothelium is in direct contact with pro-calcific stimuli in circulation, and so ECs are likely to exert their own osteogenic response to condition underlying VSMCs within the medial layer. This study aimed to address these limitations by defining multiple endothelial pro-calcific responses to RANKL, and assessing the potential for TRAIL protection in this respect.

At an mRNA level, both ALP and its upstream transcription factor Runx2 were induced by RANKL at 24 hours, but this upregulation was not sustained at 72 hours. Interestingly, however, both intra- and extra-cellular ALP activity were elevated following 72 hours' RANKL exposure, a trend previously highlighted in HASMCs (Osako *et al.*, 2010) but never before clarified in the endothelial monolayer. We therefore highlight the novel finding that *endothelial* exposure to RANKL induces active ALP, potentially contributing to VSMC extracellular matrix mineralisation and/or elevated circulating ALP noted in chronic T2DM (Hussein, 2017). Taken together, these data may suggest that, like BMP-2, early transcriptional changes in ALP/Runx2 may affect sustained responses at a protein level. Also of relevance, Sox9 chondrogenic transcription factor expression was not present in detectable quantities in

HAECs, either untreated or exposed to RANKL, suggesting a specific role for the endothelium in pro-osteogenic rather than chondrogenic processes.

With regard to TRAIL, no effect was noted on ALP/Runx2 transcription at either time point. TRAIL did, however, significantly reduce extracellular ALP activity at 72 hours, and more pertinently, *completely attenuated RANKL-induced active ALP*. In the first study to our knowledge to consider endothelial ALP as a paracrine factor, or more specifically a core contributor to VSMC matrix crystallisation, we present further novel evidence to support the protective role for TRAIL in attenuating RANKL-induced endothelial pro-calcific signalling.

3.3.5.3 The Effects of RANKL +/- TRAIL on OPG Regulation

Following quantification of extracellular OPG, neither RANKL nor TRAIL were found to affect the release of their own decoy receptor from HAECs at the employed concentrations. It has long been reported that OPG, with its well-defined cardioprotective properties, is secreted by endothelial cells (Malyankar *et al.*, 2000; Zannettino *et al.*, 2005), although many claims to date have been based on less physiologically relevant cell models (eg. HUVECs). More relevantly, previous studies in our own lab have identified endothelial release in the 20-30 pg/mL range, consistent with our own reports (Davenport *et al.*, 2016). To date, few studies have investigated the effects of RANKL/TRAIL on OPG release, potentially due to its role as a potent decoy receptor for these ligands. However, endothelial OPG secretion in the low pg/mL range is highly unlikely to exert any biologically relevant neutralising effects on excessive ng/mL concentrations of recombinant ligands employed in this case. Furthermore, anti-OPG antibodies are often employed in RANKL studies *in vitro*, in order to negate this neutralising function (Davenport *et al.*, 2016; Osako *et al.*, 2010). However, both RANKL and TRAIL exert biologically significant effects *in vivo* even in the presence of circulating OPG (Carbone *et al.*, 2016; Secchiero *et al.*, 2006). Therefore, we chose to maintain physiological relevance and exclude OPG neutralisation from our *in vitro* models.

Despite the detection of OPG protein, OPG mRNA was deemed too low to be accurately quantified in HAECs. In this regard, our finding contradicts the literature, as Osako *et al.* (2010) and Davenport *et al.* (2018) have previously identified OPG mRNA in HAECs. While the discrepancy in RANKL/TRAIL expression (whereby protein but not mRNA transcripts were detected) may be explained by population heterogeneity, we propose an environment-specific explanation for the same discrepancy with OPG. Due to the high concentration of intracellular

protein, HAECs appear to maintain a “store” of OPG for release under the appropriate conditions, and thus OPG transcription levels may not be required in measurable amounts. Furthermore, the qPCR “cut-off point” employed in this study (40 C_q) may not have been employed by the aforementioned authors, resulting in low but quantifiable OPG expression in those studies. As a final consideration, this proposed induction of stored OPG alongside the apparent low transcription rate may result in the eventual attenuation of OPG release, leaving the vasculature open to injury. Therefore, the protective effects of OPG may be short-term, rendering OPG nothing more than a marker of early endothelial dysfunction with minimal biologically significant effects. The precise nature of OPG regulation in endothelial cells, relatively understudied to date, therefore requires further clarification.

3.3.5.4 The Effects of RANKL +/- TRAIL on NF-κB Activation

The activation of NF-κB by RANKL and TRAIL under certain conditions is well established. RANKL binding to the RANK cell surface receptor is known to involve NF-κB signalling in osteoclastogenesis and vascular disease (Abu-Amer 2013; Boyce *et al.*, 2015; Otero *et al.*, 2012), and NF-κB has previously been implicated in diabetic vascular complications (Suryavanshi and Kulkarni, 2017; Zhan *et al.*, 2014; Zhao *et al.*, 2012). The literature, however, lacks clarity with respect to which pathway exerts pro-calcific functions. While the non-canonical pathway has been implicated in VC pathogenesis in VSMCs (Panizo *et al.*, 2009), no studies to our knowledge have investigated RANKL-induced NF-κB activation in vascular *endothelial* cells. In the current study, we note that RANKL activates both the canonical and non-canonical NF-κB pathway in HAECs, suggesting a potential role for both pathways in RANKL endothelial function. Interestingly, Feng and colleagues (2003) have previously linked NF-κB activation and BMP-2 gene expression in chondrocytes, involving both canonical and non-canonical signalling elements (p50/p65, p52), but this study failed to assess BMP-2 protein levels nor is it directly relevant to paracrine communication in the vasculature.

TRAIL, which can activate NF-κB through its surface receptors DcR2, DR4 and DR5 (Juan *et al.*, 2001) (all of which are expressed by HAECs), is widely known to hold a complex relationship with NF-κB signalling (Forde *et al.*, 2016). In this case, TRAIL had no effect on either the canonical or non-canonical pathway, in agreement with the same finding in HUVECs (Secchiero *et al.*, 2003), however, TRAIL has previously been shown to activate NF-κB signalling in the endothelium at higher concentrations (20 – 50 ng/mL) (Li *et al.*, 2003). Furthermore, previous research in our lab has indicated that 100 ng/mL TRAIL induces a strong

trend towards canonical activation (Forde *et al.*, unpublished observations), which may suggest a concentration-dependent NF- κ B response to TRAIL. However, the major limitation of the literature to date is the lack of specification on *which* NF- κ B pathway is activated, in our view a vital piece information in determining TRAIL function.

Moreover, we noted for the first time that endothelial co-incubation with RANKL + TRAIL can *completely attenuate RANKL-induced non-canonical, but not canonical, activation*, a finding for which the mechanism will be explored in Chapter 5. Interestingly, this coincides with TRAIL blockade of RANKL-induced paracrine BMP-2 release and ALP activity. As we know that RANKL can function via non-canonical signalling (Panizo *et al.*, 2009), this pathway may also be responsible for RANKL-induced pro-calcific action in the endothelium, and TRAIL may exert its protective effects by attenuating RANKL-induced non-canonical activation. Moreover, HAEC exposure to the calcification inducer β -glycerophosphate was noted to induce non-canonical (but not canonical) signalling alongside BMP-2/ALP induction, further implicating the former pathway in RANKL pro-calcific function.

As NF- κ B is a well-known “early responder” to its stimuli (Healy *et al.*, 2013), non-canonical signalling was monitored following 15 minutes-24 hours’ exposure to RANKL to gain a better insight into the RANKL/NF- κ B pro-calcific mechanism. We noted maximum activation at 1 hour, with an increase apparent as early as 15 minutes’ exposure. Interestingly, as NF- κ B/p52 translocation to the nucleus regulates gene transcription (Oeckinghaus and Ghosh, 2009), this may explain the early upregulation of pro-calcific genes before eventually returning to baseline alongside low-level non-canonical activation. Furthermore, RANKL-induced NF- κ B, although somewhat diminished, remains steadily active at 24-72 hours, supporting the ability of RANKL to exert sustained effects on HAECs in its role during chronic VC.

3.3.5.5 Summary: HAEC Monoculture

Overall, we present novel evidence that RANKL induces endothelial paracrine BMP-2/ALP signalling via NF- κ B non-canonical activation, and that TRAIL has the ability to attenuate these effects. While RANKL induces early maximal NF- κ B/pro-calcific gene expression, longer term protein responses are sustained at 72 hours, remaining relevant to chronic VC. This novel evidence provides valuable insight on the pro-calcific function and mechanism of RANKL in the endothelial monolayer, and supports the valuable therapeutic potential for TRAIL in the modulation of these pathophysiological effects.

3.4 HASMC Monoculture

HASMCs were also employed in monoculture, in which the same range of mRNA and protein targets were assessed for differential expression in response to RANKL +/- TRAIL. Additional investigations, incorporating the pro-calcific inducer β -glycerophosphate and the key paracrine signalling molecule BMP-2, were also employed to better define the pro-calcific events surrounding RANKL exposure in the vascular media.

3.4.1 The Effects of RANKL +/- TRAIL on the Expression of HASMC Gene Targets

RANKL +/- TRAIL exposure exerted several effects on the expression of HASMC gene targets following 72 hours' incubation. RANKL treatment was found to dose-dependently decrease OPG mRNA, and increase Runx2 transcription factor expression at 25 ng/mL (Figure 3.6A), while having no effect on ALP/BMP-2 transcript levels (Appendix 3.7A (i), (ii)) or Sox9 mRNA expression (data not shown). TRAIL treatment, on the other hand, had no effect on OPG mRNA expression, nor did it interfere with the RANKL-induced downregulation of OPG. TRAIL did, however, decrease Runx2 mRNA by approximately 40%, and maintained a 30% decrease in Runx2 expression following co-incubation with 5 ng/mL RANKL. Again, no changes in ALP or Sox9 transcript expression were noted in response to TRAIL, but TRAIL significantly decreased the abundance of BMP-2 transcripts by approximately 30% (although this trend was not maintained with RANKL co-incubation). Interestingly, with regard to IL-6, both RANKL (25 ng/mL) and TRAIL (5 ng/mL) increased mRNA levels by approximately 1.5-fold, inducing an additive effect with co-treatment (Appendix 3.7A (iii)).

Core gene targets were also assessed following 24 hours' exposure to RANKL, to address inconsistencies between mRNA and protein trends (see Section 3.4.2). Interestingly, while BMP-2, ALP and Sox9 mRNA showed no change at 72 hours, all three pro-calcific genes were upregulated following 24 hours' exposure. While BMP-2 and Runx2 transcripts were decreased in response to TRAIL at 72 hours, no change was noted in either gene at the earlier time-point of 24 hours (Appendix 3.8A). With regard to OPG, a more detailed investigation (including a 48-hour time point) was executed in an attempt to explain the complex regulation of OPG at a protein level (see Section 3.4.2). In this case, while TRAIL had no effect, RANKL induced an increase in OPG expression at 24 hours, returned to baseline at 48 hours, and ultimately decreased mRNA expression levels at a 72-hour time point (Appendix 3.8B).

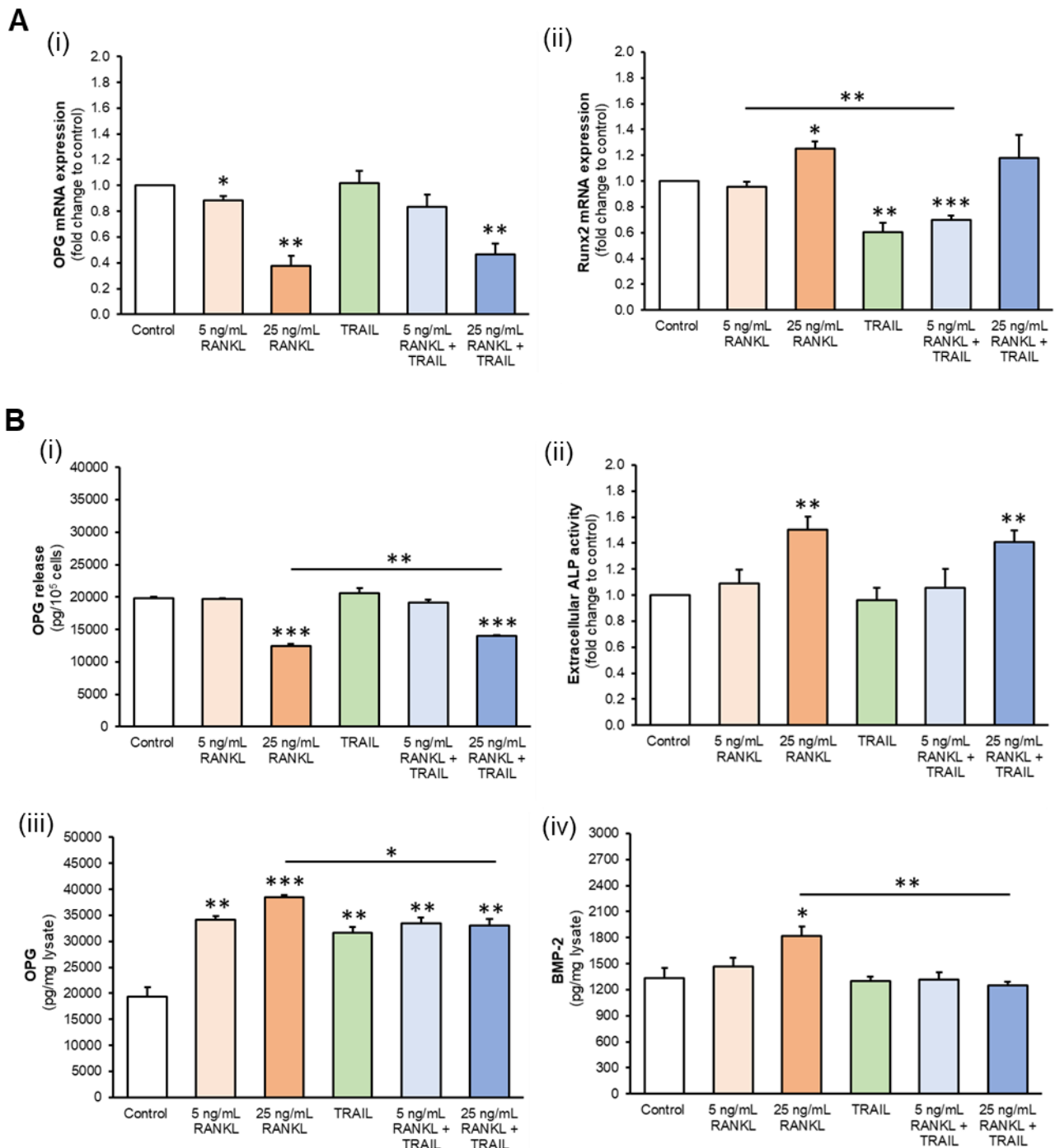


Figure 3.6. mRNA and protein analyses in HASMC monoculture. HASMCs were exposed to RANKL (5-25 ng/mL) +/- TRAIL (5 ng/mL) for 72 hours. (A) mRNA expression of (i) OPG and (ii) Runx2 were analysed by RT-qPCR; GAPDH was employed as an endogenous control. (B) (i) OPG and (ii) active ALP release were analysed by ELISA and activity assay respectively, and normalised to 10⁵ cells. Intracellular levels of (iii) OPG and (iv) BMP-2 were analysed by ELISA, normalised to total protein. * $p < 0.05$; ** $p < 0.01$; *** $p < 0.001$ compared to untreated control unless otherwise stated; bars indicate statistical significance between treatment groups.

3.4.2 The Effects of RANKL +/- TRAIL on the Expression of HASMC Protein Targets

Pertaining to extracellular protein trends, OPG (released at substantially higher levels in HASMCs than HAECs) was noted to be significantly decreased following exposure to 25 ng/mL RANKL (Figure 3.6B (i)). TRAIL treatment had no effect on OPG release, either alone or in combination with RANKL. Active ALP was also increased in the conditioned media following 25 ng/mL RANKL exposure, both alone and following co-exposure with TRAIL (Figure 3.6B (ii)). BMP-2, secreted at lower levels from HASMCs than in the vascular endothelium, remained unchanged in all cases, while extracellular IL-6 levels were elevated by 25 ng/mL RANKL both alone and in combination with TRAIL (Appendix 3.7C). Intracellularly, RANKL exposure dose-dependently increased OPG production. OPG was also induced by TRAIL, but no additive effect was noted with co-treatment; rather, TRAIL significantly diminished the effect of 25 ng/mL RANKL in this case (Figure 3.6B (iii)). Interestingly, RANKL induced BMP-2 protein levels at 25 ng/mL concentration, and while TRAIL itself had no effect, co-treatment resulted in complete attenuation of RANKL-induced BMP-2 translation (Figure 3.6B (iv)). No effects were noted in intracellular ALP activity under any of the conditions tested (Appendix 3.7B).

3.4.3 The Effects of RANKL +/- TRAIL on NF- κ B Activation

Recombinant RANKL, at both 5 and 25 ng/mL concentrations, significantly induced activation of both canonical and non-canonical NF- κ B signalling in smooth muscle cells after 72 hours. TRAIL treatment significantly induced canonical activation, but did not exert any significant effects on the non-canonical pathway. Both pathways remained similarly activated in the presence of RANKL + TRAIL (Figure 3.7).

3.4.4 The Effects of β -glycerophosphate on the Expression of Gene/Protein Targets

In order to profile an established pro-calcific response, HASMCs were exposed to 10 mM β -glycerophosphate, a key driver of calcification, for 72 hours. In this way, the effects of RANKL can be compared to that of a recognised inducer of mineralisation in vascular smooth muscle. As expected, β -glycerophosphate exposure significantly upregulated BMP-2, ALP, Runx2 and Sox9 at an mRNA level (Appendix 3.9A), while also increasing intracellular and extracellular levels of BMP-2 and ALP activity (Appendix 3.9B, C). β -glycerophosphate did not induce

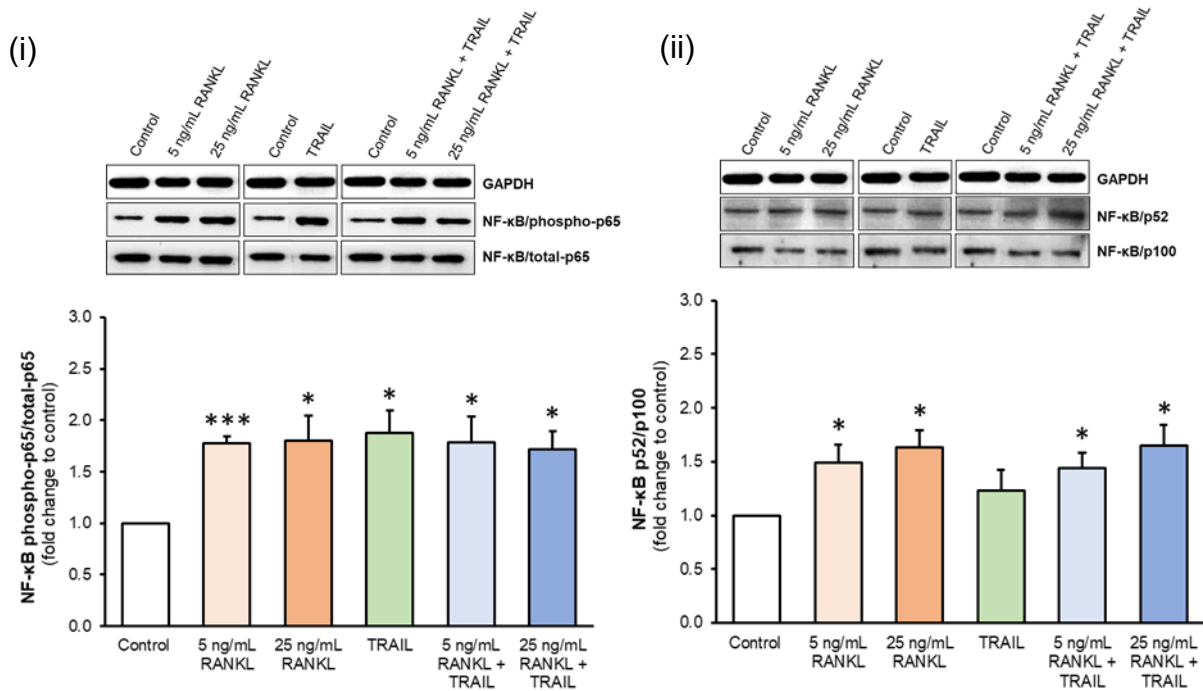


Figure 3.7. NF-κB activation in HASMC monoculture following RANKL +/- TRAIL treatment. HASMCs were exposed to RANKL (5-25 ng/mL) +/- TRAIL (5 ng/mL) for 72 hours. (i) Non-canonical and (ii) canonical NF-κB activation were determined by Western blotting, and analysed by scanning densitometry normalised to GAPDH. Blots are representative. * $p < 0.05$; *** $p < 0.001$ compared to untreated control.

activation of either the canonical or non-canonical NF-κB pathways or IL-6 regulation in HASMCs (data not shown). Interestingly, OPG release, intracellular production, and mRNA expression were significantly increased following β -glycerophosphate exposure (Appendix 3.9D). HASMC exposure to β -glycerophosphate for 72 hours did not exert any significant effects on cell morphology, viability or apoptosis, nor did it affect the suitability of GAPDH/S18 endogenous controls employed in qPCR (data not shown).

3.4.5 The Effects of BMP-2 +/- Noggin on the Expression of HASMC Gene/Protein Targets

To confirm the pro-calcific effects of paracrine BMP-2 signalling from the endothelium to smooth muscle, recombinant BMP-2 and the BMP inhibitor, noggin, were employed in HASMC monoculture. Recombinant BMP-2, at 5 ng/mL, was found to significantly increase ALP, Runx2 and Sox9 mRNA in HASMCs after 72 hours. Co-incubation with noggin (100 ng/mL) was found to completely attenuate the pro-calcific influence of BMP-2 at a transcriptional level (Appendix 3.10A). Interestingly, while a non-significant increase was noted in extracellular ALP activity following BMP-2 exposure, co-treatment with noggin

reduced active ALP by approximately 50% compared to control (Appendix 3.10B). Post-treatment increases in intracellular ALP and BMP-2 were also significantly reduced and completely attenuated by noggin co-exposure, respectively (Appendix 3.10C). BMP-2 exposure did not induce activation of either the canonical or non-canonical NF- κ B pathway (Appendix 3.10D), nor did it affect OPG (mRNA/protein) or IL-6 release (data not shown). Again, regarding preliminary controls, BMP-2 and/or noggin did not exert any significant effects on cell morphology, viability, apoptosis, or the expression of smooth muscle markers SM α -actin and SM22 α . GAPDH/S18 were also confirmed to be suitable reference genes for BMP-2/noggin analyses.

3.4.6 HASMC Monoculture: Summary of Results

The expression levels of several indices were altered in response to RANKL +/- TRAIL treatment in HASMCs, as summarised in Table 3.3 below.

Table 3.3. The effects of RANKL +/- TRAIL in HASMC monoculture.

		RANKL (25 ng/mL)	TRAIL (5 ng/mL)	RANKL + TRAIL
BMP-2	<i>mRNA</i>	–	↓	–
	<i>Intracellular Protein</i>	↑	–	–
ALP	<i>Extracellular Activity</i>	↑	–	↑
OPG	<i>mRNA</i>	↓	–	↓
	<i>Extracellular Protein</i>	↓	–	↓
	<i>Intracellular Protein</i>	↑↑	↑	↑
IL-6	<i>mRNA</i>	↑	↑	↑↑
	<i>Extracellular Protein</i>	↑	–	↑
Runx2	<i>mRNA</i>	↑	↓	–
NF-κB (p52/p100)	<i>Activation</i>	↑	–	↑
NF-κB (p-p65/t-p65)	<i>Activation</i>	↑	↑	↑

↑, upregulation; ↑↑, further upregulation relative to corresponding treatment conditions; ↓, downregulation; –, no change. p-p65, phospho-p65; t-p65, total-p65.

3.4.7 Discussion: HASMC Monoculture

The clear majority of VC research to date has been carried out in VSMCs, with varying reports. To our knowledge, however, this study is the first to assess an expansive range of indices within a human primary HASMC population. Although smooth muscle is not generally in direct contact with circulating proteins under healthy physiological conditions, in pathophysiological areas of vascular damage and EC dysfunction *in vivo*, these proteins may penetrate to the medial layer due to an increased endothelial permeability (Review: Sena *et al.*, 2013). Elevated levels of RANKL/TRAIL have been identified in calcified arteries and atherosclerotic plaque (Dhore *et al.*, 2001; Michowitz *et al.*, 2005; Morony *et al.*, 2008; Schoppet *et al.*, 2004). Therefore, it is vital to understand the function of RANKL and TRAIL in the VSMC layer, whereby these proteins may exert direct effects in addition to those paracrine signals induced by HAECs. The key findings from this study (Table 3.3) also aid our understanding of subsequent co-culture models.

There is a large body of literature regarding the effect of RANKL and TRAIL in VSMCs; however, many of these studies will not be drawn on in the current discussion (Byon *et al.*, 2011; Chasseraud *et al.*, 2011; Olesen *et al.*, 2012; Tseng *et al.*, 2010). While some divergences may be explained by a combination of methodological differences (eg. anti-OPG), variations in exposure time/dosage, donor heterogeneity and limitations in the range of calcification indices assessed, we highlight an additional confounder often employed in VC research. A number of researchers employ “calcifying” media with high levels of calcium/phosphate in VSMC studies, in order to induce/enhance mineralisation and pro-calcific responses. The inclusion of these confounders may interfere with the analysis of pro-calcific indices, as they themselves have been shown to induce Runx2, Sox9 and ALP levels (Alesutan *et al.*, 2015). As such, our own series of experiments were specifically conducted in the absence of calcifying media, in order to facilitate a clearer interpretation of HASMC responses to RANKL/TRAIL.

3.4.7.1 The Effects of RANKL +/- TRAIL on Pro-Calcific Targets

BMP-2 is primarily known to act in a paracrine manner on smooth muscle when released from ECs. In agreement with Davenport *et al.* (2016) and Osako *et al.* (2010), we found that BMP-2 is released at significantly lower levels in HASMCs compared to HAECs, and incubation with RANKL and/or TRAIL had no effect on these release levels. Again, RANKL exerted no effect on BMP-2 mRNA level at 72 hours, but significantly elevated these levels at the earlier

time point of 24 hours. In agreement, Panizo and colleagues (2009) reported no change in BMP-2 expression in rat VSMCs following 48 hours' RANKL exposure, further suggesting short-term transcriptional regulation. TRAIL, on the other hand, exerted a later response in BMP-2 mRNA and induced a down-regulation at 72 hours. While this reduction in BMP-2 mRNA was not observed in co-incubation with RANKL, TRAIL completely attenuated RANKL-induced intracellular accumulation. This novel finding may indicate a potential storage mechanism for BMP-2 in VSMCs, released under certain inflammatory/atherogenic conditions (Ikeda *et al.*, 2012; Nakagawa *et al.*, 2010; Simões Sato *et al.*, 2014), and although RANKL itself induces BMP-2 production, it does not induce this release. As with HAECs, BMP-2 appears to be regulated at a translational rather than a transcriptional level in HASMCs.

In agreement with Davenport *et al.* (2016), no effects were noted in ALP mRNA expression in response to RANKL/TRAIL in HASMCs at 72 hours, despite significant upregulation at 24 hours. Interestingly, extracellular (but not intracellular) ALP activity was also induced following 72-hour RANKL exposure, both in the presence and absence of TRAIL. Thus, while ALP is induced by RANKL in VSMCs in accordance with the literature (Liu *et al.*, 2014; Morony *et al.*, 2012; Panizo *et al.*, 2009; Yuan *et al.*, 2011; Zhan *et al.*, 2014), this induction is not modulated at a long-term transcriptional level. Furthermore, the observation that ALP activity is only increased following exposure to higher concentrations of RANKL may suggest a dose-dependent response, but may also highlight the significance of endogenous OPG protection in the vasculature *in vivo*. Overall, this data is supportive of a *direct* role for RANKL in VSMC calcification and more specifically a role in paracrine ALP regulation, although TRAIL does not exert a protective influence on RANKL function in VSMCs. We also demonstrate that TRAIL downregulates Runx2 mRNA expression at 72 hours, even in the presence of 5 ng/mL RANKL; while Runx2 has previously been implicated in the VC process/RANKL function in VSMCs (Sun *et al.*, 2012; Zhan *et al.*, 2014), we highlight for the first time the ability of TRAIL to downregulate this osteoblastic transcription factor *in vitro*.

Sox9 chondrocytic transcription factor, although undetectable at an mRNA level in HAECs, was readily detectable in HASMCs. Sox9 has been shown to occur in VSMC calcification, and is associated with many of the same gene/protein alterations as osteogenic differentiation (Speer *et al.*, 2009; Tyson *et al.*, 2003). Despite this knowledge, and as a major limitation of the literature to date, Sox9 is rarely employed as a marker of pro-calcific events in VC studies. In this series of experiments, while a non-significant increase was observed at 24 hours following RANKL exposure, neither recombinant protein affected Sox9 transcript expression

at 72 hours. This may suggest that HASMCs are not directly induced to express chondrocytic genes/proteins following exposure RANKL, or it may suggest a complete dependence on osteoblastic (rather than chondroblastic) transcription factors for calcifying VSMCs. To date, the role of Sox9 in the calcification process remains under debate (Speer *et al.*, 2009), but we propose that RANKL does not induce long-term Sox9 upregulation in VSMCs.

In order to profile a well-defined pro-calcific insult on HASMCs in monoculture, the calcification inducer β -glycerophosphate was employed for a series of control experiments (Shioi *et al.*, 1995). β -glycerophosphate was found to significantly induce all pro-calcific indices, confirming the suitability of these targets in assessing osteoblastic activity in smooth muscle. As an additional control, we investigated the effects of BMP-2 directly on HASMCs to provide preliminary insight into the potential for endothelial BMP-2 paracrine regulation in co-culture. In this case, ALP, Runx2 and Sox9 mRNA, alongside ALP/BMP-2 protein, were upregulated, and subsequently reduced/abrogated by the BMP inhibitor noggin (Krause *et al.*, 2011). Thus, endothelial paracrine BMP-2 signalling is likely to regulate these pro-calcific indices in smooth muscle both in co-culture and *in vivo*.

3.4.7.2 The Effects of RANKL +/- TRAIL on OPG Regulation

OPG, given its established role as a cardioprotective decoy receptor for RANKL and TRAIL (Collin-Osdoby, 2004; Emery *et al.*, 1998), was also assessed in HASMCs. Initially, HASMCs were noted to produce and release far greater amounts of OPG than HAECs after 72 hours, supporting the common observation that the VSMC layer is the dominant source of vascular OPG (Corallini *et al.*, 2009; Davenport *et al.*, 2016). However, as optimal RANKL/TRAIL conditions were determined in endothelial monoculture (with co-culture in mind as an end goal), and both proteins have also been shown to exert physiological responses *in vivo* despite the presence of endogenous OPG (Carbone *et al.*, 2016; Secchiero *et al.*, 2006), no action was taken to neutralise this decoy ligand. Moreover, the expression of multiple pro-calcific indices were altered in response to treatment, further supporting the ability of RANKL/TRAIL to function in the presence of substantial OPG release. Therefore, while OPG can readily bind and neutralise these proteins, recombinant RANKL/TRAIL likely exert their function uninhibited prior to OPG release and subsequent neutralisation.

In the current study, RANKL was found to decrease OPG mRNA and release, while TRAIL exposure had no effect either alone or in combination with RANKL. Interestingly, however,

RANKL and TRAIL both induced intracellular OPG production. This data may suggest alternate OPG regulatory mechanisms for both RANKL and TRAIL; as such, we propose that RANKL may block OPG release without affecting protein turnover, while TRAIL may enhance intracellular production as part of a protective storage mechanism. While TRAIL somewhat depletes RANKL-dependent intracellular accumulation of OPG, it has no effect on RANKL-inhibited OPG release, and therefore exerts minimal biological significance by way of protection against RANKL. However, no studies to our knowledge yet describe the effects of RANKL/TRAIL on OPG production in VSMCs, and so this theory cannot be confirmed.

In order to further delineate these complex trends, we assessed OPG mRNA expression at the shorter time-point of 24 hours. In this instance, while TRAIL alone had no influence, RANKL exerted a clear bimodal effect on OPG transcription, inducing OPG mRNA at 24 hours and decreasing it at 72 hours. This novel finding may highlight the potential differential effects of RANKL on OPG regulation over time, inducing a protective upregulation in acute vascular injury (potentially to protect from further damage), but exerting a long-term downregulation and depletion of OPG in chronic conditions such as VC. As a further point of interest, the calcification inducer β -glycerophosphate was noted to induce OPG at both a transcriptional and translational level, most likely as a protective mechanism to prevent inflammation and blood vessel damage similar to that of early RANKL exposure. Of importance, circulating OPG has been widely claimed to be elevated in vascular pathologies (Abedin *et al.*, 2007; O'Sullivan *et al.*, 2010; Schoppet *et al.*, 2003), consistent with that of β -glycerophosphate exposure. In this way, elevated OPG may function as a biomarker for VC while its depletion in the vasculature contributes to damage and calcification. Also of note, BMP-2 exposure had no effect on HASMCs, suggesting that OPG is not regulated by endothelial paracrine signalling.

Upon reflection, we present the first novel evidence that RANKL exerts a clear pro-calcific effect in HASMCs through maintained suppression of its own decoy receptor, allowing unopposed RANKL function to ensue. TRAIL, on the other hand, exerts minimal effect on OPG regulation in HASMCs, and does not attenuate RANKL-induced OPG depletion. It is unlikely that the proposed protective nature of TRAIL is attributable to OPG regulation, as this intracellular OPG is unavailable to bind to recombinant RANKL. However, both RANKL and TRAIL play a clear role in the complex modulation of OPG in HASMCs, in a different manner to their role in the endothelium. It is obvious that, due to the quantity of OPG produced and released, HASMCs are a key influencer in the development and progression of vascular complications.

3.4.7.3 The Effects of RANKL +/- TRAIL on NF- κ B Activation

Although we suggest a role for the non-canonical NF- κ B/p52 pathway in RANKL-induced calcification and TRAIL-mediated vasoprotection in HAECs, the function of NF- κ B in HASMCs is less clear. Both RANKL and TRAIL were shown to activate both the canonical and non-canonical NF- κ B pathway in smooth muscle, with TRAIL exerting no inhibition on RANKL-induced activation. We have confirmed that HASMCs express surface receptors for RANKL/TRAIL binding and NF- κ B activation, however, due to the inflammatory and proliferative roles for NF- κ B in VSMCs (Brasier, 2010; Mehrhof *et al.*, 2005), it is difficult to determine if the result of this activation is pro-calcific. We did, however, note that the calcification inducer β -glycerophosphate did not activate either pathway in HASMCs, nor did BMP-2, which may be suggestive that NF- κ B is *not* involved in VSMC calcification, although this finding would contradict the literature (Hénaut *et al.*, 2016; Landry *et al.*, 1997; Song *et al.*, 2017). While this may hold true for TRAIL, with its pre-established role in VSMC inflammation and proliferation (Kavurma *et al.*, 2008; Song *et al.*, 2011), RANKL activation of NF- κ B has already been implicated in VSMC calcification (Panizo *et al.*, 2009; Zhan *et al.*, 2014). What therefore appears more likely is that both NF- κ B pathways may be involved in RANKL-induced pro-calcific induction in HASMCs, but not involved in β -glycerophosphate induction (perhaps due to the absence of direct RANKL:RANK binding).

3.4.7.4 Summary: HASMC Monoculture

In a study assessing the widest range of calcification indices to date, we note that the pro-calcific nature of RANKL and the proposed protective effect of TRAIL in HASMCs is minimal compared to that observed in HAECs. We further note that, while TRAIL attenuates RANKL-induced NF- κ B signalling in endothelial cells, it does not exert the same effect in HASMCs, instead activating both NF- κ B pathways alongside RANKL. The absence of BMP-2 release was also noted in HASMCs in response to RANKL, supporting the one-way paracrine relationship between the endothelium and smooth muscle as proposed by Davenport *et al.* (2016) and Osako *et al.* (2010). We conclude that RANKL and TRAIL exert direct effects on VSMCs when in contact during vascular damage, even in the presence of excess endogenous OPG, potentially influencing the progression of VC in these areas.

3.5 HAEC:HASC Co-culture

Finally, HAECs and HASMCs were employed in co-culture to better recapitulate the paracrine communication that exists between the endothelium and smooth muscle *in vivo*. Within the semi-permeable transwell insert, HAECs were exposed to RANKL +/- TRAIL (Figure 3.8), and the underlying smooth muscle cells in the basal compartment were harvested for analysis. Paracrine signalling proteins

present in the subluminal conditioned media, along with HASMC mRNA/lysate, were analysed as appropriate for transcriptional and translational changes in response to endothelial communication. Additional control investigations, including the incorporation of the BMP inhibitor noggin, were also employed to support the theoretical basis surrounding this model.

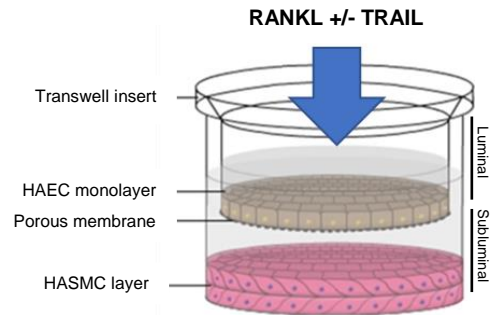


Figure 3.8. The co-culture model. HAECs in semi-permeable transwell inserts, suspended above a confluent smooth muscle layer, were exposed to RANKL +/- TRAIL for 72 hours.

3.5.1 The Effects of RANKL +/- TRAIL on the Expression of HASMC Gene Targets

Endothelial RANKL +/- TRAIL treatment was found to regulate several gene targets in the underlying HASMC layer. Firstly, RANKL exposure significantly increased ALP transcript expression; TRAIL treatment alone downregulated ALP mRNA by approximately 10%, and completely attenuated RANKL-induced expression at both concentrations (Figure 3.9 (i)). Similarly, Sox9 mRNA expression was also dose-dependently upregulated in HASMCs following endothelial RANKL treatment, and co-exposure with TRAIL exhibited complete blockade of this effect (Figure 3.9 (iii)). Thirdly, OPG mRNA levels were dose-dependently decreased following RANKL exposure, and again this expression was entirely recovered with TRAIL co-treatment (Figure 3.9 (ii)). RANKL/TRAIL treatment had no effect on BMP-2/Runx2 mRNA expression in co-culture (Appendix 3.11A).

3.5.2 The Effects of RANKL +/- TRAIL on the Expression of HASMC Protein Targets

With regard to extracellular protein in the subluminal space, endothelial treatment with RANKL was found to induce ALP and BMP-2 secretion at 5 and 25 ng/mL respectively, while TRAIL co-treatment attenuated these effects (Figure 3.10A (i), (ii)). As expected, these trends resemble that of endothelial treatment in monoculture, but may be altered by the co-secretion

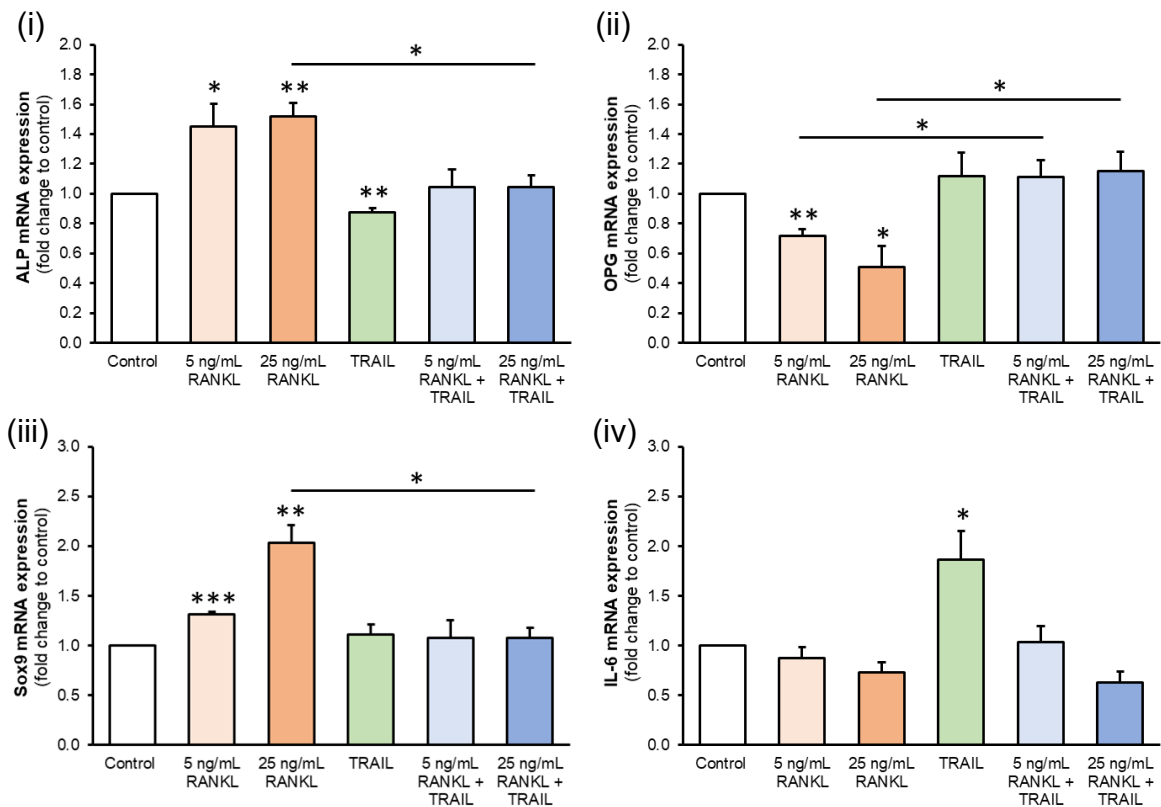


Figure 3.9. mRNA analyses of HASMCs in co-culture. HAECs in transwell inserts were exposed to RANKL (5-25 ng/mL) +/- TRAIL (5 ng/mL) for 72 hours. HASMCs in the subluminal compartment were assessed for mRNA expression of (i) ALP, (ii) OPG, (iii) Sox9 and (iv) IL-6 by RT-qPCR; GAPDH was employed as an endogenous control. * $p < 0.05$; ** $p < 0.01$; *** $p < 0.001$ compared to untreated control unless otherwise stated; bars indicate statistical significance between treatment groups.

of these molecules from underlying HASMCs. RANKL was also found to induce OPG secretion at both 5 and 25 ng/mL (Figure 3.10A (iii)), and while TRAIL alone had no effect, co-exposure with TRAIL completely attenuated RANKL-induced OPG release. Due to the almost negligible levels of OPG secreted by HAECs when exposed to RANKL +/- TRAIL, it can be expected that this trend is due to smooth muscle OPG release rather than that of the endothelial monolayer. Furthermore, while RANKL (25 ng/mL) and TRAIL (5 ng/mL) induced an apparent increase and decrease in IL-6 release respectively, no change was noted in co-treatment compared to control, and these effects remained non-significant (Figure 3.10A (iv)). It is noteworthy that both BMP-2 and IL-6 release levels are present at considerably elevated levels compared to that measured in endothelial/smooth muscle monocultures; this highlights the combined secretion of these proteins from both ECs and VSMCs in co-culture.

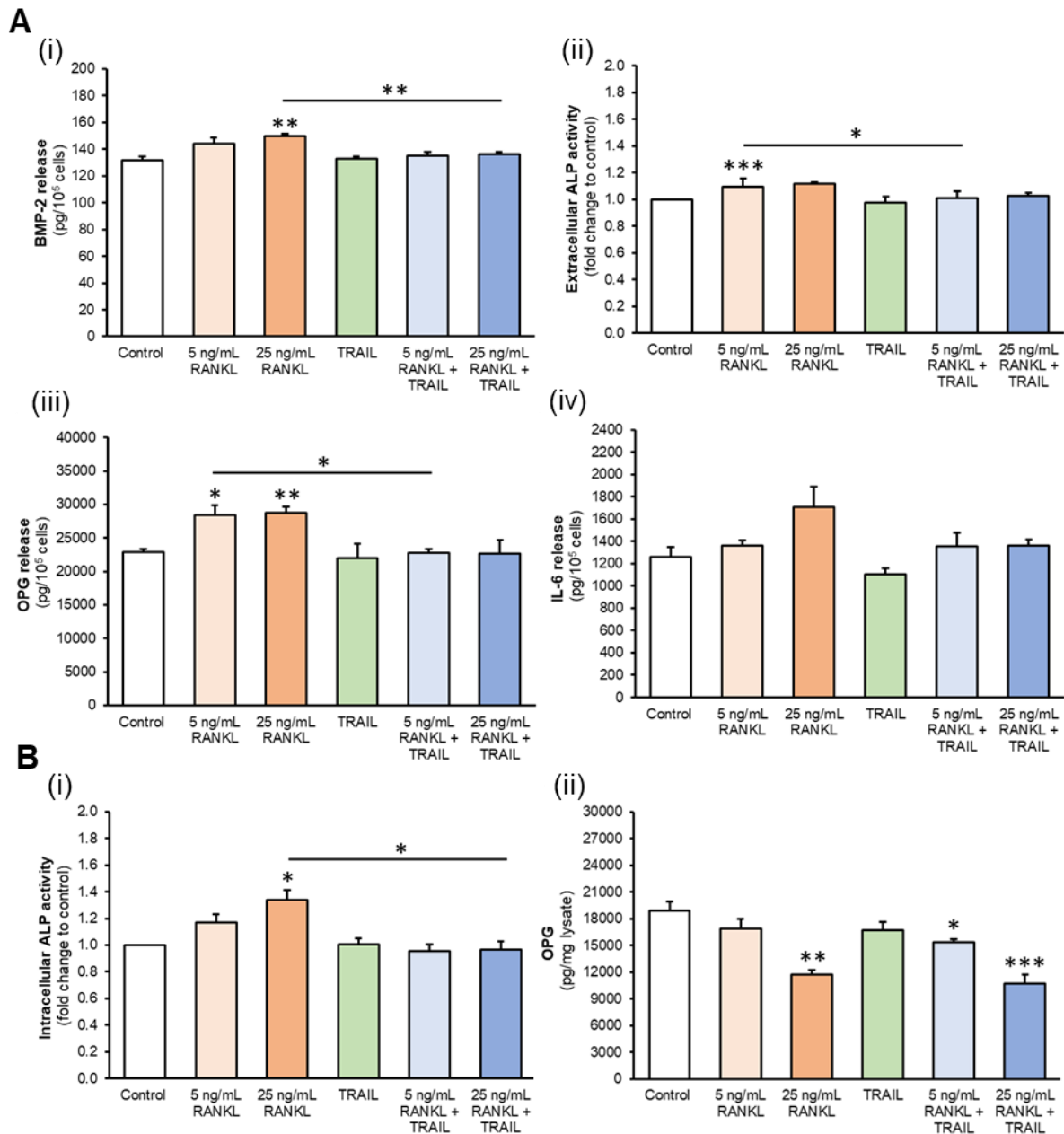


Figure 3.10. Analysis of protein targets in co-cultured HASMCs. HAECs in transwell inserts were exposed to RANKL (5-25 ng/mL) +/- TRAIL (5 ng/mL) for 72 hours. In the subluminal HASMC compartment, (A) (i) BMP-2, (ii) ALP, (iii) OPG and (iv) IL-6 release levels were measured, while (B) intracellular (i) ALP and (ii) OPG were determined in HASMC lysate. BMP-2, OPG and IL-6 levels were analysed by ELISA, while ALP activity was determined by activity assay. Conditioned media and lysate analyses were normalised to 10⁵ cells and total intracellular protein respectively. * $p < 0.05$; ** $p < 0.01$; *** $p < 0.001$ compared to untreated control unless otherwise stated; bars indicate statistical significance between treatment groups.

Regarding intracellular protein, active ALP levels in HASMCs were dose-dependently induced by RANKL, while TRAIL co-treatment again abrogated this effect (Figure 3.10B (i)). However, the reduction in smooth muscle OPG intracellular production following RANKL treatment was not significantly affected by TRAIL (Figure 3.10B (ii)). Furthermore, intracellular BMP-2 levels in HASMCs were not affected by endothelial exposure to either recombinant ligand either alone or in co-treatment (Appendix 3.11B).

As an additional control, endothelial conditioned media transfer experiments were employed as an alternative to non-contact co-culture, to confirm that endothelial paracrine signalling was indeed responsible for the observed HASMC responses. In this case, HAECs were exposed to RANKL (5-25 ng/mL) for 72 hours, conditioned media harvested and applied at a 1:1 ratio to reporter HASMCs for a further 72 hours prior to media/lysate harvesting. Following HASMC exposure, extracellular BMP-2 and ALP were dose-dependently induced by RANKL exposure, exhibiting the same trends as noted in both endothelial monoculture and co-culture. OPG release trends, however, mirrored that of HASMC monoculture, and were decreased following endothelial treatment with 25 ng/mL RANKL (Appendix 3.12A). Intracellular levels of BMP-2, ALP and OPG were dose-dependently increased following HAEC exposure to RANKL, reflecting trends noted in smooth muscle monoculture (BMP-2, OPG) and co-cultured HASMCs (ALP) (Appendix 3.12B).

3.5.3 The Effects of RANKL +/- TRAIL on HASMC NF- κ B Activation

Despite potent effects of RANKL and TRAIL exposure on NF- κ B activation in endothelial/smooth muscle monocultures, no significant effects on either canonical or non-canonical pathways were noted in co-cultured HASMCs (Appendix 3.11C). Furthermore, in the aforementioned conditioned media transfer control, no effects were noted in either canonical or non-canonical NF- κ B activation when exposed to endothelial conditioned media (Appendix 3.12C).

3.5.4 The Effects of RANKL +/- Noggin on the Expression of HASMC Targets

To determine the extent to which endothelial-secreted BMPs are responsible for smooth muscle responses in co-culture, noggin BMP inhibitor was employed. As before, HAECs cultured in transwell inserts were exposed to RANKL (5-25 ng/mL) for 72 hours, while noggin (100 ng/mL) was added to the subluminal compartment to neutralise BMP paracrine signals. Again, endothelial exposure to RANKL dose-dependently increased ALP and decreased OPG mRNA expression in HASMCs; co-incubation with noggin BMP inhibitor neutralised the effects of RANKL on ALP, but not OPG, at a transcriptional level (Appendix 3.13A).

With regard to extracellular protein, a similar trend was observed; while RANKL dose-dependently increased and decreased active ALP and OPG release respectively, noggin co-

treatment in the subluminal compartment completely abrogated RANKL-induced ALP activity but did not affect depletion of extracellular OPG (Appendix 3.13B). Interestingly, both RANKL-induced ALP activity and OPG production in HASMC lysate were completely attenuated by co-incubation with noggin in co-culture (Appendix 3.13C). No effects were noted in Runx2 or Sox9 mRNA expression with noggin addition (data not shown).

3.5.5 HAEC:HASMC Co-culture: Summary of Results

The expression of several pro-calcific indices were altered in HASMCs in response to endothelial RANKL +/- TRAIL treatment, as summarised in Table 3.4 below.

Table 3.4. The effects of RANKL +/- TRAIL in HAEC:HASMC co-culture.

		RANKL (25 ng/mL)	TRAIL (5 ng/mL)	RANKL + TRAIL
BMP-2	<i>Extracellular Protein</i>	↑	–	–
ALP	<i>mRNA</i>	↑	↓	–
	<i>Extracellular Activity</i>	↑ ^δ	–	–
	<i>Intracellular Activity</i>	↑	–	–
OPG	<i>mRNA</i>	↓	–	–
	<i>Extracellular Activity</i>	↓	–	–
	<i>Intracellular Activity</i>	↓	–	↓
IL-6	<i>mRNA</i>	↓ ^δ	↑	↓ ^δ
	<i>Extracellular Activity</i>	↑ ^δ	↓ ^δ	–
Sox9	<i>mRNA</i>	↑	–	–

↑, upregulation; ↓, downregulation; –, no change. ^δ, not significant.

3.5.6 Discussion: Co-culture

Co-culture models have previously been employed to investigate the paracrine contribution of various cell types to VSMC calcification (Deuell *et al.*, 2012; Shin *et al.*, 2004), overcoming important limitations of traditional monoculture investigations (Chiu *et al.*, 2009; Eddahibi *et al.*, 2006; Redmond *et al.*, 1995). The importance of paracrine mediation in maintaining vascular function has been highlighted previously, both in (patho-)physiological processes in general and more specifically within the context of RANKL signalling (Ardanaz *et al.*, 2006; Davenport *et al.*, 2016; Osako *et al.*, 2010; Rongen *et al.*, 1994). Given the conflicting evidence reported across endothelial and smooth muscle cell monoculture studies, a comprehensive co-culture model employing primary human vascular cells was clearly warranted. Again, co-culture experiments were conducted in the absence of pro-calcifying media and anti-OPG, maintaining maximal physiological relevance. As circulating RANKL and TRAIL are primarily in contact with the endothelial layer *in vivo*, and calcification ultimately occurs in medial smooth muscle, crucial paracrine signalling elements between the two cell types are undoubtedly central to the manifestation and progression of VC. These paracrine signals (released from the apical endothelial monolayer and functioning on the underlying smooth muscle) were assessed, alongside the effects of these signals on smooth muscle pro-calcific indices. In this respect, the pro-calcific role of RANKL and the potential protective role for TRAIL in the vasculature were investigated (results summarised in Table 3.4).

3.5.6.1 The Effects of RANKL +/- TRAIL on Endothelial Paracrine Signalling

Although the presence of paracrine communication within the vascular wall is well established, few studies to date have directly implicated endothelial BMP-2 as a potent mediator of RANKL-induced VSMC calcification. Two key studies in EC/VSMC monoculture and co-culture, by Osako *et al.* (2010) and Davenport *et al.* (2016) respectively, contributed greatly to the formation of our hypothesis. Both studies agree that endothelial release of paracrine proteins in response to RANKL subsequently induce a pro-calcific response in smooth muscle, attributable (at least in part) to BMP-2. As expected in this case, and in agreement with these studies, RANKL-induced endothelial BMP-2 release observed in HAEC monoculture was also apparent in the subluminal space in co-culture, although at a higher baseline level due to HASMC secretion. Furthermore, RANKL-induced ALP activity in the conditioned media, as a potential influencer of HASMC calcification, also displayed a similar trend in co-culture. As a key finding of this study, TRAIL co-incubation in co-culture was found to *completely*

attenuate RANKL-induced BMP-2/ALP release, enhancing the physiological relevance of this novel finding. As noted, Osako and colleagues (2010) were the first research group to study in detail the role of BMP-2 in the calcification process, providing evidence that RANKL induces endothelial BMP-2 secretion while HASMCs separately stimulated by BMP-2 acquire significant osteoblastic phenotypic alterations after 72 hours. In the study by Osako and colleagues (2010), however, a number of limitations were observed; calcifying growth media was employed, cells were assessed in isolation rather than in co-culture, and a small range of calcification indices were analysed at a transcriptional level only. Furthermore, the potential protective effects of TRAIL on HASMC calcification were not considered.

In light of these limitations, Davenport and co-workers (2016) completed a more advanced series of experiments with a focus on BMP-2 signalling. Firstly, a conditioned media model was employed whereby reporter HASMCs were exposed to HAEC conditioned media previously treated with RANKL; elevated BMP-2 release was noted from HAECs in response to RANKL, while HASMCs exposed to endothelial conditioned media displayed an increase in pro-calcific indices. Indeed, the conditioned media controls employed in the current study confirmed these results. Secondly, Davenport *et al.* (2016) also employed an advanced perfused capillary co-culture system using the CellMax®Duo bioreactor to investigate endothelial BMP-2 secretion in response to RANKL on HASMC calcification. Again, endothelial RANKL exposure was associated with increased BMP-2 release, and subsequent intracellular pro-calcific responses (ALP, Runx2, BSP upregulation) in co-cultured HASMCs. While our findings agree with these data regarding RANKL/BMP-2, Davenport *et al.* (2016) did not consider co-incubation with TRAIL in these models; we therefore expand on this study by including this co-incubation, and further extending the range of pro-calcific indices examined in both endothelial and smooth muscle cells. Within the current co-culture model, we now highlight for the first time the ability of TRAIL to completely attenuate RANKL-induced endothelial paracrine communication reported by Osako *et al.* (2010) and Davenport *et al.* (2016), shedding novel light on this complex signalling mechanism.

3.5.6.2 The Effects of Endothelial Paracrine Signalling on HASMC Pro-Calcific Indices

Firstly, despite the induction of endothelial BMP-2 when exposed to RANKL, we noted that smooth muscle cell BMP-2 remained unaffected by endothelial paracrine signalling at the transcriptional or the translational level. Also of interest, BMP blockade by the addition of noggin in co-culture induced BMP-2 mRNA and protein production, which may suggest that

HASMCs are not totally exempt from BMP-2 regulation in the vasculature. Regarding ALP, both mRNA expression and intracellular activity in HASMCs were induced by endothelial RANKL and subsequently attenuated by TRAIL co-treatment. This trend was also noted in the subluminal compartment, with ALP levels ascribed to both luminal HAECs and subluminal HASMCs. Intracellular ALP was similarly induced by HAEC conditioned media transfer in response to RANKL and attenuated at both a transcriptional and translational level when noggin was employed in co-culture. Taken together, this data strongly indicates that BMP signalling mediates the expression and production of ALP in medial HASMCs, with RANKL inducing endothelial BMP-2 paracrine signalling and ultimately smooth muscle ALP activity. We also illustrate for the first time that *endothelial co-incubation with TRAIL completely attenuates RANKL-induced ALP activity in the underlying smooth muscle*, most likely due to blockade of paracrine BMP-2. Comparatively, Osako *et al.* (2010) have previously noted that smooth muscle ALP mRNA was significantly increased following exposure to BMP-2, while Davenport *et al.* (2016) illustrated that smooth muscle exposure to endothelial conditioned media (+ RANKL) induced extracellular ALP activity and mRNA expression (subsequently blocked by noggin).

Runx2 expression, unlike ALP, was not mediated in the smooth muscle cell layer by endothelial paracrine signalling nor was it affected by noggin co-incubation; this finding indicates that HAEC communication does not modulate this osteogenic transcription factor in medial smooth muscle. Contrastingly, however, Runx2 was found to be induced in HASMCs following exposure to HAEC-conditioned media *and* in RANKL-treated capillary co-culture (Davenport *et al.*, 2016). This starkly conflicting data in extremely similar cell models is difficult to interpret. Focusing on the conditioned media model in isolation, it may be again possible that residual RANKL in the media is exerting direct effects on HASMC Runx2 expression, given that RANKL directly upregulates this transcription factor in monoculture. Indeed, given the extensive preliminary experiments conducted, the employed co-culture model does not allow the transfer of RANKL into the subluminal compartment. Moreover, with regard to the CellMax®Duo model, a higher concentration of RANKL was employed (50 ng/mL), potentially suggesting a dose-dependent effect for Runx2 in co-cultured HASMCs that we do not detect at 25 ng/mL in the current study. Phenotypic variation and donor differences between primary cells employed may also be pertinent in explaining these inconsistencies.

While RANKL-induced endothelial paracrine signalling did not affect osteogenic Runx2 expression in HASMCs, Sox9 chondrogenic transcription factor was significantly upregulated

in smooth muscle following co-culture. Furthermore, this RANKL-induced induction in Sox9 mRNA was completely attenuated by endothelial co-incubation with TRAIL, although TRAIL alone had no effect. Inclusion of noggin in the basal compartment, however, did not attenuate RANKL-induced Sox9 induction. As Sox9 was not induced following direct smooth muscle exposure to RANKL (unlike Runx2), it appears that this factor may be regulated solely through endothelial paracrine signalling. We therefore propose the following: in areas of intact endothelium in the vasculature, the initial differentiation of VSMCs in response to RANKL is predominantly chondrogenic, mediated by endothelial signalling. In areas of damaged endothelium (such as atherosclerotic plaque) where circulating RANKL may be in *direct* contact with HASMCs, Runx2 expression and resulting osteogenic activity may be prominent. In support of this theory, phenotypic alteration of smooth muscle cells in VC has been previously accepted to be chondrogenic rather than osteogenic, and as Runx2 and Sox9 exert many of the same pro-calcific functions (Luo *et al.*, 1997; Speer *et al.*, 2009; Tyson *et al.*, 2003), it may be possible that effects induced by Sox9 may be mistaken for specifically osteoblastic activity. Given that vascular monoculture studies involving Sox9 are extremely limited, and to the best of our knowledge, this is the only vascular co-culture model to date to investigate this protein, there is minimal data available with which to compare this result. Nonetheless, we present novel evidence that *TRAIL has the ability to block RANKL-induced Sox9 expression in HASMCs in co-culture*, not only supporting TRAIL's protective function but implicating Sox9 for the first time in VC pathogenesis.

3.5.6.3 The Effects of Endothelial Paracrine Signalling on HASMC OPG Regulation

In the case of co-culture, the majority of OPG is produced and secreted by HASMCs (Davenport *et al.*, 2016), but again notably different trends were observed when compared to HASMC monoculture. While OPG mRNA levels were similarly downregulated in HASMCs exposed to RANKL, TRAIL co-incubation completely attenuated this effect in co-culture. Furthermore, the *opposite* effects were noted in both intra- and extra-cellular OPG in response to endothelial RANKL exposure in co-culture; RANKL significantly induced OPG release while simultaneously reducing cellular concentration. TRAIL co-incubation fully attenuated this RANKL-induced OPG release, but interestingly, the observed depletion in intracellular protein remained. Given this data, we believe it is possible that OPG release and production are regulated by different paracrine signalling mechanisms in the smooth muscle layer. Interestingly, the inclusion of noggin in the subluminal compartment in co-culture does not

affect RANKL-induced depletion of OPG mRNA/intracellular protein, but does attenuate RANKL-induced OPG release. This finding implicates BMP paracrine signalling in the regulation of OPG secretion (but not transcription/total protein) in HASMCs, and highlights the mechanism by which TRAIL may block this effect. The observed effect of RANKL on intracellular OPG levels, however, remains to be explained, but it is possible that these levels are regulated by another paracrine molecule upon which TRAIL exerts no effect. What is also notable is that RANKL induces the release of neutralising OPG, while TRAIL inhibits this release, despite the “cardioprotective” nature of this protein. It appears, therefore, that endothelial paracrine signalling regulates a natural protective mechanism in HASMCs in response to RANKL (i.e., inducing OPG release), and TRAIL-mediated blockade of these paracrine signals eliminates this effect. This finding therefore uncovers an inherent protective response to counteract RANKL-mediated calcification, in the natural release of a potent decoy receptor for this ligand.

Of interest, neither Osako *et al.* (2010) nor Davenport *et al.* (2016) chose to assess the effects of RANKL/TRAIL on OPG in their models, and indeed both included a neutralising antibody for this protein. While OPG can bind to and attenuate the functions of both RANKL and TRAIL *in vivo*, this neutralisation is dependent on relative circulating concentrations of all three proteins in the triad (Vitovski *et al.*, 2007). We therefore believe that this co-culture study (the first to allow unimpeded OPG regulation) is the most physiologically representative study to date in which the effects of RANKL/TRAIL on the vasculature are assessed. *We present novel evidence that smooth muscle OPG may be induced by RANKL via endothelial paracrine signalling, and that TRAIL co-incubation can attenuate this effect.* This finding may also shed additional light on the regulation of circulating OPG in its role as a biomarker for vascular pathologies (Abedin *et al.*, 2007; O’Sullivan *et al.*, 2010; Schoppet *et al.*, 2003).

3.5.6.4 The Effects of Endothelial Paracrine Signalling on HASMC NF- κ B Activation

To the extent of our knowledge, while many researchers have investigated the *direct* activation of NF- κ B in response to RANKL and TRAIL in smooth muscle, this is the first study to date to assess these effects on HASMCs in co-culture. In this respect, neither the canonical nor the non-canonical pathway were activated in co-cultured HASMCs or in HASMCs exposed to HAEC-conditioned media. This data demonstrates that while endothelial paracrine signalling to the underlying smooth muscle may regulate multiple pro-calcific effects, these signals do not function via activation of NF- κ B. Furthermore, there have been no studies to date

implicating BMP-2 as a modulator of NF- κ B in vascular cells; instead, BMPs are known to function through BMP receptors and activate SMAD signalling (Hruska *et al.*, 2005). While SMAD/NF- κ B crosstalk has been reported in osteoblastic differentiation (Huang *et al.*, 2014; Mao *et al.*, 2016), no studies to date have provided significant evidence of cross-activation in smooth muscle. NF- κ B (particularly the non-canonical pathway) therefore appears to be responsible for the induction of endothelial paracrine signalling in response to RANKL, but *is not involved in underlying smooth muscle pro-calcific responses to HAEC communication.*

3.5.6.5 Summary: Co-culture

Overall, in the first physiologically relevant co-culture model to assess such a wide range of VC-related indices, we provide strong evidence that RANKL treatment of HAECs has putative pro-calcific consequences for osteoblastic activation in underlying smooth muscle, reinforcing the significance of BMP-2 communication made by Osako *et al.* (2010) and Davenport *et al.* (2016). We also present novel and translationally pertinent evidence that TRAIL can block the key paracrine signalling actions of RANKL, exerting a strong protective effect on the vasculature as a whole. We further propose that, while NF- κ B plays a key role in the induction of *endothelial* pro-calcific signalling, these paracrine signals do not directly activate NF- κ B in the underlying HASMC layer; this paracrine signalling does, however, mediate a number of pro-calcific indices directly in the underlying smooth muscle medial layer (Figure 3.11).

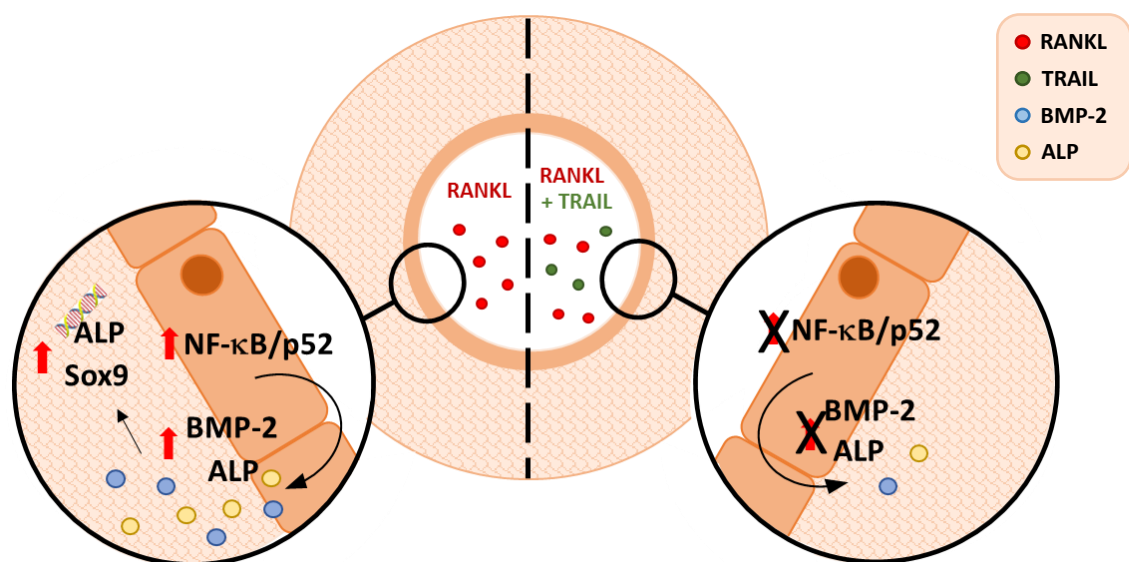


Figure 3.11. Summary of the key responses following endothelial exposure to RANKL +/- TRAIL in co-culture. Endothelial exposure to RANKL activates the non-canonical NF- κ B pathway, and induces BMP-2 and ALP release. These paracrine signals then act on the underlying smooth muscle cells to induce pro-calcific genes. The co-addition of TRAIL, however, attenuates endothelial non-canonical NF- κ B activation and paracrine signalling, thereby preventing the upregulation of smooth muscle pro-calcific genes.

3.6 Alizarin Red S Staining for End-point Calcification

Research presented in the previous sections has profiled the pro-calcific signalling events that occur in the vasculature, ultimately driving calcium deposition and vascular mineralisation. Therefore, Alizarin Red S staining for calcium deposition was next employed, in an attempt to quantify this “end-point” calcification in response to RANKL, and the potential protective effects of TRAIL co-treatment in this respect. Staining was assessed at 0X, 4X and 10X magnification to enable visualisation of extracellular matrix crystallisation.

3.6.1 Alizarin Red S Staining: MC3T3-E1 Pre-osteoblasts

To confirm successful staining, MC3T3-E1 murine pre-osteoblasts were employed as a positive control. Following osteoblastic differentiation, MC3T3-E1 cells were stained, visualised by microscopy, and quantified by absorbance (Figure 3.12A (i), B (i)) as described in Section 2.2.6.1. Compared to undifferentiated controls, differentiated MC3T3-E1 cells displayed significantly higher levels of Alizarin Red S calcium staining. This was accompanied by an increase in pro-calcific ALP, Runx2, BSP and OCN mRNA (Appendix 3.14A) and intracellular ALP activity (Figure 3.12C (i)). Extracellular activity was significantly elevated from day 7 of differentiation (Appendix 3.14B (i)).

3.6.2 Alizarin Red S Staining: HASMCs

HASMCs were also subject to 21 days’ differentiation prior to staining. Differentiated HASMCs revealed a significant 1.4-fold increase in calcium deposition (Figure 3.12A (ii), B (ii)). Again, this was concurrent with elevated intracellular ALP activity (Figure 3.12C (ii)) and extracellular activity from day 7 of differentiation (Appendix 3.14B (ii)). Differentiated HASMCs revealed significant transcriptional downregulation of smooth muscle phenotypic markers SM α -actin and SM22 α , alongside an upregulation of early osteoblastic marker BSP (but not late-stage marker OCN) at 21 days (Figure 3.12D). HASMCs were also exposed to RANKL (5-25 ng/mL) +/- TRAIL (5 ng/mL) for the final 72 hours of differentiation, both in monoculture and co-cultured with HAECs. In each case, neither RANKL nor TRAIL exerted any effect on alizarin red S staining/quantification, and thus calcium deposition (Appendix 3.14C). Moreover, no differential effects were noted in calcium deposition following exposure to BMP-2 +/- noggin under the same circumstances (data not shown).

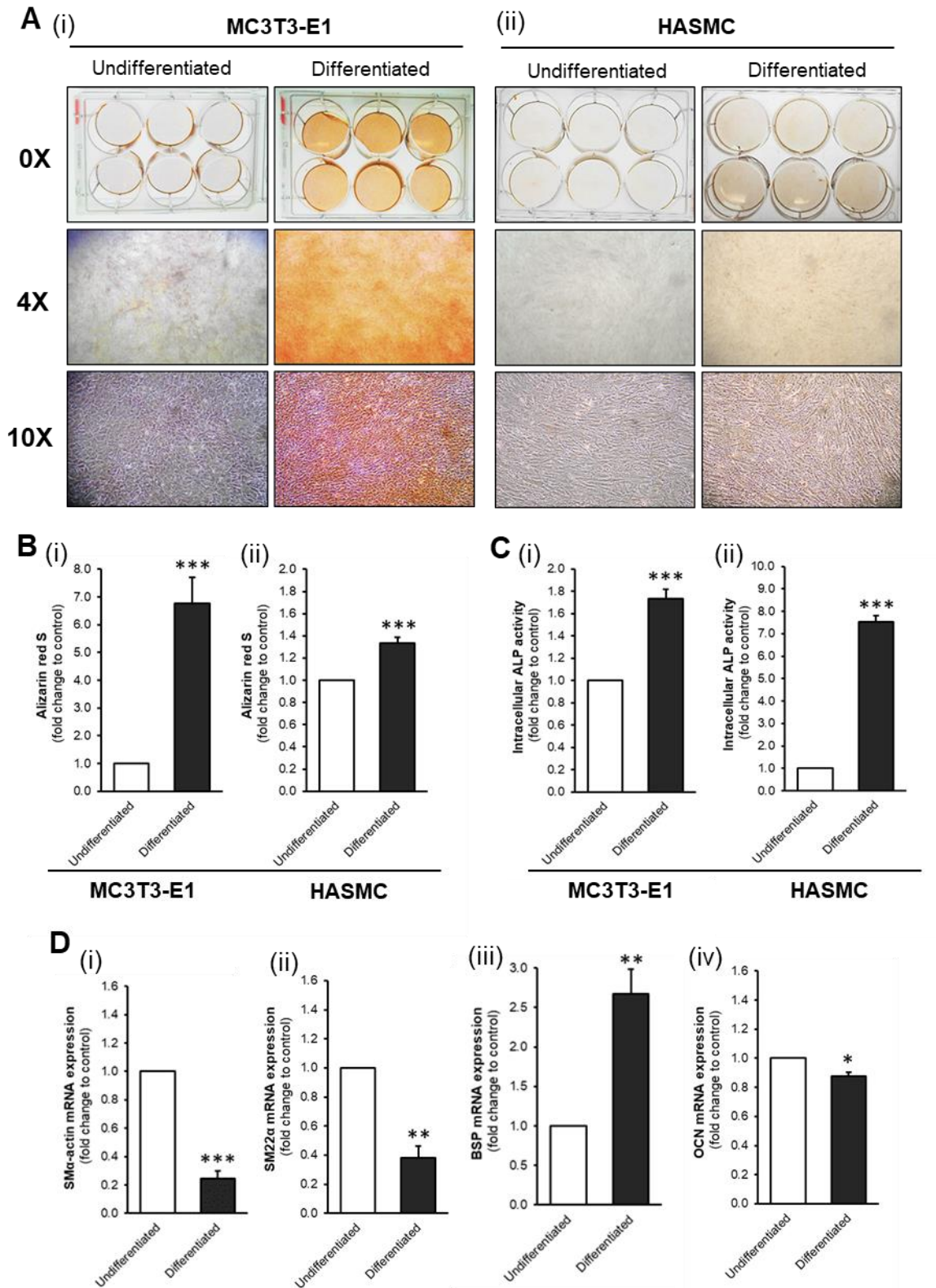


Figure 3.12. Alizarin red staining of differentiated MC3T3-E1 and HASMC cells. MC3T3-E1 and HASMCs were exposed to osteogenic differentiation media for days prior to Alizarin Red S staining and (A) analysis by light microscopy, (B) quantification of staining by absorbance, and (C) analysis of intracellular ALP activity via enzyme assay. (D) mRNA analysis of smooth muscle markers (i) SM22 α and (ii) SM α -actin, and osteogenic differentiation markers (iii) BSP and (iv) OCN, were also analysed by RT-qPCR in HASMCs; GAPDH was employed as an endogenous control. * $p < 0.05$; ** $p < 0.01$; *** $p < 0.001$ compared to undifferentiated cells cultured in control media for 21 days.

3.6.3 Discussion: End-point Calcification

In addition to the wide range of indices assessed at a gene/protein level in mono- and co-culture, Alizarin Red S staining for calcium deposition was also attempted in order to assess the effect of RANKL/TRAIL on end-point calcification in these models. For both MC3T3-E1 pre-osteoblasts and HASMCs, osteoblastic differentiation was carried out for 21 days prior to staining to ensure a positive staining response; indeed, it has been previously shown in the literature that this differentiation step is required to promote a “calcifying” phenotype (Westhrin *et al.*, 2015). Positive staining was achieved in differentiated MC3T3-E1 pre-osteoblasts, indicating a successful staining protocol and the presence of mineral deposits, however staining achieved in HASMCs following 21 days’ osteoblastic differentiation was less robust. Furthermore, no significant differences in calcium deposition were noted in differentiated HASMCs exposed directly to RANKL +/- TRAIL following differentiation either in mono- or co-culture. As noted, a 21-day incubation period has previously been employed for successful staining in VSMCs, and differentiation media components employed have been shown to induce calcification in culture (Ghali *et al.*, 2015; Westhrin *et al.*, 2015).

In light of these controls, it is likely that culture heterogeneity may be a primary contributing factor to the absence of mineralisation in our models. As discussed, HASMCs can vary considerably in their phenotypic state (Speer *et al.*, 2009), and some cultures (donor/location specific) may be more prone to calcification than others. This issue has been raised previously by Olesen *et al.* (2010), who label calcium deposition as an unreliable and unreproducible endpoint with a high degree of variability among donors. Additionally, many Alizarin Red studies to date employ a subset of HASMCs labelled “calcifying” VSMCs that have either been clonally selected for the pro-calcific phenotype or have been directly isolated from previously calcified artery (Luo *et al.*, 2009; Zhan *et al.*, 2014). While these cultures may ensure positive staining, they may mask potential pro-calcific/protective effects of RANKL and TRAIL in the development and progression of VC, as these cells are already in a calcific state.

Despite the absence of positive staining in the current study, the effects of the differentiation process highlight the transition of healthy HASMCs to pro-calcific HASMCs with an osteoblastic phenotype. In this respect, both early (BSP) and late (OCN) markers of this osteogenic process were assessed (Huang *et al.*, 2007), alongside smooth muscle markers SM α -actin and SM22 α (Zhang *et al.*, 2014). Following 21 days’ differentiation, we noted a significant decrease in both smooth muscle markers and an increase in early marker BSP but

not late marker OCN. MC3T3-E1 cells also displayed significant osteoblastic induction, with an increase in ALP, Runx2, BSP and OCN mRNA following differentiation. Both MC3T3-E1 and HASMCs also displayed substantially elevated ALP activity, a crucial marker of osteoblastic function (Shioi *et al.*, 1995), throughout the differentiation process. While both cell types therefore display a clear phenotypic transition towards an osteoblastic calcified cell, we identified an upregulation of the late calcification marker OCN (upregulated alongside mineralisation) only in MC3T3-E1 cells. The lack of OCN expression in HASMCs may further explain the less pronounced staining and end-point calcification, as these cells remain in the early stages of differentiation. Furthermore, in observing the Alizarin Red staining distribution for both cell types post-differentiation, it appears that calcium deposition is distributed evenly throughout the extracellular space. Perhaps with the employment of calcifying VSMCs and/or elevated levels of calcium and phosphate, larger mineralised nodules (such as that previously observed in VSMCs by Hénaut *et al.* (2016)) may become more apparent.

Of additional note, primary mesenchymal stem cells (MSCs) are a common ancestor of both myocytes (muscle cells) and osteocytes/chondrocytes *in vivo*. Differentiation of MSCs are dependent on their location and extracellular environment, and involve distinct processes for each cell type (Chen *et al.*, 2015; Galli *et al.*, 2014; Ullah *et al.*, 2015). It is likely that, once VSMCs differentiate towards a myocytic lineage, they can no longer return to a “pre-differentiated” state to then take on a new calcifying phenotype. Following differentiation/pro-calcific treatment (e.g. β -glycerophosphate, RANKL), these cells may instead display certain characteristics of “pro-calcific” cells (da Silva Meirelles *et al.*, 2006), including the upregulation of osteoblastic/chondroblastic genes/proteins identified throughout this chapter. To establish VC, pro-calcific paracrine signals (e.g., BMP-2) may then go on to influence the osteoblastic differentiation of pre-differentiated MSCs in the vasculature (Wei *et al.*, 2006).

Despite the absence of Alizarin Red staining, our analysis of a wide range of relevant indices provide a well-rounded view of the signalling processes that occur during VC. Assessment of these gene/protein markers are likely more reliable than end-point calcification (Olesen *et al.*, 2010), particularly at the exposure durations employed. While we can confirm that these HASMCs are responsive to an established mineralising stimulus (β -glycerophosphate), it is likely that calcium deposition may take much longer, and the differential effects of RANKL and TRAIL longer still. Undeniably, VC as a chronic condition in type-2 diabetics may take years to develop, but we provide novel evidence profiling the effects of RANKL/TRAIL on the genotypic/phenotypic alterations that contribute to its progression.

3.7 Summary and Conclusions

To summarise, this chapter profiles the effects of RANKL +/- TRAIL on the widest range of pro-calcific indices to date in primary human vascular cells. Not only do we clarify the role of these proteins (both alone and in combination) on the endothelial and smooth muscle layer in isolation, but we integrate the effects of endothelial paracrine signalling in a co-culture model that more closely resembles the structure of the vasculature. Furthermore, we attempt to assess the effects of RANKL and TRAIL on end-point calcium deposition in both cell models. Within these experiments, we eliminate a number of common confounders and limitations of the literature to date, adding novel credibility and physiological pertinence to our findings.

We have confirmed in this chapter that RANKL exerts its previously defined pro-calcific function in endothelial cells, through induction of BMP-2/ALP paracrine signalling to the underlying smooth muscle (Davenport *et al.*, 2016; Osako *et al.*, 2010). We further implicate the non-canonical NF- κ B signalling pathway as the mechanism by which RANKL induces these pro-calcific paracrine signals in the endothelium. Furthermore, and most prominently, we demonstrate for the first time that *TRAIL can completely attenuate RANKL-induced endothelial paracrine signalling, most likely via interference with the non-canonical NF- κ B pathway*. The direct effects of RANKL and TRAIL on HASMCs are vastly different however, with RANKL exerting several direct pro-calcific effects, and TRAIL exerting minimal protection; HASMCs are only in direct contact with circulating proteins in areas of endothelial damage, however, limiting the relevance of this finding to pathologies such as atherosclerosis.

Of relevance, the vast majority of VC research to date does not account for real-time communication between the endothelium and smooth muscle. We therefore employ the first in-depth physiologically relevant vascular model in which to clarify the function of RANKL and TRAIL in calcification. Within this model, we note for the first time that RANKL-induced endothelial paracrine signalling to the underlying smooth muscle layer induces strong pro-calcific effects in the underlying HASMCs, while *TRAIL co-incubation completely attenuates the majority of these effects*.

While end-point calcium staining was also attempted, this data was inconclusive, likely due to the “healthy” nature of our primary HASMCs. As the nature of VC is chronic, however, the pro-calcific effects of RANKL and TRAIL observed may ultimately influence long-term development and progression of calcium deposition. Overall, we provide novel evidence of

RANKL-induced pro-calcific signalling and TRAIL-mediated protection in VC, highlighting in particular the therapeutic potential of TRAIL in this process.

Chapter 4

Profiling the effects of RANKL and TRAIL in vascular cell models under inflammatory and hyperglycemic conditions

4.1 Introduction

4.1.1 Background and Hypothesis Development

Accelerated calcification often accompanying chronic systemic diseases has long been correlated with increased mortality rates, yet the molecular mechanisms underlying this process (that may ultimately lead to timely interventions) have yet to be defined. In Chapter 3, we profiled the pro-calcific effects of RANKL and the hypothesised protective role for TRAIL in the vasculature, highlighting the ability of TRAIL to counteract RANKL-induced calcification. Medial VC, however, in its pathogenesis in type-2 diabetes in particular, occurs alongside elevated blood glucose (hyperglycemia) and often in conjunction with atherosclerotic plaque formation (McCullough *et al.*, 2008). As such, while the effects of RANKL and TRAIL have been profiled in a “healthy” (i.e. non-pathological) environment in Chapter 3, their roles under hyperglycemic (common in diabetes) and pro-inflammatory (present in atherosclerotic plaque) conditions may vary.

Both intimal and medial VC are known to be accelerated among the T2DM population (Rubin and Silverberg, 2004); despite this, the vast majority of *in vitro* research to date assesses the effects of RANKL and TRAIL on the VC process in the absence of relevant pathological stimuli. In the context of bone turnover, glucose has been shown to induce RANKL mRNA expression alongside mineralisation in osteoblastic cells (García-Hernández *et al.*, 2012). In a vascular setting, elevated RANKL has been correlated with carotid calcification in atherosclerotic lesions (Higgins *et al.*, 2015) and RANKL inactivation reduces calcification and lesion size in OPG^{-/-} ApoE^{-/-} mice (Callegari *et al.*, 2014). ***We therefore hypothesise that elevated levels of RANKL may accelerate VC under established pathological conditions.***

With regard to TRAIL, recombinant delivery to ApoE^{-/-} diabetic mice has been shown to significantly reduce atherosclerosis progression (Secchiero *et al.*, 2006) whilst TRAIL delivery also protects against diabetic vascular injury in rats (Liu *et al.*, 2014). Also of relevance, TRAIL deficiency promotes VC and diabetes development *in vivo* (di Bartolo *et al.*, 2011; di Bartolo *et al.*, 2013). It is possible therefore that TRAIL-mediated protection from RANKL-induced pro-calcific signalling may also exist for *other* pro-calcific stimuli that accelerate VC during T2DM and CVD. Thus, ***we also hypothesise that TRAIL may abrogate pro-calcific signalling induced by inflammation and hyperglycemia.***

4.1.2 Study Aims

As discussed, the role for TRAIL in VC remains to be clarified, and while RANKL is a clear promoter of VC, its effects in the presence of established pathological stimuli observed in T2DM (hyperglycemia, inflammation) have not yet been considered *in vitro*. To date, the majority of VC studies employing RANKL and TRAIL have been carried out in “healthy” models, employing cell types of minimal physiological relevance, and analysing a limited range of pro-calcific markers (Corallini *et al.*, 2011; Osako *et al.*, 2010; Secchiero *et al.*, 2003). We therefore employ, as in Chapter 3, human primary aortic vascular cells in both mono- and co-culture models in order to thoroughly investigate the proposed roles for RANKL and TRAIL in VC under pathological conditions. This study advances on findings observed in Chapter 3, adding relevance to pathophysiological environments often present in T2DM.

A number of specific study aims were defined to address the aforementioned hypotheses:

1. To delineate the effects of hyperglycemia and inflammation on pro-calcific indices in the endothelial monolayer, the established location of intimal VC *in vivo*, and to investigate if RANKL and TRAIL can respectively accelerate or attenuate the pathological effects of these stimuli.
2. To investigate the effects of hyperglycemia and inflammation on pro-calcific indices in vascular smooth muscle, the established location of medial VC *in vivo*, and to investigate the proposed effects of RANKL and TRAIL on these stimuli.
3. To investigate the effects of hyperglycemia and inflammation on endothelial:smooth muscle paracrine signalling in our physiological co-culture model, and to profile the effects of RANKL and TRAIL under these conditions.

4.1.3. Experimental Design

To investigate study aims 1 and 2, HAECs and HASMCs were cultured in standard 6-well culture dishes, and exposed to 100 ng/mL TNF α (an established pro-inflammatory stimulus) or 15-30 mM glucose (to simulate hyperglycemia). Cells were then exposed to these pathological stimuli in the presence of RANKL (25 ng/mL) or TRAIL (5 ng/mL). To investigate study aim 3, a non-contact co-culture model was again employed to approximate the structure of the vasculature. To reiterate, HASMCs were grown in standard 6-well culture dishes, while HAECs were seeded at confluency into semi-permeable transwell inserts. HAECs

in the luminal compartment were then exposed to TNF α or glucose, in the presence of RANKL or TRAIL, and the underlying HASMCs in the subluminal compartment harvested for analysis (Figure 4.1). As previously described, mRNA, protein lysate and conditioned media were harvested for RT-qPCR, ELISA, enzyme assay and Western blotting ($n=3$ independent experiments). A comprehensive range of calcification indices, as previously listed in Section 3.1.3, were assessed (BMP-2, ALP, OPG, IL-6, Runx2, Sox9 and NF- κ B p52/p65).

To further clarify, TNF α , a well-established inflammatory cytokine, will be employed to represent the pro-inflammatory environment of an atherosclerotic plaque, alongside which medial VC often develops (McCullough *et al.*, 2008). With regard to the concentration chosen, TNF α at 100 ng/mL has previously been employed in *in vitro* vascular models of inflammation (Rastogi *et al.*, 2012; Rochfort and Cummins, 2015) and has recently been successfully used within our research group (Forde *et al.*, unpublished observations). Hyperglycemia, an intrinsic aspect of type-2 diabetes, will be utilised at two concentrations: 15 mM, representing circulatory glucose during moderate “pre-diabetes”, and 30 mM, levels common in severe diabetes. Both concentrations have been previously employed by our group in vascular cell models (Davenport *et al.*, 2018). The optimal concentrations of both RANKL and TRAIL as determined in Section 3.2.1 were preserved, alongside the 72-hour exposure time to reflect the chronic nature of VC.

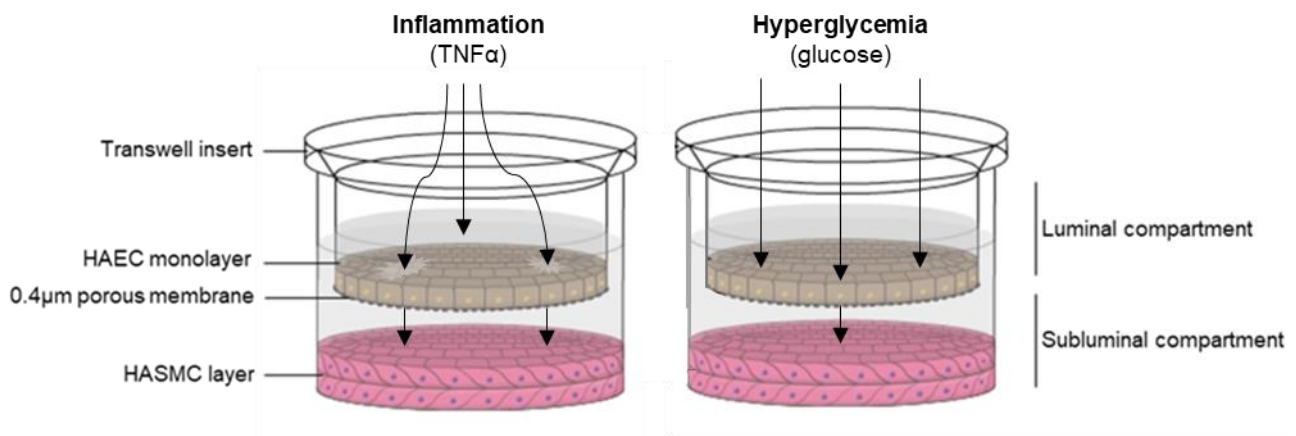


Figure 4.1. Representation of the transwell co-culture model under inflammatory and hyperglycemic conditions. HASMCs were grown to confluency in standard 6-well culture dishes. HAECs were grown to confluency in semi-permeable transwell inserts and suspended above the confluent smooth muscle layer. HAECs in the luminal compartment were exposed to 100 ng/mL TNF α (left) to simulate pro-inflammatory conditions, whereby endothelial damage/leakage may enable TNF α to act directly on underlying HASMCs. HAECs were exposed to 15-30 mM glucose (right) to simulate hyperglycemia, whereby active glucose transport across the endothelial monolayer may act directly on underlying HASMCs. Cells were incubated under these conditions for 72 hours, in the presence and absence of RANKL or TRAIL, prior to analysis of pro-calcific indices. Image adapted from Harper *et al.*, 2017.

4.2 Preliminary Investigations

As in Chapter 3, initial preliminary investigations were conducted to ensure correct interpretation of results; as such, the expression of RANKL and TRAIL in response to the employed pathological stimuli (inflammation, hyperglycemia) were assessed, alongside any potential adverse cellular effects of exposure to these stimuli. Essential methodological validations were also considered.

4.2.1 Expression of RANKL and TRAIL

RANKL and TRAIL have been shown to be expressed at a protein level in HAECs and HASMCs (Section 3.2.2). Thus, the potential effects of 100 ng/mL TNF α and 30 mM glucose on RANKL and TRAIL expression was first examined to ensure accuracy of treatment conditions during co-exposure with recombinant proteins.

4.2.1.1 HAECs

In HAECs, RANKL and TRAIL mRNA were not expressed at quantifiable levels following exposure to either TNF α or glucose (data not shown). Regarding release, RANKL levels in endothelial conditioned media were not altered following treatment with either pathological stimulus (data not shown), however, TRAIL release was induced under both inflammatory and hyperglycemic conditions (Appendix 4.1B). Furthermore, intracellular TRAIL protein production was significantly decreased by ~30% following TNF α exposure, while RANKL protein approximately doubled in both cases (Appendix 4.1D).

4.2.1.2 HASMCs

While no effect was noted in TRAIL mRNA expression, RANKL transcripts were influenced by treatment, with an approximate 2.5-fold increase and 70% decrease noted with TNF α and hyperglycemia respectively (Appendix 4.1A). A slight but insignificant increase in TRAIL release was observed in response to TNF α , alongside a significant increase in response to glucose (Appendix 4.1C). No changes were noted with regard to RANKL release (data not shown), but intracellular protein was induced by approximately one third following exposure to both pathological stimuli; TRAIL protein production was also slightly elevated following TNF α exposure (Appendix 4.1E).

4.2.2 Effects of RANKL and TRAIL on Cellular Integrity

Due to the employment of well-established injurious stimuli, the adverse effects of both TNF α and high glucose on cellular integrity were monitored. In this regard, the effects of inflammation and hyperglycemia on morphology, viability/apoptosis, endothelial barrier function and the expression of smooth muscle phenotypic markers were assessed.

4.2.2.1 Cell Morphology

HAECs and HASMCs were observed via light microscopy prior to and following exposure to TNF α and glucose for 72 hours. While no morphological differences were noted in response to glucose in either endothelial or smooth muscle cell cultures, TNF α exposure significantly altered the typical “cobblestone” morphology of HAECs (Figure 4.2). After 72 hours, HAECs exposed to this cytokine appeared contracted, elongated, and the

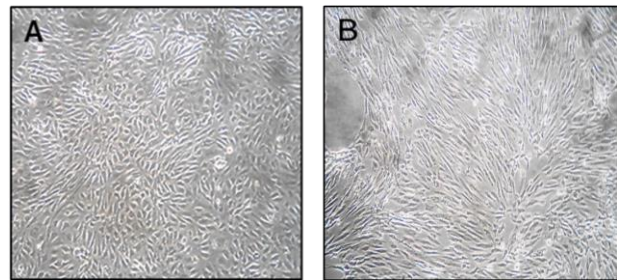


Figure 4.2. HAECs under control conditions and following exposure to TNF α . (A) Cultured HAECs under control conditions displaying typical cobblestone morphology. (B) Cultured HAECs following exposure to 100 ng/mL TNF α for 72 hours appear contracted and elongated. Images were taken using a Nikon Eclipse TS100 phase-contrast light microscope.

integrity of the endothelial barrier was compromised in several areas (Figure 4.2B, left hand side). No variations were noted in HASMCs following exposure to TNF α , as they retained their typical spindle shape.

4.2.2.2 Viability and Apoptosis

Routine viability measurements were conducted as required. Cell viability measurements for HAECs and HASMCs (in both mono- and co-culture) were maintained above 89% for all treatments employed. Due to the potent injurious nature of TNF α and hyperglycemia, apoptosis was also monitored via flow cytometry for both stimuli. In both HAECs and HASMCs, TNF α exposure induced apoptosis by approximately 10.3% and 4.3% respectively, whilst upper concentrations of glucose elicited a respective 1.7% and 4.2% increase in apoptotic cells (Figure 4.3). Average values for viability and apoptosis measurements are presented in Table 4.1.

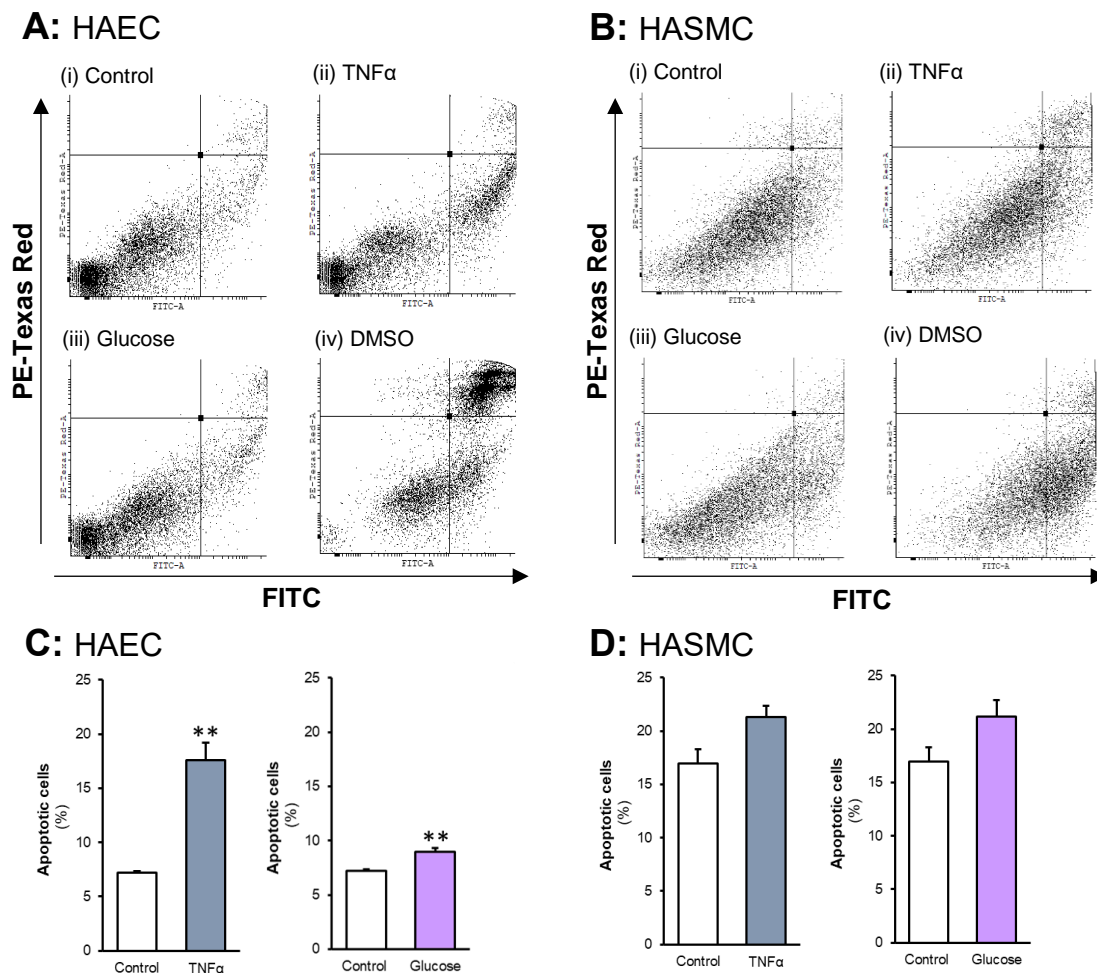


Figure 4.3. The effect of TNF α and glucose exposure on HAEC and HASMC apoptosis. (A) HAECs and (B) HASMCs were exposed to experimental concentrations of TNF α (100 ng/mL) and glucose (30 mM) for 72 hours, or 20% DMSO for 30 minutes, prior to analysis by flow cytometry. Quadrants determined by unstained control. Bar charts represent percentage apoptosis when (C) HAECs and (D) HASMCs were exposed to TNF α and glucose for 72 hours. Control and DMSO data were previously presented in Figure 3.4, included here for comparison purposes. ** $p < 0.01$ compared to untreated control.

Table 4.1. Average percentages of viable, non-viable, and apoptotic cells post-treatment.

		Viable (%)	Non-viable (%)	Apoptotic (%)
HAECs	<i>Untreated</i>	96.58	3.41	7.23
	<i>100 ng/mL TNFα</i>	94.05	5.94**	17.56***
	<i>30 mM glucose</i>	96.52	3.47	8.96*
	<i>DMSO</i>	48.42	49.15	17.8
HASMCs	<i>Untreated</i>	95.60	3.32	17.01
	<i>100 ng/mL TNFα</i>	89.63**	9.54***	21.31
	<i>30 mM glucose</i>	97.05	2.72	21.17
	<i>DMSO</i>	88.20	11.43	44.63

* $p < 0.05$; ** $p < 0.01$; *** $p < 0.001$ compared to untreated control.

4.2.2.3 Endothelial Barrier Function

Again, as HAECs will be employed in co-culture, endothelial permeability was assessed in response to inflammatory and hyperglycemic conditions. HAECs, following 72-hour exposure to TNF α or glucose in transwell inserts, were tested for barrier function using the FITC-Dextran/TEE method described in Section 2.2.5.2. Untreated cells permitted an average TEE of 3.0% FITC-dextran to the subluminal compartment after 3 hours, while TNF α and glucose treatment resulted in non-significant increases of 4.9% and 3.7% transfer respectively (Appendix 4.2A).

4.2.2.4 Phenotypic Analysis of Smooth Muscle Cells

HASMCs were characterised for both smooth muscle and osteoblastic phenotypic markers at an mRNA level following exposure to TNF α and glucose. SM α -actin and SM22 α , core smooth muscle markers, remained constitutively expressed following treatment (Appendix 4.2B (i), (ii)). BSP mRNA expression, an early marker of osteoblastic differentiation, was not affected by exposure to inflammation or hyperglycemia, while OCN, a marker of late differentiation, was significantly reduced in both cases (Appendix 4.2B (iii), (iv)). Transcript levels for all four markers remained unaffected by treatment in co-culture (data not shown).

4.2.3 Methodological Validation

Prior to exposure, it was observed that neither HAECs nor HASMCs released detectable levels of TNF α under any of the conditions tested. Regarding hyperglycemic treatments, the media formulation employed did not contain glucose prior to manual addition at the required concentrations. With respect to RT-qPCR analyses, it was confirmed that the addition of TNF α or glucose for 72 hours did not affect the mRNA expression of endogenous control genes (GAPDH, 18S) (data not shown). Furthermore, as TNF α exposure is widely known to affect endothelial barrier integrity (Marcos-Romero *et al.*, 2014), and glucose can be subject to active transport across the endothelial monolayer (Mann *et al.*, 2003), it was expected that both conditions would allow transfer to the subluminal compartment in co-culture. While percentage TEE was not quantified, this transfer acts as an integral part of inflammatory/hyperglycemic models as both pathophysiological conditions are associated with endothelial dysfunction (Hadi and Suwaidi, 2007; Marcos-Romero *et al.*, 2014).

4.2.5 Discussion: Preliminary Investigations

4.2.5.1 Expression of RANKL and TRAIL under Inflammatory/Hyperglycemic Conditions

As endothelial RANKL and TRAIL mRNA proved undetectable in Chapter 3, it is therefore unsurprising that neither transcript were quantifiable under inflammatory or hyperglycemic conditions in HAECs. As discussed, there are conflicting reports in the literature regarding the expression of these ligands in the endothelium (Collin-Osdoby *et al.*, 2001; Osako *et al.*, 2010; Pritzker *et al.*, 2004; Secchiero *et al.*, 2006; Zannettino *et al.*, 2005). Conclusions regarding RANKL mRNA responses to TNF α in ECs appear equally divisive (Collin-Osdoby *et al.*, 2001; Davenport *et al.*, unpublished observations), whilst for TRAIL are completely lacking. More relevantly, at a transcriptional level, the observed induction of RANKL protein production under inflammatory conditions has been noted previously (Collin-Osdoby *et al.*, 2001). While the effects of hyperglycemia on RANKL expression have not yet been defined in HAECs, glucose uptake has been shown to be required for RANKL protein production in osteocytic cells (Takeno *et al.*, 2018) which may partly explain the increase in RANKL observed in this study. Despite this increase, extracellular RANKL levels remained unchanged, and so are inconsequential for recombinant ligand treatment. Similarly, the release of TRAIL induced by both pathological stimuli is a significant finding, and may potentially reveal a novel aspect of endothelial vasculo-protection; however, in this case, extracellular TRAIL levels were deemed too low to affect ligand exposure in the ng/mL range. Overall, the effects of RANKL/TRAIL in response to these stimuli (TNF α , glucose) have not yet been extensively investigated in HAECs, but due to the conflicting literature listed above, we further reiterate that specific responses should be characterised for each application (Spierings *et al.*, 2004).

The expression of both RANKL and TRAIL are more widely recognised in smooth muscle (Chang *et al.*, 2015; Harith *et al.*, 2016; Li *et al.*, 2016; Tseng *et al.*, 2010). Previous unpublished studies in our laboratory have highlighted an increase in both RANKL and TRAIL mRNA in response to TNF α treatment in HASMCs, and while our findings agree with that of RANKL, the utilisation of ten-fold less recombinant TRAIL in the current study may explain the discrepancy regarding this ligand (Davenport *et al.*, unpublished observations). Interestingly, Davenport and colleagues noted that glucose exposure had no effect on RANKL/TRAIL mRNA, but hyperglycemia has previously been shown to reduce RANKL transcript expression in rat aortic VSMCs (Chang *et al.*, 2015) in agreement with our findings. Chang and colleagues (2015) did, however, report a decrease in RANKL protein production

following glucose exposure, in contrast to the increase detected in this case. Also of note, Kang *et al.* (2015) reported no effect in RANKL/TRAIL mRNA or (intracellular) protein expression following long-term hyperglycemia. It is obvious therefore that, while the expression of both ligands have been confirmed in smooth muscle, their expression under the current pathological conditions have not, with a significant level of variation still existing in the literature. It again appears likely that the expression of RANKL and TRAIL may be species, tissue and environment specific and (as for endothelial cells) should be specified prior to use.

4.2.5.2 The Effects of TNF α and Glucose on Cellular Integrity

As mentioned, TNF α , in its well-established role as a pro-inflammatory cytokine, was employed at a pre-determined concentration of 100 ng/mL often utilised in *in vitro* models of endothelial inflammation and atherosclerosis (Rastogi *et al.*, 2012; Rochfort and Cummins, 2015). Similarly, glucose was employed at both 15 and 30 mM concentrations to represent circulating concentrations during moderate “pre-diabetes” and severe diabetes respectively, levels that are again common in hyperglycemic studies (Davenport *et al.*, 2018; Kang *et al.*, 2015; Liu *et al.*, 2010). Therefore, as dosage optimisations were not required, the adverse effects of these conditions on primary HAECs and HASMCs after 72 hours were defined, similar to that of RANKL and TRAIL in Section 3.2.6.3.

As an important point central to the design of this study, it was expected that both inflammatory and hyperglycemic conditions would induce potent injurious effects on HAECs and HASMCs due to their notorious roles in multiple T2DM/CVD pathologies (Duckworth, 2001; Liu *et al.*, 2010; Popa *et al.*, 2007; Tintut *et al.*, 2000; Zhang *et al.*, 2009). Unlike Chapter 3, where a key design element was the retention of endothelial barrier integrity (and thus distinctly separate luminal and subluminal components), in this case the induced pathophysiological environments are likely to disrupt this barrier and encourage endothelial leakage (Hadi and Suwaidi, 2007; Marcos-Romero *et al.*, 2014). Not only is this damage expected, but is pertinent to the pathological relevance of these models. Furthermore, active glucose transport through the endothelial layer predominantly via glucose transporter (GLUT)-1 is prevalent in aortic ECs (Mann *et al.*, 2003; Viator and Fouty, 2009) and another mechanism by which glucose may transfer to the subluminal space in co-culture.

Firstly, with regard to HAECs under inflammatory conditions, morphological differences were observed following 72 hours’ TNF α exposure, with clear barrier degradation and breakdown

evident. As noted by Stroka and colleagues (2012), this morphological response is usual following long-term exposure to TNF α . Following these observations, it is unsurprising that an approximate 10% induction in apoptosis was measured in TNF α -treated samples compared to control; in fact, TNF α is a known inducer of apoptosis in vascular ECs (Xia *et al.*, 2006) and endothelial dysfunction responses to this pro-inflammatory cytokine are well characterised (Zhang *et al.*, 2009). Endothelial barrier integrity was also significantly compromised, albeit less than 2%, but again, TNF α has long been known to enhance vascular permeability (Royall *et al.*, 1989). Overall, the potent injurious effects of HAEC exposure to TNF α are consistent with the literature, and it is clear that this model suitably represents areas of endothelial injury that occur during (predominantly intimal) VC. Despite the employed supra-physiological concentration of 100 ng/mL TNF α , the levels of this cytokine have been shown to be significantly elevated in atherosclerotic plaque alongside which medial VC often co-develops (Barath *et al.*, 1990; McCullough *et al.*, 2008; Tintut *et al.*, 2000). On a separate note, HAECs fared well under hyperglycemic conditions, with no morphological changes and minimal apoptotic/permeability effects noted. This observation may support the more subtle effects of circulating glucose on the vasculature during chronic type-2 diabetes, whereby the endothelium remains functional despite a slight deterioration in endothelial health. Glucose therefore may not affect the integrity of the endothelial barrier in co-culture to any great extent, but due to the aforementioned nature of glucose transport through the aortic endothelium, the underlying HASMCs are likely to experience some level of hyperglycemia as they would under diabetic conditions *in vivo*.

Interestingly, no morphological effects were noted in HASMCs in response to either stimulus, nor any significant induction in apoptotic cells. Core smooth muscle markers SM α -actin and SM22 α remained constitutively expressed as part of a typical smooth muscle phenotype, despite evidence that inflammation and hyperglycemia can induce pro-calcific differentiation in VSMCs (Lee *et al.*, 2010; Liu *et al.*, 2010; Tintut *et al.*, 2000). Also of note, BSP (an early marker of osteoblastic differentiation) remained unaffected, while OCN (a late marker), was significantly downregulated under both inflammatory and hyperglycemic conditions. This novel finding has, to our knowledge, not been disclosed to date, but it is unclear as of yet what the significance of this is. This phenomenon was absent from subluminal HASMCs in co-culture, however, more physiologically representative of the vasculature *in vivo*. To conclude, therefore, HASMCs do not display any significant changes when conditioned with TNF α or glucose in culture, substantiating any potential responses in the upcoming study.

4.3 HAEC Monoculture

HAECs were first employed in standard monoculture to assess the proposed effects of RANKL and TRAIL on the endothelium under pathological (inflammatory, hyperglycemic) conditions associated with VC in T2DM. The comprehensive range of gene/protein targets employed in Chapter 3 were investigated. Given the large volume of data accrued, only the key findings will be highlighted in text, while the readers' attention will be drawn to the relevant figure panels.

4.3.1 The Effects of TNF α and Glucose on Pro-Calcific Targets in HAECs

Due to the complexity of the current model, the effects of TNF α (an inflammatory stimulus) and glucose (a hyperglycemic stimulus) were first profiled in the absence of RANKL and TRAIL recombinant ligands. As cultured cells are exposed to enhanced osmotic pressure when exposed to glucose, an osmotic control was also included. Mannitol, an organic sugar alcohol, was employed at 30 mM to mimic the osmotic pressure of glucose at upper experimental concentrations, as previously utilised by Liu *et al.* (2010). Mannitol was found to have no effect on any of the measured pro-calcific indices in HAECs (Appendix 4.3).

Following endothelial exposure to 100 ng/mL TNF α , all measured pro-calcific indices at an mRNA level were found to be upregulated (Figure 4.4A). Similarly, BMP-2, OPG and ALP activity levels were increased both in HAEC-conditioned media (Figure 4.4B) and in HAEC lysate (Figure 4.4C), alongside both canonical and non-canonical NF- κ B activation (Figure 4.4D). Following hyperglycemic treatment, BMP-2 and ALP mRNA expression levels were elevated, while Runx2 was decreased (Figure 4.5A). All measured indices in the conditioned media were elevated (Figure 4.5B), while only OPG levels were increased in endothelial lysate (Figure 4.5C). Canonical (but not non-canonical) NF- κ B activation was also significantly reduced compared to control (Figure 4.5D).

4.3.2 The Effects of RANKL and TRAIL under Inflammatory Conditions in HAECs

Next, the effects of RANKL and TRAIL on pro-calcific indices were assessed under pro-inflammatory conditions in HAECs. Both ALP and Runx2 mRNA levels were significantly downregulated by the separate addition of both ligands, with TRAIL co-incubation reducing Runx2 to baseline and ALP to below baseline in the presence of TNF α (Figure 4.6A).

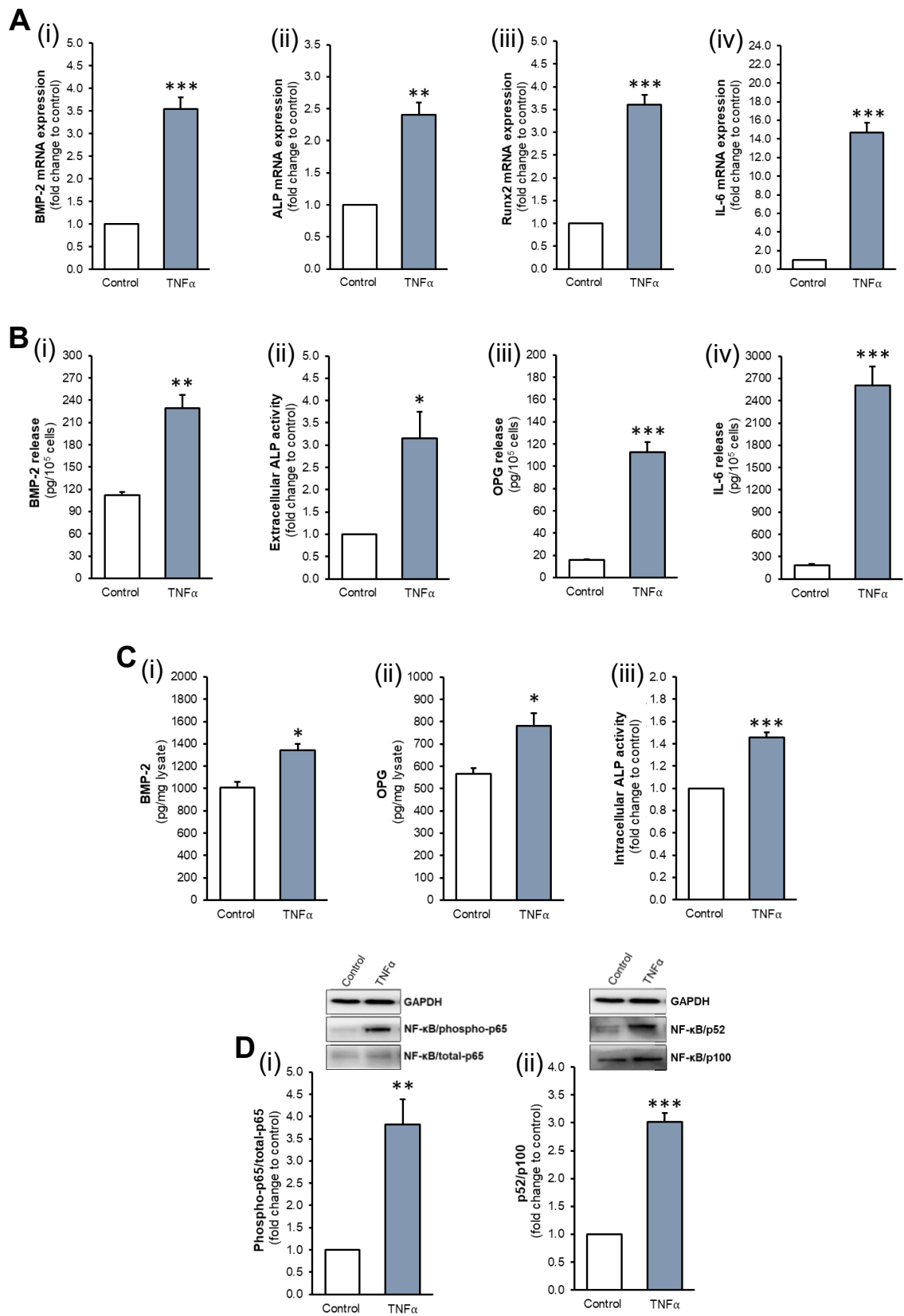


Figure 4.4. The effects of TNF α on pro-calcific indices in HAEC monoculture. HAECs were exposed to TNF α (100 ng/mL) for 72 hours. **(A)** (i) BMP-2, (ii) ALP, (iii) Runx2 and (iv) IL-6 mRNA were assessed by RT-qPCR, employing GAPDH as an endogenous control. **(B)** (i) BMP-2, (ii) ALP, (iii) OPG and (iv) IL-6 release, and **(C)** intracellular (i) BMP-2, (ii) ALP and (iii) OPG protein levels were quantified by ELISA and enzyme assay where appropriate. **(D)** (i) Canonical and (ii) non-canonical NF- κ B activation were determined by Western blotting, quantified by scanning densitometry and normalised to GAPDH. Blots are representative. Absolute values for media and protein lysate analyses are normalised to 10⁵ cells and total protein respectively. * $p < 0.05$; ** $p < 0.01$; *** $p < 0.001$ compared to untreated control.

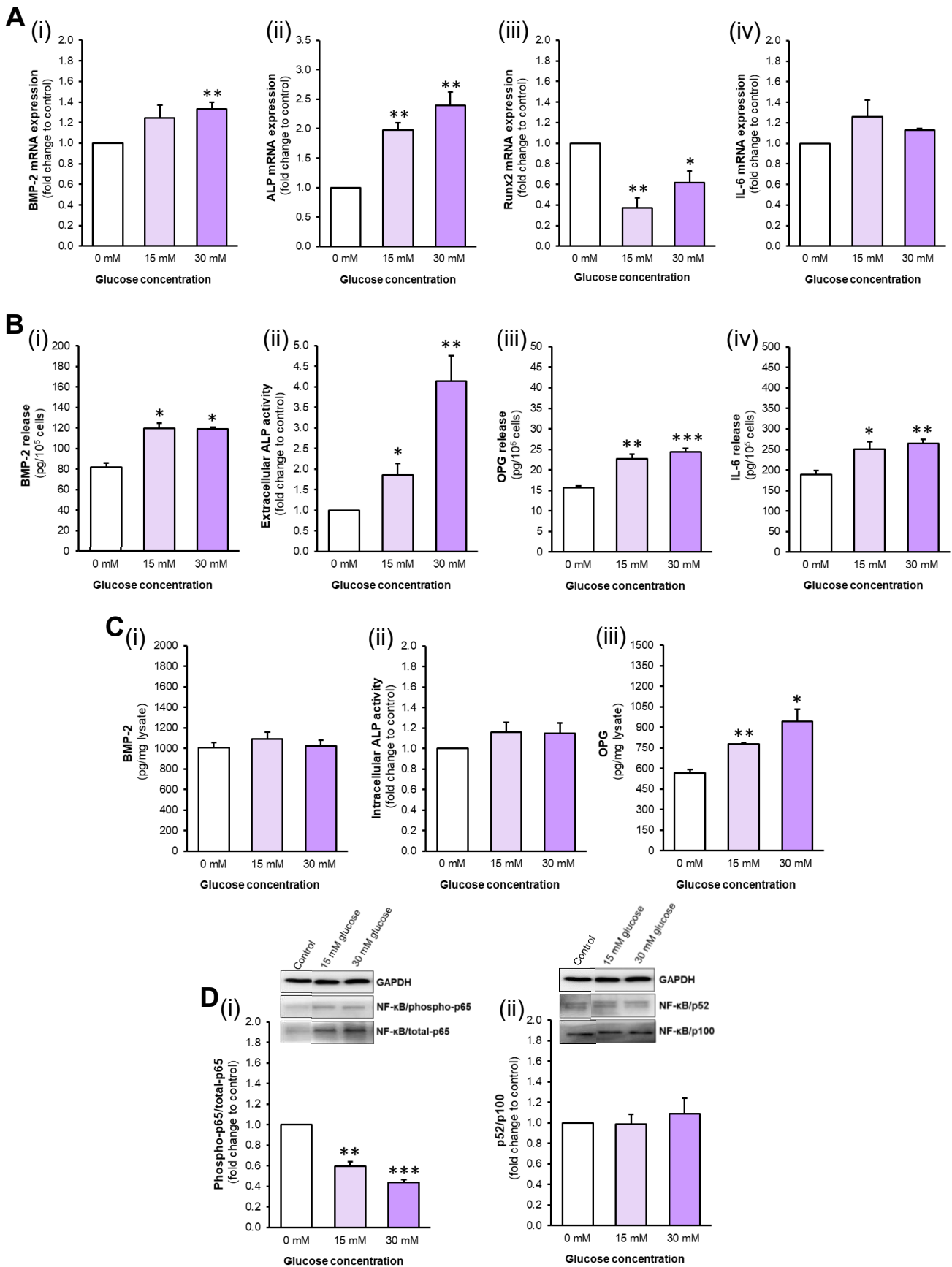


Figure 4.5. The effects of glucose on pro-calcific indices in HAEC monoculture. HAECs were exposed to glucose (15–30 mM) for 72 hours. (A) (i) BMP-2, (ii) ALP, (iii) Runx2 and (iv) IL-6 mRNA were assessed by RT-qPCR, employing GAPDH as an endogenous control. (B) (i) BMP-2, (ii) ALP, (iii) OPG and (iv) IL-6 release, and (C) intracellular (i) BMP-2, (ii) ALP and (iii) OPG protein levels were quantified by ELISA and enzyme assay where appropriate. (D) (i) Canonical and (ii) non-canonical NF- κ B activation were determined by Western blotting, quantified by scanning densitometry and normalised to GAPDH. Blots are representative (control bands previously presented in Figure 4.4). Absolute values for media and protein lysate analyses are normalised to 10⁵ cells and total protein respectively. * $p < 0.05$; ** $p < 0.01$; *** $p < 0.001$ compared to untreated control.

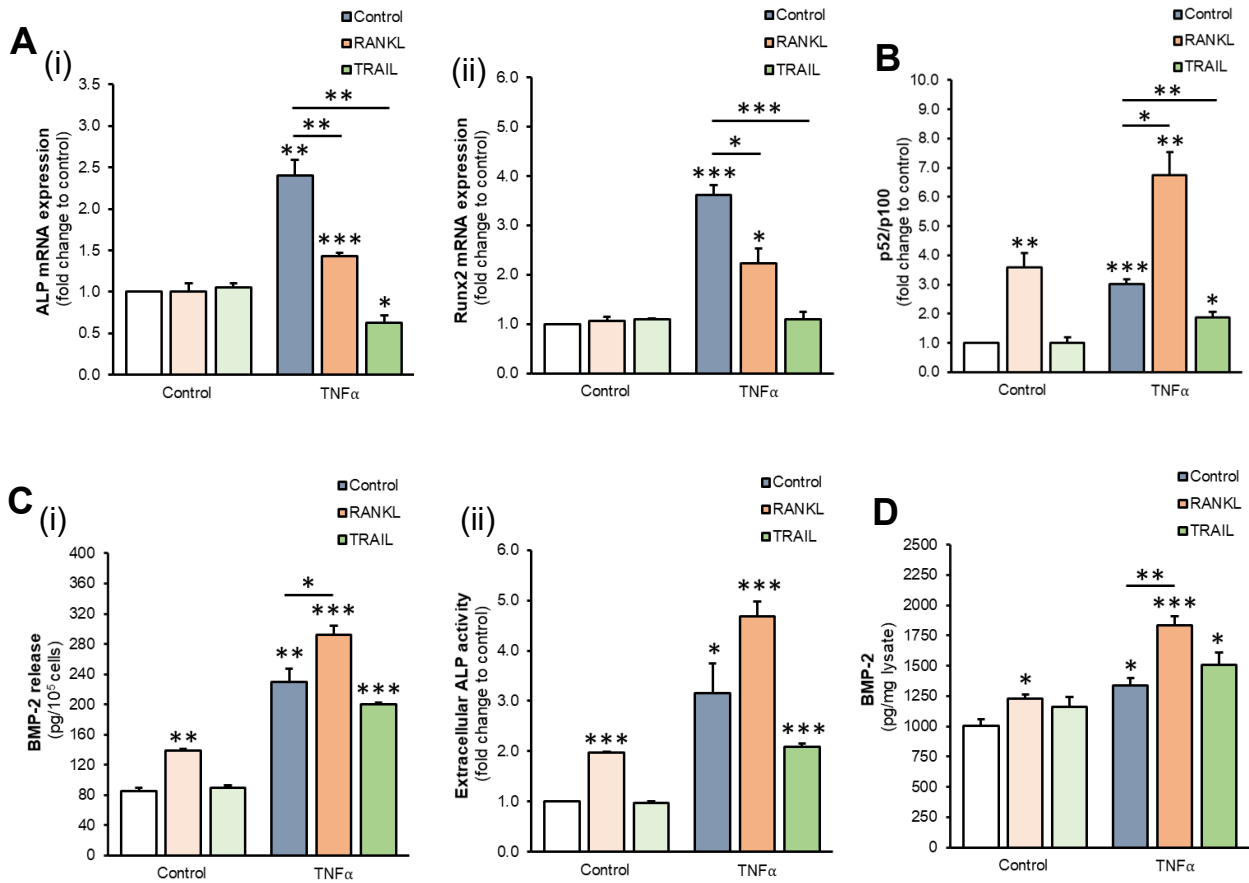


Figure 4.6. The effects of TNF α +/- RANKL/TRAIL on pro-calcific indices in HAEC monoculture. HAECs were exposed to TNF α (100 ng/mL) +/- RANKL (25 ng/mL) or TRAIL (5 ng/mL) for 72 hours. **(A)** mRNA expression of (i) ALP and (ii) Runx2 were analysed by RT-qPCR employing GAPDH as an endogenous control. **(B)** Non-canonical NF- κ B activation was determined by Western blotting, quantified by scanning densitometry and normalised to GAPDH. Representative blots are presented in Appendix 4.6. **(C)** (i) BMP-2 and (ii) ALP in the conditioned media and **(D)** intracellular BMP-2 were analysed by ELISA and activity assay where appropriate. Absolute values for media and lysate are normalised to 10⁵ cells and total protein respectively. * $p < 0.05$; ** $p < 0.01$; *** $p < 0.001$ compared to untreated control unless otherwise stated; bars indicate statistical significance between treatment groups.

Furthermore, RANKL in the presence of TNF α significantly promoted the release of BMP-2 and non-significantly accelerated ALP activity, while TRAIL did not exert any significant effects on the release profile of endothelial cells under inflammatory conditions (Figure 4.6C). Interestingly, endothelial exposure to TNF α + RANKL also significantly promoted non-canonical NF- κ B activation when compared to exposure with TNF α alone (Figure 4.6B), and further induced intracellular BMP-2 production (Figure 4.6D). Moreover, TRAIL treatment under pro-inflammatory conditions significantly reduced non-canonical NF- κ B signalling to below that of TNF α exposure alone (Figure 4.6B). Supporting material for the additional measured indices is presented in Appendix 4.4 and 4.6.

4.3.3 The Effects of RANKL and TRAIL under Hyperglycemic Conditions in HAECs

With regard to mRNA, both RANKL and TRAIL exposure under hyperglycemic conditions reduced ALP transcript expression when compared to that of glucose treatment alone (but TRAIL to a greater extent). Moreover, incubation with RANKL significantly induced Runx2 compared to control, while TRAIL co-incubation recovered expression to basal levels (Figure 4.7A). Interestingly, RANKL-induced BMP-2 release was maintained under hyperglycemic conditions, while TRAIL exposure did not affect glucose-induced BMP-2 secretion. RANKL also non-significantly promoted glucose-induced ALP activity in the conditioned media, while TRAIL attenuated this activity following severe hyperglycemia (Figure 4.7B). Supplementary material is presented in Appendix 4.5 and 4.6.

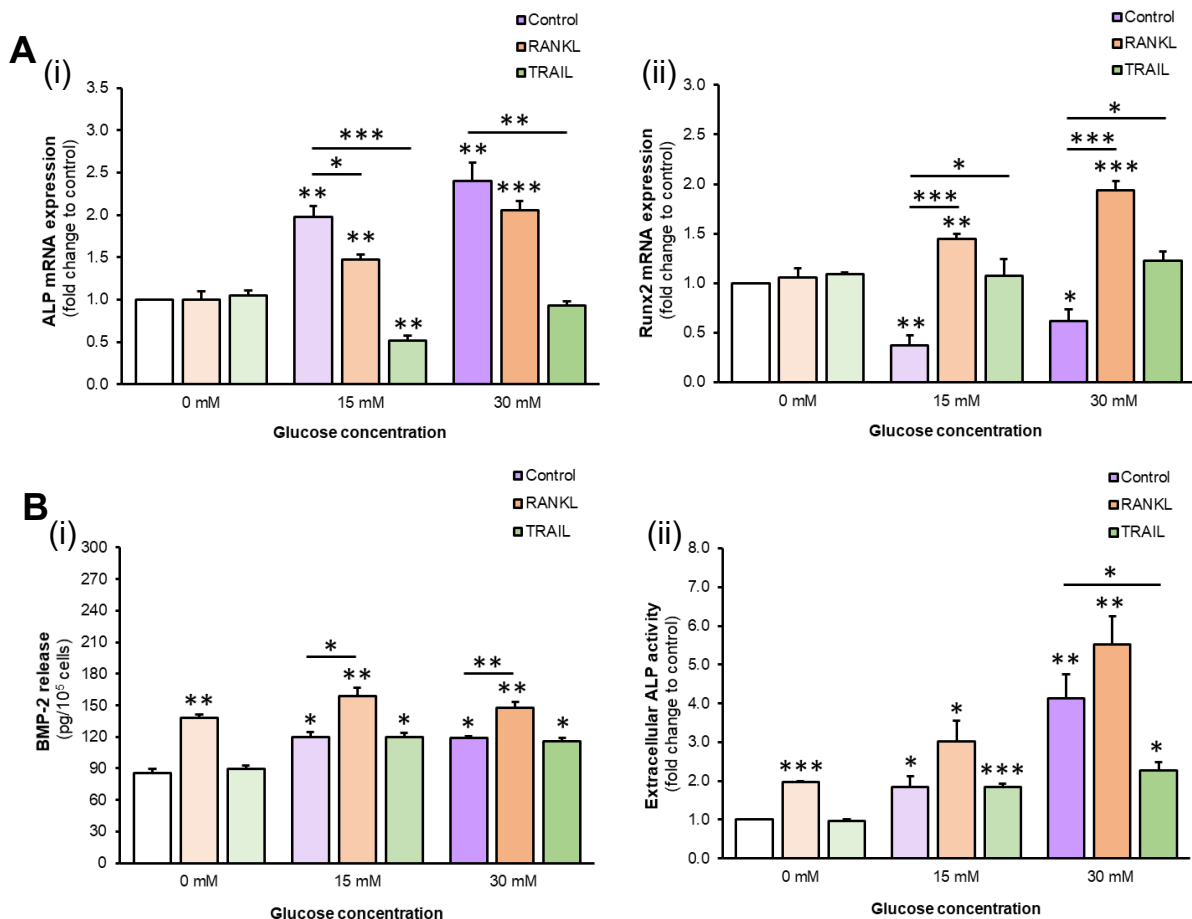


Figure 4.7. The effects of glucose +/- RANKL/TRAIL on pro-calcific indices in HAEC monoculture. HAECs were exposed to glucose (15-30 mM) +/- RANKL (25 ng/mL) or TRAIL (5 ng/mL) for 72 hours. (A) mRNA expression of (i) ALP and (ii) Runx2 were analysed by RT-qPCR employing GAPDH as an endogenous control. (B) (i) BMP-2 release and (ii) extracellular activity were quantified by ELISA and activity assay where appropriate. Absolute values are normalised to 10⁵ cells. * $p < 0.05$; ** $p < 0.01$; *** $p < 0.001$ compared to untreated control unless otherwise stated; bars indicate statistical significance between treatment groups.

4.3.4 HAEC Monoculture: Summary of Results

The effects of endothelial exposure to RANKL and TRAIL under inflammatory and hyperglycemic conditions are summarised below in Table 4.2.

Table 4.2. The effects of TNF α and glucose +/- RANKL or TRAIL in HAECs.

<i>Inflammation</i>			RANKL	TRAIL
BMP-2	<i>Extracellular Protein</i>	↑	↑↑	↑
	<i>Intracellular Protein</i>	↑	↑↑	↑
ALP	<i>mRNA</i>	↑↑	↑	↓
	<i>Extracellular Activity</i>	↑	↑↑ ^δ	↑
OPG	<i>Intracellular Protein</i>	↑	↑↑	↑
Runx2	<i>mRNA</i>	↑↑	↑	–
NF-κB (p52/p100)	<i>Activation</i>	↑↑	↑↑↑	↑
<i>Hyperglycemia</i>				
BMP-2	<i>mRNA</i>	↑	–	–
	<i>Extracellular Protein</i>	↑	↑↑	↑
	<i>Intracellular Protein</i>	–	↑	–
ALP	<i>mRNA</i>	↑	↑	–
	<i>Extracellular Activity</i>	↑↑	↑↑	↑
OPG	<i>Extracellular Protein</i>	↓	↓	–
	<i>Intracellular Protein</i>	↑	↑↑	–
IL-6	<i>mRNA</i>	–	–	↓
Runx2	<i>mRNA</i>	↓	↑	–
NF-κB (p-p65/t-p65)	<i>Activation</i>	↓	–	–

p-p65, phospho-p65; t-p65, total-p65. ↑, upregulation; ↑↑/↑↑↑, further upregulation relative to corresponding treatment conditions; ↓, downregulation; –, no change; ^δ, not significant.

4.3.5 Discussion: HAEC Monoculture

The effects of RANKL and TRAIL on the endothelial monolayer under inflammatory and hyperglycemic conditions were first assessed. Although the pathological effects of TNF α and glucose on the vasculature (particularly VSMCs) have been described previously, there is limited data regarding the specific role for these stimuli in the endothelium of large arteries during VC. Furthermore, the effects of RANKL and TRAIL have not yet been clarified in the presence of pro-inflammatory or hyperglycemic conditions common in type-2 diabetes and vascular injury. This *in vitro* study is the first to our knowledge to investigate such a comprehensive range of pro-calcific indices in human primary-derived endothelial cells under pathological conditions, and is certainly the first to incorporate RANKL and TRAIL in such models. In addition, profiling HAEC responses to these stimuli will aid in discerning the extent of endothelial pro-calcific paracrine signalling ultimately relevant in co-culture. This discussion will focus on some of the key pertinent findings regarding the endothelial response to pathological conditions (summarised in Table 4.2), beginning with the effects of TNF α and high glucose alone before focusing on the effects of RANKL and TRAIL on these stimuli.

4.3.5.1 The Effects of TNF α on VC Indices in HAECs

The process of inflammation is closely related to that of VC, as immune cells at the site of atherosclerotic plaque release inflammatory cytokines (including TNF α) that contribute to pro-calcific events. In this respect, it is known that circulating TNF α levels are elevated during T2DM/CVD (Olson *et al.*, 2012; Levine *et al.*, 1990; Mirza *et al.*, 2012), and TNF α has been shown to be highly expressed in intimal atherosclerotic plaque (Barath *et al.*, 1990). Furthermore, TNF α has been shown to induce endothelial injury/dysfunction (Zhang *et al.*, 2009), and as such, has been widely used as a model of vascular injury in many studies drawn on in this chapter. While TNF α is predominantly employed as a pro-inflammatory stimulus, the pro-calcific effects of this cytokine are also well documented (Illiantri *et al.*, 2016), but the vast majority of relevant VC research focuses on intimal rather than medial calcification. However, it should be taken into account that medial VC often coincides with atherosclerosis *in vivo* (McCullough *et al.*, 2008), leaving the role for endothelial paracrine signalling in the presence of these inflammatory conditions unclear.

Following analysis of a wide range of pro-calcific indices that regulate medial VC, *TNF α was found to induce all measured targets in HAECs*. Of particular interest, BMP-2 and active ALP

release were significantly increased, paracrine signalling elements that promote calcification in the underlying VSMC layer (Davenport *et al.*, 2016; Osako *et al.*, 2010). In support of this finding, albeit in less relevant models, TNF α has been shown to induce BMP-2 release in HUVECs (Illiandri *et al.*, 2016), while ALP activity is increased by IL-6 in pulmonary aortic ECs (Nakazato *et al.*, 1997), in turn itself upregulated by TNF α . Contrastingly, however, Illiandri and colleagues (2016) have recently reported that TNF α does not induce BMP-2 in ECs above a concentration of 5 ng/mL, although these authors note excessive levels of apoptosis in response to TNF α which may explain this discrepancy. Of additional note, whilst RANKL exposure elicited similar paracrine responses (Section 3.3.5.1), these effects did not coincide with transcriptional upregulation as seen in the case of TNF α , potentially indicating that this cytokine exerts a more potent pro-calcific phenotypic influence on HAECs.

Also noteworthy, TNF α significantly induced OPG mRNA/release from endothelial cells in accordance with the literature (Collin-Osdoby *et al.*, 2001; Olesen *et al.*, 2005); as previously noted, OPG (stored in Weibel-Palade bodies) can be rapidly released in response to inflammation (Zannettino *et al.*, 2005), which may highlight both a natural cardioprotective response to TNF α and partly explain the increase in circulating OPG observed in vascular disorders (Abedin *et al.*, 2007; O'Sullivan *et al.*, 2010; Schoppet *et al.*, 2003). Furthermore, IL-6, well known to be induced by TNF α , has also been implicated in the pathogenesis of EC dysfunction and CVD (Qu *et al.*, 2014) and has been considered a pro-calcific cytokine (Hénaut and Massy, 2018). Of further note, while TNF α is well known to function via the canonical NF- κ B pathway, the precise role for TNF α -induced non-canonical activation requires clarity, particularly with respect to VC (Kim *et al.*, 2011).

4.3.5.2 The Effects of RANKL on VC Indices under Inflammatory Conditions in HAECs

The effects of RANKL on HAECs under these conditions (i.e. RANKL + TNF α) were next assessed. As noted, RANKL has been identified in vascular cells, and has been shown to be elevated in atherosclerotic tissue (Cheng *et al.*, 2015, Higgins *et al.*, 2015; Osako *et al.*, 2010). Indeed, both RANKL and inflammatory cytokines (eg. TNF α , IL-6) can activate overlapping signalling pathways, highlighting an inter-related function for these pro-calcific stimuli (Ndip *et al.*, 2014). Of note, the current study is novel in a vascular context, with the majority of existing RANKL/TNF α studies completed with an osteoclastic focus (Kwan *et al.*, 2004; Vitale and Ribeiro, 2007). At an mRNA level, pro-calcific (ALP, Runx2) expression was upregulated

following exposure to RANKL under inflammatory conditions, although to a lesser extent than with TNF α treatment alone. It is possible, therefore, that RANKL may induce the switching of HAECs from a pro-inflammatory state to a more sustainable pro-calcific phenotype emulating the natural sequence of events in atherosclerosis (Joshi *et al.*, 2016). This effect is not reflected at a translational level, rendering this data of limited physiological value.

The observed increase in BMP-2 release and extracellular ALP activity (alongside non-canonical NF- κ B activation) following exposure to RANKL + TNF α is particularly interesting. These levels are not only accelerated compared to RANKL treatment alone, but also compared to that of TNF α exposure. It appears, therefore, that *RANKL and TNF α exert an additive effect on pro-calcific (paracrine) signalling in the endothelial layer*, a trend previously observed in osteoclastogenesis (Fuller *et al.*, 2002; Yamashita *et al.* 2015), and *these pro-calcific responses may be exerted via the non-canonical NF- κ B pathway*. RANKL's contribution to TNF α -induced BMP-2/ALP release likely enhances the VC process in the medial HASMC layer. TNF α also strongly induces BMP-2 production, accompanying the observed increase in BMP-2 release. This additive trend may be explained by the overlapping mechanisms involved in both RANKL and TNF α function, in particular the activation of pro-calcific NF- κ B activation previously associated with BMP-2 (Feng *et al.*, 2003; Kim *et al.*, 2011; Panizo *et al.*, 2009).

4.3.5.3 The Effects of TRAIL on VC Indices under Inflammatory Conditions in HAECs

As noted, TRAIL has also been identified in vascular cells, and TRAIL administration has been shown to exert a protective influence particularly during (pro-inflammatory) atherosclerotic calcification (di Bartolo *et al.*, 2013; Liu *et al.*, 2014; Secchiero *et al.*, 2006). Despite this, no studies have yet clarified the effects of TRAIL on medial VC in areas of vascular inflammation, or the role of the endothelium in this process. Under inflammatory conditions, TRAIL was found to completely attenuate TNF α -induced pro-calcific gene expression (ALP, Runx2) while also reducing non-canonical NF- κ B activation. TRAIL did not, however, attenuate TNF α -induced pro-calcific paracrine signalling, as it did when co-incubated with RANKL in Chapter 3. It seems, therefore, that TRAIL-mediated atherosclerotic protection previously observed (Liu *et al.*, 2014; Secchiero *et al.*, 2006) *may not result from the attenuation of TNF α -induced endothelial ALP/BMP-2 release*. Also of note, intracellular BMP-2 production levels remained unaffected by TRAIL, supporting a key observation from Chapter 3 that TRAIL does not affect total BMP-2 turnover but rather specifically prevents RANKL-induced release.

It remains possible that TRAIL-mediated anti-atherosclerotic activity may involve a reduction in non-canonical NF- κ B signalling, influencing genes/proteins not measured in the current study. Additionally, several signalling processes have previously been linked to TRAIL function in atherosclerosis, including anti-oxidant mechanisms and MAPK signalling (Forde *et al.*, 2016), which remain to be fully investigated in the context of TRAIL-induced protection. Interestingly, preliminary investigations within our own research group have highlighted the potential for an anti-oxidant role for TRAIL in the endothelium, which may be involved in TRAIL-mediated anti-atherosclerotic activity (Forde *et al.*, unpublished observations).

4.3.5.4 The Effects of Hyperglycemia on VC Indices in HAECs

Hyperglycemia is best recognised in a clinical setting as a key circulatory hallmark of type-2 diabetics, among which VC is particularly prevalent. Elevated glucose is a recognised promoter of endothelial dysfunction and sustained vascular inflammation, and T2DM has indeed been shown to coincide with increased risk of arterial hardening (Stabley and Towler, 2017) and atherosclerosis (Mirza *et al.*, 2012). Furthermore, elevated glucose has been shown to induce pro-calcific effects in vascular/osteoblastic cells *in vitro* (García-Hernández *et al.*, 2012; Liu *et al.*, 2010), but no studies to date have clarified the effect of hyperglycemia on pro-calcific indices in HAECs, a major contributor to vascular paracrine signalling.

Following the simulation of hyperglycemic conditions, high glucose did not promote BMP-2 protein production but slightly induced its release. Of note, BMP-2 was induced by both RANKL and TNF α alongside NF- κ B activation (not seen in response to hyperglycemia), which suggests that BMP-2 can also be induced by an NF- κ B-independent mechanism. Of note, circulating BMP-2 has been correlated with T2DM in clinical studies (Zhang *et al.*, 2015), but non-endothelial sources (eg. HASMCs) and/or the presence of other pathological stimuli (eg. RANKL, TNF α) likely contribute to this correlation. Extracellular ALP activity was also elevated, and to a much greater extent under severe hyperglycemia. Thus, *endothelial BMP-2/ALP may act in a paracrine manner on the underlying HASMCs during T2DM*, promoting extracellular matrix calcification and contributing to the long-established correlation between elevated circulating BMP-2/ALP and hyperglycemia in clinical studies (Rao and Morghom, 1986; Zhang *et al.*, 2015). Interestingly, OPG protein production/release were also significantly increased following high glucose exposure, albeit to a lesser extent than TNF α , again likely as a natural response to endothelial injury/inflammation and contributory to elevated circulating OPG in diabetics (Secchiero *et al.*, 2006).

4.3.5.5 The Effects of RANKL on VC Indices under Hyperglycemic Conditions in HAECs

The effects of RANKL under hyperglycemic conditions were next assessed. As discussed, RANKL has long been associated with the progression of VC, but the pro-calcific effects of RANKL in the endothelium have not yet been clarified in the presence of high glucose. In the presence of hyperglycemia, ALP mRNA levels were dose-dependently upregulated following RANKL treatment, but (as with TNF α) not to the same extent as with high glucose alone. Furthermore, Runx2 mRNA expression was significantly upregulated following glucose + RANKL exposure, despite being downregulated by glucose alone. This finding suggests that, while hyperglycemia alone does not promote Runx2-mediated pro-calcific activity, *RANKL-induced Runx2 expression may promote VC during both moderate and severe hyperglycemia*. Runx2 is responsible for the upregulation of several pro-calcific genes (Byon *et al.*, 2008), implicating RANKL once more in the promotion of calcification in the endothelium. Also of note, RANKL-induced non-canonical NF- κ B activation is not observed in the presence of high glucose, again implicating an NF- κ B independent mechanism for glucose-induced pro-calcific effects. Wittrant and colleagues (2008) have previously found that high glucose inhibited osteoclast formation in response to RANKL via inhibition of NF- κ B activity, suggesting that glucose-induced pro-calcific functions remain independent of NF- κ B. Thus, RANKL-induced non-canonical NF- κ B activation described in Chapter 3 may be more relevant under normoglycemic conditions.

4.3.5.6 The Effects of TRAIL on VC Indices under Hyperglycemic Conditions in HAECs

Finally, the effects of high glucose + TRAIL were assessed. As mentioned, the protective effects of TRAIL in CVD have been observed (di Bartolo *et al.*, 2013), and in Chapter 3, the ability of TRAIL to counteract RANKL-induced endothelial pro-calcific signalling was described. Thus, we investigate for the first time if TRAIL can exert anti-calcific effects on the endothelium under hyperglycemic conditions associated with T2DM. In this case, *TRAIL was found to completely attenuate glucose-induced ALP mRNA expression and significantly reduce extracellular ALP activity during severe hyperglycemia*. This observation highlights a clear protective effect of TRAIL on glucose-induced calcification, ultimately protecting from extracellular matrix calcification in the underlying HASMC layer. Interestingly, TRAIL did not attenuate glucose-induced BMP-2 release, further supporting the hypothesis that the attenuation of BMP-2 paracrine signalling is achieved via a RANKL-specific mechanism. Moreover, TRAIL attenuates glucose-induced OPG production and restores OPG release,

while also returning Runx2 expression to baseline. Taking this data together, it appears that *TRAIL* may be responsible for maintaining endothelial homeostasis under hyperglycemic conditions, counteracting glucose-specific effects. Despite this, TRAIL exerts a much more potent protective effect on RANKL-induced calcification than it does under either inflammatory or hyperglycemic conditions *in vitro*.

4.3.5.7 HAEC Monoculture: Summary

To summarise the key findings of this chapter, illustrated in Figure 4.8, TNF α and high glucose were found to exert the expected pro-calcific effects in HAECs. Pertinently, RANKL functions together with TNF α to drive BMP-2/ALP paracrine signalling, ultimately promoting calcification within the underlying smooth muscle layer. This effect coincides with elevated non-canonical NF- κ B signalling, implicating this pathway once again in the VC process, while TRAIL again attenuates TNF α -induced non-canonical activation. Both RANKL and TRAIL also exert a weakly pro-calcific and protective influence respectively on the endothelium during hyperglycemia (although to a lesser extent than that observed under inflammatory conditions), in the absence of non-canonical NF- κ B activation. It must be considered, however, that utilising HAECs in isolation only provides a one-dimensional view of the vascular environment; as such, the effects of these stimuli on HASMCs in mono- and co-culture may shed additional light on the roles of RANKL and TRAIL under pathological conditions.

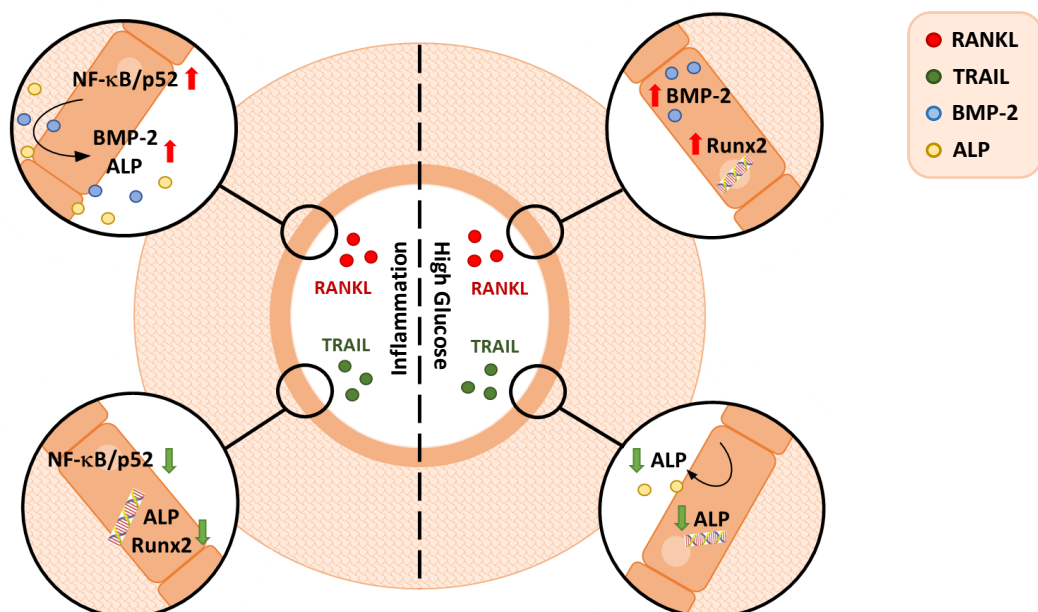


Figure 4.8. Summary of the key findings following endothelial exposure to RANKL/TRAIL +/- TNF α (inflammation) and high glucose. RANKL was found to further upregulate (red arrow) a number of pro-calcific indices when compared to TNF α or glucose treatment alone. TRAIL was found to reduce (green arrow) a number of pro-calcific indices induced by TNF α or glucose treatment.

4.4 HASMC Monoculture

HASMCs were next employed to profile the effects of RANKL and TRAIL on pro-calcific indices under pathological (inflammatory, hyperglycemic) conditions commonly associated with calcification in the vascular media. Again, only key findings will be alluded to in-text, and the readers' attention will be drawn to the corresponding figures. No notable trends were observed in cases where data is not presented.

4.4.1 The Effects of TNF α and Glucose on Pro-Calcific Targets in HASMCs

Once again, the effects of inflammation (TNF α) and hyperglycemia (glucose) were first assessed in the absence of RANKL and TRAIL to better understand natural HASMC responses to these stimuli. Mannitol was again included as a control to ensure the observed effects in response to glucose were not due to an increase in osmotic pressure. Mannitol (at 30 mM) was confirmed to have no effect on any of the measured indices in HASMCs (Appendix 4.7). At an mRNA level, ALP, OPG and Sox9 transcripts were significantly upregulated under inflammatory conditions; BMP-2 mRNA, however, was downregulated by approximately 90% (Figure 4.9A). At a protein level, TNF α induced all measured extra- and intracellular indices in HASMCs (Figure 4.9B-D). Under hyperglycemic conditions, ALP and Sox9 mRNA expression were elevated, while BMP-2 transcript expression was once again dramatically reduced (Figure 4.10A). High glucose induced the release of all measured indices in the conditioned media, while only OPG levels were increased intracellularly. Hyperglycemia also reduced activation of the canonical NF- κ B pathway (Figure 4.10B-D).

4.4.2 The Effects of RANKL and TRAIL under Inflammatory Conditions in HASMCs

Regarding mRNA, co-treatment with both TNF α and RANKL significantly reduced ALP, Runx2 and Sox9 transcript expression (Figure 4.11A) but further promoted BMP-2, OPG and IL-6 mRNA levels (Appendix 4.8A). Interestingly, the addition of TRAIL exerted a similar effect (with the exception of OPG). With respect to protein levels, co-incubation of TNF α with both RANKL and TRAIL (separately) reduced smooth muscle cell OPG release, while TNF α + TRAIL also significantly reduced extracellular ALP activity (Figure 4.11B). Both ligands exerted minimal effects on the TNF α -mediation of intracellular indices. Supporting material is presented in Appendix 4.8 and 4.10.

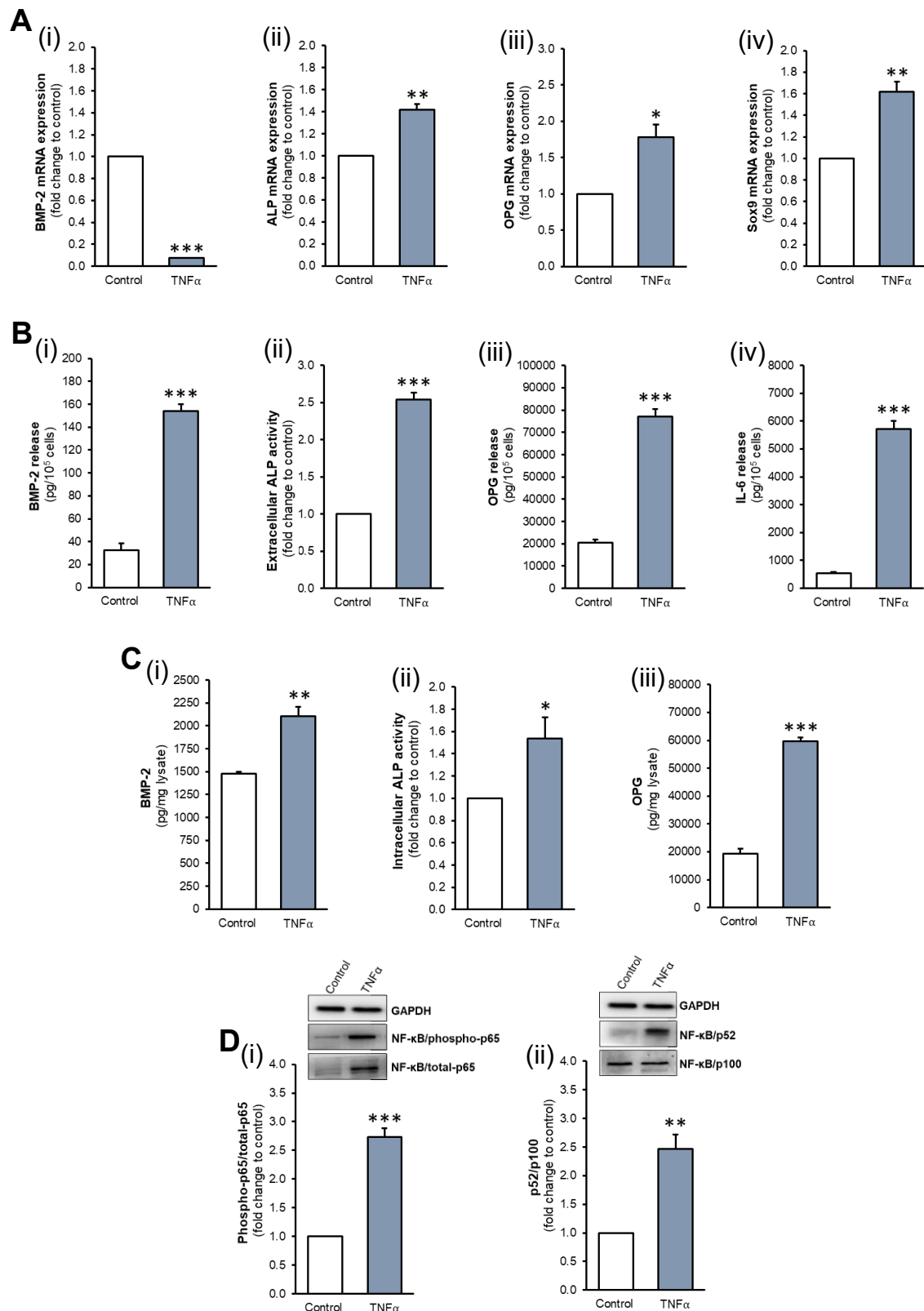


Figure 4.9. The effects of TNF α on pro-calcific indices in HASMC monoculture. HASMCs were exposed to TNF α (100 ng/mL) for 72 hours. **(A)** (i) BMP-2, (ii) ALP, (iii) OPG and (iv) Sox9 mRNA were assessed by RT-qPCR, employing GAPDH as an endogenous control. **(B)** (i) BMP-2, (ii) ALP, (iii) OPG and (iv) IL-6 release, and **(C)** intracellular (i) BMP-2, (ii) ALP and (iii) OPG protein levels were quantified by ELISA and enzyme assay where appropriate. **(D)** (i) Canonical and (ii) non-canonical NF- κ B activation were determined by Western blotting, quantified by scanning densitometry and normalised to GAPDH. Blots are representative. Absolute values for media and protein lysate analyses are normalised to 10⁵ cells and total protein respectively. * $p < 0.05$; ** $p < 0.01$; *** $p < 0.001$ compared to untreated control.

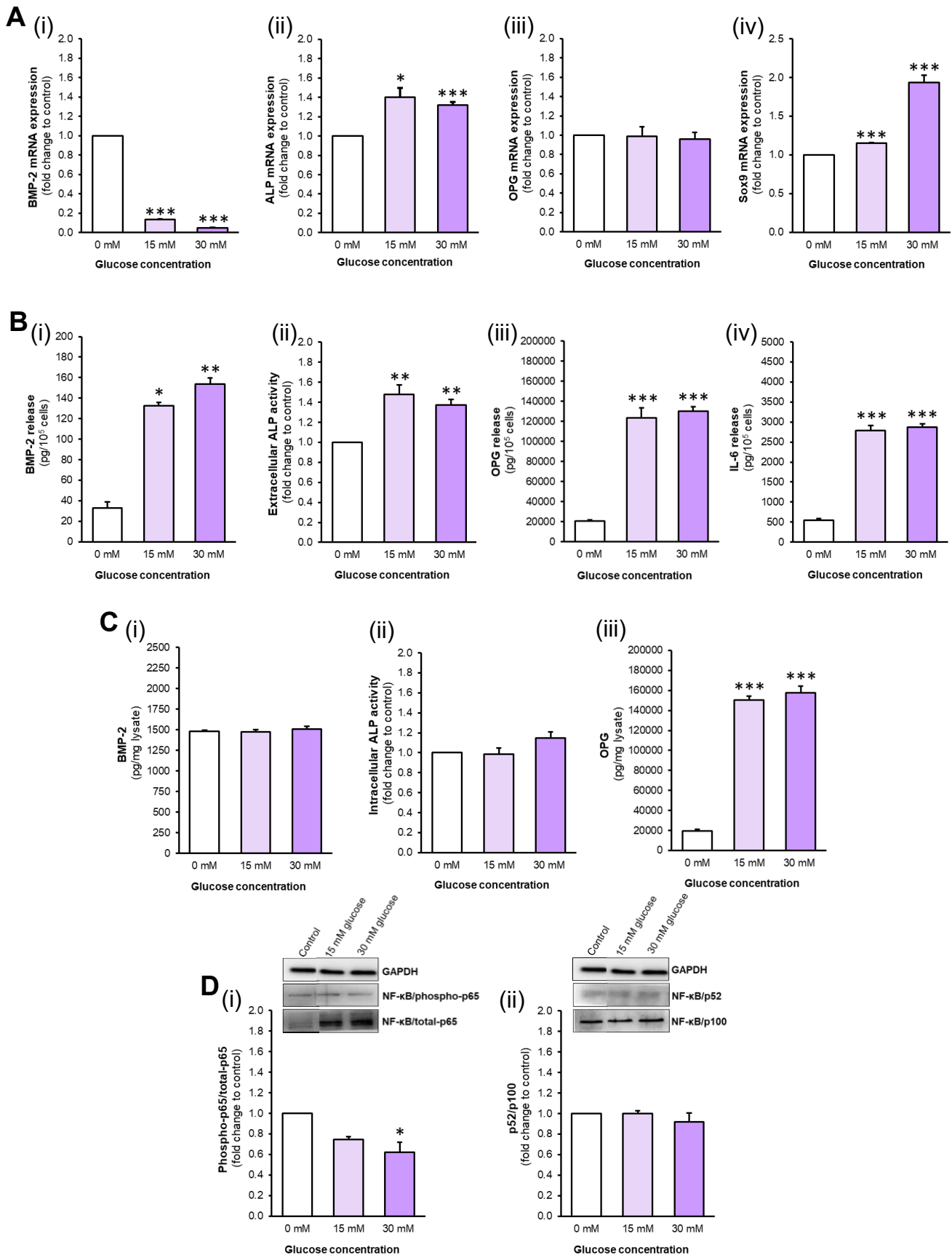


Figure 4.10. The effects of glucose on pro-calcific indices in HASMC monoculture. HASMCs were exposed to glucose (15-30 mM) for 72 hours. **(A)** (i) BMP-2, (ii) ALP, (iii) OPG and (iv) Sox9 mRNA were assessed by RT-qPCR, employing GAPDH as an endogenous control. **(B)** (i) BMP-2, (ii) ALP, (iii) OPG and (iv) IL-6 release, and **(C)** intracellular (i) BMP-2, (ii) ALP and (iii) OPG protein levels were quantified by ELISA and enzyme assay where appropriate. **(D)** (i) Canonical and (ii) non-canonical NF- κ B activation were determined by Western blotting, quantified by scanning densitometry and normalised to GAPDH. Blots are representative (control bands previously presented in Figure 4.9). Absolute values for media and protein lysate analyses are normalised to 10⁵ cells and total protein respectively. * $p < 0.05$; ** $p < 0.01$; *** $p < 0.001$ compared to untreated control.

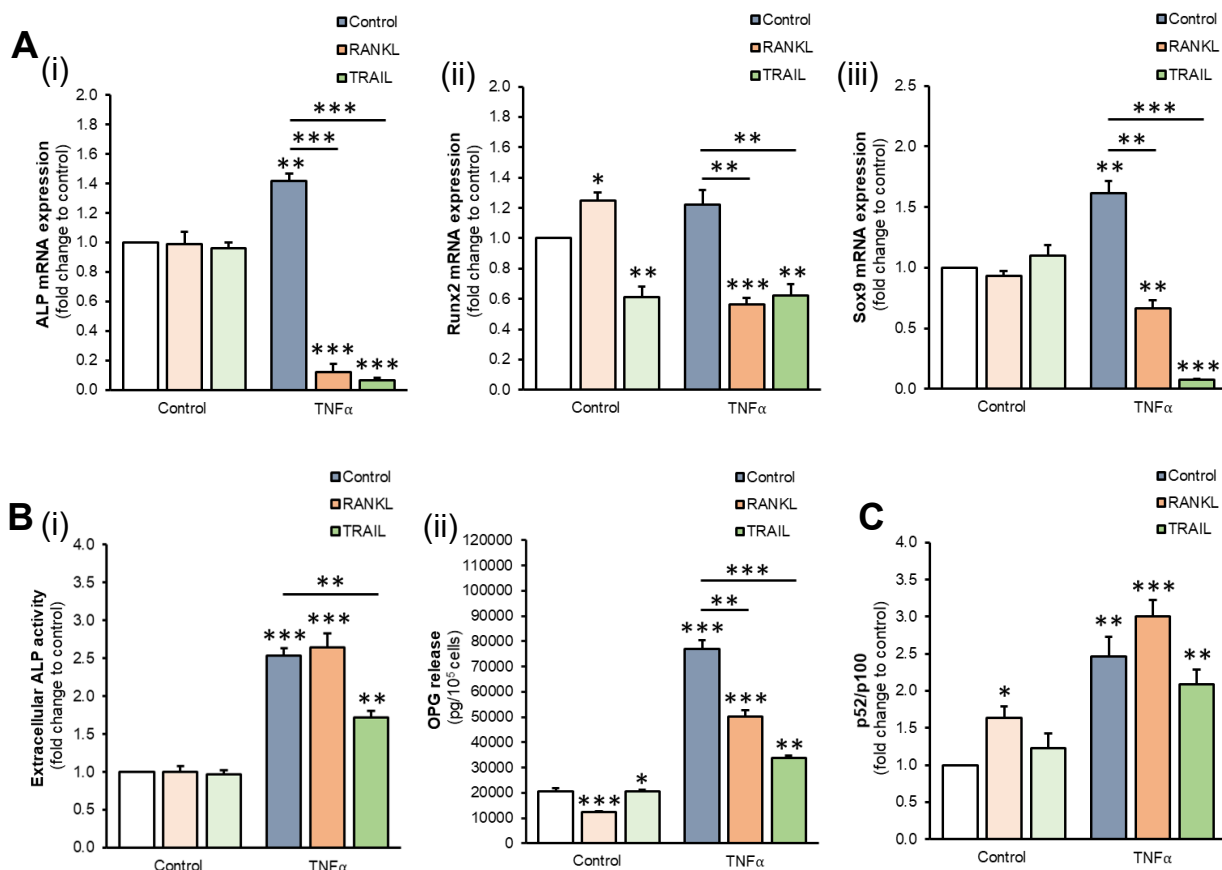


Figure 4.11. The effects of TNF α +/- RANKL/TRAIL on pro-calcific indices in HASMC monoculture. HASMCs were exposed to TNF α (100 ng/mL) +/- RANKL (25 ng/mL) or TRAIL (5 ng/mL) for 72 hours. (A) mRNA expression of (i) ALP, (ii) Runx2 and (iii) Sox9 were analysed by RT-qPCR employing GAPDH as an endogenous control. (B) (i) Extracellular ALP activity was quantified by activity assay and (ii) OPG release was quantified by ELISA, normalised to 10⁵ cells. (C) Non-canonical NF- κ B activation was determined by Western blotting, quantified by scanning densitometry and normalised to GAPDH. Representative blots are presented in Appendix 4.10. * $p < 0.05$; ** $p < 0.01$; *** $p < 0.001$ compared to untreated control unless otherwise stated; bars indicate statistical significance between treatment groups.

4.4.3 The Effects of RANKL and TRAIL under Hyperglycemic Conditions in HASMCs

At a transcriptional level, both RANKL and TRAIL attenuated the upregulation of glucose-induced ALP/Sox9 mRNA, while TRAIL also reduced Runx2 expression. Interestingly, OPG mRNA was upregulated by the co-addition of both RANKL and TRAIL under hyperglycemic conditions (Figure 4.12A). Both ligands reduced OPG release induced by hyperglycemia, while TRAIL significantly reduced IL-6 release into the conditioned media (Figure 4.12B). Neither RANKL nor TRAIL exerted any relevant effects on glucose-mediated BMP-2/ALP release or intracellular pro-calcific indices (Appendix 4.9B, C), while canonical NF- κ B induced by both ligands alone was completely attenuated in the presence of high glucose. Furthermore, non-canonical NF- κ B activation induced by RANKL was also attenuated under hyperglycemic conditions (Appendix 4.11C).

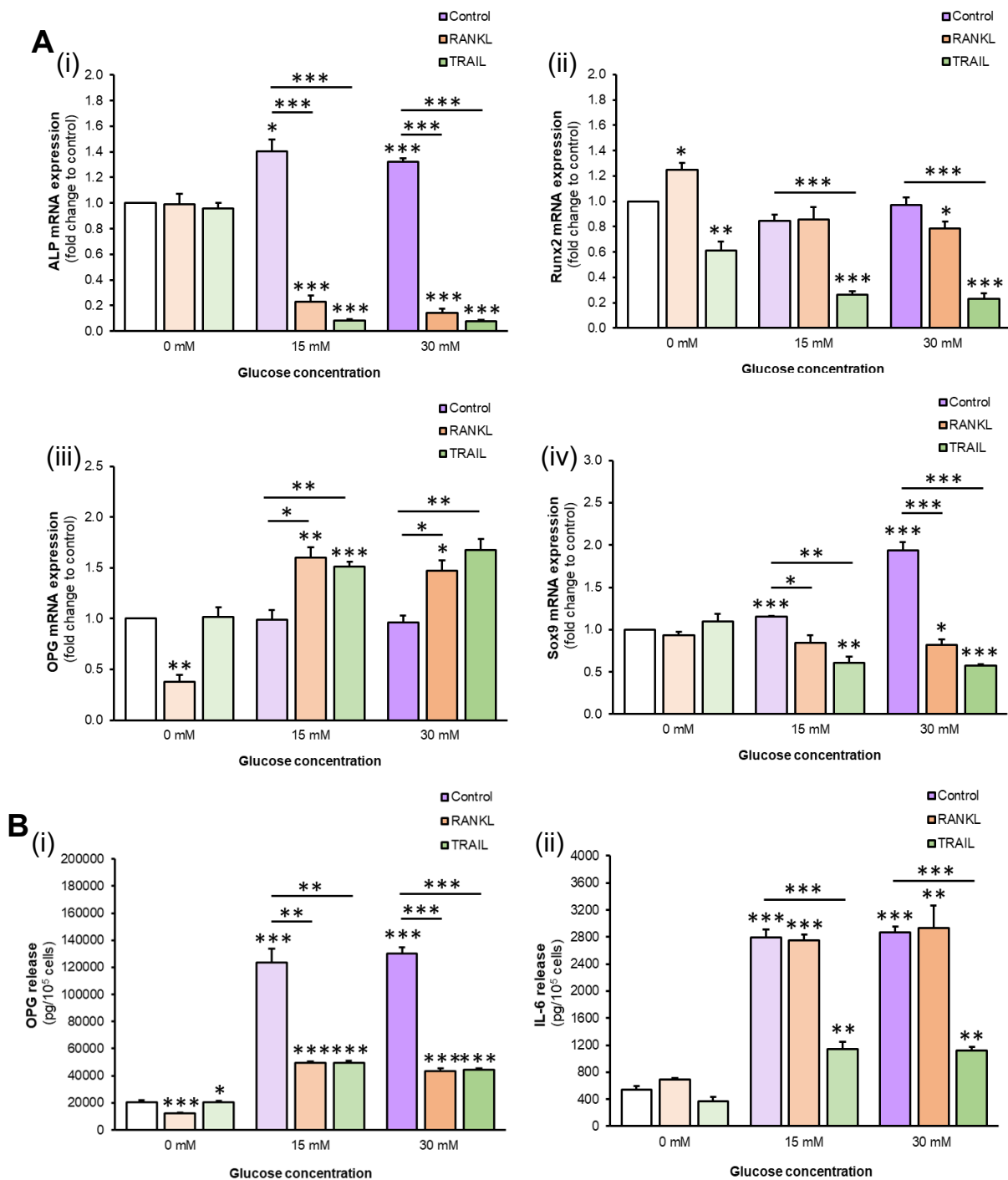


Figure 4.12. The effects of glucose +/- RANKL/TRAIL on pro-calcific indices in HASMC monoculture. HASMCs were exposed to glucose (15-30 mM) +/- RANKL (25 ng/mL) or TRAIL (5 ng/mL) for 72 hours. **(A)** mRNA expression of (i) ALP, (ii) Runx2, (iii) OPG and (iv) Sox9 were analysed by RT-qPCR employing GAPDH as an endogenous control. **(B)** (i) OPG and (ii) IL-6 release were quantified by ELISA, normalised to 10⁵ cells. * $p < 0.05$; ** $p < 0.01$; *** $p < 0.001$ compared to untreated control unless otherwise stated; bars indicate statistical significance between treatment groups.

4.4.4 HASMC Monoculture: Summary of Results

HASMC exposure to RANKL and TRAIL under inflammatory and hyperglycemic conditions influenced a number of pro-calcific indices, summarised below in Table 4.3.

Table 4.3. The effects of TNF α or glucose +/- RANKL or TRAIL in HASMCs.

<i>Inflammation</i>			RANKL	TRAIL
BMP-2	<i>mRNA</i>	↓	↑↑	↑
ALP	<i>mRNA</i>	↑	↓	↓
	<i>Extracellular Activity</i>	↑↑	↑↑	↑
OPG	<i>mRNA</i>	↑	↑↑	↓
	<i>Extracellular Protein</i>	↑↑↑	↑↑	↑
IL-6	<i>mRNA</i>	↓	↑	↑↑
Runx2	<i>mRNA</i>	–	↓	↓
Sox9	<i>mRNA</i>	↑	↓	↓↓
<i>Hyperglycemia</i>				
BMP-2	<i>mRNA</i>	↓	–	–
	<i>Intracellular Protein</i>	–	↑	–
ALP	<i>mRNA</i>	↑	↓	↓
OPG	<i>mRNA</i>	–	↑	↑
	<i>Extracellular Protein</i>	↑↑	↑	↑
	<i>Intracellular Protein</i>	↑↑	↑	↑↑
IL-6	<i>mRNA</i>	↓	↑	↑↑
	<i>Extracellular Protein</i>	↑↑	↑↑	↑
Runx2	<i>mRNA</i>	–	↓	↓↓
Sox9	<i>mRNA</i>	↑	↓	↓
NF-κB (p-p65/t-p65)	<i>Activation</i>	↓	–	–

p-p65, phospho-p65; t-p65, total-p65. ↑, upregulation; ↑↑, further upregulation relative to corresponding treatment conditions; ↓, downregulation; ↓↓, further downregulation relative to corresponding treatment conditions; –, no change.

4.4.5 HASMC Monoculture: Discussion

The pathological effects of TNF α and high glucose have previously been described in the vasculature, but few studies attempt to clarify the role of RANKL and TRAIL under inflammatory and hyperglycemic conditions in VSMCs, the primary location of medial VC *in vivo*. In this respect, we profile the most comprehensive range of pro-calcific indices in primary HASMCs under these common pathological conditions in T2DM/CVD, for the first time incorporating key ligands involved in the VC process. As noted, during TNF α -induced inflammation, the endothelial monolayer is rendered permeable to circulating proteins, while during hyperglycemia, glucose transport is facilitated by GLUT-1 transporters across the endothelial monolayer (Viator and Fouty, 2009). These pathological conditions in the vasculature may therefore exert direct pro-calcific effects on the underlying smooth muscle cell layer, and prior to analysis in co-culture, the direct effects of both TNF α and glucose must be clarified in HASMCs. Again, due to the comprehensive nature of this study, this discussion will first focus on the key relevant findings regarding the effects of inflammation and high glucose on HASMCs, prior to the incorporation of RANKL and TRAIL into these models.

4.4.5.1 The Effects of TNF α on VC Indices in HASMCs

As discussed, inflammatory cytokines such as TNF α may allow circulating proteins to exert direct effects on the medial smooth muscle layer. In this respect, serum TNF α levels are particularly elevated during T2DM/CVD (Olson *et al.*, 2012; Levine *et al.*, 1990; Mirza *et al.*, 2012) and this cytokine is highly expressed alongside atherosclerotic calcification (Barath *et al.*, 1990). Medial arterial hardening, the prime focus of this study, is indeed known to co-exist with atherosclerosis (McCullough *et al.*, 2008), and thus the pro-calcific effects of the involved cytokines at these sites cannot be ignored. Of interest, pro-inflammatory cytokines (eg. TNF α , IL-6) have been implicated in key osteogenic processes in the vasculature that drive medial VC (Al-Aly, 2008; Illiandri *et al.*, 2016; Shao *et al.*, 2010), and have been shown to induce osteogenic differentiation and mineralisation of calcifying vascular cells (Aikawa *et al.*, 2007). More specifically, TNF α has been shown to directly induce osteogenic responses and calcification in VSMCs (Liu *et al.*, 2010; Tintut *et al.*, 2000).

Following assessment of a wide range of pro-calcific indices, *TNF α was found to induce the vast majority of pro-calcific indices in HASMCs*, both at an mRNA and protein level. In consideration of the documented pro-calcific effects of this cytokine (Lee *et al.*, 2010; Tintut

et al., 2000), this result is unsurprising. Interesting trends were observed, however, regarding BMP-2, as the concurrent increase in BMP-2 release and downregulation of mRNA expression may suggest only a temporary induction of BMP-2 release in response to TNF α . Indeed, HAECs, and not HASMCs, are thought to be the primary source of BMP-2 paracrine signalling in the vasculature (Osako *et al.*, 2010; Davenport *et al.*, 2016), and minimal BMP-2 was found to be released from HASMCs (under basal conditions or following RANKL exposure) in Chapter 3. TNF α , however, strongly induced BMP-2 release, and thus HASMCs may release pro-calcific autocrine signals under pro-inflammatory conditions to promote VC. Nonetheless, further experimentation is necessary to determine if this release is maintained longer-term.

OPG levels were significantly upregulated both at an mRNA and protein level following TNF α exposure in HASMCs, a finding previously reported by multiple authors in smooth muscle (Ben-Tal Cohen *et al.*, 2007; Davenport *et al.*, 2018; Olesen *et al.*, 2005). This observation is perhaps more physiologically relevant, given that OPG release from smooth muscle is significantly greater than from the endothelium (Davenport *et al.*, 2016). It is again likely that OPG is released as part of a cardioprotective mechanism in response to vascular injury, and contributing significantly to the elevated circulating OPG noted in diabetic patients (Abedin *et al.*, 2007; O'Sullivan *et al.*, 2010; Schoppet *et al.*, 2003). On an additional note, the well-defined induction of IL-6 release in response to TNF α exposure may also contribute to the observed pro-calcific effects, as this cytokine has also been shown to induce calcification and mineralisation of vascular cells (Aikawa *et al.*, 2007).

4.4.5.2 The Effects of RANKL on VC Indices under Inflammatory Conditions in HASMCs

Of interest, many similarities in the effects of TNF α and RANKL have been observed in osteogenic and calcific processes (Shao *et al.*, 2010). While the role for RANKL in osteoclastogenesis has been described in detail, TNF α has long been known to regulate bone turnover, inhibiting osteoblastic function and promoting bone resorption (Azuma *et al.*, 2000; Gaspersic *et al.*, 2003). The upregulation of osteoblastic genes in the vasculature are responsible for driving VC, however, it seems that the paradoxical effects of RANKL in bone versus vessel (i.e. RANKL exerts osteoclastic/resorptive functions in bone, but promotes calcification in an *osteoblastic* role during VC) appear also relevant to TNF α .

Interestingly, the observed decrease in BMP-2 mRNA expression was significantly reversed following RANKL co-treatment, although paracrine levels of BMP-2 remained unchanged

compared to that induced by TNF α alone; this finding may be suggestive that the combination of both proteins exerts a longer-term upregulation of BMP-2 as part of a pro-calcific phenotypic change. The relevance of this finding is augmented by the fact that RANKL treatment alone did not induce BMP-2 expression or release in HASMCs, and as such, the proposed autocrine release of BMP-2 appears to be TNF α -dependent. It is possible, therefore, that smooth muscle BMP-2 signalling may only occur in inflamed areas of vasculature affected by atherosclerosis, as previously reported by Simões Sato *et al.* (2014). The opposite trends, however, were observed in ALP, Runx2 and Sox9 mRNA expression following TNF α + RANKL exposure. While the inclusion of RANKL significantly downregulated TNF α -induced pro-calcific gene expression, no change was noted in ALP activity, again highlighting divergent responses at a transcriptional and translational level common throughout this study. As seen with OPG regulation in Chapter 3, pro-calcific gene regulation may involve a bimodal response to these stimuli, with an initial upregulation caused by TNF α /RANKL activation followed by a subsequent downregulation as part of a natural protective mechanism.

Also of relevance, co-incubation with RANKL results in a reduction of smooth muscle OPG release, exerting the opposite effect to TNF α but exerting a similar effect to RANKL exposure alone. Of note, we have confirmed in Chapter 3 that this finding is not due to RANKL:OPG ELISA interference, and so we propose that during inflammation, the presence of RANKL renders the smooth muscle cell layer more susceptible to calcification. While this observation was of minimal relevance in Chapter 3 (where we considered an intact endothelial barrier), this data is particularly pertinent in areas of vasculature affected by EC dysfunction/atherosclerosis. With the exception of OPG, however, the presence of RANKL does not significantly affect TNF α -induced pro-calcific indices, and *the two proteins do not appear to function synergistically in the promotion of VC*, despite previous reports of synergy during osteoclastogenesis (Fuller *et al.*, 2002; Yamashita *et al.* 2015).

4.4.5.3 The Effects of TRAIL on VC Indices under Inflammatory Conditions in HASMCs

In Chapter 3, it was found that while TRAIL attenuates RANKL-induced pro-calcific signalling in the endothelium, its protective influence in the smooth muscle cell layer is minimal. TRAIL has, however, been shown to exert anti-calcific effects under pro-inflammatory atherosclerotic conditions *in vitro* and *in vivo* (di Bartolo *et al.*, 2011; di Bartolo *et al.*, 2013; Liu *et al.*, 2014), and as such, it remains to be determined if TRAIL can attenuate pro-calcific signalling in

HASMCs during inflammation. Interestingly, TRAIL was found to exert similar effects to RANKL in the presence of TNF α at an mRNA level, reversing TNF α -induced downregulation of BMP-2, and downregulating multiple pro-calcific genes. These trends are not maintained at a protein level, however, and so this finding is of minimal physiological relevance. TRAIL did, however, reduce ALP activity in VSMC-conditioned media, thereby reducing extracellular matrix calcification in the vascular media (Orimo, 2010). Furthermore, TRAIL co-incubation under inflammatory conditions significantly reduced OPG release; as for RANKL, this observation cannot be attributed to OPG:TRAIL interference, but does indicate that this effect is not RANKL-specific (and perhaps a phenomenon induced by high concentrations of extracellular OPG decoy receptors). Physiologically, the smooth muscle cell layer is rendered more susceptible to vascular injury following reduced OPG release, and as such, TRAIL does not appear to exert anti-calcific effects on the vasculature via OPG regulation under inflammatory conditions. Overall, *TRAIL does not exert a strong vasoprotective influence on the medial arterial layer in areas of dysfunctional endothelium*, suggesting that the aforementioned TRAIL protection in atherosclerosis may be exerted via a different mechanism.

4.4.5.4 The Effects of Hyperglycemia on VC Indices in HASMCs

Like TNF α , hyperglycemia is well recognized in its pathological role in T2DM and has been long associated with CVD and arterial hardening (Liu *et al.*, 2010; Stabley and Towler, 2017). Elevated glucose has been shown to elicit pro-calcific effects in VSMCs *in vitro* (Chen *et al.*, 2006; Liu *et al.*, 2010), but to date, such a wide range of pro-calcific indices have not been profiled in HASMCs under hyperglycemic conditions. In this respect, and unsurprisingly, *several key pro-calcific indices were found to be upregulated in response to moderate and severe hyperglycemia*. Most relevantly, active ALP and BMP-2 release were significantly induced following glucose treatment, suggesting that during T2DM (permitting glucose transport across the EC monolayer) HASMCs secrete autocrine factors that promote medial calcification. In agreement with this finding, BMP-2 has previously been shown to be induced in HASMCs following hyperglycemic treatment (Liu *et al.*, 2010), and Al-Aly *et al.* (2007) noted that hyperglycemia and calcification progressed alongside activation of the BMP-2 pathway *in vivo*. Additionally, ALP activity (and mRNA) have also been shown to be induced following glucose treatment in HASMCs (Chen *et al.*, 2006; Liu *et al.*, 2010), and thus hyperglycemia may contribute to explaining the elevated circulating levels of both BMP-2 and ALP observed in T2DM patients (Rao and Morghom, 1986; Zhang *et al.*, 2015).

It should be noted, however, that BMP-2 transcript expression was significantly downregulated under hyperglycemic conditions. Contrastingly, BMP-2 mRNA has previously been shown to be upregulated following exposure to high glucose (Liu *et al.*, 2010), however, this finding followed only 24 hours' incubation. The observed decrease in BMP-2 mRNA at 72 hours is less easily explained, and may suggest that the autocrine secretion of BMP-2 from HASMCs is short-lived; as mentioned, HAECs are considered to be the primary source of secretory BMP-2 in the vasculature (Davenport *et al.*, 2016; Osako *et al.*, 2010). Also of interest, Sox9 chondrocytic transcription factor appears to be a key driver of pro-calcific indices in HASMCs in response to high glucose, particularly under severe hyperglycemic conditions. As noted in Chapter 3, both Runx2 and Sox9 modulate a similar range of osteochondroblastic genes, and it has been thought in recent years that VC may more closely resemble chondrogenesis (Speer *et al.*, 2009). Indeed, previous research has implicated both Runx2 and Sox9 in HASMC trans-differentiation induced by hyperglycemia (Alesutan *et al.*, 2017; Bessueille *et al.*, 2015; Leopold, 2015), but we propose a more pronounced role for Sox9 in this process.

Interestingly, OPG production and release were significantly elevated under hyperglycemic conditions, again as a potential cardioprotective response to injurious stimuli and contributing to elevated circulating OPG during T2DM (Bjerre, 2013; Secchiero *et al.*, 2006). In contrast to TNF α -exposure, however, OPG mRNA expression was downregulated alongside this increase in protein levels. With regard to the literature, a dose-dependent increase in OPG mRNA has been associated with 48-hour high glucose treatment in VSMCs (Chang *et al.*, 2015), while in longer-term exposures (2 weeks), no change in OPG mRNA was detected (Hadi and Suwaidi, 2007). This finding may suggest that the observed induction in OPG release/production is time-dependent, with an initial upregulation of OPG mRNA subsequently followed by a reversal and ultimate loss of this effect (a phenomenon also observed in Chapter 3). As noted, transcriptional and translational pathways are often distinct from one another (Carmody and Wente, 2009; Greenbaum *et al.*, 2003), but it is as of yet unclear whether OPG acts primarily as an early-stage marker of VC or plays a longer-term role in vasoprotection.

4.4.5.5 The Effects of RANKL on VC Indices under Hyperglycemic Conditions in HASMCs

There is minimal evidence in the literature regarding the role of RANKL under hyperglycemic conditions, despite being recognised as a key promoter of VC (Collin-Osdoby, 2004); as such, the effects of RANKL on the smooth muscle cell layer remain to be defined. Interestingly, glucose-induced BMP-2 release remained unaffected by RANKL co-incubation, however,

RANKL completely recovered BMP-2 downregulation at a transcriptional level. It is unclear as of yet what the significance of this is, but it is possible that RANKL may promote the longer-term maintenance of autocrine BMP-2 signalling within the HASMC layer; indeed, RANKL also induces the production of intracellular BMP-2 in the presence of glucose. With the exception of BMP-2, *RANKL does not appear to have a synergistic effect on pro-calcific indices under hyperglycemic conditions in the smooth muscle cell layer*, but rather reduces the transcription of pro-calcific genes, perhaps as part of a compensatory mechanism designed to prevent VC. Furthermore, RANKL significantly induced OPG mRNA expression while simultaneously decreasing OPG release, despite having minimal effect on intracellular protein expression. Thus, in the presence of RANKL, the vasculature may be rendered more susceptible to injury. As a final note, RANKL does not appear to function via NF- κ B signalling in HASMCs under hyperglycemic conditions, and rather the activation of these pathways are more relevant to RANKL-induced pro-calcific signalling in areas of healthy/intact endothelium. The mechanism by which RANKL functions in the presence of glucose remains to be delineated, but this data further supports our hypothesis that *RANKL exerts its pro-calcific function predominantly via endothelial signalling*, and not directly on HASMCs.

4.4.5.6 The Effects of TRAIL on VC Indices under Hyperglycemic Conditions in HASMCs

Again, there is limited data to consider regarding the role of TRAIL in smooth muscle under hyperglycemic conditions. As noted, TRAIL has been known to exert a protective influence under hyperglycemic conditions *in vivo* (Liu *et al.*, 2014), but it is unclear if this protection is mediated via modulation of pro-calcific indices or if this effect occurs in HASMCs. Interestingly, TRAIL exerts similar effects to RANKL on the vasculature at an mRNA level in the downregulation of pro-calcific genes; TRAIL does not affect the measured pro-calcific indices at a protein level, however, and as such, *does not appear to exert a protective influence under hyperglycemic conditions in HASMCs*. Furthermore, TRAIL-induced canonical NF- κ B activation observed in healthy VSMCs does not occur during hyperglycemia, indicating that high glucose mediates pro-calcific indices via a distinct and unrelated mechanism. Like RANKL, TRAIL was also found to downregulate OPG release while simultaneously inducing its expression. Thus, while this effect may render the vasculature prone to damage, it seems to be relevant to both soluble OPG receptors rather than being RANKL- or TRAIL-specific. This finding may also contribute to explaining the contrasting data with regard to the role of TRAIL in the vasculature discussed in Chapter 3.

4.4.5.7 HASMC Monoculture: Summary

As summarised in Table 4.3 and Figure 4.13 below, it is clear that both RANKL and TRAIL exert some function in the medial smooth muscle layer under inflammatory and hyperglycemic conditions, however, these effects appear less potent than those observed in the endothelium. RANKL did not synergistically promote any of the measured pro-calcific indices under inflammatory conditions, and while TRAIL slightly reduced TNF α -induced ALP release, a strong protective influence on HASMCs was not observed. Similarly, while both moderate and severe hyperglycemia promoted many pro-calcific genes/proteins, RANKL did not accelerate this effect, nor did TRAIL protect from it. Interestingly, although TNF α may also exert its function via NF- κ B signalling in HASMCs, TRAIL co-incubation did not attenuate non-canonical activation in this case; this finding may suggest that TRAIL only attenuates this pathway in the endothelium (as a similar finding was observed in Chapter 3). Overall, it is clear that RANKL and TRAIL exert their respective pro-calcific and protective functions predominantly via endothelial signalling under pathological conditions. Therefore, it is hoped that the inclusion of this paracrine contribution in co-culture may shed additional light on the roles of both RANKL and TRAIL in VC in the presence of inflammation and hyperglycemia.

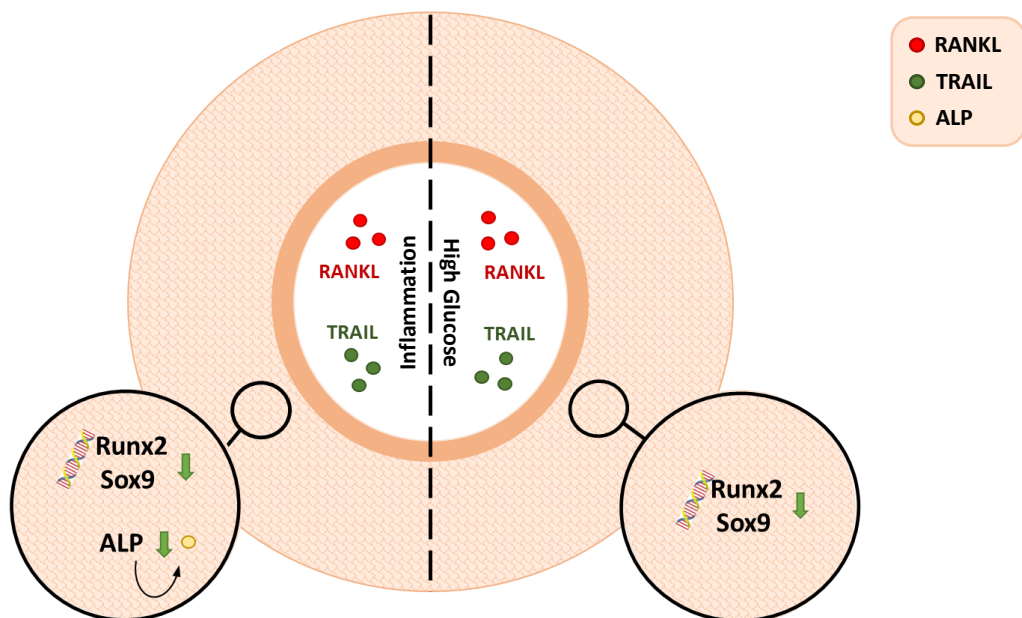


Figure 4.13. Summary of the key findings following smooth muscle exposure to RANKL/TRAIL +/- TNF α (inflammation) and high glucose. RANKL did not further promote any of the measured pro-calcific indices mediated by TNF α or glucose treatment. TRAIL was found to exert a slight protective influence (green arrow) via downregulation of both glucose- and TNF α -induced Runx2/Sox9 mRNA expression, and also slightly reduced TNF α -mediated active ALP release.

4.5 HAEC:HASC Co-culture

Finally, a co-culture model was employed to facilitate paracrine communication between the endothelium and smooth muscle cell (Figure 4.14). Following treatment of HAECs with TNF α or glucose in the absence and presence of RANKL/TRAIL, conditioned media from the *subluminal compartment* was assessed for paracrine signalling molecules, while *underlying HASMCs* were monitored for pro-calcific gene and protein expression. Once again, only the key findings from the following investigations will be discussed in-text, while the reader will be directed to the relevant figure panels. No notable trends were observed in cases where data is not presented.

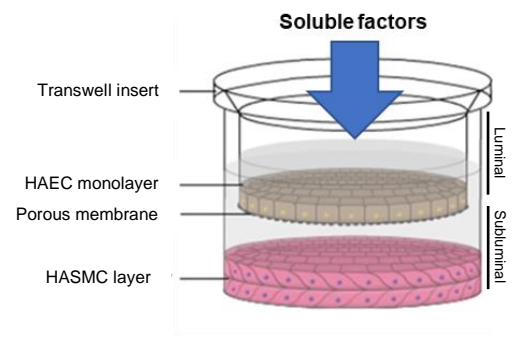


Figure 4.14. The co-culture model. HAECs in semi-permeable transwell inserts, suspended above a confluent smooth muscle layer were exposed to soluble factors (i.e. RANKL/TRAIL +/- glucose, TNF α) for 72 hours.

4.5.1 The Effects of TNF α and Glucose on Pro-Calcific Targets in Co-culture

Following endothelial treatment with TNF α , no pro-calcific genes were upregulated in HASMCs, but rather a downregulation was observed in Runx2 and OPG mRNA (Figure 4.15A). TNF α treatment also induced the release of all measured extracellular indices into the subluminal compartment (Figure 4.15B), while intracellular BMP-2 and OPG in the underlying HASMCs were also elevated (Figure 4.15C). Both NF- κ B pathways were activated in HASMCs following HAEC treatment (Figure 4.15D). With regard to endothelial glucose treatment, smooth muscle ALP/Sox9 mRNA levels were upregulated following severe hyperglycemia, while Runx2/OPG mRNA were downregulated (Figure 4.16A). High glucose also stimulated the release of BMP-2, ALP and IL-6 into the subluminal compartment (Figure 4.16B), while intracellular OPG levels in the underlying HASMCs was reduced (Figure 4.16C). Hyperglycemic treatment did not activate NF- κ B in the underlying HASMCs (Figure 4.16D).

4.5.2 The Effects of RANKL and TRAIL under Inflammatory Conditions in Co-culture

At an mRNA level, both RANKL and TRAIL downregulated TNF α -induced Runx2 and OPG, but upregulated BMP-2 mRNA in the underlying HASMCs (Appendix 4.11A). At a protein level, RANKL co-treatment further promoted TNF α -induced BMP-2 release into the subluminal space, while also further driving smooth muscle OPG. TRAIL, on the other hand,

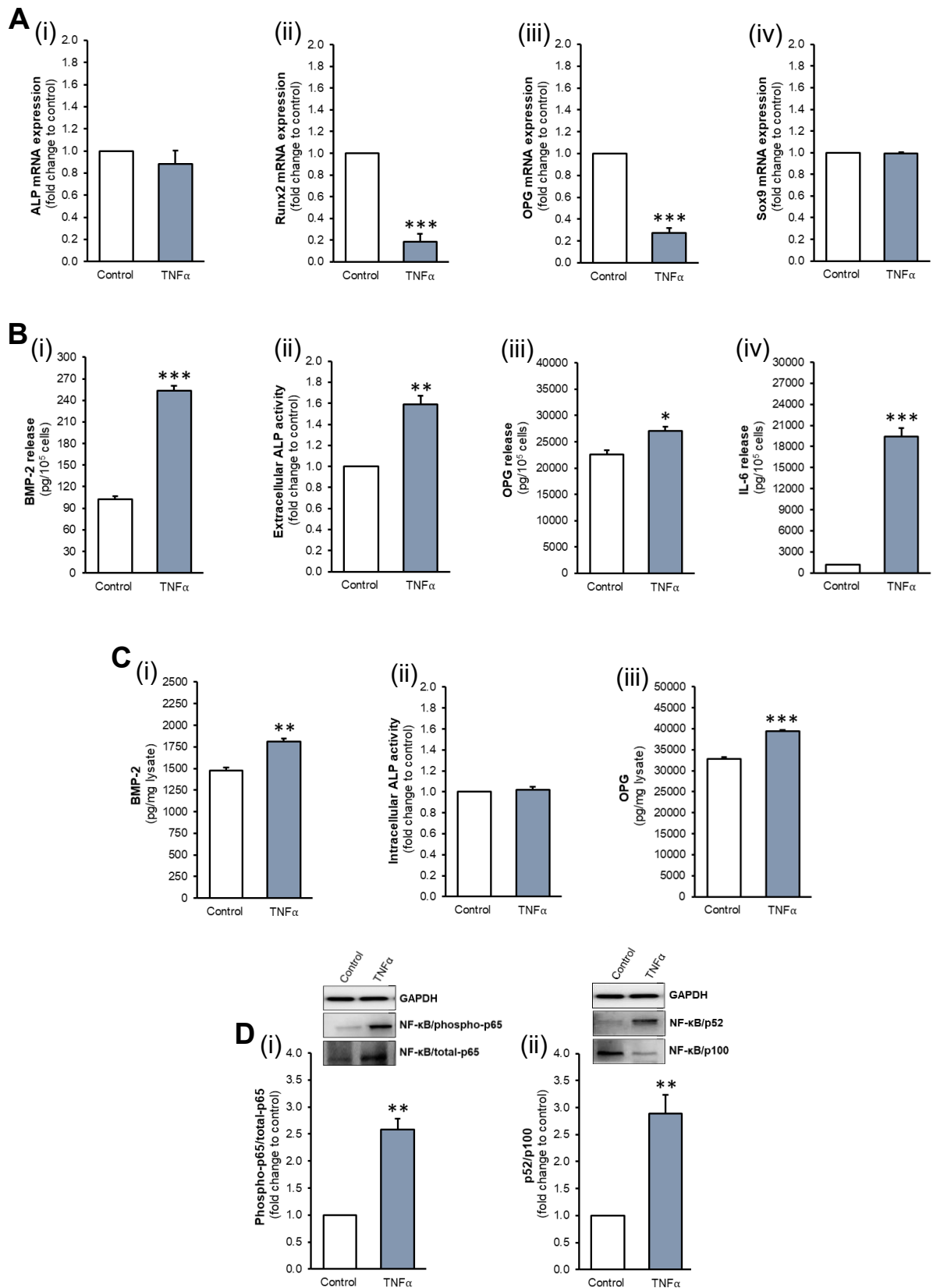


Figure 4.15. The effects of TNF α on pro-calcific indices in co-cultured HASMCs. HAECs were exposed to TNF α (100 ng/mL) for 72 hours, and the underlying HASMCs harvested for analysis. **(A)** (i) ALP, (ii) Runx2, (iii) OPG and (iv) Sox9 mRNA were assessed by RT-qPCR, employing GAPDH as an endogenous control. **(B)** (i) BMP-2, (ii) ALP, (iii) OPG and (iv) IL-6 release, and **(C)** intracellular (i) BMP-2, (ii) ALP and (iii) OPG protein levels were quantified by ELISA and enzyme assay where appropriate. **(D)** (i) Canonical and (ii) non-canonical NF- κ B activation were determined by Western blotting, quantified by scanning densitometry and normalised to GAPDH. Blots are representative. Absolute values for media and protein lysate analyses are normalised to 10⁵ cells and total protein respectively. * $p < 0.05$; ** $p < 0.01$; *** $p < 0.001$ compared to untreated control.

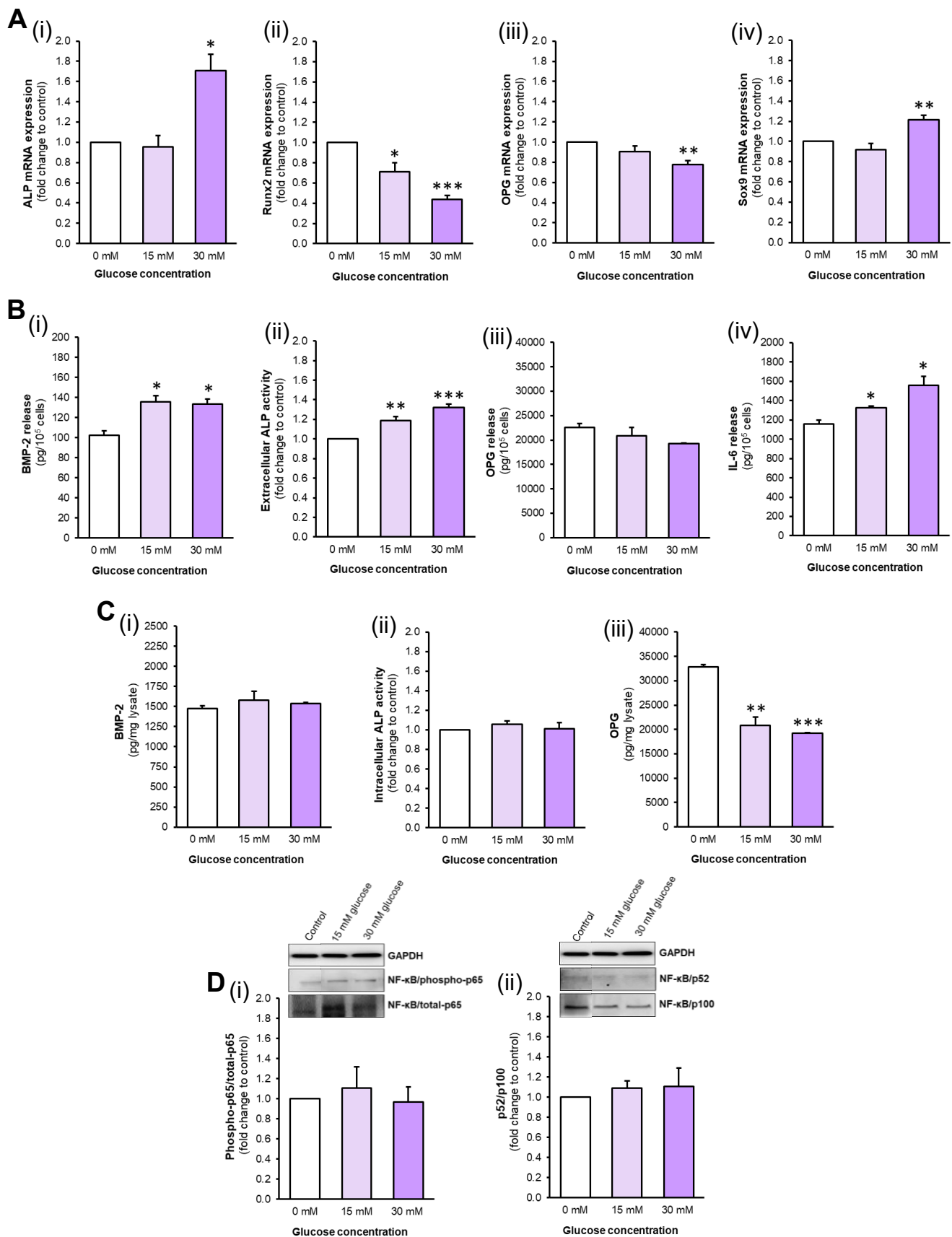


Figure 4.16. The effects of glucose on pro-calcific indices in co-cultured HASMCs. HAECs were exposed to glucose (15-30 mM) for 72 hours, and the underlying HASMCs harvested for analysis. **(A)** (i) ALP, (ii) Runx2, (iii) OPG and (iv) Sox9 mRNA were assessed by RT-qPCR, employing GAPDH as an endogenous control. **(B)** (i) BMP-2, (ii) ALP, (iii) OPG and (iv) IL-6 release, and **(C)** intracellular (i) BMP-2, (ii) ALP and (iii) OPG protein levels were quantified by ELISA and enzyme assay where appropriate. **(D)** (i) Canonical and (ii) non-canonical NF- κ B activation were determined by Western blotting, quantified by scanning densitometry and normalised to GAPDH. Blots are representative (control bands previously presented in Figure 4.15). Absolute values for media and protein lysate analyses are normalised to 10^5 cells and total protein respectively. * $p < 0.05$; ** $p < 0.01$; *** $p < 0.001$ compared to untreated control.

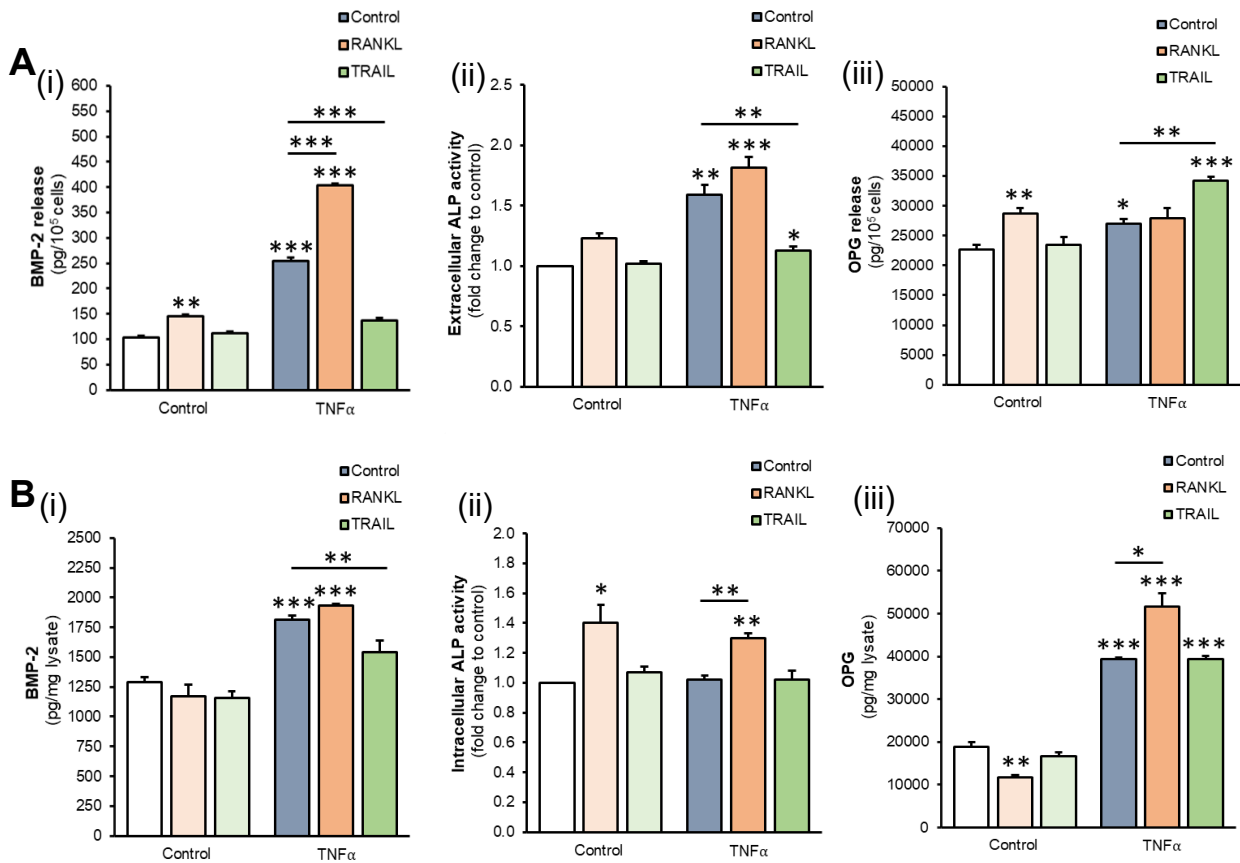


Figure 4.17. The effects of TNF α +/- RANKL/TRAIL on pro-calcific indices in co-cultured HASMCs. HAECs in transwell inserts were exposed to TNF α (100 ng/mL) +/- RANKL (25 ng/mL) or TRAIL (5 ng/mL) for 72 hours, and HASMCs in the subluminal compartment were harvested for analysis. **(A)** (i) BMP-2, (ii) ALP activity and (iii) OPG release were quantified by ELISA and enzyme assay where appropriate, normalised to 10⁵ cells. **(B)** Intracellular (i) BMP-2, (ii) ALP activity and (iii) OPG in the underlying HASMCs were assessed similarly, normalised to total cellular protein. * $p < 0.05$; ** $p < 0.01$; *** $p < 0.001$ compared to untreated control unless otherwise stated; bars indicate statistical significance between treatment groups.

significantly reduced TNF α -mediated BMP-2/ALP release, further promoted OPG release, and reduced HASMC BMP-2 production (Figure 4.17A, B). Both ligands significantly reduced smooth muscle NF- κ B/p52 activation (Appendix 4.13). Supporting data is presented in Appendix 4.11 and 4.13.

4.5.3 The Effects of RANKL and TRAIL under Hyperglycemic Conditions in Co-culture

Following hyperglycemic treatment, RANKL further promoted glucose-induced BMP-2/ALP release into the subluminal space, while TRAIL completely attenuated the release of both paracrine elements. TRAIL also promoted OPG release, and smooth muscle intracellular OPG in the presence of hyperglycemia (Figure 4.18B, C). Also of interest, at an mRNA level, TRAIL attenuated glucose-induced ALP/Sox9 transcript expression (Figure 4.18A). Additional data is presented in Appendix 4.12 and 4.13.

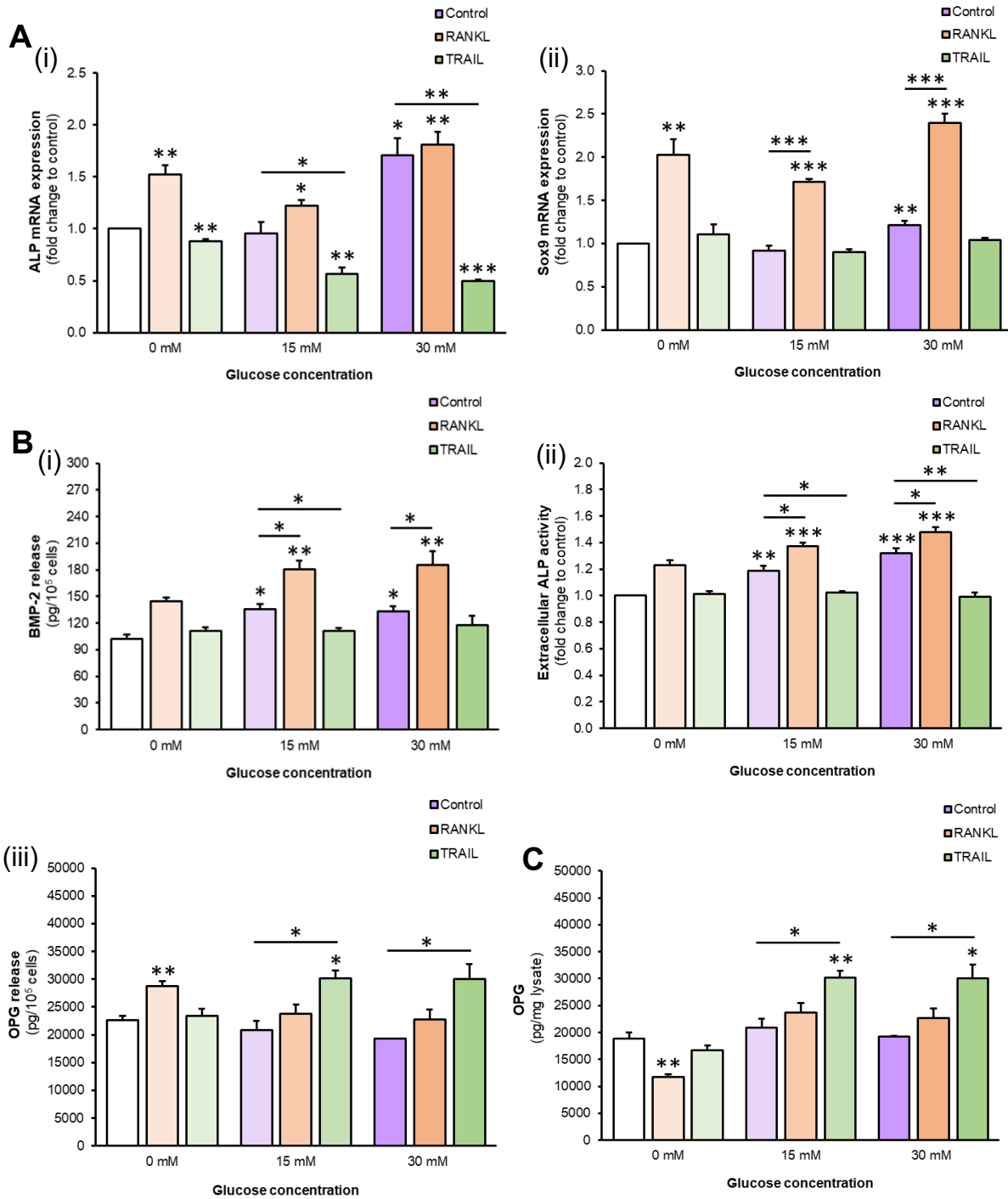


Figure 4.18. The effects of glucose +/- RANKL/TRAIL on pro-calcific indices in co-cultured HASMCs. HAECs in transwell inserts were exposed to glucose (15-30 mM) +/- RANKL (25 ng/mL) or TRAIL (5 ng/mL) for 72 hours, and HASMCs in the subluminal compartment were harvested for analysis. (A) mRNA expression of (i) ALP and (ii) Sox9 were analysed by RT-qPCR employing GAPDH as an endogenous control. (B) (i) BMP-2, (ii) ALP activity and (iii) OPG release in the subluminal compartment, and (C) intracellular OPG in HASMCs were quantified by ELISA or enzyme activity assay where appropriate. Media and lysate analyses were normalised to 10⁵ cells and total protein respectively. * $p < 0.05$; ** $p < 0.01$; *** $p < 0.001$ compared to untreated control unless otherwise stated; bars indicate statistical significance between treatment groups.

4.5.4 HAEC:HASC Co-culture: Summary of Results

RANKL and TRAIL exerted a number of effects on VC-related indices under inflammatory and hyperglycemic conditions in co-culture, both in the subluminal space and in the underlying HASMCs. These results are summarised below in Table 4.4.

Table 4.4. The effects of TNF α or glucose +/- RANKL or TRAIL in co-cultured HASMCs.

<i>Inflammation</i>			RANKL	TRAIL
BMP-2	<i>mRNA</i>	↑	↑↑	↑↑↑
	<i>Extracellular Protein</i>	↑	↑↑	–
	<i>Intracellular Protein</i>	↑	↑	–
ALP	<i>mRNA</i>	–	↑	↓
	<i>Extracellular Activity</i>	↑↑	↑↑	↑
	<i>Intracellular Activity</i>	–	↑	–
OPG	<i>Extracellular Protein</i>	↑	↑ ^δ	↑↑
	<i>Intracellular Protein</i>	↑	↑↑	↑
IL-6	<i>mRNA</i>	↑	↑	↑↑
Sox9	<i>mRNA</i>	–	↑	–
NF-κB (p52/p100)	<i>Activation</i>	↑↑	↑	↑
<i>Hyperglycemia</i>				
BMP-2	<i>mRNA</i>	–	–	↓
	<i>Extracellular Protein</i>	↑	↑↑	–
	<i>Intracellular Protein</i>	↑	↑↑	↑
ALP	<i>mRNA</i>	↑	↑	↓
	<i>Extracellular Activity</i>	↑	↑↑	–
	<i>Intracellular Activity</i>	–	↑ ^δ	–
OPG	<i>mRNA</i>	↓	↓↓	↓↓
	<i>Extracellular Protein</i>	–	–	↑
	<i>Intracellular Protein</i>	–	–	↑
IL-6	<i>mRNA</i>	↓	–	–
	<i>Extracellular Protein</i>	↑	↑	–
Sox9	<i>mRNA</i>	↑	↑↑	–

↑, upregulation; ↑↑/↑↑↑, further upregulation relative to corresponding treatment conditions; ↓, downregulation; ↓↓, further downregulation relative to corresponding treatment conditions; –, no change; ^δ, not significant.

4.5.5 Co-culture: Discussion

Co-culture models have previously been employed to investigate the paracrine contribution of various cell types to VSMC calcification, overcoming important limitations of traditional monoculture (Davenport *et al.*, 2016; Deuell *et al.*, 2012; Osako *et al.*, 2010; Shin *et al.*, 2004). Despite this, few studies consider the effects of inflammation and hyperglycemia on the progression of VC in co-culture, and the contributory effects of RANKL and TRAIL have not been considered in these models. As highlighted in Chapter 3, the vascular endothelium can exert strong pro-calcific effects via paracrine signalling on underlying HASMCs, the location of medial calcification *in vivo*. Furthermore, RANKL and TRAIL can influence these signals to promote or prevent VC respectively, and as such, likely contribute to EC:VSMC communication in the presence of TNF α or high glucose. In this study, it must also be taken into account that both ligands may also act directly on the underlying HASMCs in co-culture, as TNF α can promote endothelial permeability (Royall *et al.*, 1989) and glucose may transfer to the subluminal compartment via active transport (Viator and Fouty *et al.*, 2009). As such, communication in the subluminal space under pathological conditions may involve both paracrine (endothelial) and autocrine (smooth muscle) signalling that jointly mediate VC.

4.5.5.1 The Effects of TNF α on VC Indices in Co-culture

Following endothelial treatment with TNF α , paracrine/autocrine signalling in the subluminal space and pro-calcific mRNA/protein expression in the underlying HASMCs were assessed. As noted, TNF α is elevated in atherosclerotic lesions (Barath *et al.*, 1990), and can penetrate damaged endothelium to act directly on HASMCs (Zhang *et al.*, 2009). TNF α has been previously employed in EC/VSMC co-culture, and has been shown to increase endothelial permeability in these models (Chu *et al.*, 2018; Kerkar *et al.*, 2006; Lodi *et al.*, 2012). TNF α has also been shown to promote VSMC calcification (Liu *et al.*, 2010; Tintut *et al.*, 2000), and as such, we investigated the effects of this cytokine on pro-calcific EC:VSMC signalling in areas of the vasculature affected by atherosclerosis.

Following analysis, *TNF α was found to exert strong pro-calcific effects on the vast majority of pro-calcific indices in co-culture.* Of particular interest to paracrine signalling, the release of BMP-2/ALP were induced in the subluminal space. While unsurprising given the pro-calcific effects of TNF α noted in the literature (Illiadri *et al.*, 2016), this finding is of particular relevance to the progression of VSMC calcification in areas of damaged or dysfunctional

endothelium. As noted, both proteins have been shown to drive medial VC, and ALP is involved in extracellular matrix calcification in the smooth muscle layer (Davenport *et al.*, 2016; Osako *et al.*, 2010; Schoppet and Shanahan, 2008). It should be highlighted, however, that TNF α , while eliciting endothelial paracrine signalling, may also directly induce pro-calcific autocrine signals within the underlying HASMCs; thus, both HAECs and HASMCs may contribute to elevated levels of BMP-2/ALP in the subluminal space. Interestingly, BMP-2 mRNA/protein were upregulated in the underlying smooth muscle cells, which supports a role for HASMC BMP-2 signalling in damaged vasculature. To further support this point, both canonical and non-canonical NF- κ B activation was observed in HASMCs following endothelial exposure to TNF α , pathways previously implicated in BMP-2 signalling and VC (Panizo *et al.*, 2009, Suryavanasgi and Kulkarni, 2017, Zhan *et al.*, 2014, Zhao *et al.*, 2012).

OPG release was also elevated in the subluminal space following TNF α exposure, as was intracellular OPG in the underlying HASMCs. OPG mRNA levels, however, do not coincide with this release, but given the deviating responses between OPG transcriptional and translational levels to date, this finding is difficult to interpret accurately. Nonetheless, this data further supports the hypothesis that in areas of damaged endothelium (such as that present during atherosclerosis) inflammation may drive the release of OPG as a natural cardioprotective mechanism in response to vascular injury, ultimately increasing circulatory OPG (Abedin *et al.*, 2007; O'Sullivan *et al.*, 2010; Schoppet *et al.*, 2003).

As a final consideration, a significant amount of IL-6 release into the subluminal space in co-culture was observed, and as noted, the pro-calcific functions have been widely reported (Al-Aly, 2008; Iliandri *et al.*, 2016; Shao *et al.*, 2010). As a potential explanation for this, Wallace and Truskey (2010) have previously hypothesised (based on EC:VSMC co-culture models) that smooth muscle cells under pathological conditions induce an activated pro-inflammatory state in endothelial cells, and suggest based on pertinent evidence that they may be centrally involved in the progression of atherosclerotic disease (Chiu *et al.*, 2007; Rainger and Nash, 2001). Thus, while endothelial paracrine signalling is the core focus of current vascular research, the importance of smooth muscle signalling to the endothelium should not be overlooked in future studies. In this respect, we hypothesise that in areas of inflamed endothelium/atherosclerosis, both cell types drive the production of pro-calcific signals that drive medial VC (McCullough *et al.*, 2008), and contribute to elevated circulating BMP-2/ALP often accompanying vascular pathologies (Rao and Morghom, 1986; Zhang *et al.*, 2015).

4.5.5.2 The Effects of RANKL on VC Indices under Inflammatory Conditions in Co-culture

Several authors have recognised the comparable effects of RANKL and TNF α , and have considered inter-related functions for these proteins in co-culture models. In this respect, it has been noted that RANKL-induced pro-calcific activity in smooth muscle is dependent on TNF α (Deuell *et al.*, 2012), while RANKL-induced TNF α has been considered an autocrine factor in osteoclastic differentiation (Nakao *et al.*, 2007). As such, the pro-calcific effects of RANKL under inflammatory conditions were next assessed.

Following the addition of RANKL, a significant increase in BMP-2 release was measured in the subluminal compartment compared to TNF α treatment alone, likely a combination of both paracrine and autocrine signalling. A similar trend was observed in ALP activity following TNF α + RANKL exposure, but the effects of RANKL did not significantly elevate these levels beyond that of TNF α treatment. Despite this, ALP was significantly upregulated in the underlying HASMCs, suggesting that RANKL may be necessary to induce smooth muscle ALP production in the vasculature, and reinforcing a key observation from Chapter 3. As a pertinent finding of this chapter, *we therefore highlight the ability of RANKL to function alongside TNF α to induce BMP-2 paracrine signalling* (and to a lesser extent ALP activity), further enhancing VSMC calcification and matrix mineralisation (Davenport *et al.*, 2016; Osako *et al.*, 2010; Schoppet and Shanahan, 2008). Also of interest, while TNF α alone has no effect on Sox9 expression, RANKL promoted this chondrocytic transcription factor both alone and in the presence of inflammation; this observation may indicate that the induction of Sox9 in co-cultured HASMCs is RANKL-specific, and may be associated with the aforementioned upregulation of ALP. The TNF α -specific downregulation of Runx2, however, remains unaffected by RANKL, and as such, further implicates chondrocytic rather than osteocytic regulation during VC (Speer *et al.*, 2009). As a final note, the addition of RANKL under inflammatory conditions slightly promoted OPG production, despite RANKL treatment alone reducing it. As a potential explanation, this effect may result from residual RANKL traversing the damaged endothelial monolayer and acting directly on underlying HASMCs (a direct effect observed in Section 4.4).

4.5.5.3 The Effects of TRAIL on VC Indices under Inflammatory Conditions in Co-culture

There is limited literature to draw on regarding the role of TRAIL under inflammatory conditions *in vitro*, but the anti-atherosclerotic and anti-calcific effects of this ligand have been

highlighted *in vivo* (di Bartolo *et al.*, 2013; Liu *et al.*, 2014; Secchiero *et al.*, 2006). Therefore, this study is the first of its nature to consider the combined effects of TRAIL + TNF α in a vascular setting, and even more pertinently, in co-culture, adding to the pathophysiological relevance of these findings.

Firstly, *TRAIL was found to exert a clear protective effect by attenuating TNF α -induced pro-calcific autocrine/paracrine signalling*, as it significantly reduced BMP-2/ALP release into the subluminal space, emulating its protective influence on RANKL-induced pro-calcific signalling identified in Chapter 3. It must be noted that, in the aforementioned HAEC studies, this trend was also observed alongside an increase in non-canonical NF- κ B activation, suggesting that this pathway may also be involved in the regulation of endothelial paracrine signalling under inflammatory conditions. While TRAIL has been found to prevent endothelial BMP-2 release, it also decreases TNF α -induced BMP-2 production in co-cultured HASMCs, indicating a protective role for TRAIL in both cell types during inflammation. Furthermore, TRAIL slightly promotes TNF α -induced OPG release, that (given the significantly higher OPG production in smooth muscle compared to endothelial cells (Davenport *et al.*, 2018)) can be primarily attributed to the HASMC layer. Again, this trend is not recapitulated at an mRNA level; thus, the bimodal regulation of OPG observed in Chapter 3 remains prominent under inflammatory conditions.

4.5.5.4 The Effects of Hyperglycemia on VC Indices in Co-culture

As discussed, circulating glucose can be transported through the endothelial monolayer via active GLUT-1 transport (Viator and Fouty *et al.*, 2009) to act directly on underlying HASMCs *in vivo*, and as such, vascular issues that are common during T2DM may result from both EC and VSMC autocrine/paracrine signalling. The effects of hyperglycemia have previously been studied in EC:VSMC co-culture, but these studies focus on proliferation and inflammation and have not been completed in aortic models to date (Tarallo *et al.*, 2012; Zitman-Gal *et al.*, 2015). Thus, as we investigate the effects of high glucose on pro-calcific vascular signalling for the first time, it must be noted that there is limited data with which to compare these novel results. Unsurprisingly, *a number of pro-calcific indices were upregulated under hyperglycemic conditions*, most relevantly BMP-2/ALP in the subluminal space. As noted, these pro-calcific autocrine/paracrine signals are likely generated by both HAECs and HASMCs, contributing to elevated circulating BMP-2/ALP during T2DM (Rao and Morghom, 1986; Zhang *et al.*, 2015).

Furthermore, IL-6 release within the subluminal space was elevated during hyperglycemia, as previously observed in co-culture (Zitman-Gal *et al.*, 2015), which may further promote the aforementioned pro-calcific signals (Kurozumi *et al.*, 2016). Also, despite the role of IL-6 as a well-known inducer of NF- κ B activation (Brasier, 2010), this co-culture model further supports the observation that high glucose does not promote VC via NF- κ B signalling.

As a further note, the upregulation of Sox9 transcription factor alongside the downregulation of Runx2 again implicates chondrocytic rather than osteoblastic regulation during glucose-induced pro-calcific signalling. As discussed, both factors have been shown to exert similar pro-calcific effects (Luo *et al.*, 1997; Speer *et al.*, 2009; Tyson *et al.*, 2003), and this finding supports a key novel finding of Chapter 3 (in which RANKL-induced Sox9 was identified in co-cultured HASMCs). As an additional interesting finding, high glucose was found to decrease OPG mRNA/protein in co-cultured HASMCs, while OPG release remained unaffected, despite circulating OPG widely known to be increased during type-2 diabetes (Bjerre, 2013; Secchiero *et al.*, 2006). Therefore, from the current data, it appears that hyperglycemia itself does *not* induce OPG release in areas of healthy vasculature; rather this circulating OPG may be the result of glucose-induced secretion in areas of damaged endothelium, or induced by inflammatory cytokines that often accompany hyperglycemia in these patients (Esposito *et al.*, 2002).

4.5.5.5 The Effects of RANKL on VC Indices under Hyperglycemic Conditions in Co-culture

To our knowledge, no studies to date have considered the effects of RANKL under hyperglycemic conditions in vascular cell co-culture models. As such, the finding that *RANKL exerts an additive effect on glucose-induced BMP-2/ALP pro-calcific paracrine signalling*, promoting underlying HASMC calcification, is particularly novel. Moreover, the upregulation of Sox9 in the underlying HASMC layer, alongside decreased Runx2 expression, further suggests that both hyperglycemia and RANKL promote chondrocytic rather than osteoblastic pro-calcific signalling in smooth muscle (Speer *et al.*, 2009). Indeed, RANKL and glucose also exerted an additive effect on this transcription factor in co-cultured HASMCs, in a similar manner to BMP-2/ALP release. Again, pro-calcific IL-6 levels (Hénaut and Massy, 2018) remain unchanged in the presence of RANKL, and as such, the aforementioned promotion of BMP-2, ALP and Sox9 are RANKL-specific, emulating trends observed in Chapter 3.

As another interesting observation, while a decrease in OPG mRNA was observed, no effects were noted in OPG release levels; thus, glucose appears to interrupt RANKL-induced OPG secretion in co-culture. We therefore propose that, under healthy conditions, OPG may be released as a natural cardioprotective mechanism in response to its pro-calcific ligand; under hyperglycemic conditions, however, the vasculature is left open to injury and may be more susceptible to RANKL-induced pro-calcific effects. This finding also further supports the proposition that inflammatory rather than hyperglycemic processes may be more responsible for the increase in circulatory OPG release noted during early T2DM (Secchiero *et al.*, 2006).

4.5.5.6 The Effects of TRAIL on VC Indices under Hyperglycemic Conditions in Co-culture

Similarly, with regard to TRAIL, no studies to our knowledge have investigated the effects of this ligand on the vasculature under hyperglycemic conditions, and as such, there no data available with which to compare these results. In a significant and novel finding of this chapter, however, *TRAIL was found to completely attenuate glucose-induced BMP-2/ALP release* into the subluminal space, thus preventing pro-calcific effects in the underlying HASMCs (Davenport *et al.*, 2016; Schoppet and Shanahan, 2008). Of particular relevance, we highlighted both in Chapter 3 and in inflammatory models in the current study that non-canonical NF- κ B activation may be centrally involved in pro-calcific signalling, and that TRAIL may exert its protective effects via attenuation of this pathway. In this case, however, TRAIL exerts protective effects in the absence of non-canonical activation, and thus TRAIL-mediated protection during hyperglycemia must progress via a different mechanism. We propose that, given strong evidence in the literature that high glucose induces oxidative stress (Fiorentino *et al.*, 2013), the vasoprotective effects of TRAIL may be due to the proposed anti-oxidant properties of this ligand (Forde *et al.*, unpublished observations). TRAIL is indeed well known as a pleiotropic molecule (Forde *et al.*, 2016), and its vascular function likely involves multiple interrelated mechanisms which remain to be fully delineated (see Chapter 5).

Also of interest, the observed TRAIL protection during hyperglycemia may be mediated in part by a reduction in pro-calcific IL-6 release, known to promote VC (Hénaut and Massy, 2018). Indeed, the interrelated roles of both hyperglycemia and inflammation have recently been noted by Chu *et al.* (2018), who highlighted (in an EC:VSMC co-culture model) the importance of reduced cytokine release in the prevention vascular disorders, further supporting the key role of paracrine signalling in vascular protection (Chu *et al.*, 2018). TRAIL-induced OPG release

from HASMCs may also contribute to these vasoprotective effects, however, it must be considered that this effect may be more accurately described as a short-term cardioprotective response, contributing to the proposed role for OPG as a biomarker of vascular injury (Secchiero *et al.*, 2006). It is unlikely that OPG is fully responsible for the protective effects of TRAIL noted above, given that RANKL exerts its pro-calcific function even in the presence of excess OPG.

4.5.5.7 Co-culture: Summary

As summarised in Table 4.4, the employed inflammatory and hyperglycemic co-culture models further enforce the key findings from Chapter 3: RANKL promotes pro-calcific signalling via the induction of paracrine BMP-2/ALP release, while TRAIL exerts a protective influence via the attenuation of pro-calcific signalling under pathological conditions. It is likely that these effects are mediated at both an endothelial and smooth muscle level, secreting proteins that ultimately drive VC. Moreover, RANKL and TRAIL modulate the release of their own decoy receptor, OPG, which may further contribute to these effects. Given the physiological relevance of this co-culture model, these novel findings provide significant evidence to implicate RANKL and TRAIL in the progression and prevention of VC, respectively, under pathological conditions common during T2DM/CVD.

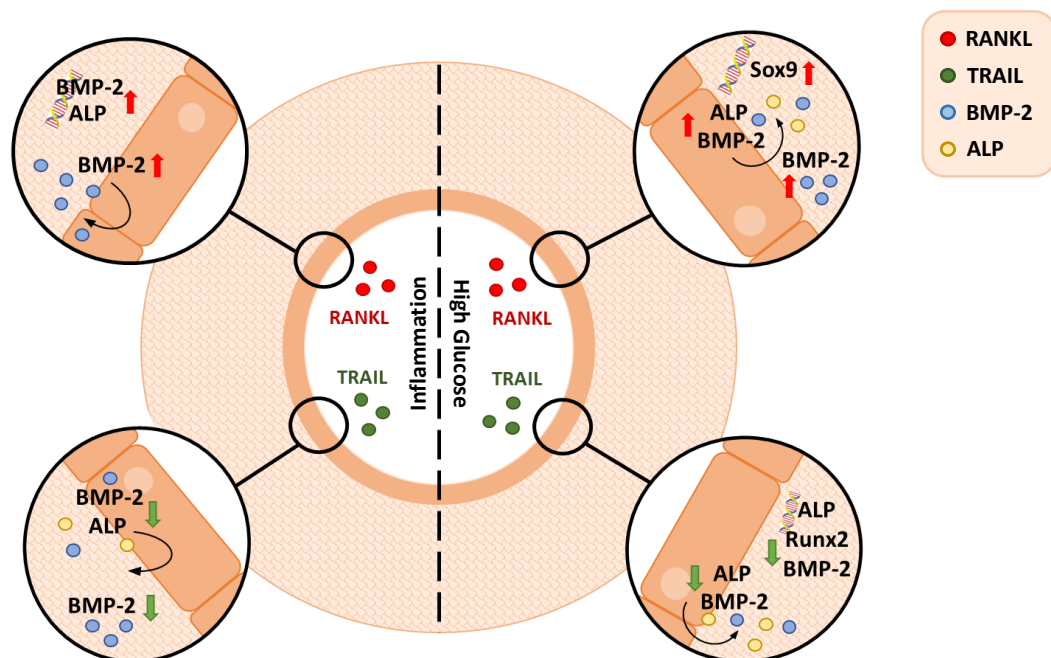


Figure 4.19. Summary of the key HASMC responses following endothelial exposure to RANKL/TRAIL +/- TNF α (inflammation) and high glucose in co-culture. RANKL was found to further upregulate (red arrow) a number of pro-calcific indices when compared to TNF α or glucose treatment alone. TRAIL was found to reduce (green arrow) a number of pro-calcific indices induced by TNF α or glucose treatment in co-culture.

4.6 Summary and Conclusions

In summary, this chapter profiles the effects of RANKL and TRAIL on pro-calcific signalling in the presence of inflammation and hyperglycemia, pathological conditions common during T2DM/CVD. Within the realm of VC, this is undoubtedly the most comprehensive study to date to be completed in primary human vascular cell mono- and co-culture models, and the first to combine known mediators of VC with these pathological stimuli. As noted, given the likelihood of endothelial dysfunction and glucose transport within these models, we build on the data observed in healthy vasculature in Chapter 3 to now consider both paracrine and autocrine signals that may regulate calcification in VSMCs under pathological conditions.

Firstly, we have confirmed the pro-calcific effects of $TNF\alpha$ and high glucose in the vascular intima and media across a wide range of indices, somewhat clarifying the pro-calcific signalling processes that occur during these pathologies. Of interest, the pro-calcific and the protective effects of RANKL and TRAIL respectively during these pathological conditions were particularly obvious in EC:VSMC co-culture. Most prevalently, *RANKL exerted an additive effect on both $TNF\alpha$ and glucose-induced BMP-2/ALP paracrine/autocrine signalling in the subluminal space, while TRAIL significantly attenuated BMP-2/ALP release induced by these stimuli.* We suggest, therefore, that RANKL may function alongside inflammation and hyperglycemia to promote medial VC via BMP-2/ALP pro-calcific signalling (Davenport *et al.*, 2016; Osako *et al.*, 2010), while we highlight for the first time the protective influence of TRAIL on pro-calcific signalling under these conditions. These effects may be mediated via the non-canonical NF- κ B signalling pathway under inflammatory conditions, previously implicated in RANKL/TRAIL function in Chapter 3. However, we can conclude that RANKL- and TRAIL-induced pro-calcific and protective effects respectively appear to be mediated by a different mechanism during hyperglycemia, which remains to be investigated.

Overall, therefore, we have profiled for the first time the pro-calcific effects of RANKL and the protective effects of TRAIL in physiologically relevant co-culture models, delineating the relevant signalling processes that exist under pathological conditions common during T2DM/CVD. These findings add significant and novel knowledge to the field of VC research, particularly with respect to the roles of RANKL and TRAIL, and most importantly emphasise the translational value of TRAIL as a potential therapeutic for cardiovascular complications associated with inflammation/hyperglycemia.

Chapter 5

Mechanisms of RANKL-induced Pro-calcific Signalling and TRAIL-mediated Protection in the Vasculature

5.1 Introduction

5.1.1 Background and Hypothesis Development

The cellular mechanisms by which RANKL and TRAIL exert their function, while clarified in other areas of research, remain largely undefined in a vascular context. RANKL is known to activate both canonical and non-canonical NF- κ B signalling via its cell surface receptor, RANK, and both pathways play important roles in osteoclastogenesis (Beristain *et al.*, 2012; Boyce *et al.*, 2015). However, the specific involvement of these pathways has not yet been clarified in VC, and although research points to a pro-calcific role for non-canonical activation in smooth muscle (Panizo *et al.*, 2009), the data presented in Chapter 3 is the first to implicate this pathway in endothelial pro-calcific signalling. Furthermore, RANKL has been shown to induce oxidative stress, a key promoter of VC (Byon *et al.*, 2008; Thummuri *et al.*, 2017), which may suggest that multiple mechanisms contribute to its pro-calcific vascular function.

TRAIL has also been associated with many pathways in its role as a pleiotropic molecule (Forde *et al.*, 2016). However, like RANKL, its precise mechanism(s) of action in the vasculature remain largely unspecified, particularly with respect to VC protection (di Bartolo *et al.*, 2013; Secchiero *et al.*, 2006). In Chapters 3 and 4, novel evidence suggested that TRAIL may attenuate non-canonical NF- κ B signalling induced by pro-calcific stimuli (RANKL, TNF α) acting upon the endothelium. Moreover, TRAIL also attenuated glucose-induced pro-calcific signalling in the absence of non-canonical activation, suggesting that additional mechanism(s) of TRAIL protection may exist. Pertinently, recent evidence has emerged within our research group that TRAIL may exert anti-oxidant effects in the endothelium (Forde *et al.*, unpublished observations). Indeed, RANKL, TNF α and glucose are all known promoters of oxidative stress (Chen *et al.*, 2008; Li *et al.*, 2017; Thummuri *et al.*, 2017), and as such, further clarification of the anti-oxidant role for TRAIL in VC is merited.

In the current chapter, an effort will be made to shed additional light on the mechanisms by which RANKL and TRAIL exert their respective pro-calcific and protective influences on the vasculature. In consideration of the key findings of Chapters 3 and 4, ***we propose that non-canonical NF- κ B signalling and oxidative stress pathways may together regulate the effects of RANKL and TRAIL in the vascular endothelium.*** Given the complex roles for both ligands *in vivo*, and the wide range of pathways with which they interact (Beristain *et al.*, 2012; Forde *et al.*, 2016), an attempt will also be made to identify novel participants that may influence RANKL/TRAIL function during VC.

5.1.2 Study Aims

As noted, the precise mechanisms underlying RANKL-induced pro-calcific signalling and TRAIL-mediated protection have yet to be fully defined in a vascular setting, although evidence points to the involvement of non-canonical NF- κ B signalling and oxidative stress. We therefore once again employ primary human vascular cells in both mono- and co-culture models in an attempt to provide novel insights into the pathways activated by these proteins during VC. Given the pertinent role for EC paracrine signalling in RANKL/TRAIL function identified in Chapters 3 and 4, a focus on the endothelium will be maintained.

Three main study objectives were developed, carried out in tandem but arranged in the following order for clarity:

1. To identify novel VC participants that may aid in delineating the mechanisms responsible for RANKL-induced calcification and TRAIL-mediated protection.
2. To investigate the involvement of oxidative stress in endothelial VC regulation, with respect to RANKL-induced pro-oxidant signalling and TRAIL-mediated anti-oxidant protection.
3. To specify the role for endothelial non-canonical NF- κ B activation in RANKL-induced pro-calcific signalling, thus clarifying the importance of TRAIL-mediated attenuation of this pathway.

5.1.3 Study Overview

Given the comprehensive nature of this study, the specific experimental approach/research background for each aim is described in the relevant sections. A brief overview is summarised overleaf in Figure 5.1, with the above objectives determining the three key investigations:

5.1.3.1 Identification of Novel VC Targets

To aid in the understanding of the mechanisms responsible for RANKL-induced pro-calcific signalling and TRAIL-mediated protection, novel participants in the VC process were investigated. Following a combination of bioinformatics and literature analyses, any proteins identified as potential contributors to the VC process would be assessed under all experimental conditions and within all cell models employed in Chapters 3 and 4.

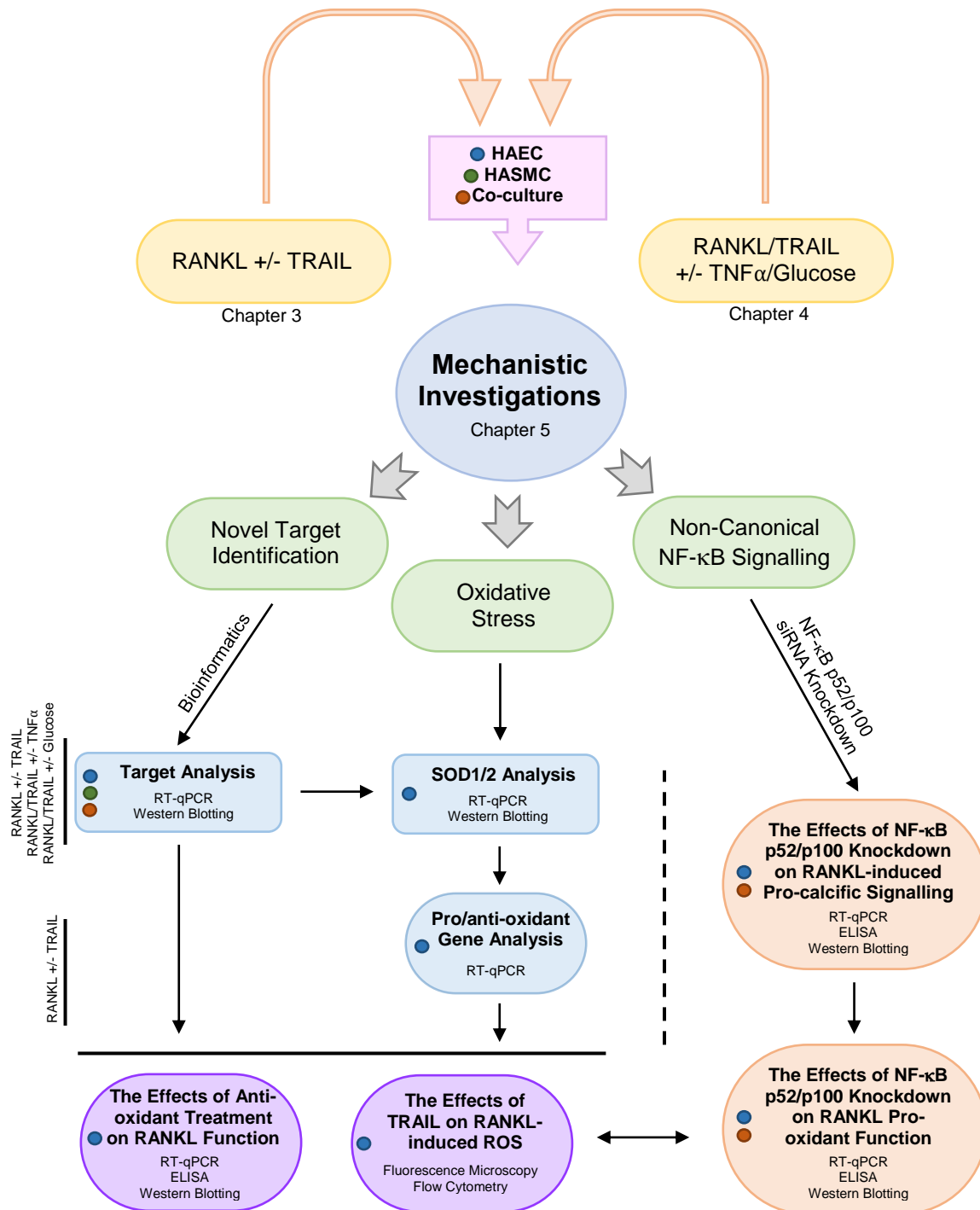


Figure 5.1. Schematic representation of the experiments and techniques employed in Chapter 5. Experimental models from Chapters 3 employing RANKL and TRAIL, and from Chapter 4 incorporating the pathological stimuli TNF α and glucose, were employed where deemed necessary for the current series of experiments. HAEC/HASMC monoculture and HAEC:HASMC co-culture models were employed/modified where required, indicated above by the relevant colour code. Three mechanistic routes were investigated; the identification of novel targets, oxidative stress pathways, and the non-canonical NF- κ B signalling pathway. Experimental targets were analysed by RT-qPCR, Western blotting, ELISA, fluorescence microscopy and flow cytometry where indicated.

5.1.3.2 Investigating the Role of Oxidative Stress in VC Regulation

As noted, recent evidence points to a pro-oxidant and anti-oxidant role for RANKL and TRAIL respectively, however, the precise role(s) for oxidative stress in VC remain to be delineated. The following experiments were carried out to clarify the involvement of pro-/anti-oxidant events in RANKL/TRAIL function in the endothelium:

- (i) The expression of SOD1 and SOD2 in HAECs, contributors to the regulation of cytoplasmic and mitochondrial ROS respectively, known for their cardioprotective effects (Fukai and Ushio-Fukai, 2011); these proteins were assessed under all conditions employed in Chapters 3 and 4.
- (ii) The expression of pro-/anti-oxidant genes in HAECs in response to RANKL +/- TRAIL, including:
 - a. the pro-oxidant genes gp91-phox and p47-phox (referred to as gp91 and p47 from this point onward), subunits of the superoxide generator NADPH oxidase;
 - b. eNOS, with cardioprotective functions ascribed to its synthesis of NO (Förstermann *et al.*, 1994);
 - c. HMOX1, induced in response to oxidative stress and believed to be protective (Gozzelino *et al.*, 2010).
- (iii) The effects of N-acetyl-L-cysteine (NAC) anti-oxidant treatment on RANKL pro-calcific function, to determine if pro-calcific and pro-oxidant pathways are inter-dependent in the endothelium.
- (iv) The effects of TRAIL on RANKL-induced ROS, to determine if the potential anti-oxidant effects of TRAIL may contribute to TRAIL-mediated protection from RANKL pro-calcific signalling.

5.1.3.3 Clarifying the Role of Endothelial Non-canonical NF- κ B Signalling during VC

In order to assess the importance of non-canonical NF- κ B activation for RANKL-induced pro-calcific signalling, co-cultured HAECs were subject to siRNA knockdown of a key component of the non-canonical pathway, namely p100/p52. Endothelial paracrine signalling, alongside all pro-calcific indices in HASMCs assessed in Chapters 3 and 4, were analysed. Furthermore, given the potential interlinked roles for pro-calcific and pro-oxidant signalling in response to RANKL, a range of targets associated with oxidative stress were also assessed.

5.1.4 Experimental Design

For the identification of novel targets involved in VC signalling, bioinformatics analyses were conducted using two databases: the Search Tool for the Retrieval of Interacting Genes/Proteins (STRING) and the Biological General Repository for Interaction Datasets (BioGRID). Proteins interacting with RANKL, TRAIL and any of the measured pro-calcific indices were of interest, alongside any predicted interactions determined via STRING computational prediction or text mining methods (Szkarczyk *et al.*, 2016). Target(s) identified were first analysed at both an mRNA level (via RT-qPCR) and protein level (via Western blotting) in HAEC/HASMC monocultures grown in standard 6-well culture dishes. Second, HAEC:HASMC co-culture was implemented, whereby HAECs in the luminal compartment were treated in semi-permeable transwell inserts, and confluent HASMCs in the subluminal compartment were harvested for analysis in response to endothelial paracrine signalling (Figure 5.2). Potential target(s) were assessed following exposure to RANKL (5-25 ng/mL) +/- TRAIL (5 ng/mL), and either RANKL (25 ng/mL) or TRAIL (5 ng/mL) under inflammatory (100 ng/mL TNF α) or hyperglycemic (15-30 mM glucose) conditions for 72 hours.

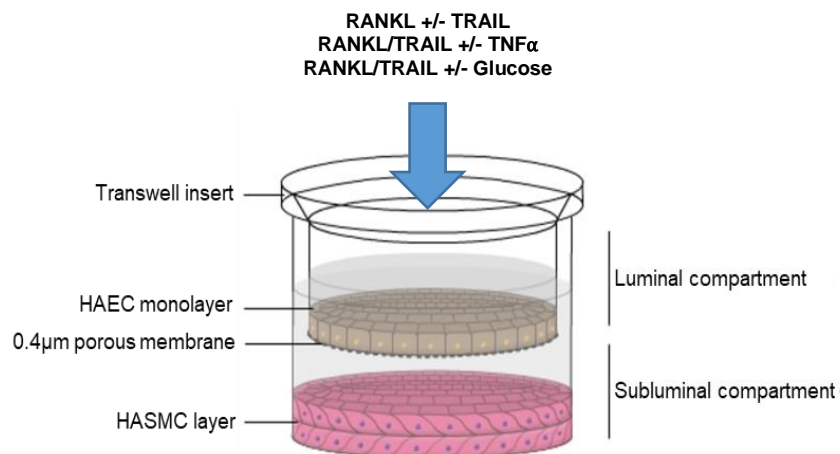


Figure 5.2. Representation of the transwell co-culture model employed for novel VC target analysis. HAECs in the luminal compartment were exposed to soluble factors for 72 hours. The HASMC transcriptome and proteome were harvested and analysed for mRNA and protein expression by RT-qPCR and Western blotting respectively. Image adapted from Harper *et al.*, 2017.

In consideration of the observed contribution of the endothelium to VC signalling in Chapters 3 and 4, the potential role for oxidative stress in RANKL/TRAIL regulation was assessed only in HAEC monoculture. SOD1 and SOD2 gene expression (via RT-qPCR) and protein expression (via Western blotting) was assessed following exposure to RANKL +/- TRAIL, and RANKL or TRAIL under inflammatory or hyperglycemic conditions for 72 hours. For the analysis of pro/anti-calcific gene expression, HAECs were exposed to RANKL +/- TRAIL for 72 hours prior to analysis by RT-qPCR.

To investigate the effects of NAC on RANKL function, HAECs were exposed to RANKL (25 ng/mL) +/- NAC (5 mM, *t* - 1 hours) for 72 hours prior to gene and protein expression analysis by RT-qPCR and ELISA/Western blotting, respectively. NAC has been successfully employed at 5 mM concentration to achieve a potent anti-oxidant effect in endothelial cells, and has been shown to be optimally functional at scavenging its target (O_2^-) in these cells when added 1 hour prior to treatment (Guinan *et al.*, 2013). All pro-calcific and pro-oxidant genes/proteins were assessed (where deemed necessary) as previously described, to investigate the potential inter-related mechanisms of VC and oxidative stress (BMP-2, ALP, Runx2, IL-6, OPG, NF- κ B/p52, SOD1/2, gp91, p47, eNOS, HMOX1). As a positive control, the effects of NAC on 100 ng/mL TNF α , a known pro-oxidant stimulus (Chen *et al.*, 2008), was included to ensure NAC exerted the desired anti-oxidant effects in the employed cell model. For ROS analyses, the effects of RANKL +/- TRAIL were assessed by fluorescence microscopy (Section 2.2.6.2) and flow cytometry (Section 2.2.7.2) following 24 and 72 hours' incubation. Once again, the effects of NAC on TNF α -induced ROS formation was assessed as a positive control for ROS induction/depletion (Chen *et al.*, 2008).

To clarify the role of non-canonical NF- κ B signalling in HAECs, siRNA knockdown of the p100 subunit (the precursor to p52) was carried out, according to the method described in Section 2.2.2.4. Following thorough transfection optimisation, HAECs were subject to non-targetting siRNA/NF κ B2 gene knockdown in transwell inserts for 48 hours. Following 6 hours' recovery in fresh media, transwell inserts were transferred to a 6-well culture dish containing confluent HASMCs, and HAECs subject to RANKL exposure for 72 hours. Conditioned media from the subluminal compartment, HAECs and HASMCs were harvested and analysed for pro-calcific and pro-oxidant indices where necessary. All relevant controls, including untransfected cells and non-targetting siRNA treatments, were included as required.

All studies presented in this chapter are conducted to *n* = 3 independent experiments.

5.2 Identification and Analysis of a Novel VC Target

Prior to the investigation of oxidative stress and non-canonical NF- κ B signalling, novel participants in the VC process that may potentially contribute to delineating the overlapping pathways involved in RANKL-induced pro-calcific signalling and TRAIL-mediated protection were considered. In this respect, bioinformatics and literature analyses were employed to identify novel protein interactions not yet assessed in the context of VC, as described in detail in Section 2.2.8.

5.2.1 Target Identification

In order to identify novel targets, the STRING database (version 10.0) was first employed within which experimentally determined protein interactions and text mining predictions are recorded (Szklarczyk *et al.*, 2016). Proteins interacting with RANKL, TRAIL and their soluble decoy receptor OPG were primarily assessed. Searches were conducted in accordance with the criteria detailed in Section 2.2.8 within both *homo sapiens* and *mus musculus* species databases in order to incorporate interactions that may not yet be identified in human studies. The primary interactions identified within the STRING database are summarised in Table 5.1 below.

Table 5.1. Key protein interactions and potential interactions with RANKL, OPG and TRAIL identified using the STRING database (version 10.0).

RANKL	OPG	TRAIL
OPG	RANKL	OPG
RANK	TRAIL	Caspase 3, 8, 10
PTH	TGF β -1	DcR1, DcR2
TRACP5	PTH	DR4, DR5
TRAF6	TRACP5	FADD
BMP-2	IL-18	
STAT3		

FADD, fas-associated protein with death domain; PTH, parathyroid hormone; TRACP5, tartrate-resistant acid phosphatase 5; TRAF, TNF receptor associated factor; TGF, transforming growth factor; STAT3, signal transducer and activator of transcription 3.

Following further analyses according to the same search criteria, only TRACP5 (identified as a potential interactant for both RANKL and OPG via STRING analysis) was found to also associate with the previously identified pro-calcific paracrine proteins BMP-2 and ALP. Moreover, following additional protein interaction analysis using the BioGRID database (version 3.4.142), TRACP5 was also listed as a potential interactant with TRAIL. As such, the target TRACP5 was subject to functional analysis using the Universal Protein (UniProt) database (entry P13686). Several key functions of interest, overlapping with those of RANKL, TRAIL, OPG and other pro-calcific indices, were computationally inferred:

- (i) Regulation of bone morphogenesis, predominantly bone resorption;
- (ii) Osteoclast differentiation and activation;
- (iii) BMP signalling;
- (iv) OPN/BSP dephosphorylation;
- (v) Negative regulation of NO biosynthesis;
- (vi) Regulation of IL-1 β ;
- (vii) Superoxide anion (O₂⁻) generation;
- (viii) Response to *L*-ascorbic acid.

Thus, the investigation of a potential role for TRACP5 in the development and progression of VC was clearly warranted on a bioinformatics basis, with protein interactions and overlapping functions with key VC-related indices identified. Following an extensive literature review, discussed in detail in Section 5.2.5, several key studies also supported the potential involvement of TRACP5 in the VC process:

- (i) While primarily expressed in bone, TRACP5 is also expressed in heart tissue, and increased expression of TRACP5 has been identified in atherosclerotic lesions compared to normal regions of human aorta (Timofeeva *et al.*, 2009);
- (ii) TRACP5 is upregulated in the artery of obese pigs, coinciding with the induction of pro-inflammatory, pro-oxidant and NF- κ B pathways (Padilla *et al.*, 2013);
- (iii) RANKL induces TRACP5 expression in osteoclastogenesis, which can be attenuated by statin treatment (Nakashima and Haneji, 2013);
- (iv) TRACP5 co-localises with OPG/RANKL in chondrocytes (Solberg *et al.*, 2015);
- (v) Recombinant TRAIL injection decreases circulating TRACP5 levels *in vivo* (Zauli *et al.*, 2008);
- (vi) TRACP5 can be activated by oxidative stress in chondrocytes (Seol *et al.*, 2009).

Given the apparent role for TRACP5 in bone morphogenesis and oxidative stress, this evidence further supports a potential role for this protein in VC, not yet investigated to date. Although the primary role for TRACP5 appears to be bone *resorption*, rather than formation, the similar paradoxical function of RANKL (i.e., exerting osteoclastic effects in bone and osteoblastic effects in vasculature) cannot be ignored; therefore, the role of TRACP5 in RANKL/TRAIL-mediated VC was next investigated.

5.2.2 The Effects of RANKL +/- TRAIL on TRACP5 Expression

First, the effects of RANKL +/- TRAIL on TRACP5 expression in both mono- and co-culture were assessed. In HAEC monoculture, 25 ng/mL RANKL increased TRACP5 mRNA expression, and also induced TRACP5 protein expression, significantly at 5 ng/mL. TRAIL was found to significantly decrease TRACP5 mRNA expression both alone and in combination with 5 ng/mL RANKL, while also decreasing RANKL-induced TRACP5 protein expression (Figure 5.3A). In HASMC monoculture, RANKL treatment was found to dose-dependently induce TRACP5 transcript expression; while TRAIL also slightly, but significantly, increased TRACP5 mRNA, it also significantly reduced RANKL-induced TRACP5 expression at 25 ng/mL. No effects, however, were noted in TRACP5 protein expression in HASMCs (Figure 5.3B), nor were any effects noted at an mRNA or protein level in co-cultured HASMCs (Figure 5.3C). The calcification inducer, β -glycerophosphate, was found to increase TRACP5 mRNA/protein expression in HAECs (Appendix 5.1A (i), (iv)) and HASMCs (data not shown).

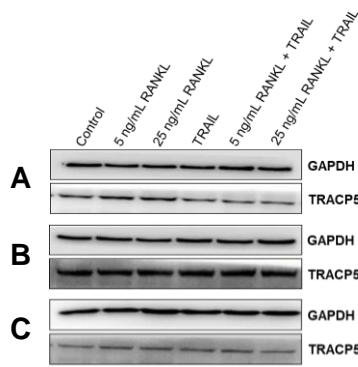
5.2.3 The Effects of RANKL/TRAIL on TRACP5 Expression during Inflammation

Following TNF α exposure, TRACP5 mRNA expression was significantly reduced in both HAECs and HASMCs in monoculture, while it was significantly upregulated in co-cultured HASMCs (Figure 5.4A-C (i)). The addition of RANKL further downregulated TRACP5 mRNA in HASMC monoculture, while TRAIL somewhat recovered the TNF α -induced downregulation of TRACP5 mRNA in the same model (Figure 5.4B (i)). Interestingly, TRAIL further upregulated TNF α -induced TRACP5 mRNA in co-cultured HASMCs (Figure 5.4C (i)). TRACP5 protein remained unaffected by TNF α treatment in both mono- and co-culture, and the addition of RANKL did not exert any effect on TRACP5 protein expression under

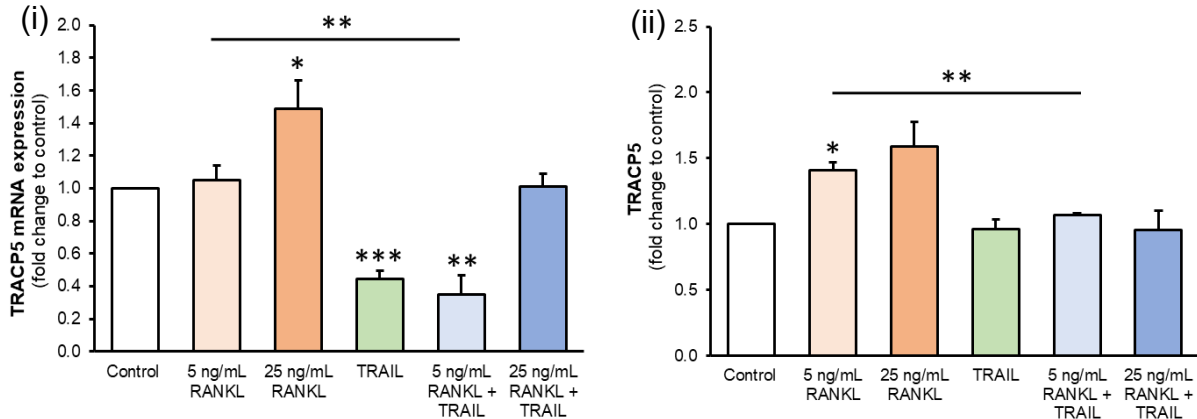
inflammatory conditions. TRAIL, however, significantly upregulated TRACP5 protein expression in all models employed (Figure 5.5A-C (i)).

5.2.4 The Effects of RANKL/TRAIL on TRACP5 Expression during Hyperglycemia

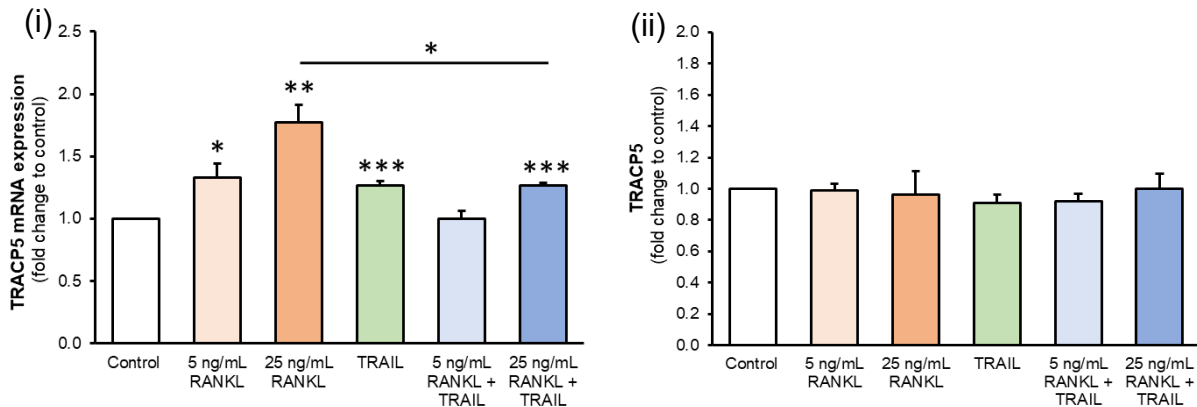
To ensure that the observed effects under hyperglycemic treatment were glucose-specific, an osmotic control was first employed; mannitol (30 mM) had no effect on TRACP5 protein mRNA/protein expression in HAECs (Appendix 5.1A (i)) or HASMCs (data not shown). At an mRNA level, high glucose significantly downregulated TRACP5 mRNA in HAECs (at 30 mM) and HASMCs, while dose-dependently upregulating TRACP5 mRNA in co-cultured HASMCs (Figure 5.4A-C (ii)). Interestingly, following RANKL addition, TRACP5 transcript expression was significantly upregulated under hyperglycemic conditions in HAECs (Figure 5.4A (ii)). High levels of glucose had no effect on TRACP5 protein expression in mono- or co-culture (Figure 5.5A-C (ii)). Exposure to TRAIL (but not RANKL) under hyperglycemic conditions, however, significantly promoted TRACP5 protein expression in both endothelial and smooth muscle monoculture. Neither ligand exerted any effects on TRACP5 protein expression under hyperglycemic conditions in co-culture.



A: HAEC



B: HASMC



C: Co-culture

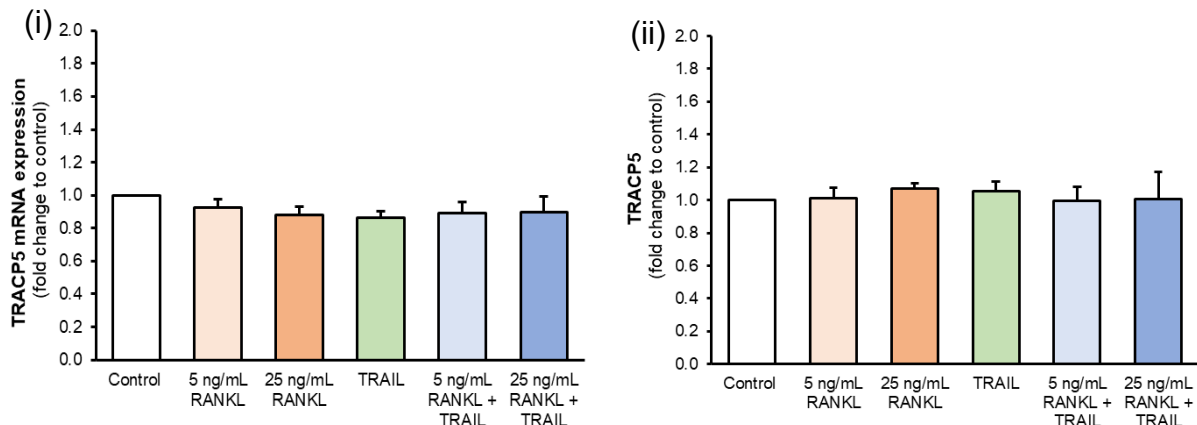


Figure 5.3. The effects of RANKL +/- TRAIL on TRACP5 expression. (A) HAECs and (B) HASMCs were exposed to RANKL (5-25 ng/mL) +/- TRAIL (5 ng/mL) for 72 hours, prior to harvesting and analysis of TRACP5 (i) mRNA and (ii) protein expression. (C) HAECs in the luminal compartment in co-culture were exposed to the same conditions, and the underlying HASMCs harvested and assessed for TRACP5 (i) mRNA and (ii) protein expression. Gene expression was analysed by RT-qPCR employing GAPDH as an endogenous control, while protein expression was assessed by Western blotting, quantified by scanning densitometry and normalised to GAPDH. Blots are representative. * $p < 0.05$; ** $p < 0.01$; *** $p < 0.001$ compared to untreated control unless otherwise stated; bars indicate statistical significance between treatment groups.

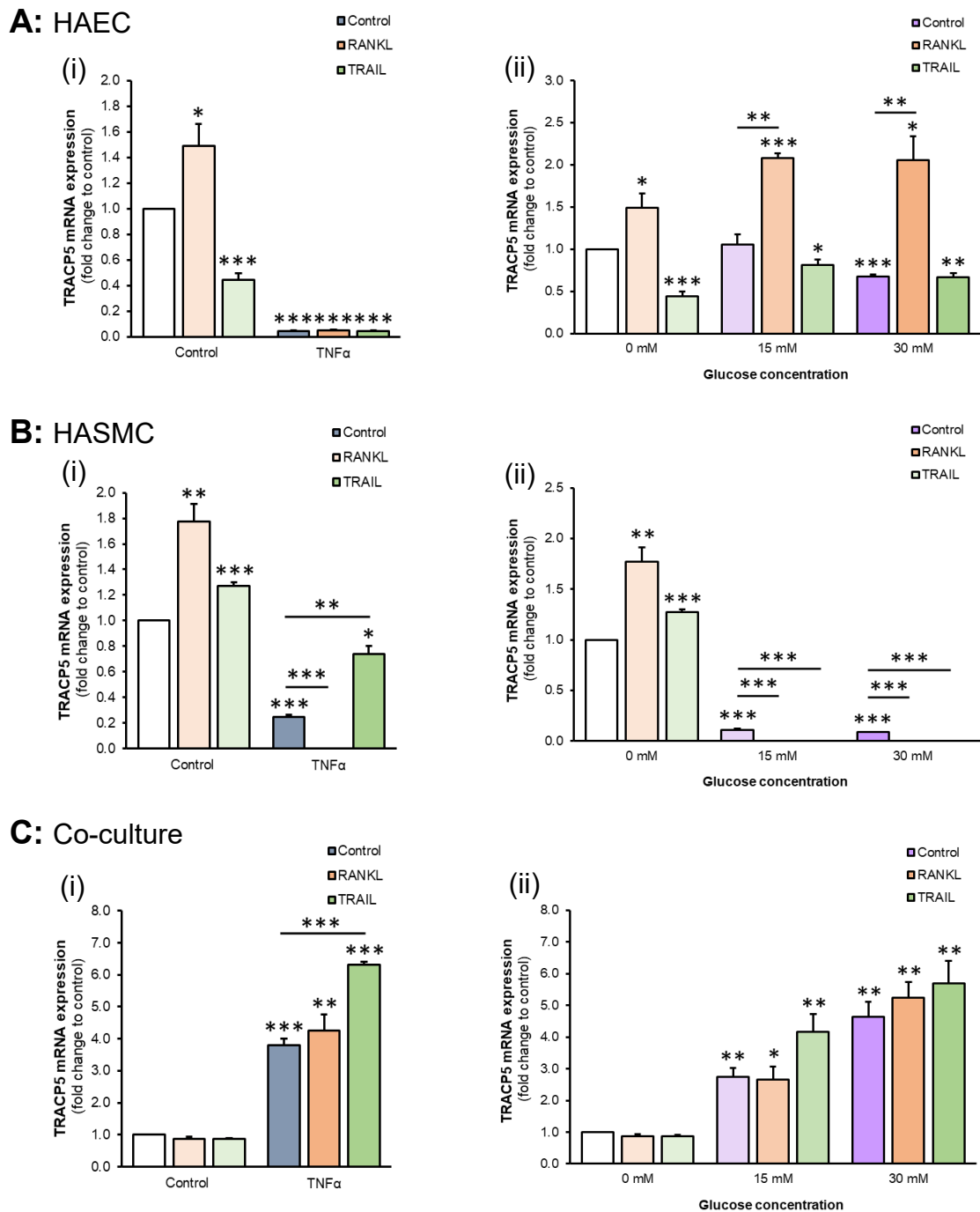


Figure 5.4. The effects of RANKL/TRAIL on TRACP5 mRNA expression under inflammatory and hyperglycemic conditions. (A) HAECs and (B) HASMCs were exposed to (i) TNF α (100 ng/mL) or (ii) glucose (15-30 mM) +/- RANKL (25 ng/mL) or TRAIL (5 ng/mL) for 72 hours, prior to analysis of TRACP5 mRNA expression. (C) HAECs in the luminal compartment in co-culture were exposed to the same conditions, and the underlying HASMCs harvested and assessed for TRACP5 mRNA expression. TRACP5 levels were determined by RT-qPCR, employing GAPDH as an endogenous control. * $p < 0.05$; ** $p < 0.01$; *** $p < 0.001$ compared to untreated control unless otherwise stated; bars indicate statistical significance between treatment groups.

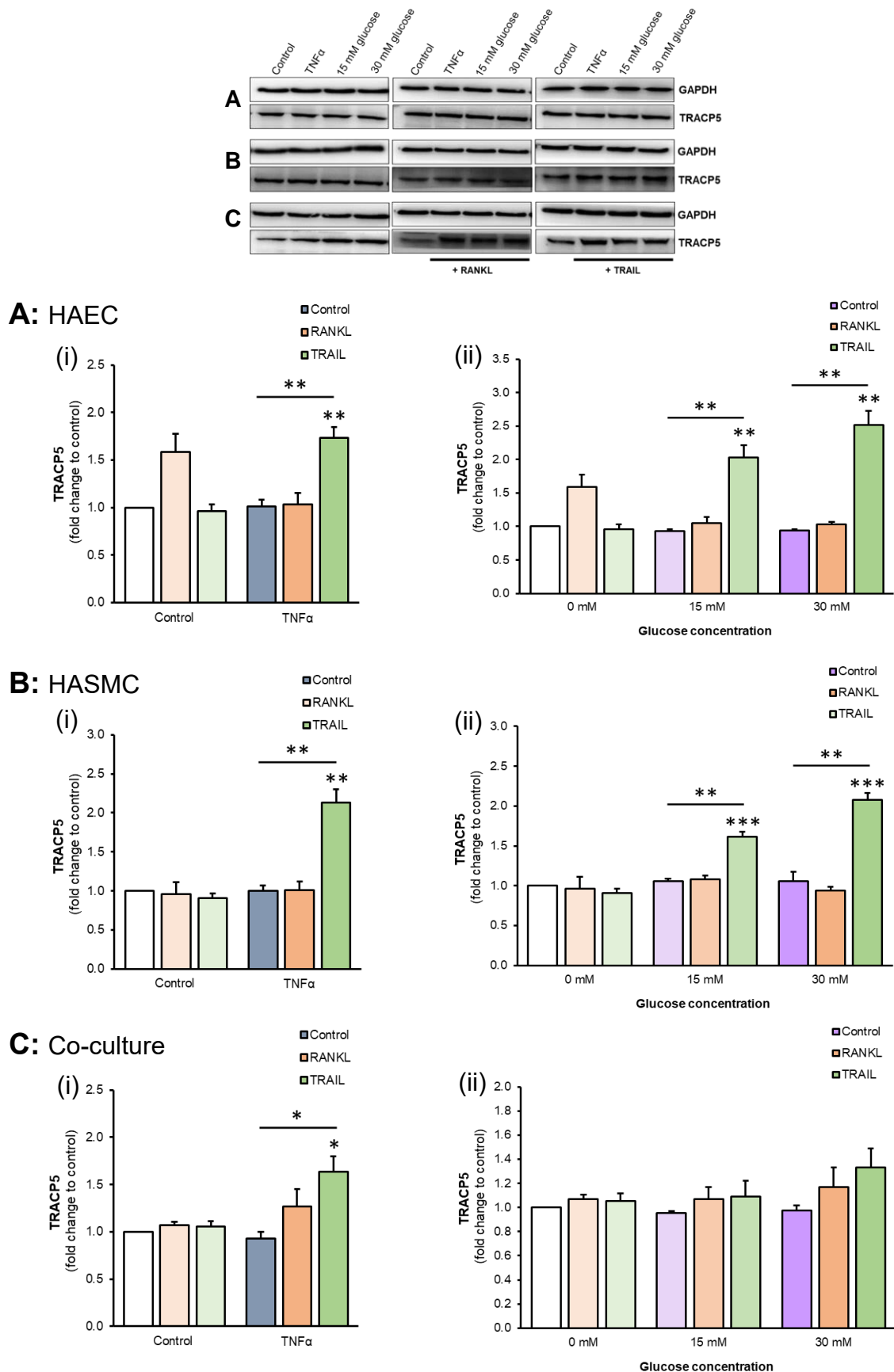


Figure 5.5. The effects of RANKL/TRAIL on TRACP5 protein expression under inflammatory and hyperglycemic conditions. (A) HAECs and (B) HASMCs were exposed to (i) TNF α (100 ng/mL) or (ii) glucose (15-30 mM) +/- RANKL (25 ng/mL) or TRAIL (5 ng/mL) for 72 hours, prior to analysis of TRACP5 protein expression. (C) HAECs in the luminal compartment in co-culture were exposed to the same conditions, and the underlying HASMCs harvested and assessed for TRACP5 protein expression. TRACP5 levels were determined by Western blotting, quantified by scanning densitometry and normalised to GAPDH. Blots are representative. * $p < 0.05$; ** $p < 0.01$; *** $p < 0.001$ compared to untreated control unless otherwise stated; bars indicate statistical significance between treatment groups.

5.2.5 Discussion: TRACP5 Analysis

It is now known that RANKL and TRAIL play central roles in the regulation of VC. However, much remains to be delineated regarding the precise molecular signalling processes and mechanisms underpinning these functions. The key aim of this investigation, given the integrated roles for these ligands identified previously, was to identify novel targets that may aid in the understanding of RANKL-induced calcification and TRAIL-mediated protection. Following in-depth bioinformatics and literature analyses, TRACP5 was identified as a potential interactant with RANKL/TRAIL, with multiple associated functions in bone morphogenesis and oxidative stress. Hence, this protein was assessed in both mono- and co-culture, following exposure to RANKL, TRAIL and pathological stimuli employed in previous chapters.

5.2.5.1 Identification of a Novel VC Target: TRACP5

Following bioinformatics analyses, a number of proteins that may potentially interact with RANKL, TRAIL and their common decoy receptor OPG were identified. As expected, RANKL and TRAIL were associated with their membrane and decoy receptors, while TRAIL's primary role as an apoptosis-inducing ligand was highlighted in its interaction with caspase proteins (Li and Yuan, 2008). The interaction between RANKL and TRAF6 is also well-established, with TRAF6 known to mediate RANKL-induced signals such as NF- κ B in bone (Armstrong *et al.*, 2002). Interestingly, text mining analyses revealed a potential interaction of RANKL/OPG with PTH; indeed, PTH has been implicated in the development of VC, particularly associated with renal failure (Neves *et al.*, 2007), but no studies to date have identified a link between PTH and TRAIL function. Of additional note, despite reports of TRAIL-mediated vasoprotection in previous studies (di Bartolo *et al.*, 2011; Liu *et al.*, 2014; Secchiero *et al.*, 2006), TRAIL has not yet been associated with any VC-related indices via bioinformatics. This finding emphasizes the novelty of the studies presented in Chapters 3 and 4, and indicates that TRAIL may indirectly mediate pro-calcific pathways (via mechanism(s) that remain to be determined) rather than through direct interaction with pro-calcific proteins. Highlighting the importance of a comprehensive bioinformatics strategy, BioGRID analysis suggested that TRACP5, identified as a potential interactant with RANKL/OPG via STRING text mining, also interacted in some way with TRAIL; furthermore, TRACP5 was associated with many of the same pathways/processes central to RANKL/TRAIL function *in vivo*.

5.2.5.2 The Function of TRACP5 in Bone and Vasculature

Several functions of TRACP5 identified in the UniProt and BioSystems databases overlap with that of RANKL and TRAIL, potentially implicating this protein in VC pathogenesis. TRACP5 is known to be expressed in a number of cell types *in vivo*, in particular osteoclasts and activated macrophages, but has also been identified in the heart, among other organs and tissues (Hayman *et al.*, 2000). In this case, the role for TRACP5 in osteoclasts, regulating bone resorption, was of particular interest. TRACP5 shares this primary function with that of RANKL, but the role for TRACP5 in the vasculature remains understudied. Given the paradoxical role for RANKL in bone and vasculature (i.e. resorbing bone while promoting VC), the potential for TRACP5 to exert similar pro-calcific effects could not be disregarded. Indeed, TRACP5 is also expressed in osteoblasts (Solberg *et al.*, 2014) and has been suggested (through bioinformatics) to regulate osteoblast differentiation/activation. In fact, Lau and Baylink (2003) have previously identified two distinct isoenzymes of TRACP5, one with osteoclastic and one with osteoblastic function, further indicating a dual role for this protein.

Moreover, computational analysis associated TRACP5 function with BMP receptor signalling. Again, the primary function for BMPs are that of bone morphogenesis, striking a balance between formation and resorption (Paul *et al.*, 2009), but their role in the regulation of VC has now been well established (Davenport *et al.*, 2016; Osako *et al.*, 2010; Panizo *et al.*, 2009). BMPs (2-7) have previously been shown to promote the formation of TRACP5-positive multinucleated osteoclasts in bone (Paul *et al.*, 2009), and as such, BMP signalling in the vasculature may also promote TRACP5 expression. Furthermore, bioinformatics analyses also identified a role for TRACP5 in extracellular matrix mineralisation, although it is not specified whether positive or negative; this function is likely linked to OPN/BSP dephosphorylation, a key process necessary for osteoclast migration (Ek-Rylander *et al.*, 1994) but also responsible for the release of free phosphate into the extracellular space in a mechanism similar to that of ALP (Linder *et al.*, 2017).

Within the literature, there are several studies that suggest a role for TRACP5 in the promotion of bone formation. In this respect, TRACP5-deficient mice have been found to develop delayed cartilaginous mineralisation alongside severe osteopetrosis, while TRACP5-overexpressing mice develop mild osteoporosis and increased osteoblastic activity (Hayman *et al.*, 1996; Angel *et al.*, 2000). These effects would appear to contradict the osteoclastic function of TRACP5, suggesting once again a potential dual function for this protein in bone morphogenesis.

Evidence also points to an integrated role for TRACP5 and RANKL/TRAIL, relevant to both bone and vasculature. RANKL has been found to induce TRACP5 expression in osteoclasts (Nakashima and Haneji, 2013), while statin treatment was found to attenuate this effect, again highlighting the link between bone turnover and cardiovascular health. TRACP5 has also been found to co-localise with OPG/RANKL in chondrocytes (Solberg *et al.*, 2015), of particular interest given the proposition that chondrocytic (rather than osteoblastic) signalling events mediate VC (Speer *et al.*, 2009). TRACP5 expression has also been associated with NF- κ B activation, a pathway which plays a key role in bone resorption (Abu-Amer, 2013) but also contributes to pro-calcific signalling (Zhao *et al.*, 2012). With regard to TRAIL, recombinant injection has been found to decrease circulating TRACP5 levels *in vivo* (Zauli *et al.*, 2008), coinciding with the previous observation that TRAIL delivery exerts a cardioprotective effect in murine models (Liu *et al.*, 2014; Secchiero *et al.*, 2006). Of further note, TRACP5 is thought to respond to *L*-ascorbic acid, a strong pro-calcific agent employed to promote osteoblastic differentiation (Ciceri *et al.*, 2012). Overall, therefore, there is strong evidence to suggest a pro-calcific role for TRACP5 in the regulation of VC.

Finally, following bioinformatics analyses, TRACP5 function was also associated with the promotion of oxidative stress, known to be involved in RANKL's vascular function and implicated in the pathogenesis of VC (Byon *et al.*, 2008; Thummuri *et al.*, 2017). Like RANKL, TRACP5 is known to promote ROS generation *in vivo* (Halleen *et al.*, 1999), and as such promotes a pro-oxidant environment. Consistent with this is the finding that TRACP5 negatively regulates NO, an anti-oxidant signalling molecule centrally involved in cardioprotection (Hummel *et al.*, 2006; Nasseem, 2005; Räsänen *et al.*, 2005). Furthermore, TRACP5 has been shown to be activated by oxidative stress in chondrocytes (Seol *et al.*, 2009), potentially suggesting a reciprocal regulatory mechanism between the two. Indeed, the aforementioned upregulation of arterial TRACP5, associated with NF- κ B signalling, was also found to coincide with pro-oxidant pathways (Padilla *et al.*, 2013). Therefore, the hypothesised pro-calcific role for TRACP5 in the vasculature may, like RANKL, be accentuated by coexistent pro-oxidant effects. As recent evidence suggests an anti-oxidant role for TRAIL in the vasculature (Forde *et al.*, unpublished observations), it may also be possible that TRAIL may interact with TRACP5 via oxidative stress mechanisms in the mediation of VC.

5.2.5.3 *The Effects of RANKL +/- TRAIL on TRACP5 Expression*

Firstly, the expression of TRACP5 was investigated in vascular cells in mono- and co-culture following exposure to RANKL +/- TRAIL to determine if these ligands may regulate TRACP5 expression during VC. As mentioned, TRACP5 has been found to be upregulated in atherosclerotic lesions compared to normal artery (Timofeeva *et al.*, 2009), but its expression has not yet been confirmed in HAECs or HASMCs; thus, the first novel finding of note is that TRACP5 is expressed at both an mRNA and protein level in both aortic ECs and VSMCs.

Following exposure to RANKL/TRAIL, the finding that RANKL promoted both TRACP5 mRNA and protein expression in HAECs was particularly noteworthy, given the prominent role for the endothelium in pro-calcific signalling identified in Chapters 3 and 4. As mentioned, RANKL has been claimed to induce TRACP5 expression in osteoclasts (Nakashima and Haneji, 2013), but this finding has not yet been confirmed in vascular cells; thus, we highlight for the first time the presence of RANKL-mediated TRACP5 regulation in the endothelium, coinciding with pro-calcific BMP-2/ALP paracrine signalling and non-canonical NF- κ B activation also induced by RANKL. With regard to the latter, TRACP5 has, unsurprisingly, been associated with NF- κ B activation in its role in osteoclastogenesis (Abu-Amer, 2013), but whether or not TRACP5 activates NF- κ B within a vascular context remains to be determined. It is likely, however, given the potential for TRACP5 to exert pro-calcific effects as discussed in Section 5.2.5.2, that RANKL-induced TRACP5 expression may further contribute to signalling events (e.g. NF- κ B activation, matrix mineralisation) during VC pathogenesis.

Even more interesting is the observed ability of TRAIL to completely attenuate RANKL-induced TRACP5 mRNA/protein in HAECs. As noted, TRAIL exerts protective effects at an endothelial level in the prevention of RANKL-induced pro-calcific BMP-2/ALP and non-canonical NF- κ B signalling. Given that TRACP5 is simultaneously attenuated suggests that TRACP5 expression may be mediated via the same pathway(s) that regulate other RANKL-induced pro-calcific signals (eg. NF- κ B). In support of this, circulatory TRACP5 levels have been shown to be reduced following TRAIL delivery (Zauli *et al.*, 2008). This finding also adds further validation to the protective nature of TRAIL in the vasculature, for which the mechanism(s) remain to be explored in the following sections; TRACP5 does, however, interact with both oxidative stress and NF- κ B pathways (Halleen *et al.*, 1999), which will be investigated as potential targets for TRAIL-mediated protection in Sections 5.3 and 5.4 respectively.

While a similar trend in TRACP5 expression was observed at an mRNA level in HASMCs, TRACP5 was not regulated at a protein level. The promotion and prevention of TRACP5 transcript expression by RANKL and TRAIL respectively, however, suggests a role for TRACP5 in smooth muscle during VC. By way of explanation, TRACP5 protein expression has been shown to be upregulated in late stage (but not early stage) calcification induced by RANKL in monocyte precursor cells (Nie *et al.*, 2015); as such, TRACP5 protein responses may vary across cell types, taking longer to exert a functional response in smooth muscle compared to endothelium. Finally, RANKL and TRAIL had no effect on TRACP5 regulation in co-culture. Thus, endothelial paracrine signalling does not mediate TRACP5 expression in HASMCs, but rather direct RANKL treatment of vascular cells.

5.2.5.4 The Effects of RANKL/TRAIL on TRACP5 Expression during Inflammation

The regulation of TRACP5 under pathological conditions is less easily explained. Despite the well-established pro-calcific, pro-oxidant and pro-inflammatory roles for TNF α , this cytokine did not exert any effect on TRACP5 protein expression in HAECs, HASMCs or HASMCs in co-culture. Contrastingly, TNF α has previously been shown to promote TRACP5 expression in osteoclastogenesis (Azuma *et al.*, 2000), again highlighting the conflicting regulation of this protein in bone and vasculature. Moreover, while RANKL treatment alone promoted TRACP5 protein expression in HAECs, this effect was not sustained under inflammatory conditions, while TRAIL treatment significantly upregulated TRACP5 in the presence of TNF α . While difficult to interpret, these findings further support a key observation of Chapter 4 that the effects of RANKL and TRAIL vary significantly under healthy and pathological conditions.

Interestingly, both TNF α and RANKL share many of the same functions and activate similar signalling pathways in bone and vasculature (Al-Aly, 2008; Azuma *et al.*, 2000; di Bartolo and Kavurma, 2014; Wada *et al.*, 2006), and as such it is unclear why the presence of TNF α attenuates RANKL-induced TRACP5 expression. By way of potential explanation, IL-6 pro-inflammatory cytokine is widely known to be induced following TNF α treatment (Modur *et al.*, 1996), a trend confirmed in HAECs and HASMCs in Chapter 4. Interestingly, IL-6 directly inhibits differentiation of osteoclast progenitor cells by inhibiting specific components of RANK signalling pathways (I κ B, c-Jun N-terminal kinase), despite being widely considered a promoter of osteoclast activity (Yoshitake *et al.*, 2008). Thus, Yoshitake and colleagues highlight a potential multifunctional role for IL-6 during osteoclast differentiation, which may

also extend to the vasculature, with IL-6 potentially attenuating RANKL-induced TRACP5 expression while maintaining its pro-calcific function via uninhibited pathways.

The observed upregulation of TRACP5 by TRAIL is also contradictory to our hypothesis; however, a potential explanation for this may lie with the regulation of TRAIL surface receptors. Previous research within our group, in accordance with the literature, have shown that TNF α promotes the expression of DR5 in endothelial cells (Sheikh *et al.*, 1998), and as such, it is possible that DR5 mediates additional signalling events in vascular cells; indeed, TRAIL has been found to induce osteoclastic activity and TRACP5 expression in monocyte/macrophage precursor cells (Yen *et al.*, 2008). While this explanation is speculative, it is well known that TRAIL-mediated signalling can exert both pathological and protective effects under specific conditions (Forde *et al.*, 2016), and thus it is possible that TRAIL promotes TRACP5 in the presence of inflammation. As suggested in previous chapters, this finding further implies that the vasoprotective effects of TRAIL may be most pertinent specifically during RANKL-induced calcification in areas of healthy, rather than atherosclerotic, vasculature.

5.2.5.5 The Effects of RANKL/TRAIL on TRACP5 Expression during Hyperglycemia

Once again, RANKL and TRAIL exert drastically different effects in the vasculature under hyperglycemic compared to normoglycemic conditions. Glucose-induced IL-6 may in part contribute to a reduction in RANKL-induced TRACP5 expression (Yoshitake *et al.*, 2008), previously suggested in Section 5.2.5.4., but this cytokine is released to a much lesser extent under hyperglycemic compared to inflammatory conditions. There is no further evidence to our knowledge to support the apparent “protective” effects of glucose on RANKL-induced TRACP5 expression. In fact, hyperglycemia in T2DM has been associated with osteoporosis (Starup-Linde and Vestergaard, 2015), and has been shown to promote VC (Besueille *et al.*, 2015), suggesting a paradoxical role in bone and vasculature similar to that of RANKL.

With regard to TRAIL, no evidence to our knowledge suggests that glucose regulates the expression of TRAIL receptors, and so the previously suggested upregulation of DR5 resulting in TRAIL-induced TRACP5 expression cannot be supported in this case. As noted, the pleiotropic role of TRAIL is well documented (Forde *et al.*, 2016), and our data suggests that it may exert different effects under normal and pathological conditions. It must be noted, however, that the varying trends between mRNA and protein levels may hinder our

understanding of TRACP5 regulation in the vasculature. It is known that mRNA and protein trends do not always coincide (Carmody and Wentz, 2009; Greenbaum *et al.*, 2003), which seems particularly true for TRACP5 under pathological conditions, making the longer-term effects of RANKL/TRAIL treatment difficult to determine. Furthermore, it is possible that the apparent upregulation of TRACP5 observed following exposure to TRAIL may actually represent a blockade of TRACP5 release, rather than an increase in expression, similar to that observed with BMP-2 in Chapter 3. These explanations require further experimentation, but given the convincing evidence to support TRAIL protection, should not be disregarded.

5.2.5.6 TRACP5: Summary of Results

Following thorough analyses, we confirm that TRACP5 (despite its primary role in osteoclastogenesis) is expressed in vascular tissue, and suggest that it may be involved in RANKL-induced calcification and TRAIL-mediated protection in healthy vasculature (particularly the endothelium). Whether or not TRACP5 is mediated by the same proposed pathways as other pathological stimuli (i.e., NF- κ B, redox signalling), or if extracellular TRACP5 may contribute to VC, remains to be determined (Figure 5.6). The effects of RANKL/TRAIL on TRACP5 expression were altered under inflammatory and hyperglycemic conditions, however, further experimentation is required to explain these discrepancies. Overall, however, we find that TRACP5, like RANKL, may exert paradoxical roles in bone and vasculature, and further investigation into its potential pro-calcific role warrants further research.

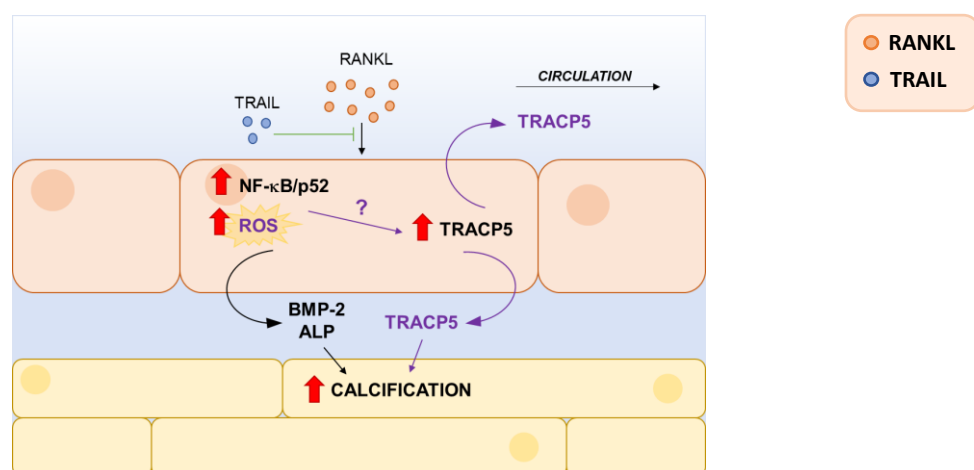


Figure 5.6. Representation of the key findings of TRACP5 investigations. Endothelial cell (upper layer) exposure to RANKL activates non-canonical NF- κ B and may also induce reactive oxygen species (ROS) generation. This leads to TRACP5 production, alongside BMP-2/ALP pro-calcific signalling, to induce calcification in the underlying (lower layer) smooth muscle. TRAIL co-incubation blocks this process thereby preventing calcification. It remains to be determined if TRACP5 is also released in a paracrine manner, or into circulation, by the endothelium. Purple text, hypothesised event: remains to be confirmed experimentally.

5.3 Identifying the Role of RANKL/TRAIL in Endothelial Oxidative Stress

Oxidative stress plays a key role in many vascular processes, and has long been implicated in vasculopathies associated with CVD/T2DM (Higashi *et al.*, 2009; Pitocco *et al.*, 2013). As oxidative stress is a major contributor to endothelial dysfunction/VC (Silva *et al.*, 2012; Singh *et al.*, 2010), and given the profound role for the endothelium in VC signalling identified in Chapters 3 and 4, oxidative stress was deemed a valid target in the investigation of RANKL/TRAIL functional mechanisms. Indeed, RANKL has been shown to induce oxidative stress, which has been implicated in the promotion of VC (Byon *et al.*, 2008; Thummuri *et al.*, 2017), while recent evidence points to an anti-oxidant role for TRAIL in the endothelium (Forde *et al.*, unpublished observations). Moreover, TRACP5, a potential player in the VC process identified in Section 5.2.1, is thought to interact with RANKL/TRAIL function and is known to regulate oxidative stress (Seol *et al.*, 2009). This finding further highlights the potential for the involvement of pro/anti-oxidant mechanisms in RANKL/TRAIL-mediated VC processes. In this section, a number of targets related to oxidative stress will be assessed, as listed in Section 5.1.3.2, while experimental approaches incorporating the anti-oxidant NAC will also be employed.

5.3.1 The Expression of SOD1/SOD2 in HAECs

First, the expression of SOD1/SOD2 in HAECs exposed to RANKL +/- TRAIL, and RANKL/TRAIL under inflammatory and hyperglycemic conditions, will be assessed. As discussed, SOD1 and SOD2 are involved in the conversion of superoxide radicals (O_2^-) into less damaging species in the cytosol and mitochondria respectively, and as such are known to exert cardioprotective effects in the vasculature (Fukai and Ushio-Fukai, 2011). The expression of SOD1/SOD2 was only assessed in HAECs, given the prominent role for the endothelium in VC regulation identified in previous chapters and in the relevant literature.

5.3.1.1 The Effects of RANKL +/- TRAIL on SOD1/SOD2 Expression

At an mRNA level, 25 ng/mL RANKL significantly downregulated SOD1 transcript expression by approximately 30%. TRAIL, on the other hand, significantly induced SOD1 expression, both alone and in combination with both concentrations of RANKL (Figure 5.7A).

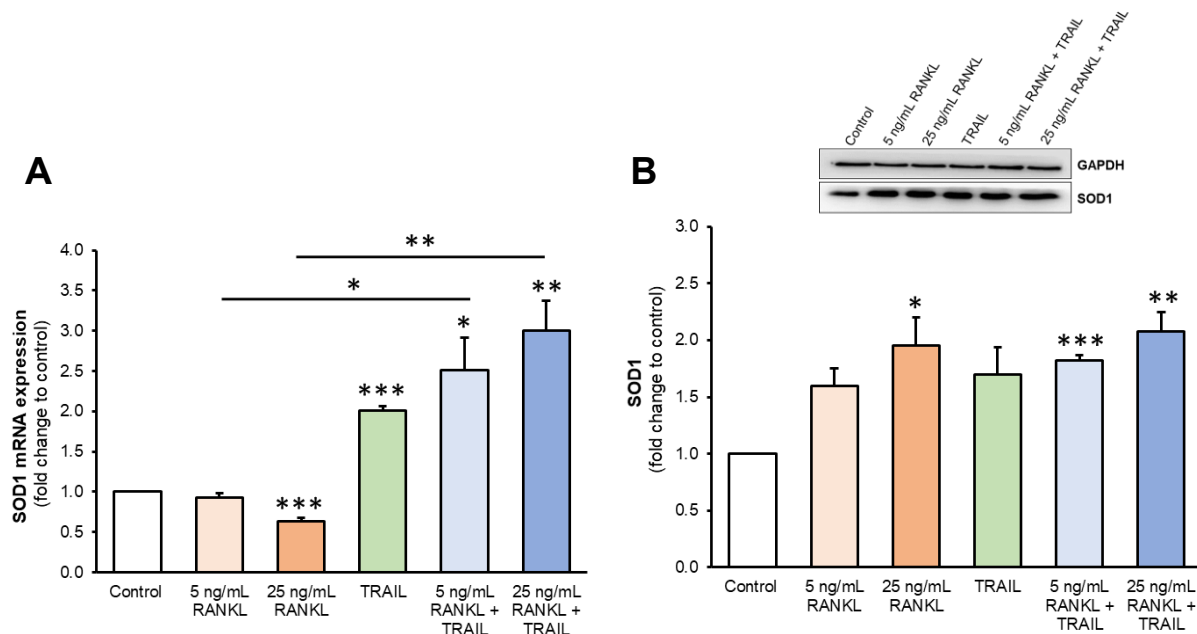


Figure 5.7. The effects of RANKL +/- TRAIL on SOD1 expression in HAECs. HAECs were exposed to RANKL (5-25 ng/mL) +/- TRAIL (5 ng/mL) for 72 hours, prior to harvesting and analysis of SOD1 (A) mRNA and (B) protein expression. Gene expression was analysed by RT-qPCR employing GAPDH as an endogenous control, while protein expression was assessed by Western blotting, quantified by scanning densitometry and normalised to GAPDH. Blots are representative. * $p < 0.05$; ** $p < 0.01$; *** $p < 0.001$ compared to untreated control unless otherwise stated; bars indicate statistical significance between treatment groups.

At a protein level, RANKL dose-dependently increased SOD1 protein expression (with a significant upregulation observed at 25 ng/mL), while TRAIL induced a non-significant upregulation of SOD1. SOD1 protein expression remained significantly upregulated in the presence of RANKL (5-25 ng/mL) + TRAIL (Figure 5.7B). Furthermore, β -glycerophosphate significantly induced SOD1 expression at both an mRNA and protein level (Appendix 5.1A (ii), (v)). Regarding SOD2, RANKL dose-dependently downregulated mRNA levels while TRAIL significantly increased its expression. SOD2 transcription levels returned to baseline, however, in the presence of both RANKL and TRAIL (Appendix 5.2). SOD2 protein expression remained undetectable by Western blotting under these conditions (data not shown), but its production was significantly induced following exposure to β -glycerophosphate (Appendix 5.1A (vi)).

5.3.1.2 The Effects of RANKL/TRAIL on SOD1/SOD2 Expression during Inflammation

Following exposure to $\text{TNF}\alpha$, SOD1 mRNA expression was significantly upregulated; while the addition of RANKL slightly (but significantly) decreased its expression, SOD1 remained upregulated to the same extent in the presence of TRAIL (Appendix 5.3A (i)). $\text{TNF}\alpha$ also upregulated SOD1 a protein level, while the addition of both RANKL and TRAIL (separately) reduced this effect by approximately 30% (Appendix 5.4A (i)). SOD2 transcript expression

was upregulated to a major extent (~60-fold) under inflammatory conditions, and again, while TRAIL had no effect on this, RANKL exposure slightly reduced these expression levels (Appendix 5.3B (i)). TNF α also increased SOD2 protein expression ~5-fold, while the separate addition of RANKL and TRAIL reduced this expression by 40-45% (Appendix 5.4B (i)).

5.3.1.3 The Effects of RANKL/TRAIL on SOD1/SOD2 Expression during Hyperglycemia

Prior to glucose treatment, HAECs were again exposed to mannitol osmotic control to ensure that any observed effects on SOD expression were glucose-specific; as such, mannitol had no effect on SOD1/SOD2 expression at an mRNA (data not shown) or protein level (Appendix 5.1B (ii), (iii)). Following hyperglycemic treatment, SOD1 mRNA expression was dose-dependently upregulated, and no significant effects were noted following treatment with RANKL or TRAIL (Appendix 5.3A (ii)). SOD1 protein expression was elevated following both moderate and severe glucose treatment; while RANKL treatment did not significantly affect this trend, the addition of TRAIL partially reduced this effect (Appendix 5.4A (ii)). SOD2 mRNA expression was also upregulated following both moderate and severe hyperglycemic treatment. RANKL treatment completely attenuated this effect, while TRAIL further promoted SOD2 transcript expression, particularly in the presence of moderate hyperglycemia (Appendix 5.3B (ii)). Contrastingly, at a protein level, SOD2 remained undetectable following both RANKL and TRAIL treatment under hyperglycemic conditions.

5.3.2 The Effects of RANKL +/- TRAIL on Pro-/Anti-oxidant Gene Expression in HAECs

A range of redox genes (gp91, eNOS, HMOX1) were next assessed in HAECs exposed to RANKL +/- TRAIL to further investigate the role of oxidative stress in RANKL/TRAIL function. Interestingly, neither ligand had any notable effects on gp91 mRNA (only a slight decrease of approximately 20% was noted with 5 ng/mL RANKL), but 25 ng/mL RANKL significantly upregulated p47 transcript expression by ~1.4-fold. Furthermore, the addition of TRAIL non-significantly attenuated this effect (Figure 5.8A). Regarding anti-oxidant genes, RANKL significantly increased and TRAIL decreased eNOS expression; during co-exposure, however, RANKL and TRAIL at these concentrations exerted a synergistic effect on eNOS transcription levels. Moreover, TRAIL (in both the presence and absence of RANKL) significantly upregulated HMOX1 mRNA expression by approximately 2.2-fold (Figure 5.8B).

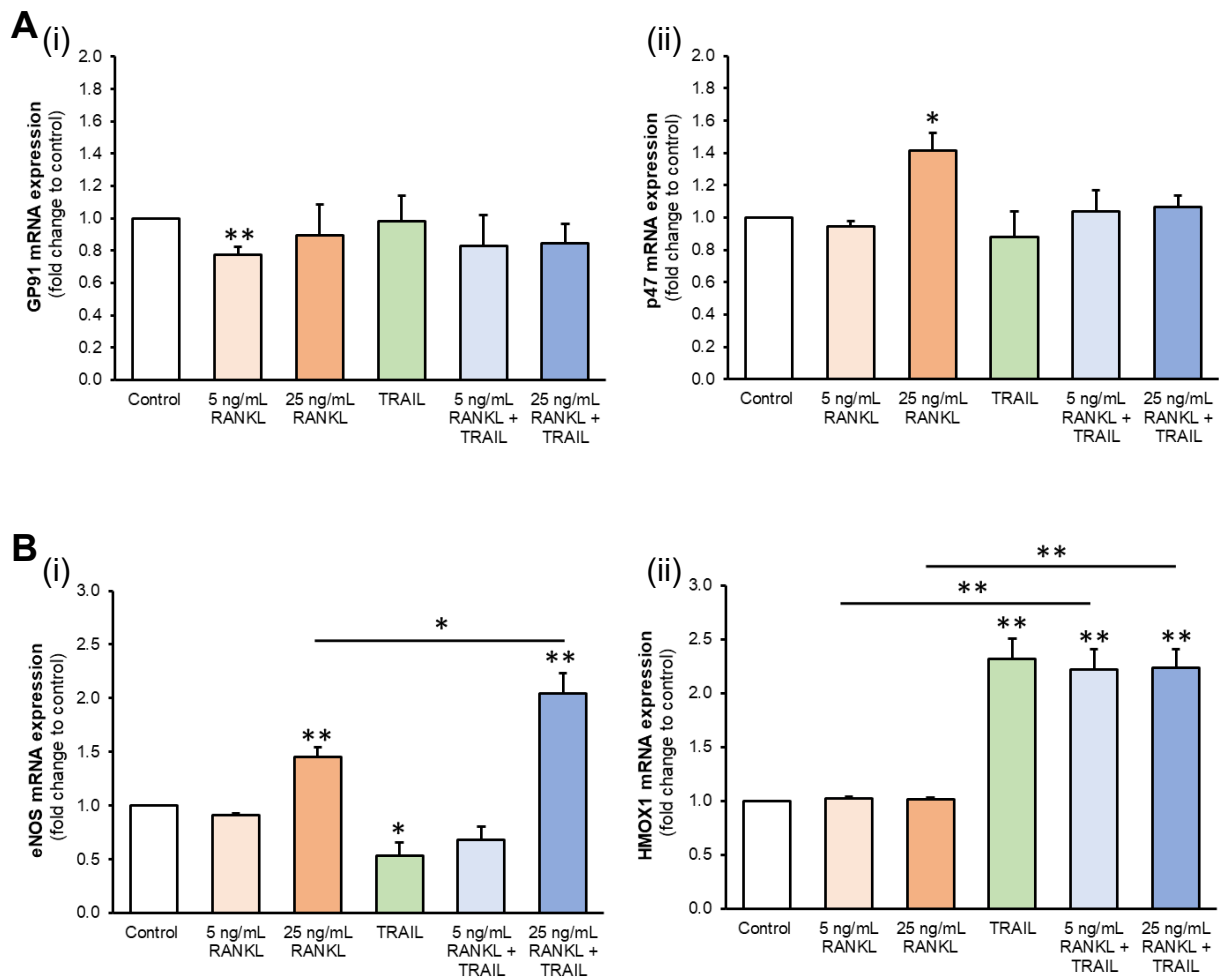


Figure 5.8. The effects of RANKL +/- TRAIL on pro/anti-oxidant mRNA expression in HAECs. HAECs were exposed to RANKL (5-25 ng/mL) +/- TRAIL (5 ng/mL) for 72 hours, prior to analysis of (A) (i) gp91 and (ii) p47 pro-oxidant genes, and (B) (i) eNOS and (ii) HMOX1 anti-oxidant genes. Gene expression was analysed by RT-qPCR employing GAPDH as an endogenous control * $p < 0.05$; ** $p < 0.01$ compared to untreated control unless otherwise stated; bars indicate statistical significance between treatment groups.

5.3.3 The Effects of the Anti-Oxidant NAC on Pro-calcific Signalling in HAECs

While studies describing the effects of RANKL and TRAIL on the aforementioned targets may be useful in delineating the pro/anti-calcific effects of these ligands, a functional study may be more beneficial in clarifying the role of oxidative stress in the endothelium during VC. As such, the anti-oxidant NAC was employed in HAEC monoculture, both alone and in combination with RANKL, to determine (i) if the pro-calcific effects of RANKL are dependent on pro-oxidant mechanisms, and (ii) if TRAIL exerts similar effects to a well-established anti-oxidant. Furthermore, $\text{TNF}\alpha$, a strong pro-oxidant/pro-calcific stimulus, was also co-treated with NAC to ensure the desired anti-oxidant effect was achieved. A wide range of genes/proteins were assessed in an attempt to clarify the inter-related roles of oxidative stress and VC.

5.3.3.1 The Effects of NAC on the Pro-calcific and Pro-oxidant Actions of RANKL

With regard to the pro-calcific effects of RANKL identified in Chapters 3 and 4, again no effects were noted on BMP-2 and ALP mRNA expression after 72 hours; NAC, however, both alone and in combination with RANKL, significantly downregulated BMP-2/ALP mRNA (Figure 5.9A). No changes were noted following NAC treatment in Runx2 or IL-6 transcript expression (data not shown). Furthermore, co-incubation with NAC completely attenuated RANKL-induced BMP-2/ALP release (Figure 5.9C). NAC also significantly attenuated intracellular ALP activity induced by RANKL (Figure 5.9B), but did not affect intracellular BMP-2 production (data not shown). Furthermore, the addition of NAC significantly increased both OPG production and release, both alone and when co-treated with RANKL (data not shown). No effects were noted in IL-6 release levels (data not shown). While the canonical NF- κ B pathway was not assessed (given the focus on pro-calcific signalling), RANKL-induced non-canonical activation was also attenuated by NAC (Figure 5.9D).

5.3.3.2 The Effects of NAC on the Pro-oxidant and Pro-calcific Actions of TNF α

With regard to oxidative stress, NAC was found to significantly reduce TNF α -induced p47 and gp91 gene expression (data not shown). Regarding pro-calcific indices, at an mRNA level, TNF α -induced ALP, BMP-2, Runx2 and IL-6 were all significantly reduced by the co-addition of NAC (data not shown). This trend was reflected at a protein level, where BMP-2 and ALP release (induced by TNF α) were significantly attenuated, and IL-6 release significantly reduced by NAC (Appendix 5.5A). Similarly, NAC attenuated TNF α -induced intracellular BMP-2 protein levels and ALP activity (Appendix 5.5B). Non-canonical NF- κ B activation was, however, only slightly reduced by NAC addition (Appendix 5.5C). Moreover, NAC was found to further promote TNF α -induced OPG production and release when compared to TNF α treatment alone (data not shown).

5.3.4 The Effects of TRAIL on RANKL-induced ROS Generation in HAECs

Finally, the effects of RANKL and TRAIL on endothelial ROS production were assessed in an effort to further clarify the role of oxidative stress during VC. Again, HAECs were treated with RANKL (25 ng/mL) both alone and in combination with TRAIL (5 ng/mL), and DHE staining was employed to quantify/visualise ROS levels by flow cytometry (Section 2.2.7.2) and by

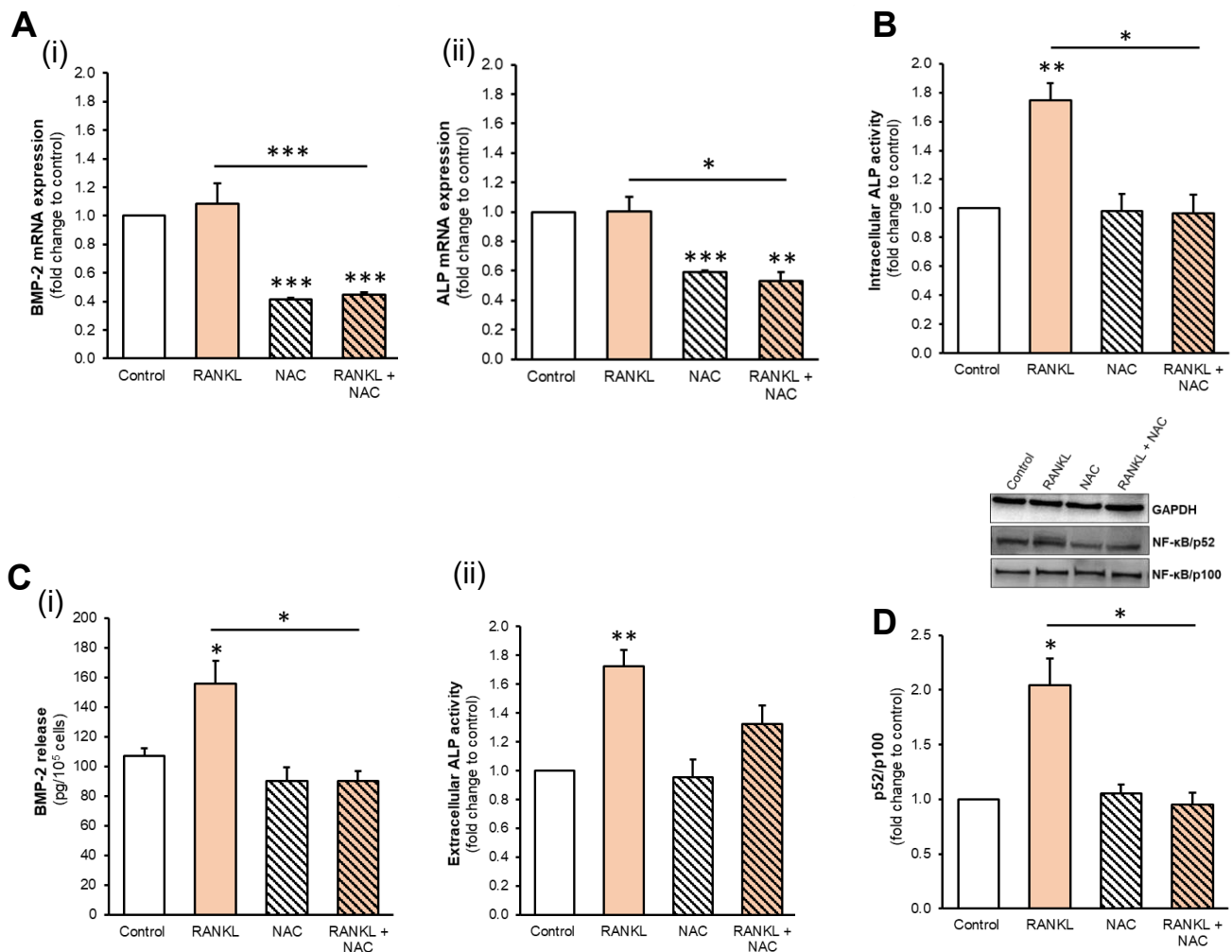


Figure 5.9. The effects of RANKL +/- NAC on gene/protein expression in HAECs. HAECs were exposed to RANKL (25 ng/mL) +/- NAC (5 mM) for 72 hours prior to analysis. **(A)** mRNA expression levels of (i) BMP-2 and (ii) ALP were analysed by RT-qPCR employing GAPDH as an endogenous control. **(B)** intracellular ALP activity and **(C)** (i) BMP-2 and (ii) ALP release were assessed by ELISA and enzyme assay where appropriate, normalized to 10⁵ cells (media) and total protein (lysate). **(D)** Non-canonical NF-κB activation was assessed by Western blotting, quantified by scanning densitometry and normalised to GAPDH. Blots are representative. * $p < 0.05$; ** $p < 0.01$; *** $p < 0.001$ compared to untreated control unless otherwise stated; bars indicate statistical significance between treatment groups.

fluorescence microscopy (Section 2.2.6.2). These experiments were conducted at both 24 and 72 hours to investigate the potential for time-dependent ROS generation in response to RANKL and TRAIL. HAECs were also treated with TNF α +/- NAC for 24 hours to ensure that ROS production/depletion could be successfully detected. Following treatment, RANKL was found to time-dependently induce ROS production, and while TRAIL alone had no effect, its co-addition significantly reduced RANKL-induced ROS after 72 hours (and non-significantly at 24 hours) (Figure 5.10A, B). TNF α , a recognised pro-oxidant stimulus, increased ROS generation, while NAC anti-oxidant treatment significantly reduced TNF α -induced ROS (Appendix 5.6A). These trends were confirmed by microscopy (Figure 5.10C, Appendix 5.6B).

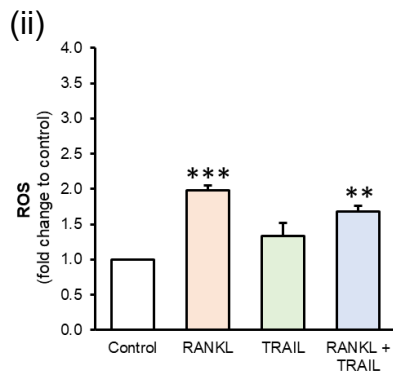
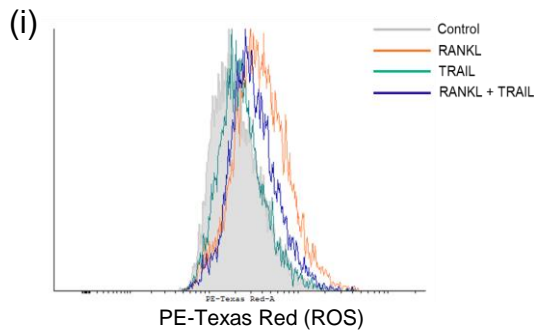
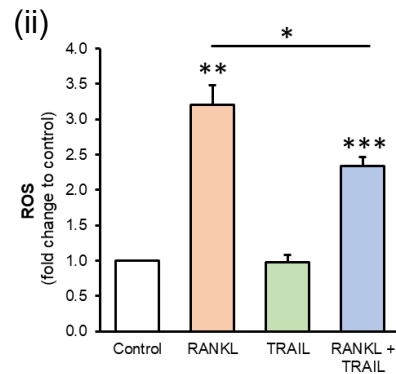
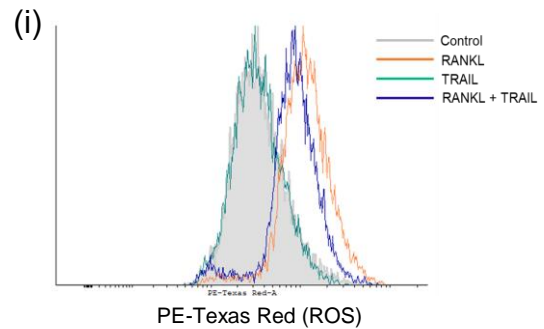
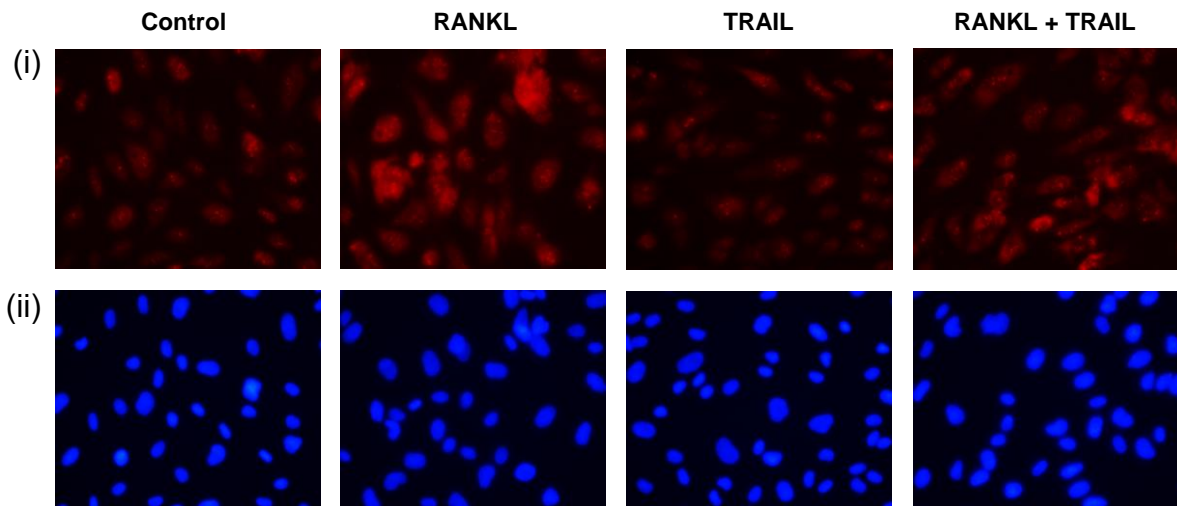
A: 24 hours**B: 72 hours****C: 72 hours**

Figure 5.10. The effects of RANKL +/- TRAIL on ROS generation in HAECs. HAECs were exposed to RANKL (25 ng/mL) +/- TRAIL (5 ng/mL) for 24 and 72 hours prior to analysis. DHE stain (3 μ M) was added 30 minutes prior to the end of the incubation period; DAPI was added 3 minutes prior to analysis for fluorescence microscopy only. (A, B) ROS generation was measured by flow cytometry, quantified by histogram area; presented histograms are representative. (C) (i) ROS generation via DHE staining and (ii) DAPI nuclear counterstain were visualised using a Nikon Eclipse Ti fluorescence microscope at 24 hours. Images (40X magnification) are representative. * $p < 0.05$; ** $p < 0.01$; *** $p < 0.001$ compared to untreated control unless otherwise stated; bars indicate statistical significance between treatment groups.

5.3.5 Discussion: Oxidative Stress

To reiterate, oxidative stress is exerted *in vivo* by the generation of ROS, by-products of metabolism resulting from the reduction of oxygen (Bayir, 2005). ROS levels are mediated by pro-oxidants (e.g. NADPH oxidase) and anti-oxidants (e.g. SOD, NO) in the modulation of multiple cellular processes (Rahal *et al.*, 2014), and the accumulation of ROS (above levels required to mediate these processes) exerts pathological effects on cells. Relevant to this study, oxidative stress has been associated with CVD/T2DM, and is known to promote endothelial dysfunction (Higashi *et al.*, 2009; Kayama *et al.*, 2015; Pitocco *et al.*, 2013). As such, the previously observed regulation of redox pathways by RANKL and TRAIL may partly explain the observed pro-calcific and protective effects of these ligands in the vasculature (Byon *et al.*, 2008; Forde *et al.*, unpublished observations; Thummuri *et al.*, 2017). In further support of this theory, TRACP5, identified as a potential contributor to VC in Section 5.2 and known to drive oxidative stress (Seol *et al.*, 2009), was regulated by RANKL/TRAIL treatment in HAECs. Thus, given the central role for the endothelium in the regulation of vascular paracrine signalling, HAECs were employed in an attempt to clarify the mechanisms by which RANKL and TRAIL exert their respective functions during VC.

5.3.5.1 The Effects of RANKL +/- TRAIL on SOD1/SOD2 Expression

Firstly, the effects of RANKL and TRAIL on endothelial SOD1/SOD2 expression were investigated. As noted, SOD enzymes catalyse superoxide dismutation, i.e., the conversion of superoxide anions into less harmful compounds, and as such are potent anti-oxidants (Ighodaro and Akinloye, 2017; Zhang *et al.*, 2003). SOD1, accounting for the vast majority of SOD activity, is responsible for scavenging cytosolic ROS, while SOD2 exerts this function exclusively in the mitochondria (Zelko *et al.*, 2002). Of relevance, cytosolic and mitochondrial ROS have been associated with vascular dysfunction (Faraci and Didion, 2004; Madamanchi *et al.*, 2007), and both SOD1 and SOD2 have been shown to exert a cardioprotective influence on the vessel wall (Ohashi *et al.*, 2006; Tribble *et al.*, 1999). SOD3, a third isoform (responsible for the dismutation of extracellular ROS) was not assessed in this study. Like SOD1 and SOD2, SOD3 is known to play a role in the mediation of vascular oxidative stress, however it is not believed to be expressed by endothelial cells (Faraci and Didion, 2004; Fukai *et al.*, 2002).

A significant and novel finding of the current study was the decrease observed in SOD1 and SOD2 mRNA expression following RANKL treatment. No studies to our knowledge have yet

assessed the effect of RANKL on SOD expression, despite RANKL being a known promoter of oxidative stress (Thummuri *et al.*, 2017). Interestingly, the NF- κ B family of transcription factors are established regulators of SOD expression, likely explaining the mechanism by which RANKL modulates these genes (Miao and St. Clair, 2010). While at an mRNA level the effects of RANKL may appear pro-oxidant, SOD1 protein expression was dose-dependently induced. By way of explanation, alongside the RANKL-induced downregulation of SOD mRNA, it is possible that the observed increase in SOD1 translation may represent a natural protective mechanism to counteract RANKL-induced oxidative stress. In support of this theory, TNF α (a potent pro-oxidant cytokine) has previously been shown to induce SOD2 protection (Warner *et al.*, 1991), but this trend has not yet been associated with SOD1.

Following TRAIL treatment, SOD1 and SOD2 mRNA were upregulated, and protein levels of SOD1 also trended upwards. While there is limited literature available to compare TRAIL-mediated SOD expression, conflicting research within our own group suggests that TRAIL had no effect on SOD1/SOD2 transcription/translation (Forde *et al.*, unpublished observations). In this particular instance, however, a higher dose of TRAIL (100 ng/mL) over a shorter incubation period (24 hours) was employed, potentially suggesting time- or dose-dependent regulation. Research presented in Chapter 3 indeed supports this proposition. Higher concentrations of TRAIL were found to induce the release of pro-inflammatory and pro-calcific proteins in HAECs (Section 3.2.1), possibly revealing that TRAIL exerts pathological effects at higher doses. Moreover, the TRAIL-induced inflammatory response was previously reported to be both time- and dose-dependent (Zoller *et al.*, 2017), again highlighting the pleiotropic nature of TRAIL and potentially explaining the above discrepancies in SOD expression.

Overall, as both RANKL and TRAIL induce SOD1 expression to a similar extent, this is likely not the mechanism responsible for TRAIL-mediated protection in the endothelium. With regard to SOD2, it has been confirmed within our research group that SOD2 protein remains undetectable in response to TRAIL treatment in HAECs (Forde *et al.*, unpublished observations). Indeed, low expression levels of SOD2 have been reported in HUVECs and BAECs (Valle *et al.*, 2005), and it has been reported that it is not uncommon for SOD2 mRNA and protein levels to deviate (Vogel *et al.*, 2011). Moreover, the short half-life of SOD2 and its complex post-translational regulation make these trends difficult to decipher (Kim *et al.*, 2011; Knirsch *et al.*, 2001; Miao and St. Clair, 2009). However, the lack of detectable protein expression also suggests that SOD2 does not mediate RANKL or TRAIL function in HAECs.

5.3.5.2 The Effects of RANKL/TRAIL on SOD1/SOD2 Expression during Inflammation

Studies have shown that endothelial dysfunction is mediated by TNF α -induced oxidative stress (Chen *et al.*, 2008) while other pro-inflammatory cytokines (e.g. IL-6) induced by TNF α further promote EC injury (Wassmann *et al.*, 2004). Circulating levels of these cytokines are known to be elevated during CVD/T2DM (Olson *et al.*, 2012; Levine *et al.*, 1990) contributing to a pro-calcific, pro-oxidant vascular environment. Thus, the effects of RANKL and TRAIL on TNF α -induced oxidative stress, such as that present during atherosclerosis, were next assessed to determine if either ligand mediates redox pathways under pathological conditions.

Interestingly, both SOD1 and SOD2 mRNA/protein levels were upregulated following TNF α exposure in HAECs. As mentioned, TNF α has previously been shown to induce SOD2 expression in ECs (Forde *et al.*, unpublished observations; He *et al.*, 2004), but conflicting data suggests that TNF α actually downregulates SOD1 mRNA/protein expression (Afonso *et al.*, 2006; Dschietzig *et al.*, 2012). These studies were, however, conducted in malignant cell lines of minimal physiological relevance to the natural vascular environment. Previous research within our own group has also indicated that TNF α exerts negligible effects on SOD1 regulation in HAECs following 24 hours' exposure. This finding suggests that the observed induction of SOD1 may only activate under chronic (>24 hour) conditions, potentially explaining the conflicting evidence presented above. Additionally, given the pro-oxidant role for TNF α , one would expect this cytokine to downregulate anti-oxidant SOD enzymes. However, this data supports the suggestion that SOD is upregulated by pro-oxidant stimuli as part of an intrinsic cardioprotective mechanism, emulating its natural function *in vivo*. Following RANKL addition, SOD1/SOD2 mRNA and protein expression were slightly reduced compared to treatment with TNF α alone. There are, as of yet, no relevant studies with which to compare this finding, but it may suggest that the presence of RANKL dampens the natural anti-oxidant response of HAECs. TRAIL addition had no effect at an mRNA level, but slightly downregulated both SOD proteins in a similar manner to RANKL. Given these findings, that TRAIL does not exert its protective influence via the upregulation of SOD in inflamed endothelium.

5.3.5.3 The Effects of RANKL/TRAIL on SOD1/SOD2 Expression during Hyperglycemia

Hyperglycemia is also considered a strong stimulus for oxidative stress and is a recognized promoter of ROS generation and endothelial dysfunction (Yano *et al.*, 2004). As noted,

elevated blood glucose is one of the key hallmarks of T2DM, and VC is known to be particularly prevalent among diabetic patients (Stabley and Towler, 2017). As such, hyperglycemia (like RANKL and TRAIL) likely contributes to the regulation of the pro-calcific and pro-oxidant vascular environment during T2DM. The effects of RANKL/TRAIL on HAECs in the presence of elevated glucose were therefore assessed to investigate whether or not these ligands mediate redox signalling pathways under hyperglycemic conditions. In this model, hyperglycemia was found to promote SOD1 expression as previously reported in vascular cells (Mahavadi *et al.*, 2017; Patel *et al.*, 2013). Interestingly, genetic disruption of SOD1 has been shown to induce glucose intolerance (Muscogiuri *et al.*, 2013), and SOD1 overexpression attenuates hyperglycemia-induced pathologies (Coucha *et al.*, 2015), providing strong evidence that glucose-induced SOD1 represents the cardioprotective anti-oxidant mechanism previously hypothesised. Regarding SOD2, while upregulated at a transcriptional level, SOD2 protein again remained undetectable. In support of this finding, the transcriptional upregulation of SOD2 under hyperglycemic conditions observed by Valle and colleagues was not accompanied by a concurrent increase in protein (Valle *et al.*, 2005).

With regard to RANKL treatment, no significant effects were noted in the presence of glucose, suggesting that RANKL does not modulate hyperglycemia-induced SOD expression during T2DM; however, this is the first study of its nature to date, and there is no evidence with which to compare this finding. Following TRAIL treatment, despite the non-significant increase observed in SOD1 mRNA, SOD1 protein was reduced when compared to hyperglycemia alone. Again, SOD2 protein remained undetectable (despite an upregulation of mRNA following moderate hyperglycemia). There is some evidence, albeit minimal, with which this data can be compared. An upregulation has previously been noted in SOD2 mRNA expression following TRAIL treatment under hyperglycemic conditions (Liu *et al.*, 2014) in conjunction with an increase in total SOD activity. Although we observed a decrease in SOD1 protein production (and undetectable SOD2 protein) compared to high-glucose alone, it must be noted that SOD activity and SOD protein expression may not coincide (indeed, enzyme activity can be mediated by a number of additional factors, e.g. levels of pro-inflammatory mediators) (Demerdash *et al.*, 2017). It is unlikely, however, based on the presented data, that TRAIL exerts a strong protective influence on HAECs under hyperglycemic conditions via the modulation of SOD expression.

5.3.5.4 The Effects of RANKL +/- TRAIL on Pro-/Anti-oxidant Gene Expression in HAECs

Next, representative pro-oxidant and anti-oxidant genes were assessed in HAECs exposed to RANKL and TRAIL, to further investigate if the respective pro-calcific/protective effects of these ligands may be mediated (at least in part) by the regulation of redox pathways. Given that neither RANKL nor TRAIL appeared to exert these effects via the regulation of SOD1/SOD2, but TRAIL was found to attenuate RANKL-induced TRACP5 in endothelial cells (a known catalyst for ROS generation), this experiment was conducted in the RANKL +/- TRAIL model only. As such, we investigate the effects of RANKL and TRAIL on the expression of oxidative stress-related genes in HAECs under physiological conditions.

Firstly, the pro-oxidant genes p47 and gp91 were assessed in HAECs following exposure to RANKL +/- TRAIL. These genes encode two phox subunits of NADPH oxidase (NOX) enzymes, a major source of ROS in endothelial cells (Pitocco *et al.*, 2013). Unsurprisingly therefore, NADPH oxidases have been associated with the progression of CVD/T2DM (Cave *et al.*, 2006; Fulton and Barman, 2016, Meyer and Schmitt, 2000). Specifically, gp91 (NOX2) mRNA expression has been positively correlated with atherosclerosis severity (Sorescu *et al.*, 2002) and relevant to this study has also been shown to promote RANKL-induced osteoclast differentiation (Kang and Kim, 2016). The p47 subunit, involved in NOX1/NOX2 signalling, has also been implicated in intimal calcification (Barry-Lane *et al.*, 2001) and is induced in endothelial cells under pro-inflammatory conditions common during VC (Li *et al.*, 2002).

In the current study, RANKL was found to upregulate p47 mRNA at the higher concentration of 25 ng/mL. While research linking RANKL with this subunit is lacking, p47 has previously been implicated in the inhibition of early bone development, emulating the natural resorptive effects of RANKL (Chen *et al.*, 2015), and TNF α has been shown to upregulate p47 (Li *et al.*, 2002), also known to exert pro-calcific effects on the vasculature. Deletion of p47 has also been found to protect against atherosclerotic calcification (Barry-Lane *et al.*, 2001; Vendrov *et al.*, 2007) further implicating this subunit in the progression of vascular pathologies. Taken together, this data may suggest that p47-mediated NOX pathways (NOX1 and NOX2) may be involved in RANKL function in the endothelium. Of note, NOX1 is not believed to be expressed in ECs (Pendyala *et al.*, 2009) potentially implicating the NOX2 pathway as a source of RANKL-induced endothelial ROS. Indeed, gp91 also modulates the NOX2 pathway, previously shown to promote atherosclerosis (Sorescu *et al.*, 2002) and RANKL-induced osteoclast differentiation (Kang and Kim, 2016). As such, the lack of upregulation of gp91

mRNA may be explained at a translational level, or may suggest that RANKL-induced p47 mediates the NOX2 pathway by promoting p47/gp91 assembly at the plasma membrane. Of further relevance, the upregulation of p47 mRNA by RANKL was completely attenuated by TRAIL. There is, however, no evidence to date to suggest that TRAIL exerts protective effects via NOX blockade; in contrast, TRAIL's apoptotic function has been positively associated with NOX1-induced superoxide production in tumour cells via DR4/DR5 signalling (Park *et al.*, 2012). However, endothelial resistance to TRAIL-induced apoptosis can be mediated by the expression of DcR1/DcR2 (Zhang *et al.*, 2000), and TRAIL is now widely accepted to exert *pleiotropic* effects *in vivo* via both death and decoy receptors (Forde *et al.*, 2016). Given the pro-calcific/pro-oxidant effects of RANKL and the anti-calcific/anti-oxidant effects of TRAIL observed in this model to date, we present novel evidence to suggest that the effects of these ligands may be mediated (in part) by the NOX2 pathway in endothelial cells.

The next gene involved in the mediation of redox signalling assessed in this study was eNOS, one of three NO synthase (NOS) isoforms. eNOS is primarily (but not exclusively) expressed in endothelial cells (Förstermann *et al.*, 2012) and plays a complex role in the regulation of ROS. Under basal conditions, eNOS produces NO, a free radical responsible for the regulation of vascular homeostasis, VSMC proliferation and vasodilation among other functions (Sena *et al.*, 2013). As such, eNOS is generally considered to exert protective effects on the vasculature. Under pathological conditions, however, eNOS can become “uncoupled”, and produce superoxide instead of NO (Yang *et al.*, 2009). eNOS uncoupling is prevalent in cardiovascular diseases and diabetes (Guzik *et al.*, 2002; Yang *et al.*, 2009), particularly under oxidative stress, thereby contributing to vascular ROS. Indeed, under these conditions, the role of eNOS may be altered, but constitutively expressed eNOS under physiological conditions is generally considered cardioprotective (Albrecht *et al.*, 2003).

Interestingly, RANKL at 25 ng/mL was found to upregulate eNOS mRNA. Given the proposed cardioprotective nature of eNOS, and the downregulation of eNOS observed during pro-calcific events (Banquet *et al.*, 2013, Oemar *et al.*, 1998), this result was surprising. By way of comparison, Min and colleagues (2007) have identified an increase in eNOS activity following RANKL treatment, but no change in eNOS mRNA/protein; however, this group stimulated HUVECs for only 30 minutes, likely explaining this discrepancy. Min *et al.* suggest that RANKL-induced eNOS/NO may play a role in the development of atherosclerosis via the promotion of vascular permeability; however, their analysis does not address the cardioprotective effects of eNOS in healthy vasculature. Therefore, we propose that RANKL-

induced eNOS may represent endothelial switching from a healthy to a pro-oxidant state, increasing oxidative stress and upregulating eNOS as previously described (Ding *et al.*, 2007). As such, RANKL treatment may provide the pro-oxidant environment necessary for eNOS uncoupling and eNOS-mediated ROS generation (Yang *et al.*, 2009).

Following TRAIL treatment, a slight downregulation in eNOS mRNA was observed, also in contrast with previous studies (Forde *et al.*, unpublished observations; Zauli *et al.*, 2003). However, these studies employed TRAIL at 20-fold higher concentrations at varying time points, and as noted, the effects of TRAIL on ECs are likely time- and dose-dependent. Following treatment with RANKL, however, the mRNA expression of eNOS was synergistically induced. This novel finding may suggest that TRAIL upregulates eNOS in an effort to counteract coexisting RANKL-induced p47 expression and ultimately ROS generation. Interestingly, Liu *et al.* (2014) note that TRAIL recovers eNOS activity in aortic cells under hyperglycemic conditions, further suggesting that TRAIL-induced eNOS may be dependent on a pro-oxidant, pathological environment. Protein analyses are required to confirm this hypothesis, but preliminary data suggests that the protective effects of TRAIL on RANKL-mediated pro-calcific/oxidant effects may involve the upregulation of eNOS.

Finally, HMOX1, an enzyme known to exert anti-oxidant effects on the vasculature in response to oxidative stress and inflammation (True *et al.*, 2007) was assessed. HMOX1 catalyses the degradation of heme, a potent pro-oxidant (Jeney *et al.*, 2002), exerting a range of cardioprotective effects (Araujo *et al.*, 2012; Juan *et al.*, 2001). As expected, RANKL did not regulate HMOX1 in the current model. TRAIL, on the other hand, was a potent inducer of HMOX1, both alone and in the presence of RANKL. Interestingly, carbon monoxide, a by-product of HMOX1 activity, has previously been shown to prevent RANKL-induced osteoclastic differentiation via NF- κ B (Bak *et al.*, 2017), and may possibly partly explain the TRAIL-mediated attenuation of RANKL effects. Overall, following gene expression analyses of redox genes in the endothelium, it appears that RANKL may modulate its pro-oxidant effects in the vasculature via upregulation of p47/NOX2 signalling, and that TRAIL may exert its anti-oxidant effects via attenuation of RANKL-induced p47, alongside the upregulation of eNOS and HMOX1 under pathological conditions. Protein analyses are required to confirm these findings, but the observed pro-/anti-oxidant effects of RANKL and TRAIL likely contribute to the respective pathological and protective effects during VC.

5.3.5.5 *The Effects of NAC on the Pro-calcific and Pro-oxidant Actions of RANKL*

As noted, RANKL has been shown to exert pro-oxidant effects on the vasculature, and pathological conditions such as EC dysfunction and VC are associated with an increase in oxidative stress (Silva *et al.*, 2012; Singh *et al.*, 2010). NAC, a well-known anti-oxidant often used *in vitro* as a negative regulator of oxidative stress (Nedeljkovic *et al.*, 2013), was next employed to further delineate the consequences of RANKL's pro-oxidant influence on the endothelium. In this way, following NAC blockade of pro-oxidant signalling by RANKL, a range of pro-calcific indices were assessed to determine if RANKL-induced redox pathways are involved in the promotion of VC.

Interestingly, the addition of NAC was found to significantly reduce BMP-2/ALP mRNA following 72 hours' incubation, indicating that (even in the absence of RANKL) attenuation of pro-oxidant pathways may exert anti-calcific protective effects on the vasculature. In accordance with this finding, co-treatment with NAC completely attenuated BMP-2 release and reduced extracellular ALP activity (alongside complete attenuation of intracellular ALP activity). Thus, we present novel evidence that RANKL-induced oxidative stress may mediate endothelial pro-calcific paracrine signalling, ultimately regulating VC in the underlying HASMC layer (Davenport *et al.*, 2016; Osako *et al.*, 2010). Indeed, the attenuation of BMP-2 mRNA expression by NAC has been reported in human epithelial cells, while BMP-2/ALP-induced mineralization (alongside ROS generation) has been blocked by NAC in pre-osteoblasts (Gustafsson *et al.*, 2005; Mandal *et al.*, 2011). NAC treatment has also been associated with reduced circulating ALP *in vivo* (Maheswari *et al.*, 2014) and has been found to attenuate dimethylnitrosamine-induced ALP in rats (Priya *et al.*, 2011).

Furthermore, the NAC-mediated reduction in BMP-2/ALP was accompanied by attenuation of RANKL-induced non-canonical NF- κ B signalling. We suggest in Chapter 3 that the non-canonical pathway may be responsible for the pro-calcific effects of RANKL, given its previous associations with VC (Panizo *et al.*, 2009), and that TRAIL-mediated vasoprotection may involve blockade of this pathway. Interestingly, NF- κ B activation and oxidative stress are known to intersect, and ROS intermediates have been shown to activate NF- κ B (Bonizzi *et al.*, 1999; Morgan and Liu, 2011). Thus, while RANKL is known to activate NF- κ B directly, RANKL-induced oxidative stress may also promote this effect, and the anti-oxidant role of TRAIL may be responsible for the attenuation of NF- κ B (and ultimately pro-calcific signalling). In further support of this proposition, NAC has been shown to attenuate NF- κ B

and protect from diabetes *in vivo* (Ho *et al.*, 1999), and more specifically, to prevent NF- κ B induced by TNF α (known to exert pro-calcific effects) (Oka *et al.*, 2000). Indeed, the similarities in the effects of TRAIL and this anti-oxidant on RANKL-induced pro-calcific signalling cannot be ignored. Thus, NF- κ B and redox pathways likely exert interlinking functions in the regulation of VC, jointly regulated by RANKL and TRAIL.

5.3.5.6 The Effects of NAC on the Pro-calcific and Pro-oxidant Actions of TNF α

To ensure NAC was exerting the desired anti-oxidant effect on HAECs, TNF α , a known pro-oxidant stimulus, was employed. Given that TNF α is known to activate p47/NOX2 signalling (Kim *et al.*, 2007; Li *et al.*, 2005), it was no surprise that p47/gp91 mRNA expression was elevated following treatment; furthermore, the observed blockade of this upregulation by NAC suggested a successful anti-oxidant effect was achieved. On an additional note, an interesting observation was made regarding the effect of NAC on TNF α -induced pro-calcific indices. In this respect, NAC co-incubation significantly attenuated/reduced all measured pro-calcific indices upregulated by TNF α at both an mRNA and protein level. However, this finding was accompanied by only a slight decrease in non-canonical NF- κ B activation, unlike the complete attenuation observed following RANKL + NAC treatment. As noted, NAC has previously been shown to attenuate NF- κ B signalling, in particular that induced by TNF α (Oka *et al.*, 2000). However, these authors demonstrate NAC-mediated attenuation of the canonical signalling pathway by Western blotting (p50/p65 subunits) and do not attempt to specify the precise effects of NAC on non-canonical activation. As such, this finding may suggest that anti-calcific effects in the vasculature under inflammatory conditions may be mediated primarily via anti-oxidant pathways, rather than attenuation of non-canonical NF- κ B signalling.

5.3.5.7 The Effects of TRAIL on RANKL-induced ROS Generation in HAECs

As a final attempt to clarify the role of oxidative stress in the regulation of VC by RANKL and TRAIL, a functional analysis to quantify ROS generation was employed. Indeed, data presented up to this point supports a pro-oxidant role for RANKL and suggests that TRAIL-mediated vasoprotection may involve anti-oxidant signalling. However, whether this proposed anti-oxidant effect of TRAIL exerts a protective effect on RANKL-induced pro-calcific signalling remains to be confirmed. In this respect, ROS levels (assessed by DHE staining) were quantified/visualised following endothelial exposure to RANKL +/- TRAIL. TNF α +/-

NAC, defined pro-oxidant and anti-oxidant stimuli respectively (Chen *et al.*, 2008; Nedeljkovic *et al.*, 2013), were also incorporated into this experiment as a positive control to ensure the generation/attenuation of ROS could be successfully detected. Furthermore, ROS generation was assessed at both 24 and 72 hours to identify potential time-dependent redox signalling.

Firstly, TNF α was confirmed to induce ROS generation at 24 hours, while NAC addition attenuated this effect. TNF α can induce both mitochondrial and NOX-mediated oxidative stress (Chen *et al.*, 2008), and NAC has been found to attenuate TNF α -mediated ROS generation in ECs (Szotowski *et al.*, 2007). Thus, both the induction and attenuation of ROS were successfully detected, verifying the suitability of the employed methodological approach. While oxidative stress has long been associated with VC (Agharazii *et al.*, 2015; Towler, 2008), no direct evidence yet suggests that ROS is mediated by RANKL in the vasculature. As such, the observed time-dependent induction of endothelial ROS following RANKL treatment is particularly significant. In support of this finding, there is compelling evidence that RANKL-mediated ROS is centrally involved in osteoclastogenesis (Kim *et al.*, 2010; Lee *et al.*, 2005; Thummuri *et al.*, 2017). In a particularly relevant study, Lee and colleagues (2005) demonstrate that RANKL-induced ROS promotes the osteoclastic differentiation of bone marrow monocyte-macrophage lineage cells, and further suggest that this ROS generation is dependent on NADPH oxidases (consistent with our previous finding that RANKL upregulates p47). Moreover, blockade of NOX (and treatment with NAC) both exert similar effects in the attenuation of RANKL-induced osteoclastic function, further implicating NOX signalling in RANKL function as previously hypothesised (Lee *et al.*, 2005).

As discussed in Chapter 1, RANKL is widely known to exert its function via RANK binding and NF- κ B activation in bone and vasculature. Of relevance, an overlap between NF- κ B and ROS signalling in the context of VC has previously been highlighted by Al-Aly and co-workers (2011). Unsurprisingly, these authors propose a pathological role for ROS in the vasculature, emphasising the therapeutic potential for anti-oxidants during VC treatment. Al-Aly *et al.* rely heavily on a study by Zhao and co-workers in this conclusion (2011), who present pertinent evidence that β -glycerophosphate, a potent inducer of calcification, promotes ROS generation in bovine VSMCs alongside canonical NF- κ B activation. Thus, taking this data together, it appears likely that RANKL mediates ROS in the promotion of VC, supporting the data presented and endorsing a role for NF- κ B in this process.

Unlike RANKL, TRAIL had no independent effect on ROS generation in HAECs, and this finding has been confirmed within our own research group by Forde *et al.* (unpublished observations). While there is little research to date attempting to clarify the effects of TRAIL on ROS generation in untransformed cells, contrasting evidence exists in malignant cells. In this respect, TRAIL-induced apoptosis is claimed to be mediated by oxidative stress, with compelling evidence that TRAIL enhances ROS-mediated apoptosis via upregulation of DR4 and DR5 (Jung *et al.*, 2005; Lee *et al.*, 2002; Park *et al.*, 2012; Yodkeeree *et al.*, 2009). As no researchers outside of our own group have yet assessed the effects of TRAIL on primary HAECs, we propose that ROS-induced apoptosis by TRAIL does not progress under healthy, physiological conditions in these cells. As an interesting observation, TRAIL has been shown to induce NOX4 signalling in an *in vivo* murine model; however, unlike NOX1 and NOX2, NOX4 has been associated with a number of protective functions, including the expression of anti-oxidant genes (eNOS, HMOX1) (Schröder *et al.*, 2012), and in one particular study, neovascularisation following ischemic injury (di Bartolo *et al.*, 2015). Thus, the regulation of oxidative stress by TRAIL may not be clear-cut, and instead may involve a complex balance of redox pathways emulating its pleiotropic function.

Following co-treatment, TRAIL significantly reduced RANKL-induced ROS at 72 hours. This novel finding is particularly pertinent given the coinciding attenuation of RANKL-induced pro-calcific signalling and non-canonical NF- κ B activation observed in Chapter 3. Thus, as RANKL/NF- κ B has previously been associated with ROS generation, we present the strongest evidence to date that TRAIL may exert an anti-calcific effect on the vasculature via a reduction in RANKL-induced ROS. In support of this finding, previous studies have revealed that TRAIL may attenuate ROS during VC pathogenesis. Research within our group suggests that TRAIL may significantly reduce both TNF α - and hyperglycemia-induced ROS in HAECs (Forde *et al.*, unpublished observations), well known promoters of VC (Besueille *et al.*, 2015; Chen *et al.*, 2008; Yano *et al.*, 2004). Indeed, TRAIL has also been shown to reduce hyperglycemia-induced ROS in diabetic rats via eNOS/NO signalling (Liu *et al.*, 2014).

5.3.5.8 Summary: Oxidative Stress

Overall, it is clear that both RANKL and TRAIL mediate redox signalling pathways in their role in the endothelium. From this data, it is unlikely that SOD enzymes, in the dismutation of ROS, are responsible for these effects, but the upregulation of pro-oxidant (NOX) and anti-oxidant (eNOS, HMOX1) genes by RANKL and TRAIL respectively may contribute to these effects. Furthermore, NAC was found to attenuate RANKL-induced pro-calcific signalling and non-canonical NF- κ B activation, supporting an anti-oxidant role of TRAIL in the mediation of RANKL-induced VC and revealing a potential mechanism by which TRAIL blocks the pro-calcific effects of RANKL. Finally, TRAIL co-incubation reduced RANKL-induced ROS, confirming a functional anti-oxidant effect on the endothelium. It is therefore our assertion that TRAIL regulates anti-oxidant genes in the endothelium, attenuating NF- κ B activation and pro-calcific signalling induced by RANKL, and ultimately preventing the progression of VC.

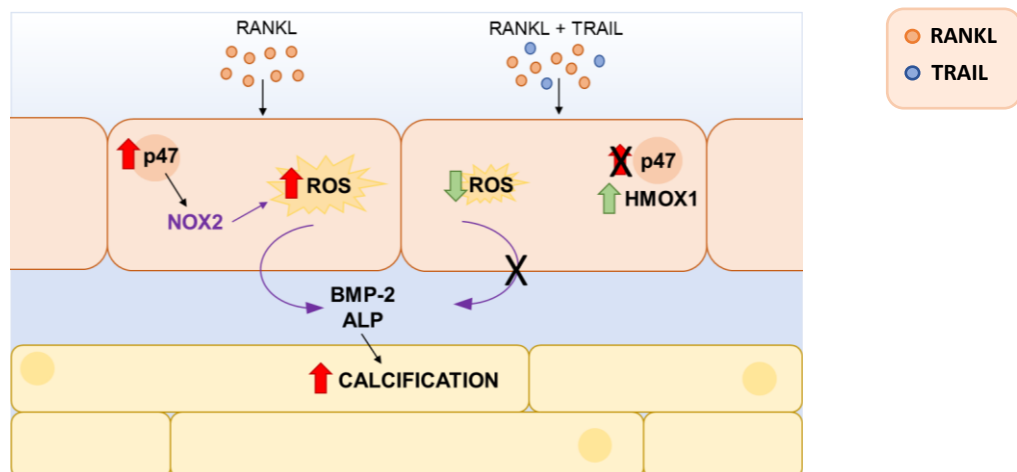


Figure 5.11. Representation of the key findings of redox investigations. Endothelial cell (upper layer) exposure to RANKL induces p47 mRNA expression, and may also promote NADPH oxidase 2 (NOX2) generation of reactive oxygen species (ROS). ROS may also contribute to the induction of endothelial pro-calcific paracrine signalling (e.g., BMP-2, ALP) to the underlying smooth muscle (bottom layer), thereby promoting calcification. Co-incubation with TRAIL attenuates RANKL-induced p47 and upregulates the anti-oxidant HMOX1, and therefore may also reduce NOX2 generation of ROS. The anti-oxidant influence of TRAIL may also attenuate pro-calcific paracrine signalling, thereby protecting from calcification. Purple text, hypothesised event: remains to be shown experimentally.

5.4 Investigating the Role of Non-canonical NF- κ B Activation in HAECs

Finally, the non-canonical NF- κ B pathway was investigated to further delineate its role in pro-calcific signalling. As noted, RANKL is known to activate NF- κ B via the RANK receptor, and the non-canonical pathway has previously been implicated in smooth muscle calcification (Beristain *et al.*, 2012; Boyce *et al.*, 2015; Panizo *et al.*, 2009). Furthermore, endothelial non-canonical NF- κ B signalling has been associated with the pro-calcific effects of RANKL in Chapters 3 and 4, while the co-addition of TRAIL attenuated RANKL-induced non-canonical activation. This follow-on study now aims to fully clarify the RANKL/TRAIL-mediated signalling processes that can be attributed to *non-canonical* NF- κ B during VC. In this regard, HAECs were subject to siRNA knockdown of the NF κ B2 gene, which encodes the p52 precursor protein, p100, and is therefore an effective method of attenuating the non-canonical NF- κ B pathway. Following optimisation, HAECs were co-cultured with HASMCs in the presence of RANKL (Figure 5.12), and a range of pro-calcific indices monitored. Moreover, given the inter-related roles for oxidative stress and pro-calcific signalling identified in Sections 5.2 and 5.3, representative pro/anti-oxidant targets were also assessed in HAECs.

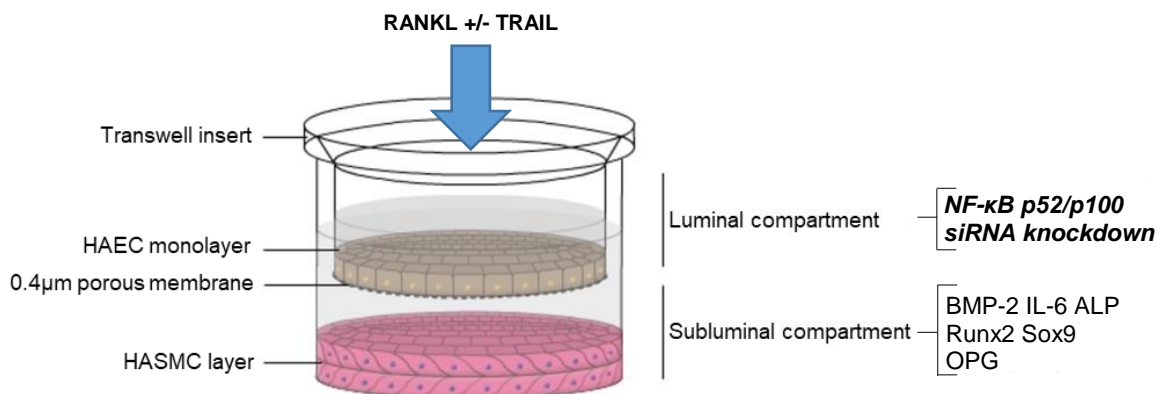


Figure 5.12. Representation of the transwell co-culture model employed following endothelial NF- κ B p52/p100 knockdown. HAECs in semi-permeable transwell inserts were subject to NF κ B2 siRNA knockdown for 48 hours, prior to suspension above the confluent smooth muscle layer. HAECs in the luminal compartment were exposed to RANKL (5-25 ng/mL) for 72 hours prior to analysis of smooth muscle pro-calcific indices. Image adapted from Harper *et al.*, 2017.

5.4.1 Optimisation of siRNA Knockdown

Firstly, to ensure valid results, an in-depth optimisation process was developed prior to co-culture analyses. To assess reagent toxicity and ensure robust gene knockdown, HAECs were

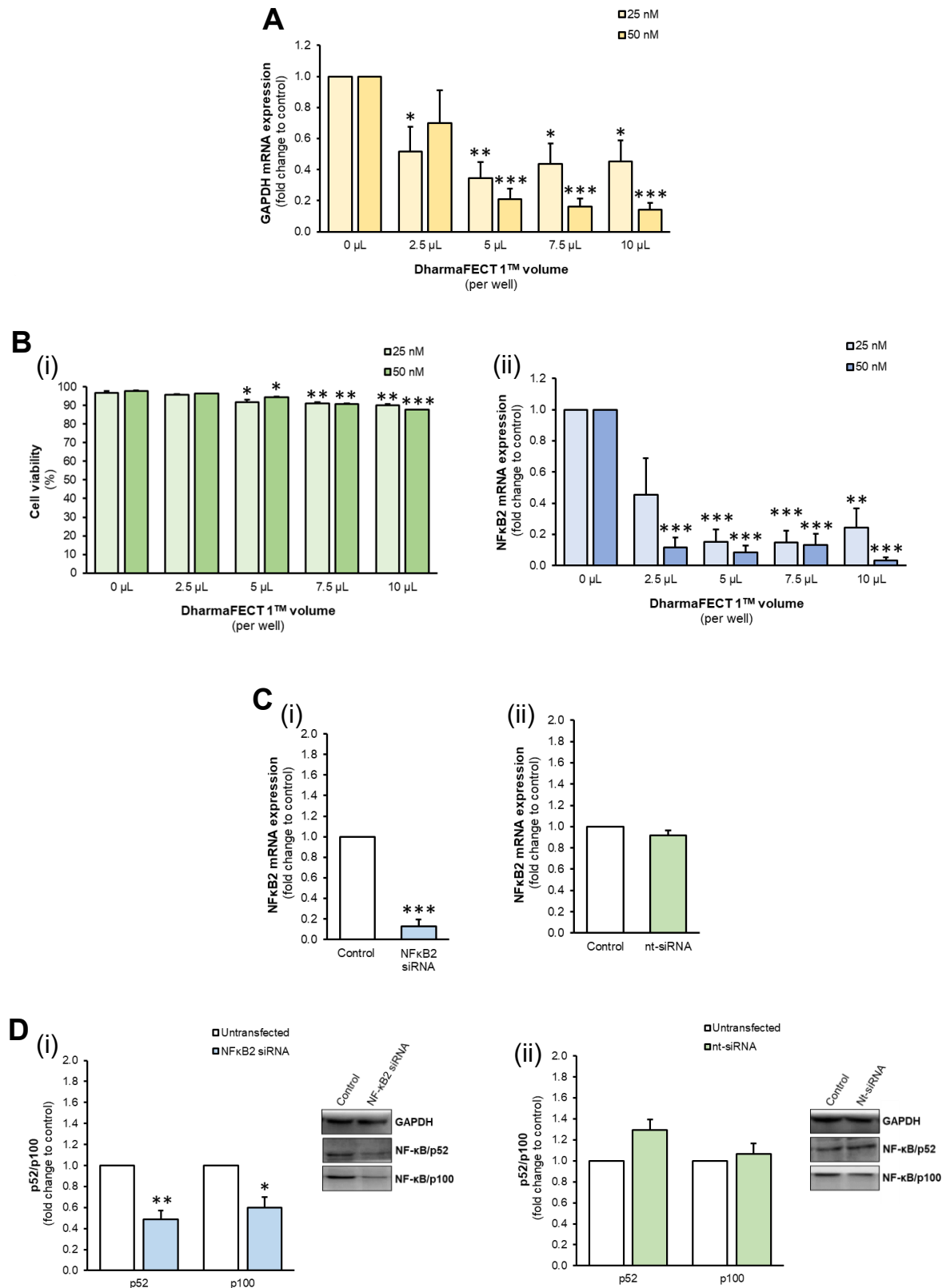


Figure 5.13. Optimisation of NF- κ B2 siRNA knockdown. (A) HAECs were subject to GAPDH knockdown for 48 hours across a range of DharmaFECT™ volumes and siRNA concentrations; GAPDH expression levels were determined by RT-qPCR, employing 18S as an endogenous control. (B) HAECs were subject to NF κ B2 siRNA knockdown across a range of DharmaFECT™ volumes and siRNA concentrations; (i) viability was assessed by ADAM™ counter and (ii) NF κ B2 mRNA expression levels were determined by RT-qPCR, employing 18S as an endogenous control. (C) HAEC NF κ B2 mRNA expression was similarly assessed following (i) NF κ B2 and (ii) non-targetting siRNA knockdown for 48 hours in transwell inserts. (D) NF- κ B p52/p100 protein expression was assessed by Western blotting following 72 hours' knockdown with (i) NF κ B2 and (ii) non-targetting siRNA in transwell inserts. Protein expression was quantified by scanning densitometry and normalised to GAPDH. Blots are representative. * $p < 0.05$; ** $p < 0.01$; *** $p < 0.001$ compared to untreated control.

subject to pre-validated GAPDH siRNA knockdown across concentration and reagent volume ranges (25-50 nM; 2.5-10 μ L DharmaFECT™ per well) as recommended by the manufacturer. A concentration of 50 nM siRNA achieved optimal GAPDH gene knockdown after 48 hours when combined with higher volume of DharmaFECT™ reagent (Figure 5.13A); HAEC viability was maintained above 85% in all cases (data not shown). Following successful siRNA silencing of a pre-validated target, DharmaFECT™ reagents were deemed suitable for gene knockdown in primary HAECs. With regard to NF κ B2 knockdown, the same range of siRNA concentrations and reagent volumes were assessed. Again, a combination of 50 nM siRNA + 10 μ L DharmaFECT™ was deemed optimal, with viability maintained above 89% (Figure 5.13B). NF κ B2 knockdown efficiency was also comparable in transwell inserts, while scrambled non-targeting siRNA (nt-siRNA) had no effect on NF κ B2 expression under the same conditions, confirming target specificity (Figure 5.13C). At a protein level, approximately 45-48% knockdown of p52 and its precursor p100 was achieved following NF κ B2 knockdown, while scrambled nt-siRNA had no significant effects on p52/p100 protein expression (Figure 5.13D).

5.4.2 The Effects of NF- κ B/p52 Knockdown on Pro-Calcific Indices in HAECs

Following endothelial NF κ B2 knockdown in transwell inserts, no significant effects were noted in BMP-2, ALP or Runx2 mRNA levels, however, IL-6 transcript expression was significantly upregulated (data not shown). NF κ B2 silencing did not affect BMP-2, ALP or OPG release, but significantly reduced IL-6 levels in the conditioned media (Appendix 5.7A (i)). Intracellularly, NF κ B2 siRNA knockdown in HAECs significantly decreased BMP-2 production by approximately 70%, but had no effect on ALP activity (Appendix 5.7B (i)). Furthermore, NF κ B2 knockdown had no effect on OPG release or protein expression in HAECs (data not shown), nor did it affect activation of the canonical NF- κ B pathway (Appendix 5.7C (i)). Following scrambled nt-siRNA treatment, no effects were noted at an mRNA expression level for any of the measured indices (data not shown). The endothelial release profile also remained unaffected (Appendix 5.7A (ii)); nt-siRNA treatment, however, slightly but significantly induced intracellular ALP activity (Appendix 5.7B (ii)). Again, no effects were noted in OPG production/release (data not shown) or canonical NF- κ B activation (Appendix 5.7C (ii)) following nt-siRNA treatment.

5.4.3 The Effects of NF- κ B/p52 Knockdown on Pro-Calcific Indices in Co-culture

Following siRNA knockdown in transwell inserts, HAECs were co-cultured with HASMCs for a further 72 hours in the presence and absence of RANKL (5-25 ng/mL) before assessing a range of pro-calcific indices in the underlying HASMCs. Prior to analysis, it was confirmed that endothelial treatment with nt-siRNA had no effect on the measured indices in HASMCs, apart from a slight increase in IL-6 release (data not shown). At an mRNA level, the previously identified upregulation of ALP/Sox9 in co-cultured HASMCs following endothelial RANKL treatment were completely attenuated by NF κ B2 knockdown; furthermore, Sox9 mRNA levels were reduced to below baseline (Figure 5.14A). Runx2 mRNA levels were slightly but significantly downregulated in co-cultured HASMCs following NF κ B2 knockdown in HAECs, while the RANKL-induced downregulation of OPG/IL-6 mRNA were completely recovered.

Regarding protein release, RANKL-induced BMP-2 secretion into the subluminal space was completely attenuated following HAEC NF κ B2 knockdown, and extracellular ALP activity (induced by 25 ng/mL RANKL) was significantly reduced (Figure 5.14B (i), (ii)). Interestingly, OPG secretion was induced following NF κ B2 silencing in HAECs, while RANKL treatment dose-dependently decreased this release (Figure 5.14B (iii)). NF κ B2 knockdown did not affect RANKL-induced IL-6 secretion (Appendix 5.8B). Intracellularly, RANKL-induced OPG production was reduced following knockdown of endothelial NF κ B2 (Appendix 5.8C), as was RANKL-induced ALP activity, at the higher concentration of 25 ng/mL (Figure 5.14C).

5.4.4 The Effects of NF- κ B/p52 Knockdown on Pro/Anti-Oxidant Indices in HAECs

Finally, the effects of endothelial NF κ B2 knockdown on pro- and anti-calcific indices were assessed, namely SOD1/2, gp91, p47, eNOS and HMOX1, in the endothelial monolayer following RANKL exposure. In this respect, neither mock-transfected (nt-siRNA) nor NF κ B2-silenced HAECs responded differently in the mRNA expression of these genes than that previously observed in response to RANKL (data not shown). SOD2 protein remained undetectable, while HAECs treated with nt-siRNA exerted the same increase in SOD1 protein expression as previously reported. Interestingly, following NF κ B2 gene silencing, SOD1 protein expression was upregulated to the same extent in both untreated and RANKL-treated HAECs (data not shown).

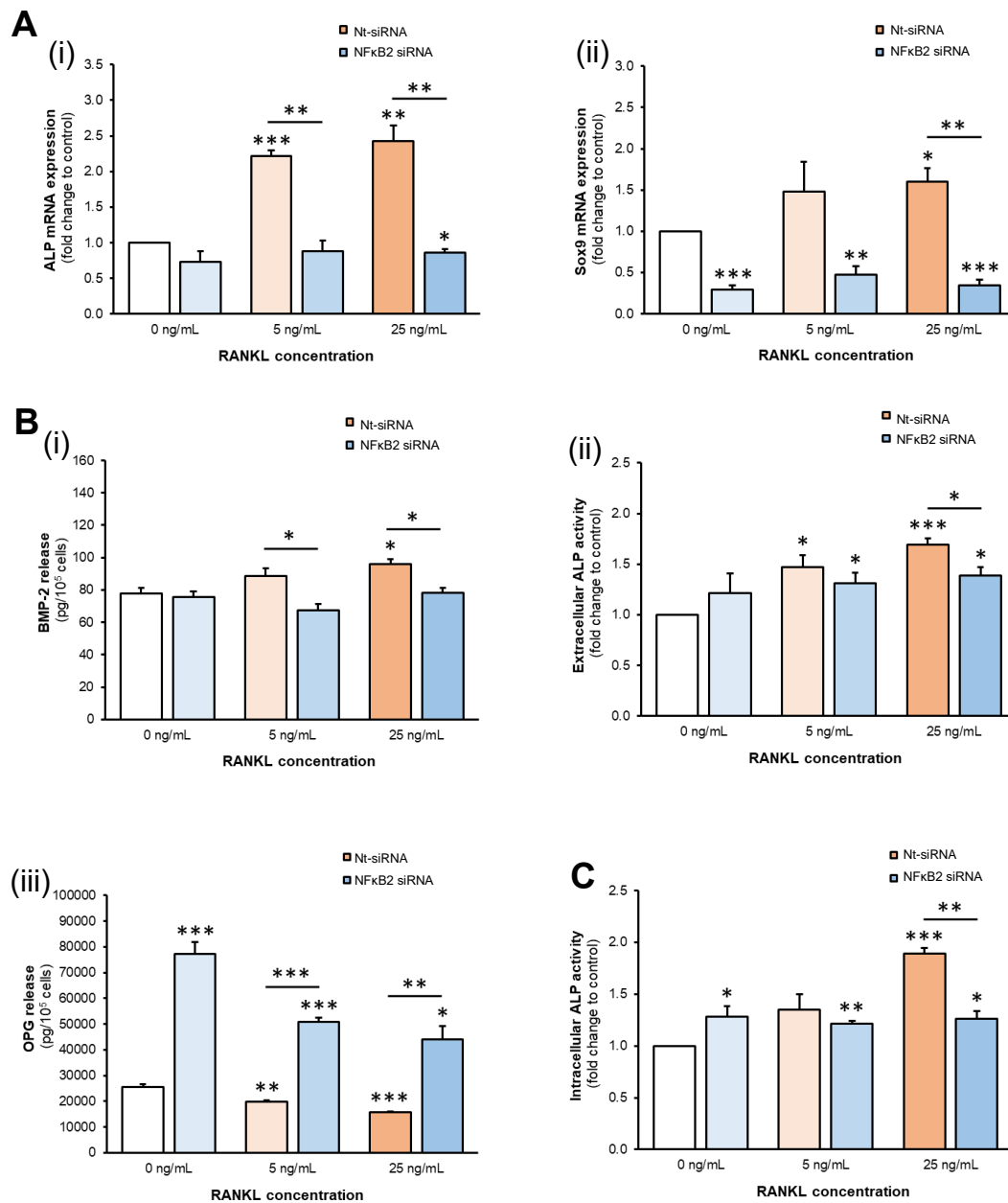


Figure 5.14. The effects of RANKL following endothelial siRNA knockdown in co-cultured HASMCs. HAECs were subject to nt-siRNA/NFκB2 knockdown in transwell inserts for 48 hours, prior to co-culture with confluent HASMCs. HAECs in the luminal compartment were then treated with RANKL (5-25 ng/mL) for 72 hours prior to analysis of protein/mRNA responses in the underlying HASMCs. **(A)** (i) ALP and (ii) Sox9 mRNA expression levels were determined by RT-qPCR, employing GAPDH as an endogenous control. **(B)** (i) BMP-2, (ii) ALP and (iii) OPG release in the subluminal space, alongside **(C)** intracellular ALP activity, were assessed by ELISA and enzyme assay where appropriate; media and lysate analysis were normalised to 10⁵ cells and total protein respectively. * $p < 0.05$; ** $p < 0.01$; *** $p < 0.001$ compared to untreated control unless otherwise stated; bars indicate statistical significance between treatment groups.

5.4.5 Discussion: Non-canonical NF- κ B Activation

To reiterate, RANKL is known to exert its osteoclastic functions in bone via NF- κ B signalling (Beristain *et al.*, 2012; Boyce *et al.*, 2015), and has been shown to induce pro-calcific effects in VSMCs both directly via NF- κ B activation (Panizo *et al.*, 2009) and indirectly via endothelial paracrine signalling (Davenport *et al.*, 2016; Osako *et al.*, 2010). In Chapter 3, we identified the non-canonical NF- κ B pathway in particular as a potential mediator of RANKL-induced pro-calcific effects, in agreement with Panizo *et al.* (2009), who have previously associated this pathway with VC progression in smooth muscle. Furthermore, we noted that TRAIL co-incubation could attenuate non-canonical signalling alongside blockade of endothelial paracrine signalling. Indeed, the protective influence of TRAIL in the vasculature has been noted previously (di Bartolo *et al.*, 2013), while TRAIL has been shown to interfere with RANKL signalling in bone (Zauli *et al.*, 2004; Zauli *et al.*, 2008). Despite this evidence, no studies to date have associated RANKL/TRAIL signalling with non-canonical NF- κ B activation in the endothelium, or assessed the implications of this in the pathogenesis of VC.

Furthermore, evidence suggests an anti-oxidant role for TRAIL in HAECs *in vitro* (Forde *et al.*, unpublished observations), a consideration thoroughly explored in Section 5.3. However, while TRAIL reduces RANKL-induced ROS generation, it does not completely attenuate it, unlike the complete blockade of pro-calcific signalling/non-canonical NF- κ B observed in Chapter 3; thus, TRAIL-mediated protection cannot be wholly attributed to the regulation of ROS. Interestingly, redox signalling and NF- κ B activation are known to reciprocally intersect (Morgan and Liu, 2011), and Zhao and colleagues have presented pertinent evidence describing the dual activation of ROS and NF- κ B following VC induction (2011). Indeed, we have observed that the anti-oxidant NAC can attenuate pro-calcific signalling and non-canonical NF- κ B, suggesting that the proposed anti-oxidant nature of TRAIL may be responsible for the attenuation of non-canonical signalling. Thus, we aimed to determine the importance of non-canonical signalling in RANKL/TRAIL-mediated VC, delineating if this pathway is central to the regulation of VC or merely a side-effect of redox signalling.

In this respect, the NF κ B2 gene was subject to siRNA silencing in co-cultured HAECs. NF κ B2 codes for the p100 fragment, and thus the cleaved p52 product, ultimately involved in nuclear translocation during non-canonical activation. A range of pro-calcific/pro-oxidant indices were assessed in HAECs and HASMCs following treatment with RANKL in co-culture, in an effort to determine the significance of non-canonical NF- κ B activation during VC pathogenesis.

5.4.5.1 The Effects of NF- κ B/p52 Knockdown on the Expression of Pro-Calcific Indices

Firstly, comprehensive control studies confirmed the employed siRNA pool was specific for the NF κ B2 gene, and knockdown did not exert adverse effects on transfected HAECs or on co-cultured HASMCs. Firstly, NF- κ B/p52 knockdown was found to significantly reduce endothelial BMP-2 production, further implicating this pathway in the regulation of BMPs as first suggested by Panizo *et al.* (2009). Importantly, NF κ B2 silencing had no effect on total or phosphorylated levels of p65, thus ruling out off-target effects. By way of knockdown efficiency, close to 90% and 50% NF κ B2 gene silencing and p52/p100 protein knockdown, respectively, were achieved, alongside minimal effects on cell viability. Indeed, recent studies have successfully achieved knockdown of NF- κ B pathways in various cell types (including vascular cells), achieving comparable levels of knockdown to that observed in this case (Hénaut *et al.*, 2016; Patel *et al.*, 2017; Wang *et al.*, 2016). Given the complex nature of NF- κ B signalling, and its role in many physiological processes including cell survival (Papa *et al.*, 2004), it was of major concern that complete p52/p100 knockdown may inadvertently exert pathological effects on HAECs. As such, the protein knockdown efficiency achieved was considered acceptable for the purpose of assessing the resulting influence on pro-calcific indices.

Following mock transfection (scrambled, nt-siRNA) and NF κ B2 silencing, HAECs in co-culture were exposed to RANKL (5-25 ng/mL) for 72 hours. A range of pro-calcific indices in both the subluminal space and the underlying HASMCs were assessed to determine the contribution of endothelial non-canonical activation in the progression of VC. As observed and discussed in Chapter 3, RANKL treatment of mock-transfected HAECs in co-culture led to pro-calcific effects in both the subluminal space (increased ALP, BMP-2 release) and in the underlying HASMCs (increased ALP, Sox9 mRNA, ALP activity, decreased OPG mRNA/release). Following NF κ B2 silencing, however, RANKL treatment of transfected HAECs in co-culture had a much less potent pro-calcific influence on the underlying HASMCs, with many of the aforementioned effects completely attenuated.

Firstly, the attenuation of BMP-2 release and the decrease in extracellular ALP activity is of particular relevance to this study. As noted, BMP-4 regulation has previously been associated with non-canonical activation in VSMCs (Panizo *et al.*, 2009), but to date, no studies have specifically associated BMP-2 release with this pathway. While extracellular ALP is not completely attenuated, it must be considered that only ~50% p52/p100 protein knockdown was

achieved, and smooth muscle ALP release also likely contributes to this trend; indeed, a similar trend in ALP activity was observed in the underlying HASMCs. Therefore, non-canonical NF- κ B activation may be responsible for BMP-2/ALP endothelial paracrine signalling, and in turn the regulation of smooth muscle ALP, ultimately contributing to smooth muscle calcification.

In the underlying HASMCs, the attenuation of RANKL-induced ALP and Sox9 mRNA, alongside a reduction in Runx2 mRNA, suggests that endothelial NF- κ B signalling (and paracrine communication) is required for smooth muscle pro-calcific gene expression. In fact, both Runx2 and Sox9, osteoblastic and chondroblastic transcription factors respectively, are responsible for the regulation of a wide range of genes during VC (including ALP) (Akiyama, 2008; Fujita *et al.*, 2004), and in the absence of endothelial NF κ B2 are now reduced to below baseline. Interestingly, Runx2 and Sox9 transcription factors have been shown to mediate BMP-2-induced gene expression (Jang *et al.*, 2012; Pan *et al.*, 2008), and thus the observed attenuation of BMP-2 paracrine signalling may be responsible for this observation.

It is also apparent that non-canonical NF- κ B activation influences vascular OPG regulation, and in particular is involved in RANKL-mediated regulation of its own decoy receptor. In this regard, NF- κ B mediates the RANKL-induced downregulation of smooth muscle OPG mRNA, and the accumulation of intracellular OPG. Interestingly, OPG release was significantly induced following NF κ B2 silencing, however this did not affect the RANKL-mediated reduction in OPG; As such, this OPG release may represent the previously hypothesised cardioprotective response to vascular stress, rather than a RANKL/NF κ B2-dependent mechanism involving ALP/BMP-2 signalling.

As discussed in our publication of this study (Harper *et al.*, 2018), there is minimal data to which we can compare these findings outside of our own results. Indeed, it was suggested in Chapter 3 that pro-calcific events may be mediated by non-canonical rather than canonical NF- κ B activation in endothelial cells, as the calcification inducer β -glycerophosphate was only found to activate the former pathway. Furthermore, the aforementioned study by Panizo *et al.* (2009), central to our hypothesis, has implicated this pathway in BMP signalling in VSMCs, while Zhan and colleagues (2014) have observed the attenuation of VC via blockade of RANKL/NF- κ B (but not specifically non-canonical signalling) by GLP-1RA treatment. Of further note, NF- κ B has also been considered a potential therapeutic target in the management of diabetic microvascular complications (Suryavanashi *et al.*, 2017), but again neither canonical nor non-canonical signalling pathways are favoured in this suggestion. In endothelial

cells, the role of NF- κ B (but not specifically non-canonical signalling) in the regulation of paracrine signalling has been previously noted. In this respect, the knockdown of canonical NF- κ B in ECs has consequences for VSMC proliferation (Patel *et al.*, 2017), further highlighting the importance of NF- κ B for vascular paracrine communication. In this study, we now present novel evidence that endothelial non-canonical NF- κ B signalling is required for pro-calcific paracrine communication in VSMCs, thereby playing a central role in the pathogenesis of medial VC.

5.4.5.2 The Effects of NF- κ B/p52 Knockdown on Anti-oxidant Expression

Finally, the effects of non-canonical NF- κ B knockdown on oxidative stress indices were assessed in order to determine if this pathway mediates redox pathways in ECs. In this respect, the previous section has clarified that non-canonical NF- κ B is responsible for pro-calcific paracrine signalling, but it has also been observed that RANKL and TRAIL mediate endothelial oxidative stress. The bi-directional relationship between NF- κ B and redox signalling is complex; ROS can induce NF- κ B, and the resulting upregulated genes can then reciprocally regulate ROS (Morgan and Liu, 2011). Indeed, several processes that mediate oxidative stress also regulate NF- κ B (including pro-inflammatory cytokines) (Brand *et al.*, 1996). Furthermore, NF- κ B can exert both pro- and anti-oxidant effects, and is known to mediate NOX (Anrather *et al.*, 2006) as well as SODs/HMOX1 (Djavaheri-Mergny *et al.*, 2004; Lavrovsky *et al.*, 1994; Rojo *et al.*, 2004), potent pro- and anti-oxidant genes respectively. Moreover, TRACP5, identified in Section 5.2 as a potential regulator of VC, is also known to induce oxidative stress (Halleen *et al.*, 1999). Thus, the inter-regulation between endothelial non-canonical NF- κ B and oxidative stress during VC requires clarification.

To reiterate, a key aim of this Chapter is to delineate the mechanism(s) by which TRAIL exerts its protective function in the vasculature, identified in Chapter 3. The majority of evidence presented in this chapter points to a role for redox pathways in the regulation of non-canonical NF- κ B (i.e., the anti-oxidant NAC was found to attenuate non-canonical activation). Thus, we propose that TRAIL may exert anti-calcific effects in the endothelium via anti-oxidant signalling, blocking non-canonical NF- κ B activation and ultimately pro-calcific paracrine signalling. As such, this investigation serves to confirm the hypothesis that redox pathways mediate NF- κ B in the promotion of VC, rather than vice-versa. In this case, a range of pro-oxidant and anti-oxidant genes were assessed in endothelial cells following NF κ B2 silencing

and RANKL exposure. Compared to mock-transfected cells, no changes were noted at an mRNA level in any of the measured oxidative stress indices in HAECs following NF κ B2 knockdown. RANKL exposure exerted the same trends on these indices (SOD1, SOD2, gp91, p47, eNOS, HMOX1) as previously identified in Section 5.3, thus remaining unaffected by NF κ B2 silencing. This finding therefore confirms that RANKL-induced non-canonical NF- κ B activation induces pro-calcific signalling in HAECs, but does not regulate the measured redox genes (which remained unaffected by NF κ B2 knockdown).

Overall, therefore, while non-canonical NF- κ B is required for endothelial pro-calcific paracrine signalling, it is not required for RANKL-mediated oxidative stress. Indeed, the stimulus that causes NF- κ B to regulate redox genes appears to be cell-specific, and relies on a number of environmental factors (Morgan and Liu, 2011; Perkins *et al.*, 2006). What we can conclude from this study is that RANKL-induced pro-calcific signalling is reliant on non-canonical NF- κ B activation, and the concurrent induction of oxidative stress is not mediated by this pathway. However, TRAIL-mediated anti-oxidant signalling can attenuate non-canonical NF- κ B, implicating a role for oxidative stress upstream of NF- κ B in the modulation of VC.

5.5 Summary and Conclusions

While RANKL is known to exert its osteoclastic function via NF- κ B signalling, its mechanism in the vasculature remains largely unclarified. This statement is even more true for TRAIL, known to activate multiple pathways in its pleiotropic functions *in vivo*, none of which have yet been experimentally associated with its protective role in the vasculature. Research from Chapter 3 suggests that RANKL may exert its pro-calcific function via non-canonical NF- κ B activation, subsequently blocked by TRAIL; however, it has also been suggested that RANKL and TRAIL can exert pro-oxidant and anti-oxidant effects respectively. In this study, the regulation of non-canonical NF- κ B/redox signalling by RANKL/TRAIL in the vasculature were clarified, and potential novel targets that may be involved in RANKL/TRAIL function were investigated.

Firstly, TRACP5, a protein with a central role in osteoclastogenesis, was identified as a potential contributor to VC pathogenesis. Our data provides strong evidence that TRACP5 is mediated by RANKL/TRAIL in the vasculature, and therefore may be pertinent in delineating the mechanisms underlying VC. Of additional note, TRACP5 is also known to exert pro-oxidant effects, known to drive VC, thereby further supporting a role for RANKL and TRAIL in vascular redox signalling.

Following analysis of a number of oxidative stress targets, the proposed pro-oxidant and anti-oxidant roles for RANKL and TRAIL respectively were confirmed, with RANKL upregulating the p47 subunit of NADPH oxidase, and TRAIL promoting HMOX1 expression. Furthermore, the TRAIL-dependent promotion of eNOS expression in the presence of RANKL, and the simultaneous reduction in RANKL-induced ROS further supports an anti-oxidant role for TRAIL in the mediation of VC.

Finally, the anti-oxidant NAC was also found to attenuate RANKL-induced pro-calcific signalling alongside non-canonical NF- κ B activation, emulating the effects of TRAIL observed in Chapter 3 and supporting a role for oxidative stress in the regulation of pro-calcific non-canonical NF- κ B signalling. Indeed, following siRNA silencing of the NF κ B2 gene, it was confirmed that the non-canonical NF- κ B pathway in endothelial cells is responsible for EC:VSMC pro-calcific paracrine communication. Thus, we can conclude that TRAIL may also exert its protective effects on the endothelium via attenuation of RANKL-induced non-canonical NF- κ B activation. In this way, we shed additional light on the mechanisms of

RANKL and TRAIL-mediated pro-calcific and protective effects during VC, respectively, highlighting a role for both redox signalling and NF- κ B activation in this process.

Chapter 6

Final Summary

6.1 Final Summary

Recent evidence now points to a role for RANKL, TRAIL and their common decoy receptor OPG in VC pathogenesis, a major cause of cardiovascular morbidity and mortality among type-2 diabetics. The primary role for RANKL *in vivo* is in the promotion of bone resorption, while for TRAIL it is the induction of apoptosis (Kim *et al.*, 2004; Wada *et al.*, 2006). In the vasculature, however, these ligands appear to exert the opposite effect, with RANKL driving calcification (a process analogous to bone *formation*), and TRAIL exerting a *cardioprotective* effect in the vasculature by preventing VC. Despite this evidence, however, the precise signalling pathways and mechanisms exerting the effects of RANKL and TRAIL in a vascular setting remain largely undefined within the scientific literature. Of interest, much evidence now highlights the therapeutic potential for TRAIL in preventing or regressing VC *in vivo* (di Bartolo *et al.*, 2013). As such, if the precise molecular events and mechanisms underpinning the VC process (and TRAIL protection in particular) can be defined, this may aid in the development of a novel treatment to ultimately reduce the morbidity and mortality associated with CVD/T2DM worldwide.

Interestingly, recent research has identified a pro-calcific role for RANKL both directly in VSMCs (Panizo *et al.*, 2009) and via endothelial paracrine signalling, promoting calcification in the underlying smooth muscle layer (Davenport *et al.*, 2016; Osako *et al.*, 2010). Furthermore, previous limited studies have indicated that TRAIL may have the ability to attenuate RANKL's effects in osteoclastogenesis (Zauli *et al.*, 2004; Zauli *et al.*, 2008). Therefore, we hypothesised that *TRAIL may exert its protective effects in the vasculature via attenuation of RANKL-induced pro-calcific signalling* (Study 1). The key findings from Study 1 are summarised in Section 6.1.1. Secondly, we noted that the vast majority of studies to date regarding the role of RANKL and TRAIL in the vasculature have been carried out in “healthy”, non-pathological models *in vitro*. In reality, however, VC progresses alongside known pathological stimuli such as hyperglycemia (a key circulatory hallmark of T2DM) and inflammation (present during atherosclerosis) (McCullough *et al.*, 2008). Thus, we investigated the effects of RANKL and TRAIL (separately) on the vasculature in the presence of these pathological stimuli, to determine if these ligands retained their respective pro-calcific and protective effects under these conditions. In this respect, we hypothesised that *RANKL may promote, and TRAIL may prevent, pro-calcific events induced by inflammation/hyperglycemia* (Study 2). The key findings from Study 2 are summarised in Section 6.1.2.

Although the mechanisms underpinning RANKL-induced osteoclastogenesis and TRAIL-mediated apoptosis are well defined, the precise signalling pathways activated by these ligands in the vasculature remain unclear. Interestingly, both NF- κ B signalling and oxidative stress have been implicated in the pathogenesis of VC, rendering these pathways of particular interest (Byon *et al.*, 2008; Zhao *et al.*, 2012). Indeed, it is known that RANKL activates NF- κ B signalling in the vasculature, but (as RANKL is one of few ligands known to activate the non-canonical NF- κ B pathway), it has not yet been clarified *which* NF- κ B pathway is responsible for RANKL-mediated pro-calcific effects. Furthermore, an anti-oxidant role for TRAIL in the vasculature has been proposed (Zauli *et al.*, 2003), but whether or not this pathway exerts an anti-calcific effect on the vasculature remains to be determined. As such, we chose to further investigate these pathways *in vitro*, with a hypothesis that *RANKL and TRAIL may mediate their respective pro-calcific and anti-calcific effects (at least in part) via NF- κ B signalling and/or oxidative stress* (Study 3). We also considered and assessed additional contributors to the VC process, not yet identified to date, in an effort to shed additional light on VC from a mechanistic perspective. The key findings from Study 3 are summarised in Section 6.1.3.

To examine these hypotheses, primary human endothelial and smooth muscle cells were assessed both in monoculture and co-culture. The employed co-culture model more closely resembles the structure of the vasculature, incorporating endothelial paracrine communication (the cells in contact with circulating proteins *in vivo*) to the underlying smooth muscle layer (the location of medial VC *in vivo*). Furthermore, the widest range of VC-related indices to date were assessed, and a number of common confounders employed in the literature were eliminated (Davenport *et al.*, 2016; Olesen *et al.*, 2012). In this respect, these studies comprise the most physiologically relevant and comprehensive investigation of its nature to date, providing valuable insight into the molecular processes and signalling pathways driving the VC process, and aiding our understanding of this complex pathology.

6.1.1 Study 1: Key Findings

In study 1, we investigated the hypothesis that TRAIL may attenuate RANKL-induced pro-calcific signalling in the vasculature. In endothelial cell monoculture, it was found that RANKL induced both BMP-2 and ALP paracrine signalling, previously observed by Davenport *et al.* (2016). We further highlighted an increase in both intracellular BMP-2/ALP. Most pertinently, *co-incubation with TRAIL completely attenuated endothelial BMP-2/ALP release, alongside intracellular ALP activity*, highlighting a protective role for this ligand in the attenuation of

RANKL-mediated pro-calcific signalling. Interestingly, RANKL also induced both canonical and non-canonical NF- κ B activation in endothelial cells, while *TRAIL completely attenuated RANKL-induced non-canonical signalling*, potentially implicating this pathway as the mechanism by which RANKL exerts its pro-calcific effects in the vasculature. In smooth muscle cell monoculture, RANKL was found to exert *direct* pro-calcific effects via the induction of ALP release, osteoblastic Runx2 mRNA expression, and decreasing cardioprotective OPG release. Minimal protective effects of TRAIL were noted in smooth muscle cells, however, indicating that *TRAIL may only exert its protective effects via endothelial paracrine signalling*, and not at the level of the underlying VSMCs.

In co-culture models, endothelial exposure to RANKL induced a number of pro-calcific effects in the underlying smooth muscle cells. In this respect, RANKL promoted the expression of ALP and Sox9 mRNA, whilst decreasing OPG mRNA. *All three transcriptional changes, however, were attenuated by TRAIL co-treatment, as was RANKL-induced intracellular ALP activity*. Once again, co-exposure with TRAIL completely attenuated RANKL-induced BMP-2/ALP paracrine signalling, suggesting that *the observed effects of RANKL and TRAIL in smooth muscle are primarily mediated by endothelial communication*. Of additional interest, RANKL was found to induce smooth muscle OPG release in co-culture, despite a decrease being observed in smooth muscle monoculture. This finding may suggest that, in areas of intact (healthy) endothelium, the vasculature exerts a natural cardioprotective mechanism to protect from RANKL-induced calcification, while in areas of damaged or dysfunctional endothelium (for example, atherosclerotic plaque) OPG levels are reduced, rendering the vessel susceptible to further damage. Furthermore, RANKL appears to induce Runx2 osteoblastic transcription factor when in *direct* contact with VSMCs, while upregulating Sox9 chondrogenic transcription factor expression via endothelial signalling; thus, we propose that RANKL may drive both osteoblastic and chondrocytic differentiation, determined by the integrity of the endothelium. Overall, however, *we highlight for the first time the pro-calcific effects of RANKL-mediated endothelial paracrine signalling on underlying VSMCs, and the ability of TRAIL to attenuate RANKL-induced calcification in a vascular setting*.

6.1.2 Study 2: Key Findings

In study 2, we investigated the role of RANKL and TRAIL under pathological conditions (inflammation, hyperglycemia) common during T2DM. In both mono- and co-culture, as expected, the employed pathological stimuli (TNF α , glucose) were found to induce a wide

range of pro-calcific effects on endothelial and smooth muscle cells. In endothelial cell monoculture, RANKL was found to further promote TNF α -induced BMP-2 release and (non-significantly) extracellular ALP; moreover, these effects were exerted alongside an increase in non-canonical NF- κ B activation, potentially implicating this pathway in the regulation of TNF α -mediated pro-calcific signalling. In smooth muscle cells, RANKL exerted minimal effects on TNF α -induced pro-calcific signalling, but again endothelial BMP-2/ALP paracrine signalling was promoted by RANKL in co-culture, alongside intracellular smooth muscle ALP activity. With regard to TRAIL, non-canonical NF- κ B activation was significantly attenuated in the endothelial layer under inflammatory conditions, and TRAIL co-treatment was also found to significantly reduce TNF α -induced BMP-2/ALP release and intracellular BMP-2 in co-culture. Thus, *RANKL and TRAIL (respectively) promote and prevent TNF α -induced endothelial BMP-2/ALP release and non-canonical NF- κ B activation*, highlighting a role for these ligands in paracrine communication under inflammatory conditions, and further implicating NF- κ B signalling in VC pathogenesis.

Under hyperglycemic conditions, RANKL further promoted endothelial BMP-2 release and (non-significantly) ALP activity, while also upregulating Runx2 mRNA expression. In HASMC monoculture, RANKL exerted minimal pro-calcific effects, but in co-culture, RANKL again promoted glucose-induced BMP-2/ALP paracrine signalling while upregulating smooth muscle Sox9 mRNA. Again, TRAIL exerted minimal direct effects on smooth muscle cells, but significantly reduced glucose-induced BMP-2/ALP paracrine signalling in co-culture. Furthermore, this effect was accompanied by a decrease in smooth muscle ALP and Sox9 mRNA, and an increase in cardioprotective OPG release (compared to glucose treatment alone). As an additional significant finding, under hyperglycemic conditions, the observed pro-calcific endothelial paracrine signalling was *not* accompanied by an increase in the activation of either NF- κ B pathway; therefore, RANKL and TRAIL exert their respective functions via an unrelated (unknown) mechanism in the presence of elevated glucose. Furthermore, in all cases, the mRNA expression trends of both RANKL and TRAIL are particularly similar, decreasing a number of pro-calcific markers. While this finding may contribute to explaining the protective nature of TRAIL, it is unclear as of yet what the significance of this is for RANKL, as this ligand exerts simultaneous pro-calcific effects at a protein level; therefore, further experimentation is required to delineate these trends. Overall, however, it is clear that *both RANKL and TRAIL promote and prevent glucose-induced pro-calcific paracrine signalling, respectively, via a mechanism unrelated to non-canonical NF- κ B*.

6.1.3 Study 3: Key Findings

In study 3, we investigated the key molecular mechanisms underpinning VC, focusing on oxidative stress and non-canonical NF- κ B signalling. Furthermore, we investigated new targets as of yet unrelated to VC, that may aid in delineating the molecular events and signalling mechanisms behind this process. With respect to the latter, TRACP5, a protein central to bone resorption, was identified and assessed as a potential contributor to VC pathogenesis. Our findings suggest that *TRACP5 may be involved in RANKL/TRAIL-mediated pro-calcific signalling in the endothelium*, given that RANKL promotes, and TRAIL attenuates, the TRACP5 expression. Further research is therefore warranted to delineate the precise role of this enzyme during VC, and to investigate its contribution to the calcification process.

Secondly, a number of pro- and anti-oxidant targets were assessed to determine the role of oxidative stress in RANKL/TRAIL-mediated endothelial paracrine signalling. SOD1, a potent anti-oxidant enzyme, was elevated in response to both RANKL and TRAIL, and therefore does not appear to be responsible for the observed effects of RANKL and TRAIL in endothelial cells. Interestingly, RANKL was found to upregulate p47 mRNA, a central subunit involved in NOX2 ROS generation, while also significantly inducing intracellular ROS levels. Thus, *RANKL appears to exert a net pro-oxidant effect on the endothelium, which may contribute to RANKL-induced pro-calcific signalling*. TRAIL, on the other hand, completely attenuated RANKL-induced p47 mRNA expression while upregulating the anti-oxidant HMOX1 mRNA, and co-treatment with RANKL + TRAIL significantly induced eNOS mRNA expression. Furthermore, these effects were accompanied by a decrease in RANKL-induced intracellular ROS levels. Therefore, *TRAIL exerts a net anti-oxidant effect on the endothelium, which may contribute to TRAIL-mediated endothelial protection*.

To better understand the pro-oxidant and anti-oxidant nature of RANKL and TRAIL, respectively, NAC was employed to determine the effects of anti-oxidant treatment on RANKL-induced pro-calcific signalling. Interestingly, *NAC treatment was found to completely attenuate endothelial pro-calcific paracrine signalling and non-canonical NF- κ B activation, suggesting that anti-oxidant mechanisms may mediate calcification upstream of NF- κ B*. Indeed, the effects of NAC were similar to that of TRAIL co-treatment, further suggesting that *TRAIL may exert an anti-oxidant effect on endothelial cells to prevent pro-calcific signalling*.

To better understand the importance of non-canonical NF- κ B signalling in this process, a key element of this pathway was subject to siRNA knockdown. It was determined that *non-*

canonical activation is indeed necessary for RANKL-induced endothelial pro-calcific signalling, and the induction of pro-calcific events in the underlying smooth muscle. However, NF- κ B/p52 knockdown did not affect any of the measured redox indices in endothelial cells; therefore, it can be concluded that RANKL-induced oxidative stress activates non-canonical NF- κ B and subsequent pro-calcific endothelial paracrine signalling in the mediation of VC. Furthermore, the anti-calcific nature of TRAIL may be dependent on anti-oxidant signalling, potentially explaining its protective effects under inflammatory (NF- κ B-dependent) and hyperglycemic (NF- κ B-independent) conditions. The proposed effects of RANKL and TRAIL under physiological and pathological conditions from a mechanistic perspective are summarised below in Figure 6.1.

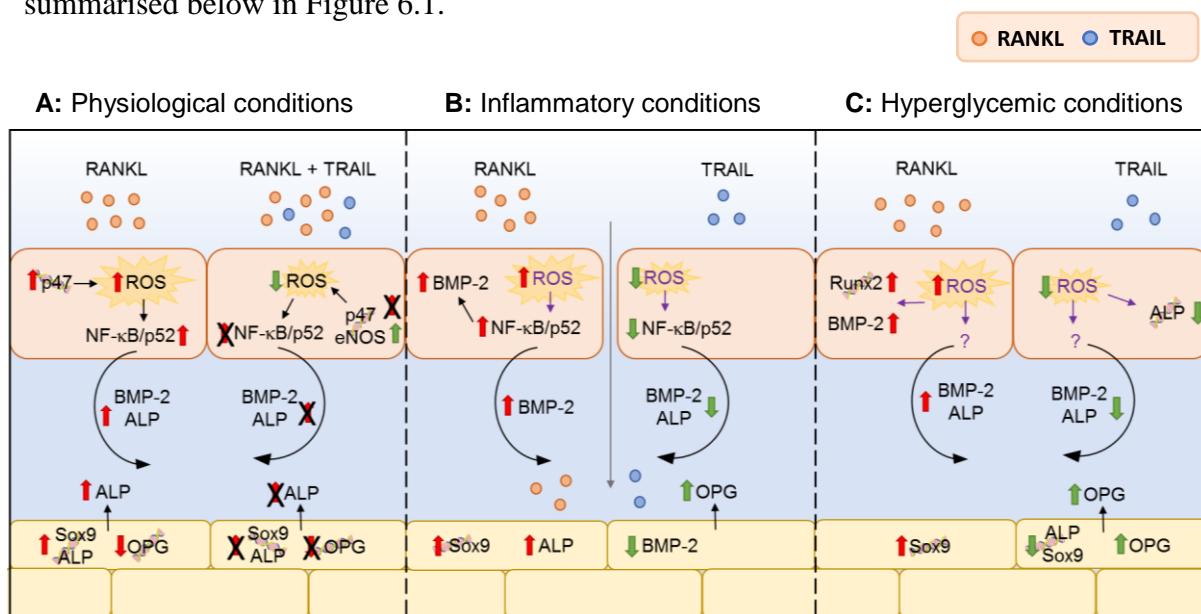


Figure 6.1. Visual interpretation of the key findings from Studies 1-3. (A) Under physiological conditions, our data suggests that RANKL induces oxidative stress (via NOX2/p47) upstream of non-canonical NF- κ B activation (NF- κ B/p52) in endothelial cells. This activation results in endothelial paracrine signalling (BMP-2/ALP) driving pro-calcific effects in the underlying smooth muscle cells. When co-incubated with TRAIL, this oxidative stress is reduced (via a NOX2/eNOS-dependent mechanism), non-canonical NF- κ B signalling is attenuated, and the subsequent paracrine signalling/smooth muscle calcification prevented. (B) Under inflammatory conditions (TNF α exposure), we suspect that RANKL further promotes TNF α -induced oxidative stress in endothelial cells, thereby driving non-canonical NF- κ B activation and pro-calcific paracrine signalling/smooth muscle calcification. TRAIL, however, likely exerts an anti-oxidant effect on the endothelium, preventing TNF α -induced non-canonical NF- κ B activation and the downstream pro-calcific cascade. (C) Under hyperglycemic conditions (glucose exposure), we suspect that RANKL amplifies the pro-oxidant influence of hyperglycemia, thereby accentuating pro-calcific paracrine signalling via an (as yet) unknown mechanism. These paracrine signals then drive chondrocytic (Sox9) differentiation in the underlying smooth muscle cells. We also propose that TRAIL exerts an anti-oxidant effect under hyperglycemic conditions, thereby preventing glucose-induced paracrine signalling via an unknown mechanism. Glucose-induced pro-calcific effects in the underlying smooth muscle layer are therefore reduced. Thus, RANKL and TRAIL may promote and prevent, respectively, pro-calcific signalling events mediated by pathological stimuli. RANKL, receptor activator of NF- κ B ligand; TRAIL, tumour necrosis factor-related apoptosis-inducing ligand; ROS, reactive oxygen species; eNOS, endothelial nitric oxide synthase; BMP, bone morphogenetic protein; ALP, alkaline phosphatase; OPG, osteoprotegerin; Sox9, sex determining region Y box-9; Runx2, runt-related transcription factor 2. Purple text, hypothesised event: data not shown experimentally in the current thesis.

6.2 Future Directions

Despite the comprehensive nature of this study, there are several questions that remain unanswered regarding the role of RANKL and TRAIL, and their mechanisms of action, in the vasculature. In this respect, a common trend throughout this research was the divergent responses of mRNA and protein, a likely contributor to the conflicting evidence identified in the literature to date. It is well known that mRNA and protein trends do not always coincide (Carmody and Wente, 2009; Greenbaum *et al.*, 2003), and indeed, protein measurements more accurately represent the functional outcome of RANKL/TRAIL treatment. However, the longer-term effects of the diverging mRNA responses on vascular cells remain to be clarified to determine if these protein responses are retained. In particular, the bimodal response of OPG identified in Chapter 3, and the complex trends identified in the regulation of this ligand throughout this thesis, requires further clarification. Indeed, a key limitation of this study is the employment of only one endothelial cell and one smooth muscle cell donor; thus, repeat experiments with multiple cell donors may shed additional light on these discrepancies.

From a mechanistic perspective, the effects of RANKL and TRAIL on oxidative stress under pathological conditions remain to be fully delineated. We propose in Figure 6.1 that RANKL promotes, and TRAIL reduces, ROS generation induced by hyperglycemia and inflammation. Recent research within our group indeed suggests that TRAIL (at 100 ng/mL) can reduce both TNF α - and glucose-induced ROS (Forde *et al.*, unpublished observations), but additional experiments are required to confirm this at 5 ng/mL, and to investigate the effects of RANKL under these conditions. Furthermore, the specific redox mechanism(s) by which RANKL and TRAIL mediate pro-calcific signalling under *hyperglycemic* conditions are of particular interest, as non-canonical NF- κ B signalling was not observed in these models. As an additional oversight of this study, only SOD mRNA/protein expression were assessed following endothelial exposure to the aforementioned stimuli. To further clarify the role of SOD1/2 in the regulation of calcification, SOD *enzyme activity* should also be assessed, which may provide additional mechanistic information into the role of oxidative stress in VC.

Furthermore, clarification is required regarding the regulation of RANK and TRAIL receptors during RANKL/TRAIL-mediated VC. It has been considered that TRAIL may exert its protective effects on RANKL-induced pro-calcific signalling via the downregulation of RANK in endothelial cells, although preliminary evidence at an mRNA level suggests that this is not the case (data not shown). Despite this, RANK and TRAIL receptors will be assessed at a

protein level (via receptor quantification/flow cytometry) to determine the potential influence of receptor regulation during VC. Indeed, following these mechanistic investigations, additional pathways associated with RANKL/TRAIL signalling (e.g. MAPK, ERK) may be investigated to determine their contribution to VC regulation.

Of note, it is known that VC progresses under *both* hyperglycemic and inflammatory conditions *in vivo* (Olson *et al.*, 2012), and in the presence of a complex balance of soluble factors including RANKL and TRAIL. Moreover, multiple cell types contribute to VC, including the release of pro-inflammatory cytokines from immune cells at atherosclerotic sites (Gotsman *et al.*, 2008). The inclusion of all of these factors would be too complex *in vitro*, and as such, a murine model of diabetic calcification would be ideal for future VC investigations (such as that employed by Liu *et al.* (2014)). Additionally, *in vivo* models incorporate the physiological element of shear stress exerted on the vasculature by the flow of blood, which may potentially alter the effects observed for RANKL and TRAIL under static conditions *in vitro*. Within a diabetic murine model, the precise effects of recombinant RANKL and TRAIL under pathological conditions may be more accurately determined, and may shed light on the potential therapeutic value for TRAIL during VC.

Finally, the role for TRACP5 as a potential contributor to RANKL/TRAIL function in VC warrants further investigation. In this regard, whether or not TRACP5 is actively involved in the progression of calcification/pro-calcific signalling remains to be determined (e.g. via TRACP5 siRNA knockdown). Furthermore, extracellular TRACP5 measurements *in vitro*, not assessed in the current investigation, may highlight a role for this enzyme as a circulatory biomarker for VC, as TRACP5 has previously been identified as a marker of bone pathologies (Seol *et al.*, 2009). Interestingly, two circulatory isoforms of TRACP5 have been identified (Halleen *et al.*, 2009), and the relevance of each to VC pathogenesis remain to be defined.

On a similar note, the potential for TRAIL as a circulatory biomarker for cardiovascular complications during T2DM has been investigated within our own research group by Forde *et al.* (unpublished observations). Indeed, circulating TRAIL levels were found to accurately distinguish between patients with newly diagnosed T2DM, and diabetic patients with underlying CVD complications. Further collaborative research is now underway to design and implement a mass spectrometry immunoassay to examine specific circulatory isoforms of TRAIL (and related VC indices), adding further value to T2DM/CVD diagnostics in the prevention of diabetic cardiovascular events.

6.3 Concluding Remarks

Overall, this research has provided valuable insight into the roles of RANKL and TRAIL in the pathogenesis of VC from both a molecular signalling and mechanistic perspective, clarifying much debate remaining in the literature. We highlight the significance of endothelial paracrine signalling in the mediation of VC, and the importance of incorporating vascular cell communication *in vitro*. We report that RANKL-induced pro-calcific effects are exerted predominantly at an endothelial level, and that RANKL can also promote VC in the presence of pathological stimuli common during T2DM. Significantly, we present novel evidence that TRAIL exerts a protective, anti-calcific effect on the vasculature via the attenuation of RANKL-induced endothelial paracrine signalling, and also reduces the potent pro-calcific effects induced by pathological stimuli. Furthermore, this research provides important insight into the mechanisms underpinning VC in vascular cells; in this respect, we implicate for the first time the non-canonical NF- κ B pathway as a key driver of endothelial pro-calcific signalling. Furthermore, we show that RANKL exerts a pro-oxidant effect on the vasculature in the promotion of VC, while TRAIL exerts an anti-oxidant effect on the vasculature in the prevention of VC; moreover, these effects appear to be upstream of NF- κ B signalling, subsequently activated by RANKL and attenuated by TRAIL. Therefore, while this research provides necessary clarification regarding the complex signalling events underpinning VC, we also highlight the therapeutic value of TRAIL in this context, potentially reducing the growing mortality rates associated with diabetic cardiovascular complications in the future.

Bibliography

Abedin M, Omland T, Ueland T, Khera A, Aukrust P, Murphy SA, Jain T, Gruntmanis U, McGuire DK, de Lemos JA. Relation of osteoprotegerin to coronary calcium and aortic plaque (from the Dallas Heart Study). *Am J Cardiol* 2007;**99**:513-518.

Abu-Amer Y. NF- κ B signaling and bone resorption. *Osteoporos Int* 2013;**24**:2377-2386.

Acierno LJ. The History of Cardiology. New York: Parthenon Publishing Group Inc. *Atherosclerosis (arteriosclerosis)* 1994;109-126.

Afonso V, Champy R, Mitrovic D, Collin P, Lomri A. Reactive oxygen species and superoxide dismutases: role in joint diseases. *Joint Bone Spine* 2007;**74**(4):324-9.

Agharazii M, St-Louis R, Gautier-Bastien A, Ung RV, Mokas S, Larivière R, Richard DE. Inflammatory cytokines and reactive oxygen species as mediators of chronic kidney disease-related vascular calcification. *Am J Hypertens* 2015;**28**:746-755.

Aikawa E, Nahrendorf M, Figueiredo JL, Swirski FK, Shtatland T, Kohler RH, Jaffer FA, Aikawa M, Weissleder R. Osteogenesis associates with inflammation in early-stage atherosclerosis evaluated by molecular imaging in vivo. *Circulation* 2007;**116**:2841-2850.

Akiyama H, Chaboissier MC, Martin JF, Schedl A, de Crombrughe B. The transcription factor Sox9 has essential roles in successive steps of the chondrocyte differentiation pathway and is required for expression of Sox5 and Sox6. *Genes Dev* 2002;**16**:2813-2828.

Akiyama H. Control of chondrogenesis by the transcription factor Sox9. *Mod Rheumatol* 2008;**18**:213-219.

Al-Aly Z, Shao JS, Lai CF, Huang E, Cai J, Behrmann A, Cheng SL, Towler DA. Aortic Msx2-Wnt calcification cascade is regulated by TNF- α -dependent signals in diabetic Ldlr^{-/-} mice. *Arterioscler Thromb Vasc Biol* 2007;**27**:2589-2596.

Al-Aly Z. Arterial calcification: a tumor necrosis factor- α mediated vascular Wnt-opathy. *Transl Res* 2008;**151**:233-239.

Al-Aly Z. Phosphate, oxidative stress, and nuclear factor- κ B activation in vascular calcification. *Kidney Int* 2011;**79**:1044-1047.

Albrecht EW, Stegeman CA, Heeringa P, Henning RH, van Goor H. Protective role of endothelial nitric oxide synthase. *J Pathol* 2003;**199**:8-17.

Albrecht S. The Pathophysiology and Treatment of Stable Angina Pectoris. *US Pharm* 2013;**38**:43-60.

Alesutan I, Musculus K, Castor T, Alzoubi K, Voelkl J, Lang F. Inhibition of Phosphate-Induced Vascular Smooth Muscle Cell Osteo-/Chondrogenic Signaling and Calcification by Bafilomycin A1 and Methylamine. *Kidney Blood Press Res* 2015;**40**:490-499.

Alesutan I, Tuffaha R, Auer T, Feger M, Pieske B, Lang F, Voelkl J. Inhibition of osteo/chondrogenic transformation of vascular smooth muscle cells by MgCl₂ via calcium-sensing receptor. *J Hypertens* 2017;**35**:523-532.

- Allison MA, Criqui MH, Wright CM. Patterns and risk factors for systemic calcified atherosclerosis. *Arterioscler Thromb Vasc Biol* 2004;**24**:331-336.
- Almasan A, Ashkenazi A. Apo2L/TRAIL: apoptosis signaling, biology, and potential for cancer therapy. *Cytokine & Growth Factor Rev* 2003;**14**:337-348.
- Anand DV, Lahiri A, Lim E, Hopkins D, Corder R. The relationship between plasma osteoprotegerin levels and coronary artery calcification in uncomplicated type 2 diabetic subjects. *J Am Coll Cardiol* 2006;**47**:1850-1857.
- Anand DV, Lim E, Darko D, Bassett P, Hopkins D, Lipkin D, Corder R, Lahiri A. Determinants of progression of coronary artery calcification in type 2 diabetes role of glycemic control and inflammatory/vascular calcification markers. *J Am Coll Cardiol* 2007;**50**:2218-2225.
- Andrade MC, Carmo LS, Farias-Silva E, Liberman M. Msx2 is required for vascular smooth muscle cells osteoblastic differentiation but not calcification in insulin-resistant ob/ob mice. *Atherosclerosis* 2017;**265**:14-21.
- Angel NZ, Walsh N, Forwood MR, Ostrowski MC, Cassady AI, Hume DA. Transgenic mice overexpressing tartrate-resistant acid phosphatase exhibit an increased rate of bone turnover. *J Bone Miner Res* 2000;**15**:103-110.
- Anrather J, Racchumi G, Iadecola C. NF- κ B regulates phagocytic NADPH oxidase by inducing the expression of gp91phox. *J Biol Chem* 2006;**281**:5657-67.
- Araujo JA, Zhang M, Yin F. Heme oxygenase-1, oxidation, inflammation, and atherosclerosis. *Front Pharmacol* 2012;**3**:119.
- Arch RH, Gedrich RW, Thompson CB. Tumor necrosis factor receptor-associated factors (TRAFs)-a family of adapter proteins that regulates life and death. *Genes Dev* 1998;**12**:2821-2830.
- Ardanaz N, Pagano PJ. Hydrogen peroxide as a paracrine vascular mediator: regulation and signaling leading to dysfunction. *Exp Biol Med* (Maywood) 2006;**231**:237-251.
- Armstrong AP, Tometsko ME, Glaccum M, Sutherland CL, Cosman D, Dougall WC. A RANK/TRAF6-dependent signal transduction pathway is essential for osteoclast cytoskeletal organization and resorptive function. *J Biol Chem* 2002;**277**:44347-44356.
- Aronson D, Rayfield EJ. How hyperglycemia promotes atherosclerosis: molecular mechanisms. *Cardiovasc Diabet* 2002;**1**:1.
- Atkins GJ, Kostakis P, Vincent C, Farrugia AN, Houchins JP, Findlay DM, Evdokiou A, Zannettino AC. RANK Expression as a cell surface marker of human osteoclast precursors in peripheral blood, bone marrow, and giant cell tumors of bone. *J Bone Miner Res* 2006;**21**:1339-1349.
- Awan Z, Denis M, Roubtsova A, Essalmani R, Marcinkiewicz J, Awan A, Gram H, Seidah NG, Genest J. Reducing Vascular Calcification by Anti-IL-1 β Monoclonal Antibody in a Mouse Model of Familial Hypercholesterolemia. *Angiology* 2016;**67**:157-167.

- Azuma Y, Kaji K, Katogi R, Takeshita S, Kudo A. Tumor necrosis factor-alpha induces differentiation of and bone resorption by osteoclasts. *J Biol Chem* 2000;**275**:4858-4864.
- Bak SU, Kim S, Hwang HJ, Yun JA, Kim WS, Won MH, Kim JY, Ha KS, Kwon YG, Kim YM. Heme oxygenase-1 (HO-1)/carbon monoxide (CO) axis suppresses RANKL-induced osteoclastic differentiation by inhibiting redox-sensitive NF- κ B activation. *BMB Rep* 2017;**50**:103-108.
- Baker RG, Hayden MS, Ghosh S. NF- κ B, inflammation, and metabolic disease. *Cell Metab* 2011;**13**:11-22.
- Banegas JR, López-García E, Dallongeville J, Guallar E, Halcox JP, Borghi C, Massó-González EL, Jiménez FJ, Perk J, Steg PG, De Backer G, Rodríguez-Artalejo F. Achievement of treatment goals for primary prevention of cardiovascular disease in clinical practice across Europe: the EURIKA study. *Eur Heart J* 2011;**32**:2143-2152.
- Banquet S, Bourguignon MP, Garry A, Royere E, Crespo C, Lapret I, Simonet S, Gosgnach W, Thollon C, Villeneuve N, Vilaine JP. Reduced no bioavailability, oxidative stress and alteration of calcium homeostasis in vascular endothelium from diabetic mice. *FASEB J* 2013;**27Suppl1**:1138-1188.
- Barath P, Fishbein MC, Cao J, Berenson J, Helfant RH, Forrester JS. Detection and localization of tumor necrosis factor in human atheroma. *Am J Cardiol* 1990;**65**:297-302.
- Barry-Lane PA, Patterson C, Van Der Merwe M, Hu Z, Holland SM, Yeh ET, Runge MS. p47phox is required for atherosclerotic lesion progression in ApoE^{-/-} mice. *Journal Clin Invest* 2001;**108**:1513-1522.
- Bauer M, Kristensen BW, Meyer M, Gasser T, Widmer HR, Zimmer J, Ueffing M. Toxic effects of lipid-mediated gene transfer in ventral mesencephalic explant cultures. *Basic Clin Pharmacol Toxicol* 2006;**98**:395-400.
- Baumgartl J, Baudler S, Scherner M, Babaev V, Makowski L, Suttles J, McDuffie M, Tobe K, Kadowaki T, Fazio S, Kahn CR, Hotamisligil GS, Krone W, Linton M, Brüning JC. Myeloid lineage cell-restricted insulin resistance protects apolipoproteinE-deficient mice against atherosclerosis. *Cell Metab* 2006;**3**:247-256.
- Bayir H. Reactive oxygen species. *Crit Care Med* 2005;**33**:S498-501.
- Ben-Tal Cohen E, Hohensinner PJ, Kaun C, Maurer G, Huber K, Wojta J. Statins decrease TNF-alpha-induced osteoprotegerin production by endothelial cells and smooth muscle cells in vitro. *Biochem Pharmacol* 2007;**73**:77-83.
- Beristain AG, Narala SR, Di Grappa MA, Khokha R. Homotypic RANK signaling differentially regulates proliferation, motility and cell survival in osteosarcoma and mammary epithelial cells. *J Cell Sci* 2012;**125**:943-955.
- Bessueille L, Fakhry M, Hamade E, Badran B, Magne D. Glucose stimulates chondrocyte differentiation of vascular smooth muscle cells and calcification: A possible role for IL-1 β . *FEBS Lett* 2015;**589**:2797-2804.

- Bharti AC, Takada Y, Shishodia S, Aggarwal BB. Evidence that receptor activator of nuclear factor (NF)-kappaB ligand can suppress cell proliferation and induce apoptosis through activation of a NF-kappaB-independent and TRAF6-dependent mechanism. *J Biol Chem* 2004;**279**:6065-6076.
- Bilgir O, Yavuz Z, Bilgir F, Akan OY, Bayindir AG, Calan M, Bozkaya G, Yuksel A. Relationship between insulin resistance, hs-CRP, and body fat and serum osteoprotegerin/RANKL in prediabetic patients. *Minerva Endocrinol* 2018;**43**:19-26.
- Bjerre M. Osteoprotegerin (OPG) as a biomarker for diabetic cardiovascular complications. *Springerplus* 2013;**2**:658.
- Blumer MJ, Hausott B, Schwarzer C, Hayman AR, Stempel J, Fritsch H. Role of tartrate-resistant acid phosphatase (TRAP) in long bone development. *Mech Dev* 2012;**129**:162-176.
- Bolon B, Campagnuolo G, Feige U. Duration of bone protection by a single osteoprotegerin injection in rats with adjuvant-induced arthritis. *Cell Mol Life Sci* 2002;**59**:1569-1576.
- Bonizzi G, Piette J, Schoonbroodt S, Greimers R, Havard L, Merville MP, Bours V. Reactive oxygen intermediate-dependent NF-kappaB activation by interleukin-1beta requires 5-lipoxygenase or NADPH oxidase activity. *Mol Cell Biol* 1999;**19**:1950-1960.
- Boskey A. Bone mineral crystal size. *Osteoporos Int* 2003;**14**:S16-21.
- Boström K, Tsao D, Shen S, Wang Y, Demer LL. Matrix GLA protein modulates differentiation induced by bone morphogenetic protein-2 in C3H10T1/2 cells. *J Biol Chem* 2001;**276**:14044-14052.
- Boyce BF, Xing L. Biology of RANK, RANKL, and osteoprotegerin. *Arthritis Res Ther* 2007;**9**:S1.
- Boyce BF, Xiu Y, Li J, Xing L, Yao Z. NF-κB-Mediated Regulation of Osteoclastogenesis. *Endocrinol Metab* 2015;**30**:35-44.
- Boyce BF, Yao Z, Xing L. Functions of nuclear factor kappaB in bone. *Ann N Y Acad Sci* 2010;**1192**:367-375.
- Brand K, Page S, Rogler G, Bartsch A, Brandl R, Knuechel R, Page M, Kaltschmidt C, Baeuerle PA, Neumeier D. Activated transcription factor nuclear factor-kappa B is present in the atherosclerotic lesion. *J Clin Invest* 1996;**97**:1715.
- Brandes RP, Kreuzer J. Vascular NADPH oxidases: molecular mechanisms of activation. *Cardiovasc Res* 2005;**65**:16-27.
- Brasier AR. The nuclear factor-kappaB-interleukin-6 signalling pathway mediating vascular inflammation. *Cardiovasc Res* 2010;**86**:211-218.
- Bryant PW, Zheng Q, Pumiglia KM. Focal adhesion kinase is a phospho-regulated repressor of Rac and proliferation in human endothelial cells. *Biol Open* 2012;**1**:723-730.

- Bucay N, Sarosi I, Dunstan CR, Morony S, Tarpley J, Capparelli C, Scully S, Tan HL, Xu W, Lacey DL, Boyle WJ, Simonet WS. Osteoprotegerin-deficient mice develop early onset osteoporosis and arterial calcification. *Genes Dev* 1998;**12**:1260-1268.
- Budoff MJ, Hokanson JE, Nasir K, Shaw LJ, Kinney GL, Chow D, Demoss D, Nuguri V, Nabavi V, Ratakonda R, Berman DS, Raggi P. Progression of coronary artery calcium predicts all-cause mortality. *JACC Cardiovasc Imaging* 2010;**3**:1229-1236.
- Budoff MJ. Atherosclerosis imaging and calcified plaque: coronary artery disease risk assessment. *Prog Cardiovasc Dis* 2003;**46**:135-148.
- Bunting C. The formation of true bone with cellular (red) marrow in a sclerotic aorta. *J Exp Med* 1906;**8**:365-376.
- Byon CH, Javed A, Dai Q, Kappes JC, Clemens TL, Darley-Usmar VM, McDonald JM, Chen Y. Oxidative stress induces vascular calcification through modulation of the osteogenic transcription factor Runx2 by AKT signaling. *J Biol Chem* 2008;**283**:15319-15327.
- Byon CH, Sun Y, Chen J, Yuan K, Mao X, Heath JM, Anderson PG, Tintut Y, Demer LL, Wang D, Chen Y. Runx2-upregulated receptor activator of nuclear factor κ B ligand in calcifying smooth muscle cells promotes migration and osteoclastic differentiation of macrophages. *Arterioscler Thromb Vasc Biol* 2011;**31**:1387-1396.
- Callaghan MJ, Ceradini DJ, Gurtner GC. Hyperglycemia-induced reactive oxygen species and impaired endothelial progenitor cell function. *Antioxid Redox Signal* 2005;**7**:1476-1482.
- Callegari A, Coons ML, Ricks JL, Rosenfeld ME, Scatena M. Increased calcification in osteoprotegerin-deficient smooth muscle cells: Dependence on receptor activator of NF- κ B ligand and interleukin 6. *J Vasc Res* 2014;**51**:118-131.
- Callegari A, Coons ML, Ricks JL, Yang HL, Gross TS, Huber P, Rosenfeld ME, Scatena M. Bone marrow- or vessel wall-derived osteoprotegerin is sufficient to reduce atherosclerotic lesion size and vascular calcification. *Arterioscler Thromb Vasc Biol* 2013;**33**:2491-2500.
- Carbone F, Crowe LA, Roth A, Burger F, Lenglet S, Braunersreuther V, Brandt KJ, Quercioli A, Mach F, Vallée JP, Montecucco F. Treatment with anti-RANKL antibody reduces infarct size and attenuates dysfunction impacting on neutrophil-mediated injury. *J Mol Cell Cardiol* 2016;**94**:82-94.
- Carmody SR, Wenthe SR. mRNA nuclear export at a glance. *J Cell Sci* 2009;**122**:1933-1937.
- Cave AC, Brewer AC, Narayanapanicker A, Ray R, Grieve DJ, Walker S, Shah AM. NADPH oxidases in cardiovascular health and disease. *Antioxid Redox Signal* 2006;**8**:691-728.
- Chang HJ, Li TF, Guo JL, Lan YL, Kong YQ, Meng X, Ma XJ, Lu XL, Lu WY, Zheng SJ. Effects of high glucose on expression of OPG and RANKL in rat aortic vascular smooth muscle cells. *Asian Pac J Trop Med* 2015;**8**:209-213.

- Chasseraud M, Liabeuf S, Mozar A, Mentaverri R, Brazier M, Massy ZA, Kamel S. Tumor necrosis factor-related apoptosis-inducing ligand and vascular calcification. *Ther Apher Dial* 2011;**15**:140-146.
- Chen J, Li C, Chen L. The Role of Microvesicles Derived from Mesenchymal Stem Cells in Lung Diseases. *Biomed Res Int* 2015;**2015**:985814.
- Chen NX, Duan D, O'Neill KD, Moe SM. High glucose increases the expression of Cbfa1 and BMP-2 and enhances the calcification of vascular smooth muscle cells. *Nephrol Dial Transplant* 2006;**21**:3435-3442.
- Chen X, Andresen¹ BT, Hill M, Zhang J, Booth F, Zhang C. Role of Reactive Oxygen Species in Tumor Necrosis Factor-alpha Induced Endothelial Dysfunction. *Curr Hypertens Rev* 2008;**4**:245-255.
- Chen X, Kandasamy K, Srivastava RK. Differential roles of RelA (p65) and c-Rel subunits of nuclear factor- κ B in tumor necrosis factor-related apoptosis-inducing ligand signaling. *Cancer Res* 2003;**63**:1059-1066.
- Chendrimada TP, Gregory RI, Kumaraswamy E, Norman J, Cooch N, Nishikura K, Shiekhattar R. TRBP recruits the Dicer complex to Ago2 for microRNA processing and gene silencing. *Nature* 2005;**436**:740–744.
- Cheng A, Genever PG. SOX9 determines RUNX2 transactivity by directing intracellular degradation. *J Bone Miner Res* 2010;**25**:2680-2689.
- Cheng W, Liu F, Wang Z, Zhang Y, Zhao YX, Zhang Q, Jiang F. Soluble TRAIL concentration in serum is elevated in people with hypercholesterolemia. *PLoS One* 2015;**10**:e0144015.
- Cheng W, Zhao Y, Wang S, Jiang F. Tumor necrosis factor-related apoptosis-inducing ligand in vascular inflammation and atherosclerosis: a protector or culprit? *Vascul Pharmacol* 2014;**63**:135-144.
- Chiang C, Flint M, Lin JS, Spiropoulou CF. Endocytic Pathways Used by Andes Virus to Enter Primary Human Lung Endothelial Cells. *PLoS One* 2016;**11**:e0164768.
- Chiu JJ, Chen LJ, Lee CI, Lee PL, Lee DY, Tsai MC, Lin CW, Usami S, Chien S. Mechanisms of induction of endothelial cell E-selectin expression by smooth muscle cells and its inhibition by shear stress. *Blood* 2007;**110**:519-528.
- Chiu JJ, Usami S, Chien S. Vascular endothelial responses to altered shear stress: pathologic implications for atherosclerosis. *Ann Med* 2009;**41**:19-28.
- Chomczynski P, Sacchi N. Single-step method of RNA isolation by acid guanidinium thiocyanate-phenol-chloroform extraction. *Anal Biochem* 1987;**162**:156-159.
- Chu F, Wang M, Ma H, Zhu J. Simvastatin Modulates Interaction Between Vascular Smooth Muscle Cell / Macrophage and TNF- α -activated Endothelial Cell. *J Cardiovasc Pharmacol* 2018. doi: 10.1097/FJC.0000000000000567 [Epub ahead of print].

- Ciceri P, Volpi E, Brenna I, Arnaboldi L, Neri L, Brancaccio D, Cozzolino M. Combined effects of ascorbic acid and phosphate on rat VSMC osteoblastic differentiation. *Nephrol Dial Transplant* 2012;**27**:122-127.
- Clempus RE, Griending KK. Reactive oxygen species signaling in vascular smooth muscle cells. *Cardiovasc Res* 2006;**71**:216-225.
- Collin-Osdoby P, Rothe L, Anderson F, Nelson M, Maloney W, Osdoby P. Receptor activator of NF-kappa B and osteoprotegerin expression by human microvascular endothelial cells, regulation by inflammatory cytokines, and role in human osteoclastogenesis. *J Biol Chem* 2001;**276**:20659-20672.
- Collin-Osdoby P. Regulation of vascular calcification by osteoclast regulatory factors RANKL and osteoprotegerin. *Circ Res* 2004;**95**:1046-1057.
- Corallini F, Celeghini C, Rimondi E, di Iasio MG, Gonelli A, Secchiero P, Zauli G. Trail down-regulates the release of osteoprotegerin (OPG) by primary stromal cells. *J Cell Physiol* 2011;**226**:2279-2286.
- Corallini F, Gonelli A, D'Aurizio F, di Iasio MG, Vaccarezza M. Mesenchymal stem cells-derived vascular smooth muscle cells release abundant levels of osteoprotegerin. *Eur J Histochem* 2009;**53**:19-24.
- Coucha M, Li W, Hafez S, Abdelsaid M, Johnson MH, Fagan SC, Ergul A. SOD1 overexpression prevents acute hyperglycemia-induced cerebral myogenic dysfunction: relevance to contralateral hemisphere and stroke outcomes. *Am J Physiol Heart Circ Physiol* 2015;**308**:H456-466.
- Cunningham KS, Gotlieb AI. The role of shear stress in the pathogenesis of atherosclerosis. *Lab Invest* 2005;**85**:9-23.
- da Silva Meirelles L, Chagastelles PC, Nardi NB. Mesenchymal stem cells reside in virtually all post-natal organs and tissues. *J Cell Sci* 2006;**119**:2204-2213.
- Daniels RA, Turley H, Kimberley FC, Liu XS, Mongkolsapaya J, Paul CE, Xiao Ning X, Jin B, Pizella F, Screaton GR. Expression of TRAIL and TRAIL receptors in normal and malignant tissues. *Cell Res* 2005;**15**:430-438.
- Darnay BG, Ni J, Moore PA, Aggarwal BB. Activation of NF-kappaB by RANK requires tumor necrosis factor receptor-associated factor (TRAF) 6 and NF-kappaB-inducing kinase. Identification of a novel TRAF6 interaction motif. *J Biol Chem* 1999;**274**:7724-7731.
- Davenport C, Harper E, Forde H, Rochfort KD, Murphy RP, Smith D, Cummins PM. RANKL promotes osteoblastic activity in vascular smooth muscle cells by upregulating endothelial BMP-2 release. *Int J Biochem Cell Biol* 2016;**77(Pt A)**:171-180.
- Davenport C, Harper E, Rochfort KD, Forde H, Smith D, Cummins PM. RANKL Inhibits the Production of Osteoprotegerin from Smooth Muscle Cells under Basal Conditions and following Exposure to Cyclic Strain. *J Vasc Res* 2018;**55**:111-123.

Davenport C, Mahmood WA, Forde H, Ashley DT, Agha A, McDermott J, Sreenan S, Thompson CJ, McGrath F, McAdam B, Cummins PM, Smith D. The effects of insulin and liraglutide on osteoprotegerin and vascular calcification in vitro and in patients with type 2 diabetes. *Eur J Endocrinol* 2015;**173**:53-61.

Degli-Esposti MA, Dougall WC, Smolak PJ, Waugh JY, Smith CA, Goodwin RG. The novel receptor TRAIL-R4 induces NF-kappaB and protects against TRAIL-mediated apoptosis, yet retains an incomplete death domain. *Immunity* 1997;**7**:813-820.

Delgi-Esposti M. To die or not to die-the quest of the TRAIL receptors. *J Leukoc Biol* 1999;**65**:535-542.

Demer LL. Effect of calcification on in vivo mechanical response of rabbit arteries to balloon dilation. *Circulation* 1991;**83**:2083-2093.

Demer LL. Cholesterol in vascular and valvular calcification. *Circulation* 2001;**104**:1881-1883.

Demer LL, Tintut Y. Vascular calcification: pathobiology of a multifaceted disease. *Circulation* 2008;**117**:2938-2948.

Demerdash HM. Role of Oxidative Stress and Associated Alteration in Enzyme Activities in Obesity Comorbidities. *Obesity Res* 2017;**4**:32-43.

Detrano R, Guerci AD, Carr JJ, Bild DE, Burke G, Folsom AR, Liu K, Shea S, Szklo M, Bluemke DA, O'Leary DH, Tracy R, Watson K, Wong ND, Kronmal RA. Coronary calcium as a predictor of coronary events in four racial or ethnic groups. *N Engl J Med* 2008;**358**:1336-1345.

Deuell KA, Callegari A, Giachelli CM, Rosenfeld ME, Scatena M. RANKL enhances macrophage paracrine pro-calcific activity in high phosphate-treated smooth muscle cells: dependence on IL-6 and TNF- α . *J Vasc Res* 2012;**49**:510-521.

Dharmacon. *Recommended DharmaFECT Formulation for Various Cell Lines*. 2015. Available at: <http://dharmacon.horizondiscovery.com/uploadedFiles/Resources/dharmafect-customer-recommend-productbulletin.pdf> [Accessed 9 May 2018].

Dhore CR, Cleutjens JP, Lutgens E, Cleutjens KB, Geusens PP, Kitslaar PJ, Tordoir JH, Spronk HM, Vermeer C, Daemen MJ. Differential expression of bone matrix regulatory proteins in human atherosclerotic plaques. *Arterioscler Thromb Vasc Biol* 2001;**21**:998-2003.

di Bartolo BA, Cartland SP, Harith HH, Bobryshev YV, Schoppet M, Kavurma MM. TRAIL-deficiency accelerates vascular calcification in atherosclerosis via modulation of RANKL. *PloS One* 2013;**8**:e74211.

di Bartolo BA, Cartland SP, Prado-Lourenco L, Griffith TS, Gentile C, Ravindran J, Azahri NS, Thai T, Yeung AW, Thomas SR, Kavurma MM. Tumor Necrosis Factor-Related Apoptosis-Inducing Ligand (TRAIL) Promotes Angiogenesis and Ischemia-Induced Neovascularization Via NADPH Oxidase 4 (NOX4) and Nitric Oxide-Dependent Mechanisms. *J Am Heart Assoc* 2015;**4**:e002527.

di Bartolo BA, Chan J, Bennett MR, Cartland S, Bao S, Tuch BE, Kavurma MM. TNF-related apoptosis-inducing ligand (TRAIL) protects against diabetes and atherosclerosis in Apoe^{-/-} mice. *Diabetologica* 2011;**54**:3157-3167.

di Bartolo BA, Kavurma MM. Regulation and function of Rankl in arterial calcification. *Curr Pharm Des* 2014;**20**:5853-5861.

di Bartolo BA, Schoppet M, Mattar MZ, Rachner TD, Shanahan CM, Kavurma MM. Calcium and osteoprotegerin regulate IGF1R expression to inhibit vascular calcification. *Cardiovasc Res* 2011;**91**:537-545.

Diabetes Ireland. *Diabetes Prevalence in Ireland*. 2018. Available at: <https://www.diabetes.ie/about-us/diabetes-in-ireland/> [Accessed 8 May 2018].

Ding H, Aljofan M, Triggle CR. Oxidative stress and increased eNOS and NADPH oxidase expression in mouse microvessel endothelial cells. *J Cell Physiol* 2007;**212**:682-689.

Djavaheri-Mergny M, Javelaud D, Wietzerbin J, Besançon F. NF-κB activation prevents apoptotic oxidative stress via an increase of both thioredoxin and MnSOD levels in TNFα-treated Ewing sarcoma cells. *FEBS letters* 2004;**578**:111-115.

Doherty TM, Asotra K, Fitzpatrick LA, Qiao JH, Wilkin DJ, Detrano RC, Dunstan CR, Shah PK, Rajavashisth TB. Calcification in atherosclerosis: bone biology and chronic inflammation at the arterial crossroads. *Proc Natl Acad Sci USA* **100**:11201-11206.

Domazetovic V, Marcucci G, Iantomasi T, Brandi ML, Vincenzini MT. Oxidative stress in bone remodeling: role of antioxidants. *Clin Cases Miner Bone Metab* 2017;**14**:209-216.

Dschietzig T, Brecht A, Bartsch C, Baumann G, Stangl K, Alexiou K. Relaxin improves TNF-α-induced endothelial dysfunction: the role of glucocorticoid receptor and phosphatidylinositol 3-kinase signalling. *Cardiovasc Res* 2012;**95**:97-107.

Duckworth WC. Hyperglycemia and cardiovascular disease. *Curr Atheroscler Rep* 2001;**3**:383-391.

Ducy P, Schinke T, Karsenty G. The osteoblast: A sophisticated fibroblast under central surveillance. *Science* 2000;**289**:1501-1504.

Eddahibi S, Guignabert C, Barlier-Mur AM, Dewachter L, Fadel E, Dartevielle P, Humbert M, Simonneau G, Hanoun N, Saurini F, Hamon M, Adnot S. Cross talk between endothelial and smooth muscle cells in pulmonary hypertension: critical role for serotonin-induced smooth muscle hyperplasia. *Circulation* 2006;**113**:1857-1864.

Ehrlich S, Infante-Duarte C, Seeger B, Zipp F. Regulation of soluble and surface-bound TRAIL in human T cells, B cells, and monocytes. *Cytokine* 2003;**24**:244-253.

Ek-Rylander B, Flores M, Wendel M, Heinegård D, Andersson G. Dephosphorylation of osteopontin and bone sialoprotein by osteoclastic tartrate-resistant acid phosphatase. Modulation of osteoclast adhesion in vitro. *J Biol Chem* 1994;**269**:14853-14856.

- Eldor R, Raz I. American Diabetes Association indications for statins in diabetes: is there evidence? *Diabetes Care* 2009;**32**:S384-391.
- Emery JG, McDonnell P, Burke MB, et al. Osteoprotegerin is a receptor for the cytotoxic ligand TRAIL. *J Biol Chem* 1998;**273**:14363–14367.
- Esposito K, Nappo F, Marfella R, Giugliano G, Giugliano F, Ciotola M, Quagliaro L, Ceriello A, Giugliano D. Inflammatory cytokine concentrations are acutely increased by hyperglycemia in humans: role of oxidative stress. *Circulation* 2002;**106**:2067-2072.
- Essalihi R, Ouellette V, Dao HH, McKee MD, Moreau P. Phenotypic modulation of vascular smooth muscle cells during medial arterial calcification: a role for endothelin? *J Cardiovasc Pharmacol* 2004;**44**:S147-50.
- Falschlehner C, Emmerich CH, Gerlach B, Walczak H. TRAIL signalling: decisions between life and death. *Int J Biochem Cell Biol* 2007;**39**:1462-1475.
- Falschlehner C, Schaefer U, Walczak H. Following TRAIL's path in the immune system. *Immunology* 2009;**127**:145-154.
- Faraci FM, Didion SP. Vascular protection: superoxide dismutase isoforms in the vessel wall. *Arterioscler Thromb Vasc Biol* 2004;**24**:1367-1373.
- Farrar EJ, Huntley GD, Butcher J. Endothelial-derived oxidative stress drives myofibroblastic activation and calcification of the aortic valve. *PLoS One* 2015;**10**:e0123257.
- Feng JQ, Xing L, Zhang JH, Zhao M, Horn D, Chan J, Boyce BF, Harris SE, Mundy GR, Chen D. NF-kappaB specifically activates BMP-2 gene expression in growth plate chondrocytes in vivo and in a chondrocyte cell line in vitro. *J Biol Chem* 2003;**278**:29130-29135.
- Fernández-González FJ, Cañigral A, López-Caballo JL, Brizuela A, Cobo T, de Carlos F, Suazo I, Pérez-González Y, Vega JA. Recombinant osteoprotegerin effects during orthodontic movement in a rat model. *Eur J Orthod* 2015;**38**:379-385.
- Finn AV, Nakano M, Narula J, Kolodgie FD, Virmani R. Concept of vulnerable/unstable plaque. *Arterioscler Thromb Vasc Biol* 2010;**30**:1282-1292.
- Fiorentino TV, Prioleta A, Zuo P, Folli F. Hyperglycemia-induced oxidative stress and its role in diabetes mellitus related cardiovascular diseases. *Curr Pharm Des* 2013;**19**:5695-5703.
- Folli F, Corradi D, Fanti P, Davalli A, Paez A, Giaccari A, Perego C, Muscogiuri G. The role of oxidative stress in the pathogenesis of type 2 diabetes mellitus micro- and macrovascular complications: avenues for a mechanistic-based therapeutic approach. *Curr Diabetes Rev* 2011;**7**:313-324.
- Ford TJ, Corcoran D, Berry C. Stable coronary syndromes: pathophysiology, diagnostic advances and therapeutic need. *Heart* 2017;**0**:1-9.
- Forde H, Harper E, Davenport C, Rochfort KD, Wallace R, Murphy RP, Smith D, Cummins PM. The beneficial pleiotropic effects of tumour necrosis factor-related apoptosis-inducing

ligand (TRAIL) within the vasculature: A review of the evidence. *Atherosclerosis* 2016;**247**:87-96.

Förstermann U, Closs EI, Pollock JS, Nakane M, Schwarz P, Gath I, Kleinert H. Nitric oxide synthase isozymes. Characterization, purification, molecular cloning, and functions. *Hypertension* 1994;**23**:1121-1131.

Förstermann U, Sessa WC. Nitric oxide synthases: regulation and function. *Eur Heart J* 2012;**33**:829-837.

Freise C, Kretzschmar N, Querfeld U. Wnt signaling contributes to vascular calcification by induction of matrix metalloproteinases. *BMC Cardiovasc Disord* 2016;**16**:185.

Fujita T, Azuma Y, Fukuyama R, Hattori Y, Yoshida C, Koida M, Ogita K, Komori T. Runx2 induces osteoblast and chondrocyte differentiation and enhances their migration by coupling with PI3K-Akt signaling. *J Cell Biol* 2004;**166**:85-95.

Fukai T, Folz RJ, Landmesser U, Harrison DG. Extracellular superoxide dismutase and cardiovascular disease. *Cardiovasc Res* 2002;**55**:239-249.

Fukai T, Ushio-Fukai M. Superoxide dismutases: role in redox signaling, vascular function, and diseases. *Antioxid Redox Signal* 2011;**15**:1583-1606.

Fuller K, Murphy C, Kirstein B, Fox SW, Chambers TJ. TNFalpha potently activates osteoclasts, through a direct action independent of and strongly synergistic with RANKL. *Endocrinology* 2002;**143**:1008-1018.

Fulton DJ, Barman SA. Clarity on the Isoform-Specific Roles of NADPH Oxidases and NADPH Oxidase-4 in Atherosclerosis. *Arterioscler Thromb Vasc Biol* 2016;**36**:579-581.

Galeone A, Brunetti G, Oranger A, Greco G, Di Benedetto A, Mori G, Colucci S, Zallone A, Paparella D, Grano M. Aortic valvular interstitial cells apoptosis and calcification are mediated by TNF-related apoptosis-inducing ligand. *Int J Cardiol* 2013;**169**:296-304.

Galli D, Vitale M, Vaccarezza M. Bone Marrow-Derived Mesenchymal Cell Differentiation toward Myogenic Lineages: Facts and Perspectives. *Biomed Res Int* 2014;**2014**:762695.

Ganz P, Hsue PY. Endothelial dysfunction in coronary heart disease is more than a systemic process. *Eur Heart J* 13;**34**:2025-2027.

García-Hernández A, Arzate H, Gil-Chavarría I, Rojo R, Moreno-Fierros L. High glucose concentrations alter the biomineralization process in human osteoblastic cells. *Bone* 2012;**50**:276-288.

Gaspersic R, Stiblar-Martincic D, Osredkar J, Skaleric U. In vivo administration of recombinant TNF-alpha promotes bone resorption in mice. *J Periodontal Res* 2003;**38**:446-448.

Gaudio A, Privitera F, Pulvirenti I, Canzonieri E, Rapisarda R, Fiore CE. Relationships between osteoprotegerin, receptor activator of the nuclear factor kB ligand and serum levels

and carotid intima-media thickness in patients with type 2 diabetes mellitus. *Panminerva Med* 2014;**56**:221-225.

Ghali O, Broux O, Falgayrac G, Haren N, van Leeuwen J, Penel G, Hardouin P, Chauveau C. Dexamethasone in osteogenic medium strongly induces adipocyte differentiation of mouse bone marrow stromal cells and increases osteoblast differentiation. *BMC Cell Biol* 2015;**16**:9.

Giaginis C, Papadopouli A, Zira A, Katsargyris A, Klonaris C, Theocharis S. Correlation of plasma osteoprotegerin (OPG) and receptor activator of the nuclear factor κ B ligand (RANKL) levels with clinical risk factors in patients with advanced carotid atherosclerosis. *Med Sci Monit* 2012;**18**:CR597-604.

Gochuico BR, Zhang J, Ma BY, Marshak-Rothstein A, Fine A. TRAIL expression in vascular smooth muscle. *Am J Physiol Lung Cell Mol Physiol* 2000;**278**:L1045-1050.

Goettsch C, Rauner M, Hamann C, Sinnigen K, Hempel U, Bornstein SR, Hofbauer LC. Nuclear factor of activated T cells mediates oxidised LDL-induced calcification of vascular smooth muscle cells. *Diabetologia* 2011;**54**:2690-2701.

Golub EE, Boesze-Battaglia K. The role of alkaline phosphatase in mineralization. *Curr Opin Orthopaedics* 2007;**18**:444-448.

Gotsman I, Sharpe AH, Lichtman AH. T-cell costimulation and coinhibition in atherosclerosis. *Circ Res* 2008;**103**:1220-1231.

Gozzelino R, Jeney V, Soares MP. Mechanisms of cell protection by heme oxygenase-1. *Annu Rev Pharmacol Toxicol* 2010;**50**:323-354.

Greenbaum D, Colangelo C, Williams K, Gerstein M. Comparing protein abundance and mRNA expression levels on a genomic scale. *Genome Biol* 2003;**4**:117.

Guicciardi ME, Gores GJ. Life and death bly receptors. *FASEB J* 2009;**23**:1625-1637.

Guinan AF, Rochfort KD, Fitzpatrick PA, Walsh TG, Pierotti AR, Phelan S, Murphy RP, Cummins PM. Shear stress is a positive regulator of thimet oligopeptidase (EC3.4.24.15) in vascular endothelial cells: consequences for MHC1 levels. *Cardiovasc Res* 2013;**99**:545-554.

Gustafsson AC, Kupersmidt I, Edlundh-Rose E, Greco G, Serafino A, Krasnowska EK, Lundeberg T, Bracci-Laudiero L, Romano MC, Parasassi T, Lundeberg J. Global gene expression analysis in time series following N-acetyl L-cysteine induced epithelial differentiation of human normal and cancer cells in vitro. *BMC Cancer* 2005;**5**:75.

Guzik TJ, Mussa S, Gastaldi D, Sadowski J, Ratnatunga C, Pillai R, Channon KM. Mechanisms of increased vascular superoxide production in human diabetes mellitus Role of NAD(P)H oxidase and endothelial nitric oxide synthase. *Circulation* 2002;**105**:1656-1662.

Hadi H, Suwaidi JA. Endothelial dysfunction in diabetes mellitus. *Vasc Health Risk Manag* 2007;**3**:853-876.

Halleen JM, Räsänen S, Salo JJ, Reddy SV, Roodman GD, Hentunen TA, Lehenkari PP, Kaija H, Vihko P, Väänänen HK. Intracellular fragmentation of bone resorption products by reactive

oxygen species generated by osteoclastic tartrate-resistant acid phosphatase. *J Biol Chem* 1999;**274**:22907-22910.

Harith HH, Di Bartolo BA, Cartland S, Genner S, Kavurma MM. Insulin promotes vascular smooth muscle cell proliferation and apoptosis via differential regulation of tumor necrosis factor-related apoptosis-inducing ligand. *J Diabetes* 2016;**8**:568-578.

Harper E, Forde H, Davenport C, Rochfort KD, Smith D, Cummins PM. Vascular calcification in type-2 diabetes and cardiovascular disease: Integrative roles for OPG, RANKL and TRAIL. *Vascul Pharmacol* 2016;**82**:30-40.

Harper E, Rochfort KD, Forde H, Davenport C, Smith D, Cummins PM. Activation of the non-canonical NF- κ B/p52 pathway in vascular endothelial cells by RANKL elicits pro-calcific signalling in co-cultured smooth muscle cells. *Cell Signal* 2018;**47**:142-150.

Harper E, Rochfort KD, Forde H, Davenport C, Smith D, Cummins PM. TRAIL attenuates RANKL-mediated osteoblastic signalling in vascular cell mono-culture and co-culture models. *PLoS One* 2017;**12**:e0188192.

Harris MI. Diabetes in America: epidemiology and scope of the problem. *Diabetes Care* 1998;**21**:C11–C14.

Harrison TA, Hindorff LA, Kim H, Wines RC, Bowen DJ, McGrath BB, Edwards KL. Family history of diabetes as a potential public health tool. *Am J Prev Med* 2003;**24**:152-159.

Hashizume M, Hayakawa N, Suzuki M, Mihara M. IL-6/sIL-6R trans-signalling, but not TNF- α induced angiogenesis in a HUVEC and synovial cell co-culture system. *Rheumatol Int* 2009;**29**:1449–1454.

Hausenloy DJ, Yellon DM. New directions for protecting the heart against ischaemia–reperfusion injury: targeting the Reperfusion Injury Salvage Kinase (RISK)-pathway. *Cardiovasc Res* 2004;**61**:448-460.

Hayden MR, Tyagi SC, Kolb L, Sowers JR, Khanna R. Vascular ossification-calcification in metabolic syndrome, type 2 diabetes mellitus, chronic kidney disease, and calciphylaxis-calcific uremic arteriopathy: the emerging role of sodium thiosulfate. *Cardiovasc Diabetol* 2005;**4**:4.

Hayman AR, Bune AJ, Bradley JR, Rashbass J, Cox TM. Osteoclastic tartrate-resistant acid phosphatase (Acp 5): its localization to dendritic cells and diverse murine tissues. *J Histochem Cytochem* 2000;**48**:219-228.

Hayman AR, Jones SJ, Boyde A, Foster D, Colledge WH, Carlton MB, Evans MJ, Cox TM. Mice lacking tartrate-resistant acid phosphatase (Acp 5) have disrupted endochondral ossification and mild osteopetrosis. *Development* 1996;**122**:3151-3162.

He T, Peterson TE, Holmuhamedov EL, Terzic A, Caplice NM, Oberley LW, Katusic ZS. Human endothelial progenitor cells tolerate oxidative stress due to intrinsically high expression of manganese superoxide dismutase. *Arterioscler Thromb Vasc Biol* 2004;**24**:2021-2027.

- Healy S, Khan P, Davie JR. Immediate early response genes and cell transformation. *Pharmacol Therap* 2013;**137**:64-77.
- Helas S, Goettsch C, Schoppet M, Zeitz U, Hempel U, Morawietz H, Kostenuik PJ, Erben RG, Hofbauer LC. Inhibition of receptor activator of NF-kappaB ligand by denosumab attenuates vascular calcium deposition in mice. *Am J Pathol* 2009;**175**:473-478.
- Hénaut L, Massy ZA. New insights into the key role of interleukin 6 in vascular calcification of chronic kidney disease. *Nephrol Dial Transplant* 2018. doi: 10.1093/ndt/gfx379 [Epub ahead of print].
- Hénaut L, Sanz AB, Martin-Sanchez D, Carrasco S, Villa-Bellosta R, Aldamiz-Echevarria G, Massy ZA, Sanchez-Nino MD, Ortiz A. TWEAK favors phosphate-induced calcification of vascular smooth muscle cells through canonical and non-canonical activation of NFκB. *Cell Death Dis* 2016;**7**:e:2305.
- Higashi Y, Noma K, Yoshizumi M, Kihara Y. Endothelial function and oxidative stress in cardiovascular diseases. *Circ J* 2009;**73**:411-418.
- Higgins CL, Isbilir S, Basto P, Chen IY, Vaduganathan M, Vaduganathan P, Reardon MJ, Lawrie G, Peterson L, Morrisett JD. Distribution of alkaline phosphatase, osteopontin, rank ligand and osteoprotegerin in calcified human carotid atheroma. *Protein J* 2015;**34**:315-328.
- Ho E, Chen G, Bray TM. Supplementation of N-acetylcysteine inhibits NFkappaB activation and protects against alloxan-induced diabetes in CD-1 mice. *FASEB J* 1999;**13**:1845-1854.
- Hofbauer LC, Schoppet M. Clinical implications of the osteoprotegerin/RANKL/RANK system for bone and vascular diseases. *JAMA* 2004;**292**:490-495.
- Hoffmann A, Natoli G, Ghosh G. Transcriptional regulation via the NFκB signaling module. *Oncogene* 2006;**25**:6706–6716.
- Hruska KA, Mathew S, Saab G. Bone morphogenetic proteins in vascular calcification. *Circ Res* 2005;**97**:105-114.
- Huang J, Yuan L, Wang X, Zhang TL, Wang K. Icaritin and its glycosides enhance osteoblastic, but suppress osteoclastic, differentiation and activity in vitro. *Life Sci* 2007;**81**:832-840.
- Huang RL, Yuan Y, Zou GM, Liu G, Tu J, Li Q. LPS-stimulated inflammatory environment inhibits BMP-2-induced osteoblastic differentiation through crosstalk between TLR4/MyD88/NF-κB and BMP/Smad signaling. *Stem Cells Dev* 2014;**23**:277-289.
- Huh YJ, Kim JM, Kim H, Song H, So H, Lee SY, Kwon SB, Kim HJ, Kim HH, Lee SH, Choi Y, Chung SC, Jeong DW, Min BM. Regulation of osteoclast differentiation by the redox-dependent modulation of nuclear import of transcription factors. *Cell Death Differ* 2006;**13**:1138-1146.
- Hui M, Tenenbaum HC. New face of an old enzyme: alkaline phosphatase may contribute to human tissue aging by inducing tissue hardening and calcification. *Anat Rec* 1998;**253**:91-94.

- Hummel SG, Fischer AJ, Martin SM, Schafer FQ, Buettner GR. Nitric oxide as a cellular antioxidant: a little goes a long way. *Free Radic Biol Med* 2006;**40**:501-506.
- Hunter GK, Goldberg HA. Modulation of crystal formation by bone phosphoproteins: role of glutamic acid-rich sequences in the nucleation of hydroxyapatite by bone sialoprotein. *Biochem J* 1994;**302**:175-179.
- Hussein, RM. Biochemical relationships between bone turnover markers and blood glucose in patients with type 2 diabetes mellitus. *Diabetes Metab Syndr* 2017;**11 Supp1**:S369-372.
- Huxford T, Malek S, Ghosh G. Structure and Mechanism in NF- κ B/I κ B Signaling. *Cold Spring Harb Symp Quant Biol* 1999;**64**:533-540.
- Ighodaro OM, Akinloye OA. First line defence antioxidants-superoxide dismutase (SOD), catalase (CAT) and glutathione peroxidase (GPX): Their fundamental role in the entire antioxidant defence grid. *Alex J Med* 2017. In Press, Corrected Proof. Available at: <https://doi.org/10.1016/j.ajme.2017.09.001> [Accessed 9 May 2018].
- Iijima K, Ito Y, Son BK, Akishita M, Ouchi Y. Pravastatin and olmesartan synergistically ameliorate renal failure-induced vascular calcification. *J Atheroscler Thromb* 2014;**21**:917-929.
- Ikeda K, Souma Y, Akakabe Y, Kitamura Y, Matsuo K, Shimoda Y, Ueyama T, Matoba S, Yamada H, Okigaki M, Matsubara H. Macrophages play a unique role in the plaque calcification by enhancing the osteogenic signals exerted by vascular smooth muscle cells. *Biochem Biophys Res Commun* 2012;**425**:39-44.
- Ikeda T, Kasai M, Utsuyama M, Hirokawa K. Determination of three isoforms of the receptor activator of nuclear factor-kappaB ligand and their differential expression in bone and thymus. *Endocrinology* 2001;**142**:1419-1426.
- Illiandri O, Sujuti H, Permatasari N, Soeharto S. Moderate Concentrations of TNF- α Induce BMP-2 Expression in Endothelial Cells. *Int J Pharm Clin Res* 2016;**8**:1669-1672.
- Israël A. The IKK Complex, a Central Regulator of NF- κ B Activation. *Cold Spring Harb Perspect Biol* 2010;**2**:a000158.
- Jang WG, Kim EJ, Kim DK, Ryoo HM, Lee KB, Kim SH, Choi HS, Koh JT. BMP2 protein regulates osteocalcin expression via Runx2-mediated Atf6 gene transcription. *J Biol Chem* 2012;**287**:905-915.
- Jeney V, Balla J, Yachie A, Varga Z, Vercellotti GM, Eaton JW, Balla G. Pro-oxidant and cytotoxic effects of circulating heme. *Blood* 2002;**100**:879-887.
- Jimi E, Aoki K, Saito H, D'Acquisto F, May MJ, Nakamura I, Sudo T, Kojima T, Okamoto F, Fukushima H, Okabe K, Ohya K, Ghosh S. Selective inhibition of NF-kappa B blocks osteoclastogenesis and prevents inflammatory bone destruction in vivo. *Nat Med* 2004;**10**:617-624.

Johnson RC, Leopold JA, Loscalzo J. Vascular calcification: pathobiological mechanisms and clinical implications. *Circ Res* 2006;**99**:1044-1059.

Joshi FR, Rajani NK, Abt M, Woodward M, Bucarius J, Mani V, Tawakol A, Kallend D, Fayad ZA, Rudd JH. Does Vascular Calcification Accelerate Inflammation?: A Substudy of the dal-PLAQUE Trial. *J Am Coll Cardiol* 2016;**67**:69-78.

Juan SH, Lee TS, Tseng KW, Liou JY, Shyue SK, Wu KK, Chau LY. Adenovirus-mediated heme oxygenase-1 gene transfer inhibits the development of atherosclerosis in apolipoprotein E-deficient mice. *Circulation* 2001;**104**:1519-1525.

Jun JH, Lee SH, Kwak HB, Lee ZH, Seo SB, Woo KM, Ryoo HM, Kim GS, Baek JH. N-acetylcysteine stimulates osteoblastic differentiation of mouse calvarial cells. *J Cell Biochem* 2008;**103**:1246-1255.

Jung CH, Lee WY, Kim SY, Jung JH, Rhee EJ, Park CY, Mok JO, Oh KW, Kim CH, Park SW, Kim SW. The relationship between coronary artery calcification score, plasma osteoprotegerin level and arterial stiffness in asymptomatic type 2 DM. *Acta Diabetol* 2010;**47**:145-152.

Jung EM, Lim JH, Lee TJ, Park JW, Choi KS, Kwon TK. Curcumin sensitizes tumor necrosis factor-related apoptosis-inducing ligand (TRAIL)-induced apoptosis through reactive oxygen species-mediated upregulation of death receptor 5 (DR5). *Carcinogenesis* 2005;**26**:1905-1913.

Kaden JJ, Bickelhaupt S, Grobholz R, Haase KK, Sarikoç A, Kiliç R, Brueckmann M, Lang S, Zahn I, Vahl C, Hagl S, Dempfle CE, Borggreffe M. Receptor activator of nuclear factor kappaB ligand and osteoprotegerin regulate aortic valve calcification. *J Mol Cell Cardiol* 2004;**36**:57-66.

Kamohara H, Matsuyama W, Shimozato O, Abe K, Galligan C, Hashimoto SI, Matsushima K, Yoshimura T. Regulation of tumour necrosis factor-related apoptosis-inducing ligand (TRAIL) and TRAIL receptor expression in human neutrophils. *Immunol* 2004;**111**:186-194.

Kang IS, Kim C. NADPH oxidase gp91phox contributes to RANKL-induced osteoclast differentiation by upregulating NFATc1. *Sci Rep* 2016;**6**:38014.

Kang YH, Park MG, Noh KH, Park HR, Lee HW, Son SM, Park, KP. Low serum TNF-related apoptosis-inducing ligand (TRAIL) levels are associated with acute ischemic stroke severity. *Atherosclerosis* 2015;**240**:228-233.

Kapustin A, Shanahan CM. Targeting vascular calcification: softening-up a hard target. *Curr Opin Pharmacol* 2009;**9**:84-89.

Kauffmanstein G, Pizard A, Le Corre Y, Vessières E, Grimaud L, Toutain B, Labat C, Murras Y, Gorgels TG, Bergen AA, Le Saux O, Lacolley P, Lefthériotis G, Henrion D, Martin L. Disseminated arterial calcification and enhanced myogenic response are associated with abcc6 deficiency in a mouse model of pseudoxanthoma elasticum. *Arterioscler Thromb Vasc Biol* 2014;**34**:1045-1056.

- Kavurma MM, Schoppet M, Bobryshev YV, Khachigian LM, Bennett MR. TRAIL stimulates proliferation of vascular smooth muscle cells via activation of NF-kappaB and induction of insulin-like growth factor-1 receptor. *J Biol Chem* 2008;**283**:7754-7762.
- Kawano N, Mori K, Emoto M, Lee E, Kobayashi I, Yamazaki Y, Urata H, Morioka T, Koyama H, Shoji T, Nishizawa Y, Inaba M. Association of serum TRAIL levels with atherosclerosis in patients with type 2 diabetes mellitus. *Diabetes Res Clin Pract* 2011;**91**:316-320.
- Kayagaki N, Yamaguchi N, Nakayama M, Eto H, Okumura K, Yagita H. Type I interferons (IFNs) regulate tumor necrosis factor-related apoptosis-inducing ligand (TRAIL) expression on human T cells: A novel mechanism for the antitumor effects of type I IFNs. *J Exp Med* 1999;**189**:1451-1460.
- Kayama Y, Raaz U, Jagger A, Adam M, Schellinger IN, Sakamoto M, Suzuki H, Toyama K, Spin JM, Tsao PS. Diabetic cardiovascular disease induced by oxidative stress. *Int J Mol Sci* 2015;**16**:25234-25263.
- Kearns AE, Khosla S, Kostenuik PJ. Receptor activator of nuclear factor kappaB ligand and osteoprotegerin regulation of bone remodeling in health and disease. *Endocr Rev* 2008;**29**:155-192.
- Kerkar S, Williams M, Blocksom JM, Wilson RF, Tyburski JG, Steffes CP. TNF-alpha and IL-1beta increase pericyte/endothelial cell co-culture permeability. *J Surg Res* 2006;**132**:40-45.
- Khavandgar Z, Roman H, Li J, Lee S, Vali H, Brinckmann J, Davis EC, Murshed M. Elastin haploinsufficiency impedes the progression of arterial calcification in MGP-deficient mice. *J Bone Miner Res* 2014;**29**:327-337.
- Kim CW, Song H, Kumar S, Nam D, Kwon HS, Chang KH, Son DJ, Kang DW, Brodie SA, Weiss D, Vega JD, Alberts-Grill N, Griendling K, Taylor WR, Jo H. Anti-inflammatory and antiatherogenic role of BMP receptor II in endothelial cells. *Arterioscler Thromb Vasc Biol* 2013;**33**:1350-1359.
- Kim JY, Morgan M, Kim DG, Lee JY, Bai L, Lin Y, Liu ZG, Kim YS. TNF α induced noncanonical NF- κ B activation is attenuated by RIP1 through stabilization of TRAF2. *J Cell Sci* 2011;**124**:647-656.
- Kim M, Park SY, Pai HS, Kim TH, Billiar TR, Seol DW. Hypoxia inhibits tumor necrosis factor-related apoptosis-inducing ligand-induced apoptosis by blocking Bax translocation. *Cancer res* 2004;**64**:4078-4081.
- Kim MS, Ramakrishna S, Lim KH, Kim JH, Baek KH. Protein stability of mitochondrial superoxide dismutase SOD2 is regulated by USP36. *J Cell Biochem* 2011;**112**:498-508.
- Kim MS, Yang YM, Son A, Tian YS, Lee SI, Kang SW, Muallem S, Shin DM. RANKL-mediated reactive oxygen species pathway that induces long lasting Ca²⁺ oscillations essential for osteoclastogenesis. *J Biol Chem* 2010;**285**:6913-6921.

- Kim YS, Morgan MJ, Choksi S, Liu ZG. TNF-induced activation of the Nox1 NADPH oxidase and its role in the induction of necrotic cell death. *Mol Cell* 2007;**26**:675-687.
- Knirsch L, Clerch LB. Tyrosine phosphorylation regulates manganese superoxide dismutase (MnSOD) RNA-binding protein activity and MnSOD protein expression. *Biochemistry* 2001;**40**:7890-7895.
- Kong YY, Yoshida H, Sarosi I, Tan HL, Timms E, Capparelli C, Morony S, Oliveira-dos-Santos AJ, Van G, Itie A, Khoo W, Wakeham A, Dunstan CR, Lacey DL, Mak TW, Boyle WJ, Penninger JM. OPG is a key regulator of osteoclastogenesis, lymphocyte development and lymph-node organogenesis. *Nature* 1999;**397**:315-323.
- Kostenuik PJ, Nguyen HQ, McCabe J, Warmington KS, Kurahara C, Sun N, Chen C, Li L, Cattley RC, Van G, Scully S, Elliott R, Grisanti M, Morony S, Tan HL, Asuncion F, Li X, Ominsky MS, Stolina M, Dwyer D, Dougall WC, Hawkins N, Boyle WJ, Simonet WS, Sullivan JK. Denosumab, a fully human monoclonal antibody to RANKL, inhibits bone resorption and increases BMD in knock-in mice that express chimeric (murine/human) RANKL. *J Bone Miner Res* 2009;**24**:182-195.
- Krause C, Guzman A, Knaus P. Noggin. *Int J Biochem Cell Biol* 2011;**43**:478-481.
- Kurozumi A, Nakano K, Yamagata K, Okada Y, Nakayamada S, Tanaka Y. IL-6/STAT3 pathway is critically involved in vascular calcification via histone modification of the RUNX2 promoter in vascular smooth muscle cells. *Bone Abstracts* 2016;**5**:425.
- Kwan TS, Padrines M, Théoleyre S, Heymann D, Fortun Y. IL-6, RANKL, TNF-alpha/IL-1: interrelations in bone resorption pathophysiology. *Cytokine Growth Factor Rev* 2004;**15**:49-60.
- Lacey DL, Boyle WJ, Simonet WS, Kostenuik PJ, Dougall WC, Sullivan JK, San Martin J, Dansey R. Bench to bedside: elucidation of the OPG-RANK-RANKL pathway and the development of denosumab. *Nat Rev Drug Discov* 2012;**11**:401-419.
- Lacey DL, Timms E, Tan HL, Kelley MJ, Dunstan CR, Burgess T, Elliott R, Colombero A, Elliott G, Scully S, Hsu H, Sullivan J, Hawkins N, Davy E, Capparelli C, Eli A, Qian YX, Kaufman S, Sarosi I, Shalhoub V, Senaldi G, Guo J, Delaney J, Boyle WJ. Osteoprotegerin ligand is a cytokine that regulates osteoclast differentiation and activation. *Cell* 1998;**93**:165-176.
- Laemmli UK. Cleavage of structural proteins during the assembly of the head of bacteriophage T4. *Nature* 1970;**227**:680-685.
- Landry DB, Couper LL, Bryant SR, Lindner V. Activation of the NF-kappa B and I kappa B system in smooth muscle cells after rat arterial injury. Induction of vascular cell adhesion molecule-1 and monocyte chemoattractant protein-1. *Am J Pathol* 1997;**151**:1085-1095.
- Langenbach F, Handschel J. Effects of dexamethasone, ascorbic acid and β -glycerophosphate on the osteogenic differentiation of stem cells in vitro. *Stem Cell Res Ther* 2013;**4**:117.

- Lassègue B, Griendling KK. NADPH oxidases: functions and pathologies in the vasculature. *Arterio Thromb Vasc Biol* 2010;**30**:653-661.
- Lau KW, Baylink DJ. Osteoblastic Tartrate-Resistant Acid Phosphatase: Its Potential Role in the Molecular Mechanism of Osteogenic Action of Fluoride. *J Bone Min Res* 2003;**18**:1897-1900.
- Lavrovsky Y, Schwartzman ML, Levere RD, Kappas A, Abraham NG. Identification of binding sites for transcription factors NF-kappa B and AP-2 in the promoter region of the human heme oxygenase 1 gene. *Proc Nat Acad Sci* 1994;**91**:5987-5991.
- Lee HL, Woo KM, Ryoo HM, Baek JH. Tumor necrosis factor-alpha increases alkaline phosphatase expression in vascular smooth muscle cells via MSX2 induction. *Biochem Biophys Res Commun* 2010;**391**:1087-1092.
- Lee MH, Kwon TG, Park HS, Wozney JM, Ryoo HM. BMP-2-induced Osterix expression is mediated by Dlx5 but is independent of Runx2. *Biochem Biophys Res Com* 2003;**309**:689-694.
- Lee MW, Park SC, Kim JH, Kim IK, Han KS, Kim KY, Lee WB, Jung YK, Kim SS. The involvement of oxidative stress in tumor necrosis factor (TNF)-related apoptosis-inducing ligand (TRAIL)-induced apoptosis in HeLa cells. *Cancer Letters* 2002;**182**:75-82.
- Lee NK, Choi YG, Baik JY, Han SY, Jeong DW, Bae YS, Kim N, Lee SY. A crucial role for reactive oxygen species in RANKL-induced osteoclast differentiation. *Blood* 2005;**106**:852-859.
- Lehto S, Niskanen L, Suhonen M, Ronnema T, Laakso M. Medial artery calcification. A neglected harbinger of cardiovascular complications in non-insulin-dependent diabetes mellitus. *Arterioscler Thromb Vasc Biol* 1996;**16**:978-983.
- Lenglet S, Quercioli A, Fabre M, Galan K, Pelli G, Nencioni A, Bauer I, Pende A, Python M, Bertolotto M, Spinella G, Pane B, Palombo D, Dallegri F, Mach F, Vuilleumier N, Montecucco F. Statin treatment is associated with reduction in serum levels of receptor activator of NF- κ B ligand and neutrophil activation in patients with severe carotid stenosis. *Mediators Inflamm* 2014. Available at: <https://doi.org/10.1155/2014/720987> [Accessed 8 May 2018].
- Leopold JA. Vascular calcification: Mechanisms of vascular smooth muscle cell calcification. *Trends Cardiovasc Med* 2015;**25**:267-274.
- Levine B, Kalman J, Mayer L, Fillit HM, Packer M. Elevated circulating levels of tumor necrosis factor in severe chronic heart failure. *N Engl J Med* 1990;**323**:236-241.
- Li H, Cheng Y, Simoncini T, Xu S. 17 β -Estradiol inhibits TNF- α -induced proliferation and migration of vascular smooth muscle cells via suppression of TRAIL. *Gynecol Endocrinol* 2016;**32**:581-586.
- Li J, Yuan J. Caspases in apoptosis and beyond. *Oncogene* 2008;**27**:6194-6206.
- Li JH, Kirkiles-Smith NC, McNiff JM, Pober JS. TRAIL induces apoptosis and inflammatory gene expression in human endothelial cells. *J Immunol* 2003;**171**:1526-1533.

- Li JM, Fan LM, Christie MR, Shah AM. Acute tumor necrosis factor alpha signaling via NADPH oxidase in microvascular endothelial cells: role of p47phox phosphorylation and binding to TRAF4. *Mol Cell Biol* 2005;**25**:2320-2330.
- Li JM, Mullen AM, Yun S, Wientjes F, Brouns GY, Thrasher AJ, Shah AM. Essential role of the NADPH oxidase subunit p47(phox) in endothelial cell superoxide production in response to phorbol ester and tumor necrosis factor-alpha. *Circ Res* 2002;**90**:143-150.
- Li JM, Shah AM. Endothelial cell superoxide generation: regulation and relevance for cardiovascular pathophysiology. *Am J Physiol Regul Integr Comp Physiol* 2004;**287**:R1014-1030.
- Li Q, Lin Y, Wang S, Zhang L, Guo L. GLP-1 Inhibits High-Glucose-Induced Oxidative Injury of Vascular Endothelial Cells. *Sci Rep* 2017;**7**:8008.
- Li X, Han WQ, Boini KM, Xia M, Zhang Y, Li PL. TRAIL death receptor 4 signaling via lysosome fusion and membrane raft clustering in coronary arterial endothelial cells: evidence from ASM knockout mice. *J Mol Med* 2013;**91**:25-36.
- Liao J, Hu N, Zhou N, Lin L, Zhao C, Yi S, Fan T, Bao W, Liang X, Chen H, Xu W, Chen C, Cheng Q, Zeng Y, Si W, Yang Z, Huang W. Sox9 potentiates BMP2-induced chondrogenic differentiation and inhibits BMP2-induced osteogenic differentiation. *PLoS One* 2014;**9**:e89025.
- Lieberman M, Johnson RC, Handy DE, Loscalzo J, Leopold JA. Bone morphogenetic protein-2 activates NADPH oxidase to increase endoplasmic reticulum stress and human coronary artery smooth muscle cell calcification. *Biochem Biophys Res Commun* 2011;**413**:436-441.
- Lieberman M, Pesaro AE, Carmo LS, Serrano CV Jr. Vascular calcification: pathophysiology and clinical implications. *Einstein (Sao Paulo)* 2013;**11**:376-382.
- Lin ME, Chen T, Leaf EM, Speer MY, Giachelli CM. Runx2 Expression in Smooth Muscle Cells Is Required for Arterial Medial Calcification in Mice. *Am J Pathol* 2015;**185**:1958-1969.
- Linder HC, Ek-Rylander B, Krumpel M, Norgård M, Narisawa S, Millán JL, Andersson G, Magnusson P. Bone Alkaline Phosphatase and Tartrate-Resistant Acid Phosphatase: Potential Co-regulators of Bone Mineralization. *Calcif Tissue Int* 2017;**101**:92-101.
- Liu F, Zhong H, Liang JY, Fu P, Luo ZJ, Zhou L, Gou R, Huang J. Effect of high glucose levels on the calcification of vascular smooth muscle cells by inducing osteoblastic differentiation and intracellular calcium deposition via BMP-2/Cbfa-1 pathway. *J Zhejiang Univ Sci B* 2010;**11**:905-911.
- Liu GY, Liang QH, Cui RR, Liu Y, Wu SS, Shan PF, Yuan LQ, Liao EY. Leptin promotes the osteoblastic differentiation of vascular smooth muscle cells from female mice by increasing RANKL expression. *Endocrinology* 2014;**155**:558-567.
- Liu H, Yuan L, Xu S, Wang K. Endothelial cell and macrophage regulation of vascular smooth muscle cell calcification modulated by cholestane-3beta, 5alpha, 6beta-triol. *Cell Biol Int* 2007;**31**:900-907.

- Liu M, Xiang G, Lu J, Xiang L, Dong J, Mei W. TRAIL protects against endothelium injury in diabetes via Akt-eNOS signaling. *Atherosclerosis* 2014;**237**:718-724.
- Liu T, Zhang L, Joo D, Sun S. NF- κ B signaling in inflammation. *Sig Trans Targ Ther* 2017;**2**:17023.
- Livak KJ, Schmittgen TD. Analysis of relative gene expression data using realtime quantitative PCR and the 2(-Delta Delta C(T)) Method. *Methods* 2001;**25**:402-408.
- Lodi F, Winterbone MS, Tribolo S, Needs PW, Hughes DA, Kroon PA. Human quercetin conjugated metabolites attenuate TNF- α -induced changes in vasomodulatory molecules in an HUASMCs/HUVECs co-culture model. *Planta Med* 2012;**78**:1571-1573.
- Loncar G, Bozic B, Cvorovic V, Radojicic Z, Dimkovic S, Markovic N, Prodanovic N, Lepic T, Putnikovic B, Popovic-Brkic V. Relationship between RANKL and neuroendocrine activation in elderly males with heart failure. *Endocrine* 2010;**37**:148-156.
- Looma RS, Arora R. Statin therapy and aortic stenosis: a systematic review of the effects of statin therapy on aortic stenosis. *Am J Ther* 2010;**17**:e110-114.
- Luan X, Lu Q, Jiang Y, Zhang S, Wang Q, Yuan H, Zhao W, Wang J, Wang X. Crystal structure of human RANKL complexed with its decoy receptor osteoprotegerin. *J Immunol* 2012;**189**:245-252.
- Luo G, Ducy P, McKee MD, Pinero GJ, Loyer E, Behringer RR, Karsenty G. Spontaneous calcification of arteries and cartilage in mice lacking matrix GLA protein. *Nature* 1997;**386**:78-81.
- Luo XH, Zhao LL, Yuan LQ, Wang M, Xie H, Liao EY. Development of arterial calcification in adiponectin-deficient mice: adiponectin regulates arterial calcification. *J Bone Miner Res* 2009;**24**:1461-1468.
- Mackey RH, Venkitachalam L, Sutton-Tyrrell K. Calcifications, arterial stiffness and atherosclerosis. *Adv Cardiol* 2007;**44**:234-244.
- Madamanchi NR, Runge MS. Mitochondrial dysfunction in atherosclerosis. *Circ Res* 2007;**100**:460-473.
- Madamanchi NR, Vendrov A, Runge MS. Oxidative stress and vascular disease. *Arterio Thromb Vasc Biol* 2005;**25**:29-38.
- Mafong DD, Henry RR. Exenatide as a treatment for diabetes and obesity: implications for cardiovascular risk reduction. *Curr Atheroscler Rep* 2008;**10**:55-60.
- Mahavadi S, Sriwai W, Manion O, Grider JR, Murthy KS. Diabetes-induced oxidative stress mediates upregulation of RhoA/Rho kinase pathway and hypercontractility of gastric smooth muscle. *PLoS One* 2017;**12**:e0178574.
- Maheswari E, Saraswathy GR, Santhranii T. Hepatoprotective and antioxidant activity of N-acetyl cysteine in carbamazepine-administered rats. *Indian J Pharmacol* 2014;**46**:211-215.

- Malyankar UM, Scatena M, Suchland KL, Yun TJ, Clark EA, Giachelli CM. Osteoprotegerin is an alpha v beta 3-induced, NF-kappa B-dependent survival factor for endothelial cells. *J Biol Chem* 2000;**275**:20959-20962.
- Mandal CC, Ganapathy S, Gorin Y, Mahadev K, Block K, Abboud HE, Harris SE, Ghosh-Choudhury G, Ghosh-Choudhury N. Reactive oxygen species derived from Nox4 mediate BMP2 gene transcription and osteoblast differentiation. *Biochem J* 2011;**433**:393-402.
- Mann GE, Yudilevich DL, Sobrevia L. Regulation of amino acid and glucose transporters in endothelial and smooth muscle cells. *Physiol Rev* 2003;**83**:183-252.
- Mao CY, Wang YG, Zhang X, Zheng XY, Tang TT, Lu EY. Double-edged-sword effect of IL-1 β on the osteogenesis of periodontal ligament stem cells via crosstalk between the NF- κ B, MAPK and BMP/Smad signaling pathways. *Cell Death Dis* 2016;**7**:e2296.
- Marcos-Ramiro B, García-Weber D, Millán J. TNF-induced endothelial barrier disruption: beyond actin and Rho. *Thromb Haemost* 2014;**112**:1088-1102.
- Mathew S, Davies M, Lund R, Saab G, Hruska KA. Function and effect of bone morphogenetic protein-7 in kidney bone and the bone-vascular links in chronic kidney disease. *Eur J Clin Invest* 2006;**36Suppl2**:43-50.
- McCullough PA, Agrawal V, Danielewicz E, Abela GS. Accelerated atherosclerotic calcification and Monckeberg's sclerosis: a continuum of advanced vascular pathology in chronic kidney disease. *Clin J Am Soc Nephrol* 2008;**3**:1585-1598.
- McLaren JE, Michael DR, Ashlin TG, Ramji DP. Cytokines, macrophage lipid metabolism and foam cells: implications for cardiovascular disease therapy. *Prog Lipid Res* 2011;**50**:331-347.
- Mehrfhof FB, Schmidt-Ullrich R, Dietz R, Scheidereit C. Regulation of vascular smooth muscle cell proliferation: role of NF-kappaB revisited. *Circ Res* 2005;**96**:958-964.
- Meyer JW, Schmitt ME. A central role for the endothelial NADPH oxidase in atherosclerosis. *FEBS Letters* 2000;**472**:1-4.
- Miao L, St. Clair DK. Regulation of superoxide dismutase genes: implications in disease. *Free Rad Biol Med* 2009;**47**:344-356.
- Michowitz Y, Goldstein E, Roth A, Afek A, Abashidze A, Ben Gal Y, Keren G, George J. The involvement of tumor necrosis factor-related apoptosis-inducing ligand (TRAIL) in atherosclerosis. *J Am Coll Cardiol* 2005;**45**:1018-1024.
- Min J, Cho Y, Choi J, Kim Y, Kim JH, Yu YS, Rho J, Mochizuki N, Kim Y, Oh GT, Kwon Y. Receptor activator of nuclear factor (NF)- κ B ligand (RANKL) increases vascular permeability: impaired permeability and angiogenesis in eNOS-deficient mice. *Blood* 2007;**109**:1495-1502.
- Mirza S, Hossain M, Mathews C, Martinez P, Pino P, Gay JL, Rentfro A, McCormick JB, Fisher-Hoch SP. Type 2-diabetes is associated with elevated levels of TNF-alpha, IL-6 and

adiponectin and low levels of leptin in a population of Mexican Americans: a cross-sectional study. *Cytokine* 2012;**57**:136-142.

Miura Y, Tsujioka T, Nishimura Y, Sakaguchi H, Maeda M, Hayashi H, Dong M, Hyodoh F, Yata K, Wada H, Sugihara T, Otsuki T. TRAIL expression up-regulated by interferon-gamma via phosphorylation of STAT1 induces myeloma cell death. *Anticancer Res* 2006;**26**:4115-4124.

Miyazaki T, Tokimura F, Tanaka S. A review of denosumab for the treatment of osteoporosis. *Patient Prefer Adherence* 2014;**8**:463-471.

Mizobuchi M, Towler D, Slatopolsky E. Vascular calcification: the killer of patients with chronic kidney disease. *J Am Soc Nephrol* 2009;**20**:1453-1464.

Modur V, Zimmerman GA, Prescott SM, McIntyre TM. Endothelial cell inflammatory responses to tumor necrosis factor alpha. Ceramide-dependent and -independent mitogen-activated protein kinase cascades. *J Biol Chem* 1996;**271**:13094-13102.

Mody N, Parhami F, Sarafian TA, Demer LL. Oxidative stress modulates osteoblastic differentiation of vascular and bone cells. *Free Radic Biol Med* 2001;**31**:509-519.

Moe SM, Duan D, Doehle BP, O'Neill KD, Chen NX. Uremia induces the osteoblast differentiation factor Cbfa1 in human blood vessels. *Kidney Int* 2003;**63**:1003-1011.

Mohler ER, Gannon F, Reynolds C, Zimmerman R, Keane MG, Kaplan FS. Bone formation and inflammation in cardiac valves. *Circulation* 2001;**103**:1522-1528.

Moore KJ, Sheedy FJ, Fisher EA. Macrophages in atherosclerosis: a dynamic balance. *Nat Rev Immunol* 2013;**13**:709-721.

Morgan MJ, Liu ZG. Crosstalk of reactive oxygen species and NF- κ B signaling. *Cell Res* 2011;**21**:103-115.

Mori K, Ikari Y, Jono S, Shioi A, Ishimura E, Emoto M, Inaba M, Hara K, Nishizawa Y. Association of serum TRAIL level with coronary artery disease. *Thromb Res* 2010;**125**:322-325.

Mori K, Jono S, Emoto M, Kawagishi T, Yasumoto H, Konishi T, Furumitsu Y, Shioi A, Shoji T, Inaba M, Nishizawa Y. Effects of pravastatin on serum osteoprotegerin levels in patients with hypercholesterolemia and type 2 diabetes. *Angiology* 2010;**61**:86-91.

Morony S, Sage AP, Corbin T, Lu J, Tintut Y, Demer LL. Enhanced mineralization potential of vascular cells from SM22 α -Rankl (tg) mice. *Calcif Tissue Int* 2012;**91**:379-396.

Morony S, Tintut Y, Zhang Z, Cattley RC, Van G, Dwyer D, Stolina M, Kostenuik PJ, Demer LL. Osteoprotegerin inhibits vascular calcification without affecting atherosclerosis in *ldlr*^{-/-} mice. *Circulation* 2008;**117**:411-420.

Morrish NJ, Wang SL, Stevens LK, Fuller JH, Keen H. Mortality and causes of death in the WHO Multinational Study of Vascular Disease in Diabetes. *Diabetologica* 2001;**44**:S14-21.

- Moynagh PN. The NF κ B pathway. *J Cell Sci* 2005;**118**:4389–4392.
- Muscogiuri G, Salmon AB, Aguayo-Mazzucato C, Li M, Balas B, Guardado-Mendoza R, Giaccari A, Reddick RL, Reyna SM, Weir G, Defronzo RA, Van Remmen H, Musi N. Genetic disruption of SOD1 gene causes glucose intolerance and impairs β -cell function. *Diabetes* 2013;**62**:4201-4207.
- Muthu V. Vascular and renal problems associated with poorly controlled diabetes. *BMJ* 2013;**346**:f1911.
- Myers DE, Collier FM, Minkin C, Wang H, Holloway WR, Malakellis M, Nicholson GC. Expression of functional RANK on mature rat and human osteoclasts. *FEBS Letters* 1999;**463**:295-300.
- Nakagawa Y, Ikeda K, Akakabe Y, Koide M, Uraoka M, Yutaka KT, Kurimoto-Nakano R, Takahashi T, Matoba S, Yamada H, Okigaki M, Matsubara H. Paracrine osteogenic signals via bone morphogenetic protein-2 accelerate the atherosclerotic intimal calcification in vivo. *Arterioscler Thromb Vasc Biol* 2010;**30**:1908-1915.
- Nakao A, Fukushima H, Kajiya H, Ozeki S, Okabe K. RANKL-stimulated TNF α production in osteoclast precursor cells promotes osteoclastogenesis by modulating RANK signaling pathways. *Biochem Biophys Res Commun* 2007;**357**:945-950.
- Nakashima T, Hayashi M, Fukunaga T, Kurata K, Oh-Hora M, Feng JQ, Bonewald LF, Kodama T, Wutz A, Wagner EF, Penninger JM, Takayanagi H. Evidence for osteocyte regulation of bone homeostasis through RANKL expression. *Nat Med* 2011;**17**:1231-1234.
- Nakashima Y, Haneji T. Stimulation of Osteoclast Formation by RANKL Requires Interferon Regulatory Factor-4 and Is Inhibited by Simvastatin in a Mouse Model of Bone Loss. *PLoS One* 2013;**8**:e72033.
- Nakazato H, Deguchi M, Fujimoto M, Fukushima H. Alkaline phosphatase expression in cultured endothelial cells of aorta and brain microvessels: induction by interleukin-6-type cytokines and suppression by transforming growth factor betas. *Life Sci* 1997;**61**:2065-2072.
- Nam MH, Lee HS, Seomun Y, Lee Y, Lee KW. Monocyte-endothelium-smooth muscle cell interaction in co-culture: proliferation and cytokine productions in response to advanced glycation end products. *Biochim Biophys Acta* 2011;**1810**:907-912.
- Nasseem KM. The role of nitric oxide in cardiovascular diseases. *Mol Aspects Med* 2005;**26**:33-65.
- Ndip A, Wilkinson FL, Jude EB, Boulton AJ, Alexander MY. RANKL-OPG and RAGE modulation in vascular calcification and diabetes: novel targets for therapy. *Diabetologica* 2014;**57**:2251-2260.
- Ndip A, Williams A, Jude EB, Serracino-Inglott F, Richardson S, Smyth JV, Boulton AJ, Alexander MY. The RANKL/RANK/OPG signaling pathway mediates medial arterial calcification in diabetic Charcot neuroarthropathy. *Diabetes* 2011;**60**:2187-2196.

- Nedeljkovic ZS, Gokce N, Loscalzo J. Mechanisms of oxidative stress and vascular dysfunction. *Postgrad Med J* 2003;**79**:195-199.
- Neven E, Persy V, Dauwe S, De Schutter T, De Broe ME, D'Haese PC. Chondrocyte rather than osteoblast conversion of vascular cells underlies medial calcification in uremic rats. *Arterioscler Thromb Vasc Biol* 2010;**30**:1741-1750.
- Neves KR, Graciolli FG, dos Reis LM, Graciolli RG, Neves CL, Magalhães AO, Custódio MR, Batista DG, Jorgetti V, Moysés RM. Vascular calcification: contribution of parathyroid hormone in renal failure. *Kidney Int* 2007;**71**:1262-1270.
- Nguyen CH, Senfter D, Basilio J, Holzner S, Stadler S, Krieger S, Huttary N, Milovanovic D, Viola K, Simonitsch-Klupp I, Jäger W, de Martin R, Krupitza G. NF- κ B contributes to MMP1 expression in breast cancer spheroids causing paracrine PAR1 activation and disintegrations in the lymph endothelial barrier in vitro. *Oncotarget* 2015;**6**:39262–39275.
- Nguyen KQ, Olesen P, Ledet T, Rasmussen LM. Bone morphogenetic proteins regulate osteoprotegerin and its ligands in human vascular smooth muscle cells. *Endocrine* 2007;**32**:52-58.
- Nie B, Zhou SQ, Fang X, Zhang SY, Guan SM. The function and meaning of receptor activator of NF- κ B ligand in arterial calcification. *J Huazhong Univ Sci Technolog Med Sci* 2015;**35**:666-671.
- Niessner A, Hohensinner PJ, Rychli K, Neuhold S, Zorn G, Richter B, Hülsmann M, Berger R, Mörtl D, Huber K, Wojta J, Pacher R. Prognostic value of apoptosis markers in advanced heart failure patients. *Eur Heart J* 2009;**30**:789-796.
- Nishio Y, Dong Y, Paris M, O'Keefe RJ, Schwarz EM, Drissi H. Runx2-mediated regulation of the zinc finger Osterix/Sp7 gene. *Gene* 2006;**372**:62-70.
- Nitta K, Akiba T, Suzuki K, Uchida K, Watanabe R, Majima K, Aoki T, Nihei H. Effects of cyclic intermittent etidronate therapy on coronary artery calcification in patients receiving long-term hemodialysis. *Am J Kidney Dis* 2004;**44**:680-688.
- Novaro GM, Tiong IY, Pearce GL, Lauer MS, Sprecher DL, Griffin BP. Effect of hydroxymethylglutaryl coenzyme a reductase inhibitors on the progression of calcific aortic stenosis. *Circulation* 2001;**104**:2205-2209.
- O'Sullivan EP, Ashley DT, Davenport C, Devlin N, Crowley R, Agha A, Thompson CJ, O'Gorman D, Smith D. Osteoprotegerin and biomarkers of vascular inflammation in type 2 diabetes. *Diabetes Metab Res Rev* 2010;**26**:496-502.
- Oeckinghaus A, Ghosh S. The NF- κ B Family of Transcription Factors and Its Regulation. *Cold Spring Harb Perspect Biol* 2009;**1**:a000034.
- Oemar BS, Tschudi MR, Godoy N, Brovkovich V, Malinski T, Lüscher TF. Reduced endothelial nitric oxide synthase expression and production in human atherosclerosis. *Circulation* 1998;**97**:2494-2498.

- Ohashi M, Runge MS, Faraci FM, Heistad DD. MnSOD deficiency increases endothelial dysfunction in ApoE-deficient mice. *Arterio Thromb Vasc Biol* 2006;**26**:2331-2336.
- Oka S, Kamata H, Kamata K, Yagisawa H, Hirata H. N-acetylcysteine suppresses TNF-induced NF-kappaB activation through inhibition of IkappaB kinases. *FEBS Lett* 2000;**472**:196-202.
- Olesen M, Skov V, Mechta M, Mumm BH, Rasmussen LM. No influence of OPG and its ligands, RANKL and TRAIL, on proliferation and regulation of the calcification process in primary human vascular smooth muscle cells. *Mol Cell Endocrinol* 2012;**362**:149-156.
- Olesen P, Ledet T, Rasmussen LM. Arterial osteoprotegerin: increased amounts in diabetes and modifiable synthesis from vascular smooth muscle cells by insulin and TNF- α . *Diabetologica* 2005;**48**:561-568.
- Olson NC, Callas PW, Hanley AJ, Festa A, Haffner SM, Wagenknecht LE, Tracy RP. Circulating levels of TNF- α are associated with impaired glucose tolerance, increased insulin resistance, and ethnicity: the Insulin Resistance Atherosclerosis Study. *J Clin Endocrinol Metab* 2012;**97**:1032-1040.
- Omland T, Ueland T, Jansson AM, Persson A, Karlsson T, Smith C, Herlitz J, Aukrust P, Hartford M, Caidahl K. Circulating osteoprotegerin levels and long-term prognosis in patients with acute coronary syndromes. *J Am Coll Cardiol* 2008;**51**:627-633.
- Orimo H. The mechanism of mineralization and the role of alkaline phosphatase in health and disease. *J Nippon Med Sch* 2010;**77**:4-12.
- Osako MK, Nakagami H, Koibuchi N, Shimizu H, Nakagami F, Koriyama H, Shimamura M, Miyake T, Rakugi H, Morishita R. Estrogen inhibits vascular calcification via vascular RANKL system: common mechanism of osteoporosis and vascular calcification. *Circ Res* 2010;**107**:466-475.
- Otero JE, Chen T, Zhang K, Abu-Amer Y. Constitutively active canonical NF- κ B pathway induces severe bone loss in mice. *PLoS One* 2012;**7**:e38694.
- Padilla J, Jenkins NT, Lee S, Zhang H, Cui J, Zuidema MY, Zhang C, Hill MA, Perfield JW 2nd, Ibdah JA, Booth FW, Davis JW, Laughlin MH, Rector RS. Vascular transcriptional alterations produced by juvenile obesity in Ossabaw swine. *Physiol Genomics* 2013;**45**:434-446.
- Pamukcu B, Lip GY, Shantsila E. The nuclear factor--kappa B pathway in atherosclerosis: a potential therapeutic target for atherothrombotic vascular disease. *Thromb Res* 2011;**128**:117-123.
- Pan G, Ni J, Yu GL, Wei YF, Dixit VM. TRUNDD, a new member of the TRAIL receptor family that antagonizes TRAIL signalling. *FEBS Letters* 1998;**424**:41-45.
- Pan Q, Yu Y, Chen Q, Li C, Wu H, Wan Y, Ma J, Sun F. Sox9, a key transcription factor of bone morphogenetic protein-2-induced chondrogenesis, is activated through BMP pathway and a CCAAT box in the proximal promoter. *J Cell Physiol* 2008;**217**:228-241.

- Panizo S, Cardus A, Encinas M, Parisi E, Valcheva P, López-Ongil S, Coll B, Fernandez E, Valdivielso JM. RANKL increases vascular smooth muscle cell calcification through a RANK-BMP4-dependent pathway. *Circ Res* 2009;**104**:1041-1048.
- Papa S, Zazzeroni F, Pham CG, Bubici C, Franzoso G. Linking JNK signaling to NF-kappaB: a key to survival. *J Cell Sci* 2004;**117**:5197-5208.
- Papadopouli AE, Klonaris CN, Theocharis SE. Role of OPG/RANKL/RANK axis on the vasculature. *Histol Histopathol* 2008;**23**:497-506.
- Park KJ, Lee CH, Kim A, Jeong KJ, Kim CH, Kim YS. Death receptors 4 and 5 activate Nox1 NADPH oxidase through riboflavin kinase to induce reactive oxygen species-mediated apoptotic cell death. *J Biol Chem* 2012;**287**:3313-3325.
- Pasch A, Schaffner T, Huynh-Do U, Frey BM, Frey FJ, Farese S. Sodium thiosulfate prevents vascular calcifications in uremic rats. *Kidney Int* 2008;**74**:1444-1445.
- Patel H, Chen J, Das KC, Kavdia M. Hyperglycemia induces differential change in oxidative stress at gene expression and functional levels in HUVEC and HMVEC. *Cardiovasc Diabetol* 2013;**12**:142.
- Patel H, Zaghoul N, Lin K, Liu SF, Miller EJ, Ahmed M. Hypoxia-induced activation of specific members of the NF-kB family and its relevance to pulmonary vascular remodeling. *Int J Biochem Cell Biol* 2017;**92**:141-147.
- Patel J, Zhu D, Wheeler-Jones C, Arnett T, MacRae V, Orriss I. Differing mechanisms of mineralisation in vascular smooth muscle cells and osteoblasts. *Bone Abstracts* 2016;**5**:432.
- Patel S, Santini D. Role of NF-kappa B in the pathogenesis of diabetes and its associated complications. *Pharmacol Rep* 2009;**61**:595-603.
- Paul S, Lee JC, Yeh LC. A comparative study on BMP-induced osteoclastogenesis and osteoblastogenesis in primary cultures of adult rat bone marrow cells. *Growth Factors* 2009;**27**:121-131.
- Pendyala S, Usatyuk PV, Gorshkova IA, Garcia JG, Natarajan V. Regulation of NADPH oxidase in vascular endothelium: the role of phospholipases, protein kinases, and cytoskeletal proteins. *Antioxid Redox Signal* 2009;**11**:841-860.
- Perkins ND, Gilmore TD. Good cop, bad cop: the different faces of NF-[kappa]B. *Cell Death Differ* 2006;**13**:759.
- Persy V, De Broe M, Ketteler M. Bisphosphonates prevent experimental vascular calcification: Treat the bone to cure the vessels? *Kidney Int* 2006;**70**:1537-1538.
- Pitocco D, Tesouro M, Alessandro R, Ghirlanda G, Cardillo C. Oxidative stress in diabetes: implications for vascular and other complications. *Int J Mol Sci* 2013;**14**:21525-21550.
- Poornima IG, Mackey RH, Buhari AM, Cauley JA, Matthews KA, Kuller LH. Relationship between circulating serum osteoprotegerin and total receptor activator of nuclear factor κB

ligand levels, triglycerides, and coronary calcification in postmenopausal women. *Menopause* 2014;**21**:702-710.

Popa C, Netea MG, van Riel PL, van der Meer JW, Stalenhoef AF. The role of TNF-alpha in chronic inflammatory conditions, intermediary metabolism, and cardiovascular risk. *J Lipid Res* 2007;**48**:751-762.

Popov, D. Endothelial cell dysfunction in hyperglycemia: Phenotypic change, intracellular signaling modification, ultrastructural alteration, and potential clinical outcomes. *Int J Diab Mell* 2010;**2**:189-195.

Poulsen MK, Nybo M, Dahl J, Hosbond S, Poulsen TS, Johansen A, Højlund-Carlsen PF, Beck-Nielsen H, Rasmussen LM, Henriksen JE. Plasma osteoprotegerin is related to carotid and peripheral arterial disease, but not to myocardial ischemia in type 2 diabetes mellitus. *Cardiovasc Diabetol* 2011;**10**:76.

Pratap J, Galindo M, Zaidi SK, Vradii D, Bhat BM, Robinson JA, Choi JY, Komori T, Stein JL, Lian JB, Stein GS, van Wijnen AJ. Cell growth regulatory role of Runx2 during proliferative expansion of preosteoblasts. *Cancer Res* 2003;**63**:5357-5362.

Pritzker LB, Scatena M, Giachelli CM. The role of osteoprotegerin and tumor necrosis factor-related apoptosis-inducing ligand in human microvascular endothelial cell survival. *Mol Biol Cell* 2004;**15**:2834-2841.

Priya S, Vijayalakshmi P, Vivekanandan P, Karthikeyan S. Priya S1, Vijayalakshmi P, Vivekanandan P, Karthikeyan S. *Toxic Ind Health* 2011;**27**:914-922.

Proudfoot D, Shanahan CM. Biology of calcification in vascular cells: intima versus media. *Herz* 2001;**26**:245-251.

Puchtler H, Meloan SN, Terry MS. On the history and mechanism of alizarin and alizarin red S stains for calcium. *J Histochem Cytochem* 1969;**17**:110-24.

Puri R, Nicholls SJ, Shao M, Kataoka Y, Uno K, Kapadia SR, Tuzcu EM, Nissen SE. Impact of statins on serial coronary calcification during atheroma progression and regression. *J Am Coll Cardiol* 2015;**65**:1273-1282.

Qu D, Liu J, Lau CW, Huang Y. IL-6 in diabetes and cardiovascular complications. *Br J Pharmacol* 2014;**171**:3595-3603.

Raaz U, Toh R, Maegdefessel L, Adam M, Nakagami F, Emrich FC, Spin JM, Tsao PS. Hemodynamic regulation of reactive oxygen species: implications for vascular diseases. *Antioxid Redox Signal* 2014;**20**:914-928.

Rahal A, Kumar A, Singh V, Yadav B, Tiwari R, Chakraborty S, Dhama K. Oxidative stress, prooxidants, and antioxidants: the interplay. *Biomed Res Int* 2014;**2014**:761264.

Rainger GE, Nash, GB. Cellular pathology of atherosclerosis: smooth muscle cells prime cocultured endothelial cells for enhanced leukocyte adhesion. *Circ Res* 2001;**88**:615-622.

- Räisänen SR, Alatalo SL, Ylipahkala H, Halleen JM, Cassady AI, Hume DA, Väänänen HK. Macrophages overexpressing tartrate-resistant acid phosphatase show altered profile of free radical production and enhanced capacity of bacterial killing. *Biochem Biophys Res Commun* 2005;**331**:120-126.
- Rao GM, Morghom LO. Correlation between serum alkaline phosphatase activity and blood glucose levels. *Enzyme* 1986;**35**:57-57.
- Rastogi S, Rizwani W, Joshi B, Kunigal S, Chellappan SP. TNF- α response of vascular endothelial and vascular smooth muscle cells involve differential utilization of ASK1 kinase and p73. *Cell Death Differ* 2012;**19**:274-283.
- Ravi R, Bedi GC, Engstrom LW, Zeng Q, Mookerjee B, Gélinas C, Fuchs EJ, Bedi A. Regulation of death receptor expression and TRAIL/Apo2L-induced apoptosis by NF- κ B. *Nat Cell Biol* 2001;**3**:409-416.
- Redmond EM, Cahill PA, Sitzmann JV. Perfused transcapillary smooth muscle and endothelial cell co-culture-a novel in vitro model. *In Vitro Cell Dev Biol Anim* 1995;**31**:601-9.
- Reinhard H, Lajer M, Gall MA, Tarnow L, Parving HH, Rasmussen LM, Rossing P. Osteoprotegerin and mortality in type 2 diabetic patients. *Diabetes Care* 2010;**33**:2561-2566.
- Rennenberg RJ, Kessels AG, Schurgers LJ, van Engelshoven JM, de Leeuw PW, Kroon AA. Vascular calcifications as a marker of increased cardiovascular risk: a meta-analysis. *Vasc Health Risk Manag* 2009;**5**:185-197.
- Rocha VZ, Libby P. Obesity, inflammation, and atherosclerosis. *Nat Rev Cardiol* 2009;**6**:399-409.
- Rochfort KD, Collins LE, Murphy RP, Cummins PM. Downregulation of blood-brain barrier phenotype by proinflammatory cytokines involves NADPH oxidase-dependent ROS generation: consequences for interendothelial adherens and tight junctions. *PLoS One* 2014;**9**:e101815.
- Rochfort KD, Cummins PM. Cytokine-mediated dysregulation of zonula occludens-1 properties in human brain microvascular endothelium. *Microvasc Res* 2015;**100**:48-53.
- Rojo AI, Salinas M, Martín D, Perona R, Cuadrado A. Regulation of Cu/Zn-superoxide dismutase expression via the phosphatidylinositol 3 kinase/Akt pathway and nuclear factor- κ B. *J Neurosci* 2004;**24**:7324-7334.
- Rongen GA, Smits P, Thien T. Endothelium and the regulation of vascular tone with emphasis on the role of nitric oxide. Physiology, pathophysiology and clinical implications. *Neth J Med* 1994;**44**:26-35.
- Ross R. Atherosclerosis - an inflammatory disease. *N Engl J Med* 1999;**340**:115-126.
- Royall JA, Berkow RL, Beckman JS, Cunningham MK, Matalon S, Freeman BA. Tumor necrosis factor and interleukin 1 alpha increase vascular endothelial permeability. *Am J Physiol* 1989;**257**:L399-410.

- Rozas Moreno P, Reyes García R, García-Martín A, Varsavsky M, García-Salcedo JA, Muñoz-Torres M. Serum osteoprotegerin: bone or cardiovascular marker in Type 2 diabetes males? *J Endocrinol Invest* 2013;**36**:16-20.
- Rubin MR, Silverberg SJ. Vascular calcification and osteoporosis--the nature of the nexus. *J Clin Endocrinol Metab* 2004;**89**:4243-4245.
- Ruland J. Return to homeostasis: downregulation of NF- κ B responses. *Nat Immunol* 2011;**12**:709-714.
- Sage AP, Tintut Y, Demer LL. Regulatory mechanisms in vascular calcification. *Nat Rev Cardiol* 2010;**7**:528-536.
- Samelson EJ, Miller PD, Christiansen C, Daizadeh NS, Grazette L, Anthony MS, Egbuna O, Wang A, Siddhanti SR, Cheung AM, Franchimont N, Kiel DP. RANKL inhibition with denosumab does not influence 3-year progression of aortic calcification or incidence of adverse cardiovascular events in postmenopausal women with osteoporosis and high cardiovascular risk. *J Bone Miner Res* 2014;**29**:450-457.
- Sato K, Niessner A, Kopecky SL, Frye RL, Goronzy JJ, Weyand CM. TRAIL-expressing T cells induce apoptosis of vascular smooth muscle cells in the atherosclerotic plaque. *J Exp Med* 2006;**203**:239-250.
- Schieber M, Chandel NS. ROS function in redox signaling and oxidative stress. *Curr Biol* 2014;**24**:R453-462.
- Schinke T, Karsenty G. Vascular calcification-a passive process in need of inhibitors. *Nephrol Dial Transplant* 2000;**15**:1272-1274.
- Schoppet M, Al-Fakhri N, Franke FE, Katz N, Barth PJ, Maisch B, Preissner KT, Hofbauer LC. Localization of osteoprotegerin, tumor necrosis factor-related apoptosis-inducing ligand, and receptor activator of nuclear factor- κ B ligand in Mönckeberg's sclerosis and atherosclerosis. *J Clin Endocrinol Metab* 2004;**89**:4104-4112.
- Schoppet M, Sattler AM, Schaefer JR, Herzum M, Maisch B, Hofbauer LC. Increased osteoprotegerin serum levels in men with coronary artery disease. *J Clin Endocrinol Metab* 2003;**88**:1024-1028.
- Schoppet M, Shanahan CM. Role for alkaline phosphatase as an inducer of vascular calcification in renal failure? *Kidney Int* 2008;**73**:989-991.
- Schröder K, Zhang M, Benkhoff S, Mieth A, Pliquet R, Kosowski J, Kruse C, Lüdike P, Michaelis UR, Weissmann N, Dimmeler S. Nox4 is a protective reactive oxygen species generating vascular NADPH oxidase. *Circ Res* 2012;**110**:1217-1225.
- Secchiero P, Candido R, Corallini F, Zacchigna S, Toffoli B, Rimondi E, Fabris B, Giacca M, Zauli G. Systemic tumor necrosis factor-related apoptosis-inducing ligand delivery shows antiatherosclerotic activity in apolipoprotein E-null diabetic mice. *Circulation* 2006;**114**:1522-1530.

- Secchiero P, Corallini F, Ceconi C, Parrinello G, Volpato S, Ferrari R, Zauli G. Potential prognostic significance of decreased serum levels of TRAIL after acute myocardial infarction. *PLoS One* 2009;**4**:e4442.
- Secchiero P, Corallini F, di Iasio MG, Gonelli A, Barbarotto E, Zauli, G. TRAIL counteracts the proadhesive activity of inflammatory cytokines in endothelial cells by down-modulating CCL8 and CXCL10 chemokine expression and release. *Blood* 2005;**105**:3413-3419.
- Secchiero P, Corallini F, Pandolfi A, Consoli A, Candido R, Fabris B, Celeghini C, Capitani S, Zauli G. An increased osteoprotegerin serum release characterizes the early onset of diabetes mellitus and may contribute to endothelial cell dysfunction. *Am J Pathol* 2006;**169**:2236-2244.
- Secchiero P, Gonelli A, Carnevale E, Milani D, Pandolfi A, Zella D, Zauli G. TRAIL promotes the survival and proliferation of primary human vascular endothelial cells by activating the Akt and ERK pathways. *Circulation* 2003;**107**:2250-2256.
- Secchiero P, Zauli G. The puzzling role of TRAIL in endothelial cell biology. *Arterioscler Thromb Vasc Biol* 2008;**22**:e4.
- Secchiero P, Zerbinati C, Rimondi E, Corallini F, Milani D, Grill V, Forti G, Capitani S, Zauli G. TRAIL promotes the survival, migration and proliferation of vascular smooth muscle cells. *Cell Mol Life Sci* 2004;**61**:1965-1974.
- Sena CM, Pereira AM, Seça R. Endothelial dysfunction — A major mediator of diabetic vascular disease. *Biochim Biophys Acta* 2013;**1832**:2216-2231.
- Seol JW, Lee HB, Kim NS, Park SY. Tartrate-resistant acid phosphatase as a diagnostic factor for arthritis. *Int J Mol Med* 2009;**24**:57-62.
- Shanahan CM, Proudfoot D, Tyson KL, Cary NRB, Edmonds M, Weissberg PL. Expression of mineralisation-regulating proteins in association with human vascular calcification. *Zeitschrift für Kardiologie* 2000;**89Supp 2**:S063-S068.
- Shao JS, Cheng SL, Charlton-Kachigian N, Loewy AP, Towler DA. Teriparatide (human parathyroid hormone (1-34)) inhibits osteogenic vascular calcification in diabetic low density lipoprotein receptor-deficient mice. *J Biol Chem* 2003;**278**:50195-50202.
- Shao JS, Cheng SL, Sadhu J, Towler DA. Inflammation and the osteogenic regulation of vascular calcification: a review and perspective. *Hypertension* 2010;**55**:579-592.
- Sheen CR, Kuss P, Narisawa S, Yadav MC, Nigro J, Wang W, Chhea TN, Sergienko EA, Kapoor K, Jackson MR, Hoylaerts MF, Pinkerton AB, O'Neill WC, Millán JL. Pathophysiological role of vascular smooth muscle alkaline phosphatase in medial artery calcification. *J Bone Miner Res* 2015;**30**:824-836.
- Sheikh MS, Burns TF, Huang Y, Wu GS, Amundson S, Brooks KS, Fornace AJ, El-Deiry WS. p53-dependent and-independent regulation of the death receptor KILLER/DR5 gene expression in response to genotoxic stress and tumor necrosis factor- α . *Cancer Res* 1998;**58**:1593-1598.

- Shi Y, Vanhoutte PM. Macro- and microvascular endothelial dysfunction in diabetes. *J Diabetes* 2017;**9**:434-449.
- Shin V, Zebboudj AF, Boström K. Endothelial cells modulate osteogenesis in calcifying vascular cells. *J Vasc Res* 2004;**41**:193-201.
- Shioi A, Nishizawa Y, Jono S, Koyama H, Hosoi M, Morii H. Betaglycerophosphate accelerates calcification in cultured bovine vascular smooth muscle cells. *Arterioscler Thromb Vasc Biol* 1995;**15**:2003-2009.
- Silva BR, Pernomian L, Bendhack LM. Contribution of oxidative stress to endothelial dysfunction in hypertension. *Front Physiol* 2012;**3**:441.
- Simões Sato AY, Bub GL, Campos AH. BMP-2 and -4 produced by vascular smooth muscle cells from atherosclerotic lesions induce monocyte chemotaxis through direct BMPRII activation. *Atherosclerosis* 2014;**235**:45-55.
- Singh DK, Winocour P, Farrington K. Review: Endothelial cell dysfunction, medial arterial calcification and osteoprotegerin in diabetes. *Br J Diabetes Vasc Dis* 2010;**10**:71-77.
- Singh DK, Winocour P, Summerhayes B, Kaniyur S, Viljoen A, Sivakumar G, Farrington K. Prevalence and progression of peripheral vascular calcification in type-2 diabetes subjects with preserved kidney function. *Diabetes Res Clin Pract* 2012;**97**:158-165.
- Singh DK, Winocour P, Summerhayes B, Viljoen A, Sivakumar G, Farrington K. Are low erythropoietin and 1,25-dihydroxyvitamin D levels indicative of tubulo-interstitial dysfunction in diabetes without persistent microalbuminuria? *Diabetes Res Clin Pract* 2009;**85**:258-264.
- Smith PK, Krohn RI, Hermanson GT, Mallia AK, Gartner FH, Provenzano MD, Fujimoto EK, Goeke NM, Olson BJ, Klenk DC. Measurement of protein using bicinchoninic acid. *Anal Biochem* 1985;**150**:76-85.
- Smulders YM, Thijs A, Twisk JW. New cardiovascular risk determinants do exist and are clinically useful. *Eur Heart J* 2008;**29**:436-440.
- Sodek J, Ganss B, McKee MD. Osteopontin. *Crit Rev Oral Biol Med* 2000;**11**:279-303.
- Solberg LB, Brorson SH, Stordalen GA, Bækkevold ES, Andersson G, Reinholt FP. Increased tartrate-resistant Acid phosphatase expression in osteoblasts and osteocytes in experimental osteoporosis in rats. *Calcif Tissue Int* 2014;**94**:510-521.
- Solberg LB, Stang E, Brorson SH, Andersson G, Reinholt FP. Tartrate-resistant acid phosphatase (TRAP) co-localizes with receptor activator of NF- κ B ligand (RANKL) and osteoprotegerin (OPG) in lysosomal-associated membrane protein 1 (LAMP1)-positive vesicles in rat osteoblasts and osteocytes. *Histochem Cell Biol* 2015;**143**:195-207.
- Song HY, Régnier CH, Kirschning CJ, Goeddel DV, Rothe M. Tumor necrosis factor (TNF)-mediated kinase cascades: bifurcation of nuclear factor- κ B and c-jun N-terminal kinase (JNK/SAPK) pathways at TNF receptor-associated factor 2. *Proc Natl Acad Sci USA* 1997;**94**:9792-9796.

- Song S, Choi K, Ryu SW, Kang SW, Choi C. TRAIL promotes caspase-dependent pro-inflammatory responses via PKC δ activation by vascular smooth muscle cells. *Cell Death Dis* 2011;**2**:e223.
- Song Y, Hou M, Li Z, Luo C, Ou JS, Yu H, Yan J, Lu L. TLR4/NF- κ B/Ceramide signaling contributes to Ox-LDL-induced calcification of human vascular smooth muscle cells. *Eur J Pharmacol* 2017;**794**:45-51.
- Sorescu D, Weiss D, Lassègue B, Clempus RE, Szöcs K, Sorescu GP, Valppu L, Quinn MT, Lambeth JD, Vega JD, Taylor WR. Superoxide production and expression of nox family proteins in human atherosclerosis. *Circulation* 2002;**105**:1429-1435.
- Speer MY, Yang HY, Brabb T, Leaf E, Look A, Lin WL, Frutkin A, Dichek D, Giachelli CM. Smooth muscle cells give rise to osteochondrogenic precursors and chondrocytes in calcifying arteries. *Circ Res* 2009;**104**:733-741.
- Spencer SL, Gaudet S, Albeck JG, Burke JM, Sorger PK. Non-genetic origins of cell-to-cell variability in TRAIL-induced apoptosis. *Nature* 2009;**459**:428.
- Spierings DC, de Vries EG, Vellenga E, van den Heuvel FA, Koornstra JJ, Wesseling J, Hollema H, de Jong S. Tissue distribution of the death ligand TRAIL and its receptors. *J Histochem Cytochem* 2004;**52**:821-831.
- Stabley JN, Towler DA. Arterial Calcification In Diabetes: Preclinical Models And Translational Implications. *Arterioscler Thromb Vasc Biol* 2017;**37**:205-217.
- Starup-Linde J, Vestergaard P. Diabetes and osteoporosis: cause for concern? *Front Endocrinol (Lausanne)* 2014;**5**:53.
- Steitz SA, Speer MY, Curinga G, Yang HY, Haynes P, Aebersold R, Schinke T, Karsenty G, Giachelli CM. Smooth muscle cell phenotypic transition associated with calcification: upregulation of Cbfa1 and downregulation of smooth muscle lineage markers. *Circ Res* 2001;**89**:1147-1154.
- Stroka KM, Vaitkus JA, Aranda-Espinoza H. Endothelial cells undergo morphological, biomechanical, and dynamic changes in response to tumor necrosis factor- α . *Eur Biophys J* 2012;**41**:939-947.
- Suliman A, Lam A, Datta R, Srivastava RK. Intracellular mechanisms of TRAIL: apoptosis through mitochondrial-dependent and-independent pathways. *Oncogene* 2001;**20**:2122-2133.
- Sun SC. Non-canonical NF- κ B signaling pathway. *Cell Res* 2011;**21**:71-85.
- Sun SC. The non-canonical NF- κ B pathway in immunity and inflammation. *Nat Rev Immunol* 2017;**17**:545-558.
- Sun Y, Byon CH, Yuan K, Chen J, Mao X, Heath JM, Javed A, Zhang K, Anderson PG, Chen Y. Smooth muscle cell-specific runx2 deficiency inhibits vascular calcification. *Circ Res* 2012;**111**:543-552.

- Suresh E, Abrahamsen B. Denosumab: a novel antiresorptive drug for osteoporosis. *Cleve Clin J Med* 2015;**82**:105-114.
- Suryavanshi SV, Kulkarni YA. NF- κ B: A Potential Target in the Management of Vascular Complications of Diabetes. *Front Pharmacol* 2017;**8**:798.
- Sykaras N, Opperman LA. Bone morphogenetic proteins (BMPs): how do they function and what can they offer the clinician? *J Oral Sci* 2003;**45**:57-73.
- Szklarczyk D, Morris JH, Cook H, Kuhn M, Wyder S, Simonovic M, Santos A, Doncheva NT, Roth A, Bork P, Jensen LJ, von Mering C. The STRING database in 2017: quality-controlled protein-protein association networks, made broadly accessible. *Nucleic Acids Res* 2017;**45**:D362-368.
- Szotowski B, Antoniak S, Goldin-Lang P, Tran QV, Pels K, Rosenthal P, Bogdanov VY, Borchert HH, Schultheiss HP, Rauch U. Antioxidative treatment inhibits the release of thrombogenic tissue factor from irradiation- and cytokine-induced endothelial cells. *Cardiovasc Res* 2007;**73**:806-812.
- Takeno A, Kanazawa I, Notsu M, Tanaka KI, Sugimoto T. Glucose uptake inhibition decreases expressions of receptor activator of nuclear factor-kappa B ligand (RANKL) and osteocalcin in osteocytic MLO-Y4-A2 cells. *Am J Physiol Endocrinol Metab* 2018;**314**:E115-123.
- Tanaka T, Narazaki M, Kishimoto T. IL-6 in Inflammation, Immunity, and Disease. *Cold Spring Harb Perspect Biol* 2014;**6**:a016295.
- Tang W, Wang W, Zhang Y, Liu S, Liu Y, Zheng D. TRAIL receptor mediates inflammatory cytokine release in an NF-kappaB-dependent manner. *Cell Res* 2009;**19**:758-767.
- Tarallo S, Beltramo E, Berrone E, Porta M. Human pericyte-endothelial cell interactions in co-culture models mimicking the diabetic retinal microvascular environment. *Acta Diabetol* 2012;**49 Suppl1**:S141-151.
- Tavintharan S, Pek LT, Liu JJ, Ng XW, Yeoh LY, Su Chi L, Chee Fang S. Osteoprotegerin is independently associated with metabolic syndrome and microvascular complications in type 2 diabetes mellitus. *Diab Vasc Dis Res* 2014;**11**:359-362.
- Teitelbaum, SL. Bone resorption by osteoclasts. *Science* 2000;**289**:1504-1508.
- Thapar A, Jenkins IH, Mehta A, Davies AH. Diagnosis and management of carotid atherosclerosis. *BMJ* 2013;**346**:f1485.
- Thummuri D, Naidu VGM, Chaudhari P. Carnosic acid attenuates RANKL-induced oxidative stress and osteoclastogenesis via induction of Nrf2 and suppression of NF- κ B and MAPK signalling. *J Mol Med (Berl)* 2017;**95**:1065-1076.
- Timofeeva AV, Goriunova LE, Khaspekov GL, Il'inskaia OP, Sirotkin VN, Andreeva ER, Tararak EM, Bulkina OS, Buza VV, Britareva VV, Karpov IuA, Bibilashvili RSh. [Comparative transcriptome analysis of human aorta atherosclerotic lesions and peripheral blood leukocytes from essential hypertension patients]. *Kardiologiia* 2009;**49**:27-38.

- Tintut Y, Demer L. Role of osteoprotegerin and its ligands and competing receptors in atherosclerotic calcification. *J Investig Med* 2006;**54**:395-401.
- Tintut Y, Patel J, Parhami F, Demer LL. Tumor necrosis factor- α promotes in vitro calcification of vascular cells via the cAMP pathway. *Circulation* 2000;**102**:2636-2642.
- Tobwin H, Staehelin T, Gordon J. Electrophoretic transfer of proteins from polyacrylamide gels to nitrocellulose sheets: procedure and some applications. *Proc Natl Acad Sci USA* 1979;**76**:4350-4354.
- Toussaint ND, Lau KK, Strauss BJ, Polkinghorne KR, Kerr PG. Effect of alendronate on vascular calcification in CKD stages 3 and 4: a pilot randomized controlled trial. *Am J Kidney Dis* 2010;**56**:57-68.
- Towler DA. Oxidation, inflammation, and aortic valve calcification peroxide paves an osteogenic path. *J Am Coll Cardiol* 2008;**52**:851-854.
- Tribble DL, Barcellos-Hoff MH, Chu BM, Gong EL. Ionizing radiation accelerates aortic lesion formation in fat-fed mice via SOD-inhibitable processes. *Arterio Thromb Vasc Biol* 1999;**19**:1387-1392.
- Trouvin AP, Goëb V. Receptor activator of nuclear factor- κ B ligand and osteoprotegerin: maintaining the balance to prevent bone loss. *Clin Interv Aging* 2010;**5**:345-354.
- True AL, Olive M, Boehm M, San H, Westrick RJ, Raghavachari N, Xu X, Lynn EG, Sack MN, Munson PJ, Gladwin MT, Nabel EG. Heme oxygenase-1 deficiency accelerates formation of arterial thrombosis through oxidative damage to the endothelium, which is rescued by inhaled carbon monoxide. *Circ Res* 2007;**101**:893-901.
- Tseng W, Graham LS, Geng Y, Reddy A, Lu J, Effros RB, Demer L, Tintut Y. PKA-induced receptor activator of NF κ B ligand (RANKL) expression in vascular cells mediates osteoclastogenesis but not matrix calcification. *J Biol Chem* 2010;**285**:29925-29931.
- Tsong TY. Electroporation of cell membranes. *Biophys J* 1991;**60**:297-306.
- Tyson KL, Reynolds JL, McNair R, Zhang Q, Weissberg PL, Shanahan CM. Osteo/chondrocytic transcription factors and their target genes exhibit distinct patterns of expression in human arterial calcification. *Arterioscler Thromb Vasc Biol* 2003;**23**:489-494.
- Ullah I, Subbarao RB, Rho GJ. Human mesenchymal stem cells - current trends and future prospective. *Biosci Rep* 2015;**35**:e00191.
- Valdivielso JM. [Vascular calcification: types and mechanisms]. *Nefrologia* 2011;**31**:142-147.
- Valle I, Álvarez-Barrientos A, Arza E, Lamas S, Monsalve M. PGC-1 α regulates the mitochondrial antioxidant defense system in vascular endothelial cells. *Cardiovasc Res* 2005;**66**:562-573.
- Van Campenhout A, Golledge J. Osteoprotegerin, vascular calcification and atherosclerosis. *Atherosclerosis* 2009;**204**:321-329.

- Vara D, Pula G. Reactive oxygen species: physiological roles in the regulation of vascular cells. *Curr Mol Med* 2014;**14**:1103-1125.
- Vendrov AE, Hakim ZS, Madamanchi NR, Rojas M, Madamanchi C, Runge MS. Atherosclerosis is attenuated by limiting superoxide generation in both macrophages and vessel wall cells. *Arterioscler Thromb Vasc Biol* 2007;**27**:2714-2721.
- Venuraju SM, Yerramasu A, Corder R, Lahiri A. Osteoprotegerin as a predictor of coronary artery disease and cardiovascular mortality and morbidity. *J Am Coll Cardiol* 2010;**55**:2049-2061.
- Versari D, Daghini E, Viridis A, Ghiadoni L, Taddei S. Endothelial dysfunction as a target for prevention of cardiovascular disease. *Diabetes Care* 2009;**32Suppl2**:S314-321.
- Viator RJ, Fouty BW. Aortic endothelial cells transport more glucose than pulmonary endothelial cells in vitro. *The FASEB Journal* 2009;**23**:Suppl1.
- Vik A, Mathiesen EB, Brox J, Wilsgaard T, Njølstad I, Jørgensen L, Hansen JB. Serum osteoprotegerin is a predictor for incident cardiovascular disease and mortality in a general population: the Tromsø Study. *J Thromb Haemost* 2011;**9**:638-644.
- Virmani R, Burke AP, Farb A. Plaque morphology in sudden coronary death. *Cardiologia* 1998;**43**:267-271.
- Vitale RF, Ribeiro FA. The role of tumor necrosis factor-alpha (TNF-alpha) in bone resorption present in middle ear cholesteatoma. *Braz J Otorhinolaryngol* 2007;**73**:117-121.
- Vitovski S, Phillips JS, Sayers J, Croucher PI. Investigating the interaction between osteoprotegerin and receptor activator of NF-kappaB or tumor necrosis factor-related apoptosis-inducing ligand: evidence for a pivotal role for osteoprotegerin in regulating two distinct pathways. *J Biol Chem* 2007;**282**:31601-31609.
- Vogel C, Silva GM, Marcotte EM. Protein expression regulation under oxidative stress. *Mol Cell Proteomics* 2011;**10**:M111-009217.
- Volpato S, Ferrucci L, Secchiero P, Corallini F, Zuliani G, Fellin R, Guralnik JM, Bandinelli S, Zauli G. Association of tumor necrosis factor-related apoptosis-inducing ligand with total and cardiovascular mortality in older adults. *Atherosclerosis* 2011;**215**:452-458.
- Wada T, Nakashima T, Hiroshi N, Penninger JM. RANKL-RANK signalling in osteoclastogenesis and bone disease. *Trends Mol Med* 2006;**12**:17-25.
- Wallace CS, Truskey GA. Direct-contact co-culture between smooth muscle and endothelial cells inhibits TNF-alpha-mediated endothelial cell activation. *Am J Physiol Heart Circ Physiol* 2010;**299**:H338-346.
- Walsh TG, Murphy RP, Fitzpatrick P, Rochfort KD, Guinan AF, Murphy, A, Cummins PM. Stabilization of brain microvascular endothelial barrier function by shear stress involves VE-cadherin signalling leading to modulation of pTyr-occludin levels. *J Cell Physiol* 2011;**226**:3053-3063.

- Wang J, Yi S, Zhou J, Zhang Y, Guo F. The NF- κ B subunit RelB regulates the migration and invasion abilities and the radio-sensitivity of prostate cancer cells. *Int J Oncol* 2016;**49**:381-392.
- Wang LY, Zhang DL, Zheng JF, Zhang Y, Zhang QD, Liu WH. Apelin-13 passes through the ADMA-damaged endothelial barrier and acts on vascular smooth muscle cells. *Peptides* 2011;**32**:2436-2443.
- Wang S, El-Deiry WS. TRAIL and apoptosis induction by TNF-family death receptors. *Oncogene* 2003;**22**:8628-8633.
- Warner BB, Burhans MS, Clark JC, Wispé JR. Tumor necrosis factor-alpha increases Mn-SOD expression: protection against oxidant injury. *Am J Physiol* 1991;**260**:L296-301.
- Wassmann S, Stumpf M, Strehlow K, Schmid A, Schieffer B, Böhm M, Nickenig G. Interleukin-6 induces oxidative stress and endothelial dysfunction by overexpression of the angiotensin II type 1 receptor. *Circ Res* 2004;**94**:534-541.
- Watt V, Chamberlain J, Steiner T, Francis S, Crossman D. TRAIL attenuates the development of atherosclerosis in apolipoprotein-E deficient mice. *Atherosclerosis* 2011;**215**:348-354.
- Wei Y, Hu Y, Lv R, Li D. Regulation of adipose-derived adult stem cells differentiating into chondrocytes with the use of rhBMP-2. *Cytotherapy* 2006;**8**:570-579.
- Weng JJ, Su Y. Nuclear matrix-targeting of the osteogenic factor Runx2 is essential for its recognition and activation of the alkaline phosphatase gene. *Biochim Biophys Acta* 2013;**1830**:2839-2852.
- Westhrin M, Xie M, Olderøy MØ, Sikorski P, Strand BL, Standal T. Osteogenic differentiation of human mesenchymal stem cells in mineralized alginate matrices. *PLoS One* 2015;**10**:e0120374.
- Wexler L, Brundage B, Crouse J, Detrano R, Fuster V, Maddahi J, Rumberger J, Stanford W, White R, Taubert K. Coronary artery calcification: pathophysiology, epidemiology, imaging methods, and clinical implications - A statement for health professionals from the American Heart Association Writing Group. *Circulation* 1996;**94**:1175-1192.
- Widmer RJ, Lerman A. Endothelial dysfunction and cardiovascular disease. *Glob Cardiol Sci Pract* 2014;**2014**:291-308.
- Wiley SR, Schooley K, Smolak PJ, Din WS, Huang CP, Nicholl JK, Sutherland GR, Smith TD, Rauch C, Smith CA, Goodwin RG. Identification and characterization of a new member of the TNF family that induces apoptosis. *Immunity* 1995;**3**:673-682.
- Wittrant Y, Lamoureux F, Mori K, Riet A, Kamijo A, Heymann D, Redini F. RANKL directly induces bone morphogenetic protein-2 expression in RANK-expressing POS-1 osteosarcoma cells. *Int J Oncol* 2006;**28**:261-269.

- Wong BR, Josien R, Lee SY, Vologodskaja M, Steinman RM, Choi Y. The TRAF family of signal transducers mediates NF-kappaB activation by the TRANCE receptor. *J Biol Chem* 1998;**273**:28355-28359.
- Wong ET, Tergaonkar V. Roles of NF-kappaB in health and disease: mechanisms and therapeutic potential. *Clin Sci (Lond)* 2009;**116**:451-465.
- World Heart Federation. *Cardiovascular Risk Factors*. 2017. Available at: <http://www.world-heart-federation.org/cardiovascular-health/cardiovascular-disease-risk-factors/> [Accessed 8 May 2018].
- Wu M, Rementer C, Giachelli CM. Vascular calcification: an update on mechanisms and challenges in treatment. *Calcif Tissue Int* 2013;**93**:365-373.
- Wurzer WJ, Ehrhardt C, Pleschka S, Berberich-Siebelt F, Wolff T, Walczak H, Planz O, Ludwig S. NF- κ B-dependent induction of tumor necrosis factor-related apoptosis-inducing ligand (TRAIL) and Fas/FasL is crucial for efficient influenza virus propagation. *J Biol Chem* 2004;**279**:30931-30937.
- Xia Z, Liu M, Wu Y, Sharma V, Luo T, Ouyang J, McNeill JH. N-acetylcysteine attenuates TNF-alpha-induced human vascular endothelial cell apoptosis and restores eNOS expression. *Eur J Pharmacol* 2006;**550**:134-142.
- Xiao G, Fong A, Sun SC. Induction of p100 processing by NF-kappaB-inducing kinase involves docking IkappaB kinase alpha (IKKalpha) to p100 and IKKalpha-mediated phosphorylation. *J Biol Chem* 2004;**279**:3099-30105.
- Yamaguchi K, Kinoshita M, Goto M, Kobayashi F, Tsuda E, Morinaga T, Higashio K. Characterization of structural domains of human osteoclastogenesis inhibitory factor. *J Biol Chem* 1998;**273**:5117-5123.
- Yamashita Y, Ukai T, Nakamura H, Yoshinaga Y, Kobayashi H, Takamori Y, Noguchi S, Yoshimura A, Hara Y. RANKL pretreatment plays an important role in the differentiation of pit-forming osteoclasts induced by TNF- α on murine bone marrow macrophages. *Archives Oral Biol* 2015;**60**:1273-1282.
- Yang L, Butcher M, Simon RR, Osip SL, Shaughnessy SG. The effect of heparin on osteoblast differentiation and activity in primary cultures of bovine aortic smooth muscle cells. *Atherosclerosis* 2005;**179**:79-86.
- Yang YM, Huang A, Kaley G, Sun D. eNOS uncoupling and endothelial dysfunction in aged vessels. *Am J Physiol Heart Circ Physiol* 2009;**297**:H1829-1836.
- Yano M, Hasegawa G, Ishii M, Yamasaki M, Fukui M, Nakamura N, Yoshikawa T. Short-term exposure of high glucose concentration induces generation of reactive oxygen species in endothelial cells: implication for the oxidative stress associated with postprandial hyperglycemia. *Redox Report* 2004;**9**:111-116.
- Yao Y, Jumabay M, Ly A, Radparvar M, Cubberly MR, Boström KI. A role for the endothelium in vascular calcification. *Circ Res* 2013;**113**:495-504.

Yao Y, Wang G, Wang Z, Wang C, Zhang H, Liu C. Synergistic enhancement of new bone formation by recombinant human bone morphogenetic protein-2 and osteoprotegerin in trans-sutural distraction osteogenesis: a pilot study in dogs. *J Oral Maxillofac Surg* 2011;**69**:e446-455.

Yasuda H, Shima N, Nakagawa N, Mochizuki SI, Yano K, Fujise N, Sato Y, Goto M, Yamaguchi K, Kuriyama M, Kanno T, Murakami A, Tsuda E, Morinaga T, Higashio K. Identity of osteoclastogenesis inhibitory factor (OCIF) and osteoprotegerin (OPG): a mechanism by which OPG/OCIF inhibits osteoclastogenesis in vitro. *Endocrinology* 1998;**139**:1329-1337.

Yen ML, Tsai HF, Wu YY, Hwa HL, Lee BH, Hsu PN. TNF-related apoptosis-inducing ligand (TRAIL) induces osteoclast differentiation from monocyte/macrophage lineage precursor cells. *Mol Immunol* 2008;**45**:2205-2213.

Yodkeeree S, Sung B, Limtrakul P, Aggarwal BB. Zerumbone enhances TRAIL-induced apoptosis through the induction of death receptors in human colon cancer cells: Evidence for an essential role of reactive oxygen species. *Cancer Res* 2009;**69**:6581-6589.

Yoshitake F, Itoh S, Narita H, Ishihara K, Ebisu S. Interleukin-6 directly inhibits osteoclast differentiation by suppressing receptor activator of NF-kappaB signaling pathways. *J Biol Chem* 2008;**283**:11535-11540.

Yu M, Qi X, Moreno JL, Farber DL, Keegan AD. NF- κ B signaling participates in both RANKL- and IL-4-induced macrophage fusion: receptor cross-talk leads to alterations in NF- κ B pathways. *J Immunol* 2011;**187**:1797-1806.

Yu PB, Deng DY, Beppu H, Hong CC, Lai C, Hoyng SA, Kawai N, Bloch KD. Bone morphogenetic protein (BMP) type II receptor is required for BMP-mediated growth arrest and differentiation in pulmonary artery smooth muscle cells. *J Biol Chem* 2008;**283**:3877-3888.

Yuan LQ, Zhu JH, Wang HW, Liang QH, Xie H, Wu XP, Zhou H, Cui RR, Sheng ZF, Zhou HD, Zhu X, Liu GY, Liu YS, Liao EY. RANKL is a downstream mediator for insulin-induced osteoblastic differentiation of vascular smooth muscle cells. *PloS One* 2011;**6**:e29037.

Zannettino AC, Holding CA, Diamond P, Atkins GJ, Kostakis P, Farrugia A, Gamble J, To LB, Findlay DM, Haynes DR. Osteoprotegerin (OPG) is localized to the Weibel-Palade bodies of human vascular endothelial cells and is physically associated with von Willebrand factor. *J Cell Physiol* 2005;**204**:714-723.

Zauli G, Pandolfi A, Gonelli A, Di Pietro R, Guarnieri S, Ciabattoni G, Rana R, Vitale M, Secchiero P. Tumor necrosis factor-related apoptosis-inducing ligand (TRAIL) sequentially upregulates nitric oxide and prostanoid production in primary human endothelial cells. *Circ Res* 2003;**92**:732-740.

Zauli G, Rimondi E, Nicolini V, Melloni E, Celeghini C, Secchiero P. TNF-related apoptosis-inducing ligand (TRAIL) blocks osteoclastic differentiation induced by RANKL plus M-CSF. *Blood* 2004;**104**:2044-2050.

- Zauli G, Rimondi E, Stea S, Baruffaldi F, Stebel M, Zerbinati C, Corallini F, Secchiero P. TRAIL inhibits osteoclastic differentiation by counteracting RANKL-dependent p27Kip1 accumulation in pre-osteoclast precursors. *J Cell Physiol* 2008;**214**:117-125.
- Zauli G, Secchiero P. The role of the TRAIL/TRAIL receptors system in hematopoiesis and endothelial cell biology. *Cytokine Growth Factor Rev* 2006;**17**:245-257.
- Zelko IN, Mariani TJ, Folz RJ. Superoxide dismutase multigene family: a comparison of the CuZn-SOD (SOD1), Mn-SOD (SOD2), and EC-SOD (SOD3) gene structures, evolution, and expression. *Free Rad Biol Med* 2002;**33**:337-349.
- Zhan JK, Tan P, Wang YJ, Wang Y, He JY, Tang ZY, Huang W, Liu YS. Exenatide can inhibit calcification of human VSMCs through the NF-kappaB/RANKL signaling pathway. *Cardiovasc Diabetol* 2014;**13**:153.
- Zhang C. The role of inflammatory cytokines in endothelial dysfunction. *Basic Res Cardiol* 2008;**103**:398-406.
- Zhang D, Bi X, Liu Y, Huang Y, Xiong J, Xu X, Xiao T, Yu Y, Jiang W, Huang Y, Zhang J, Zhang B, Zhao J. High Phosphate-Induced Calcification of Vascular Smooth Muscle Cells is Associated with the TLR4/NF- κ B Signaling Pathway. *Kidney Blood Press Res* 2017;**42**:1205-1215.
- Zhang H, Park Y, Wu J, ping Chen X, Lee S, Yang J, Dellsperger KC, Zhang C. Role of TNF- α in vascular dysfunction. *Clinical Science* 2009;**116**:219-30.
- Zhang J, Zheng B, Zhou PP, Zhang RN, He M, Yang Z, Wen JK. Vascular calcification is coupled with phenotypic conversion of vascular smooth muscle cells through Klf5-mediated transactivation of the Runx2 promoter. *Biosci Rep* 2014;**34**:e00148.
- Zhang M, Sara JD, Wang FL, Liu LP, Su LX, Zhe J, Wu X, Liu JH. Increased plasma BMP-2 levels are associated with atherosclerosis burden and coronary calcification in type 2 diabetic patients. *Cardiovasc Diabetol* 2015;**14**:64.
- Zhang Q, Lenardo MJ, Baltimore D. 30 Years of NF- κ B: A Blossoming of Relevance to Human Pathobiology. *Cell* 2017;**168**:37-57.
- Zhang XD, Nguyen T, Thomas WD, Sanders JE, Hersey P. Mechanisms of resistance of normal cells to TRAIL induced apoptosis vary between different cell types. *FEBS Lett* 2000;**482**:193-199.
- Zhang Y, Gu Y, Lucas MJ, Wang Y. Antioxidant superoxide dismutase attenuates increased endothelial permeability induced by platelet-activating factor. *J Soc Gynecol Investig* 2003;**10**:5-10.
- Zhang Y, Khan D, Delling J, Tobiasch E. Mechanisms underlying the osteo- and adipodifferentiation of human mesenchymal stem cells. *Scientific World Journal* 2012;**2012**:793823.

Zhang Y, Lau P, Pansky A, Kassack M, Hemmersbach R, Tobiasch E. The influence of simulated microgravity on purinergic signaling is different between individual culture and endothelial and smooth muscle cell coculture. *Biomed Res Int* 2014;**2014**:413708.

Zhao G, Xu MJ, Zhao MM, Dai XY, Kong W, Wilson GM, Guan Y, Wang CY, Wang X. Activation of nuclear factor-kappa B accelerates vascular calcification by inhibiting ankylosis protein homolog expression. *Kidney Int* 2012;**82**:34-44.

Zhao MM, Xu MJ, Cai Y, Zhao G, Guan Y, Kong W, Tang C, Wang X. Mitochondrial reactive oxygen species promote p65 nuclear translocation mediating high-phosphate-induced vascular calcification in vitro and in vivo. *Kidney Int* 2011;**79**:1071-1079.

Ziegler S, Kudlacek S, Luger A, Minar E. Osteoprotegerin plasma concentrations correlate with severity of peripheral artery disease. *Atherosclerosis* 2005;**182**:175-180.

Zitman-Gal T, Green J, Korzets Z, Bernheim J, Benchetrit S. Kruppel-like factors in an endothelial and vascular smooth muscle cell coculture model: impact of a diabetic environment and vitamin D. *In Vitro Cell Dev Biol Anim* 2015;**51**:470-478.

Zoller V, Funcke JB, Roos J, Dahlhaus M, El Hay MA, Holzmann K, Marienfeld R, Kietzmann T, Debatin KM, Wabitsch M, Fischer-Posovszky P. Trail (TNF-related apoptosis-inducing ligand) induces an inflammatory response in human adipocytes. *Scientific Reports* 2017;**7**:5691.

Appendices

Table of Contents

Appendix 1

Appendix 1.1 Therapies under investigation for the inhibition/reversal of VC.

Appendix 2

Appendix 2.1 Primer efficiency values for all primer sets employed in standard PCR and qPCR.

Appendix 2.2 Typical standard curves for ELISA and alizarin red S staining.

Appendix 3

Appendix 3.1 RANKL and TRAIL release and intracellular protein expression in HAEC and HASMC monoculture.

Appendix 3.2 The effects of RANKL and TRAIL on endothelial barrier function and smooth muscle phenotype in monoculture.

Appendix 3.3 Methodological validation.

Appendix 3.4 Pro-calcific mRNA expression and OPG protein production in HAEC monoculture.

Appendix 3.5 Non-canonical NF- κ B activation and pro-calcific gene expression in HAECs at various time points.

Appendix 3.6 HAEC responses to β -glycerophosphate exposure.

Appendix 3.7 Pro-calcific mRNA expression and protein production in HASMC monoculture.

Appendix 3.8 Expression of mRNA indices in HASMCs over a 72-hour time course.

Appendix 3.9 HASMC responses to β -glycerophosphate exposure.

Appendix 3.10 HASMC responses to BMP-2 +/- noggin exposure.

Appendix 3.11 HASMC gene expression, protein production and NF- κ B activation following endothelial treatment in co-culture.

Appendix 3.12 HASMC responses post-exposure to HAEC-conditioned media following endothelial RANKL treatment.

Appendix 3.13 HASMC responses in co-culture following endothelial RANKL treatment, +/- noggin.

Appendix 3.14 Osteogenic differentiation of MC3T3-E1 and HASMC, and alizarin red S staining of HASMCs in mono- and co-culture.

Appendix 4

- Appendix 4.1** RANKL and TRAIL expression in HAECs and HASMCs exposed to TNF α or glucose.
- Appendix 4.2** The effects of TNF α and glucose on endothelial barrier function and smooth muscle phenotype in monoculture.
- Appendix 4.3** The effect of mannitol exposure on pro-calcific indices in HAECs.
- Appendix 4.4** The effects of TNF α +/- RANKL/TRAIL on pro-calcific indices in HAEC monoculture.
- Appendix 4.5** The effects of glucose +/- RANKL/TRAIL on pro-calcific indices in HAEC monoculture.
- Appendix 4.6** The effects of TNF α and glucose +/- RANKL/TRAIL on NF- κ B activation in HAEC monoculture.
- Appendix 4.7** The effect of mannitol exposure on pro-calcific indices in HASMCs.
- Appendix 4.8** The effects of TNF α +/- RANKL/TRAIL on pro-calcific indices in HASMC monoculture.
- Appendix 4.9** The effects of glucose +/- RANKL/TRAIL on pro-calcific indices in HASMC monoculture.
- Appendix 4.10** The effects of TNF α and glucose +/- RANKL/TRAIL on NF- κ B activation in HASMC monoculture.
- Appendix 4.11** The effects of TNF α +/- RANKL/TRAIL on pro-calcific indices in co-cultured HASMCs.
- Appendix 4.12** The effects of glucose +/- RANKL/TRAIL on pro-calcific indices in co-cultured HASMCs.
- Appendix 4.13** The effects of TNF α and glucose +/- RANKL/TRAIL on NF- κ B activation in co-cultured HASMCs.

Appendix 5

- Appendix 5.1** The effects of β -glycerophosphate and mannitol on TRACP5, SOD1 and SOD2 expression in HAECs.
- Appendix 5.2** The effects of RANKL +/- TRAIL on SOD2 mRNA expression in HAECs.
- Appendix 5.3** The effects of RANKL/TRAIL on SOD1/SOD2 mRNA expression under inflammatory and hyperglycemic conditions.

- Appendix 5.4** The effects of RANKL/TRAIL on SOD1/SOD2 protein expression under inflammatory and hyperglycemic conditions.
- Appendix 5.5** The effects of TNF α +/- NAC on mRNA and protein expression levels in HAECs.
- Appendix 5.6** The effects of TNF α +/- NAC on ROS generation in HAECs.
- Appendix 5.7** The effects of siRNA knockdown on pro-calcific indices in HAECs.
- Appendix 5.8** The effects of RANKL following endothelial siRNA knockdown in co-cultured HASMCs.

Appendix 1.1. Therapies under investigation for the inhibition/reversal of VC.

Therapy	Mode of Action	Results To Date	References
<i>OPG/RANKL/TRAIL-Related Therapies</i>			
Denosumab*	Neutralizes RANKL; prevents phenotypic transformation of vascular cells.	Decreased aortic VC in a murine study; no effect on calcification in a human sub-analysis of a larger trial.	Helas <i>et al.</i> , 2009 Samelson <i>et al.</i> , 2014
Recombinant OPG Therapy	Neutralizes RANKL; prevents phenotypic transformation of vascular cells.	Inhibited VC in a murine study.	Morony <i>et al.</i> , 2008
TRAIL Administration	Unclear	Reduced atherosclerosis progression in a murine model; protected against diabetic vascular injury in a rat model.	Secchiero <i>et al.</i> , 2006 Liu <i>et al.</i> , 2014
<i>Osteoporosis Therapies</i>			
Bisphosphonates	Prevents calcium and phosphate release from bone; inhibits crystal nucleation and propagation.	Suppressed calcification in a rat model; conflicting data in human studies.	Persy <i>et al.</i> , 2006 Nitta <i>et al.</i> , 2004 Toussaint <i>et al.</i> , 2010
Teriparatide	Upregulates circulating concentrations of osteopontin, a calcification inhibitor.	Decreased valve calcification in murine studies.	Shao <i>et al.</i> , 2003
<i>Cardiovascular Disease Therapies</i>			
Statins	Prevent dyslipidemia and inflammation, risk factors for VC.	Protective effects on VC in a rat model; conflicting data in human studies.	Novaro <i>et al.</i> , 2001 Iijima <i>et al.</i> , 2014 Loomba and Arora, 2010 Puri <i>et al.</i> , 2015
Endothelin Receptor Agonists	Reduces hypertension, a risk factor for VC.	Significantly reduced VC in a rat model.	Essalihi <i>et al.</i> , 2004
Antibody to IL-1 β	Reduces inflammation, a risk factor for VC.	Attenuated calcification in a murine model.	Awan <i>et al.</i> , 2015

T2DM Therapies

Exenatide (GLP-1RA)	Enhances glucose-dependent insulin secretion to reduce T2DM symptoms.	Attenuated VSMC calcification <i>in vitro</i> ; no <i>in vivo</i> studies completed to date.	Zhan <i>et al.</i> , 2014
Liraglutide (GLP-1RA)	Enhances glucose-dependent insulin secretion to reduce T2DM symptoms.	No decrease in calcification noted in one prospective observational study to date.	Davenport <i>et al.</i> , 2015

Chronic Kidney Disease Therapies

Phosphate binders	Decreases circulating concentrations of phosphate.	Conflicting data, but favouring reduced progression of calcification with non-calcium based phosphate binders.	Jamal <i>et al.</i> , 2013
Calcimimetics	Lower circulating calcium levels.	Reduced mortality in uremic rats; reduced VC in humans in combination with low-dose vitamin D.	Jung <i>et al.</i> , 2012 Raggi <i>et al.</i> , 2011 Rodriguez <i>et al.</i> , 2008
Vitamin D Receptor Agonists	Mechanism not fully understood, but shown to increase osteopontin expression.	Significantly reduced aortic calcification in a murine model.	Lau <i>et al.</i> , 2012
Vitamin K	Upregulates production of MGP, which binds calcium ions.	Prevented arterial calcification in a rat model; slowed the progression of CAC in healthy older adults with pre-existing CAC in one human study.	Shea <i>et al.</i> , 2009 Spronk <i>et al.</i> , 2003
Sodium Thiosulfate	Chelates calcium, reduces inflammation.	Prevented calcification in a uremic rat model; uncertain if suitable for VC treatment in humans. Recognised treatment for calciphylaxis.	Auriemma <i>et al.</i> , 2011 Mathews <i>et al.</i> , 2011 Pasch <i>et al.</i> , 2008

CAC, coronary artery calcification; GLP-1RA, glucagon-like peptide-1 receptor agonist; OPG, osteoprotegerin; RANKL, receptor activator of nuclear factor kappa-beta ligand; T2DM, type-2 diabetes mellitus; TRAIL, tumour necrosis factor-related apoptosis-inducing ligand; VC, vascular calcification; VSMC, vascular smooth muscle cell. *Denosumab can be classified as both an OPG/RANKL/TRAIL-related and osteoporosis therapy. Harper *et al.*, 2016.

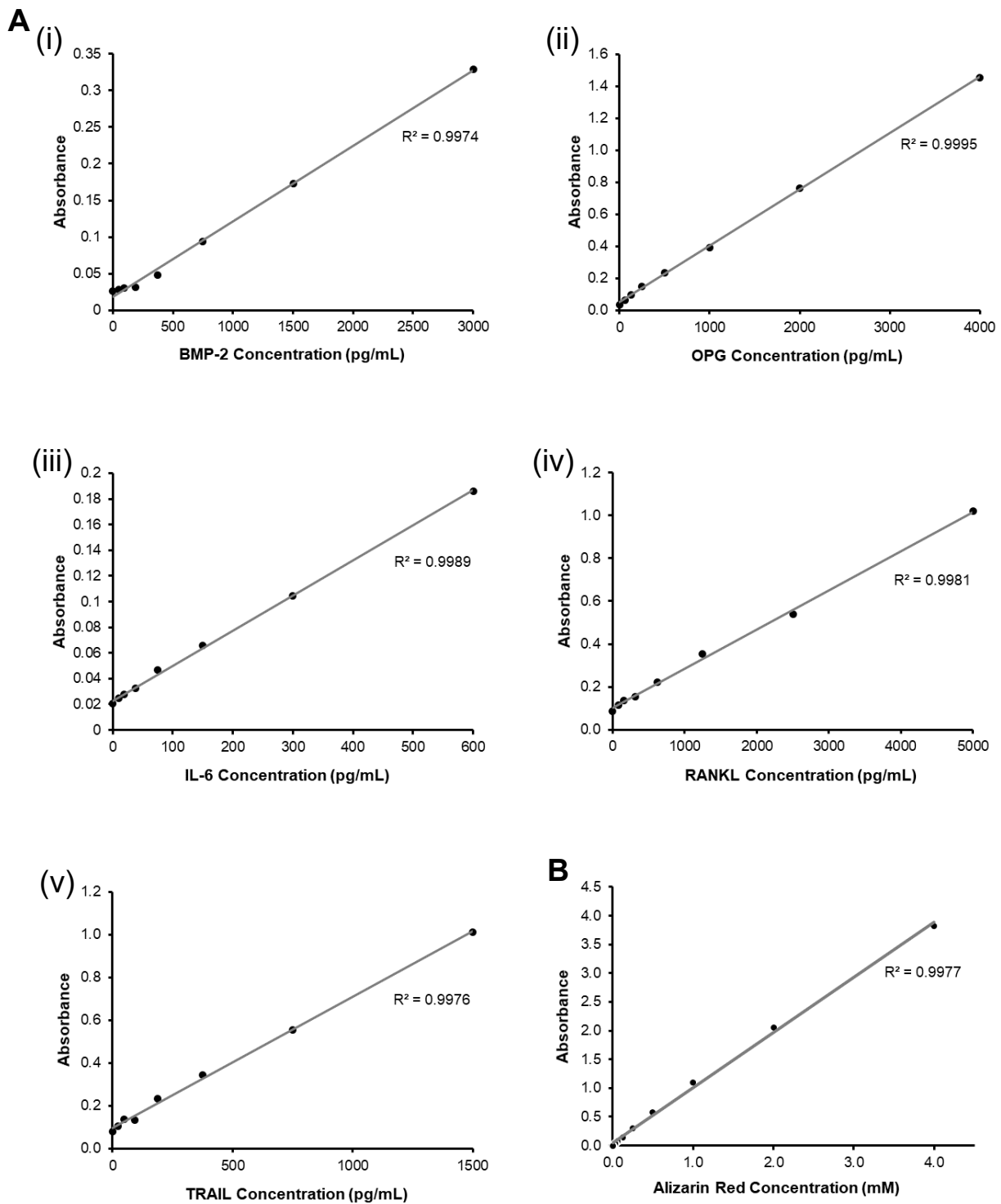
Appendix 2

Appendix 2.1. Primer efficiency values for all primer sets employed in PCR.

Target Gene	Primer Efficiency (%)
GAPDH	97
18S	98
OPG	100
RANKL	98
TRAIL	98
ALP	104
BMP-2	101
Runx2	98
Sox9	95
IL-6	95
p52/p100	98
TRACP5	94
SOD1	97
SOD2	100
eNOS	92
SM α -actin	100
SM22 α	100
RANK	100
DcR1	101
DcR2	104
DR4	101
DR5	94
gp91	96
p47	101
HMOX1	100
BSP	99
OCN	104
BSP (murine)	95
OCN (murine)	96

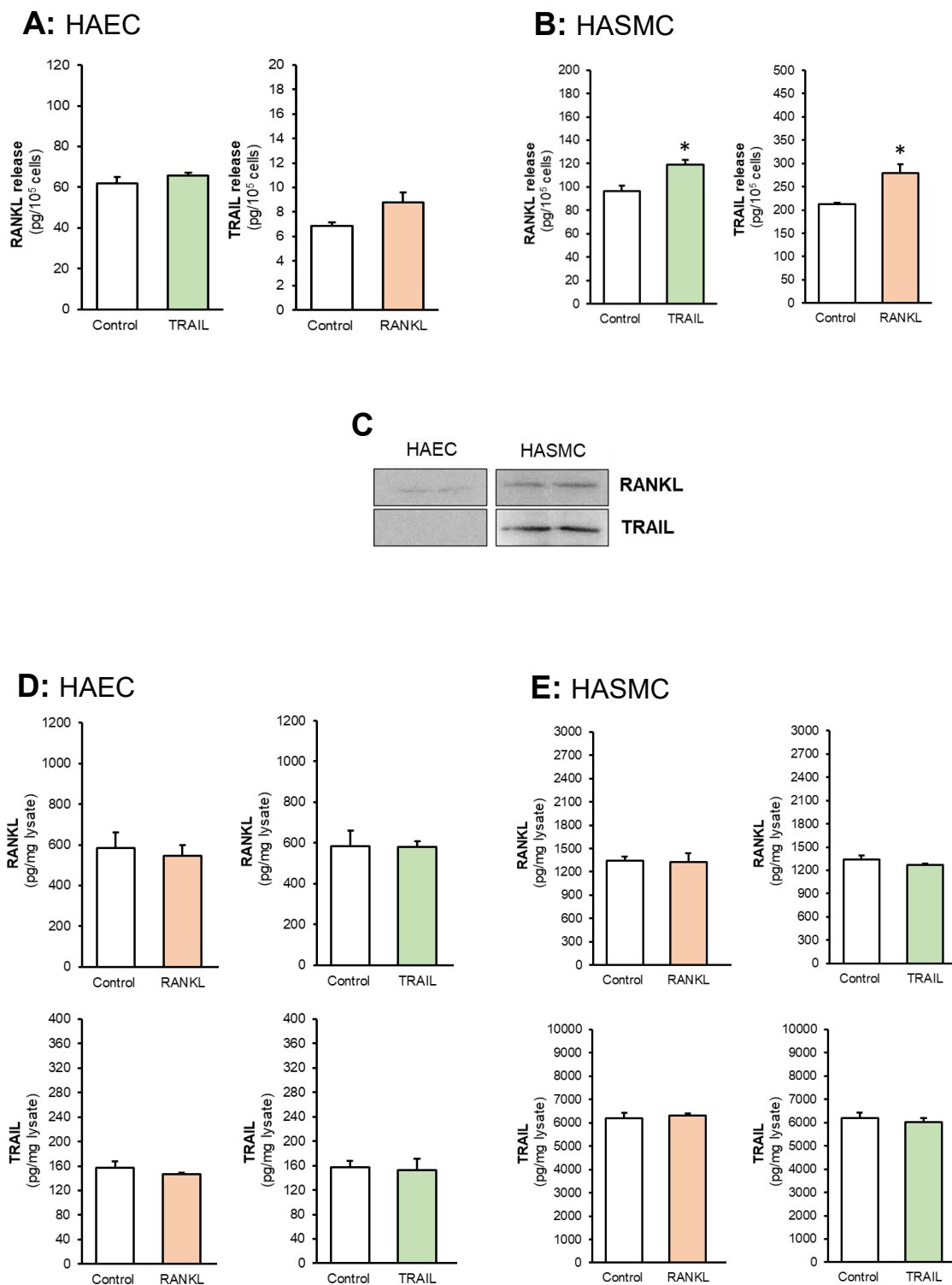
Prior to gene expression analysis, all primer sets were assessed for primer efficiency (Section 2.2.3.8). It was ensured that all efficiency values fell between the accepted range of 90-105% as specified by the MIQE guidelines.

Appendix 2



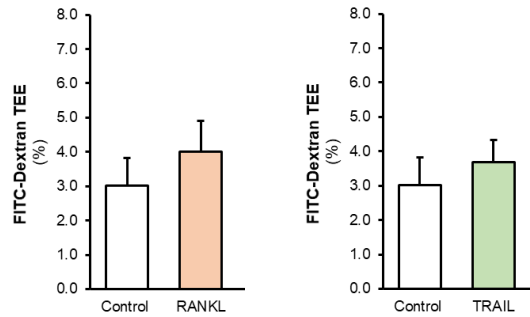
Appendix 2.2. Typical standard curves for ELISA and alizarin red S staining. (A) In order to enable protein quantification, standard curves were included for ELISA experiments. Fresh standard curves were included for each ELISA run, with representative curves for (i) BMP-2, (ii) OPG, (iii) IL-6, (iv) RANKL and (v) TRAIL presented above. (B) For quantification of alizarin red S stain for calcium deposition, a fresh standard curve was also employed for each run; a typical standard curve is presented above.

Appendix 3

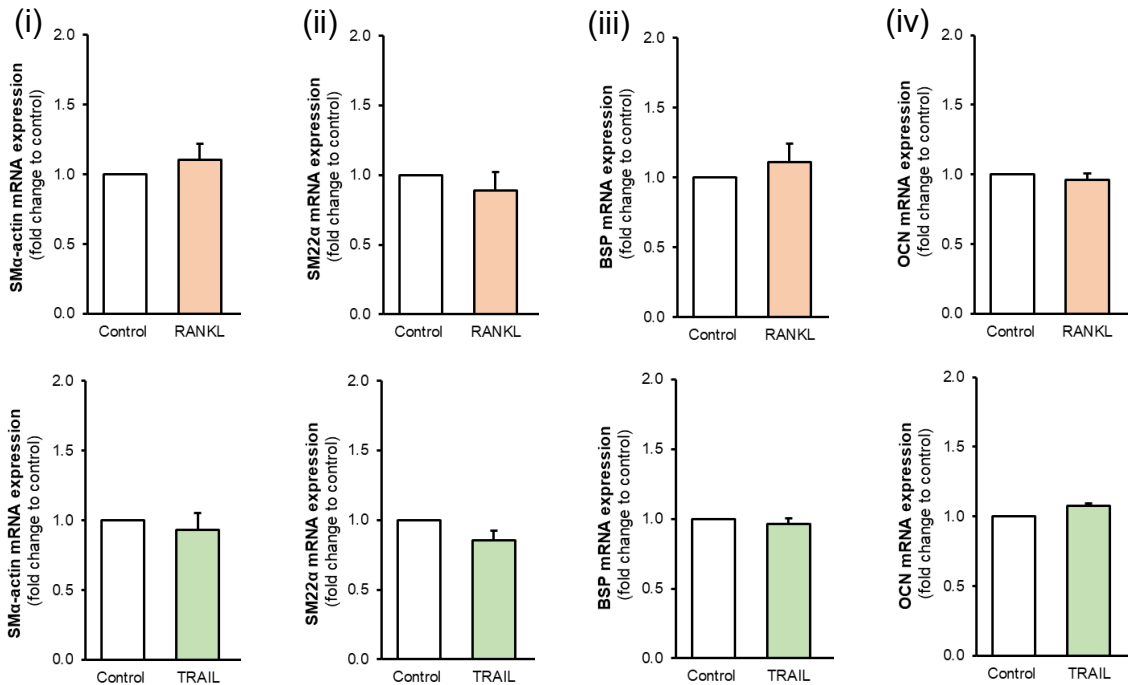


Appendix 3.1. RANKL and TRAIL release and intracellular protein expression in HAEC and HASMC monoculture. (A, B) RANKL and TRAIL release and (D, E) intracellular protein concentrations were determined by ELISA; (C) lysates were also analysed by Western blotting. HAECs (A, D) and HASMCs (B, E) were exposed to 25 ng/mL RANKL or 5 ng/mL TRAIL for 72 hours prior to analysis. Absolute values normalised to 10⁵ cells (release) or mg total protein (lysate). * $p < 0.05$ compared to untreated control.

A: HAEC

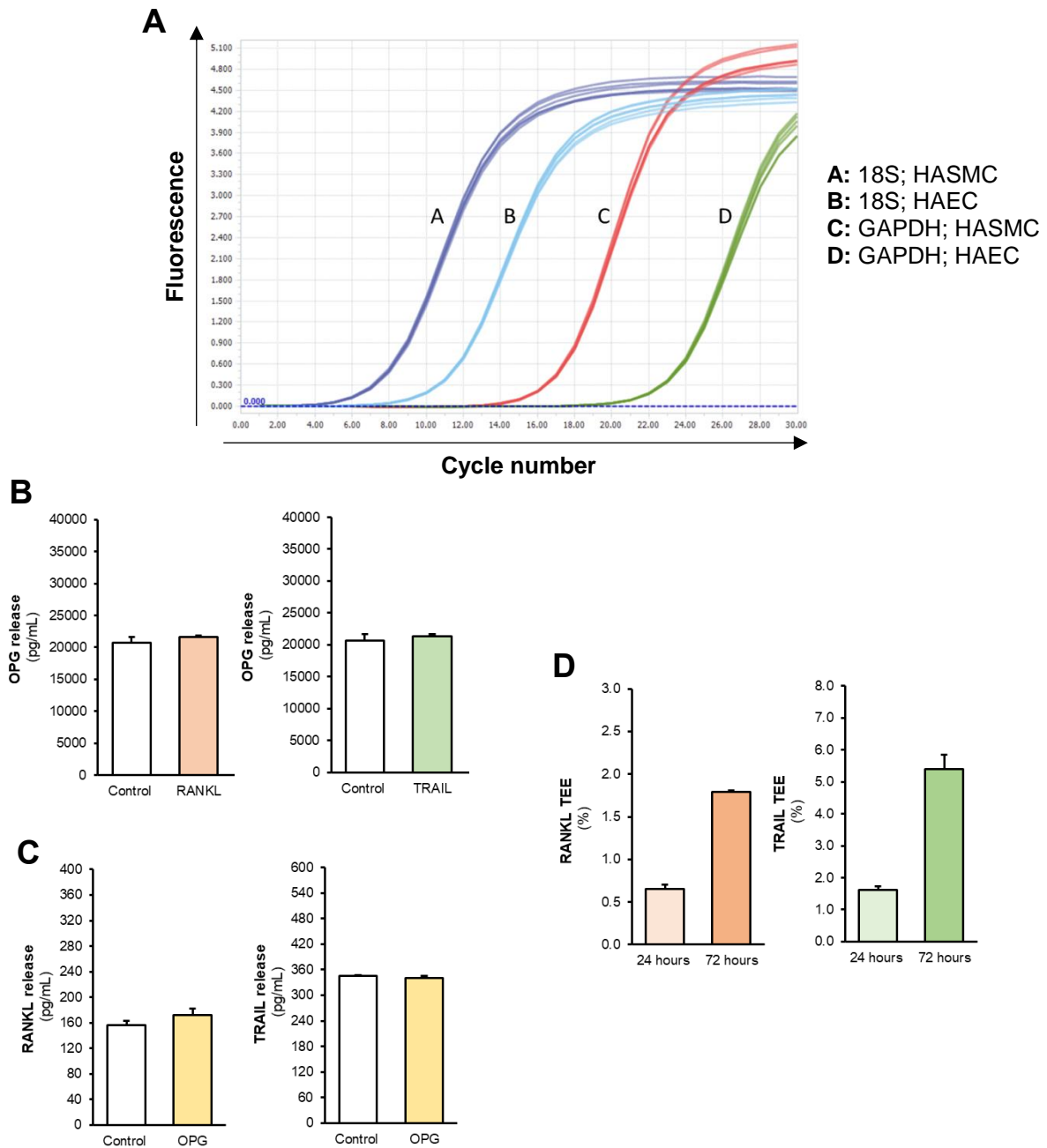


B: HASMC



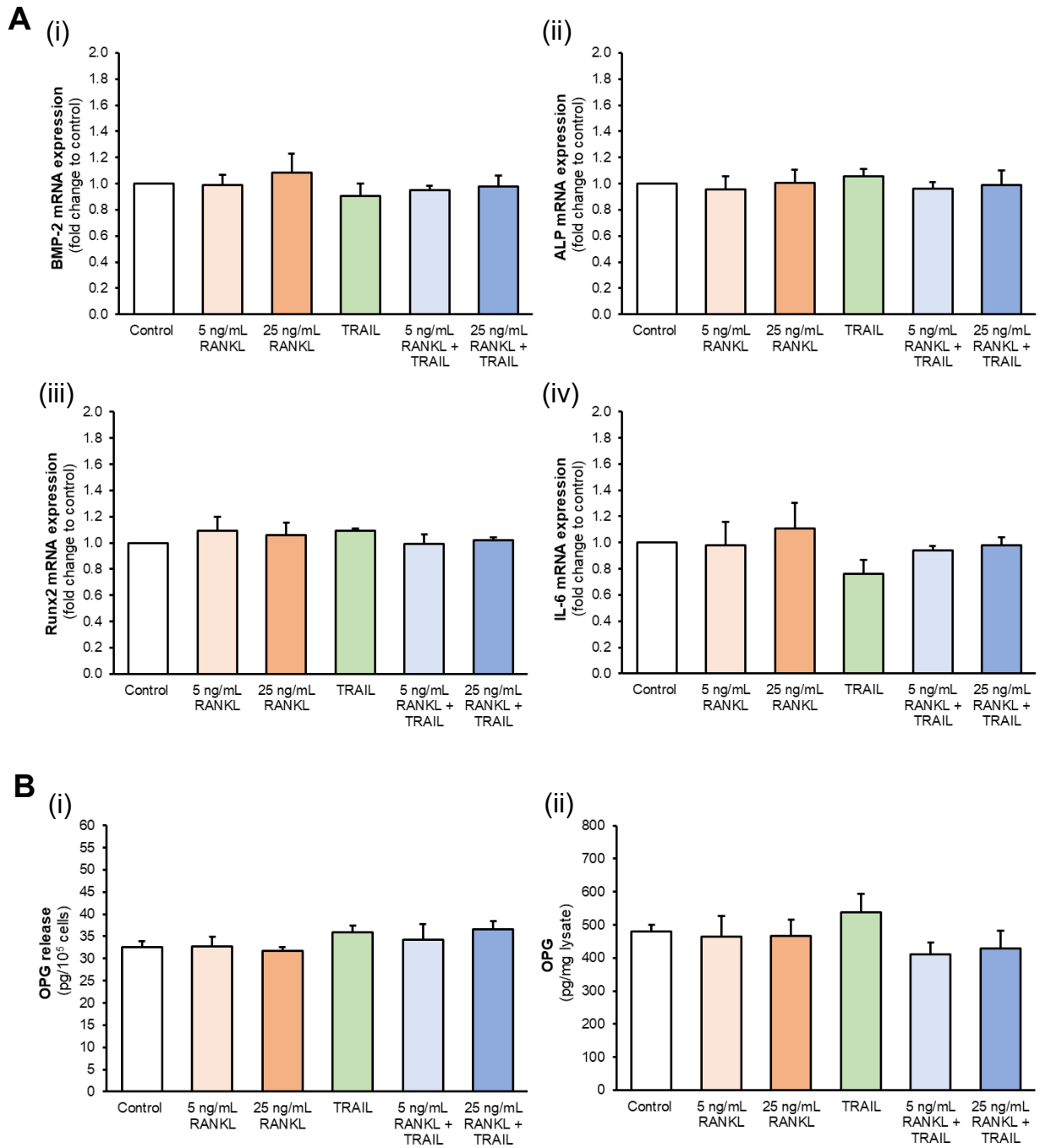
Appendix 3.2. The effects of RANKL and TRAIL on endothelial barrier function and smooth muscle phenotype in monoculture. (A) Percentage trans-endothelial exchange (TEE) of FITC-dextran from the luminal to the subluminal compartment as determined by permeability assay ($t = 3$ hours). HAECs were subject to 72-hour RANKL (25 ng/mL) or TRAIL (5 ng/mL) exposure prior to barrier analysis. Results presented as fold change to untreated control. (B) HASMCs were subject to RANKL (25 ng/mL) or TRAIL (5 ng/mL) treatment for 72 hours prior to mRNA analysis of (i) SM α -actin, (ii) SM22 α , (iii) BSP and (iv) OCN levels by RT-qPCR. Results presented as fold change to untreated control; 18S was employed as an endogenous control.

Appendix 3

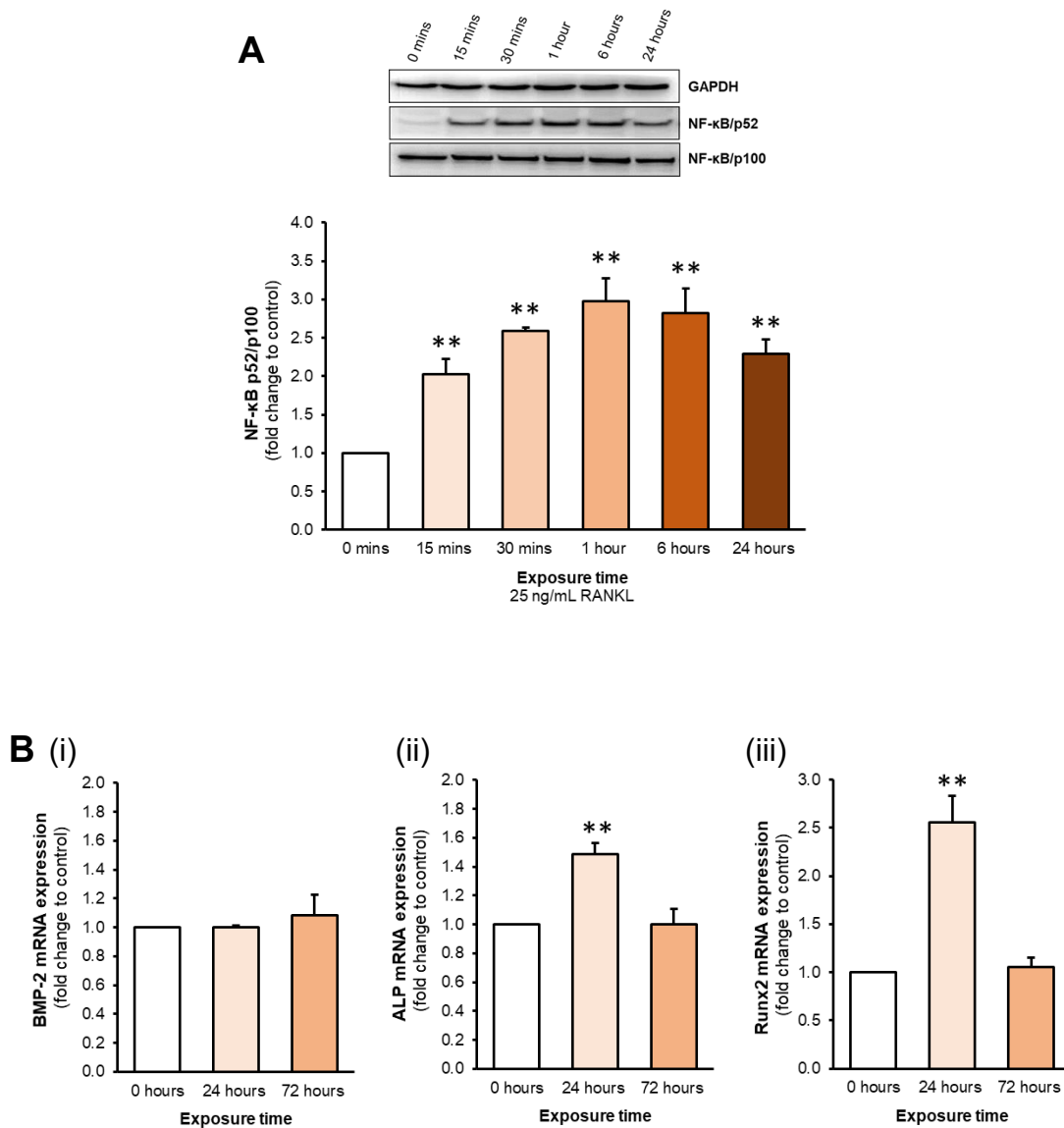


Appendix 3.3. Methodological validation. (A) Amplification curves for endogenous controls (18S, GAPDH) employed in qPCR. HAECs and HASMCs were exposed to RANKL (25 ng/mL) and TRAIL (5 ng/mL) for 72 hours prior to analysis. Samples were assayed in duplicate; control, RANKL and TRAIL amplification curves are overlapping. (B) OPG concentrations as determined by ELISA for HASMC-conditioned media (CM) and HASMC CM spiked with recombinant RANKL (25 ng/mL) and TRAIL (5 ng/mL). (C) RANKL and TRAIL concentrations as determined by ELISA for HASMC CM and HASMC CM spiked with recombinant OPG (20 ng/mL). ELISA results are presented as pg/mL absolute concentrations. (D) Percentage trans-endothelial exchange of recombinant RANKL and TRAIL from the luminal to the subluminal compartment in co-culture format after 24 and 72 hours.

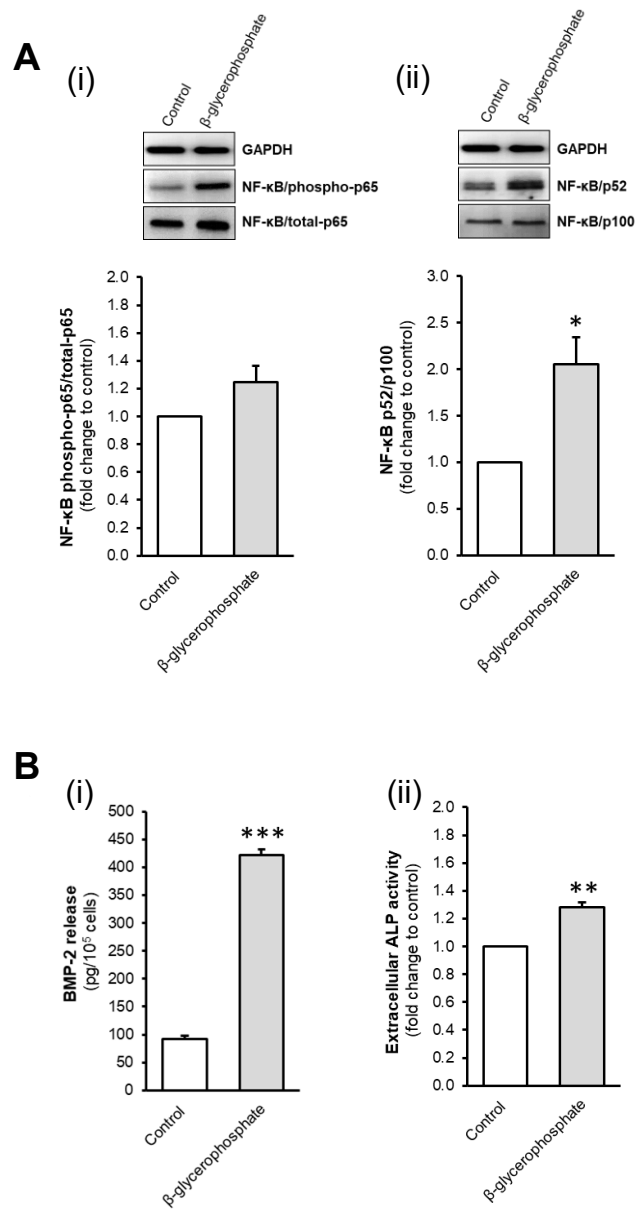
Appendix 3



Appendix 3.4. Pro-calcific mRNA expression and OPG protein production in HAEC monoculture. HAECs were exposed to RANKL (5-25 ng/mL) +/- TRAIL (5 ng/mL) for 72 hours. **(A)** (i) BMP-2, (ii) ALP, (iii) Runx2 and (iv) IL-6 mRNA expression levels were determined by RT-qPCR, with GAPDH employed as an endogenous control. **(B)** OPG (i) release and (ii) intracellular production were analysed by ELISA; absolute values for media and lysate are normalised to 10⁵ cells and total protein respectively.

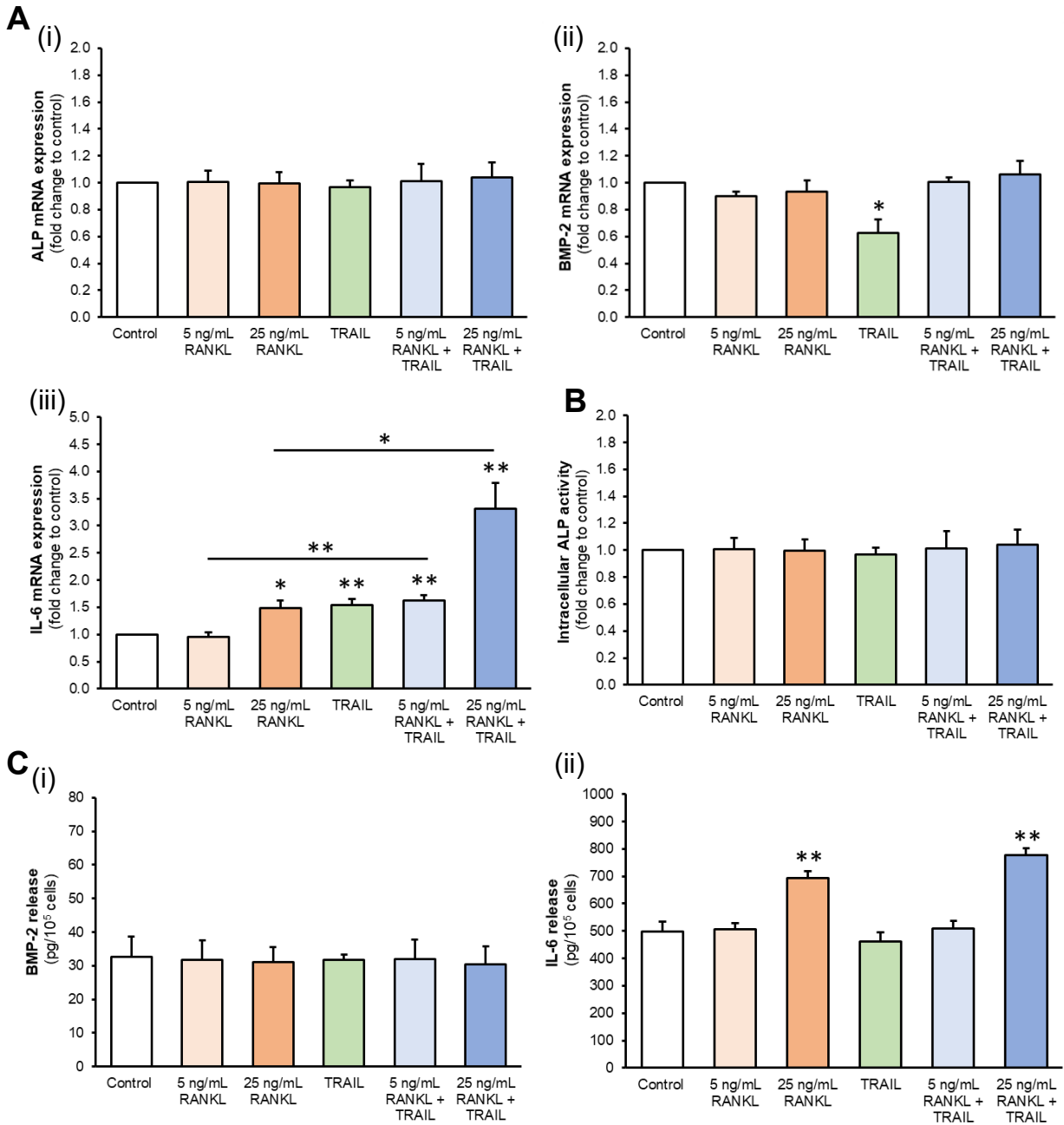


Appendix 3.5. Non-canonical NF- κ B activation and pro-calcific gene expression in HAECs at various time points. (A) HAECs were exposed to 25 ng/mL RANKL over a 0-24 hour time course. Lysates were assessed for non-canonical NF- κ B activation by Western blotting, and analysed by scanning densitometry normalised to GAPDH. Blots are representative. (B) HAECs were exposed to 25 ng/mL RANKL for 0, 24 and 72 hours. (i) BMP-2, (ii) ALP and (iii) Runx2 mRNA expression was evaluated by RT-qPCR, with GAPDH employed as a reference gene. * $p < 0.05$; ** $p < 0.01$ compared to the 0-hour time point.



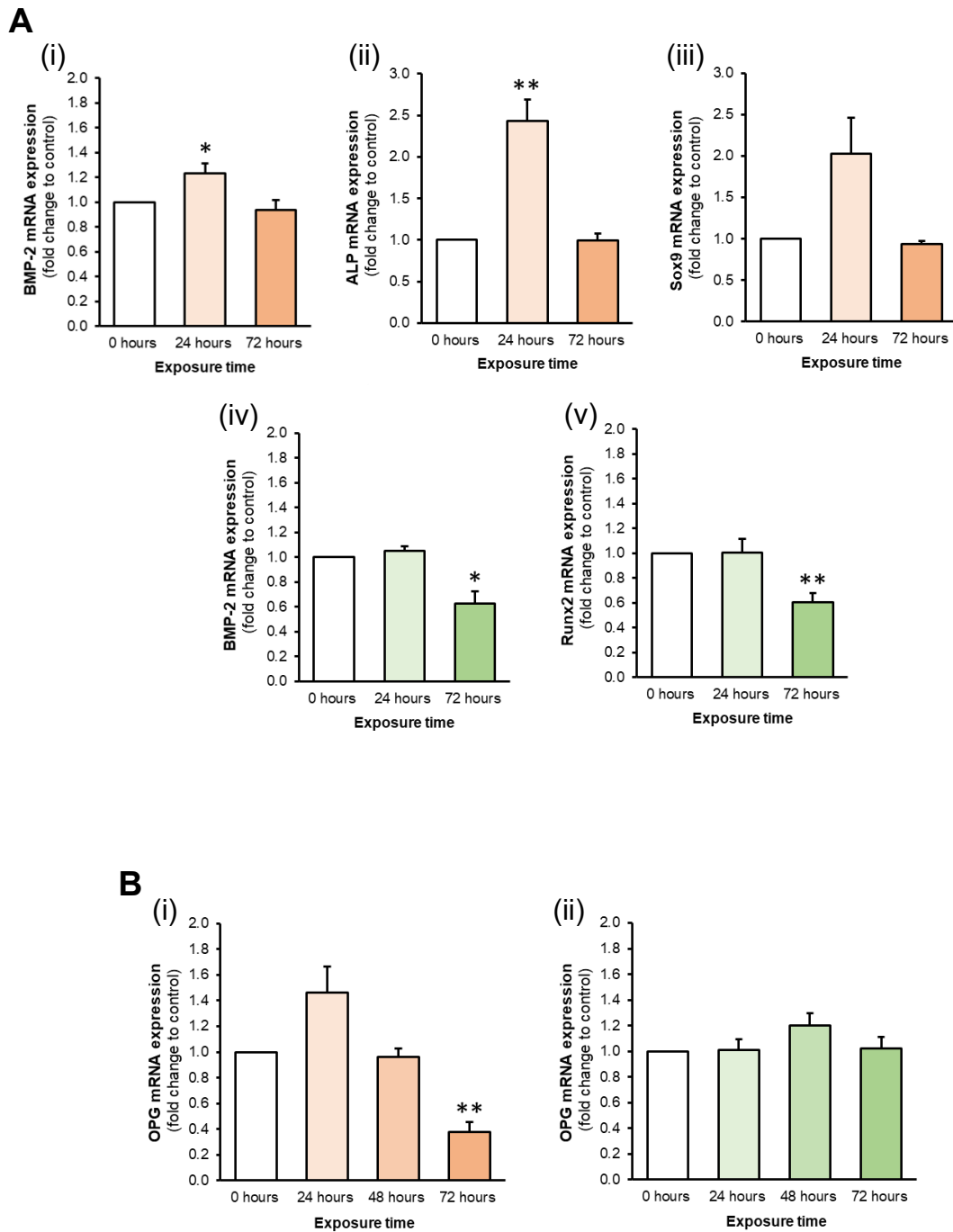
Appendix 3.6. HAEC responses to β-glycerophosphate exposure. HAECs were treated with 10 mM β-glycerophosphate for 72 hours. **(A)** Lysates were analysed for (i) canonical and (ii) non-canonical NF-κB activation by Western blotting, quantified by scanning densitometry and normalised to GAPDH. Blots are representative. **(B)** Conditioned media was assayed for (i) BMP-2 release by ELISA and (ii) ALP activity by enzyme activity assay. Absolute values are normalised to 10⁵ cells. * $p < 0.05$; ** $p < 0.01$; *** $p < 0.001$ compared to untreated control.

Appendix 3



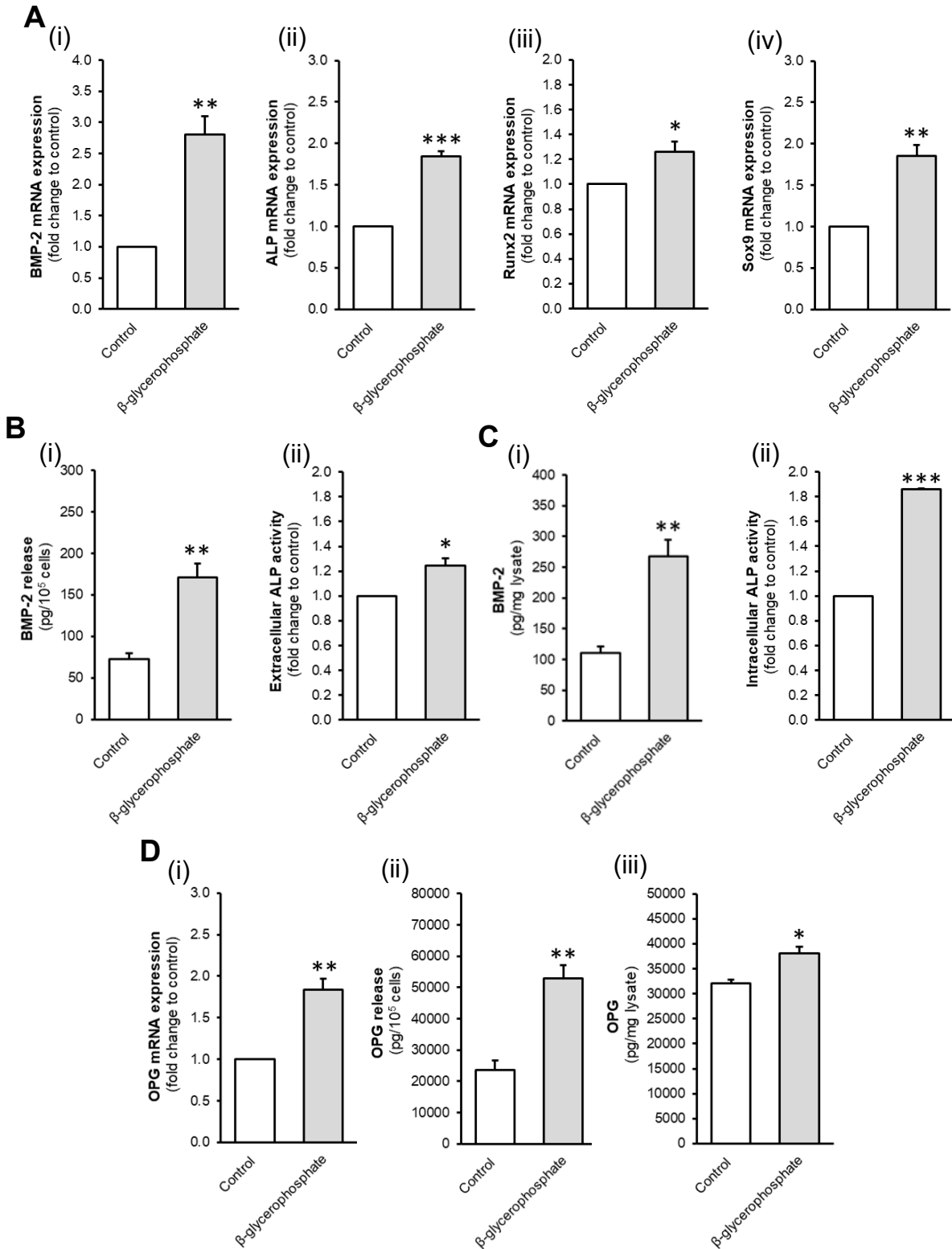
Appendix 3.7. Pro-calcific mRNA expression and protein production in HASMC monoculture. HASMCs were exposed to RANKL (5-25 ng/mL) +/- TRAIL (5 ng/mL) for 72 hours. **(A)** (i) ALP, (ii) BMP-2 and (iii) IL-6 mRNA expression levels were determined by RT-qPCR, with GAPDH employed as an endogenous control. **(B)** Intracellular ALP activity was determined via enzyme assay while **(C)** (i) BMP-2 and (ii) IL-6 release were quantified by ELISA. Absolute values for media and lysate are and normalised to 10⁵ cells and total protein respectively. * $p < 0.05$; ** $p < 0.01$ compared to untreated control unless otherwise stated; bars indicate statistical significance between treatment groups.

Appendix 3



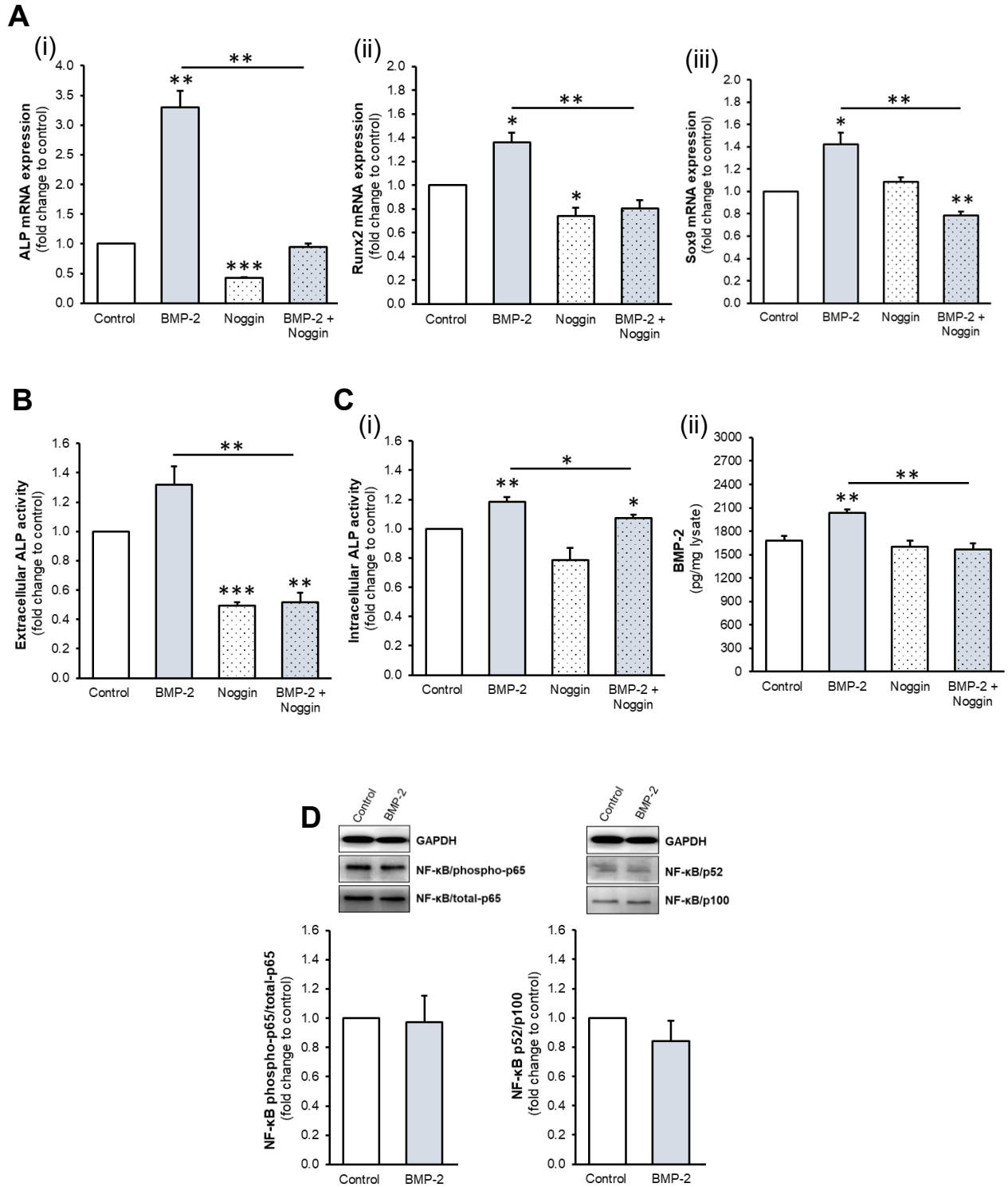
Appendix 3.8. Expression of mRNA indices in HASMCs over a 72-hour time course. (A) HASMCs were exposed to RANKL (25 ng/mL) or TRAIL (5 ng/mL) for 0, 24 and 72 hours. (i) BMP-2, (ii) ALP and (iii) Sox9 mRNA levels were investigated by RT-qPCR in response to RANKL, while (iv) BMP-2 and (v) Runx2 mRNA levels were analysed in response to TRAIL. (B) HASMCs were exposed to RANKL (25 ng/mL) or TRAIL (5 ng/mL) for 0, 24, 48 and 72 hours. OPG mRNA was analysed by RT-qPCR in response to (i) RANKL and (ii) TRAIL. GAPDH was employed as a reference gene. * $p < 0.05$; ** $p < 0.01$ compared to the 0-hour time point.

Appendix 3



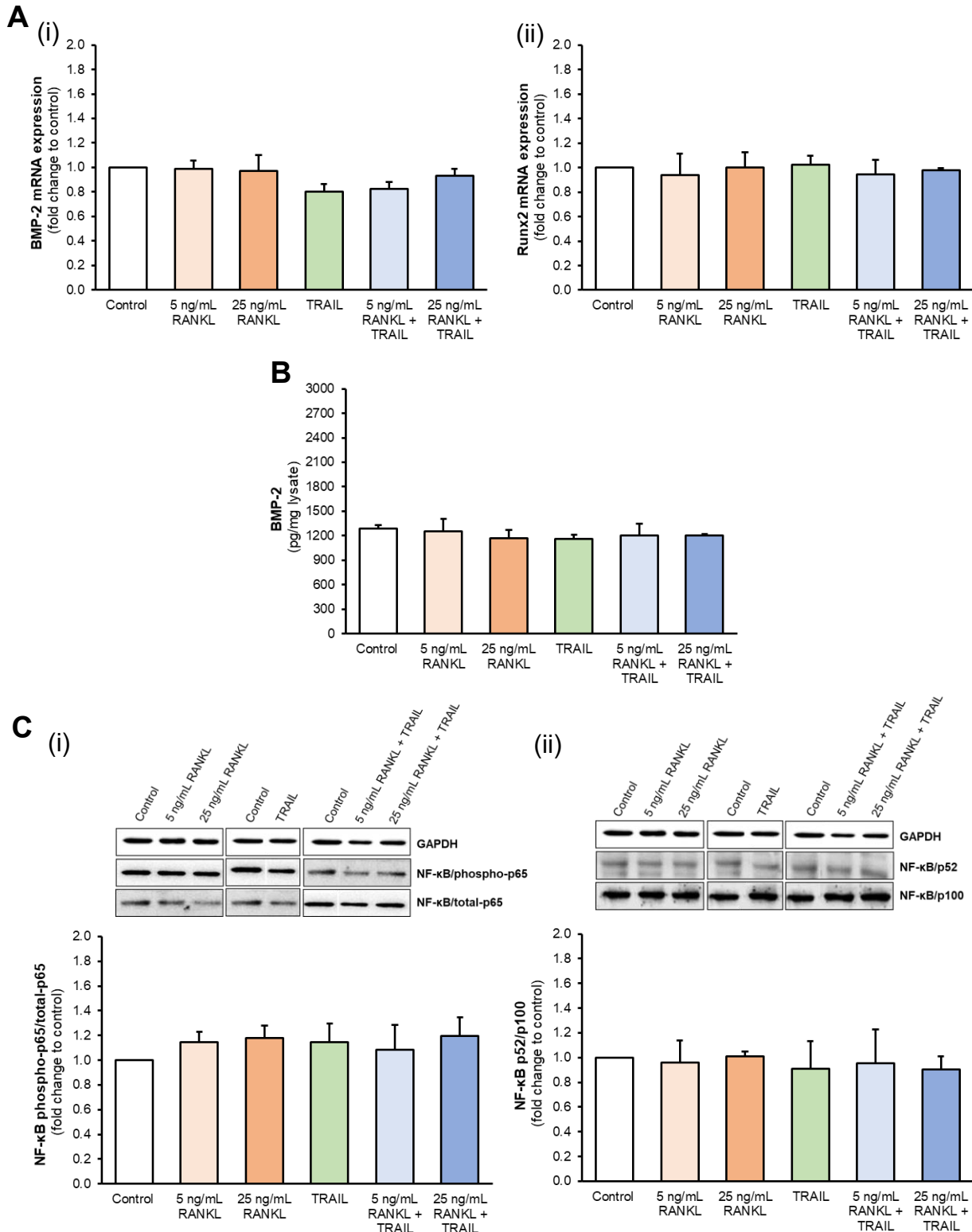
Appendix 3.9. HASMC responses to β -glycerophosphate exposure. HASMCs were treated with 10 mM β -glycerophosphate for 72 hours. (A) Pro-calcific transcripts (i) BMP-2, (ii) ALP, (iii) Runx2 and (iv) Sox9 were analysed. (B) Conditioned media was assayed for (i) BMP-2 release by ELISA and (ii) ALP activity by enzyme activity assay. (C) Lysates were analysed for (i) BMP-2 and (ii) ALP activity by ELISA and enzyme assay respectively. (D) OPG (i) mRNA, (ii) release and (iii) intracellular protein were analysed by RT-qPCR and ELISA where appropriate. GAPDH was employed as a reference gene for all RT-qPCR analyses. Absolute values are normalised to 10^5 cells and total cell protein for extra- and intracellular analyses respectively. * $p < 0.05$; ** $p < 0.01$; *** $p < 0.001$ compared to untreated control.

Appendix 3



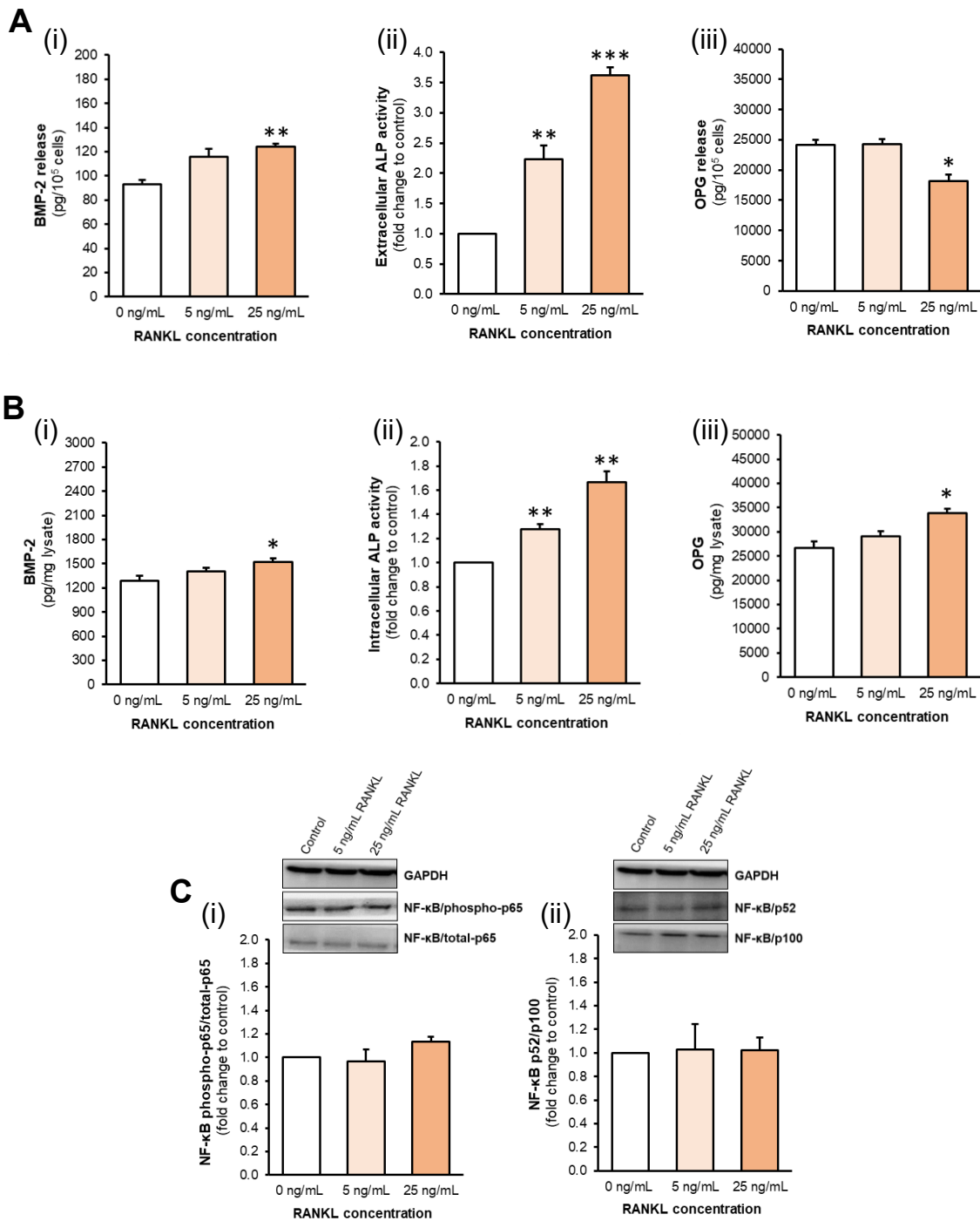
Appendix 3.10. HASMC responses to BMP-2 +/- noggin exposure. HASMCs were exposed to BMP-2 (5 ng/mL) and/or noggin (100 ng/mL) for 72 hours. **(A)** mRNA transcripts were assessed for (i) ALP, (ii) Runx2 and (iii) Sox9 by RT-qPCR, employing GAPDH as a reference gene. **(B)** Conditioned media was assessed for ALP activity via enzyme assay, normalising to 10^5 cells. **(C)** Intracellular (i) ALP and (ii) BMP-2 were analysed by activity assay and ELISA respectively, normalising to total cell protein. **(D)** Canonical and non-canonical NF- κ B activation were monitored by Western blotting and analysed by scanning densitometry, normalised to GAPDH. Blots are representative. * $p < 0.05$; ** $p < 0.01$; *** $p < 0.001$ compared to untreated control unless otherwise stated; bars indicate statistical significance between treatment groups.

Appendix 3

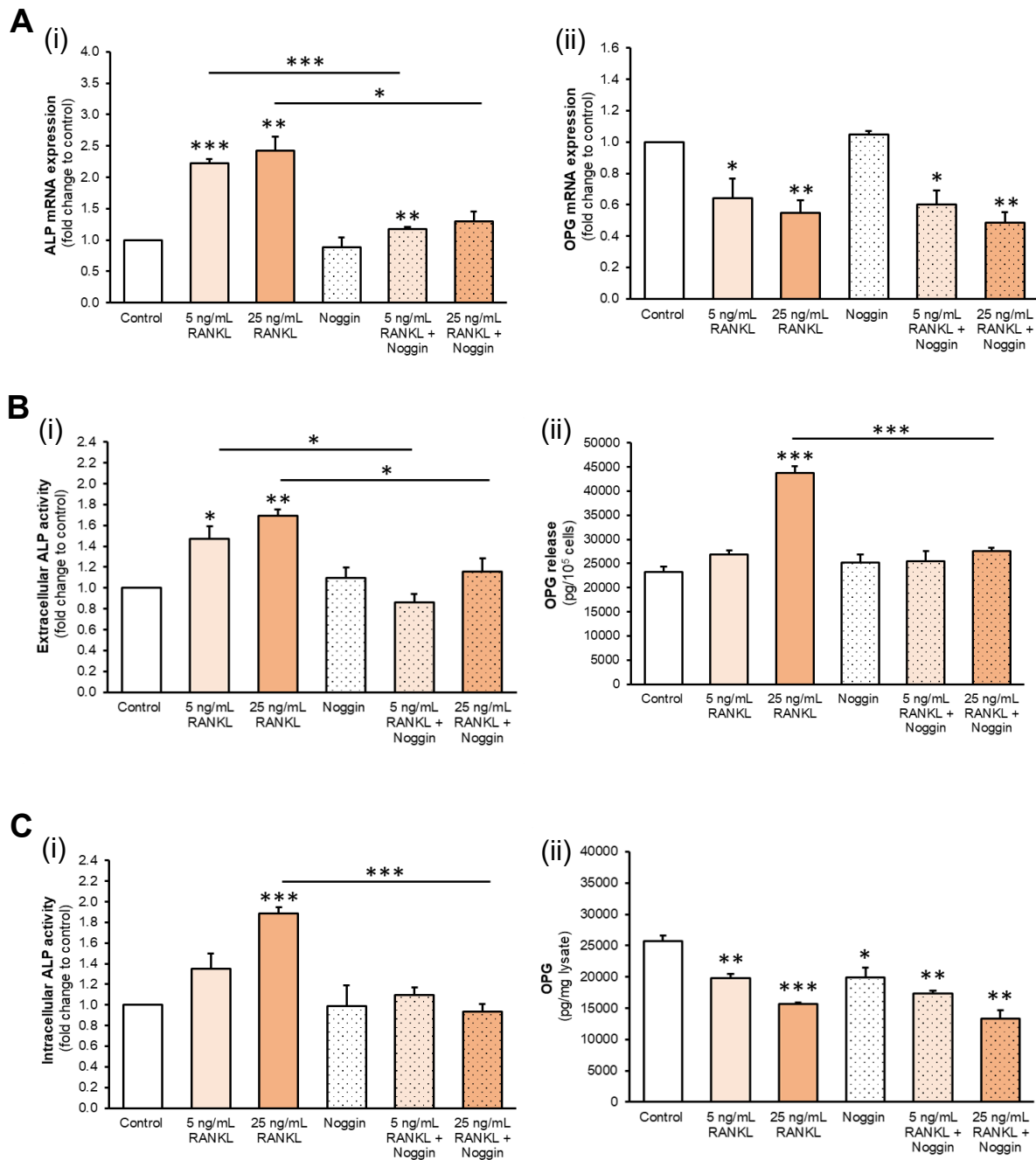


Appendix 3.11. HASMC gene expression, protein production and NF- κ B activation following endothelial treatment in co-culture. HAECs in transwell inserts were exposed to RANKL (5-25 ng/mL) +/- TRAIL (5 ng/mL) for 72 hours. In the underlying co-cultured HASMCs, (A) (i) BMP-2 and (ii) Runx2 mRNA expression levels were determined by RT-qPCR, with GAPDH employed as an endogenous control. (B) Intracellular BMP-2 was quantified by ELISA, normalised to total protein levels. (C) (i) Canonical and (ii) non-canonical NF- κ B activation was analysed by Western blotting and quantified by scanning densitometry, normalised to GAPDH. Blots are representative.

Appendix 3



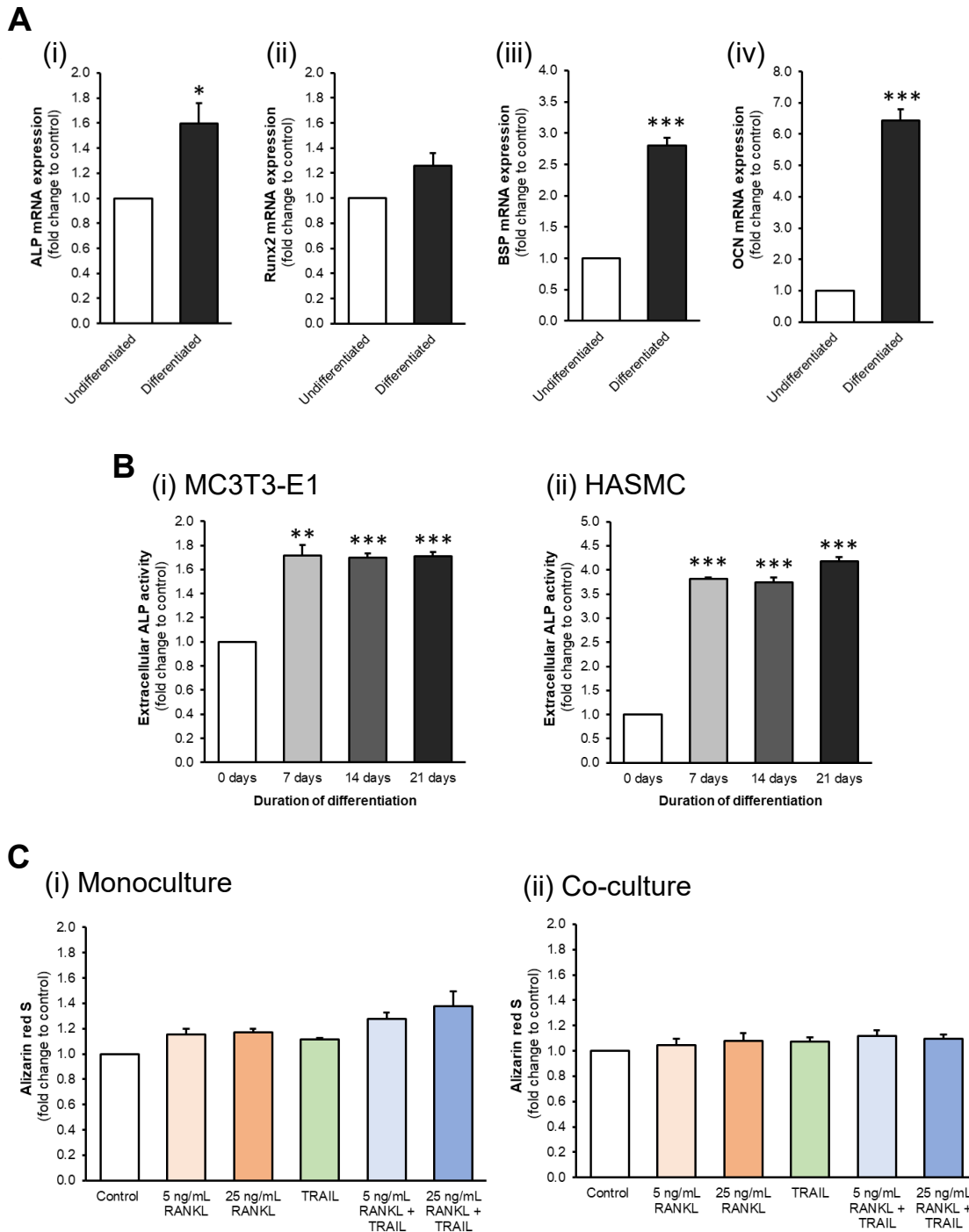
Appendix 3.12. HASMC responses post-exposure to HAEC-conditioned media following endothelial RANKL treatment. HAECs were treated with 25 ng/mL RANKL for 72 hours; HAEC conditioned media was then transferred to reporter HASMCs in culture for a further 72 hours. (A) Extracellular (i) BMP-2, (ii) ALP activity and (iii) OPG were measured by ELISA (BMP-2, OPG) and activity assay (ALP), normalised to 10⁵ cells (HASMCs). (B) Intracellular (i) BMP-2, (ii) ALP activity and (iii) OPG were quantified in a similar manner, normalised to total cell protein. (C) (i) Canonical and (ii) non-canonical NF-κB activation was analysed by Western blotting and quantified by scanning densitometry, normalised to GAPDH. Blots are representative. * $p < 0.05$; ** $p < 0.01$; *** $p < 0.001$ compared to control (0 ng/mL RANKL) HAEC-conditioned media.



Appendix 3.13. HASMC responses in co-culture following endothelial RANKL treatment, +/- noggin.

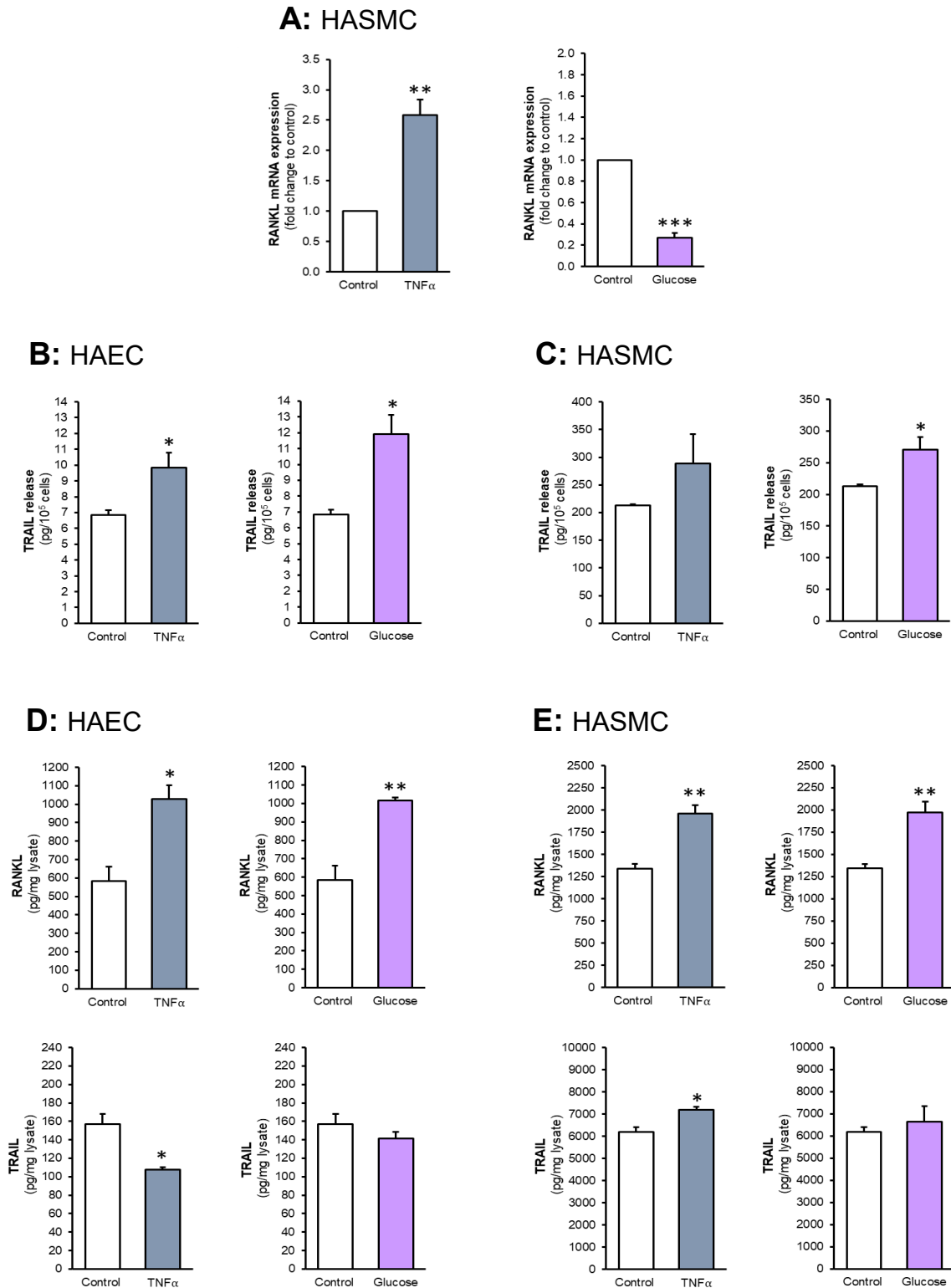
HAECs in transwell inserts were exposed to RANKL (5-25 ng/mL) for 72 hours, +/- noggin (100 ng/mL) in the subluminal compartment. **(A)** mRNA transcripts for (i) ALP and (ii) OPG were analysed in co-cultured HASMCs by RT-qPCR, normalised to GAPDH. **(B)** Extracellular (i) ALP activity and (ii) OPG release were quantified by activity assay and ELISA respectively, normalised to 10⁵ cells (HASMCs). **(C)** Intracellular (i) ALP activity and (ii) OPG were quantified in a similar manner, normalised to total cell protein. * *p* < 0.05; ** *p* < 0.01; *** *p* < 0.001 compared to untreated control unless otherwise stated; bars indicate statistical significance between treatment groups.

Appendix 3



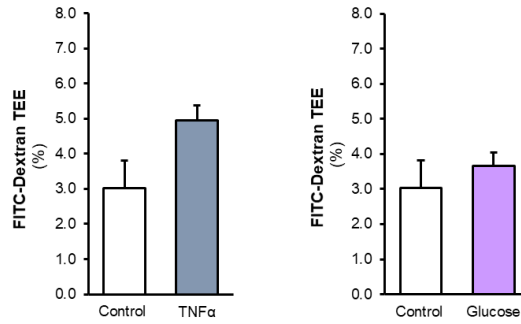
Appendix 3.14. Osteogenic differentiation of MC3T3-E1 and HASMC, and alizarin red S staining of HASMCs in mono- and co-culture. MC3T3-E1 and HASMCs were exposed to osteogenic differentiation media for 21 days prior to analysis. **(A)** Pro-calcific markers (i) ALP and (ii) Runx2, and osteogenic differentiation markers (iii) BSP and (iv) OCN were assessed by RT-qPCR in MC3T3-E1 cells; GAPDH was employed as an endogenous control. **(B)** Extracellular ALP activity was monitored at 7, 14 and 21 days' differentiation via activity assay for (i) MC3T3-E1 and (ii) HASMCs. **(C)** HASMCs in (i) monoculture and (ii) co-culture were exposed to RANKL (5-25 ng/mL) +/- TRAIL (5 ng/mL) for the final 72 hours of differentiation, prior to alizarin red S staining and quantification by absorbance. * $p < 0.05$; ** $p < 0.01$; *** $p < 0.001$ compared to control (undifferentiated cells).

Appendix 4

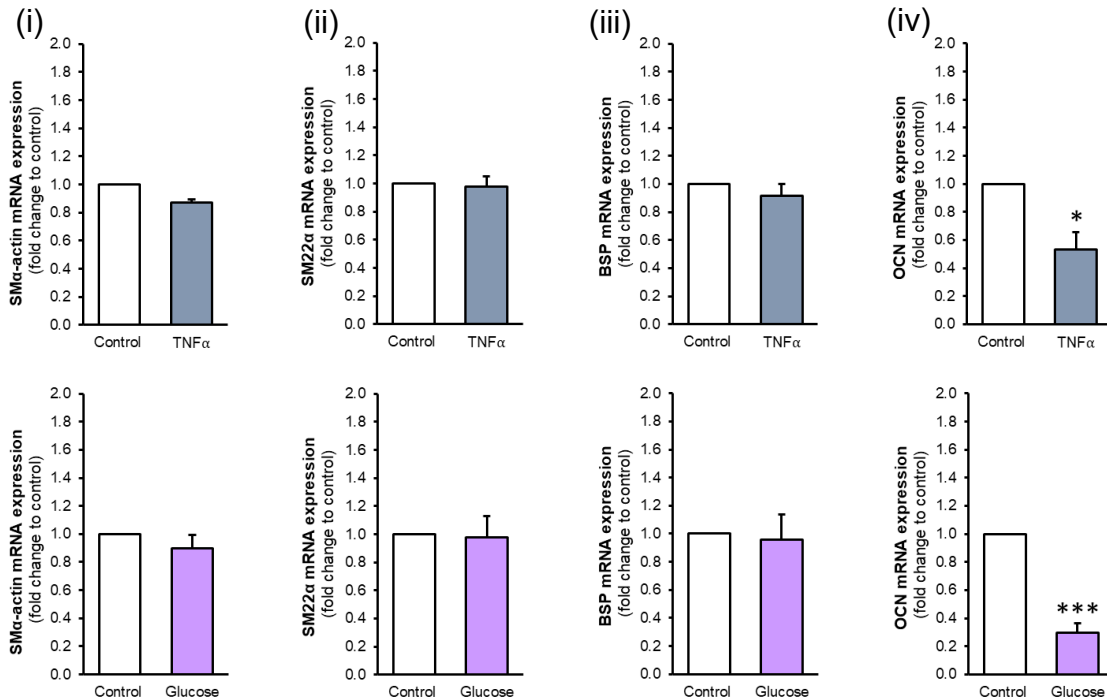


Appendix 4.1. RANKL and TRAIL expression in HAECs and HASMCs exposed to TNF α or glucose. HAECs and HASMCs were exposed to TNF α (100 ng/mL) or glucose (30 mM) for 72 hours. (A) HASMC RANKL mRNA expression was analysed by RT-qPCR, employing 18S as an endogenous control. TRAIL release from (B) HAECs and (C) HASMCs were quantified by ELISA, normalised to 10^5 cells. Intracellular RANKL and TRAIL from (D) HAECs and (E) HASMCs were quantified by ELISA, normalised to total cellular protein. * $p < 0.05$; ** $p < 0.01$; *** $p < 0.001$ compared to untreated control.

A: HAEC

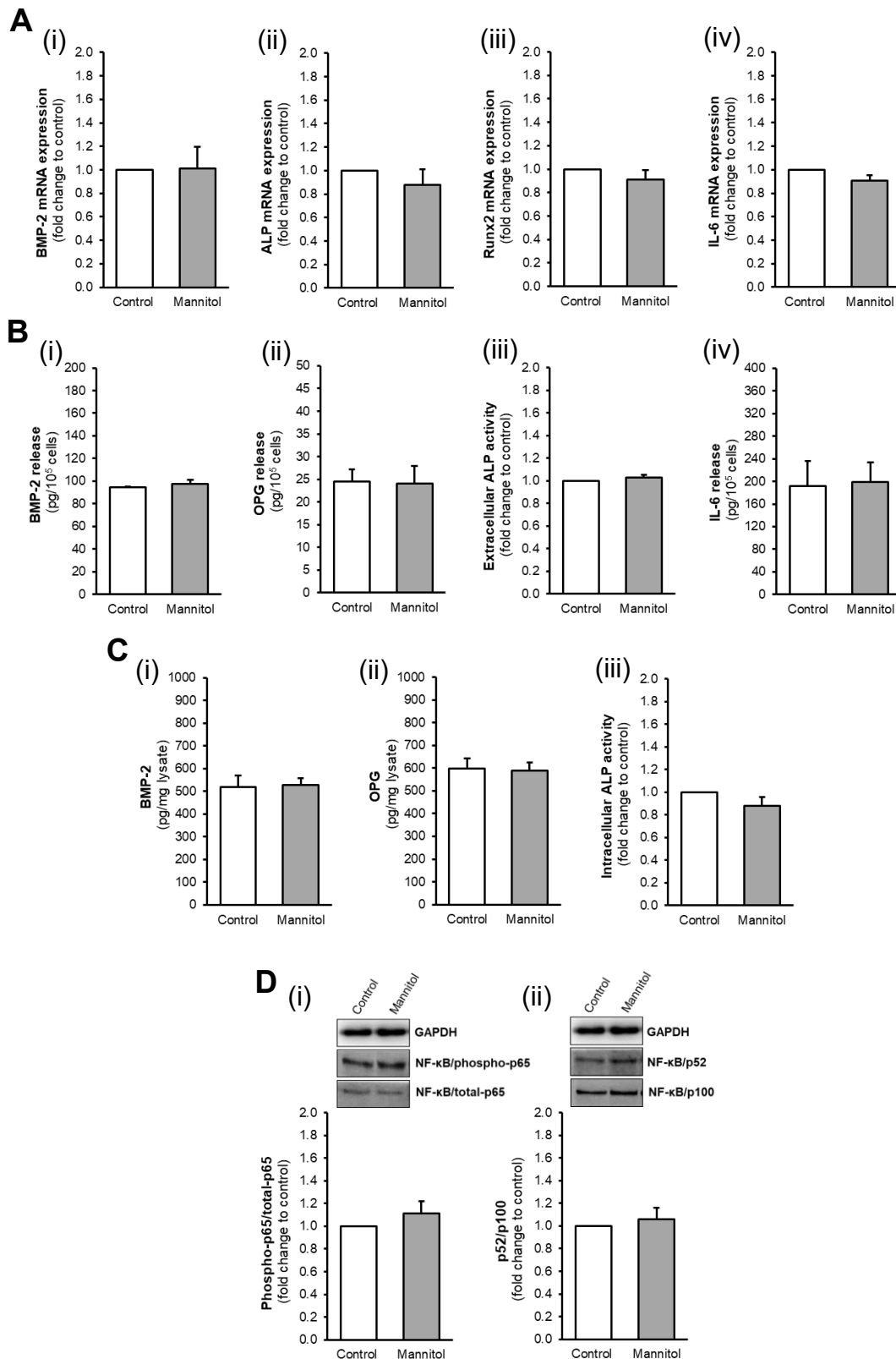


B: HASMC



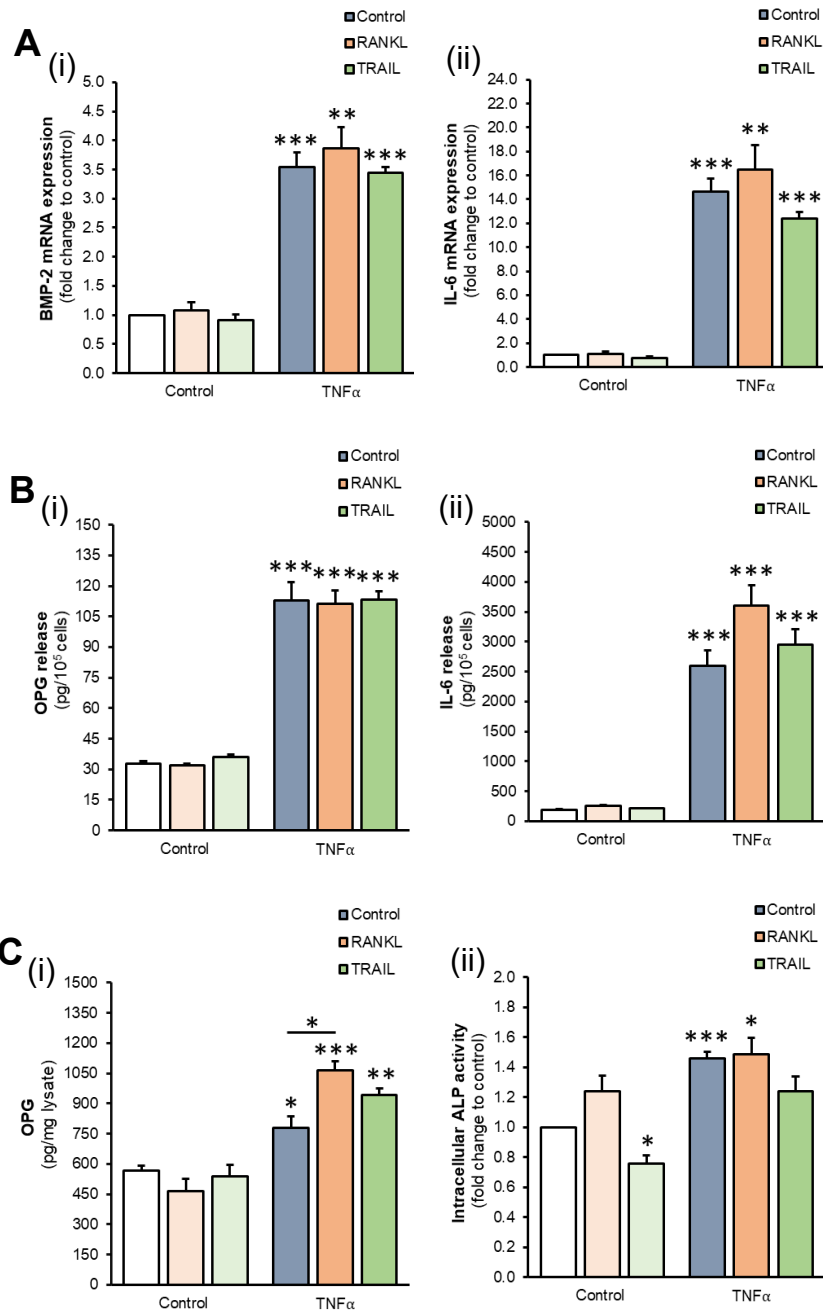
Appendix 4.2. The effects of TNF α and glucose on endothelial barrier function and smooth muscle phenotype in monoculture. (A) Percentage trans-endothelial exchange (TEE) of FITC-dextran from the apical to the basolateral compartment as determined by permeability assay ($t = 3$ hours). HAECs were subject to 72-hour TNF α (100 ng/mL) or glucose (30 mM) exposure prior to barrier analysis. Results presented as fold change to untreated control. (B) HASMCs were subject to TNF α (100 ng/mL) or glucose (30 mM) treatment for 72 hours prior to mRNA analysis of (i) SM α -actin, (ii) SM22 α , (iii) BSP and (iv) OCN levels by RT-qPCR. Results presented as fold change to untreated control; 18S was employed as an endogenous control.

Appendix 4



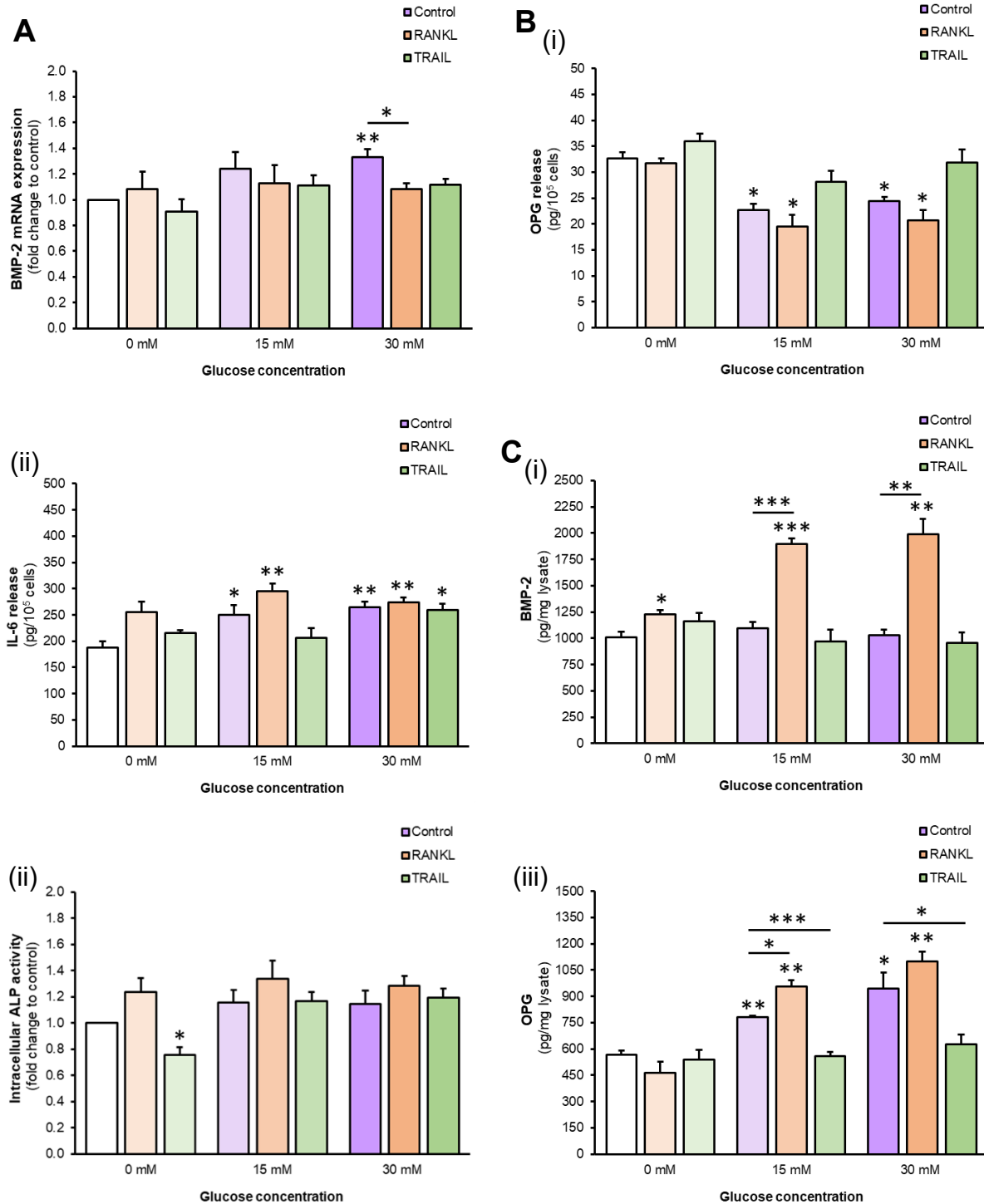
Appendix 4.3. The effect of mannitol exposure on pro-calcific indices in HAECs. HAECs were exposed to mannitol (30 mM) for 72 hours prior to analysis. **(A)** (i) BMP-2, (ii) ALP, (iii) Runx2 and (iv) IL-6 mRNA expression was determined by RT-qPCR, employing GAPDH as a reference gene. **(B)** Extracellular (i) BMP-2, (ii) OPG, (iii) ALP activity and (iv) IL-6 in the conditioned media and **(C)** intracellular (i) BMP-2, (ii) OPG and (iii) ALP activity were determined by ELISA and enzyme assay as appropriate. **(D)** (i) Canonical and (ii) non-canonical NF-κB activation were determined by Western blotting, quantified by scanning densitometry and normalised to GAPDH. Blots are representative. Media and lysate analyses are normalised to 10⁵ cells and pg lysate respectively.

Appendix 4



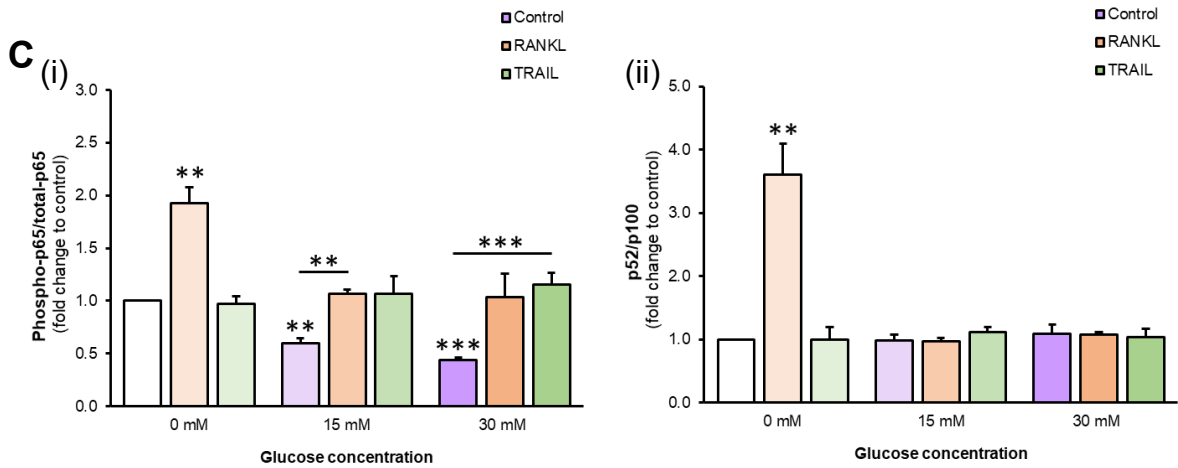
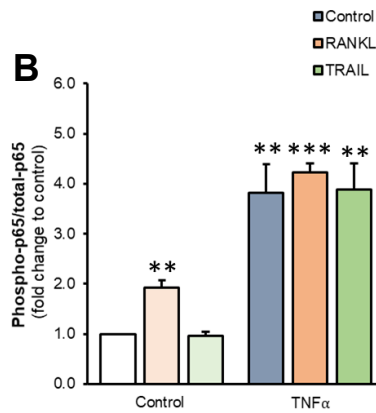
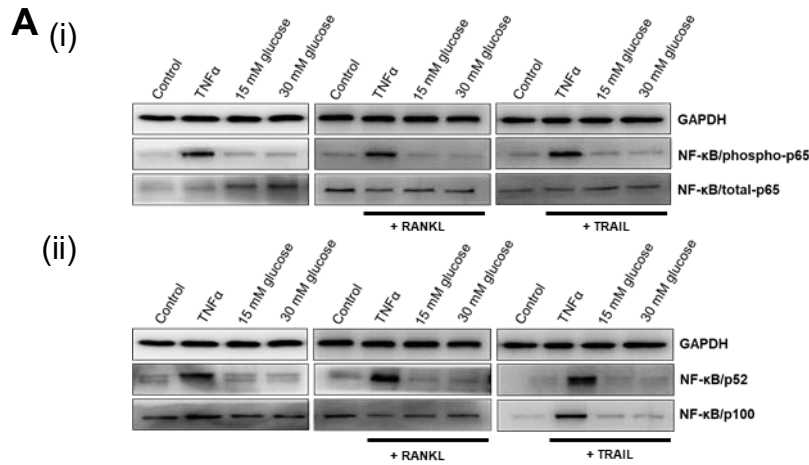
Appendix 4.4. The effects of TNF α +/- RANKL/TRAIL on pro-calcific indices in HAEC monoculture. HAECs were exposed to TNF α (100 ng/mL) +/- RANKL (25 ng/mL) or TRAIL (5 ng/mL) for 72 hours. (A) mRNA expression of (i) BMP-2 and (ii) IL-6 were analysed by RT-qPCR employing GAPDH as an endogenous control. (B) (i) OPG and (ii) IL-6 release and (C) intracellular (i) OPG and (ii) ALP activity were determined by ELISA and enzyme assay as appropriate, and normalised to 10⁵ cells (media) or total cell protein (lysate). * $p < 0.05$; ** $p < 0.01$; *** $p < 0.001$ compared to untreated control.

Appendix 4



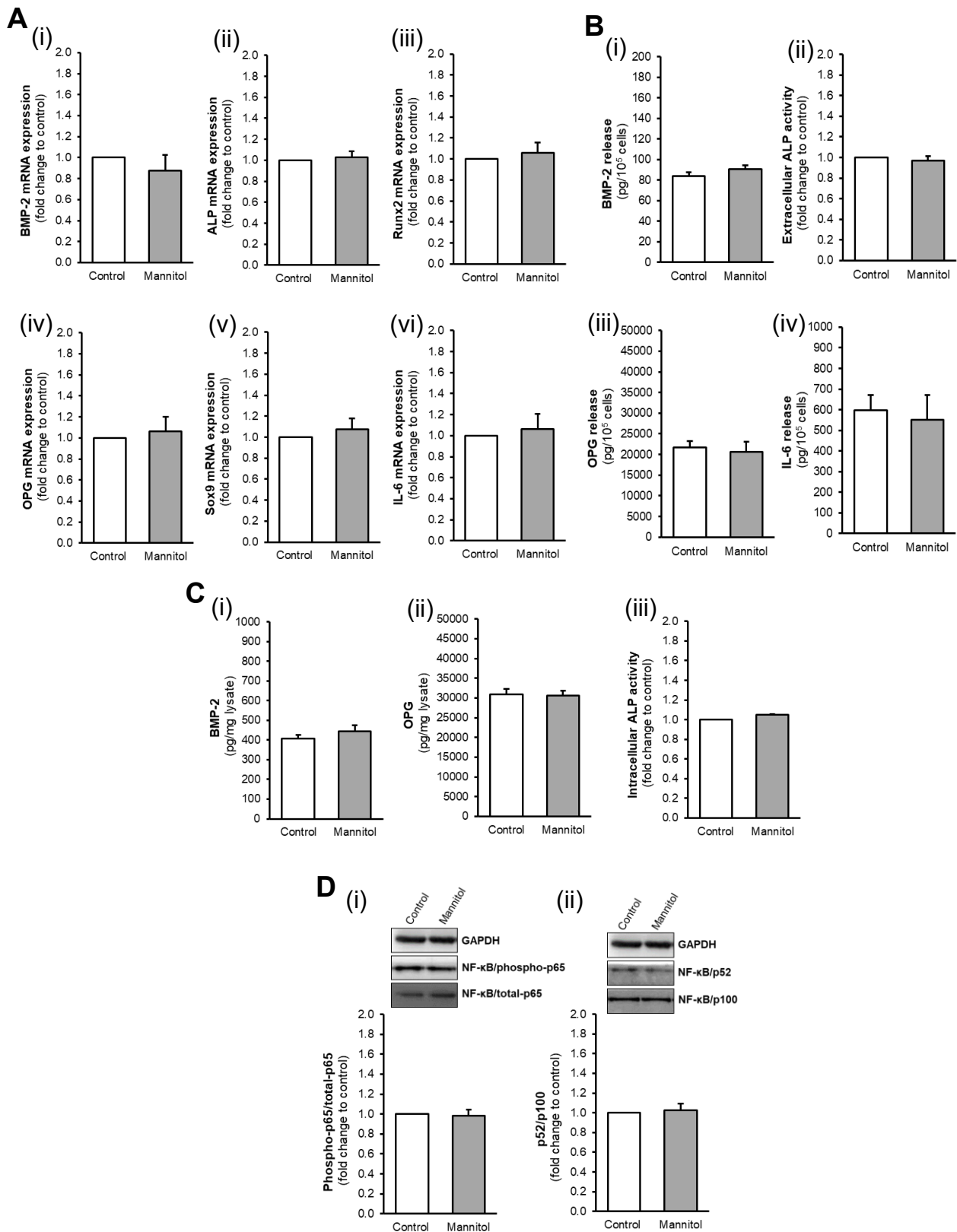
Appendix 4.5. The effects of glucose +/- RANKL/TRAIL on pro-calcific indices in HAEC monoculture.

HAECs were exposed to glucose (15-30 mM) +/- RANKL (25 ng/mL) or TRAIL (5 ng/mL) for 72 hours. (A) mRNA expression of BMP-2 was analysed by RT-qPCR employing GAPDH as an endogenous control. (B) (i) OPG and (ii) IL-6 release, and (C) intracellular (i) BMP-2, (ii) ALP activity and (iii) OPG were determined by activity assay and ELISA as appropriate, normalised to 10^5 cells (media) or total cell protein (lysate). * $p < 0.05$; ** $p < 0.01$; *** $p < 0.001$ compared to untreated control unless otherwise stated; bars indicate statistical significance between treatment groups.



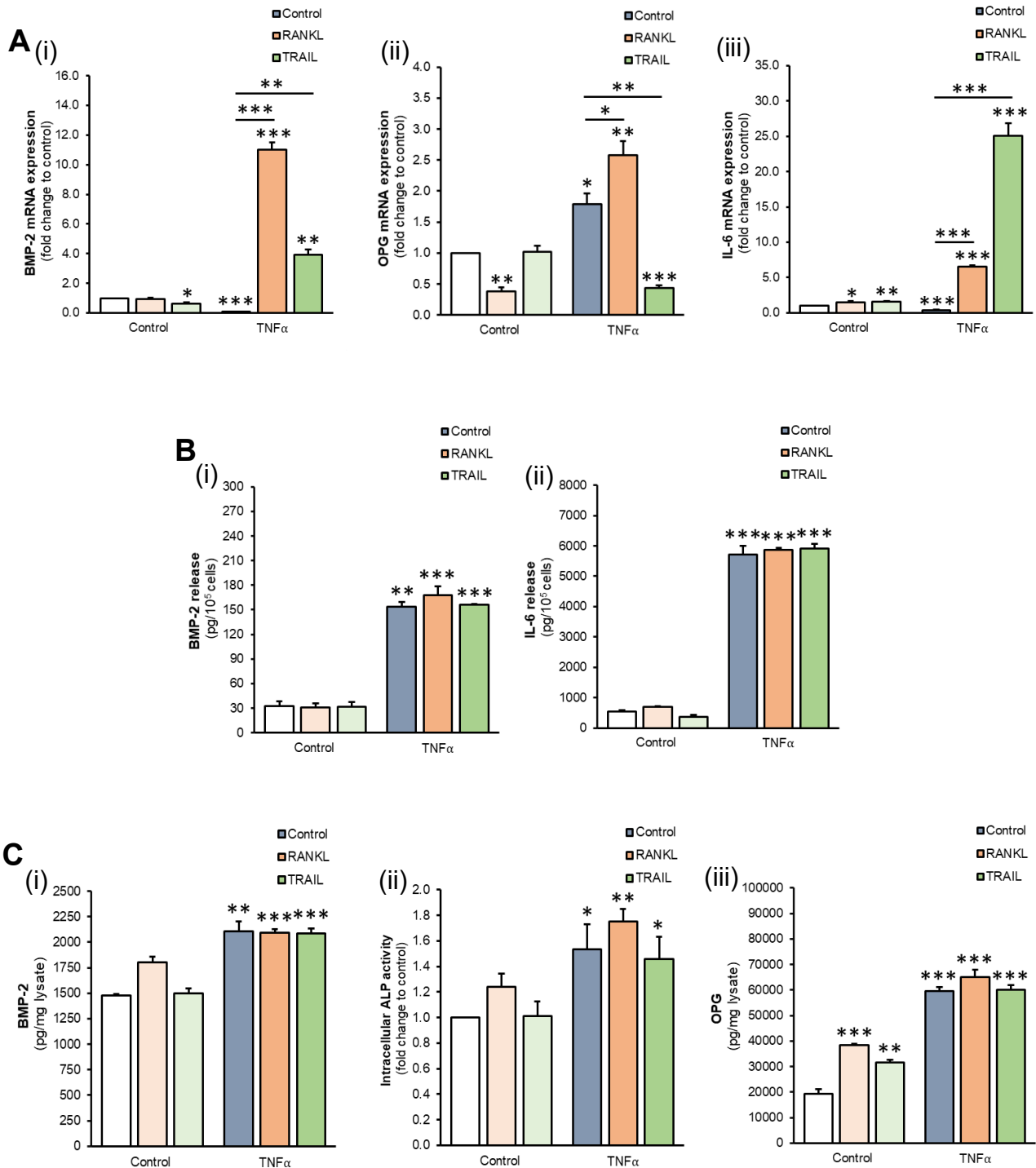
Appendix 4.6. The effects of TNF α and glucose +/- RANKL/TRAIL on NF- κ B activation in HAEC monoculture. HAECs were exposed to TNF α (100 ng/mL) or glucose (15-30 mM) +/- RANKL (25 ng/mL) or TRAIL (5 ng/mL) for 72 hours. **(A)** Representative blots for NF- κ B activation are presented for all conditions tested. **(B)** Canonical NF- κ B activation was assessed following exposure to TNF α +/- RANKL/TRAIL, and **(C)** (i) Canonical and (ii) non-canonical NF- κ B activation was assessed following exposure to glucose +/- RANKL/TRAIL. NF- κ B activation was determined by Western blotting, quantified by scanning densitometry and normalised to GAPDH. Absolute values are normalised to total protein. ** $p < 0.01$; *** $p < 0.001$ compared to untreated control unless otherwise stated; bars indicate statistical significance between treatment groups.

Appendix 4



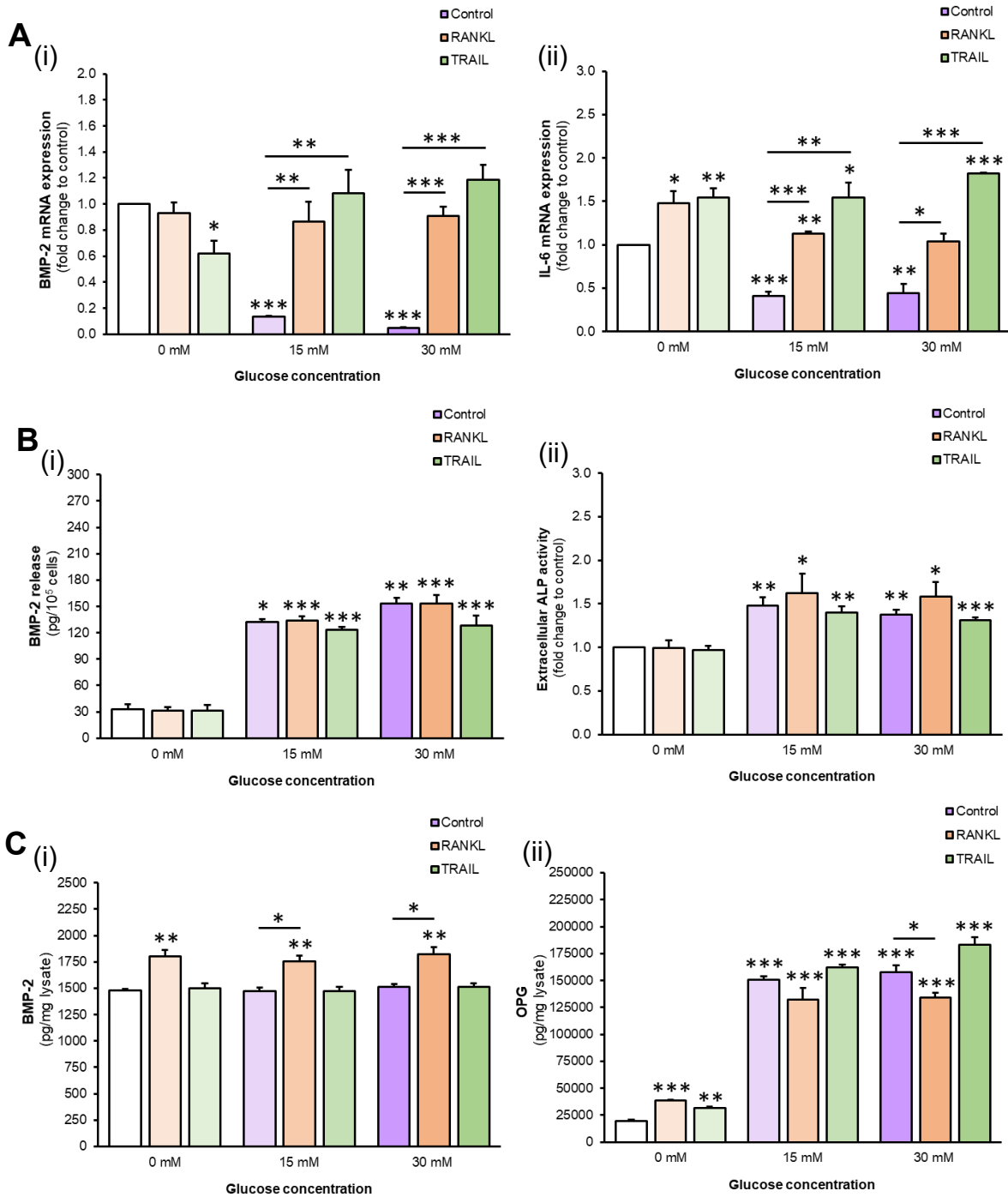
Appendix 4.7. The effect of mannitol exposure on pro-calcific indices in HASMCs. HASMCs were exposed to mannitol (30 mM) for 72 hours prior to analysis. (A) (i) BMP-2, (ii) ALP, (iii) Runx2, (iv) OPG, (v) Sox9 and (vi) IL-6 mRNA expression was determined by RT-qPCR, employing GAPDH as a reference gene. (B) (i) BMP-2, (ii) ALP activity, (iii) OPG, (iv) IL-6 in the conditioned media, and (C) intracellular (i) BMP-2, (ii) OPG and (iii) ALP activity were determined by ELISA and enzyme assay as appropriate. (D) (i) Canonical and (ii) non-canonical NF-κB activation was determined by Western blotting, quantified by scanning densitometry and normalised to GAPDH. Blots are representative. Media and lysate analyses are normalised to 10⁵ cells and pg lysate respectively.

Appendix 4

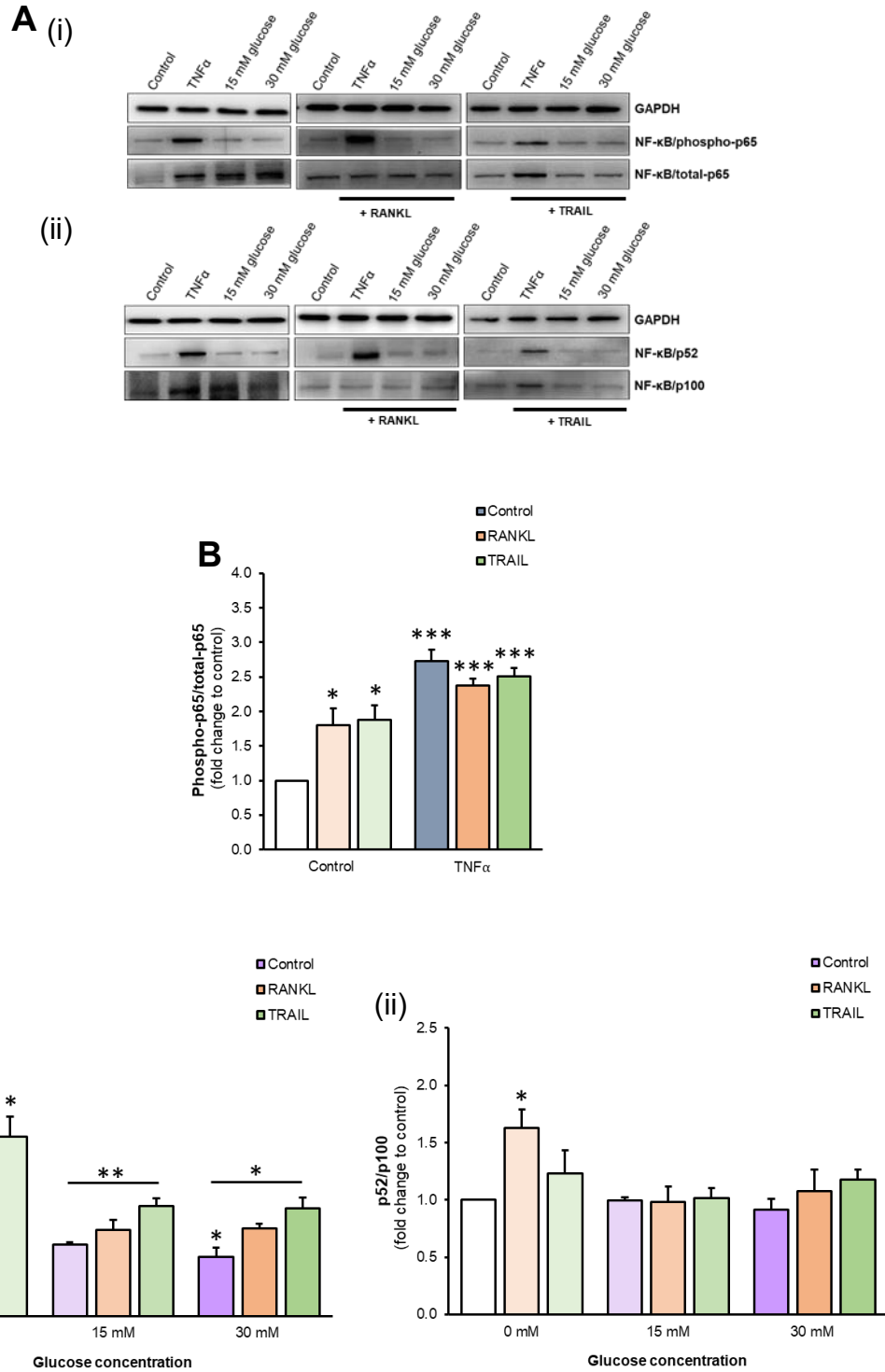


Appendix 4.8. The effects of TNF α +/- RANKL/TRAIL on pro-calcific indices in HASMC monoculture. HASMCs were exposed to TNF α (100 ng/mL) +/- RANKL (25 ng/mL) or TRAIL (5 ng/mL) for 72 hours. **(A)** (i) BMP-2, (ii) OPG and (iii) IL-6 mRNA expression was assessed by RT-qPCR, employing GAPDH as a reference gene. **(B)** (i) BMP-2 and (ii) IL-6 release and **(B)** intracellular (i) BMP-2, (ii) ALP activity and (iii) OPG were analysed by ELISA and enzyme assay as appropriate. Absolute values normalised to 10⁵ cells. * $p < 0.05$; ** $p < 0.01$; *** $p < 0.001$ compared to untreated control.

Appendix 4

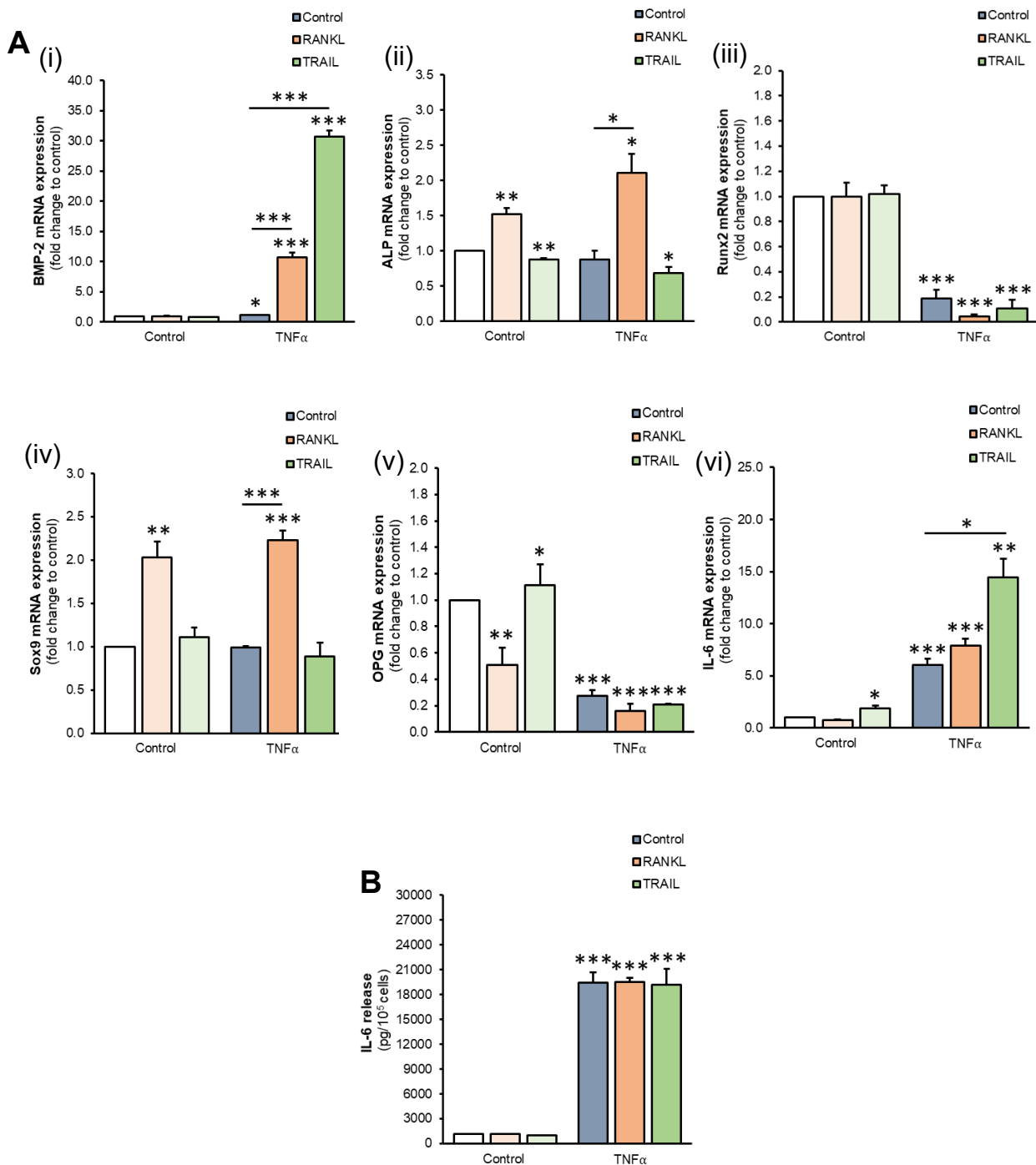


Appendix 4.9. The effects of glucose +/- RANKL/TRAIL on pro-calcific indices in HASMC monoculture. HASMCs were exposed to glucose (15-30 mM) +/- RANKL (25 ng/mL) or TRAIL (5 ng/mL) for 72 hours. (A) mRNA expression of (i) BMP-2 and (ii) IL-6 were analysed by RT-qPCR employing GAPDH as an endogenous control. (B) (i) BMP-2 and (ii) ALP activity were assessed in the conditioned media, and (C) intracellular (i) BMP-2 and (ii) OPG were determined by ELISA and activity assay as appropriate. Media and lysate analyses were normalised to 10⁵ cells and total protein respectively. * $p < 0.05$; ** $p < 0.01$; *** $p < 0.001$ compared to untreated control unless otherwise stated; bars indicate statistical significance between treatment groups.



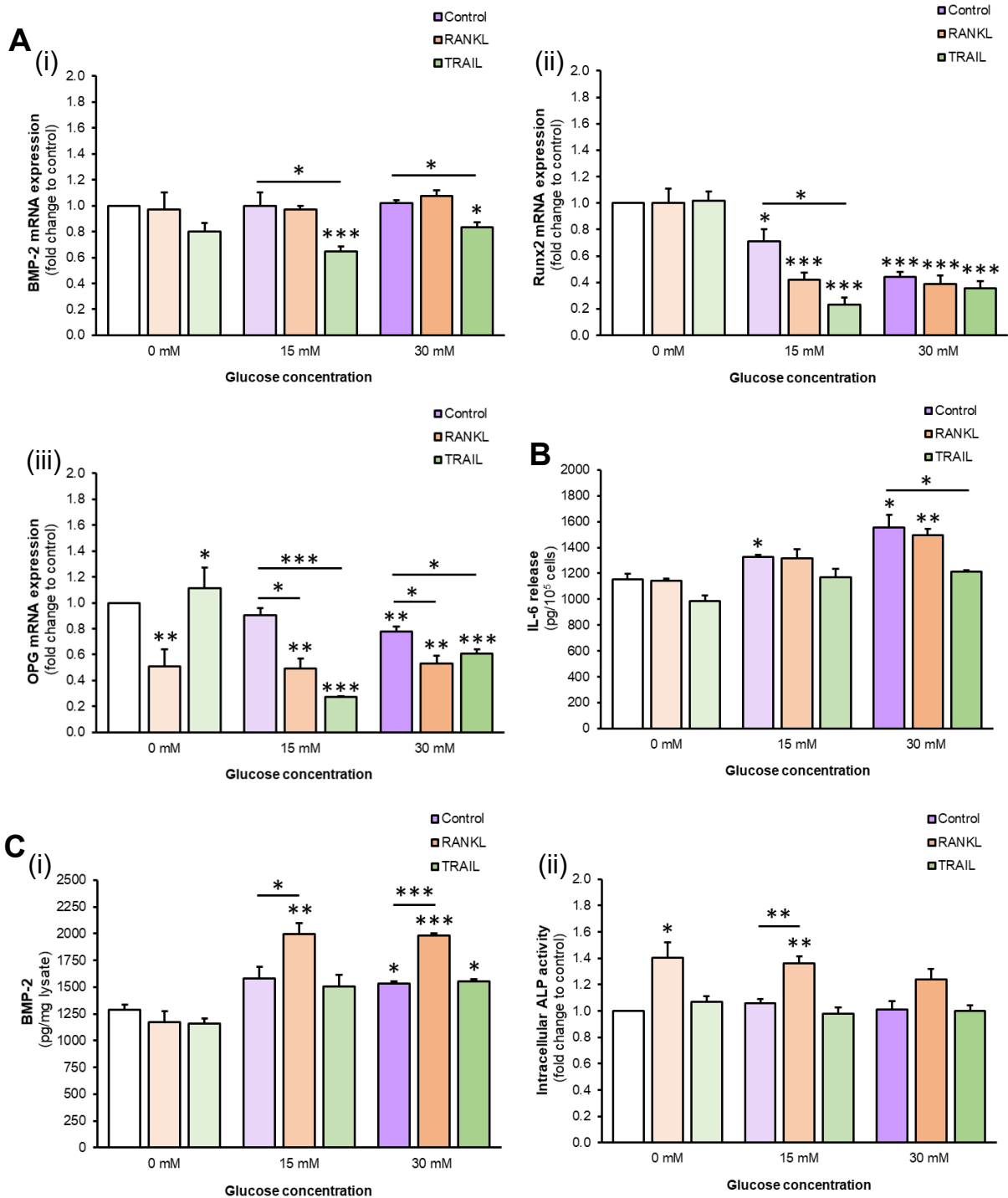
Appendix 4.10. The effects of TNF α and glucose +/- RANKL/TRAIL on NF- κ B activation in HASMC monoculture. HASMCs were exposed to TNF α (100 ng/mL) or glucose (15-30 mM) +/- RANKL (25 ng/mL) or TRAIL (5 ng/mL) for 72 hours. (A) Representative blots for NF- κ B activation are presented for all conditions tested. (B) Canonical NF- κ B activation was assessed following exposure to TNF α +/- RANKL/TRAIL, and (C) (i) canonical and (ii) non-canonical NF- κ B activation was assessed following exposure to glucose +/- RANKL/TRAIL. NF- κ B activation was determined by Western blotting, quantified by scanning densitometry and normalised to GAPDH. Absolute values are normalised to total protein. * $p < 0.05$; ** $p < 0.01$; *** $p < 0.001$ compared to untreated control unless otherwise stated; bars indicate statistical significance between treatment groups.

Appendix 4

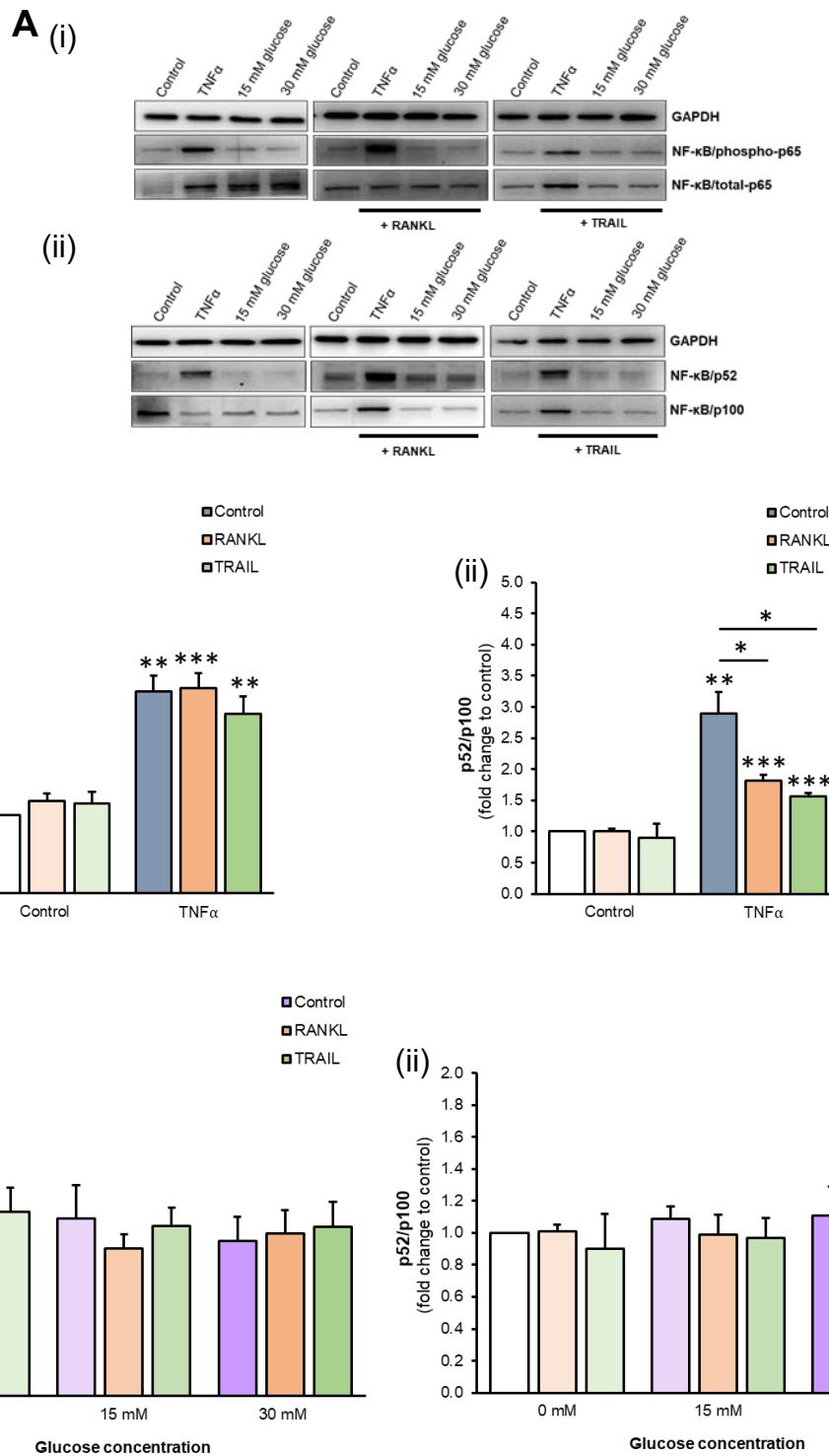


Appendix 4.11. The effects of TNF α +/- RANKL/TRAIL on pro-calcific indices in co-cultured HASMCs. HAECs in transwell inserts were exposed to TNF α (100 ng/mL) +/- RANKL (25 ng/mL) or TRAIL (5 ng/mL) for 72 hours, and the underlying HASMCs harvested for analysis. (A) mRNA expression of (i) BMP-2, (ii) ALP, (iii) Runx2, (iv) Sox9, (v) OPG and (vi) IL-6 were analysed by RT-qPCR employing GAPDH as an endogenous control. (B) IL-6 release levels were determined by ELISA, normalised to 10⁵ cells. * $p < 0.05$; ** $p < 0.01$; *** $p < 0.001$ compared to untreated control unless otherwise stated; bars indicate statistical significance between treatment groups.

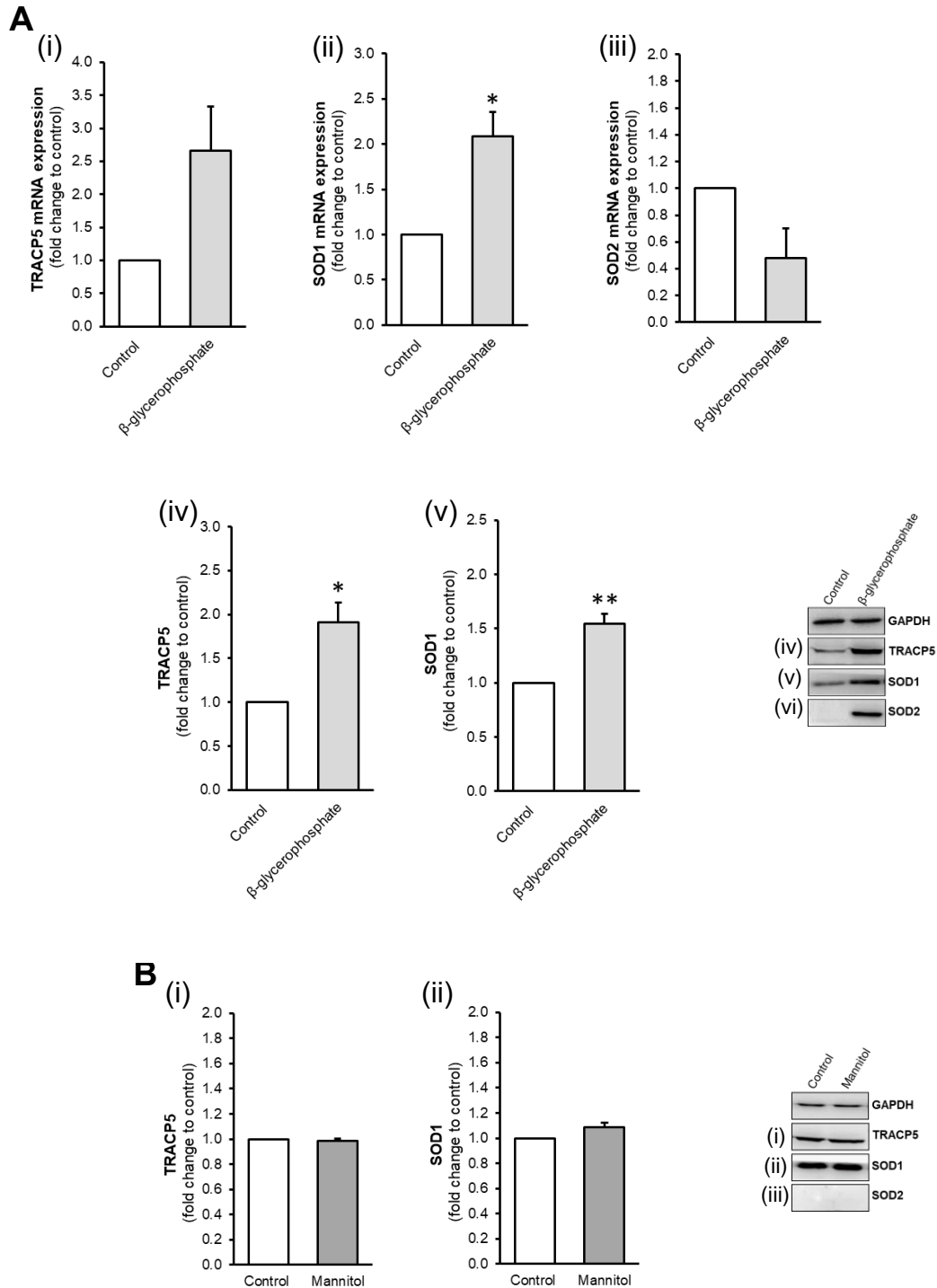
Appendix 4



Appendix 4.12. The effects of glucose +/- RANKL/TRAIL on pro-calcific indices in co-cultured HASMCs. HAECs in transwell inserts were exposed to glucose (15-30 mM) +/- RANKL (25 ng/mL) or TRAIL (5 ng/mL) for 72 hours, and the underlying HASMCs harvested for analysis. (A) mRNA expression of (i) BMP-2, (ii) Runx2 and (iii) OPG were analysed by RT-qPCR employing GAPDH as an endogenous control. (B) IL-6 release and (C) intracellular (i) BMP-2 and (ii) ALP activity were determined by ELISA and activity assay where appropriate, and normalised to 10⁵ cells (media) or total protein (lysate). * $p < 0.05$; ** $p < 0.01$; *** $p < 0.001$ compared to untreated control unless otherwise stated; bars indicate statistical significance between treatment groups.

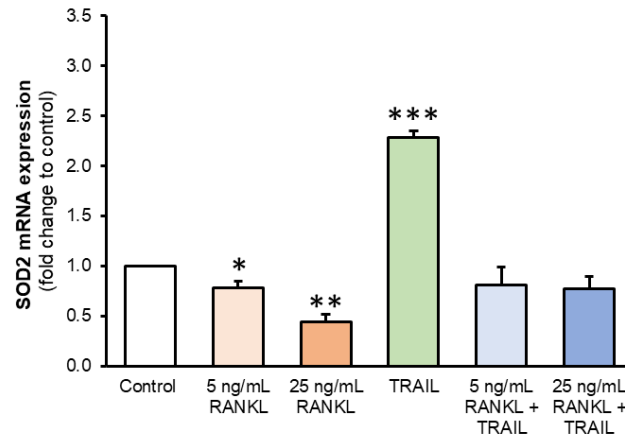


Appendix 4.13. The effects of TNF α and glucose +/- RANKL/TRAIL on NF- κ B activation in co-cultured HASMCs. HAECs were exposed to TNF α (100 ng/mL) or glucose (15-30 mM) +/- RANKL (25 ng/mL) or TRAIL (5 ng/mL) for 72 hours, and the underlying HASMCs harvested for analysis. (A) Representative blots for NF- κ B activation are presented for all conditions tested. (B) (i) Canonical and (ii) non-canonical NF- κ B activation was assessed following exposure to TNF α +/- RANKL/TRAIL, and (C) (i) canonical and (ii) non-canonical NF- κ B activation was assessed following exposure to glucose +/- RANKL/TRAIL. NF- κ B activation was determined by Western blotting, quantified by scanning densitometry and normalised to GAPDH. Absolute values are normalised to total protein. * $p < 0.05$; ** $p < 0.01$; *** $p < 0.001$ compared to untreated control unless otherwise stated; bars indicate statistical significance between treatment groups.

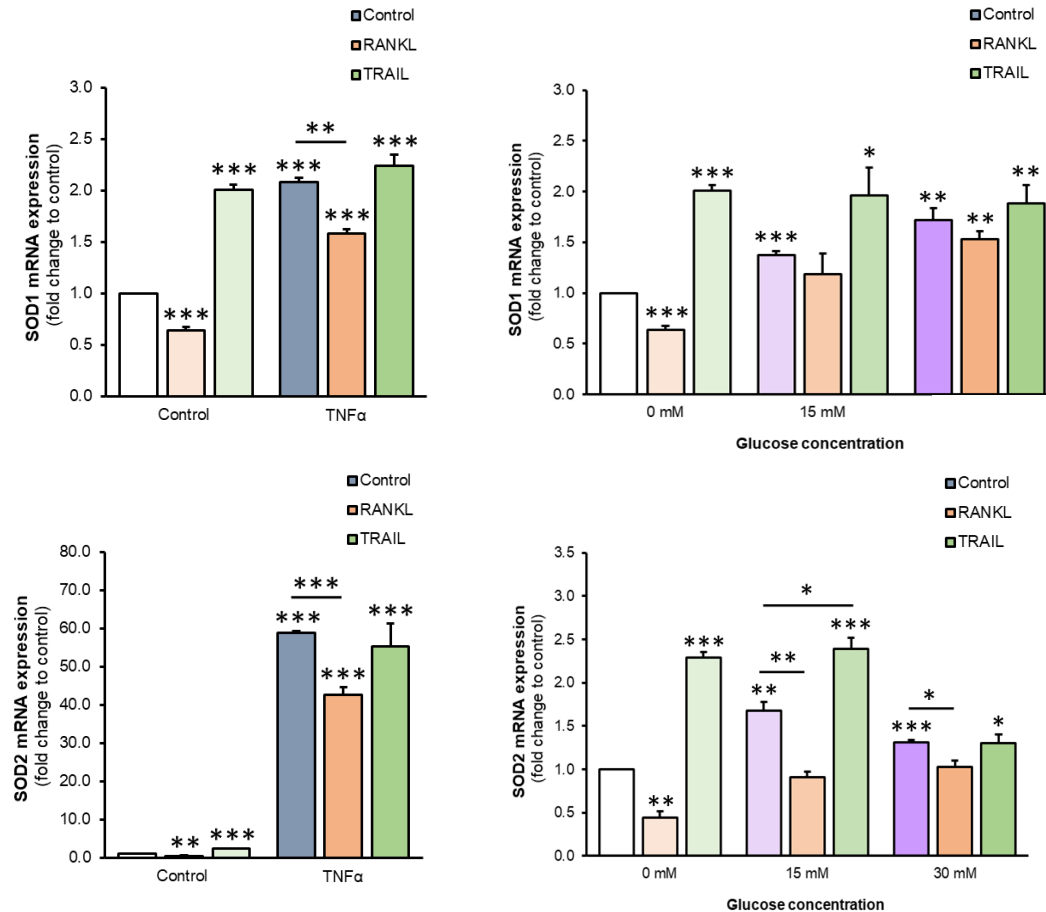


Appendix 5.1. The effects of β -glycerophosphate and mannitol on TRACP5, SOD1 and SOD2 expression in HAECs. HAECs were exposed to (A) 10 mM β -glycerophosphate for 72 hours prior to analysis of (i) TRACP5, (ii) SOD1 and (iii) SOD2 mRNA expression via RT-qPCR employing 18S as an endogenous control, or (iv) TRACP5, (v) SOD1 and (vi) SOD2 protein expression via Western blotting. (B) HAECs were exposed to 30 mM mannitol prior to analysis of (i) TRACP5, (ii) SOD1 and (iii) SOD2 protein expression by Western blotting. Blots are normalised to GAPDH, quantified by scanning densitometry where possible. Presented blots are representative. * $p < 0.05$; ** $p < 0.01$; compared to untreated control.

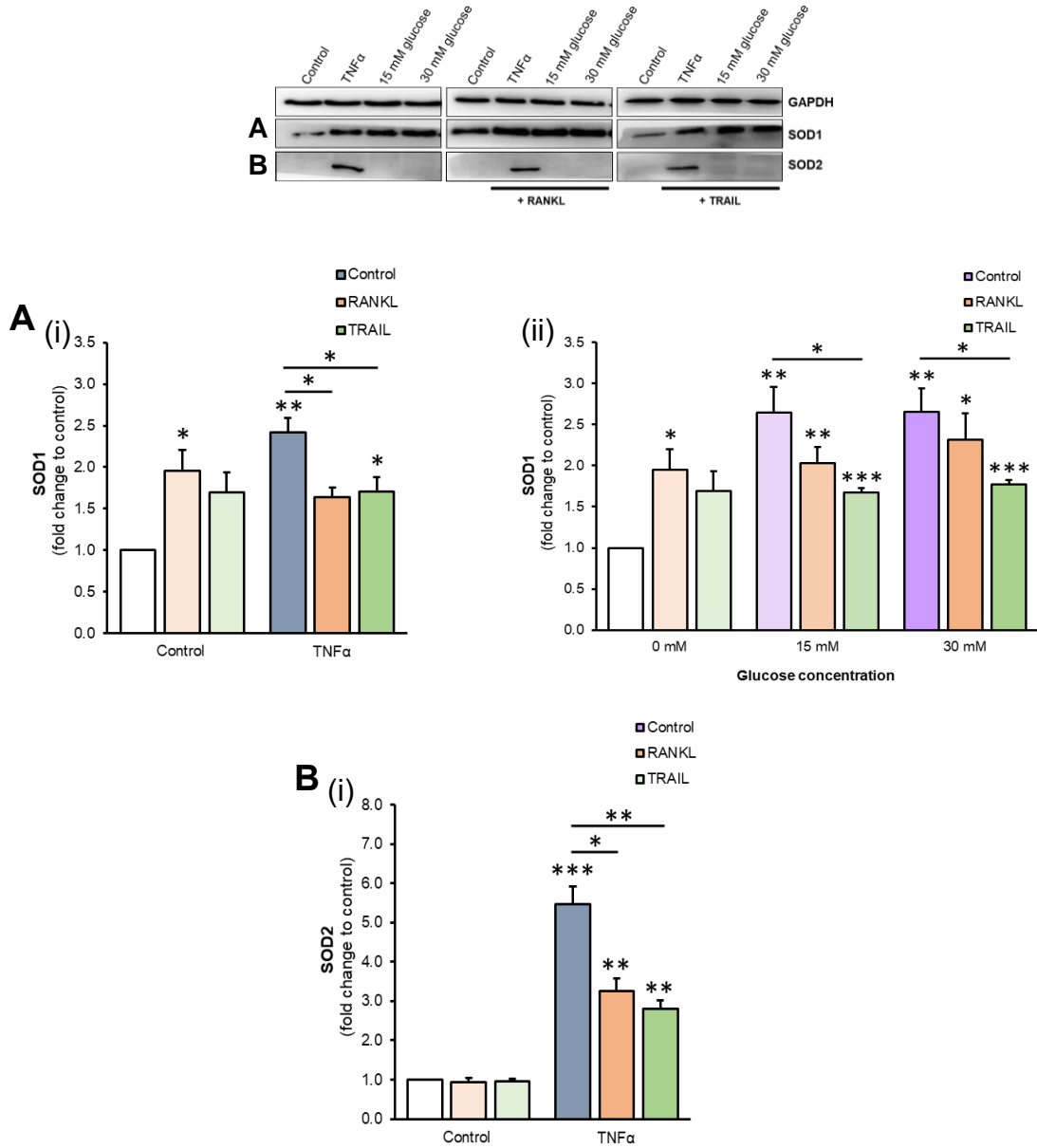
Appendix 5



Appendix 5.2. The effects of RANKL +/- TRAIL on SOD2 mRNA expression in HAECs. HAECs were exposed to RANKL (5-25 ng/mL) +/- TRAIL (5 ng/mL) for 72 hours prior to analysis. SOD2 gene expression was analysed by RT-qPCR employing GAPDH as an endogenous control. * $p < 0.05$; ** $p < 0.01$; *** $p < 0.001$ compared to untreated control.

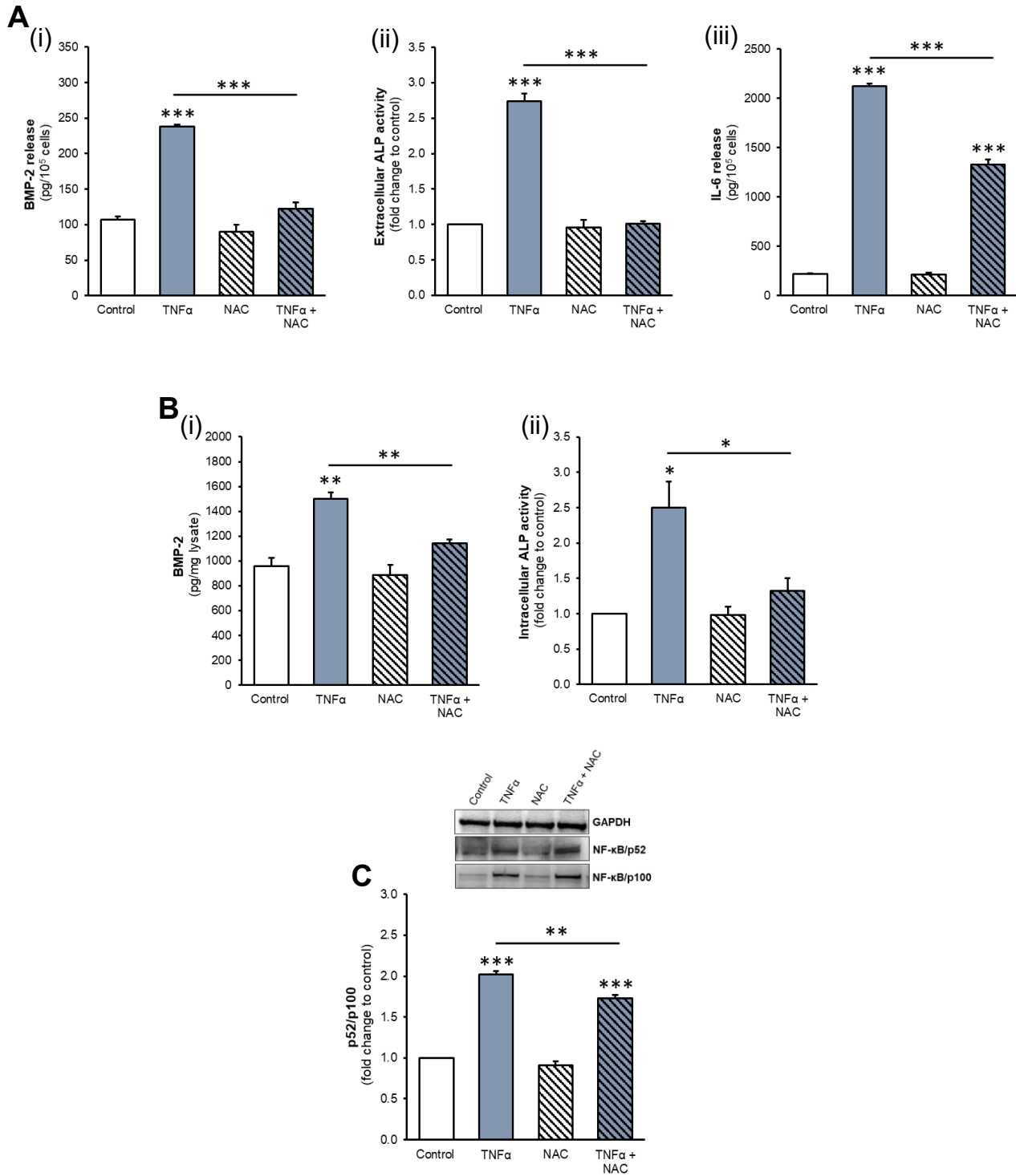


Appendix 5.3. The effects of RANKL/TRAIL on SOD1/SOD2 mRNA expression under inflammatory and hyperglycemic conditions. HAECs were exposed to (i) TNF α (100 ng/mL) or (ii) glucose (15-30 mM) +/- RANKL (25 ng/mL) or TRAIL (5 ng/mL) for 72 hours, prior to analysis of (A) SOD1 and (B) SOD2 mRNA expression. SOD1/SOD2 levels were determined by RT-qPCR, employing GAPDH as an endogenous control. * $p < 0.05$; ** $p < 0.01$; *** $p < 0.001$ compared to untreated control unless otherwise stated; bars indicate statistical significance between treatment groups.

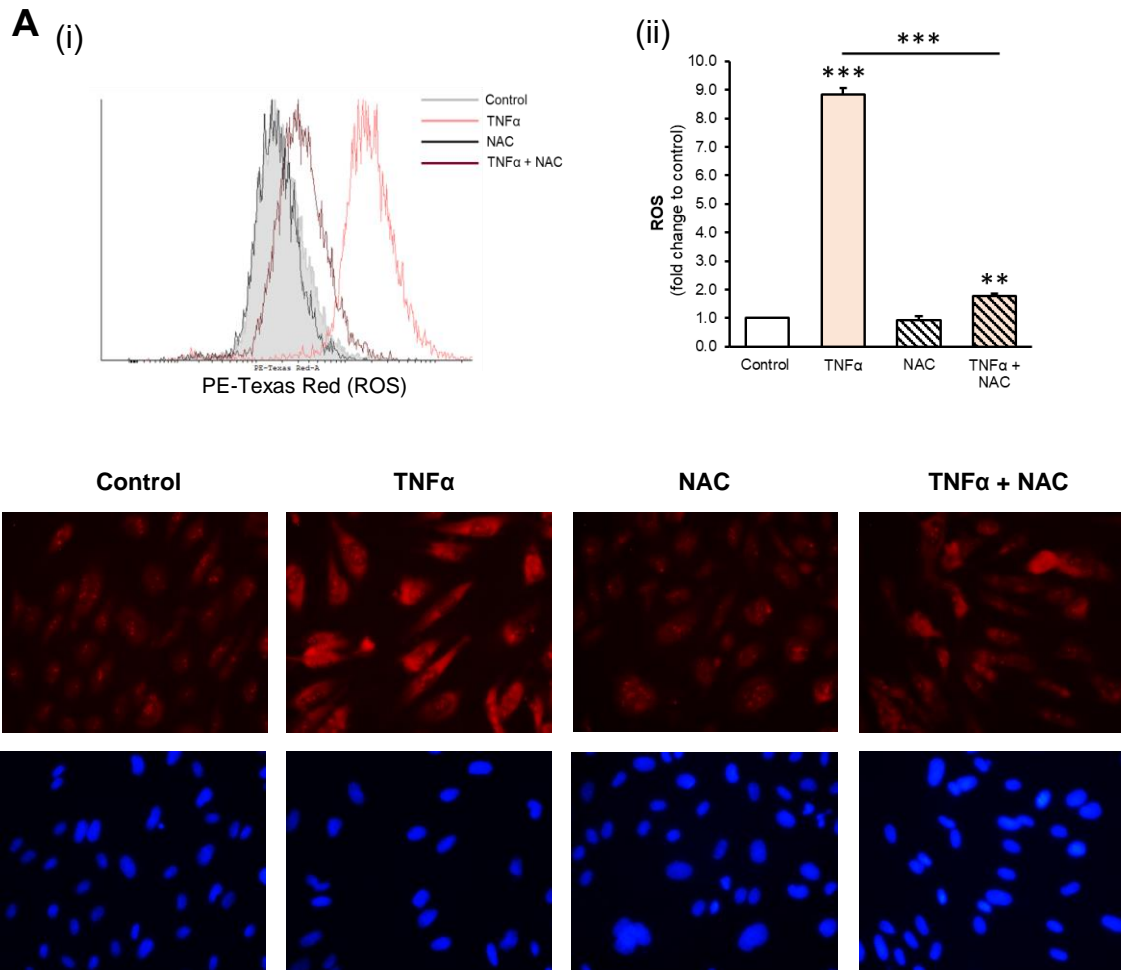


Appendix 5.4. The effects of RANKL/TRAIL on SOD1/SOD2 protein expression under inflammatory and hyperglycemic conditions. HAECs were exposed to (i) TNF α (100 ng/mL) or (ii) glucose (15-30 mM) +/- RANKL (25 ng/mL) or TRAIL (5 ng/mL) for 72 hours, prior to analysis of (A) SOD1 and (B) SOD2. Protein expression levels were determined by Western blotting, quantified by scanning densitometry and normalised to GAPDH. Blots are representative. * $p < 0.05$; ** $p < 0.01$; *** $p < 0.001$ compared to untreated control unless otherwise stated; bars indicate statistical significance between treatment groups.

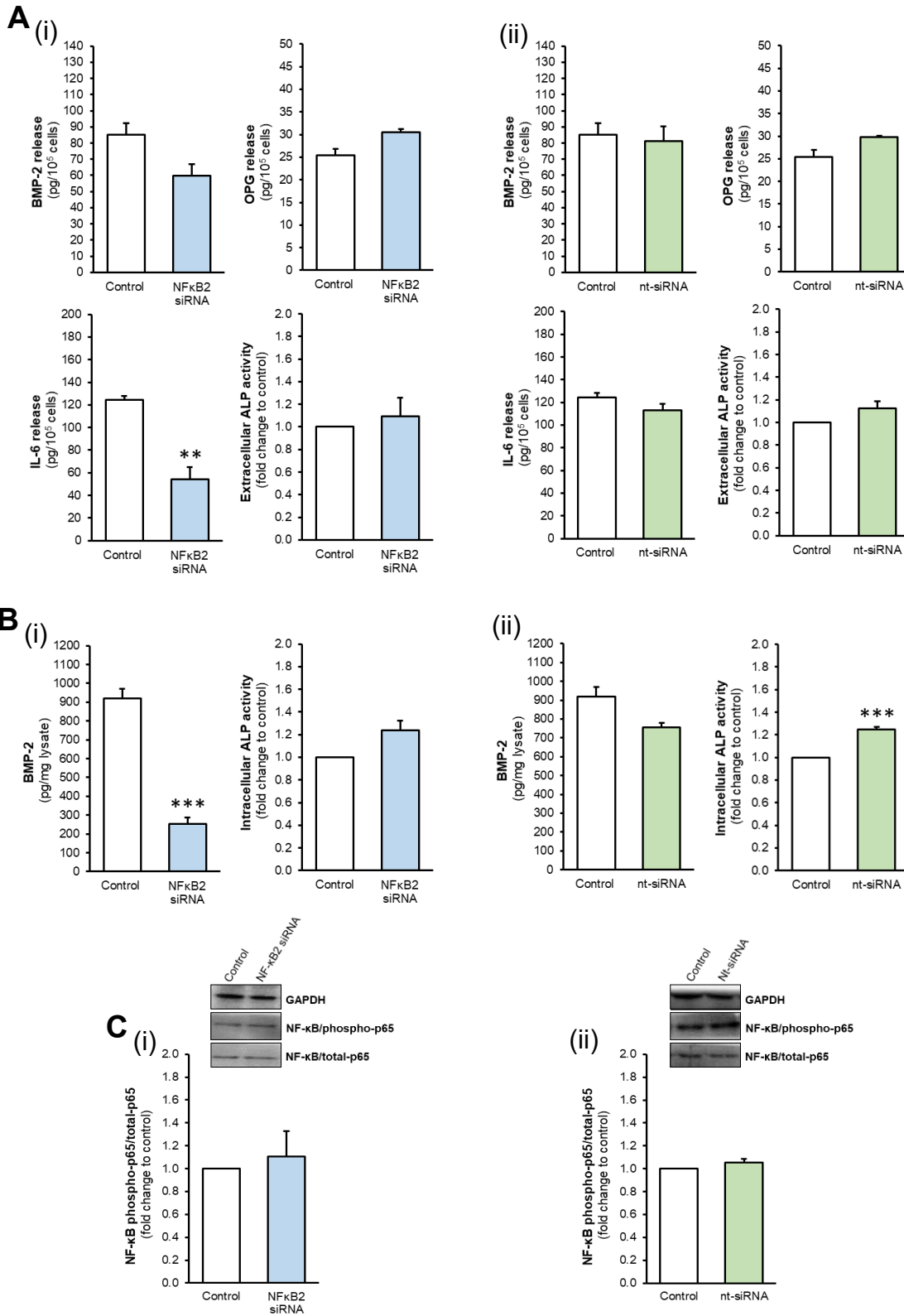
Appendix 5



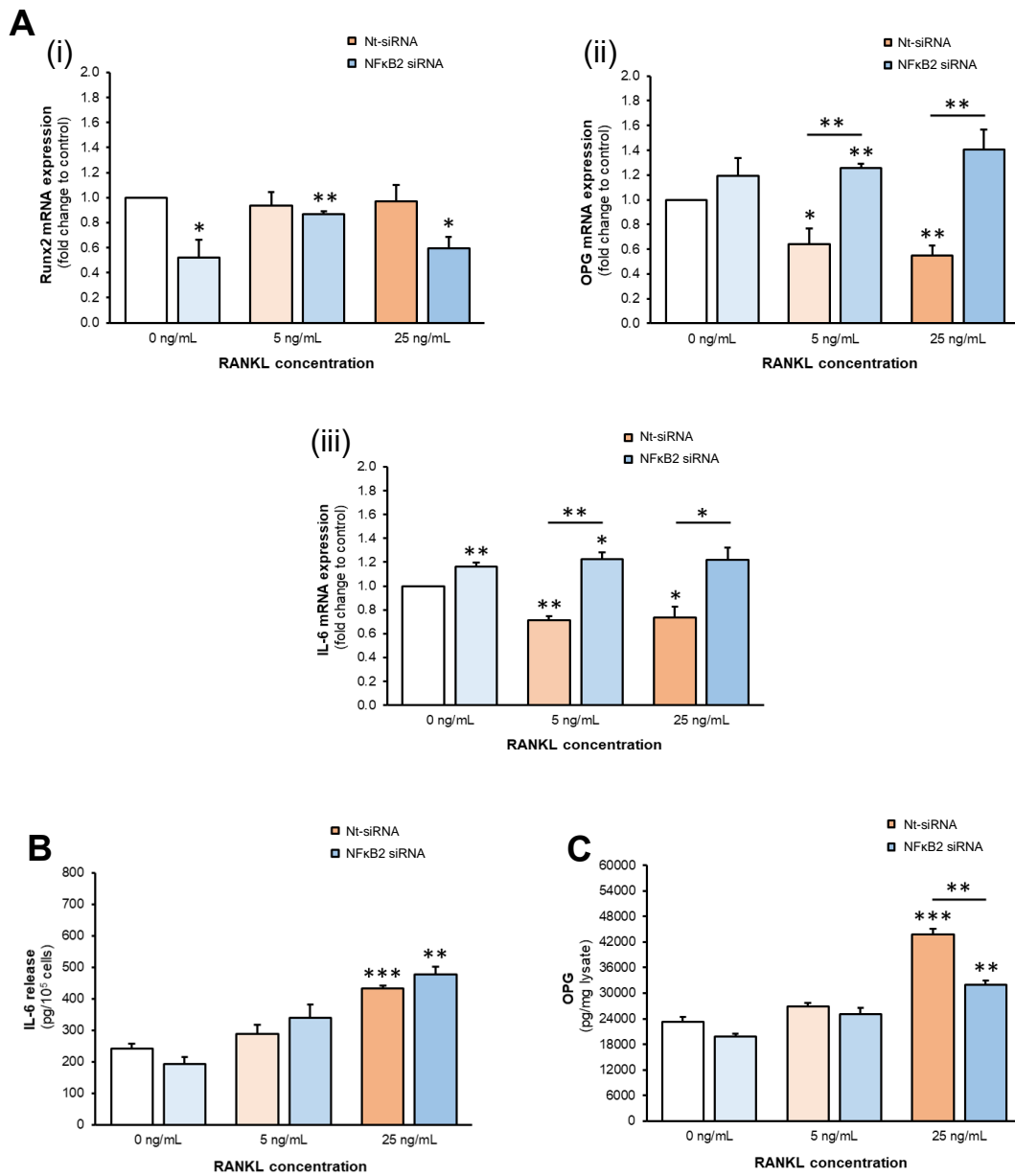
Appendix 5.5. The effects of TNF α +/- NAC on mRNA and protein expression levels in HAECs. HAECs were exposed to TNF α (100 ng/mL) +/- NAC (5 mM) for 72 hours prior to analysis. **(A)** Release levels of (i) BMP-2, (ii) ALP and (iii) IL-6, and **(B)** intracellular levels of (i) BMP-2 and (ii) ALP were determined by ELISA and enzyme activity where appropriate. Media and lysate values are normalised to 10^5 cells and total protein respectively. **(C)** Non-canonical NF- κ B activation was determined by Western blotting, quantified by scanning densitometry and normalised to GAPDH. Blots are representative. * $p < 0.05$; ** $p < 0.01$; *** $p < 0.001$ compared to untreated control unless otherwise stated; bars indicate statistical significance between treatment groups.



Appendix 5.6. The effects of TNF α +/- NAC on ROS generation in HAECs. HAECs were exposed to TNF α (100 ng/mL) +/- NAC (5 mM) for 24 hours prior to analysis. DHE stain (3 μ M) was added 30 minutes prior to the end of the incubation period; DAPI was added 3 minutes prior to analysis for fluorescence microscopy only. **(A)** ROS generation was measured by flow cytometry, quantified by histogram area; presented histograms are representative. **(B)** (i) ROS generation via DHE staining and (ii) DAPI nuclear counterstain were visualised using a Nikon Eclipse Ti fluorescence microscope. Images (40X magnification) are representative. ** $p < 0.01$; *** $p < 0.001$ compared to untreated control unless otherwise stated; bars indicate statistical significance between treatment groups.



Appendix 5.7. The effects of siRNA knockdown on pro-calcific indices in HAECs. HAECs were subject to (i) NFκB2 or (ii) non-targeting siRNA knockdown for 72 hours prior to analysis. (A) HAEC release profile of pro-calcific indices, and (B) intracellular BMP-2/ALP were assessed by ELISA and enzyme assay where appropriate. (C) Canonical NF-κB activation was determined by Western blotting, quantified by scanning densitometry and normalised to GAPDH. Blots are representative. ** $p < 0.01$; *** $p < 0.001$ compared to untreated control.



Appendix 5.8. The effects of RANKL following endothelial siRNA knockdown in co-cultured HASMCs. HAECs were subject to nt-siRNA/NFκB2 knockdown in transwell inserts for 48 hours, prior to co-culture with confluent HASMCs. HAECs in the luminal compartment were then treated with RANKL (5-25 ng/mL) for 72 hours prior to analysis of protein/mRNA responses in the underlying HASMCs. **(A)** (i) Runx2, (ii) OPG and (iii) IL-6 mRNA expression levels were determined by RT-qPCR, employing GAPDH as an endogenous control. **(B)** IL-6 release in the subluminal space, alongside **(C)** intracellular OPG, were assessed by ELISA; media and lysate analysis were normalised to 10⁵ cells and total protein respectively. * *p* < 0.05; ** *p* < 0.01; *** *p* < 0.001 compared to untreated control unless otherwise stated; bars indicate statistical significance between treatment groups.